Springer Transactions in Civil
and Environmental Engineering

Sharad Manohar
Suhasini Madhekar

# Seismic Design of RC Buildings

## Theory and Practice

Springer

# Springer Transactions in Civil and Environmental Engineering

More information about this series at http://www.springer.com/series/13593

Sharad Manohar • Suhasini Madhekar

# Seismic Design of RC Buildings

## Theory and Practice

Springer

Sharad Manohar
Structural and Training Consultant
Formerly with Tata Consulting Engineers
Pune, Maharashtra, India

Suhasini Madhekar
Civil Engineering
College of Engineering Pune
Pune, Maharashtra, India

ISSN 2363-7633 ISSN 2363-7641 (electronic)
Springer Transactions in Civil and Environmental Engineering
ISBN 978-81-322-2318-4 ISBN 978-81-322-2319-1 (eBook)
DOI 10.1007/978-81-322-2319-1

Library of Congress Control Number: 2015945961

Springer New Delhi Heidelberg New York Dordrecht London


Printed on acid-free paper

Springer (India) Pvt. Ltd. is part of Springer Science+Business Media (www.springer.com)

# Foreword

In recent years, earthquake engineering has been introduced as a subject at undergraduate and postgraduate levels. However, a beginner, with only an elementary knowledge of the theory of vibrations, finds it difficult to grasp the concepts of inertia forces, ductility, etc. Secondly, because of the vastness of the subject and its complexity, most practicing engineers find it difficult to access and comprehend the analytical process. Thus, at present, there is a clear need for a book which will explain the fundamentals of earthquake-resistant design in such a manner that students as well as practicing engineers can absorb them with ease. It is my strong belief that this book will meet such a requirement.

The authors are well known for their ability to present complex concepts in a simple manner. Mr. Manohar is known for his consultancy work at both national and international levels and is the recipient of the Indian Concrete Institute's Lifetime Achievement Award. He has also trained a large cross-section of professional engineers, architects, students, and supervisors in concepts of structural engineering and earthquake-resistant design. Professor Madhekar is dedicated to her work as a faculty for this subject. It is not without reason that she is held in high esteem by her students and employers. In addition, both authors have delivered lectures under the "Capacity Development Programme" of the Government of Maharashtra, sponsored by UNDP as well as by many other organisations. Teaching is a passion for both authors, and these qualities are effectively reflected in this publication.

Some of the attractive features of this book are as follows:

1. The fundamentals of structural dynamics and their practical applications to earthquake-resistant design of buildings are dealt with side by side. This unified approach is very useful to fully understand the practical implications of theoretical concepts. I am confident that students and practicing engineers will appreciate this approach.

2. In this book, the reader is initiated into the subject of response evaluation of structures' under ground motion excitation through an "easy-to-understand" concept, namely, simple harmonic motion. This simple theoretical approach is gradually extended to cover linear single-degree-of-freedom systems under earthquake excitation and then continues systematically right up to the nonlinear analysis of multistorey buildings. The mathematical content is highly focused and comprehensive. In my opinion, the book satisfies virtually all the needs of students, teaching faculty, and professional engineers.
3. There are several solved examples which cover the evaluation of forces and moments for which various types of practical structures, such as RC buildings, masonry structures, shear walls, retaining walls, and piles, need to be designed. Also included are members such as drag struts and collectors. It also deals with the subjects of soil-structure interaction and the effect of passive base isolation on the response of a building. This will definitely assist the professional engineers reading this book.
4. Earthquake engineering is a multifaceted subject requiring inputs from various disciplines to create a sound earthquake-resistant structure. For instance, it encompasses subjects such as inelastic material properties of primary building materials, important geotechnical aspects that play a role in soil-structure coupling and lateral loads on retaining walls, and importance of ductility, to name just a few. The authors have done well to include the right quantum of information from such topics to aid the designer in the design process.
5. It covers the subject of modal analysis in depth including the important missing mass correction approach. The authors have also provided a theoretical background to formulae used for evaluation of modal mass, participation factor, etc. This highly mathematical topic is developed in a systematic and easy-to-understand fashion which will benefit faculty and students alike.
6. The authors have drawn readers attention to a possible tension shift in shear walls and beams. This has an important bearing on reinforcement detailing.
7. Brick adobes are often badly hit during an earthquake because of their heavy weight and inadequate attention paid to incorporate anti-seismic measures. I am glad the authors have included requirements for "confined brickwork," as these are relatively inexpensive to implement and can certainly improve a building's performance during an earthquake.
8. The authors have used the medium of an illustrative example to explain the manner of conducting a nonlinear time history analysis for both a SDOF as well as a MDOF system. As a result, this difficult area is presented in a very clear, step-by-step manner, which is very easy to follow for a student.
9. The student as well as the professional designer will benefit greatly from coverage of topics such as (1) pushover analysis, (2) soil structure coupling, (3) piles exposed to lateral loads, (4) limit state design of brick masonry, and (5) performance-based design.

This book is well suited for senior-level graduate and postgraduate courses in Structural Dynamics and Earthquake Engineering. The book contains a wealth of information which is very difficult to obtain, and thus it will be an excellent reference document for both students and practicing professionals. It will provide a vital link between theory and practice.

Professor, Department of Civil Engineering, R.S. Jangid
Indian Institute of Technology Bombay,
Powai, Mumbai, India
15 September 2014

# Preface

The writing of this book has been both a joy and a challenge. Decades of our combined experience in consulting and teaching at postgraduate level in earthquake-resistant design has given us an opportunity to bring the complex theoretical concepts of earthquake engineering within easy reach of students, teaching faculty, and practicing professionals in a user-friendly manner. It is our belief that when theoretical concepts are well understood, it gives an impetus to put them into practice. The real challenge has been to address a wide spectrum of readers ranging from architects to structural engineers and from students to teaching faculty.

Over the centuries, mankind has had to deal with many natural hazards, such as cyclones, floods, droughts, and volcanic eruptions, which cause huge losses in terms of lives lost and property destroyed, but the one most feared is an earthquake. This fear stems principally from the totally unpredictable nature of this hazard, its suddenness, and the colossal destruction of life and property that it can cause. Contrary to common belief, a very large number of detectable earthquakes occur annually in the world, of which only about 20 % are felt and cause varying degrees of damage. That one can build an earthquake-proof structure is only an idealistic thought. Apart from the fact that such a structure could be economically unviable, one cannot guarantee the safety of a structure against a motion whose characteristics at best can only be an informed guess. Hence, in seismic-resistant design, the primary aim is to minimize damage and thus also save lives.

The Indian subcontinent is under a real threat of a moderate or major earthquake, and over the years, the country has experienced its share of seismic activity. Some of these have caused severe damage to property and loss of life. For a country as densely populated as ours, the need for affordable space for urban expansion will drive human habitat into regions with high seismic risk. It is therefore very important that we develop a clear understanding of the concepts of earthquake-resistant design and implement the correct design and construction practices in order to minimize damage and loss of life, should an earthquake strike.

Adobes are at a disadvantage during an earthquake because of their heavy weight. Secondly, in rural areas, where brick housing is common, there is still considerable lack in understanding of the provisions required to improve their seismic resistance. However, such structures would continue to be built in large measure because of their relatively low cost, availability of materials locally, and their thermal insulation and fire-resistant properties. It is for this reason that we have included a chapter dealing with confined masonry. Such masonry can bring about improvement in seismic resistance of such abodes, at minimal extra cost. The subject is then extended to cover design aspects of reinforced brickwork to tackle higher-end masonry buildings.

The primary user group envisaged includes students, teaching faculty, and professional engineers. This book is our small contribution towards achieving good quality in the design and construction of buildings and for students and professionals to clearly understand the concepts of sound earthquake engineering. Some recent developments, as far as India is concerned, have also been included to provide the student and practicing engineer an insight into these areas, comprising (1) base-isolated buildings, (2) strength design of brick masonry, (3) concepts of performance-based design, (4) principles of capacity-based design, etc.

This book deals with the design and detailing requirements for seismic resistance of new buildings. The normal design of buildings is well understood. Hence, this book focuses only on seismic engineering aspects of the design process. A large number of examples on important topics are included for the benefit of students and practicing engineers. The examples are chosen to illustrate specific areas of design fundamentals. It is not the intention of this book to present exhaustive step-by-step calculations while solving examples. We believe that understanding the right approach to problem solution is more important. The illustrative examples are structured accordingly.

There are two important relatively recent developments which are covered in this book: (1) There is a growing demand to move away from strength-based design towards performance-based design. This subject has been introduced in the book. (2) There is greater awareness among owners to minimize earthquake-related damage to property and consequently prevent loss of life. As a result, there are increasing calls for checking the adequacy of existing buildings to meet current seismic codal stipulations. For this purpose, the pushover analysis technique is handy. Literature on this subject is very limited and, moreover, not readily available. The methodology of undertaking such an exercise is presented in the book with solved examples.

We have delivered many presentations across the country to a wide cross-section of technical personnel in an effort to disseminate knowledge in this field and to provide solutions to practical problems faced by designers, contractors, and architects while implementing theoretical concepts in their designs. From exchanges with participants, we realized that there was a definite need to translate the concepts of earthquake-resistant design from the laboratories to students, teaching faculty, and practicing professionals in a manner they would readily relate to. That is what this book attempts to achieve.

We wish to acknowledge that this book builds its foundations on the technical works of veritable giants such as Prof. James M. Kelly, Prof. Gary C. Hart and Kevin Wong as well as Prof. Tushar Kanti Datta and others. Many of the publications are referenced in the bibliography, but space restrictions do not permit inclusion of all. We also wish to express our gratitude to Prof. R.S. Jangid of IIT Bombay for his kind words of appreciation in his Foreword to this book. We are grateful to those who may have been of help but whose names have been inadvertently left out. Some photographs have been included to highlight certain key aspects of earthquake damage as well as concepts. We are grateful to Mr. C.M. Dordi and M/s Ambuja Cements Ltd. for making most of them available for use in this book.

Every effort has been made to ensure the correctness of various facets of earthquake-resistant design and detailing and examples covered in this book. In spite of that, it is inevitable that some errors or misprints may still be found. We will be grateful to the users of this book for conveying to us any error that they may find. We would also welcome any suggestions and comments offered. We would like to thank the M.Tech. students from the College of Engineering Pune who assisted in solving some of the example problems.

We would like to express our gratitude to our respective families for their unstinted support and encouragement without which this publication would not have been possible.

Pune, India
15 September 2014

Sharad N. Manohar
Suhasini N. Madhekar

# Contents


**1 Earthquakes** ..... 1
- 1.1 Concise Historical Review of Seismic Design ..... 1
- 1.2 Understanding Earthquakes ..... 4
  - 1.2.1 Earth Interior ..... 4
  - 1.2.2 Plate Tectonics ..... 5
  - 1.2.3 Faults ..... 5
  - 1.2.4 Predicting Earthquake Occurrence ..... 6
  - 1.2.5 Earthquake Effects ..... 7
  - 1.2.6 Seismic Zoning ..... 8
- 1.3 Earthquake Features ..... 8
  - 1.3.1 Seismic Waves ..... 8
  - 1.3.2 Locating an Earthquake's Epicentre ..... 9
- 1.4 Quantification of the Shake ..... 11
  - 1.4.1 Measuring Ground Motion ..... 11
  - 1.4.2 Intensity Scale ..... 12
  - 1.4.3 Magnitude Scale ..... 13
- 1.5 Illustrative Examples ..... 14
- Ex 1.5.1 Locating the Epicenter ..... 14
- Ex 1.5.2 Evaluating Moment Magnitude ..... 14

**2 Important Attributes for Seismic Design** ..... 15
- 2.1 Introduction ..... 15
- 2.2 Material Attributes ..... 16
  - 2.2.1 Need for Yogic Concrete ..... 16
  - 2.2.2 Steel Reinforcement ..... 18
  - 2.2.3 Bond and Shear ..... 19
  - 2.2.4 Masonry Components ..... 20
- 2.3 Damping ..... 21
  - 2.3.1 Types of Damping ..... 21
  - 2.3.2 Damping Ratio ..... 22
  - 2.3.3 Critical Damping ..... 23

2.3.4 Logarithmic Decrement (δ) ..... 24
2.3.5 Magnitude of Damping ..... 26
2.3.6 Proportional Damping ..... 26
2.4 Ductility ..... 28
2.4.1 Importance of Ductility ..... 28
2.4.2 Classification of Ductility ..... 29
2.4.3 Ensuring Adequate Ductility ..... 34
2.5 Lateral Stiffness ..... 35
2.5.1 Nature of Stiffness ..... 35
2.5.2 Lateral Stiffness Values ..... 38
2.6 Strength ..... 42
2.6.1 Characteristic Strength ..... 43
2.6.2 Target Strength ..... 43
2.6.3 Overstrength ..... 43
2.7 Mass ..... 44
2.7.1 Lumped Mass ..... 44
2.7.2 Mass Moment of Inertia ($m_\theta$) ..... 45
2.8 Degrees of Freedom (DOF) ..... 46
2.8.1 Description of Degrees of Freedom ..... 46
2.8.2 Natural Vibration Frequencies in Six DOF ..... 47
2.9 Illustrative Examples ..... 48
Ex 2.9.1 Determination of Nature of Damping and Damped Frequency ..... 48
Ex 2.9.2 Calculation of Critical Damping, Damping Coefficient and Logarithmic Decrement ..... 49
Ex 2.9.3 Obtaining Undamped and Damped Frequencies and Vibration Period with Damping ..... 49
Ex 2.9.4 Finding Time Period required for Specified Reduction in Amplitude ..... 50
Ex 2.9.5 Calculating Energy Dissipated in a Cycle ..... 50
Ex 2.9.6 Deriving Damping Ratios and Rayleigh Damping Matrix ..... 50
Ex 2.9.7 Calculation of Curvature Ductility ..... 52
Ex 2.9.8 Calculation of Rotational Ductility ..... 52
Ex 2.9.9 Evaluation of Frequencies for Six Degrees of Freedom ..... 53

**3 Vibration Concepts: *Linear Systems*** ..... 57
3.1 Introduction ..... 57
3.2 Simple Harmonic Motion (SHM) ..... 58
3.2.1 Equation of a Simple Harmonic Motion ..... 59
3.3 Combining Gravity and Dynamic Loads ..... 60
3.4 Single Degree-of-Freedom (SDOF) Systems ..... 62
3.4.1 Equation of Motion of a SDOF System ..... 62
3.4.2 Undamped Free Vibrations ..... 64

3.4.3 Damped Free Vibrations ..... 65
3.4.4 Damped Free Vibrations Under Impulse Loading ..... 66
3.4.5 Damped Free Vibrations Under Earthquake Excitation ..... 67
3.4.6 Resonance ..... 69
3.5 Two Degree-of-Freedom (Two DOF) System ..... 69
3.5.1 Undamped Free Vibrations ..... 69
3.6 Multi-Degree-of-Freedom (MDOF) System ..... 73
3.6.1 Undamped Free Vibrations ..... 74
3.6.2 Damped System Under Free Vibrations ..... 74
3.6.3 Damped Vibrations Under Earthquake Excitation ..... 75
3.7 Torsional Vibrations ..... 77
3.7.1 Equations of Motion for an Undamped System ..... 77
3.8 Rocking Motion ..... 79
3.9 Illustrative Examples ..... 83
Ex 3.9.1 Evaluation of Frequency and Frame Side Sway ..... 83
Ex 3.9.2 Computation of Displacement Response due to a Seismic Impulse ..... 84
Ex 3.9.3 Calculation of Inertia Forces, Base Shear, Displacement and Drift for a Two DOF Shear Frame ..... 85
Ex 3.9.4 Calculation of Frequencies with Torsion ..... 87
Ex 3.9.5 Computation of Rocking Frequency ..... 88

**4 Response Evaluation** ..... 89
4.1 Introduction ..... 89
4.2 Elastic Response Spectrum ..... 90
4.2.1 Concept ..... 90
4.2.2 Relationship Between Spectral Quantities ..... 91
4.2.3 Linear Design Acceleration Spectrum ..... 93
4.2.4 Tripartite Plot ..... 93
4.2.5 Merits and Limitations of a Design Response Spectrum ..... 95
4.2.6 Effect of Vertical Ground Motion ..... 95
4.3 Inelastic Response Spectrum ..... 97
4.3.1 Effect of Ductility ..... 97
4.3.2 Deducing Inelastic Design Response Spectrum ..... 99
4.4 Estimate of Fundamental Time Period of Vibration ..... 99
4.4.1 Effect of Masonry Infill ..... 100
4.4.2 Effect of Shear Walls ..... 101
4.5 Linear Static Procedure (LSP) ..... 101
4.5.1 Design Horizontal Seismic Coefficient ..... 101
4.5.2 Response Reduction Factor ..... 103
4.5.3 Evaluation of Base Shear ..... 105

4.5.4 Distribution of Base Shear ..... 105
4.5.5 Linear Static Design Procedure ..... 106
4.6 Modal Analysis ..... 107
4.6.1 Basic Principles ..... 107
4.6.2 Modal Equation of Motion ..... 107
4.6.3 Mode Shapes ..... 109
4.6.4 Modal Frequencies ..... 110
4.6.5 Orthogonality of Modes ..... 110
4.6.6 Normalisation of Modes ..... 111
4.6.7 Modal Participation Factor ..... 112
4.6.8 Modal Mass ..... 112
4.6.9 Modal Height and Moment ..... 114
4.6.10 Combining Modal Responses ..... 114
4.6.11 Modal Analysis Procedure ..... 116
4.6.12 Missing Mass Correction ..... 118
4.7 Numerical Time History Analysis ..... 118
4.7.1 Newmark's Numerical Methods ..... 119
4.7.2 Linear Acceleration Method ..... 120
4.7.3 Average Acceleration Method ..... 122
4.8 Nonlinear Time History Analysis ..... 123
4.8.1 Nonlinear SDOF System ..... 123
4.8.2 Nonlinear MDOF System ..... 125
4.9 Illustrative Examples ..... 127
Ex 4.9.1 Use of Tripartite Plot ..... 127
Ex 4.9.2 Effect of Ductility on Magnitude of Lateral Force ..... 127
Ex 4.9.3 Evaluation of Mode Shapes and Modal Frequencies ..... 128
Ex 4.9.4 Demonstration of Mode Orthogonality ..... 130
Ex 4.9.5 Different Methods for Normalizing Mode Shape ..... 131
Ex 4.9.6 Calculation of Participation Factors ..... 132
Ex 4.9.7 Determining Modal Masses and Modal Height ..... 133
Ex 4.9.8 Comparison of SRSS and CQC Methods ..... 134
Ex 4.9.9 Use of Missing Mass Method ..... 135
Ex 4.9.10 Time History Calculations for a Linear SDOF System using Linear Acceleration Method ..... 138
Ex 4.9.11 Time History Calculations for an Elasto - Plastic SDOF System ..... 141
Ex 4.9.12 Time History Computation for a MDOF system ..... 147

**5 Planning for Aseismic Buildings** ..... 155
5.1 Introduction ..... 155
5.2 Building Configuration ..... 156
5.2.1 Architectural Planning for Earthquakes ..... 156
5.2.2 Structural Planning ..... 158
5.2.3 Irregularity ..... 160
5.3 Pounding ..... 165

5.4 Horizontal Torsion ..... 167
5.4.1 Torsion Computation for a Multi-storey Building ..... 167
5.4.2 Design Forces Including for Torsion ..... 171
5.4.3 Effects of Horizontal Torsion ..... 173
5.5 Structural Anatomy ..... 174
5.5.1 Soft and Weak Storeys ..... 174
5.5.2 Short Column ..... 176
5.5.3 Floating Column ..... 178
5.5.4 Load Path Integrity and Redundancy ..... 179
5.5.5 Staircases ..... 181
5.6 Force-Based Design ..... 184
5.6.1 Design Philosophy ..... 184
5.6.2 Selection of a Design Earthquake ..... 185
5.6.3 Direction of Ground Motion ..... 185
5.6.4 Inertia Effects ..... 185
5.6.5 Load Combinations ..... 189
5.7 Illustrative Examples ..... 190
Ex 5.7.1 Effect of Vertical Irregularity ..... 190
Ex 5.7.2 Evaluation of Torsional Moment at a Floor in a Multistorey Building ..... 190
Ex 5.7.3 Sharing of Forces among Walls due to Torsion ..... 193
Ex 5.7.4 Checking for Existence of a Soft Storey ..... 196
Ex 5.7.5 Checking for Existence of a Weak Storey ..... 196

**6 Frames and Diaphragms: *Design and Detailing*** ..... 199
6.1 Introduction ..... 199
6.2 Moment-Resisting Frames (MRFs) ..... 200
6.2.1 Types of Moment-Resisting Frames ..... 200
6.2.2 Seismic Analysis Procedures ..... 201
6.2.3 Design and Ductile Detailing Principles ..... 204
6.3 Diaphragms ..... 206
6.3.1 Flexible Diaphragm ..... 207
6.3.2 Rigid Diaphragm ..... 207
6.3.3 Flat Slab Diaphragm ..... 210
6.3.4 Transfer Diaphragm ..... 212
6.3.5 Collectors and Chord Elements ..... 212
6.4 Beams ..... 214
6.4.1 Design for Moment ..... 214
6.4.2 Design for Shear ..... 216
6.4.3 Design for Bond ..... 217
6.4.4 Tension Shift ..... 218
6.4.5 Ductile Detailing ..... 219
6.5 Columns ..... 220
6.5.1 Column Design ..... 220
6.5.2 Ductile Detailing ..... 224

6.6 Beam–Column Joints ..... 225
6.6.1 Joint Types ..... 227
6.6.2 Joint Behaviour Mechanism ..... 228
6.6.3 Joint Design ..... 231
6.6.4 Ductile Detailing of a Joint ..... 233
6.6.5 Joint Constructability ..... 234
6.7 Facade Skin ..... 235
6.7.1 Rigid Masonry Infill ..... 235
6.7.2 Curtain Wall ..... 236
6.8 Tall Frames ..... 238
6.8.1 Introduction ..... 238
6.8.2 Structural Forms ..... 239
6.9 Special Aspects Relevant to Tall Frames ..... 242
6.9.1 Damping ..... 242
6.9.2 Effect of Higher Modes ..... 243
6.9.3 Reduction of Frames ..... 243
6.9.4 Shear Lag Effect ..... 247
6.9.5 P-Δ Translational Effect ..... 248
6.9.6 P-Δ Torque Effect ..... 251
6.9.7 Drift and Deformation ..... 251
6.9.8 Podium ..... 252
6.10 Illustrative Examples ..... 253
Ex 6.10.1 Analysis using Linear Static Procedure ..... 253
Ex 6.10.2 Evaluation of vibration frequencies ..... 256
Ex 6.10.3 Analysis using Linear Dynamic Procedure ..... 256
Ex 6.10.4 Load Distribution among Walls Depending on Diaphragm Rigidity ..... 259
Ex 6.10.5 Analysis of a Collector and a Chord ..... 261
Ex 6.10.6 Design of a Beam-Column Joint ..... 262
Ex 6.10.7 Evaluation of P-Delta Translational Effect ..... 265

**7 Shear Walls: *Aseismic Design and Detailing*** ..... 269
7.1 Introduction ..... 269
7.2 Functional Layout and Configuration ..... 270
7.3 Classification of Shear Walls ..... 272
7.3.1 Aspect Ratio ..... 272
7.3.2 Shape in Plan ..... 273
7.3.3 Ductility Class ..... 273
7.4 Design of Cantilever Walls in Flexure ..... 274
7.4.1 Important Design Considerations ..... 274
7.4.2 Flexural Stress Analysis ..... 275
7.4.3 Detailing for Flexure ..... 279
7.4.4 Boundary Elements ..... 282
7.5 Capacity-Based Shear Design of Cantilever Walls ..... 284
7.5.1 Design for Diagonal Tension ..... 284
7.5.2 Design for Sliding Shear ..... 286

7.6 Design of Squat Walls ..... 287
7.6.1 Design for Flexure ..... 287
7.6.2 Design for Diagonal Tension ..... 287
7.7 Coupled Shear Walls ..... 289
7.7.1 Degree of Coupling ..... 290
7.7.2 Design of Coupling Beams ..... 290
7.8 Walls with Openings ..... 293
7.9 Illustrative Examples ..... 294
Ex 7.9.1 Design of a Cantilever Shear Wall ..... 294
Ex 7.9.2 Design of a Squat Wall ..... 298

**8 Substructure Design and Soil–Structure Coupling** ..... 301
8.1 Introduction ..... 301
8.2 Parameters of Strong Ground Motion ..... 302
8.2.1 Amplitude and Frequency Content ..... 303
8.2.2 Effective Duration of Strong Motion ..... 304
8.2.3 Time History of Motion ..... 304
8.3 Important Subsoil Parameters ..... 305
8.3.1 Depth of Soil Overlay and Its Stratification ..... 305
8.3.2 Dynamic Shear Modulus ($G$) ..... 306
8.3.3 Poisson's Ratio ..... 306
8.3.4 Particle Grain Size Distribution ..... 307
8.3.5 Soil Damping ..... 307
8.3.6 Relative Density ..... 308
8.3.7 Water Depth ..... 308
8.3.8 Soil Bearing Capacity ..... 309
8.4 Soil Liquefaction ..... 309
8.4.1 Causes of Liquefaction ..... 309
8.4.2 Determining Liquefaction Potential ..... 310
8.5 Open Foundations ..... 310
8.5.1 Tie Beams ..... 312
8.6 Piles ..... 314
8.6.1 Pile Loads ..... 314
8.6.2 Pile Design Criteria ..... 315
8.6.3 Analysis of Laterally Loaded Piles ..... 316
8.6.4 Pile Group Effect ..... 321
8.6.5 Pile and Pile Cap Details ..... 322
8.7 Retaining Walls ..... 323
8.7.1 Yielding Walls (Cantilever Walls) ..... 323
8.7.2 Non-yielding Walls (Basement Walls) ..... 328
8.8 Soil–Structure Coupling (SSC) ..... 329
8.8.1 Dynamics of Soil–Structure Coupling ..... 330
8.8.2 Evaluating Effect of Soil–Structure Coupling ..... 331

8.9 Illustrative Examples ..... 340
Ex 8.9.1 Characteristic Load Method for Piles ..... 340
Ex 8.9.2 Active Earth Pressure and Base Moment on a Retaining Wall ..... 341
Ex 8.9.3 Active Earth Pressure on a Retaining Wall with Submerged Soil ..... 342
Ex 8.9.4 Soil Structure Interaction for a MDOF System ..... 343

**9 Confined and Reinforced Masonry Buildings** ..... 349
9.1 Introduction ..... 349
9.2 Seismic Considerations ..... 351
9.2.1 Building Configuration ..... 351
9.2.2 Walls ..... 352
9.2.3 Roofs ..... 353
9.3 Confined Masonry ..... 354
9.3.1 Tie Columns ..... 355
9.3.2 Tie Beams ..... 355
9.4 Sharing of Lateral Force Among Co-planer Walls ..... 355
9.4.1 Rigidity of a Solid Cantilever Shear Wall ..... 357
9.4.2 Rigidity of a Wall with Openings ..... 358
9.4.3 Distribution of Lateral Force Among Masonry Piers ..... 359
9.4.4 Walls Connected by a Drag Member ..... 360
9.4.5 Design of a Wall Pier ..... 360
9.5 Reinforced Masonry ..... 361
9.5.1 Wall Formation ..... 361
9.5.2 Special Reinforced Masonry Shear Wall ..... 362
9.6 Shear Wall: Working Stress Design ..... 363
9.6.1 Design Parameters ..... 363
9.6.2 Design of a Wall Subjected to Axial Load and In-Plane Flexure ..... 365
9.6.3 Design of a Wall Subjected to Out-of-Plane Forces ..... 368
9.6.4 Flanged Wall ..... 368
9.7 Slender Shear Wall: Strength Design ..... 369
9.7.1 Limit States ..... 369
9.7.2 Strength Design for Flexure ..... 370
9.8 Illustrative Examples ..... 372
Ex 9.8.1 Sharing of Inertia Forces between Piers ..... 372
Ex 9.8.2 Drag Forces in Member Connecting Masonry Shear Walls ..... 375
Ex 9.8.3 Checking Adequacy of a Selected Pier ..... 377
Ex 9.8.4 Design of a Masonry Shear Wall – Working Stress Method ..... 380
Ex 9.8.5 Design of a Wall For Out Of Plane Forces ..... 381
Ex 9.8.6 Strength Design of a Masonry Shear Wall ..... 382

**10 Base Isolation** ..... 387
10.1 Introduction ..... 387
10.2 Brief History ..... 388
10.3 Concept of Base Isolation ..... 389
10.4 Passive Base Isolators ..... 391
10.4.1 Elastomeric Isolators ..... 392
10.4.2 Sliding Isolators ..... 392
10.4.3 Primary Isolator Requirements ..... 393
10.5 Merits and Demerits of Isolators ..... 394
10.5.1 Merits ..... 394
10.5.2 Demerits ..... 395
10.6 Characteristics of Elastomeric Isolators ..... 395
10.6.1 Isolator Stiffness ..... 396
10.6.2 Isolator Damping ..... 397
10.6.3 Time Period of Isolator Supported Building ..... 397
10.7 Analysis of a SDOF Frame on Elastomeric Isolators ..... 397
10.7.1 Equation of Motion ..... 398
10.7.2 Evaluation of Natural Frequencies ..... 399
10.7.3 Mode Shapes ..... 400
10.7.4 Roof Displacement ..... 401
10.8 Analysis of a MDOF Frame on Elastomeric Isolators ..... 401
10.8.1 Equations of Motion ..... 402
10.8.2 Evaluation of Natural Frequencies ..... 403
10.9 Analysis of a SDOF Building Frame on Sliding (FPS) Isolators ..... 405
10.9.1 Evaluation of Slider Parameters ..... 405
10.9.2 Equations of Motion in Different Phases ..... 408
10.10 Analysis of a MDOF Building Frame on Sliding (FPS) Isolators ..... 410
10.10.1 Equation of Motion in Different Phases ..... 410
10.11 Illustrative Examples ..... 412
Ex 10.11.1 Determining Elastomeric Isolator Stiffness ..... 412
Ex 10.11.2 Frequencies of an Isolator Supported Building ..... 412
Ex 10.11.3 Evaluation of Displacement, Stiffness and Damping of a FPS Isolator ..... 415

**11 Performance-Based Seismic Design** ..... 417
11.1 Introduction ..... 417
11.2 Description of the Procedure ..... 418
11.2.1 Need for This Approach ..... 418
11.2.2 Performance Levels ..... 419
11.2.3 Hazard Levels ..... 421
11.2.4 Quantifying Performance Objectives ..... 422
11.2.5 Preliminary Building Design ..... 422

11.3 Nonlinear Static Procedure (NSP) – *Pushover Analysis* ..... 423
11.3.1 Capacity Evaluation ..... 423
11.3.2 Demand Evaluation ..... 427
11.3.3 Conducting a Pushover Analysis ..... 427
11.4 Capacity Spectrum Method ..... 429
11.4.1 Conversion of Spectra to ADRS Format ..... 430
11.4.2 Conversion of Demand Spectrum ..... 430
11.4.3 Conversion to Capacity Spectrum ..... 431
11.4.4 Locating the Performance Point ..... 432
11.5 Seismic Coefficient Method ..... 434
11.5.1 Equivalent Stiffness and Equivalent Time Period ..... 434
11.5.2 Prediction of Target Displacement ..... 435
11.5.3 Evaluation of Performance ..... 436

**References** ..... 439

**Index** ..... 445

# About the Authors

**Sharad Manohar** holds an MSc (Structural Engineering) degree from Imperial college, University of London. He is a graduate of the College of Engineering Pune, FIE (India), and was Chief Civil Engineer with Tata Consulting Engineers. He has extensive experience of over five decades in the construction, design, management, and handling of national and international contracts of a wide range of structures, including those in high seismic areas. He has worked with Gammon India Ltd. and Tata Consulting Engineers as Chief Civil Engineer and continues to provide consulting services and training in Structural Engineering and Management. He played a key role in the implementation of training centers for the entire cement industry in India. Mr. Manohar is a recipient of the Lifetime Achievement Award from the Indian Concrete Institute and a Gourav award from Association of Consulting Civil Engineers (India) for outstanding contribution over a lifetime of achievement. He has authored a book *Tall Chimneys – Design and Construction* and published several technical journal papers. He is a member of a national committee appointed by the Reserve Bank of India to develop guidelines for assessment of the structural safety of their existing buildings.

**Suhasini Madhekar** holds a PhD in Structural Engineering from IIT Bombay. She is presently working as a faculty member in the Department of Applied Mechanics at the College of Engineering Pune. She is FIE (India) and life member of ISTE, ISSE, INDIAN ASTR, IIBE, and ICI. Dr. Madhekar has teaching experience of over 24 years at undergraduate and postgraduate levels. She has published several papers in reputed journals and proceedings. She is the recipient of the COEP Star Award, an Excellence in Teaching Award from the College of Engineering Pune. She was awarded the Alumni Distinguished Faculty Fellowship by the Alumni Association of the College of Engineering Pune.

# Chapter 1
# Earthquakes

**Abstract** The chapter begins with a brief historical development of the science of earthquake-resistant design. Earth interior, plate tectonics and different types of faults are explained. Then it touches upon seismogenesis, the basis of zoning map in IS 1893, the characteristics of seismic waves and methods of measuring ground motion. Thereafter is explained the method adopted for locating an earthquakes' epicentre. The intensity and magnitude scales are described as well as the present-day moment scale. The chapter concludes with illustrative examples on how to locate the epicentre of an earthquake and calculation of moment magnitude of an earthquake.

**Keywords** Earthquake causes • Seismic zoning • Seismic waves • Locating the epicentre • Earthquake intensity and magnitude

## 1.1 Concise Historical Review of Seismic Design

Over centuries, man has been searching for credible answers to combat the earthquake hazard. It has been a long and arduous journey commencing from the Lisbon earthquake of 1755 (Ari Ben Menahem 1995). The first seismicity map of the world was published by Mallet in 1860, and in 1872 Gilbert reported (Otani 2003) that earthquakes are usually centred on a fault line.

Further progress over the years gave birth to the subject of earthquake engineering near the end of nineteenth century (Bozorgnia and Bertero 2004). Following the large-magnitude Messina earthquake of 1908, serious studies were commissioned to arrive at recommendations to mitigate such disasters (Bozorgnia and Bertero 2004). Based on recommendations that followed and supported by further research, modern earthquake-resistant design had its initial conceptualisation in the 1920s and 1930s. This formed the foundation of methods for practical earthquake-resistant design of structures.

However, to achieve a good measure of ground success in combating this hazard, there was a need to accurately understand the causes and nature of ground movements, develop analytical tools to evaluate structural response to an essentially dynamic random phenomenon and evolve codal provisions for designers to follow. An important step in this direction was the development of instruments to measure



S. Manohar, S. Madhekar, *Seismic Design of RC Buildings*, Springer Transactions in Civil and Environmental Engineering, DOI 10.1007/978-81-322-2319-1_1

earthquake ground motion. One of the first such instruments was Anderson and Wood torsion seismometer developed in 1925 (Ari Ben Menahem 1995).

The first significant ground motion records of Richter magnitude M 6.2 were obtained during the 1933 Long Beach earthquake (Bozorgnia and Bertero 2004). This proved to be a turning point in the field of earthquake-resistant design. With experience gained from this event, superior instruments were developed to measure earthquake motion. Their deployment in large numbers significantly enhanced seismologists' ability to accurately record ground motions. It was during the San Fernando earthquake of 1971 (Hart and Wong 2000) that accurate acceleration time histories were first recorded.

As far as structural dynamics is concerned, Newton published the first law of motion in 1687. D'Alembert's principle was published in 1743 (Otani 2003). In the nineteenth century, theory of structural mechanics developed rapidly, and in 1877 Rayleigh discussed vibration issues of a single degree-of-freedom (SDOF) system. After the 1906 San Francisco earthquake, interest was centred on developing methods to evaluate the dynamic response of a building to random ground motion. It was only after many decades of theoretical work that in the twentieth century an acceptable practical method emerged. With this method, approximate response of a structure to random dynamic ground motion could be obtained. This was largely assisted by the introduction of the acceleration response spectra method by Biot in 1934 (Trifunac 2006) and its further development by Housner 15 years later. He was also instrumental in propagating the merits of this method leading to its widespread acceptance.

In spite of considerable loss of life and property suffered in the San Francisco earthquake, call for action through codal provisions came only after the Santa Barbara earthquake of 1925 (FEMA 454 2006). In late 1920s the Structural Engineers Association of California (SEAOC) was formed and they made significant contributions to the California codal specifications. Later, codal provisions accounting for building height and flexibility were introduced in USA in 1943. In 1952 ASCE together with members of SEAOC formed a committee that presented the first formal recommendations which included the concepts of response spectrum, and these were incorporated into the 1958 edition of the UBC (Chen and Scawthorn 2003).

On the construction front, at beginning of the nineteenth century, early masonry buildings gave way to more flexible steel-framed structures with perimeter infill brick walls. Concrete framed buildings soon followed, and the first steps were taken in the 1920s to use shear walls to resist lateral loads. Recent growth of tall buildings brought with it tubular structural frameworks and other complex building forms with irregularities, multilevel automobile parking spaces requiring long span prestressed concrete beams and so on. This triggered dedicated research efforts to find analytical solutions to solve the increasingly complex structural problems.

Emergence of seismic analysis tools has been the outcome of theoretical progress, inference drawn from observed earthquake-related damages and experimental studies. The development of finite element method of analysis in late 1950s, followed by the introduction of matrix methods in the 1960s and acceptance of

risk-based approach in structural dynamics, were instrumental in designers being able to better tackle hurdles in the path of constructing superior earthquake-resistant abodes.

Research in the recent past resulted in a shift in design focus towards using ductility as a means to dissipate seismic energy leading to the concept, in late 1960s and early 1970s, of using confined concrete to counter damage caused by heavy inertia forces. Computer programs to analyse structures based on the concept of ductility were introduced in late 1970s. To incorporate ductility in structural members and also to achieve specified performance goals, form the keystone of present-day earthquake-resistant design. Increasing capability and diminishing cost of computational aids has enabled engineers to use numerical techniques to evaluate a structure's response to ground motion time histories.

In India, the earliest recorded earthquake known as the Rann of Kutch earthquake occurred in 1819 followed by those in Assam in 1897 (Richter magnitude M8.7) and at Kangra in 1905 (M 7.8). More recent major earthquakes in India are the ones in Bihar in 1934 and 1988 (M 8.4 and M 6.5) and Assam in 1950 (M 8.7) followed by those at Koyna 1967(M 6.7), Killari 1993 (M 6.3) and Bhuj in 2001(M 6.9). The code for seismic-resistant design of structures (IS 1893) was first published in 1962. The concept of ductility was first introduced in Indian codes in the latter half of the twentieth century and other codes covering ductile detailing requirements soon followed.

It was observed that some buildings survived a major earthquake even when the estimated inertia forces were far in excess of the resisting elastic capability of its structural elements. At the same time some other buildings experienced brittle collapse. It led to the realisation that the nature of post-elastic strength was an important ingredient which enabled buildings to survive. On further examination of the subject, it was apparent that certain types of post-elastic behaviour, such as in shear, culminated in sudden brittle failure. Clearly such mechanisms were to be suppressed in favour of those that did not lead to sudden failure, such as in flexure.

Over the last two decades there have been significant developments the world over in various facets of this multidisciplinary subject of earthquake engineering, e.g. better prediction of likely ground motion, availability of software to undertake three-dimensional dynamic analyses of structures inclusive of soil–structure interaction effects and an enhanced understanding of base isolation and dampers as practical techniques to minimise seismic vulnerability. The next few decades are likely to witness rapid strides in our capability to deal with high-order 3D structural dynamic problems. It will enable designers to tackle the dual problem of evaluating responses of buildings with complex structural forms and meeting the emerging codal demands arising from a performance-based design approach.

It must be realised that just following seismic-related codes is not a guarantee in itself to achieving a sound earthquake-resistant building. It requires the services of competent geophysicists and design professionals in many fields with a sound knowledge of earthquake engineering, coupled with strict inspection of construction work by trained and qualified persons who display a will to produce a superior product.

## 1.2 Understanding Earthquakes

An earthquake is a spasm of ground shaking which generates random oscillatory movements. The primary cause of earthquakes and other related issues are briefly discussed below.

### *1.2.1 Earth Interior*

It is recognised that the earth is composed of following three broadly distinct regions:

*The Core*: Central region of the earth composed mostly of iron, is called the core. This can be subdivided into two portions – (1) inner solid core which is under enormous pressure and has a radius of about 1,250 km and (2) an outer molten core which is about 2,200 km thick.

*The Mantle*: The core is surrounded by another main layer termed as mantle which is about 2,900 km thick and contains most of the earth's mass. It is solid but can deform in a plastic manner.

*The Crust*: The Mantle is sheathed by a relatively thin layer which is known as the crust. It is about 35–60 km thick under continents and about 6–10 km thick under ocean floors. This layer is much thinner than the other layers and it is brittle and susceptible to fracture. Different earth layers with their approximate thicknesses are shown in Fig. 1.1.

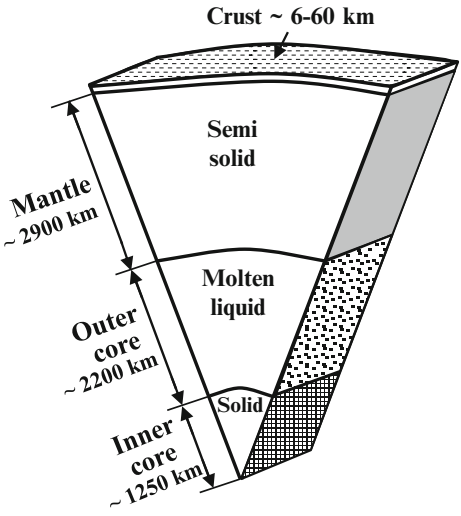


**Fig. 1.1** Earth layers

### 1.2.2 Plate Tectonics

Crust and a portion of the upper mantle are together termed as the lithosphere (from the Greek word lithos for stone). This layer appears on the surface as land masses called continents. Satellite observations confirm that the brittle lithosphere is fragmented into several large land masses called plates fitting together like a spherical jigsaw puzzle. The notion that these continents are not fixed in position was proposed by a Dutch map maker Ortelius way back in 1596.

The next significant contribution was by Wegener around 1915 (Otani 2003) when he expounded his theory of continental drift implying that continents were bodily moving. However, his fellow scientists were not convinced and it was only much later that he was proved right when in the 1960s the concept of sea floor spreading was proposed by Hess (Otani 2003). These two concepts provided the spark that generated considerable interest in this field resulting in the emergence, in the 1960s, of a plate tectonic theory. It postulates that the lithosphere, which is partly over land and partly under oceans, is broken into a mosaic of oceanic and continental plates that slide over a plastic layer of the mantle known as the asthenosphere.

Earthquakes can be caused by various reasons such as tectonic, volcanic, due to an explosion, etc. The most prevalent cause is tectonic movements. There exists enormous pressure and temperature gradients between the lithosphere and the earth's core causing convective currents in the mantle which force the brittle lithosphere to move in fits and starts. Almost all major earthquakes are tectonic in origin and occur at plate boundaries due to inter-plate (i.e. between plates) activity. Earthquakes can also occur due to intra-plate activity (i.e. local activity) within a plate because of local geological forces.

When one plate tries to grind past an adjoining one, an enormous amount of inter-plate strain develops. When the brittle rock's elastic limit is exceeded, a slip occurs along the plate boundaries and the elastic energy stored in the rock is suddenly and dynamically released, after which the fractured portions snap back into a relaxed state, known as rebound. This release of energy causes sudden relative movement between adjoining tectonic plates resulting in ground shaking that radiates outward (in the form of waves) from the location where slip occurred. This is termed as an earthquake.

### 1.2.3 Faults

Fracture between two rock masses is termed as a fault and its extent is the surface along which movement occurred. Most of these fault alignments cannot be seen because they are below ocean beds but they can be mapped by satellite measurements. Movement at a fault can be either in a horizontal or in a vertical direction or both. A fault can be described in a simple manner based on its geometry

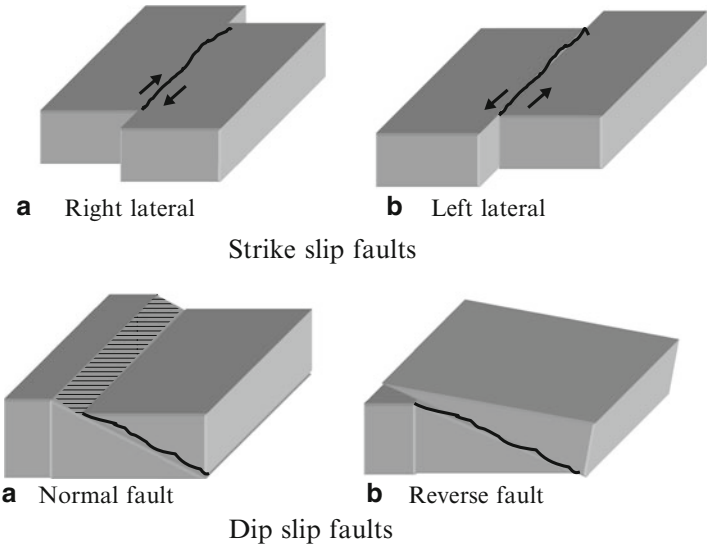


**Fig. 1.2** Types of faults

as dip, strike, and slip. The horizontal line interface relative to the North between the fault plane and a horizontal plane is called its *strike* (FEMA 454 2006) and the angle between these planes is called its *dip*. A few typical fault types are described below and depicted in Fig. 1.2.

1. *Strike-slip fault*: This type of fault occurs when movement is parallel to the strike. Usually the fault plane is nearly vertical and the plate surface on one side of the fault slides horizontally past the other. If the block opposite an observer looking across a fault moves to the right, it is termed as right lateral, and if the block moves to the left, the motion is termed as left lateral.
2. *Dip-slip fault*: This occurs when rocks on either side of a fault slip relative to each other along an inclined vertical plane. If the rock mass above an inclined fault moves down, it is termed as a normal fault; otherwise, it is termed a reverse fault.

### *1.2.4 Predicting Earthquake Occurrence*

For over a century, scientists have postulated many triggers that may predict an earthquake such as the position of the planets, abnormal weather conditions, unusual animal behaviour, volcanic activity, the extent of ground movement along identified fault planes, etc. However, no definite dependable conclusion has been drawn regarding the time interval between noticing of a trigger and occurrence of an earthquake. The only recorded prediction based on observed micro-seismic activity

and unusual animal behaviour is when Chinese authorities of Liaoning province issued a warning to the populace of Haicheng and Yingkou cities on 4 February 1975 to remain outdoors as a major earthquake was expected within 24 h. As predicted, an earthquake of Richter magnitude M 7.3 struck this region.

Because of their potential to cause devastation, there is tremendous interest to arrive at a methodology by which large-magnitude earthquakes could be predicted reasonably accurately in terms of space, time and size. Towards this end, various lines of reasoning have been tried, e.g. whether there is an *earthquake weather* meaning possible greater likelihood of its occurrence in a particular portion of the day or night or in a particular month or season, whether there is a reproducible correlation between a specific behaviour amongst animals and the occurrence of an earthquake and whether there are any noticeable changes in groundwater chemistry or surface levels or any evidence of recognisable foreshock activity prior to a major earthquake. Unfortunately, the precise prediction of an earthquake occurrence has not been possible so far.

The primary goal of any prediction would be to forewarn the public of a potentially damaging earthquake so that they can initiate appropriate response such as evacuation from their homes, alert children about steps they should take during shaking, keep an emergency medical kit handy and so on. If this is not accurately possible with virtually zero tolerance for error, then any such warnings could lead to false alarms which could make society even more complacent. Towards this end it can be said that for the present, an important requirement of predicting an earthquake accurately, in terms of time and location, still eludes seismologists.

There is now a general consensus that designs may be based on a probabilistic prediction of a seismic hazard (Booth and Key 2006). If $P_1$ represents annual probability of exceedance of a design earthquake, then the return period $T$, in years, is given by $T = 1/P_1$. Mathematically, the probability of exceedance $P_n$ during a period of $n$ years (where $n$ could be the design life of a building) is given by

$$P_n = 1 - \left(1 - \frac{1}{T}\right)^n \tag{1.1.1}$$

Thus, from life safety considerations, if the return period chosen is 475 years and design life of the building as 50 years ($n = 50$), the probability of exceedance of an earthquake of a given magnitude is

$$P_{50} = 1 - \left(1 - \frac{1}{475}\right)^{50} = 0.10 \quad \text{i.e. } 10\ \% \tag{1.1.2}$$

### *1.2.5 Earthquake Effects*

Although detailed seismicity is outside the scope of this book, a mention of some salient features is appropriate for overall understanding. There can be several

damaging after-effects of an earthquake apart from damage to man-made structures. For instance, a major earthquake can lead to a tsunami which is a sea wave triggered by large scale upward movement of the sea floor. Shallow crevasses can form during an earthquake or the ground may rupture engulfing any structure or vehicles standing there, and mountainous regions may experience debris avalanches. A closed body of water can experience sloshing and low-density saturated sands of relatively uniform size can suddenly lose their capacity to support loads. For the latter hazard, great care should be exercised in designing buildings in the vicinity of river banks and sea shores.

The damage that a structure will sustain depends on a unique combination of geological and structural factors. The former relate to nature of soil under the foundation, depth to bedrock, groundwater table, land features, etc. Structural factors could encompass a degree of confinement of concrete, slenderness of the building and its components and quality of its design and construction.

### *1.2.6 Seismic Zoning*

Based on considerable collated data regarding magnitude, intensity, location of epicentre, etc. of recorded earthquakes coupled with seismic risk perception studies from geotectonic considerations; the BIS has prepared a zoning map for India having Zones II to V. It is a qualitative representation of the probable degree of seismic hazard in different regions and forms the basis for evaluating likely seismic acceleration for which a structure needs to be designed. Even then, seismic hazard prediction for a particular site is fraught with uncertainties because of the many variables involved which are difficult to assess precisely.

## 1.3 Earthquake Features

### *1.3.1 Seismic Waves*

When a large pebble is dropped into a pond, it generates ripples which fan out in all directions. Similarly, when an earthquake occurs, energy is released in the form of elastic waves known as seismic waves. These waves radiate outward in all directions and they combine, refract and reflect off the earth's surface and cause the shaking that we perceive. Simultaneously, as these waves radiate outwards, their amplitude and frequency of oscillation also undergo changes. Essentially there are two types of seismic waves, viz. *body waves* and *surface waves*. The former travel within the earth, whereas the latter travel near the earths' surface. Each type of wave vibrates the soil in a different way.

#### 1.3.1.1 Body Waves

These can be subdivided into two categories:

1. *Primary waves*: These are also known as *P* waves (FEMA 454 2006). They vibrate the medium in the direction of their propagation with alternating compression and dilation. They are the fastest moving seismic waves which can travel through solids, liquids and gases.
2. *Secondary waves*: Also known as *S* waves or shear waves. These are slower than *P* waves. They cause the medium through which they travel to vibrate transverse to their direction of propagation. These waves are dependent on elastic shear resistance and hence cannot propagate through liquids or gases.

#### 1.3.1.2 Surface Waves

These waves have a longer vibration period and attenuate more slowly than body waves. Hence, high-rise buildings (which have a longer period than low-rise ones) are more at risk from such waves striking them at some distance away from the epicentre. These waves can also be subdivided into two categories:

1. *Love waves*: These waves are similar to shear waves but their motion is horizontal and lateral, perpendicular to the direction of wave propagation. Their amplitude is largest at the surface and decreases with depth.
2. *Rayleigh waves*: These waves have an elliptical vertical motion at the earth's surface. Amongst the four types of waves mentioned above, these waves have the slowest speed of propagation but are often largest in amplitude and are most destructive.

*P* waves are the first to arrive and are often felt as a thud. Next, *S* waves herald their arrival in the form of vertical vibrations and *Love* waves as horizontal vibrations. *Rayleigh* waves are usually felt as rocking and rolling motions. Amplitude of motion of surface waves diminishes less rapidly than that of body waves, and hence, far from the epicentre, the former are the more important source of ground movement.

### *1.3.2 Locating an Earthquake's Epicentre*

The location where rock yields resulting in an earthquake is termed as the focus (also called hypocentre), and a geographical point on the earths' surface vertically above the focus is termed as its epicentre. This is shown in Fig. 1.3. As mentioned above, when an earthquake occurs, it releases energy in the form of waves. *P* and *S* waves travel at different speeds in the body of the earth. Thus, knowing the elapsed time between arrival of the first *P* wave and the first *S* wave at a monitoring station (*lag* in travel time in Fig. 1.4), the distance from the station up to earthquake epicentre

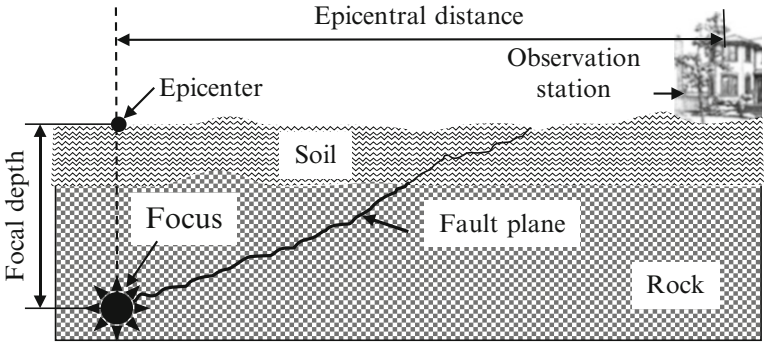


**Fig. 1.3** Focus and epicentre

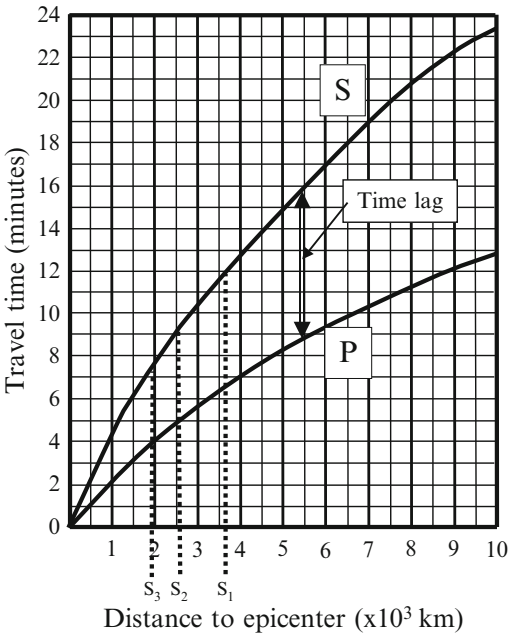


**Fig. 1.4** *P* and *S* wave travel time (diagram is only indicative)

can be estimated. The actual epicentre could lie anywhere on a great circle drawn with its centre as the monitoring station ($S_1$ in Fig. 1.5) and estimated distance to the epicentre as its radius.

There are many earthquake monitoring stations spread throughout the world from which two suitable non-collinear station locations are chosen (e.g. $S_2$, $S_3$) where arrival times of *P* and *S* waves have also been noted. Generally the sites selected are at substantial distance from likely epicentre so that epicentral and

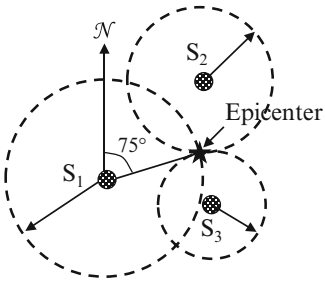


**Fig. 1.5** Plot for locating the epicentre

hypocentral distances are nearly the same (Paulay and Priestley 1992). Noting the time lag between the arrival of first $P$ and $S$ waves at these two stations, their epicentral distances can also be calculated. Then circles are drawn around these two chosen monitoring stations and the point where these three circles intersect is the approximate location of the epicentre. This is a simplistic portrayal of a highly sophisticated methodology. The procedure for locating the epicentre is depicted in *Ex* 1.5.1.

## 1.4 Quantification of the Shake

### *1.4.1 Measuring Ground Motion*

Seismology includes the study of propagation of seismic waves and this science has a long history dating back to over two centuries. All instruments for measuring ground motion are based on a fundamental principle that differential motion between a suspended mass of an oscillator and a structure fixed to the ground (thus moving with the vibrating earth) can represent motion of seismic waves. Such an instrument is called a seismometer and the earth's vibrations that it records are termed as a seismogram. From a structural engineering standpoint, it is important to measure seismic acceleration, because it dictates the magnitude of inertia forces which a mass will experience.

If the natural period of the oscillator is long relative to the period of ground motion, then recorded displacement is closely proportional to ground movement. If it is short relative to that of the ground, then measured displacement is proportional to ground acceleration and the instrument is called an accelerograph or an accelerometer. It can be shown that by choosing appropriate damping, if oscillator frequency ($\omega$) is made to be much larger than ground motion frequency, then its output is proportional to ground acceleration.

Since $\omega = \sqrt{k/m}$ (refer to Eq. 3.4.4), it follows that an accelerograph should have a small mass ($m$) and a stiff ($k$) spring. It will then record only strong ground motions which are the ones of interest in structural design since they could inflict

considerable damage. Modern digital accelerographs are rugged instruments which are activated by a trigger and when placed in a group, they can capture strong motion acceleration in three directions – two along orthogonal horizontal axes and one vertical. Results so obtained can be viewed either in the time domain or can be readily converted to frequency domain in real time.

### *1.4.2 Intensity Scale*

An earthquake is normally spoken of either in terms of its intensity or its magnitude. The former gives an indication of the extent of damage that the earthquake caused and the latter represents the magnitude of the shock. An intensity scale is not based on any instrument measurements and does not have a mathematical basis. It is an arbitrary qualitative ranking reflecting the perceived degree to which the environment and humanity have been affected by the earthquake. This scale does not correlate with actual maximum acceleration. Thus, intensity ascribed to a particular seismic event will vary depending on epicentral distance, ground conditions, quality of building construction, extent of population and other factors.

Rossi–Forel proposed a 10-point intensity scale in late nineteenth century which was enhanced to a 12-point scale by Mercalli in 1902 only to be modified by Neuman and others in 1931. This came to be known as the Modified Mercalli (MM) scale which is commonly referenced in many countries. Another scale appeared in 1964 which was developed by Medvedev, Sponheuer and Karnik which is now called the MSK scale. This intensity scale is widely used in India and a short characterisation of this scale is given in Table 1.1.

**Table 1.1** MSK intensity scale

| Scale | A short characterisation |
|---|---|
| I | Recorded only by seismographs |
| II | Felt only by individual people at rest |
| III | Felt only by a few people |
| IV | Felt by many people. Dishes and doors rattle |
| V | Hanging objects swing; many people asleep wake up |
| VI | Slight damages in buildings and small cracks in plaster |
| VII | Cracks in plaster; gaps in walls and chimneys |
| VIII | Wide gaps in masonry; parts of gables and cornices fall off |
| IX | In some buildings walls and roof collapse; landslides occur |
| X | Collapse of many buildings; cracks in ground up to widths of 1 m |
| XI | Many cracks in ground; landslides and rock falls occur |
| XII | Strong changes in the surface of the ground |

Source: International Association of Seismology and Physics

### 1.4.3 Magnitude Scale

The magnitude of an earthquake is a measure of the seismic energy released at source and hence is independent of the place of observation. In 1935 Charles Richter developed a local magnitude scale (denoted as $M_L$) for medium-sized earthquakes as

$$M_L = \log (A/A_0) \tag{1.2.1}$$

where $A$ is the maximum trace amplitude in microns recorded on a standard Wood–Anderson short seismometer and $A_0$ is a standard value as a function of distance within 100 km. Although this scale is widely used today to describe the magnitude of an earthquake, it is not popular in scientific circles. This is because it suffers, like many other prevalent scales, from early saturation at higher values of earthquake magnitude.

In the 1970s, a moment magnitude scale (denoted as $M_w$) was introduced (Hanks and Kanamori 1979). It is a measure which is based on seismic moment $M_0$ of the earthquake which has a physical significance. It is taken as the product of rigidity of the fault zone, the average area that slipped and the distance over which the fault displaced. It is not determined from instrumental recordings of a quake but on area of the fault that ruptured and its movement as a result of the quake, and hence this scale relates directly to physical properties of the fault medium. It is thus a measure of total energy released in an earthquake. Its merit over other methods is that it is valid over a wide range of magnitudes and it does not suffer from saturation (FEMA 454 2006).

This method has gained increasing acceptance amongst seismologists and is now the preferred measure to specify quantitatively the earthquake magnitude, particularly for medium- and large-magnitude earthquakes. Utilising input data from many sensors, researchers can infer a *moment tensor* which provides information regarding the fault's orientation as well as direction and magnitude of the slip.

Moment magnitude $M_w$ is based on the earthquake moment $M_0$ (Naeim 2001) which is given by (Datta 2010)

$$M_0 = \mu\, AD \tag{1.2.2}$$

where

$\mu$ : shear modulus of the medium (usually taken as $3 \times 10^{10}$ N/m$^2$ for the crust and $7 \times 10^{10}$ N/m$^2$ for the mantle)
$A$ : area of the dislocation, m$^2$
$D$ : average longitudinal displacement of rupture, m
$M_0$: seismic moment, N–m

Moment magnitude $M_w$ which is a dimensionless number is given by

$$M_w = \frac{2}{3}\log_{10} M_0 - 6.0 \tag{1.2.3}$$

The procedure for evaluating moment magnitude $M_w$ is shown in example *Ex* 1.5.2.

From the above description it can be deduced that a major earthquake occurring deep below the surface of the earth and in a remote region will rank high on moment magnitude scale but low on the MSK scale since there will usually be very little damage to environment or loss of life and property. On the other hand, a small-magnitude earthquake occurring at shallow depth but in a densely populated area will be rated as low on moment magnitude scale but is likely to rank high on the MSK scale. Thus, both scales, by themselves, are not comprehensive indicators.

## 1.5 Illustrative Examples

***Ex 1.5.1*** Determine the location and epicentral distance of an earthquake if the time lags between the arrival of *P* and *S* waves at seismic monitoring stations $S_1$, $S_2$ and $S_3$ are 5 min–26 s, 4 min–11 s and 3 min–38 s, respectively. For the purpose of this example, assume that Fig. 1.4 represents the seismic wave travel time plot.

**Solution** At monitoring station $S_1$, the time lag is 5 min–26 s. On a piece of paper draw a vertical line representing 5 min–26 s based on vertical scale of the travel time plot (Fig. 1.4). Move the paper up the curves until the length of the line matches the gap between the curves. Drop a vertical from this spot to read the distance to the epicentre from station $S_1$, which in this case is 3,600 km. Similarly proceeding in other two cases, distances to stations $S_2$ and $S_3$ are 2,500 and 1,900 km, respectively. From location of station $S_1$ a circle with a radius of 3,600 km is drawn as shown in Fig. 1.5. Similar circles are drawn around stations $S_2$ and $S_3$ with radii as 2,500 and 1,900 km, respectively. The location where these three circles intersect is shown as (*) in Fig. 1.5. The epicentre is therefore located at a distance of 3,600 km from monitoring station $S_1$ at 75° NE from it.

***Ex 1.5.2*** Calculate the moment magnitude $M_w$ of an earthquake with the following information regarding ruptured area at the fault:

| | | |
|---|---|---|
| Length of rupture area ($L$) | : | 39 km |
| Width of rupture ($W$) | : | 12 km |
| Length of slip ($D$) | : | 0.9 m |
| Average modulus of rigidity of fractured medium ($\mu$) | : | $3.1 \times 10^{10}$ N/m$^2$ |

**Solution** Area of rupture $A = L \times W = \left(39 \times 10^3\right) \times \left(12 \times 10^3\right) = 468 \times 10^6 \text{m}^2$

From Eq. 1.4, seismic moment $M_0 = \mu\, AD = 3.1 \times 10^{10} \times 468 \times 10^6 \times 0.9$
$= 1.306 \times 10^{19}$ Nm

From Eq. 1.5,

$$\text{Moment magnitude } M_W = \frac{2}{3}\left\{\log_{10}\left(1.306 \times 10^{19}\right)\right\} - (6.0) = 6.7$$

# Chapter 2
# Important Attributes for Seismic Design

**Abstract** The attributes, relevant to earthquake resistant design, are described. The reader will get acquainted with properties of reinforced concrete and masonry units to the extent that they relate to cyclic loading. Other attributes that are described in detail are damping, ductility, mass, lateral stiffness and strength. After a precise definition of degree of freedom, the methods of evaluating distortions under various modes of vibration are explained. Examples at end of the chapter illustrate the methods for evaluation of various damping parameters such as critical damping, logarithmic decrement and damping coefficient. These examples cover evaluation of energy dissipation, obtaining damped and undamped frequencies of vibration and calculation of various forms of ductility such as curvature ductility, rotational ductility, etc., as well as frequencies of vibration along six degrees of freedom.

**Keywords** Mass • Lateral stiffness • Strength • Damping • Mass moment of inertia • Ductility • Degrees of freedom

## 2.1 Introduction

Principal attributes, which dictate the satisfactory or otherwise performance of a building under earthquake impact, are its strength, stiffness, ductility and configuration. Briefly, a building should possess:

(a) Sufficient strength to withstand forces and moments induced by inertial effects under a seismic environment
(b) Adequate stiffness to contain drift within prescribed limits
(c) Appropriate ductile capacity at specified locations to withstand inelastic excursions
(d) Sound configuration

The first three aspects are covered here and the last requirement is discussed in Chap. 5.

Many of the attributes depend on characteristics of materials employed in the works. Concrete, steel reinforcement and masonry units are the basic building materials used in construction of reinforced concrete and masonry buildings. Hence, attributes for these materials are considered first. This is followed by other structural



S. Manohar, S. Madhekar, *Seismic Design of RC Buildings*, Springer Transactions in Civil and Environmental Engineering, DOI 10.1007/978-81-322-2319-1_2

attributes, viz. damping, ductility, stiffness and strength. Thereafter are discussed two aspects, viz. (1) lumping of building masses and (2) various degrees of freedom of a vibrating reinforced concrete building.

## 2.2 Material Attributes

Reinforced concrete emerged as a construction material at the beginning of the twentieth century. It soon gained ascendancy over other materials because of its many advantages, and today it is the predominant material used, other than structural steel, for the main supporting framework in urban building construction. The properties of concrete and steel and those of reinforced concrete play a vital role in the well-being of a structure during a seismic event.

### *2.2.1 Need for Yogic Concrete*

The minimum grade of concrete recommended (Jain et al. 2005) is M25 for buildings which are either more than four storeys or more than 15 m in height in Zones IV and V. Concrete is strong in compression but weak in tension, and as a result, its tensile strength is normally ignored during design. From stress–strain curves for unconfined concrete under uniaxial compression (for a range of concrete strengths), it is observed that with higher grade of concrete, a larger stress is permissible for a given strain. However, after the peak stress, the curve has a steeper drop as compared to that for a lower grade of concrete.

High-strength concrete ($f_{ck} > 40$ N/mm$^2$) provides an economic edge over normal concrete by way of higher strength per unit cost as well as improved durability. The stronger concrete permits a reduction in member sizes leading to a reduction in weight and hence in inertia forces. Also, it is reported that the strain at which longitudinal rebars buckle is independent of the concrete strength (Mendis and Panagopoulos 2000) due to which the spacing of transverse stirrups can remain the same as that for lower grade concrete. However, the design of slender high-rise building frames could be governed by stiffness considerations (storey drift limits) rather than strength. In such cases, the use of high-grade concrete could aggravate the problem as it leads to slimmer structures.

Under seismic conditions, a member experiences very high compressive strains which can result in spalling of concrete due to its transverse dilation. Concrete is neither homogenous nor isotropic, and although it can sustain cycles of compressive strain, it is inherently a brittle material. Therefore, there is a need for *Yogic concrete* – a term the authors have taken the liberty to coin – meaning concrete that has adequate strength coupled with flexibility in the inelastic range. This requirement is similar to that for a ballerina (Picture 2.1) who has to have adequate strength as well as flexibility to perform satisfactorily. It is for this reason


**Picture 2.1** Demand on concrete in seismic environment

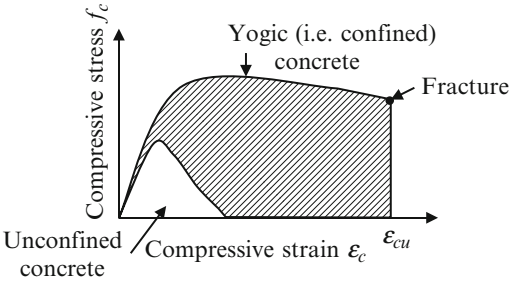


**Fig. 2.1** Stress–strain plot for Yogic and unconfined concrete

that concrete has to be confined if it is to perform satisfactorily under seismic excursions. In practice, such effective confinement is essentially achieved through the use of closely spaced stirrups.

Concrete behaviour is neither elastic nor fully plastic. The stress–strain curve of concrete (which depends on its mix proportions and physical properties of its ingredients) is non-linear at all stress levels. The non-linearity is small at low stresses and may be ignored. Typical monotonic stress–strain plot for *Yogic* and unconfined concrete is shown in Fig. 2.1. It will be seen that, compared to normal concrete, *Yogic* concrete can sustain much higher compressive stress as well as larger strain at failure which is desirable from considerations of ductility. Through tests on *Yogic* and unconfined concrete, researchers (Paulay and Priestley 1992) have reported that the monotonic stress–strain curve forms an envelope to the response

ordinates under cyclic loading, and hence the former can be used to represent concrete stress–strain profile under cyclic loads.

Confinement increases the strain capacity of concrete and thereby it is compressive, shear and bond strengths. Confining effect of stirrups, as the concrete dilates under compression, is mobilised only after concrete undergoes sufficient lateral expansion under longitudinal compressive stress at which stage the concrete cover starts to spall. However, as a result of confinement, the increase in ductility of the reinforced concrete member is very substantial.

### *2.2.2 Steel Reinforcement*

Steel is inherently a ductile material which is capable of withstanding high cyclic strains without significant reduction in strength and forms the prime source of ductility in reinforced concrete members. In the past, mild steel rebars of grade Fe 250 were commonly used as reinforcement. Such steel is characterised by a long yield plateau as well as substantial capability to withstand inelastic strains. Over the years, the strength of rebars in use has grown steadily, and today the use of Fe 415 grade rebars is common place. The Indian code IS 13920 (BIS 2003) now permits the use of Fe 500 and Fe 550 grade deformed rebars in an earthquake environment provided they are produced by the TMT process and meet the provisions of IS 1786 and it being demonstrated, through tests, that their elongation is more than 14.5 %.

General observations regarding use of rebars in concrete in a seismic environment are summarised below:

- Actual yield stress observed during tests should not exceed the specified yield stress by more than a specific margin as otherwise there is the possibility of shear or bond failure preceding plastic hinge formation in beams.
- It has been suggested that the ratio of actual ultimate strength to actual yield strength of mild steel rebars should not be less than 1.25 so as to allow adequate inelastic rotation capacity (Jain et al. 2005). For high-yield bars, this ratio will be with respect to 0.2 % proof stress.
- Rebars should demonstrate satisfactory bend and re-bend properties during controlled tests.
- For a given grade of concrete, to transfer the larger force from concrete to high-grade steel and vice versa requires longer development lengths, but there is difficulty in implementing this solution particularly at beam column joints (Brooke et al. 2005).
- When a rebar is stressed beyond yield, then de-stressed and restressed after some time has elapsed, there is an increase in its yield strength with consequent reduction in ductility. This is termed as strain hardening (Fig. 2.2) and has to be accounted for in column/beam design.
- Steel has substantial tensile strength but rebars may buckle when in compression, and hence they need to be confined as buckled bars are vulnerable to rupture.

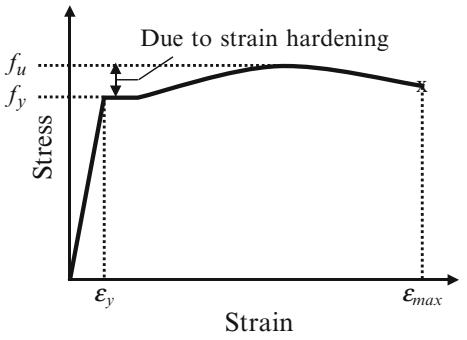


**Fig. 2.2** Effect of strain hardening of steel rebars

- Welding of rebars could lead to embrittlement, and hence their chemical composition should be checked prior to welding, to ensure that the steel is amenable to welding. Actual work should be executed by qualified welders under careful supervision.
- There is a difference between stress–strain relationship and ductile properties of Fe 250 mild steel and Fe 415 high-yield deformed rebars. Hence, it is not advisable to combine the use of such rebars as longitudinal steel in a frame column (Joshi et al. 2001).
- There has to be a minimum quantity of rebars in the compression zone of a plastic hinge as concrete strength degrades under high cyclic reversible loading.
- It has been evaluated (Brooke et al. 2005) that yield displacement of a concrete beam section with high-grade rebars (Fe 500) can be much larger than that using lower grade steel (Fe 250). Thus, the use of high-grade rebars in yielding members (e.g. beams of a moment frame) leads to a reduction in the useable displacement ductility, thereby attracting higher seismic forces to be resisted by the frame (Brooke et al. 2005).

### *2.2.3 Bond and Shear*

Under severe cyclic loading, longitudinal steel yields and concrete spalls which results in loss of bond. Hence, the use of ribbed bars is advantageous. These bars produce better bond because the ribs bear against surrounding concrete but at the expense of requiring a larger anchorage length which can be a problem at beam column joints. It should be noted that anchorage length has to cater to the maximum likely force in rebars including overstrength.

Under gravity and live loads, shear forces in beams remain essentially unidirectional. Even if they change sign, this change is usually insignificant. However, this is not the case under seismic excitation when significant shear stress reversals can take place over a substantial length of a member. During such cyclic loading, concrete will experience diagonal cracks due to shear reversal, leading to rapid degeneration

of shear transfer capability along the cracks. Further, it will affect the compressive response capacity of concrete across alternately opening and closing cracks, and as a result the effective bond strength diminishes.

Brittle failure is commonly associated with compression failure due to heavy axial forces as well as failure in shear, anchorage and bond. Because of the cyclic nature of shear stress, diagonal bars are not effective in resisting shear. However, confinement of concrete in the form of transverse reinforcement can delay its failure in compression as well as in shear. Safety against anchorage failure can be incorporated through the increase in anchorage length or by providing mechanical anchorage. Bond failure can be prevented by providing adequate bond length and selecting the right number and diameter of rebars.

### *2.2.4 Masonry Components*

Masonry walls are commonly constructed from bricks or concrete blocks (hollow or solid). These building blocks need to conform to relevant Indian Standards. The quality of in situ masonry primarily depends on the quality of bricks or blocks, on the mix proportions of the jointing mortar as well as on workmanship.

#### 2.2.4.1 Brick Units

Bricks are the traditionally used units for masonry construction. There is not enough documentation about proven properties of bricks in India nor, for that matter, about in situ masonry. The strength of bricks, employing commonly known methods for moulding and burning, varies over a wide range (Rai et al. 2005b), viz. 3–25 N/mm$^2$. Machine-made bricks with strengths in the range of 17.5–25 N/mm$^2$ are available, but any design based on such high-strength bricks must be subject to the consistency of their supply being regularly tested and proven.

Another important aspect in the selection of bricks is to make sure that they are of regular size and shape in order to achieve high-strength brickwork. For reinforced brickwork, brick units with hollow cores are preferred as they facilitate placement of reinforcement. These units are usually 10 mm less in size than their specified nominal size to allow for mortar joints. It is essential that units for reinforced masonry are of uniformly good quality with a minimum consistent compressive strength of at least 7 N/mm$^2$ on the net area (BIS 2002c).

#### 2.2.4.2 Concrete Blocks

Such units were first introduced for use in masonry construction in the early 1900s. They can be either solid or hollow. They should have a density of not less than 1,500 kg/m$^3$ (BIS 2005) and a minimum average compressive strength preferably not less than 7 N/mm$^2$. Steam-cured fly ash bricks are also available with a minimum compressive strength of 5.5 N/mm$^2$ and a density of 1,800–1,850 kg/m$^3$.

#### 2.2.4.3 Masonry Mortar

Mortar binds masonry units together and also compensates for their dimensional tolerance. The preferred mortar is a mixture of cement, lime, sand and water. Cement provides the strength, bond and durability characteristics; lime is useful as it helps the mix to retain its moisture and elasticity, improves its workability and reduces cracking because of a decrease in shrinkage. Sand, apart from its contribution to mortar strength, decreases the setting time and cracking as the mortar sets. Also, sand enables the mortar to retain its shape and thickness under the weight of several courses of masonry. Water of course provides workability and hydrates the cement. The strength of the selected mortar should be less than that of the bricks to ensure that any movement does not result in visible cracks in brickwork.

Due to an earthquake, the common mode of failure of masonry is cracking of mortar joints and sliding of the masonry along bed joints. To diminish this problem, the mortar should have adequate bond strength, and through sound workmanship, a good frictional capacity between mortar and the masonry units should be achieved. Generally a mortar mix that provides higher bond will also lead to greater shear strength. For unreinforced masonry walls, the mortar mix can be of cement/lime/sand (1:1:6) (Rai et al. 2005a), and for bedding grout in which reinforcement is embedded, it should not be leaner than cement/sand 1:3 (BIS 2001). Concrete for filling of holes should not be leaner than 1:2:4 with an aggregate size limited to 20 mm for 100 mm voids.

#### 2.2.4.4 Masonry Reinforcement

It is recommended (Rai et al. 2005b) that reinforcement shall be only of grade Fe 415 or less, and it is preferable to use deformed bars. For bed joints, reinforcement prefabricated in truss or ladder form is commonly used.

## 2.3 Damping

Damping is a key physical attribute of a vibrating system. The various facets of this parameter are discussed below.

### *2.3.1 Types of Damping*

When a building is displaced laterally and released, it is observed that its amplitude of vibration gradually reduces until it eventually comes to rest. This phenomenon is attributed to the capacity of building elements to absorb vibration energy by dissipating it through the material used and through joints. This is termed as damping, and its presence is inferred as it brings vibrations to a quiescent state. Buildings experi-

ence damping due to a variety of reasons such as cracking of concrete and inelastic movement of its structural components. Damping could be classified as under:

(a) External viscous damping: this can be caused by air surrounding a building. Its value is negligible and is usually ignored.
(b) Internal viscous damping: it manifests due to material viscosity, and its magnitude is taken as being proportional to system velocity.
(c) Friction damping: this is due to friction at connections and at supports and is constant for a particular system. This form of damping is prevalent in steel building frameworks.
(d) Hysteresis damping: it is due to dissipation of some portion of the energy input into the structure when it undergoes load reversals in the inelastic range.
(e) Radiation damping: it is due to energy released in the ground from soil–structure interaction by way of motion of the foundation relative to the free-field seismic motion. It is a function of subsoil characteristics.

When a body is restrained in its motion by a viscous fluid surrounding it, the resulting dynamic force is nearly proportional to the body's velocity. This type of damping of the motion is known as viscous damping. In dynamic analysis, for mathematical convenience rather than accuracy, it is common practice to club the effects of all types of damping mentioned above into an equivalent viscous damping with its magnitude being proportional to system velocity and having an instantaneous direction opposite to that of the vibrating system. This assumption, that all damping is viscous, permits decomposition of the equations of motion as will be seen later. Damping is expressed in units of Ns/m.

Buildings are often provided with supplementary damping for which a wide range of mechanical damping devices are commercially available. These can be grouped as: active dampers, passive dampers and semi-active dampers. In active dampers, the extent of damping is controlled by a sensor which provides a feedback so as to create optimum damping to keep the dynamic motions and stresses at acceptable levels. The passive dampers, in which typically the mechanical properties of these systems are fixed, are favoured as they do not require an external source of energy. The popular form among them is the viscous damper which consists essentially of a piston having a head with orifices, moving inside a tube filled with a fluid. Thus, the damper generates resistance to motion of the piston rod on its inward as well as outward strokes. The semi-active damper has been developed to take advantage of the best features of both active and passive dampers. The use of any form of mechanical dampers, other than isolators, is outside the scope of this book.

### *2.3.2 Damping Ratio*

Damping ratio is denoted as $\xi$. It is the ratio of actual viscous damping prevalent in the system ($c$) to critical damping ($c_{cr}$) for the system (i.e. $\xi = c/c_{cr}$). It is a useful nondimensional measure of damping in a structure and is usually expressed as a percentage of critical damping.

### 2.3.3 Critical Damping

The second-order differential equation of motion (Eq. 3.4.1) for a damped free-vibrating single degree-of-freedom (SDOF) system is

$$m\ddot{u}(t) + c\dot{u}(t) + ku(t) = 0$$

The suffix $(t)$ denotes motion parameters at any given instant of time $(t)$. In dynamic analysis, the motion is transient as a result of which the above suffix will be applicable to all motions. Since this is well understood, suffix $(t)$ is dropped in further equations for convenience, except in special cases.

This equation can be solved by assuming a solution in the form $u = Ae^{\lambda t}$ which leads to

$$m\lambda^2 + c\lambda + k = 0 \tag{2.1.1}$$

The two roots of this equation are

$$\lambda_{1,2} = -\frac{c}{2m} \pm \frac{\sqrt{c^2 - 4mk}}{2m} \tag{2.1.2}$$

The critical damping is defined as that value of $c$ (i.e. $c_{cr}$) which makes the radical zero:

$$\text{i.e.} \quad c_{cr} = 2\sqrt{mk} \tag{2.1.3}$$

It is at this damping level that the two roots in Eq. 2.1.2 are equal.

Substituting $k = m\omega^2$ from Eq. 3.4.4 gives

$$c_{cr} = 2m\omega \tag{2.1.4}$$

Introducing the damping ratio $\xi = c/c_{cr}$, Eq. 2.1.1 can be written as

$$m\lambda^2 + 2\,\xi m\omega\,\lambda + m\omega^2 = 0 \tag{2.1.5}$$

Solving, the two roots of this equation are

$$\lambda_{1,2} = \omega\,\left\{-\xi \pm i\,\sqrt{1-\xi^2}\right\} \tag{2.1.6}$$

Numerical value of the radical defines the dynamic behaviour of a vibrating system. Solutions to the above equation take different forms depending on the value of $\xi$. For instance, when:

1. $\xi > 1$, $\lambda_1$ and $\lambda_2$ are real and the system will not oscillate because damping effects overshadow the force causing vibrations. The structure is then said to be overdamped.

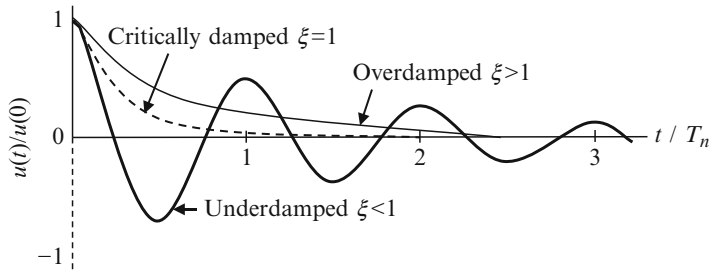


**Fig. 2.3** Damped oscillations

2. $\xi = 1$, $\lambda_1 = \lambda_2 = -\omega$ . The system is said to be critically damped which is a theoretical damping level. It represents the limit of periodic motion. The system loses its vibration characteristics and returns to its equilibrium position in the shortest time. The free vibratory motion will no longer be oscillatory.
3. $\xi < 1$, $\lambda_1$ and $\lambda_2$ are complex. The system oscillates about an equilibrium position for quite some time and gradually comes to rest. The system is said to be underdamped.
4. $\xi = 0$. The system oscillates at its natural resonant frequency ($\omega$), and it is said to be undamped.

The first three forms of oscillations are shown in Fig. 2.3. The usual example to illustrate these forms of damping is a car shock absorber. If it is highly overdamped, the car ride will be hard as the shock absorber will not absorb the shocks. If it is critically damped, the ride will be comfortable as impacts will be absorbed and the suspension spring will return quickly to its equilibrium position. If it is highly underdamped, the vehicle will experience several vertical oscillations while crossing even a small bump.

The method to determine the nature of a given damped system and its damped frequency of vibration is illustrated in *Ex* 2.9.1.

### *2.3.4 Logarithmic Decrement (δ)*

While a structure oscillates with a regular time period $T_d$ during underdamped motion, its amplitude of vibration is not constant but decreases with each successive cycle. The oscillation amplitudes will be bounded by a decay envelope given by the equation

$$u = A\mathrm{e}^{-\xi\omega t} \tag{2.2.1}$$

The rate of decay of vibration amplitude is signified by another convenient measure of damping termed logarithmic decrement ($\delta$). It is defined as the natural

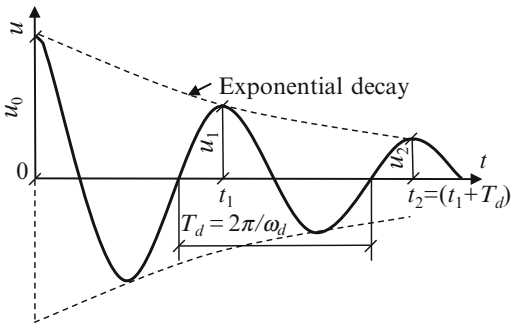


**Fig. 2.4** Decay of oscillations

logarithm of the ratio of amplitudes of vibration of a structure for two successive cycles. If $u_1$ and $u_2$ are vibration amplitudes of an underdamped SDOF system, at first and second cycles, i.e. at times $t_1$ and $[t_2 = (t_1 + T_d)]$, respectively, (Fig. 2.4) then from Eq. 3.5.8,

$$u_1 = u\,(t_1) = \mathrm{e}^{-\xi\omega t_1}\left\{u_0 \cos\ \omega_d t_1 + \left(\frac{\dot{u}_0 + u_0\omega\xi}{\omega_d}\right)\sin\ \omega_d t_1\right\}$$

and

$$u_2 = u\,(t_2) = \mathrm{e}^{-\xi\omega t_2}\left\{u_0 \cos\ \omega_d t_2 + \left(\frac{\dot{u}_0 + u_0\omega\xi}{\omega_d}\right)\sin\ \omega_d t_2\right\} \tag{2.2.2}$$

Noting that $T_d = (t_2 - t_1) = 2\pi/\omega_d$

$$\cos\ \omega_d\,(t_2) = \cos\ \omega_d\,(t_1 + T_d) = \cos\,(\omega_d t_1 + 2\pi) = \cos\ \omega_d t_1$$

Similarly, $\sin\ \omega_d t_2 = \sin\ \omega_d t_1$

This leads to

$$\frac{u_1}{u_2} = \frac{\mathrm{e}^{-\xi\omega t_1}}{\mathrm{e}^{-\xi\omega t_2}} = \mathrm{e}^{\xi\omega\left(t_2 - t_1\right)} = \mathrm{e}^{\xi\omega T_d} \tag{2.2.3}$$

From definition,

$$\delta = \ln\left(\frac{u_1}{u_2}\right) = \ln\ \mathrm{e}^{\xi\omega T_d} = \xi\omega T_d \tag{2.2.4}$$

The logarithmic decrement and damping ratio are thus related as under:

$$\delta = \xi\omega T_d = 2\pi\xi\omega/\omega_d$$

From Eq. 3.5.3, $\omega_d = \omega\sqrt{1-\xi^2}$;

hence

$$\delta = \frac{2\pi\xi}{\sqrt{1-\xi^2}} \tag{2.2.5}$$

For reinforced concrete buildings, the damping ratio ($\xi$) is small, which yields

$$\delta \simeq 2\pi\xi \quad \text{and} \quad T_d \simeq T \tag{2.2.6}$$

Hence, the period of vibration of a lightly damped concrete building can be considered nearly the same as that for an undamped one. Examples 2.9.2, 2.9.3, 2.9.4 and 2.9.5 illustrate the evaluation of various damping parameters discussed above.

### 2.3.5 Magnitude of Damping

The magnitude of damping in a building cannot be mathematically derived on the basis of member sizes or their configuration. It can be approximately assessed experimentally by measuring amplitude decay of a structure set into free vibration. Consider that for a test structure, the amplitudes of vibration measured $N$ cycles apart are $u_0$ and $u_N$, respectively. From Eqs. 2.2.4 and 2.2.6,

$$\ln\left[\frac{u_0}{u_N}\right] = \ln\left[\frac{u_0}{u_1} \times \frac{u_1}{u_2} \times \cdots \frac{u_{N-1}}{u_N}\right] = N\delta = N\,(2\pi\xi) \tag{2.3.1}$$

From which it follows that

$$\xi = \frac{\ln\,(u_0/u_N)}{2\pi\ N} \tag{2.3.2}$$

The value of damping in a building depends on many factors such as type of construction material used, nature of soil on which the structure is founded, building form, rigidity of the cladding employed, amplitude of vibration, etc. Even a small amount of damping can lead to substantial reduction in lateral displacements. For concrete and reinforced brick buildings, damping ratio is generally taken in the range of 5–8 % with the lower value for buildings with flexible cladding and higher value for those with stiff cladding and for shear wall-supported buildings. The reasonable damping ratio for a tall building (height in the range of 50–250 m) appears to be between 1 and 2 % (Wood 1973). For reasons mentioned in Sect. 6.9.1, a default value of 2.5 % is suggested.

### 2.3.6 Proportional Damping

For mathematical convenience, damping is assumed to be viscous, and its value is taken to be proportional to the velocity of motion. Mathematical models are built

on the premise that Rayleigh damping prevails, i.e. damping is proportional to both mass and stiffness of the structure which implies that for mode $i$, the damping matrix is

$$\boldsymbol{C_i} = \alpha \boldsymbol{M_i} + \beta \boldsymbol{K_i} \tag{2.4.1}$$

where $\alpha$ and $\beta$ are empirical scalar multipliers and $\boldsymbol{M_i}$ and $\boldsymbol{K_i}$ are mass and stiffness matrices. From Eqs. 3.11.7 and 3.11.8,

$$\boldsymbol{C_i} = 2\xi_i \omega_i \boldsymbol{M_i}, \quad \boldsymbol{K_i} = \omega_i^2 \boldsymbol{M_i}.$$

Substituting in Eq. 2.4.1,

$$2\xi_i \omega_i \boldsymbol{M_i} = \alpha \boldsymbol{M_i} + \beta \omega_i^2 \boldsymbol{M_i}$$

Dividing by $2\omega_i \boldsymbol{M_i}$,

$$\xi_i = \frac{\alpha}{2\omega_i} + \frac{\beta \omega_i}{2} \tag{2.4.2}$$

For any two modes of vibration $i$ and $j$,

$$\xi_i = \frac{\alpha}{2\omega_i} + \frac{\beta \omega_i}{2} \text{ and } \xi_j = \frac{\alpha}{2\omega_j} + \frac{\beta \omega_j}{2} \tag{2.4.3}$$

It can be readily shown that

$$\alpha = \frac{2\omega_i \omega_j}{\omega_j^2 - \omega_i^2} \left\{ \omega_j \xi_i - \omega_i \xi_j \right\} \text{ and } \beta = \frac{2}{\omega_i^2 - \omega_j^2} \left\{ \omega_i \xi_i - \omega_j \xi_j \right\} \tag{2.4.4}$$

In matrix form,

$$\begin{Bmatrix} \alpha \\ \beta \end{Bmatrix} = 2 \begin{pmatrix} 1/\omega_i & \omega_i \\ 1/\omega_j & \omega_j \end{pmatrix}^{-1} \begin{Bmatrix} \xi_i \\ \xi_j \end{Bmatrix} \tag{2.4.5}$$

which can be written as

$$\begin{Bmatrix} \alpha \\ \beta \end{Bmatrix} = \frac{2\omega_i \omega_j}{\omega_j^2 - \omega_i^2} \begin{pmatrix} \omega_j & -\omega_i \\ -1/\omega_j & 1/\omega_i \end{pmatrix} \begin{Bmatrix} \xi_i \\ \xi_j \end{Bmatrix} \tag{2.4.6}$$

For the condition,

$$\xi_i = \xi_j = \xi; \ \alpha = \frac{2\omega_i \omega_j \xi}{\omega_j + \omega_i} \ and \ \beta = \frac{2\xi}{\omega_j + \omega_i} \tag{2.4.7}$$

Values of $\alpha$ and $\beta$ can be obtained based on the desired damping ratio for any two modes that make a significant contribution to response. Apart from the fundamental mode, the second mode should be chosen with care so that the higher mode response is not unduly damped when significant higher mode response is anticipated. Once $\alpha$ and $\beta$ are determined, damping in any other elastic mode $\varphi_k$ can be readily obtained from the equation:

$$\xi_k = \frac{\alpha}{2\omega_k} + \frac{\beta\omega_k}{2} \tag{2.4.8}$$

This technique permits the designer to choose a damping value for any particular mode. Considering the many uncertainties involved in the choice of a damping value to adopt, the common practice is to use, for low-and medium-rise buildings, a uniform damping value (generally 5 %) for all modes even during an inelastic analysis. Method of evaluation of damping ratio and determination of damping matrix are demonstrated through *Ex* 2.9.6.

## 2.4 Ductility

The concept of ductility was introduced in 1961. It is the capacity to dissipate energy while undergoing large inelastic deformations, without significant loss of strength or stiffness (BIS 2002a). It is a very important attribute in earthquake engineering. Ductility is a measure of the reserve capacity in a structure to sustain sudden short-term overload. This permits buildings to be designed such that, in rare cases, when there is overload during a major seismic event, the structure can dissipate input seismic energy such that the building, though damaged, remains standing.

Based on this reasoning, the concept of ductility was introduced into the codes. It is now accepted that it is lateral displacement and not force alone, which invariably leads to serious structural distress during an earthquake. As a result, displacement-based design criteria have been evolved which are still being fine-tuned. Notwithstanding this development, for loads other than seismic, it is generally sufficient to design structures to have adequate stiffness and strength. Thus, force-based design will continue to be used, particularly because it is a procedure designers are familiar with. At the same time, ductility-related detailing of members is being incorporated. This allows seismic design to be based on reduced inertia forces corresponding to an assumed achievable ductility.

### *2.4.1 Importance of Ductility*

Lateral forces on buildings are generally those due to wind and earthquake. To cater to the former, one needs to provide sufficient structural strength and stiffness. In

the latter case, however, there is an additional demand to provide adequate ductility. This is to permit dissipation of seismic energy through inelastic deformations due to sudden overload from an unexpected spike in the magnitude of seismic ground motion. Just as flexibility deals with elastic deformation, ductility relates to inelastic deformations.

If the building supporting framework is ductile, then collapse is delayed through redistribution of overstress from one section to another (such as rotations in plastic hinge regions) until there is eventual crushing of concrete and buckling of reinforcement. If frames are not ductile, then failure could be sudden and disastrous. In such cases, the building often experiences what is known as a pancake-type failure ending up in a pile on the ground. Thus, existence of ductility is an essential attribute to enable a building structure to absorb major seismic shocks and thus survive. Clearly, higher the inbuilt ductility, the higher is the margin to exploit. Thus, ductility is an effective defence against random ground motion.

## *2.4.2 Classification of Ductility*

Ductility is the capability of a material, element or structure to withstand substantial inelastic deformations, while largely maintaining its initial load-carrying capacity. It is usually quantified as the ratio of deformation at near failure to deformation at first yield. Ductility is classified according to the nature of deformation being considered, e.g. whether it is strain, curvature, rotation or displacement. These are described below.

### 2.4.2.1 Structural Ductility

In Fig. 2.5 the relationship between an applied lateral force at roof level of a SDOF system and its horizontal displacement is shown. If the structure behaves elastically, then it would need to be designed for an inertia force $F_a$ when its displacement will be $\Delta_a$. On the other hand, if the structure follows an elasto-plastic (commonly assumed as elasto-fully plastic) response regime, then at yield of steel, the inertia force for the same earthquake would be $F_y$ with a displacement $\Delta_y$, but thereafter it would displace plastically to a displacement limit of $\Delta_u$. Structural ductility would be given by $\Delta_u/\Delta_y$.

From this diagram, it can be seen that if the structure can dissipate energy (input into it from seismic waves) through deformation but without failure, then it can be designed for a lower lateral force $F_y$. If, however, it has to remain elastic up to near-collapse condition, then it will need to be designed for a much larger force $F_a$ which would clearly be commercially prohibitive. It follows that much is to be gained if the structure as a whole, as well as its elements together with their connections, are designed so as to be capable of dissipating seismic energy through inelastic deformations.

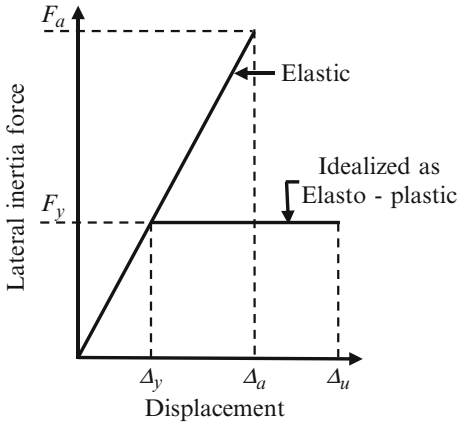


**Fig. 2.5** Force–displacement diagram

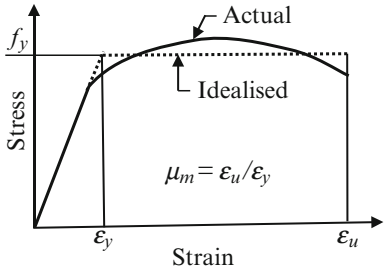


**Fig. 2.6** Material ductility

#### 2.4.2.2 Material Ductility ($\mu_m$)

Material ductility is measured as the ratio of ultimate strain ($\varepsilon_u$) to that at first yield ($\varepsilon_y$) (Fig. 2.6). It denotes the capacity of a material to withstand plastic deformations before failure. A low value of $\mu_m$ ($= \varepsilon_u/\varepsilon_y$) signifies a brittle material. Unconfined concrete exhibits very little material ductility (Paulay and Priestley 1992), but for *Yogic concrete* (i.e. confined concrete), $\mu_m$ is substantially higher.

#### 2.4.2.3 Curvature Ductility ($\mu_c$; also termed Section Ductility)

Curvature ductility relates to the plastic deformation of a cross section and is a ratio of the curvatures (rotation per unit length) at the end of the inelastic range to that at first yield point of tension steel. Consider the cross section of a singly reinforced rectangular beam under flexure (Fig. 2.7a). The elastic strain diagram at yield of steel and the limit state strain diagram are shown in Fig. 2.7b, c, respectively. If maximum achievable curvature is $\varphi_u$ and that at first yield of tension steel is $\varphi_y$, then curvature ductility is given by $\mu_c = \varphi_u/\varphi_y$.

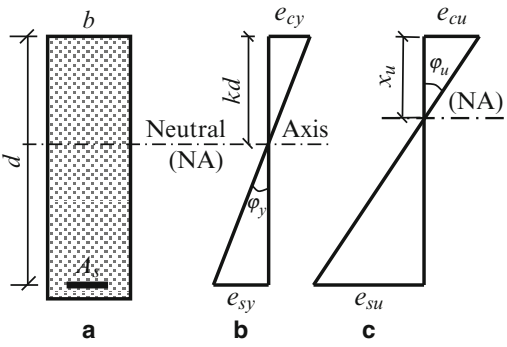


**Fig. 2.7** Curvature ductility. (**a**) Beam section, (**b**) elastic strain diagram at yield and (**c**) ultimate limit strain diagram

From design principles of elastic and limit state theories, for singly reinforced rectangular sections under flexure, one can readily derive the following:

(a) *From theory of limit state design*:

$$\tan\ \varphi_u \simeq \varphi_u = \varepsilon_{cu}/x_u \tag{2.5.1}$$

The ultimate concrete strain $\varepsilon_{cu}$ is taken as 0.0035 for unconfined concrete. If concrete is confined, then the ultimate compressive strain can be much larger. It is apparent that at that stage, spalling of concrete cover is to be expected, and the concrete outside of the confining stirrups will need to be ignored. Hence, in the analysis below, the full section is considered but the ultimate strain is limited to 0.0035.

$$\frac{x_u}{d} = \frac{0.87\ f_y\, p}{0.36\ f_{ck}} \quad \text{where}\ \ p = \frac{A_s}{bd} \quad \text{i.e.} \quad \frac{x_u}{d} = 2.417\frac{p.f_y}{f_{ck}} \tag{2.5.2}$$

$$\text{Ultimate curvature} = \varphi_u = \frac{\varepsilon_{cu}}{x_u} = \frac{0.0035\ f_{ck}}{2.417\ p.d.f_y} = 1.448 \times 10^{-3}\frac{f_{ck}}{p.d.f_y} \tag{2.5.3}$$

(b) *From elastic design principles*:

$$\text{Yield curvature}\ \ \varphi_y = \varepsilon_{sy}/\,(d - kd) \tag{2.5.4}$$

Taking modulus of elasticity of steel $E_s = 2 \times 10^5$ N/mm$^2$,

$$\varphi_y = 5 \times 10^{-6}\frac{f_y}{d\,(1-k)} \tag{2.5.5}$$

$$\text{Curvature ductility} = \mu_c = \frac{\varphi_u}{\varphi_y} = \frac{290\,(1-k)\ f_{ck}}{p.f_y^2} \tag{2.5.6}$$

where, from principles of working stress design, coefficient $k$ locating the neutral axis is given by

$$k = -m'p + \sqrt{(m'p)^2 + 2m'p} \tag{2.5.7}$$

$\varepsilon_{cu}$: maximum compressive strain in concrete at limit state
$\varepsilon_{sy}$: yield strain in steel
$A_s$: area of tensile reinforcement
$x_u$: depth of neutral axis at limit state
$kd$: depth of neutral axis at yield of steel
$f_{ck}$: characteristic strength of concrete
$f_y$: yield stress of steel
$m'$: modular ratio
$d$: effective depth of beam
$b$: width of beam
$\varphi_y$: elastic curvature
$\varphi_u$: ultimate curvature

Curvature ductility reduces with the use of higher yield strength rebars. Secondly, it increases with an increase in compression steel content and decreases with an increase in tensile steel content (Joshi et al. 2001). Example 2.9.7 illustrates the method for evaluating curvature ductility. From Eq. 2.5.6, it is evident that lower the value of $k$, higher the ductility. Hence T beams, with their large compression flange, have a higher ductility than rectangular beams.

#### 2.4.2.4 Rotational Ductility ($\mu_\theta$; also termed Joint Ductility)

Rotational ductility is the ductile rotational capacity of a joint between members or at the plastic hinge within a member, where rotation is invariably concentrated. The ratio of rotation of such a member at ultimate ($\theta_u$) to that at first yield ($\theta_y$) is a measure of its rotational ductility $\mu_\theta = \theta_u/\theta_y$.

Consider that the beam span of a moment frame is subjected to equal seismic end moments with values of $M_y$ at elastic yield and $M_u$ at inelastic limit state as shown in Fig. 2.8a. Maximum elastic curvature at the support at yield is $\varphi_y$ (Fig. 2.8b). It is further assumed that curvature in the inelastic range varies linearly from $\varphi'_y$ at commencement of the plastic hinge to $\varphi_u$ at the support (Fig. 2.8c). The length of the plastic hinge formed at the support is taken as $L_p$ (Kheyroddin and Naderpour 2007). With this proviso, the value of $\varphi'_y$ is given by

$$\varphi'_y = \frac{\varphi_y}{L}\left(L - 2L_p\right) \tag{2.6.1}$$

From Eqs. 2.5.3 and 2.5.5, $\varphi_u = 1.448 \times 10^{-3}\dfrac{f_{ck}}{p.d.f_y}$ and $\varphi_y = 5 \times 10^{-6}\left[\dfrac{f_y}{d\,(1-k)}\right]$

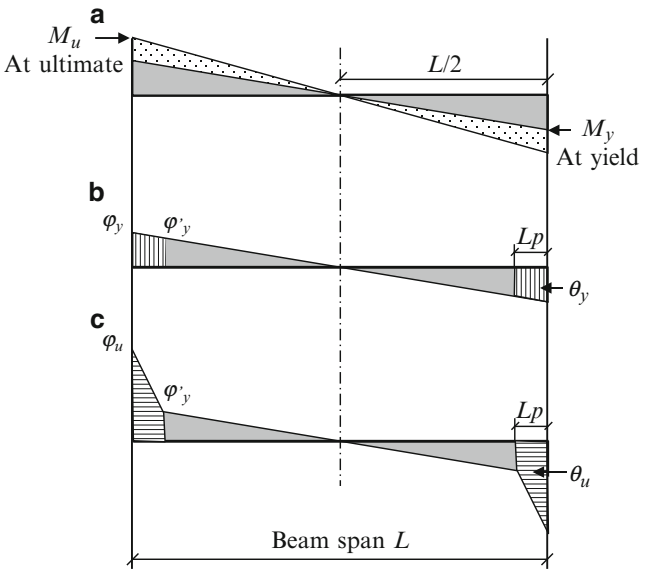


**Fig. 2.8** Rotational ductility. (**a**) Moment diagram at yield and at ultimate, (**b**) curvature diagram at yield and (**c**) curvature diagram at ultimate (Based on FEMA (FEMA 451B 2007))

Rotation at the plastic hinge will be obtained by integrating beam curvature over the length of the plastic hinge ($L_p$) which is assumed to be equal to the effective beam depth (FEMA 451B 2007). It follows that

$$\theta_y = d\left[\frac{\varphi_y + \varphi'_y}{2}\right] \quad \text{and} \quad \theta_u = d\left[\frac{\varphi_u + \varphi'_y}{2}\right] \tag{2.6.2}$$

Rotational ductility within the plastic hinge region is

$$\mu_\theta = \left[\frac{\varphi_u + \varphi'_y}{\varphi_y + \varphi'_y}\right] = \frac{\theta_u}{\theta_y} \tag{2.6.3}$$

The evaluation of rotational ductility is demonstrated through *Ex.* 2.9.8.

#### 2.4.2.5 Displacement Ductility ($\mu_\Delta$)

Displacement ductility is a measure of the lateral inelastic deflection capacity of a member. A well-engineered reinforced concrete member can undergo substantial inelastic deformation after first yield prior to its ultimate failure (Fig. 2.9). For an element, the displacement ductility factor is given by $\mu_\Delta = u_u / u_y$, where $u_u$ is the

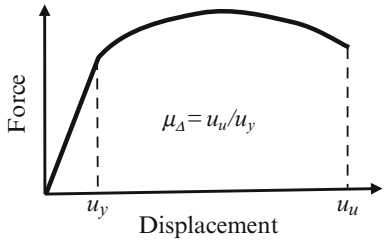


**Fig. 2.9** Displacement ductility

displacement at ultimate and $u_y$ is the displacement at yield. While low ductility can lead to brittle failure, high ductility can cause damage to nonstructural components and services, as the structure deforms.

A displacement ductility factor of 1.0 signifies a non-ductile structure. Typical structural ductility is of the order of 3–5. It is suggested (FEMA 306 1998) that displacement ductility capacity may be classified as: *Low* for $\mu_\Delta < 2$, *Moderate* for $2 \leq \mu_\Delta \leq 5$ and *High* for $\mu_\Delta > 5$. Broadly speaking, structures may be classified as elastic if $\mu = 1$, may be said to possess restricted ductility if $2 \leq \mu_\Delta \leq 5$ and may be considered as ductile if $\mu_\Delta > 5$.

### *2.4.3 Ensuring Adequate Ductility*

A typical ordinary reinforced concrete moment frame lacks adequate ductility. To site an example, the beams of such a frame are designed for gravity and seismic loads where the latter are reduced through a code-specified reduction factor. The shear design for beams corresponds to the beam support moments. However, when a major earthquake occurs, the beam moments and the corresponding shear forces will far exceed design values. Since shear failure is brittle, the building could experience a sudden collapse.

Through careful detailing, the structure can develop a capability to deform beyond the elastic limit in a controlled manner and thus avoid serious distress. To incorporate adequate ductility, the following measures should be taken:

- Adopt a regular structural configuration, e.g. avoid sudden changes in column sections.
- Avoid large windows particularly in only a few bays.
- Avoid windows stretching column to column over part of the storey height.
- Avoid brittle compression failure of concrete by confining both concrete as well as compression reinforcement in regions that are likely to develop plastic hinges and along lap joints.
- Provide protection against shear failure through closely spaced stirrups.
- Provide appropriate development and lap lengths or well-engineered mechanical splices for rebars to prevent their brittle failure in bond and/or anchorage.

- Limit the quantum of tensile steel to avoid compression failure in bending. One must resist the temptation to over reinforce concrete. The higher the tensile strength, the greater will be the compressive strain in concrete and hence the lesser the ductility.
- Ensure that bond and shear failures do not precede failure in flexure. Hence, design members in flexure as under reinforced with adequate compression reinforcement. To prevent shear failure in beams, designers should provide for an overstrength in shear.
- Ductility should be concentrated at locations where it would be effective.
- Choose a strong-column weak-beam design.

## 2.5 Lateral Stiffness

Lateral stiffness is the force required to achieve unit lateral displacement in a member. The inertia force from an earthquake can act in any direction, and hence it is important that the structure has adequate stiffness in all directions. Stiffness plays an important role in controlling deformations and in maintaining the vibration frequency of a structure away from the seismic forcing frequency, thereby avoiding large responses.

Low lateral stiffness could result in large displacements with consequent heavy damage to nonstructural elements in the event of strong shaking. It can also aggravate the danger from pounding and can cause significant $P$-$\triangle$ effects with possible danger to lateral stability of the structure. Although stiff structures will attract larger inertia forces, it is observed that they have generally performed better in past earthquakes.

During design, the stiffness contribution of nonstructural elements is not usually included because of their uncertain effectiveness under large displacements. However, the effect of joint rotations as well as flexural and axial deformations should be allowed for where relevant. In brief, a structure must have sufficient stiffness to avoid large displacements which can lead to significant $P$-$\triangle$ effects, problem of pounding and formation of a column-sway mechanism.

### *2.5.1 Nature of Stiffness*

Lateral stiffness can be looked at as a reciprocal of flexibility. It defines a relationship between force and displacement, be it in bending or rotation, and thus lays down the dynamic characteristics of a system. It is important to differentiate between flexibility and ductility. The former refers to the extent by which a member will deform due to a lateral force. The more the displacement for a given force, the larger is the flexibility. On the other hand, ductility refers to the extent by which a member can deform after yielding, before it collapses.

For a building element, the degree of lateral stiffness depends on many factors such as member sectional properties, its end conditions, its orientation with respect to direction of load and amount of reinforcement. For the structure as a whole, its value depends further on the nature of load-resisting system employed, e.g. moment frames or shear walls. Axial stiffness of a reinforced concrete member depends on whether the member is in compression or tension, which is sometimes difficult to predetermine as it will depend on the magnitude of inertia forces. In the former case, stiffness depends on material properties, member dimensions and state of cracking, and in the latter case, it depends primarily on the deformation characteristics of rebars.

From serviceability limit state considerations, structural systems and their members must possess sufficient lateral stiffness to limit storey drift and displacements. This also prevents adverse psychological effects on human occupants in addition to ensuring satisfactory performance of a building. Human response to vibration amplitude differs depending upon whether it is due to wind or earthquake. This is because, unlike in an earthquake, vibrations due to wind can be frequent, and hence their magnitude must not cross the human tolerance threshold level. During an earthquake, however, the instantaneous human concern is one of survival. Hence, in this case, deformation has to be contained primarily to prevent failure of structural and nonstructural components which could block passage ways or cause injuries due to falling ceilings and other components.

Lateral stiffness of a building significantly affects its vibration period and consequently its response parameters such as base shear, storey drift and others. Lower the stiffness, higher the natural period of a building and hence the lower the seismic forces that the structure will attract. In spite of this, the resulting deformation is generally larger leading to higher $P$-$\Delta$ effects enhancing the displacements further. Hence codes specify permissible drift limits, thereby ensuring a reasonable minimum stiffness.

During a strong motion earthquake, a structure will deform beyond its elastic range where the ratio of force to the deformation it causes is not single valued but will depend on the stage of loading and on whether deformation is increasing or decreasing. Inelastic behaviour is characterised by degradation of stiffness, strain hardening of steel and energy dissipation. The initial slope of the load displacement curve is termed as elastic stiffness of the structure for which normally the secant stiffness value is used and for non-linear portion, tangent stiffness value is recommended.

Principally, stiffness has two ranges: (1) elastic and (2) post-yield. A structure behaves elastically until yield. Later during the inelastic stage, stiffness reduces and the force–displacement curve is marked as $a$ in Fig. 2.10. For mathematical convenience, it is often presumed that the post-elastic stiffness is zero. Such a force–displacement regime is termed as being elastic–fully plastic (Fig. 2.10 curve 1). Alternatively, for response history analysis, it could be idealised as a bilinear form. This leads to a model where the initial stiffness up to first yield is linear with stress being proportional to strain followed by a lower linear stiffness up to reaching the

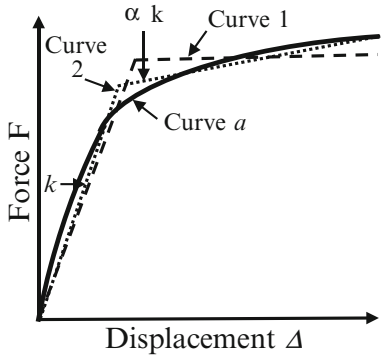


**Fig. 2.10** Stiffness degradation

limiting deformation (Fig. 2.10 curve 2). The line slopes are chosen such that areas under curves *a*, 1 and 2 remain unchanged. The two important factors that affect stiffness value are described below.

#### 2.5.1.1 Moment of Inertia (MI)

For a frame with rigid beams, storey lateral stiffness can be the summation of stiffness of its individual vertical load-bearing members in that storey. The stiffness of each such member is dependent on its MI which can be based on a cracked, gross or transformed section. Thus, the value of effective MI to consider for design varies between that for a gross section and that for a fully cracked section. Further, inertia of a beam is difficult to determine since it varies due to factors like T beam effect along the beam length, stiffness contribution from the slab and location and extent of cracking. As a result, the analytical determination of a precise moment of inertia is impractical.

For a preliminary dynamic analysis, *gross concrete section* (neglecting steel) is generally the assumption made for evaluating MI, but it should be based on a cracked section for final design. It is assumed that the effects of cracking in reinforced concrete members of an SMRF due to flexural tensile stresses can be represented by a reduced moment of inertia. The gross inertia of reinforced concrete beams are usually reduced to 50 % of their uncracked values, while the gross inertia of columns is reduced to 50–70 % of their uncracked value depending on the degree of compression (BIS 2013).

For a shear wall in flexure, Moehle et al. (2010a) have mentioned that the MI to be considered may be 50 % of its gross value. It is pointed out that coupling beams are designed to sustain damage prior to significant yielding of the wall piers. Further, they experience concentrated rotations at their junctions with wall piers. In view of the above, it is mentioned (Moehle et al. 2010a) that their stiffness be reduced to 0.15 of their gross value while calculating shear deformations. Values that may be taken for the Shear modulus ($G$) are also given.

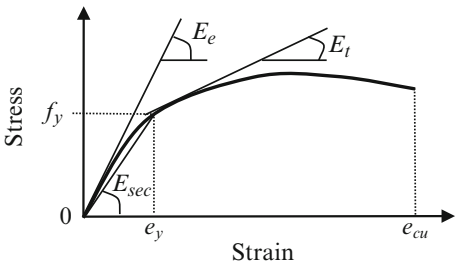


**Fig. 2.11** Concrete moduli

#### 2.5.1.2 Modulus of Elasticity ($E_c$ for Concrete and $E_m$ for Masonry)

Concrete is a complex heterogeneous material. Elastic modulus of concrete is difficult to specify since it depends on factors such as stress level, material grade, age of loading, shear span ratio, amount of reinforcement and state of cracking. Slope of the stress – strain curve during the initial elastic range – is termed as elastic modulus ($E_c$) which is generally assumed to be related to concrete compressive strength. The slope of a line joining the origin with a point on the stress – strain curve – is termed as the secant modulus ($E_{\text{sec}}$), and its instantaneous value at any given stage of loading is defined as tangent modulus ($E_t$) (Fig. 2.11).

The value of $E_c$ normally specified in codes is the secant modulus. If the initial tangent modulus is assumed, which is higher, it will prove to be unconservative for drift prediction. On the other hand, a lower value will yield a longer time period and a lower seismic force which is also unconservative. Further, under dynamic conditions, the value of $E_c$ for concrete tends to be higher than its static value, and the former depends on whether vibrations are in the elastic or in the inelastic range. Thus, there is no simple answer to the value of $E_c$ to adopt. As a compromise, the code recommends adopting the static modulus under dynamic conditions also (BIS 2002a).

Researchers have pointed out (Rai et al. 2005b) that based on their studies the elastic modulus of masonry may be taken as $E_m = 550\ f_m^{'}$ where $f_m^{'}$ is the maximum compressive prism strength of masonry. The modulus of rigidity ($G_m$) of masonry may be taken as 0.4 $E_m$.

### *2.5.2 Lateral Stiffness Values*

As detailed above, the value of stiffness depends on many variables. Further, it depends on the strength of the member which is not known at commencement of design. Thus, there are significant uncertainties in arriving at the stiffness of a system, and engineering judgement prevails in the selection of stiffness values. For linear design procedures, it is common to consider the secant stiffness value corresponding to the yield point of the component. Formulae for evaluation of approximate gross linear stiffness for commonly adopted lateral load-resisting

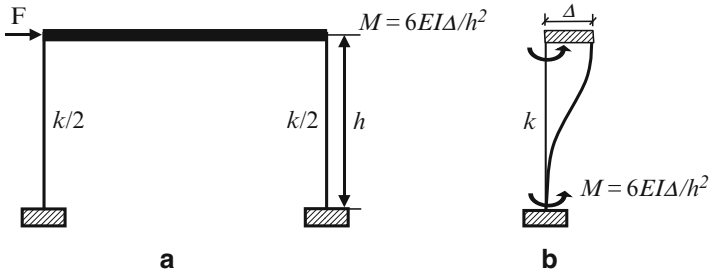


**Fig. 2.12** Lateral stiffness of a SDOF system. (**a**) Frame and (**b**) displaced column

systems of a building structure are given in the following sections. Cyclic deformation can cause deterioration of strength or stiffness or both. Hence, for final design the moment of inertia needs to be reduced as indicated in Sect. 2.5.1.1.

#### 2.5.2.1 Single Degree-of-Freedom (SDOF) Frame

Consider a SDOF frame as shown in Fig. 2.12a. For such a frame, the beam is considered to be infinitely rigid, and thus the columns can be considered as fixed at both ends. When this frame deflects laterally by an amount $\Delta$ due to a force $F$ at roof level, bending moments are generated as shown in Fig. 2.12b. Total shear force at the top would be $F = 12\ EI\Delta/h^3$, and column stiffness, for unit lateral displacement, will be given by $k = 12\ EI/h^3$.

#### 2.5.2.2 Multi-Degree-of-Freedom (MDOF) Frame

Consider a three-storey building frame with rigid floors and lumped masses ($m$) and storey stiffness ($k$) as shown in Fig. 2.13a under a seismic-base excitation $\ddot{u}_g$. When floor 1 displaces laterally, an amount $u_1$ due to inertia forces at that level, while holding the other levels in position; the resistive forces generated due to stiffness of the supporting members will be as shown in Fig. 2.13b. Similarly, when each of the floors at levels 2 and 3 displaces by $u_2$ and $u_3$, respectively, one at a time (holding the remaining two floors in position), the corresponding resistive forces are shown in Fig. 2.13c, d respectively. The net forces at different floors (as the structure deforms) will be as shown in Fig. 2.13e. The undamped equation of motion for each floor under seismic ground motion will be:

$$
\begin{aligned}
&m_1\ddot{u}_1 + (k_1 + k_2)\,u_1 - k_2u_2 = -m_1\ddot{u}_g \\
&m_2\ddot{u}_2 - k_2u_1 + (k_2 + k_3)\,u_2 - k_3u_3 = -m_2\ddot{u}_g \\
&m_3\ddot{u}_3 - k_3u_2 + k_3u_3 = -m_3\ddot{u}_g
\end{aligned}
$$

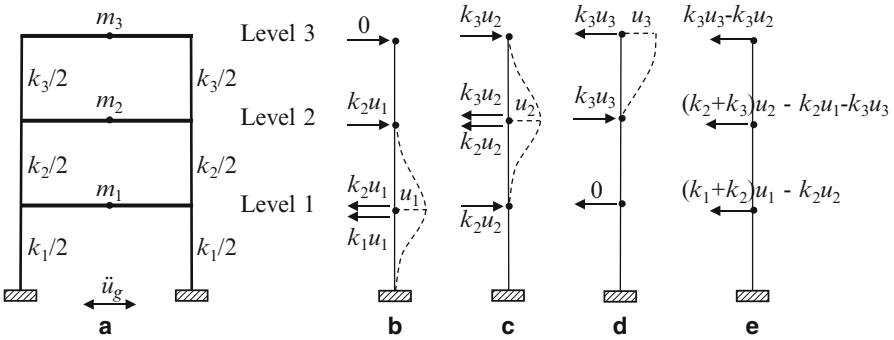


**Fig. 2.13** Stiffness matrix of a MDOF system

written in matrix form

$$\begin{pmatrix} m_1 & 0 & 0 \\ 0 & m_2 & 0 \\ 0 & 0 & m_3 \end{pmatrix} \begin{Bmatrix} \ddot{u}_1 \\ \ddot{u}_2 \\ \ddot{u}_3 \end{Bmatrix} + \begin{pmatrix} k_1+k_2 & -k_2 & 0 \\ -k_2 & k_2+k_3 & -k_3 \\ 0 & -k_3 & k_3 \end{pmatrix} \begin{Bmatrix} u_1 \\ u_2 \\ u_3 \end{Bmatrix} = - \begin{pmatrix} m_1 & 0 & 0 \\ 0 & m_2 & 0 \\ 0 & 0 & m_3 \end{pmatrix} \begin{Bmatrix} 1 \\ 1 \\ 1 \end{Bmatrix} \ddot{u}_g \tag{2.7.1}$$

The stiffness matrix is

$$\boldsymbol{K} = \begin{pmatrix} k_1+k_2 & -k_2 & 0 \\ -k_2 & k_2+k_3 & -k_3 \\ 0 & -k_3 & k_3 \end{pmatrix} \tag{2.7.2}$$

On similar lines, the stiffness matrix can be developed for an $N$ storey MDOF frame.

### 2.5.2.3 Cantilever Shear Wall

Consider a solid rectangular cantilever shear wall of uniform thickness $t$, height $h$ and length $d$. Such a wall derives its stiffness both from shear and flexural strengths. Its lateral deflection due to a force $F$ at the top is given by

$$\Delta = \frac{F h^3}{3\,E I} + \frac{1.2 F.h}{A.G} \quad \text{where } G = \frac{E}{2\,(1+\nu)} \tag{2.8.1}$$

With $G = 0.4\,E$ for concrete and Poisson's ratio $\nu \approx 0.22$,

$$\text{Stiffness } \frac{F}{\Delta} = \frac{E\,t}{4\,\alpha^3 + 2.93\,\alpha} \quad \text{where} \quad \alpha = h/d \tag{2.8.2}$$

A shear wall supported on relatively soft soil can experience significant displacement at its top due to rotation at base as soil compresses from large bending moments. This displacement should be taken into account when calculating wall stiffness. In coupled shear walls, the stiffness of coupling beams may be evaluated on the same lines as for beams. In the case of columns supporting discontinuous shear walls (which incidentally is a condition that should be avoided), their stiffness values will change depending upon whether they are in compression or tension during cyclic loading.

#### 2.5.2.4 Brick/Block Masonry Walls

Any cracking of masonry significantly reduces the stiffness of a masonry structure. However, it is opined (Rai et al. 2005b) that identifying members that are cracked is an elaborate iterative procedure, and hence for analysis purposes, the stiffness of a load-bearing masonry wall is generally based on its uncracked sectional properties.

#### 2.5.2.5 Stiffness in Torsion

Consider a rigid rectangular slab supported on $N$ number of rectangular columns each of height $h$. Distances, along orthogonal axes $x$ and $y$, of a typical column $C_n$ from the centre of rotation $O$ are $x_n$ and $y_n$ respectively and radial distance $r_n$ as shown in Fig. 2.14. When the slab rotates by an amount $u_\theta$ due to torsion, this column will translate along orthogonal axes $x$ and $y$ and rotate about its vertical axis as well. Let the stiffness against displacements along $x$ and $y$ directions be $k_x$ and $k_y$, respectively, where

$$k_x = \left(12\, E I_y\right) / h^3 \quad \text{and} \quad k_y = (12\, E I_x) / h^3 \tag{2.9.1}$$

Column stiffness against rotation about its own vertical axis is given by (Beards 1996)

$$k_{\theta\, z} = \frac{G.J_n}{h} \tag{2.9.2}$$

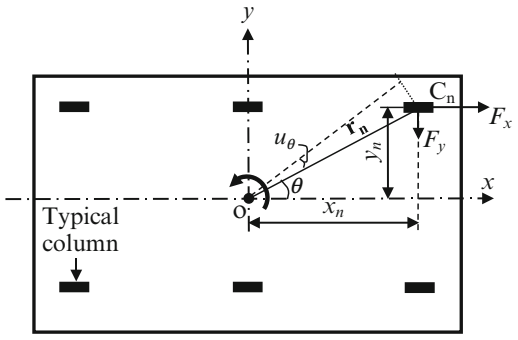


**Fig. 2.14** Torsional stiffness

where $G$ is modulus of rigidity, $J_n$ is the polar moment of inertia and $h$ is the column height. When the rigid slab rotates an angle $u_\theta$, displacement of column $C_n$ is $r_n u_\theta$. This displacement can be resolved along the two axes, and the respective resistive forces $F_n$ can be obtained as under:

$$\text{displacement along } x \text{ axis} = r_n.u_\theta \sin\theta = u_\theta y_n \text{ and force } F_x = u_\theta y_n k_x \text{ and} \tag{2.9.3}$$

$$\text{displacement along } y \text{ axis} = r_n.u_\theta \cos\theta = u_\theta x_n \text{ and force } F_y = u_\theta x_n k_y \tag{2.9.4}$$

The active and resistive torques about the centre of rotation $O$ will be

$$\text{Active torque} = k_\theta.u_\theta \tag{2.9.5}$$

$$\text{Resistive torque} = u_\theta \sum_{n=1}^{N} \left\{ F_x y_n + F_y x_n + \frac{G.J_n}{h} \right\} \tag{2.9.6}$$

Substituting values of $F_x$ and $F_y$ from Eqs. 2.9.3 and 2.9.4 and equating the above two torques,

$$k_\theta.u_\theta = u_\theta \sum_{n=1}^{N} \left\{ k_x y_n^2 + k_y x_n^2 + \frac{G.J_n}{h} \right\} \tag{2.9.7}$$

Substituting values from Eq. 2.9.1, the rotational stiffness will be

$$k_\theta = \sum_{n=1}^{N} \left[ 12 \frac{E}{h^3} \left\{ I_y y_n^2 + I_x x_n^2 \right\} + \frac{G.J_n}{h} \right] \tag{2.9.8}$$

## 2.6 Strength

Stiffness is the property of a member to resist displacement, whereas strength is its property to resist force. Lateral stiffness of a member will dictate the amount of seismic load that it will attract and consequently the strength that needs to be provided.

The strength must be such that it satisfies both the serviceability as well as near-collapse limit states at all levels of the building. An increase in flexibility is not always conservative while at the same time, under seismic excursion, stronger is not always better if the element does not possess ductility.

Englekirk (2003) has stated – 'an increase in system strength does not assure improved system behavior'. The overall strength of a structure against seismic forces depends on the strength of its individual components (both horizontal and vertical) that resist lateral forces. Adequate strength is essential to prevent serious structural damage and to limit ductility demand during a major earthquake.

### *2.6.1 Characteristic Strength*

The characteristic strength of a material typically corresponds to its strength below which not more than 5 % of the test results are expected to fall. For concrete it is based on the 28-day compressive strength of properly prepared and cured 150 mm concrete cubes. In the design of members, this strength is used but reduced by appropriate partial safety factors whose values depend on whether the member is in direct compression or in flexure. For reinforcement it is based on the direct tensile strength of steel reinforcement bars.

### *2.6.2 Target Strength*

The characteristic strength of concrete is enhanced to arrive at its target strength. The degree of enhancement is normally based on a Gaussian probability distribution, the concrete mix design and the degree of quality control expected.

### *2.6.3 Overstrength*

Overstrength came into focus in the 1970s with the introduction in New Zealand of a capacity-based approach to design. Overstrength is a measure of the amount by which the prevailing strength in a system or its elements exceeds the specified strength and can be represented as:

$$\text{Overstrength} = \frac{\text{Maximum lateral strength of the structure}}{\text{Unfactored design strength as per code}}$$

Overstrength could be due to reasons such as (Elnashai and Mwafy 2002):

- Partial load factors that are applied to gravity loads and safety factors applied to material strengths.
- Sometimes member sizes provided from serviceability (e.g. drift) and architectural considerations are larger than those required from strength considerations.
- Confinement of concrete and ductile detailing specified in codes adds to strength.

- Additional strength is available due to strain hardening of steel.
- Strength margins prevalent in design.
- Rebars present in a portion of the slab which will add to beam strength.
- Actual material strengths being higher than nominally specified ones.
- Contribution to strength from nonstructural elements which is not taken cognizance of in design.
- Degree of redundancy prevailing in the system.

The advantages of overstrength are obvious, but on the flip side, if a beam possesses large flexural overstrength, it could lead to brittle shear failure under high seismic displacements. Secondly, since column failure has serious consequences, it is clear that the strength of a column, at its junction with frame beams, must exceed that of the beams inclusive of their overstrength. In seismic design both overstrength and understrength can prove to be detrimental to structural safety.

## 2.7 Mass

The mass of a building should be kept to a minimum since the larger the mass, the greater the inertia force and greater the risk of instability due to $P$-$\Delta$ effects. Reduction of mass can be achieved by limiting slab thickness, adopting composite construction, using light-weight cladding and partitions, avoiding swimming pools particularly at high elevations and so on. The vertical members of a moment-resisting frame do not contribute much to the building mass (Fardis 2009), and hence they should be sized from considerations of stiffness, strength and displacement with little consideration for their mass.

### *2.7.1 Lumped Mass*

In a building, the mass is distributed over its entire geometry which implies a continuum system with its infinite degrees of freedom. To make the analysis manageable but still relevant, a structure is modelled as under:

- Self weight of a floor is considered positioned at that floor level, which is largely the practical situation.
- Self weight of columns and walls in a storey height is distributed equally between the upper and lower floors of that storey.
- After distributing the column masses as mentioned above, the columns are treated as massless springs providing the required lateral stiffness.
- Superloads in buildings are generally considered as being concentrated at floor levels.
- Masses at a floor level are then assumed as lumped into a single mass at that level.

Thus, for dynamic analysis purposes, a continuum system having masses distributed over its height is replaced by a lumped mass system with masses (with no physical size) concentrated at floor levels, thus reducing a structure with infinite degrees of freedom to one with drastically reduced number of degrees of freedom. This is justified for evaluating lateral inertia forces because masses in buildings are practically concentrated at floor levels. For vertical inertia forces, however, the masses need to be lumped at several intermediate points (Fardis 2009) along the horizontal elements.

A lumped mass does not undergo any rotation and its position at any time can be represented by a single kinematic displacement quantity $u$. Similar to the procedure adopted for generating the stiffness matrix (Sect. 2.5.2.2), the mass matrix for a multistorey building is obtained by applying a unit acceleration at each floor level in turn while holding the remaining floors in position. It is assumed that there is no interaction between masses at different floor levels with the result that the mass matrix $\boldsymbol{M}$ for the frame structure shown in Fig. 2.13a becomes a diagonal one as given below:

$$\boldsymbol{M} = \begin{pmatrix} m_1 & 0 & 0 \\ 0 & m_2 & 0 \\ 0 & 0 & m_3 \end{pmatrix} \tag{2.10.1}$$

The calculated storey force can be distributed among the masses at that storey, in proportion to their magnitudes. The method of evaluating the lumped masses is included as part of *Ex.* 2.9.9. The seismic mass is that which is effective in the building oscillations during an earthquake and is the sum total of the gravity load and that fraction of the live load as identified in IS 1893.

### 2.7.2 Mass Moment of Inertia ($m_\theta$)

For a two dimensional translatory motion without torsional coupling, the lumped mass approach is adequate. However, in the case of a three-dimensional analysis or when torsional effects of a rigid slab have to be evaluated, the mass moment of inertia ($\boldsymbol{m_\theta}$) for a typical rectangular floor slab about its vertical axis is required. This is obtained as under:

Consider a rectangular slab (Fig. 2.15) of uniform thickness $t$, density $\rho$ and mass $m$ rotating about a vertical axis through its centroid $O$. Mass of an element $(dx \times dy)$ of this slab will be $dm = \rho.dx.dy.t$. The rotational inertia (i.e. $m_\theta$) of all such masses located at a distance $r$ from point $O$ will be

$$m_\theta = \int r^2 dm = \rho\, t \int_{-a/2}^{a/2} \int_{-b/2}^{b/2} \left(x^2 + y^2\right) dy\ dx = m_s.\frac{\left(a^2 + b^2\right)}{12} \tag{2.11.1}$$

where $m_s$ is the mass of the slab of dimensions $a \times b$ and thickness $t$.

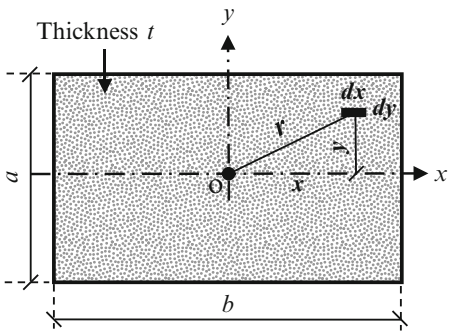


**Fig. 2.15** Evaluation of mass moment of inertia

## 2.8 Degrees of Freedom (DOF)

A portal frame is a set of members which are rigidly joined together at nodes. When this framework is set in motion, the number of attributes required to specify displaced locations of all its masses with respect to their original positions is termed as its degrees of freedom. For ease of analysis, the numbers of degrees of freedom are restricted as detailed in Sect. 2.8.1. It is shown that a single-storey plane frame may be considered to be one which has a single degree of freedom. If the frame has $N$ storeys with rigid floors, then the number of degrees of freedom will be $N$. The larger the number of degrees of freedom, the greater is the complexity of frame analysis.

### *2.8.1 Description of Degrees of Freedom*

Consider a single-storey planer portal frame with fixed bases as shown in Fig. 2.16. All masses are assumed lumped together into a single nondimensional mass $m$ at roof level and that the columns are massless. Such a structure has six degrees of freedom, viz. displacements along $x$ and $z$ directions at joints 2 and 3 and rotations ($\theta_2$ and $\theta_3$) at these two joints. If it is assumed that the beam has a very large axial stiffness, then lateral displacements at joints 2 and 3 (viz. $\Delta u$) will be the same. Secondly, if we consider that columns have a very large axial stiffness, then vertical displacements of joints 2 and 3 are zero since displacements at bases 1 and 4 are zero. Thus, the system reduces to a three degrees of freedom system. It has been shown that for most cases, rotations at joints 2 and 3 can be taken as equal without significant loss in accuracy of system response. This leads to a system with two degrees of freedom

Further, it is assumed that the beam has a very large moment of inertia compared to the columns, and as a result, rotations $\theta_2$ and $\theta_3$ are zero. The lumped mass at roof level now has only one lateral motion possible. For analysis purposes, such a plane frame structure is termed as a single degree-of-freedom (SDOF) system with a

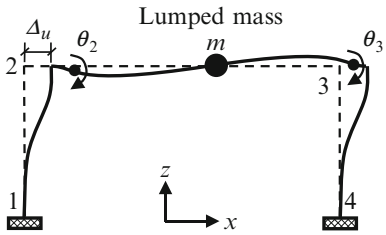


**Fig. 2.16** Plane frame

single mode of vibration. If the frame is a multistorey one, then it will have freedom for lateral translation at floor levels where lumped masses are located. This is termed as a multi-degree-of-freedom system (MDOF).

### *2.8.2 Natural Vibration Frequencies in Six DOF*

Now consider a three-dimensional single-storey frame structure (Fig. 2.17a) consisting of a rigid slab supported on four-corner columns. Each joint between the columns and the slab (e.g. $C$) will have six degrees of freedom, viz. three translations along the $X$, $Y$ and $Z$ axes and rotations about each of these axes giving a total of 24 DOF. We now introduce the reasonable kinematic constrain that the floor slab is rigid, which signifies rigid body translation and rotation of the slab. As a result, all column-slab joints translate by the same amount, and the slab rotates as a rigid body. Thus, we are left with three rigid body translations and three rigid body rotations of the slab (about $O$) reducing the total DOF to six.

The number of vibration frequencies to deal with will be three translational and three rotational. The manner of evaluating natural frequencies in each of the translational degrees of freedom is identical to that detailed in Sect. 3.4.2 of Chap. 3. When a body of mass $m$ is rotating about an axis at a radial distance $r$, then the mass moment of inertia is $m_\theta = mr^2$, and for a rotation $\theta$, the equation of motion for a free rotation will be (Beards 1996)

$$m_\theta.\ddot{\theta} + k_\theta.\theta = 0 \quad \text{i.e.} \quad \ddot{\theta} + \left(\frac{k_\theta}{m_\theta}\right)\theta = 0 \tag{2.12.1}$$

This equation is of the same form as Eq. 3.4.2 for an SHM, and hence the rotational frequency can be written as

$$\omega_\theta = \sqrt{\frac{k_\theta}{m_\theta}} \tag{2.12.2}$$

In *Ex.* 2.9.9 the frequencies for all six degrees of freedom are calculated for a rectangular slab supported on columns as shown in Fig. 2.17.

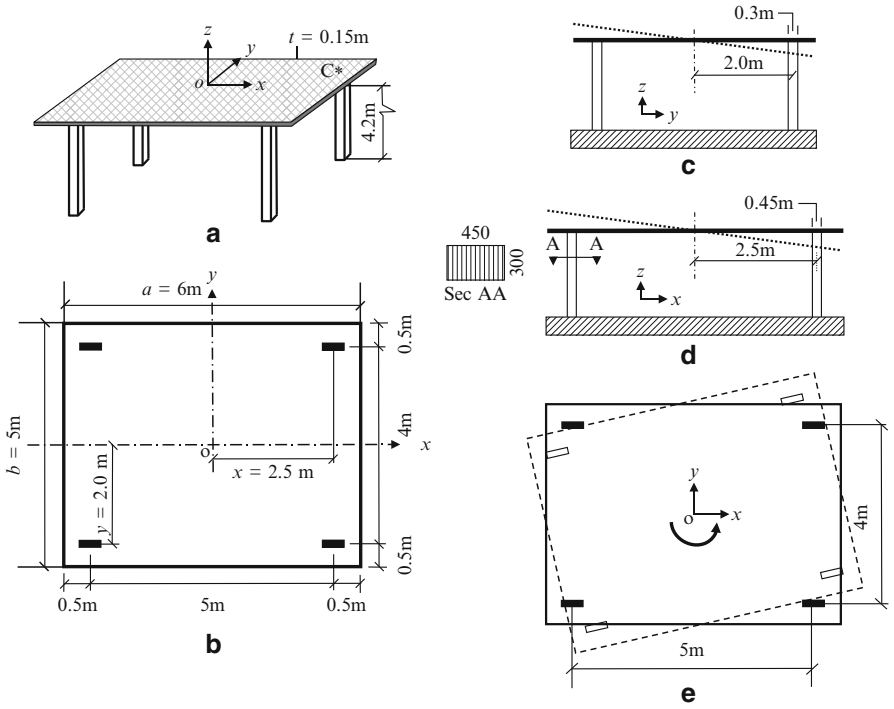


**Fig. 2.17** Degrees of freedom. (**a**) 3D frame, (**b**) plan view, (**c**) rotation about $x$ axis, (**d**) rotation about $y$ axis and (**e**) rotation about $z$ axis

## 2.9 Illustrative Examples

***Ex 2.9.1*** A SDOF system under free vibrations has a mass $m = 0.9$ kg, damping coefficient $c = 0.65$ N s/m and stiffness $k = 2.8$ N/m. Determine the nature of damped motion and frequency of vibration of the system under a lateral seismic excitation.

**Solution** For such a vibrating system, the equation of motion is given by

$$0.9\,\ddot{u} + 0.65\,\dot{u} + 2.8\,u = 0$$

From Eq. 3.4.4, $\omega = \sqrt{k/m}$ and substituting values,

$$\omega = \sqrt{2.8/0.9} = 1.764 \text{ rad/ s}$$

From Eq. 2.1.4, $c_{cr} = 2m\omega = 2 \times 0.9 \times 1.764 = 3.175$ N s/m.

From Sect. 2.3.2, damping factor $\xi = c/c_{cr} = 0.65/3.175 = 0.2047$.

Since $\xi < 1$, the motion is under damped.

From Eq. 3.5.3, the damped frequency is

$$\omega_d = 1.764 \sqrt{1 - 0.2047^2} = 1.727 \text{ rad/s}$$

Thus, it is an underdamped system with a vibration frequency of 1.727 rad/s.

***Ex 2.9.2*** A RCC slab of 3 kN weight is supported on four square columns with a total stiffness against lateral translation of 250 kN/m. Damping ratio for the structure is 6 % of critical damping. Determine (a) the critical damping and (b) damping coefficient and logarithmic decrement.

**Solution** Mass of slab $m = 3{,}000/9.81 = 305.81$ kg:

(a) *Critical damping ($c_{cr}$)*

From Eq. 2.1.3,

$$c_{cr} = 2\sqrt{km} = 2\sqrt{250,000 \times 305.81} = 17.5 \times 10^3 \text{ Ns/m}$$

(b) *Damping coefficient (c)*

$$c = \xi c_{cr} = 0.06 \times 17.5 \times 10^3 = 1,050 \text{ Ns/m}$$

(c) *Logarithmic decrement ($\delta$)*

From Eq. 2.2.6,

$$\delta \simeq 2\pi\xi = 2\pi \times 0.06 = 0.377$$

***Ex 2.9.3*** For the problem in *Ex.* 2.9.2, determine: (a) natural undamped frequency, (b) damped natural frequency and (c) vibration time period with damping.

**Solution**

(a) *Natural undamped frequency ($\omega$)*

The circular frequency is given by

$$\omega = \sqrt{\frac{k}{m}} = \sqrt{\frac{250,000}{305.81}} = 28.59 \text{ rad/s} \quad \text{i.e.} \quad f = \omega/2\pi = 4.55 \text{ Hz}$$

(b) *Damped natural frequency ($\omega_d$)*

$$\omega_d = \omega\sqrt{1 - \xi^2} = 28.59\sqrt{1 - 0.06^2} = 28.54 \text{ rad/s}$$

(c) *Period with damping ($T_d$)*

$$T_d = 2\pi/\omega_d = 2\pi/28.54 = 0.22 \text{ s}$$

***Ex 2.9.4*** For the problem in *Ex.* 2.9.2, determine the number of cycles and time required for the vibration amplitude to reduce to forty-fifth of its original value.

**Solution** From Eq. 2.3.1,

$$\ln [u_0/u_N] = N\ \delta$$

where $u_0$ is initial amplitude and $u_N$ is the amplitude after $N$ cycles. Taking $u_0 = 45\ u_N$,

$\ln [45] = 0.377$ N,

i.e. number of cycles required $N = 10.09$, say 10 cycles.

Time required $= 0.22 \times 10 = 2.2$ s.

***Ex 2.9.5*** For the problem in *Ex.* 2.9.2, determine the percentage strain energy dissipated during the first cycle.

**Solution** Ratio of energies ($E$) is proportional to square of the amplitudes.

From Eq. 2.2.4, $\delta = \ln\left(\dfrac{u_1}{u_2}\right)$ i.e. $\left(\dfrac{u_1}{u_2}\right) = \mathrm{e}^{\delta}$

Substituting values, $\dfrac{u_2}{u_1} = \mathrm{e}^{-\delta} = \mathrm{e}^{-0.377} = 0.686$

Ratio of energy after the first cycle to that at the commencement

$$E = \frac{u_2^2}{u_1^2} = 0.686^2 = 0.47$$

Hence, energy lost is $100(1 - 0.47) = 53$ %.

***Ex 2.9.6*** Properties of the three-storey shear building shown in Fig. 2.18 are summarised below:

Mass $m = 1.522 \times 10^5$ kg; stiffness factor $k = 77.16 \times 10^6$ N/m, $\omega_1 = 10.59$ rad/s, $\omega_2 = 27.45$ rad/s and $\omega_3 = 51.46$ rad/s. Evaluate the following:

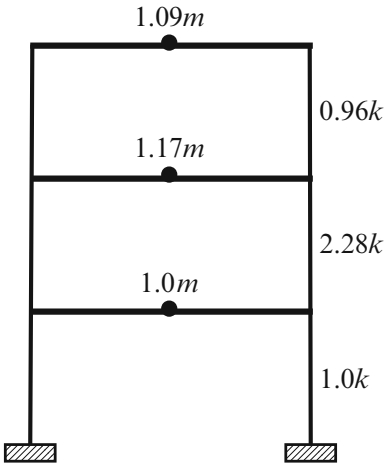


**Fig. 2.18** Three-storey frame

1. If damping ratios for the first and the third modes are chosen as 5 %, determine the damping ratio for the 2nd mode.
2. Repeat the same for the third mode if the damping ratios for the first two modes are 5 %.
3. Derive the Rayleigh damping matrix for the second case.

**Solution** Substituting values in Eqs. 2.7.2 and 2.10.1, the stiffness and mass matrices are

$$\boldsymbol{K} = k\begin{pmatrix} 3.28 & -2.28 & 0 \\ -2.28 & 3.24 & -0.96 \\ 0 & -0.96 & 0.96 \end{pmatrix} \quad \text{and} \quad \boldsymbol{M} = m\begin{pmatrix} 1.0 & 0 & 0 \\ 0 & 1.17 & 0 \\ 0 & 0 & 1.09 \end{pmatrix}$$

**Case (i)**

$$\xi_1 = \xi_3 = \xi = 0.05; \;\; \omega_1 = 10.59 \text{ rad/s}, \;\; \omega_3 = 51.46 \text{ rad/s}$$

Substituting values in Eq. 2.4.7,

$$\alpha = 0.05\left[\frac{(2 \times 10.59 \times 51.46)}{(10.59 + 51.46)}\right] = 0.8783 \quad \text{and} \quad \beta = 0.05\left[\frac{2}{(10.59 + 51.46)}\right] = 0.001612$$

Utilising Eq. 2.4.2 the damping ratio for the second mode,

$$\xi_2 = \left\{\frac{0.8783}{(2 \times 27.45)}\right\} + \left\{\frac{(0.001612 \times 27.45)}{2}\right\} = 0.038 \quad \text{i.e. } 3.8\ \%$$

**Case (ii)**

$$\xi_1 = \xi_2 = \xi = 0.05; \;\; \omega_1 = 10.59 \text{ rad/s}, \;\; \omega_2 = 27.45 \text{ rad/s}$$

Proceeding as above, $\alpha = 0.7642$, $\beta = 0.002629$ and damping ratio for the third mode $\xi_3 = 0.075$ i.e. 7.5 %

**(iii) Evaluating the Damping Matrix for Case (ii)**
$\alpha.m = 0.7642(1.522 \times 10^5) = 1.1631 \times 10^5$ and
$\beta k = 0.002629(77.16 \times 10^6) = 2.0285 \times 10^5$.

For the MDOF system,

$$\alpha\boldsymbol{M} = 10^5\begin{pmatrix} 1.1631 & 0 & 0 \\ 0 & 1.3608 & 0 \\ 0 & 0 & 1.2678 \end{pmatrix} \quad \text{and} \quad \beta\boldsymbol{K} = 10^5\begin{pmatrix} 6.6535 & -4.6250 & 0 \\ -4.6250 & 6.5723 & -1.9474 \\ 0 & -1.9474 & 1.9474 \end{pmatrix}$$

From Eq. 2.4.1, the damping matrix will be given by

$$\boldsymbol{C} = 10^5 \begin{pmatrix} 7.817 & -4.625 & 0 \\ -4.625 & 7.933 & -1.947 \\ 0 & -1.947 & 3.215 \end{pmatrix} \text{ Ns/m}$$

***Ex 2.9.7*** A $250 \times 500$ mm singly reinforced continuous M20 concrete beam has $2-\varphi$ 20 mm and $2-\varphi$ 16 mm Fe 250 top rebars at the support with 30 mm clear cover. With a modular ratio $m' = 13.33$, calculate the curvature ductility.

**Solution** Effective depth $d = 500 - 40 = 460$ mm.

$A_s = 1{,}030$ mm$^2$ and $p = A_s/bd = 0.009$ and $m'p = 0.12$.

Substituting these values in Eq. 2.5.7, $k = 0.384$, and introducing this value in Eq. 2.5.5,

$$\text{Yield curvature} = \varphi_y = 5 \times 10^{-6} \frac{250}{460\,(1 - 0.384)} = 4.411 \times 10^{-6}$$

From Eq. 2.5.3,

$$\text{Ultimate curvature} = \varphi_u = 1.448 \times 10^{-3} \left\{ \frac{20}{(0.009 \times 460 \times 250)} \right\} = 27.981 \times 10^{-6}$$

$$\text{Curvature ductility} \quad \mu_c = \frac{27.981}{4.411} = 6.34$$

***Ex 2.9.8*** For the beam in *Ex.* 2.9.7, evaluate the rotational ductility in the plastic hinge region if beam span is 12 m and the beam is subjected to a skew symmetrical linearly varying moment along its span. Assume that the plastic hinge length is same as the effective depth of the beam.

**Solution** From *Ex* 2.9.7, $\varphi_y = 4.411 \times 10^{-6}$ and $\varphi_u = 27.981 \times 10^{-6}$

Substituting values in Eqs. 2.6.1 and 2.6.2,

$$\varphi'_y = \frac{4.411}{12} \{12 - 2\,(0.46)\} \times 10^{-6} = 4.073 \times 10^{-6}$$

$$\theta_u = \frac{460}{2} \{27.981 + 4.073\} \times 10^{-6} = 7.372 \times 10^{-3}$$

and

$$\theta_y = \frac{460}{2} \{4.411 + 4.073\} \times 10^{-6} = 1.951 \times 10^{-3}$$

From Eq. 2.6.3, rotational ductility

$$\mu_\theta = \left[\frac{7.372 \times 10^{-3}}{1.951 \times 10^{-3}}\right] = 3.78$$

***Ex 2.9.9*** A 150 mm thick RCC rigid slab of overall dimensions (5 m × 6 m) is supported on four 300 × 450 mm size columns, 4.2 m long as shown in Fig. 2.17a, b. Concrete grade is M30 with Poisson's ratio $\nu = 0.3$. This system has six dynamic degrees of freedom, viz. three translations and three rotations. For each degree of freedom, evaluate the natural circular frequency of vibration $\omega$ and fundamental time period *T*. Assume that net compression prevails in the columns after rotation.

**Solution** The various parameters are as under:

*Column parameters:*

$I_{xx} = (0.45)(0.3)^3/12 = 1.013 \times 10^{-3}$ m$^4$

$I_{yy} = (0.3)(0.45)^3/12 = 2.278 \times 10^{-3}$ m$^4$

$A = (0.3)(0.45) = 0.135$ m$^2$

$E = 5,000\sqrt{f_{ck}} = 5,000\sqrt{30} = 2.739 \times 10^4$ N/mm$^2$

$G = E/2\ (1 + \nu) = 1.053 \times 10^4$ N/mm$^2$

$J$ = Polar moment of inertia for a rectangular column with sides $c \times d$ $(c > d)$ is

$$cd^3\left[\frac{1}{3} - 0.21\frac{d}{c}\left\{1 - \frac{d^4}{12c^4}\right\}\right] = 0.45 \times 0.3^3\left[\frac{1}{3} - \left\{\frac{0.21 \times 0.3}{0.45}\right\}\left\{1 - \frac{0.3^4}{12 \times 0.45^4}\right\}\right]$$
$$= 2.377 \times 10^{-3} \text{ m}^4$$

*Lumped mass at slab level*:

$$\text{Mass of slab} \quad m_s = 25,000\,(0.15 \times 5 \times 6)\,/9.81 = 11{,}468 \text{ kg}$$

Half the mass of each column is assumed lumped at slab level

$$m_c = [4.2\,(0.3 \times 0.45) \times 25,000]\,/\,(9.81 \times 2) = 722 \text{ kg}$$
$$\text{Total massmat slab level} \quad = m_s + 4m_c = 14{,}356 \text{ kg}$$

(a) *Translational degrees of freedom*:

1. *Translation in x direction (surging)*
   For a column with fixed ends, stiffness $k = 12\ E\ I_{yy}/h^3$

In $x$ direction, $k_x = \left(12 \times 2.739 \times 2.278 \times 10^7\right)/4.2^3 = 1.01 \times 10^7$ N/m, and for four columns, $\sum k_x = 4.04 \times 10^7$ N/m.

Natural circular frequency $\omega_x = \sqrt{\Sigma k_x/m} = \sqrt{4.04 \times 10^7/14,356} = 53.05$ rad/$s$.

Natural period $T_x = 2\pi/\omega_x = 0.118$ s.

2. *Translation in y direction (swaying)*

Proceeding as above,

$$k_y = 0.449 \times 10^7 \text{ N/m} \quad \text{and} \quad \sum k_y = 1.796 \times 10^7 \text{ N/m}$$

$$\text{Natural circular frequency } \omega_y = \sqrt{\Sigma k_y/m} = \sqrt{1.796 \times 10^7/14,356} = 35.37 \text{ rad/s}$$

$$\text{Natural period } T_y = 2\pi/\omega_y = 0.178 \text{ s}$$

3. *Translation in z direction (heaving)*

Axial stiffness of column $k_z = AE/h = \left(0.135 \times 2.739 \times 10^{10}\right)/4.2 = 0.880 \times 10^9$ N/m and for four columns $\Sigma k_z = 3.52 \times 10^9$ N/m

It follows that $\omega_z = \sqrt{\Sigma k_z/m} = \sqrt{3.52 \times 10^9/14,356} = 495.17$ rad/s and $T_z = 2\pi/\omega_z = 0.0127$ s

(b) *Rotational degrees of freedom:*
*Column stiffness*

Vertical rotation of the rigid slab causes axial compression in columns on one side of the axis of rotation and tension on the other side. Since it is specified that net compression prevails in the columns, axial stiffness of a column, as before $k_z = 0.88 \times 10^9$ N/m :

1. *Stiffness against rotation about x axis* (Fig. 2.17c)

$$\sum k_{\theta x} = 4k_z y^2 = 4\left[0.88 \times 10^9 \times 2^2\right] = 1.408 \times 10^{10} \text{ Nm}$$

2. *Stiffness against rotation about y axis* (Fig. 2.17d)

$$\sum k_{\theta y} = 4k_z x^2 = 4\left[0.88 \times 10^9 \times 2.5^2\right] = 2.2 \times 10^{10} \text{ Nm}$$

3. *Stiffness against rotation about z axis* (Fig. 2.17e)

In this case, the columns displace along $x$ and $y$ directions as well as rotate about their vertical axes due to the rotation of the slab

$k_{\theta z}$ due to column translation (caused by slab rotation) $= k_x y^2 + k_y x^2$

$k_{\theta z}$ (due to column rotation) $= G\,J/h$

Hence, total rotational stiffness of four columns

$$\sum k_{\theta z} = 4\left(k_x y^2 + k_y x^2 + G\ J/h\right)$$

Substituting values,

$$\sum k_{\theta z} = 4\left[\left\{\left(1.01 \times 10^7 \times 2^2\right) + \left(0.449 \times 10^7 \times 2.5^2\right) + \frac{1.053 \times 2.377 \times 10^7}{4.2}\right\}\right]$$
$$= 29.768 \times 10^7 \text{ Nm}$$

*Slab stiffness*

1. For the slab, mass moments of inertia about the three centroidal axes are given by Eq. 2.11.1, viz.

$$m_{\theta xs} = m_s\left(b^2 + t^2\right)/12 = 11,468\left(5^2 + 0.15^2\right)/12 = 23,913 \text{ kg m}^2$$
$$m_{\theta ys} = m_s\left(a^2 + t^2\right)/12 = 11,468\left(6^2 + 0.15^2\right)/12 = 34,425 \text{ kg m}^2$$
$$m_{\theta zs} = m_s\left(a^2 + b^2\right)/12 = 58,296 \text{ kg m}^2$$

2. For the four columns about the three centroidal axes:

$$m_{\theta xc} = 4m_c y^2 = 4 \times 722 \times 2^2 = 11,552 \text{ kg m}^2$$
$$m_{\theta yc} = 4m_c x^2 = 4 \times 722 \times 2.5^2 = 18,050 \text{ kg m}^2$$
$$m_{\theta zc} = 4m_c\left(x^2 + y^2\right) = 29,602 \text{ kg m}^2$$

Total mass moment of inertia values about the three axes of rotation are:

$$\sum m_{\theta x} = m_{\theta xs} + m_{\theta xc} = 23,913 + 11,552 = 35,465 \text{ kg m}^2 \quad \text{and}$$
$$\sum m_{\theta y} = 52,475 \text{ kg m}^2 \quad \text{and} \quad \sum m_{\theta z} = 87,898 \text{ kg m}^2$$

Substituting values in Eq. 2.12.2, the rotational frequencies are as under:
For rotation about $x$ axis (pitching), the frequency is

$$\omega_{\theta x} = \sqrt{\frac{\Sigma\, k_{\theta x}}{\Sigma\, m_{\theta x}}} = \sqrt{\frac{1.408 \times 10^{10}}{35,465}} = 630.088 \text{ rad/s} \quad \text{and} \quad T_{\theta x} = 0.01 \text{ s}$$

For rotation about y axis (rolling), the frequency is

$$\omega_{\theta y} = \sqrt{\frac{\Sigma\, k_{\theta y}}{\Sigma\, m_{\theta y}}} = \sqrt{\frac{2.20 \times 10^{10}}{52,475}} = 647.493 \text{ rad/s} \quad \text{and} \quad T_{\theta y} = 0.0097 \text{ s}$$

For rotation about z axis (yawing), the frequency is

$$\omega_{\theta z} = \sqrt{\frac{\Sigma\, k_{\theta z}}{\Sigma\, m_{\theta z}}} = \sqrt{\frac{29.768 \times 10^7}{87,898}} = 58.195 \text{ rad/s} \quad \text{and} \quad T_{\theta z} = 0.108 \text{ s}$$

# Chapter 3
# Vibration Concepts: *Linear Systems*

**Abstract** The intention in this chapter is to first enunciate the equation of motion of a single degree-of-freedom (SDOF) oscillator vibrating in simple harmonic motion. This theoretical base is then extended to encompass undamped free vibrations, followed by damped free vibrations. Thereafter, a structure's response to an impulse is evaluated, and it is shown how this technique can be used to determine the response to earthquake excitation. This leads up to the well-known Duhamel's integral. This basic approach is then systematically expanded to arrive at equations of motion to determine the response of two degree-of-freedom and multi-degree-of-freedom (MDOF) systems. Subsequently, torsional and rocking vibrations are also addressed. The response equations developed herein are later utilised in Chaps. 4 and 6 to demonstrate how they can be applied to analyse building frameworks under seismic excitation.

**Keywords** Simple harmonic motion • Single degree-of-freedom systems • Duhamel's integral • Multi-degree-of-freedom systems • Torsional vibrations • Rocking motion

## 3.1 Introduction

A building structure is an assembly of elements, which can vibrate due to a number of reasons, viz. fluctuating winds, earthquake ground motion, dynamic forces from equipment and others. Earthquake-induced random ground motion drags the building foundations along with it, but the superstructure prefers to stay at rest. This reluctance to move induces lateral inertia forces. The building framework has to withstand effects of these dynamic forces in addition to those from gravity, wind and other loads. In order to ensure satisfactory performance of a building, a structural engineer's goal has to be that such induced forces and vibrations do not cause unacceptable structural distress nor do they lead to movements that exceed acceptable human threshold levels and permissible drift limits.

Since ground motion is oscillatory, the induced inertia forces likewise vary with time, i.e. they are dynamic. It follows that response of a structure to such time-varying loads will also be dynamic in character with values being dependent on the ground motion signature. Until recently, equivalent static loads were used to



S. Manohar, S. Madhekar, *Seismic Design of RC Buildings*, Springer Transactions in Civil and Environmental Engineering, DOI 10.1007/978-81-322-2319-1_3

avoid complex analysis which is necessary for a dynamic analysis. With the advent of high-rise buildings having complex forms and footprints coupled with high slenderness ratios, it has become imperative to undertake a comprehensive dynamic analysis in many cases.

This change has been facilitated with the availability of powerful computational capability at diminishing costs coupled with user-friendly analysis software and a realisation that such an analysis can provide a safer and perhaps an economical solution.

The inertia forces and displacements that a structure will experience are dependent on natural frequencies of the vibrating system. These frequencies can be obtained from a dynamic analysis. Hence, it is important for structural engineers to have a thorough understanding of conducting a dynamic analysis which is normally implemented in four stages:

Stage 1: Fully define the structure as well as the exciting motions and forces.
Stage 2: Create an idealised mathematical model – this is invariably a compromise solution between the demands for accuracy and those for simplicity and computational cost-effectiveness. There are many approximations that need to be made regarding the values to use for strength, stiffness, damping and so on. This is compounded with randomness of ground motion both in magnitude and spatial distribution.
Stage 3: Write down equations of motion for the model structure using established methods.
Stage 4: Evaluate the response.

The intention in this chapter is to first enunciate the equation of motion of a single degree-of-freedom oscillator vibrating in simple harmonic motion, and then systematically proceed to arrive at equations of motion to determine the response of a multi-degree-of-freedom system under seismic excitation. In the process are analysed undamped and damped free vibrations of a single degree-of-freedom (SDOF) system as well as its damped free vibrations under impulse loading and earthquake excitation.

Thereafter, the analysis procedure is applied to obtain the response of two degree- and multi-degree-of-freedom (MDOF) system. Subsequently torsional and rocking vibrations are also addressed. The equations developed herein are later utilised in Chaps. 4 and 6 to demonstrate their application to analyse building frameworks.

## 3.2 Simple Harmonic Motion (SHM)

Vibration is a complex phenomenon. Broadly speaking, vibratory motion can be periodic or aperiodic. Periodic motion is that which repeats itself at regular time intervals (e.g. simple harmonic), and an aperiodic motion is one that does not fulfil this criterion (e.g. response to earthquake motion). Both these forms are shown in Fig. 3.1a and b, respectively.

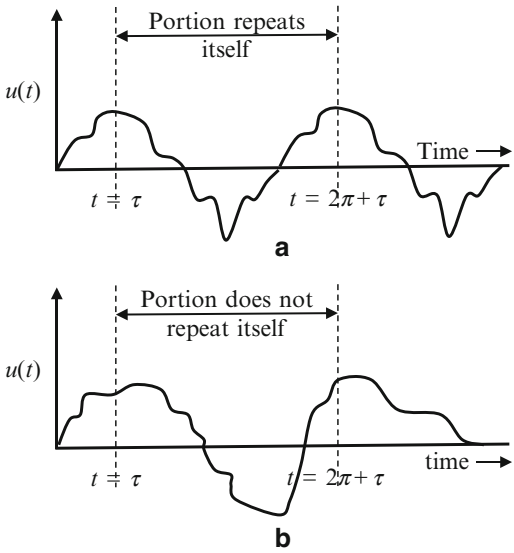


**Fig. 3.1** Vibratory motion. (**a**) Periodic motion. (**b**) Aperiodic motion

SHM, which represents a sinusoidal motion at constant frequency, is the simplest form of periodic motion. Other forms of periodic motion can also be represented as a number of simple harmonic motions. Even aperiodic motions (e.g. those due to impulse loads) can be represented as a combination of harmonic motions of different frequencies and varying amplitudes. As a result, SHM forms a powerful tool to analyse linear dynamic motions. Its study will help the reader to understand concepts of amplitude, frequency, phase and period as related to a vibrating body.

Any object, which is initially displaced slightly from its position of stable equilibrium and then released, will oscillate about its position of equilibrium. Such a body will, in general, experience a restoring force, which is linearly proportional to displacement from its position of equilibrium. This type of oscillation is termed as being simple harmonic.

### *3.2.1 Equation of a Simple Harmonic Motion*

Consider a mass $m$ at a distance A from point O (Fig. 3.2a) about which it rotates anticlockwise at a uniform angular velocity of $\omega$ rad/s which is termed as its circular frequency. The motion is deemed to commence at an angle $\varphi$ (termed phase angle) from the $x$-axis, and the angle swept by passage of mass $m$ around the circle is $\omega t$. The time that it takes the mass to complete one cycle of its motion is its period $T$. Equilibrium position of this mass at time $t = 0$ is taken as the $x$-axis and projection of its motion on the $z$-axis represents an SHM given by the displacement $u$ as

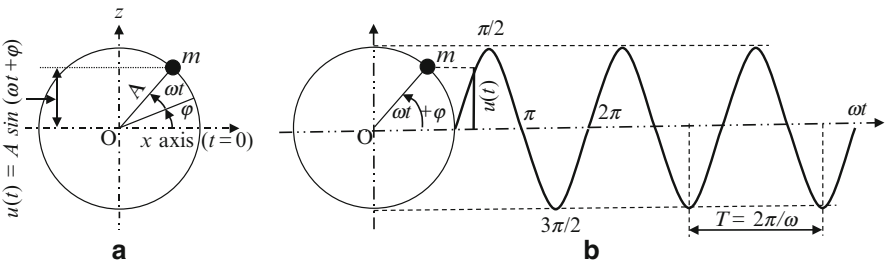


**Fig. 3.2** Free undamped simple harmonic motion

$$u(t) = A \ \sin \ (\omega t + \varphi) \tag{3.1.1}$$

where $A$ is the maximum displacement amplitude that occurs when $(\omega t + \varphi) = \pi/2$. Time history of such a motion can be graphically represented as a sine wave as shown in Fig. 3.2b. Expanding Eq. 3.1.1 and introducing $A \sin \varphi = a$ and $A \cos \varphi = b$, the equation for a SHM can be written as

$$u(t) = a \cos \ \omega t + b \sin \omega t \tag{3.1.2}$$

where $a$ and $b$ are constants and amplitude of motion

$$A = \sqrt{a^2 + b^2} \tag{3.1.3}$$

The period of vibration denotes angular distance of one revolution divided by the angular velocity, i.e. $T = 2\pi \ /\omega$. Since mass $m$ traverses a distance of one cycle in period $T$, it follows that its cyclic frequency of oscillation $f$ expressed in cycles/s will be $f = 1/T = \omega/2\pi$. Phase angle $\varphi = \tan^{-1}(a/b)$. Differentiating Eq.3.1.1, the velocity and acceleration of motion can be represented, respectively, as

$$\dot{u}(t) = \omega A \cos (\omega t + \varphi) \tag{3.1.4}$$

$$\ddot{u}(t) = -\omega^2 A \sin (\omega t + \varphi) = -\omega^2 u(t) \tag{3.1.5}$$

The above are characteristics of motion of a mass vibrating in SHM.

## 3.3 Combining Gravity and Dynamic Loads

Gravity forces are static in nature, while during an earthquake, inertia forces generated are dynamic. Consider that a static gravity load $W$ is supported by a spring providing a resistance $f_s$ given by $f_s = k v_s = W$ (Fig. 3.3a).

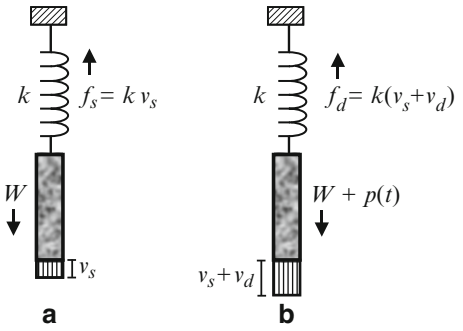


**Fig. 3.3** Gravity and dynamic loads. (**a**) Gravity load. (**b**) Gravity plus dynamic load

Next consider that this body is acted upon by a vertical dynamic force $p(t)$ (Fig. 3.3b).

$m$ : mass of the body $= W/g$ (kg)
$k$ : spring stiffness against vertical displacement (N/m)
$v_s$ & $v_d$ : static and dynamic vertical displacements, respectively (m)
$c$ : damping coefficient (N s/m)
$v_t$ : total displacement $= v_s + v_d$ (m)

It follows that $\dot{v}_t = \dot{v}_s + \dot{v}_d$. Since $v_s$ is invariant with time, $\dot{v}_t = \dot{v}_d$ and $\ddot{v}_t = \ddot{v}_d$ The dynamic equation of motion of such a body is

$$m\ddot{v}_t + c\dot{v}_t + kv_t = p(t) + W \tag{3.2.1}$$

Substituting values derived above, we get

$$m\ddot{v}_d + c\dot{v}_d + kv_s + kv_d = p(t) + W$$

and since

$$kv_s = W; \quad m\ddot{v}_d + c\dot{v}_d + kv_d = p(t) \tag{3.2.2}$$

which is the dynamic equation of motion without considering the static effect.

This demonstrates that the dynamic equation of motion with reference to the system's static equilibrium position is unaffected by gravity forces (Clough and Penzien 2003). It follows that in any linear dynamic problem, the total displacement can be obtained by adding, at any instant of time, the corresponding static and dynamic quantities evaluated separately. It will be observed that the difference between static and dynamic equilibrium is that in the latter case both excitation and response are time dependent.

## 3.4 Single Degree-of-Freedom (SDOF) Systems

For analytical purposes, there is a need to represent the complex structural configuration of a building by a simple mathematical model which can be used to obtain answers of acceptable accuracy regarding the structure's performance during an earthquake. In its simplest form, a single-storey moment frame structure is idealised as a SDOF system as explained in Sect. 2.8.1.

### *3.4.1 Equation of Motion of a SDOF System*

As shown in Fig. 3.4, consider a SDOF system with the following properties:

#### 3.4.1.1 Mass ($m$)

The entire mass of the slab is assumed as being a discrete lump concentrated at roof level. Half of the column masses are considered as being lumped at roof level and the balance half at foundation level. The total mass at roof level is lumped as a mass $m$.

Columns are then treated as massless springs providing the lateral stiffness and possessing an infinite vertical stiffness.

#### 3.4.1.2 Stiffness ($k$)

The lateral stiffness of columns provides resistance $f_s$ against lateral storey displacement $u$. Thus, it represents a linear spring:

$$f_s = k.u(t)$$

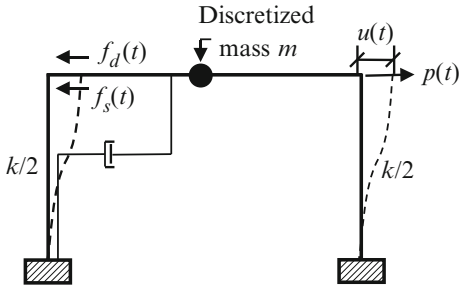


**Fig. 3.4** Lateral loading

#### 3.4.1.3 Damping Coefficient (*c*)

As a simplifying assumption, damping force $f_d$ opposing the motion is assumed to act at roof level and is taken to be proportional to the velocity of motion of the structure:

$$f_d = c\dot{u}(t)$$

#### 3.4.1.4 Lateral Dynamic Force

This is represented as a time variant force $p\,(t)$ at roof level, causing translation $u(t)$ of the roof in the direction of this force. To analyse such a mathematical model, we need to link its dynamic displacement to the excitation force taking cognizance of resistance offered by the vibrating system. This is achieved through an expression known as the equation of motion. At any instant of time, such displacement $u(t)$ is resisted by forces due to damping $f_d$ and by lateral stiffness of the frame $f_s$, resulting in a net force

$$\{p(t) - f_d(t) - f_s(t)\}$$

As per Newton's second law of motion, for linear systems, a body acted upon by a force moves such that time rate of change of its linear momentum is equal to the net force applied:

$$p(t) - f_d(t) - f_s(t) = \frac{d}{dt}\left(m\,\dot{u}(t)\right) \tag{3.3.1}$$

Since building mass $m$ is constant, the right-hand side of the above equation reduces to $m\,\ddot{u}$ leading to D'Alembert's principle of dynamic equilibrium. It states that 'a mass subjected to an acceleration produces an inertial opposing force proportional to its acceleration' {i.e. net force – (mass × acceleration) = 0)} or

$$p(t) - f_d(t) - f_s(t) = m\ddot{u}(t) \tag{3.3.2}$$

Substituting values of $f_s$ and $f_d$,

$$m\ddot{u}(t) + c\dot{u}(t) + ku(t) = p(t) \tag{3.3.3}$$

Thus, the sum of all resistive forces (i.e. due to inertia + damping + stiffness) is equal to external force. This is an equation of dynamic equilibrium, which is referred to as an equation of motion for a SDOF system under a lateral force $p(t)$. In the following sections, the equations of motion for free vibrations of a SDOF system under different types of excitation forces are developed.

### 3.4.2 *Undamped Free Vibrations*

When a mass $m$ of an idealised system is initially displaced from its neutral equilibrium position and then released (i.e. $p(t) = 0$), the system will vibrate freely about its initial equilibrium position. This response is termed as free vibrations and is represented by the equation (Chopra 1995)

$$m\ddot{u} + c\dot{u} + ku = 0 \tag{3.4.1}$$

Since there is no damping, $c = 0$ in Eq. 3.4.1 and the equation becomes

$$m\ddot{u} + ku = 0 \quad i.e. \quad \ddot{u} + \frac{k}{m}u = 0 \tag{3.4.2}$$

Assume that its solution is of the form

$$u(t) = A\mathrm{e}^{\lambda t} \tag{3.4.3}$$

where $A$ and $\lambda$ are constants. Substituting for $u$ in Eq. 3.4.2,
$A\mathrm{e}^{\lambda t}\left\{\lambda^2 + \frac{k}{m}\right\} = 0$, and since $A\mathrm{e}^{\lambda t}$ is never zero,

$$\lambda = \pm i\omega \quad \text{where } \omega = \sqrt{k/m} \tag{3.4.4}$$

Since the free vibratory motion for a given mode shape is harmonic, the general solution of Eq. 3.4.2 can be taken in the form

$$u(t) = A_1\mathrm{e}^{i\omega t} + A_2\mathrm{e}^{-i\omega t} \tag{3.4.5}$$

where $A_1$ and $A_2$ are constants.

Using Euler's theorem, Eq. 3.4.5 can be written as

$$u(t) = (A_1 + A_2)\cos\ \omega t + (A_1 - A_2)\sin\ \omega t$$

Introducing constants $C_1$ and $C_2$, such that $C_1 = (A_1 + A_2)$ and $C_2 = (A_1 - A_2)$,

$$u(t) = C_1\cos\ \omega t + C_2\sin\ \omega t \tag{3.4.6}$$

Comparing this equation with Eq. 3.1.2 of SHM, it can be said that $\omega$ is the circular frequency of a SDOF system which, for an undamped free vibration, is given by

$$\omega = \sqrt{k/m}$$

Differentiating Eq. 3.4.6,

$$\dot{u}(t) = \omega\,(-C_1\sin\ \omega t + C_2\cos\ \omega t) \tag{3.4.7}$$

If at $t = 0$, $u = u_0$ and $\dot{u} = \dot{u}_0$, then it follows from the above that $C_1 = u_0$ and $C_2 = \dot{u}_0/\omega$

The equation of motion for an undamped free vibration of a SDOF system becomes

$$u(t) = u_0 \cos\ \omega t + \frac{\dot{u}_0}{\omega} \sin\ \omega t \tag{3.4.8}$$

and the amplitude of motion is

$$A = \sqrt{u_0{}^2 + (\dot{u}_0/\omega)^2} \tag{3.4.9}$$

### 3.4.3 Damped Free Vibrations

As per Eq. 3.4.1,

$$m\ddot{u} + c\dot{u} + ku = 0$$

Substituting from Eqs. 3.4.3 and 3.4.4, $u = Ae^{\lambda t}$, $\omega = \sqrt{\frac{k}{m}}$, and introducing $\xi = \dfrac{c}{2\,m\omega}$, the above equation reduces to

$$\lambda^2 + 2\xi\omega\lambda + \omega^2 = 0 \tag{3.5.1}$$

This equation has two roots

$$\lambda_{1,2} = \omega\left\{-\xi \pm i\sqrt{1-\xi^2}\right\} \tag{3.5.2}$$

Defining the circular frequency under damped conditions as

$$\omega_d = \omega\sqrt{1-\xi^2} \tag{3.5.3}$$

$$\lambda_{1,2} = -\omega\xi \pm i\,\omega_d \tag{3.5.4}$$

and proceeding as for Eq. 3.4.5,

$$\begin{aligned} u(t) &= \left\{A_1 e^{(-\xi\omega + i\omega_d)t} + A_2 e^{(-\xi\omega - i\omega_d)t}\right\} \\ i.e.\quad u(t) &= e^{-\xi\omega t}\left\{A_1 e^{i\omega_d t} + A_2 e^{-i\omega_d t}\right\} \end{aligned} \tag{3.5.5}$$

As in Sect. 3.4.2, the equation of motion for a damped SDOF system can be written as

$$u(t) = \mathrm{e}^{-\xi\omega t}\{C_1 \cos\ \omega_d t + C_2 \sin\ \omega_d t\} \tag{3.5.6}$$

$$\text{If at } t = 0,\ u = u_0 \text{ and } \dot{u} = \dot{u}_0,\ \text{then } C_1 = u_0 \text{ and } C_2 = \frac{\dot{u}_0 + u_0\xi\omega}{\omega_d} \tag{3.5.7}$$

Thus, the expression for displacement $u(t)$ becomes

$$u(t) = \mathrm{e}^{-\xi\omega t}\left\{u_0 \cos\ \omega_d t + \frac{\dot{u}_0 + u_0\xi\omega}{\omega_d} \sin\ \omega_d t\right\} \tag{3.5.8}$$

The amplitude of vibration will be given by

$$A = \sqrt{C_1^2 + C_2^2} = \sqrt{u_0^2 + \left\{\frac{\dot{u}_0 + u_0\xi\omega}{\omega_d}\right\}^2} \tag{3.5.9}$$

This is known as damped harmonic motion. Its natural period of vibration is given by

$$T_d = \frac{2\pi}{\omega_d} \tag{3.5.10}$$

Generally for buildings, $\xi << 1$, hence $\omega_d \cong \omega$ and $T_d \cong T$. This enables the period $T$ to be determined without considering damping. Accordingly, for buildings, the equation of motion for a SDOF system with damping can be written as

$$u(t) = \mathrm{e}^{-\xi\omega t}\left\{u_0 \cos\ \omega t + \frac{\dot{u}_0 + u_0\xi\omega}{\omega} \sin\ \omega t\right\} \tag{3.5.11}$$

The application of this analysis is demonstrated through *Ex.* 3.9.1.

### *3.4.4 Damped Free Vibrations Under Impulse Loading*

A deterministic load is one where the variation of load with time is fully known even if it is highly oscillatory in character. On the other hand, if the load needs to be defined through statistical means, then it is termed as stochastic. Such a loading is a series of random impulses. An impulse is the product of a very short duration load and the minute time interval over which it acts. Consider that a body of mass $m$ is at rest until a time $t = \tau$ (i.e. $u\ (\tau) = 0$). At this juncture, it is subjected to an impulse which can be considered as an instantaneous force $p(\tau)$ for an infinitesimal period $d\tau$ whose value is zero at all other times (Fig. 3.5). From impulse–momentum compatibility with a constant mass,

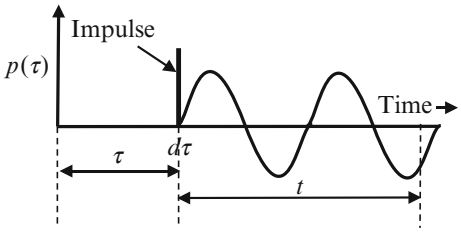


**Fig. 3.5** Impulse loading

$$p(\tau) = \frac{d}{d\tau}\{m.\dot{u}(\tau)\} = m\frac{d}{d\tau}\{\dot{u}(\tau)\}, \tag{3.6.1}$$

$$\text{i.e.} \quad \dot{u}(\tau) = \frac{p(\tau)\,d\tau}{m} \tag{3.6.2}$$

At commencement of impulse $u_0 = 0$ and the impulse acting over an infinitesimal time $d\tau$ imparts to mass $m$, a velocity $\dot{u}(\tau)$. Thereafter, the system undergoes free vibrations. Noting that at $t = 0, u(\tau) = 0$ and $\dot{u}(\tau) = \frac{p(\tau)d\tau}{m}$, then by substituting these values in Eq. 3.5.8, the displacement at time $t \geq \tau$ is obtained as

$$u(t) = e^{-\xi\omega(t-\tau)}\left\{\frac{p(\tau)}{m\omega_d}\right\} \sin\ \omega_d\,(t-\tau)\,d\tau \tag{3.6.3}$$

This is an equation of displacement at time $t$ (after the impulse), for a mass at rest experiencing an impulse load of $p(\tau)$ at time $t = \tau$.

### *3.4.5 Damped Free Vibrations Under Earthquake Excitation*

Horizontal ground motion displaces the base of a structure by an amount $u_g(t)$. There will be relative displacement $u(t)$, at time $t$, between mass $m$ at a roof level and base of the structure resulting in a total displacement of the mass as $\{u(t) + u_g(t)\}$. This is shown in Fig. 3.6. The rigid body movement $u_g(t)$ does not produce resistive forces. Hence, displacement that features in stiffness calculation is relative displacement of the roof with respect to the ground. However, spectral acceleration of the mass is a sum total of the acceleration of a body relative to the ground and ground acceleration itself. Thus, the total acceleration of the mass is $\left(\ddot{u} + \ddot{u}_g\right)$. Substituting this value in Eq. 3.4.1 leads to

$$m\ddot{u} + c\dot{u} + ku = -m\ddot{u}_g \tag{3.7.1}$$

Value of seismic acceleration cannot be predicted at any instant of time since it varies arbitrarily in the time domain. Such random ground motion induces randomly

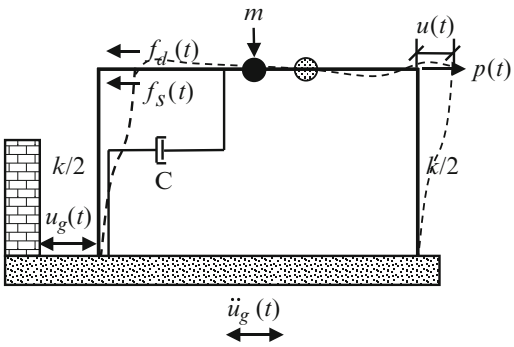


**Fig. 3.6** Ground motion

varying inertial forces which can be considered as composed of a train of piecewise impulses caused by a force $p(\tau)$, each of an infinitesimal duration $d\tau$. At any instant $t = \tau$, if the ground acceleration is $\ddot{u}_g(\tau)$, then the infinitesimal force experienced by mass $m$ would be $p(\tau) = m\ddot{u}_g(\tau)$. If this force acts for an infinitesimal time $d\tau$, then the response caused by this force at a later time $t$ is given by substituting the above value of force $p(\tau)$ in Eq. 3.6.3 giving

$$\Delta u(t) = e^{-\xi\omega(t-\tau)}\left[\frac{-\ddot{u}_g(\tau)}{\omega_d}\sin\ \omega_d(t-\tau)\,d\tau\right] \tag{3.7.2}$$

The response induced by a train of such impulses can be obtained by summing over the entire period of ground shaking, given by

$$u(t) = -\frac{1}{\omega_d}\int_0^t \ddot{u}_g(\tau)\,e^{-\xi\omega(t-\tau)}\sin\ \omega_d(t-\tau)\,d\tau \tag{3.7.3}$$

In this solution, it is assumed that the system is at rest both in terms of displacement and velocity prior to application of the impulse, which is generally the case at the commencement of seismic ground motion. If this is not the case then, initial values of displacement and velocity should be included to arrive at $u(t)$. Further, Eq. 3.7.3 is valid only for linear systems as it is based on the principle of superposition. The right-hand side is known as a convolution integral because the forcing function is entwined with the impulse response function. It is more commonly known as the Duhamel's integral. For an undamped system, the response equation reduces to

$$u(t) = -\frac{1}{\omega}\int_0^t \ddot{u}_g(\tau)\sin\ \omega(t-\tau)\,d\tau \tag{3.7.4}$$

The explicit solution of this integral can provide an exact solution for the simplest of loading cases. However, earthquake excitation is complex and numerical methods

will need to be used if it is desired to solve this integral. A typical computation of displacement response for a seismic impulse is shown in *Ex* 3.9.2. Typical numerical methods are described in Chap. 4.

### *3.4.6 Resonance*

Dynamic amplification is the increase in response of a structure at roof level in comparison with the ground motion initiating it. The degree of amplification will depend on vibration characteristics of the structure and frequency content of ground shaking. When the latter is centred around the building's natural frequency, the two are likely to resonate. For resonance to occur, there has to be a sustained harmonic force. Such a force does not generally build up during an earthquake since the motion is highly random and complex.

However, there could be significant damage if the shaking – typically from long-distance waves – contains significant energy at frequencies close to the natural frequency of the structure. This could occur in the case of a tall structure founded on a thick layer of soft soil. This is one of the reasons why some buildings shake more than others and consequently suffer more damage. A structure needs to be so designed that resonance is avoided as otherwise building displacements can be amplified resulting in aggravated damage.

## 3.5 Two Degree-of-Freedom (Two DOF) System

A two DOF system is analysed as a transition from a SDOF system to a MDOF system. This will provide the reader with a better understanding of the concepts involved as well as it will be beneficial later when examining the impact of a soft storey as well as base isolation.

### *3.5.1 Undamped Free Vibrations*

Consider a two DOF system as illustrated in Fig. 3.7a. Masses $m_1$ and $m_2$ are depicted as lumped masses at respective rigid floor levels. At any time instant $t$, these masses are acted upon by forces $p_1(t)$ and $p_2(t)$ causing displacements $u_1(t)$ and $u_2(t)$, respectively (Fig. 3.7b).

When a floor displaces laterally with respect to the floor below it, a resistive shear force $f_s = k.u$ is induced in the supporting columns which is proportional to lateral displacement $u$. The resistance force due to damping is $f_d = c\dot{u}$. These forces act at respective floor levels as the masses are assumed to be concentrated there. Inertia

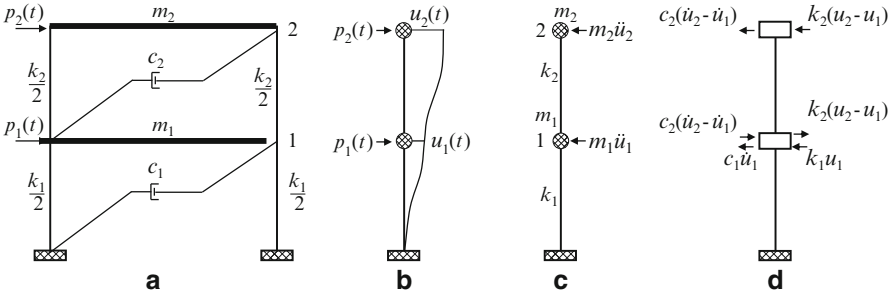


**Fig. 3.7** Two DOF system. (**a**) Schematic. (**b**) Storey displacements. (**c**) Inertia forces. (**d**) System resistance

forces generated as well as the stiffness and damping forces are shown in Fig. 3.7c, d respectively. Equations of motion for each mass at any instant $t$ can be written as laid down by Hart and Wong (2000):

$$p_1 - m_1\ddot{u}_1 + c_2\{\dot{u}_2 - \dot{u}_1\} - c_1\{\dot{u}_1\} + k_2\{u_2 - u_1\} - k_1u_1 = 0 \tag{3.8.1}$$

$$p_2 - m_2\ddot{u}_2 - c_2\{\dot{u}_2 - \dot{u}_1\} - k_2\{u_2 - u_1\} = 0 \tag{3.8.2}$$

Rearranging terms, the equations in matrix form are

$$\boldsymbol{M}\ddot{\boldsymbol{U}} + \boldsymbol{C}\dot{\boldsymbol{U}} + \boldsymbol{K}\boldsymbol{U} = \boldsymbol{P} \tag{3.8.3}$$

where

$$\boldsymbol{M} = \begin{bmatrix} m_1 & 0 \\ 0 & m_2 \end{bmatrix},\ \boldsymbol{C} = \begin{bmatrix} c_1 + c_2 & -c_2 \\ -c_2 & c_2 \end{bmatrix},\ \boldsymbol{K} = \begin{bmatrix} k_1 + k_2 & -k_2 \\ -k_2 & k_2 \end{bmatrix},\ \boldsymbol{U} = \begin{Bmatrix} u_1 \\ u_2 \end{Bmatrix},$$
$$\boldsymbol{P} = \begin{Bmatrix} p_1 \\ p_2 \end{Bmatrix} \tag{3.8.4}$$

For an undamped system under free vibrations (i.e. $\boldsymbol{C} = 0, \boldsymbol{P} = 0$),

$$\boldsymbol{M}\ddot{\boldsymbol{U}} + \boldsymbol{K}\boldsymbol{U} = 0 \tag{3.8.5}$$

and the resulting equations are

$$\begin{bmatrix} m_1 & 0 \\ 0 & m_2 \end{bmatrix} \begin{Bmatrix} \ddot{u}_1 \\ \ddot{u}_2 \end{Bmatrix} + \begin{bmatrix} k_1 + k_2 & -k_2 \\ -k_2 & k_2 \end{bmatrix} \begin{Bmatrix} u_1 \\ u_2 \end{Bmatrix} = \begin{Bmatrix} 0 \\ 0 \end{Bmatrix} \tag{3.8.6}$$

As in Eq. 3.4.6, the lateral displacements will be given by

$$\begin{Bmatrix} u_1 \\ u_2 \end{Bmatrix} = \begin{Bmatrix} A_1 \\ A_2 \end{Bmatrix} \cos\ \omega t + \begin{Bmatrix} B_1 \\ B_2 \end{Bmatrix} \sin\ \omega t \tag{3.8.7}$$

Noting that $\ddot{u}_1 = -\omega^2 u_1$ and $\ddot{u}_2 = -\omega^2 u_2$ and introducing these values in Eq. 3.8.6,

$$\begin{bmatrix} -m_1\omega^2 + k_1 + k_2 & -k_2 \\ -k_2 & -m_2\omega^2 + k_2 \end{bmatrix} \left[ \begin{Bmatrix} A_1 \\ A_2 \end{Bmatrix} \cos\ \omega t + \begin{Bmatrix} B_1 \\ B_2 \end{Bmatrix} \sin\ \omega t \right] = 0 \tag{3.8.8}$$

Neglecting the trivial solution $A_1 = A_2 = 0$ and $B_1 = B_2 = 0$, the other solution is that the determinant of the left side matrix is zero (Hart and Wong 2000),

$$\text{i.e.} \quad m_1 m_2 \omega^4 - \omega^2 \{(k_1 + k_2) m_2 + k_2 m_1\} + k_1 k_2 = 0 \tag{3.8.9}$$

The solution of this quadratic equation yields two values of $\omega^2$ as

$$\begin{aligned} {\omega^2}_{2,1} = \frac{1}{2m_1 m_2} \Big\{ & (k_1 + k_2) m_2 + k_2 m_1 \\ & \pm \sqrt{\{(k_1 + k_2) m_2 + k_2 m_1\}^2 - 4 m_1 m_2 k_1 k_2} \Big\} \end{aligned} \tag{3.8.10}$$

From this equation are obtained the two natural frequencies $\omega_1$ and $\omega_2$ of this two DOF system. Since both these frequencies satisfy Eq. 3.8.8, an additional suffix is introduced to the constants resulting in constants $A_{11}$, $B_{11}$ for frequency $\omega_1$ and $A_{12}$, $B_{12}$ for frequency $\omega_2$. This leads to two equations:

$$\begin{bmatrix} -m_1\omega_1^2 + k_1 + k_2 & -k_2 \\ -k_2 & -m_2\omega_1^2 + k_2 \end{bmatrix} \left[ \begin{Bmatrix} A_{11} \\ A_{21} \end{Bmatrix} \cos\ \omega_1 t + \begin{Bmatrix} B_{11} \\ B_{21} \end{Bmatrix} \sin\ \omega_1 t \right] = 0 \tag{3.8.11}$$

and

$$\begin{bmatrix} -m_1\omega_2^2 + k_1 + k_2 & -k_2 \\ -k_2 & -m_2\omega_2^2 + k_2 \end{bmatrix} \left[ \begin{Bmatrix} A_{12} \\ A_{22} \end{Bmatrix} \cos\ \omega_2 t + \begin{Bmatrix} B_{12} \\ B_{22} \end{Bmatrix} \sin\ \omega_2 t \right] = 0 \tag{3.8.12}$$

Equation 3.8.11 can be rewritten as two separate equations:

$$\begin{aligned} & \left(-m_1\omega_1^2 + k_1 + k_2\right) (A_{11} \cos\ \omega_1 t + B_{11} \sin\ \omega_1 t) - \\ & \quad k_2 (A_{21} \cos\ \omega_1 t + B_{21} \sin\ \omega_1 t) = 0 \end{aligned} \tag{3.8.13}$$

and

$$-k_2\left(A_{11}\cos\ \omega_1 t + B_{11}\sin\ \omega_1 t\right) + \left(k_2 - m_2\omega_1^2\right)\left(A_{21}\cos\ \omega_1 t + B_{21}\sin\ \omega_1 t\right) = 0 \tag{3.8.14}$$

Solving these equations separately and proceeding similarly for Eq. 3.8.12 and introducing factors $\alpha_1$ and $\alpha_2$, as shown by Hart and Wong (2000), as under

$$\alpha_1 = \frac{-m_1\omega_1^2 + k_1 + k_2}{k_2} = \frac{k_2}{-m_2\omega_1^2 + k_2} \tag{3.8.15}$$

$$\alpha_2 = \frac{-m_1\omega_2^2 + k_1 + k_2}{k_2} = \frac{k_2}{-m_2\omega_2^2 + k_2} \tag{3.8.16}$$

results in the following equations:

$$\begin{Bmatrix} u_1 \\ u_2 \end{Bmatrix} = \begin{Bmatrix} 1 \\ \alpha_1 \end{Bmatrix} \left(A_{11}\cos\ \omega_1 t + B_{11}\sin\ \omega_1 t\right) \tag{3.8.17}$$

$$\begin{Bmatrix} u_1 \\ u_2 \end{Bmatrix} = \begin{Bmatrix} 1 \\ \alpha_2 \end{Bmatrix} \left(A_{12}\cos\ \omega_2 t + B_{12}\sin\ \omega_2 t\right) \tag{3.8.18}$$

For any value of the constants, the determinant will be zero for both frequencies $\omega_1$ and $\omega_2$. The total response for the two frequencies together will be a sum of the two responses, i.e.

$$u_1 = A_{11}\cos\ \omega_1 t + B_{11}\sin\ \omega_1 t + A_{12}\cos\ \omega_2 t + B_{12}\sin\ \omega_2 t \tag{3.8.19}$$

$$u_2 = \alpha_1\left\{A_{11}\cos\ \omega_1 t + B_{11}\sin\ \omega_1 t\right\} + \alpha_2\left\{A_{12}\cos\ \omega_2 t + B_{12}\sin\ \omega_2 t\right\} \tag{3.8.20}$$

This demonstrates that the displacement of a storey of a two DOF system can be represented as a sum of displacements during the two vibrating modes. Values of the constants can be obtained from initial conditions which are taken as $u_1 = u_{1o}$, $u_2 = u_{2o}$, $\dot{u}_1 = \dot{u}_{1o}, \dot{u}_2 = \dot{u}_{2o}$ which gives

$$A_{11} = \frac{u_{2o} - \alpha_2 u_{1o}}{\alpha_1 - \alpha_2}, \qquad A_{12} = \frac{\alpha_1 u_{1o} - u_{2o}}{\alpha_1 - \alpha_2}$$

$$B_{11} = \frac{\dot{u}_{2o} - \alpha_2\dot{u}_{1o}}{\omega_1\left(\alpha_1 - \alpha_2\right)} \quad \text{and} \quad B_{12} = \frac{\alpha_1\dot{u}_{1o} - \dot{u}_{2o}}{\omega_2\left(\alpha_1 - \alpha_2\right)} \tag{3.8.21}$$

For the condition when the system is given an initial displacement and then released from rest (i.e. initial velocities, $\dot{u}_1 = \dot{u}_2 = 0$), the displacements are

$$\begin{Bmatrix} u_1 \\ u_2 \end{Bmatrix} = \frac{1}{(\alpha_1 - \alpha_2)} \left[ \begin{Bmatrix} 1 \\ \alpha_1 \end{Bmatrix} (u_{2o} - \alpha_2 u_{1o}) + \begin{Bmatrix} 1 \\ \alpha_2 \end{Bmatrix} (\alpha_1 u_{1o} - u_{2o}) \right] \quad (3.8.22)$$

The evaluation of inertia forces, storey shears and drift for a two DOF system is depicted in *Ex* 3.9.3.

## 3.6 Multi-Degree-of-Freedom (MDOF) System

A multistoreyed building shear frame is commonly modelled as a series of lumped masses concentrated at respective rigid floor levels with resistance to lateral motion being provided by lateral stiffness of massless columns, equivalent viscous damping in the system (Fig. 3.8) and inertia forces. An equation of motion can be written for a mass at each floor level. These equations are coupled because a force applied to any one mass will cause forces on masses at other levels, and thus it complicates the analysis process. Such a system will have a number of degrees of freedom (DOF) equal to the number of floors. As a result it will have more than one resonant frequency.

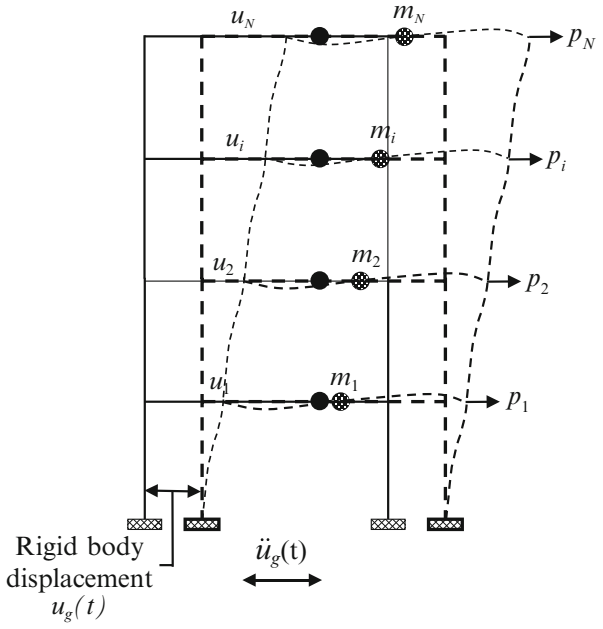


**Fig. 3.8** MDOF system

### 3.6.1 Undamped Free Vibrations

The theory presented in the previous sections is now extended to a MDOF system. A model of a MDOF system is shown in Fig. 3.8. It is shown as a single-bay structure but it may consist of any number of bays. Eq. 3.8.7 for a two DOF undamped system under free vibrations when extended to an undamped MDOF system with $N$ degrees of freedom, the equations of motion can be written as

$$\boldsymbol{U} = \begin{Bmatrix} u_1 \\ u_2 \\ \vdots \\ u_N \end{Bmatrix} = \begin{Bmatrix} A_1 \\ A_2 \\ \vdots \\ A_N \end{Bmatrix} \cos\ \omega t + \begin{Bmatrix} B_1 \\ B_2 \\ \vdots \\ B_N \end{Bmatrix} \sin\ \omega t, \tag{3.9.1}$$

$$\text{i.e.} \quad \boldsymbol{U} = \boldsymbol{A} \cos\ \omega t + \boldsymbol{B} \sin\ \omega t \tag{3.9.2}$$

Substituting Eq. 3.9.2 into Eqs. 3.8.5 and 3.8.7,

$$\left[-\boldsymbol{M}\omega^2 + \boldsymbol{K}\right][\boldsymbol{A} \cos\ \omega t + \boldsymbol{B} \sin\ \omega t] = 0, \tag{3.9.3}$$

$$\text{i.e.} \quad \left[-\boldsymbol{M}\omega^2 + \boldsymbol{K}\right][\boldsymbol{A} \cos\ \omega t] + \left[-\boldsymbol{M}\omega^2 + \boldsymbol{K}\right][\boldsymbol{B} \sin\ \omega t] = 0 \tag{3.9.4}$$

Since at any instant of time $t$, both $\sin\omega t$ and $\cos\omega t$ are not zero, it follows that

$$\left[-\boldsymbol{M}\omega^2 + \boldsymbol{K}\right]\boldsymbol{A} = 0 \quad \text{and} \quad \left[-\boldsymbol{M}\omega^2 + \boldsymbol{K}\right]\boldsymbol{B} = 0 \tag{3.9.5}$$

Using the derivation in Sect. 4.6.2 and Eq. 4.10.10, the equation of motion for mode $i$ of a MDOF system will be

$$\ddot{q}_i + \frac{k_i}{m_i} q_i = 0 \quad i = 1 \text{ to } N \tag{3.9.6}$$

This is of the same form as Eq. 3.4.2 and it follows from Eq. 3.4.4 that the $N$ natural frequencies will be given by

$$\omega_i = \sqrt{\frac{k_i}{m_i}} \quad i = 1 \text{ to } N \tag{3.9.7}$$

### 3.6.2 Damped System Under Free Vibrations

For a proportionately damped MDOF system under free vibrations, the equation of motion in mode $i$ will be as per Eq. 3.11.10 with $\ddot{u}_g = 0$, i.e.

$$\ddot{q}_i + 2\xi_i \omega_i \dot{q}_i + \omega_i^2 q_i = 0 \quad i = 1 \text{ to } N \tag{3.10.1}$$

Using the procedure adopted in Sect. 3.4.3 for damped vibrations of a SDOF system,

$$q_i(t) = e^{-\xi_i \omega_i t} \left\{ q_{i0} \cos\ \omega_{id} t + \frac{\dot{q}_{i0} + q_{i0} \xi_i \omega_i}{\omega_{id}} sin\ \omega_{id} t \right\} \tag{3.10.2}$$

where the initial displacement vector is $q_{io}$ and the $i$th natural frequency with damping will be $\omega_{id} = \omega_i \sqrt{1 - \xi_i^2}$

The total displacement $u(t)$ is obtained by summation over all modes. Hence,

$$u(t) = \sum_{i=1}^{N} \mathrm{e}^{-\xi_i \omega_i t} \left\{ q_{i0} \cos\ \omega_{id} t + \frac{\dot{q}_{i0} + q_{i0} \xi_i \omega_i}{\omega_{id}} \sin\ \omega_{id} t \right\} \tag{3.10.3}$$

### 3.6.3 *Damped Vibrations Under Earthquake Excitation*

The equation of motion due to earthquake excitation of a MDOF system can be written as in Eq. 3.8.3, but substituting the lateral forces $\boldsymbol{P}$ by that due to an earthquake,

$$\boldsymbol{M}\ddot{\boldsymbol{U}} + \boldsymbol{C}\dot{\boldsymbol{U}} + \boldsymbol{K}\boldsymbol{U} = -\boldsymbol{M}\{\boldsymbol{r}\}\ddot{u}_g \tag{3.11.1}$$

where $\{\boldsymbol{r}\}$ is a column matrix representing the excitation influence vector. For a translatory seismic planer motion, it has a value '1' for all storeys in the direction of motion and a value '0' for other degrees of freedom.

Utilising the value of $\boldsymbol{U}$ from Eq. 4.10.3 and substituting it and its derivatives in Eq. 3.11.1 and taking $\{\boldsymbol{r}\} = 1$,

$$\sum_{i=1}^{N} \boldsymbol{M}\varphi_i \ddot{q}_i + \sum_{i=1}^{N} \boldsymbol{C}\varphi_i \dot{q}_i + \sum_{i=1}^{N} \boldsymbol{K}\varphi_i q_i = -\boldsymbol{M}\ddot{u}_g \tag{3.11.2}$$

Premultiplying with a particular mode shape transpose $\varphi_j^T$, the above equation reduces to

$$\sum_{i=1}^{N} \varphi_j^T \boldsymbol{M}\varphi_i \ddot{q}_i + \sum_{i=1}^{N} \varphi_j^T \boldsymbol{C}\varphi_i \dot{q}_i + \sum_{i=1}^{N} \varphi_j^T \boldsymbol{K}\varphi_i q_i = -\varphi_j^T \boldsymbol{M}\ddot{u}_g \tag{3.11.3}$$

Here, recourse is taken of the mode orthogonality property (which is explained in Sect. 4.6.5), i.e. $\varphi_j^{\mathrm{T}} \boldsymbol{M}\varphi_i = 0 \quad and \quad \varphi_j^{\mathrm{T}} \boldsymbol{K}\varphi_\iota = 0$ for all values of $j$ other than $j = i$. Further, for ease of analysis, a reasonable idealisation for multistorey buildings is made (Chopra 1995) that classical damping exists. This implies that orthogonality

condition applies to the damping matrix also, i.e. $\varphi_j^{\mathrm{T}} \boldsymbol{C} \varphi_i = 0 \quad \text{for } j \neq i$. Then Eq. 3.11.3 reduces to

$$\left(\varphi_i^{\mathrm{T}} \boldsymbol{M} \varphi_i\right) \ddot{q}_i + \left(\varphi_i^{\mathrm{T}} \boldsymbol{C} \varphi_i\right) \dot{q}_i + \left(\varphi_i^{\mathrm{T}} \boldsymbol{K} \varphi_i\right) q_i = -\varphi_i^{\mathrm{T}} \boldsymbol{M} \ddot{u}_g \tag{3.11.4}$$

$$\text{Denoting} \quad \boldsymbol{M}_i = \left(\varphi_i^{\mathrm{T}} \boldsymbol{M} \varphi_i\right), \quad \boldsymbol{C}_i = \left(\varphi_i^{\mathrm{T}} \boldsymbol{C} \varphi_i\right) \quad \text{and} \quad \boldsymbol{K}_i = \left(\varphi_i^{\mathrm{T}} \boldsymbol{K} \varphi_i\right), \tag{3.11.5}$$

$$\boldsymbol{M}_i \ddot{q}_i + \boldsymbol{C}_i \dot{q}_i + \boldsymbol{K}_i q_i = -\varphi_i^{\mathrm{T}} \boldsymbol{M} \ddot{u}_g \tag{3.11.6}$$

The left-hand side of this equation is of the same form as that in Sect. 3.4.3. Hence, the damping ratio for mode $i$ can be defined in an analogous manner, i.e.

$$\xi_i = \frac{\boldsymbol{C}_i}{2\omega_i \boldsymbol{M}_i} \tag{3.11.7}$$

From Eq. 4.13.1,

$$\boldsymbol{K} \varphi_i = \omega_i^2 \boldsymbol{M} \varphi_i \tag{3.11.8}$$

Substituting this value in Eq. 3.11.5,

$$\boldsymbol{K}_i = \omega_i^2 \left(\varphi_i^{\mathrm{T}} \boldsymbol{M} \varphi_i\right) = \omega_i^2 \boldsymbol{M}_i \tag{3.11.9}$$

Substituting for $\boldsymbol{C}_i$ and $\boldsymbol{K}_i$ in Eq. 3.11.6 and dividing by $\boldsymbol{M}_i$,

$$\ddot{q}_i + 2\omega_i \xi_i \dot{q}_i + \omega_i^2 q_i = \frac{-\varphi_i^{\mathrm{T}} \boldsymbol{M}}{\left(\varphi_i^{\mathrm{T}} \boldsymbol{M} \varphi_i\right)} \ddot{u}_g, \tag{3.11.10}$$

$$\text{i.e.} \quad \ddot{q}_i + 2\omega_i \xi_i \dot{q}_i + \omega_i^2 q_i = -P_i \ddot{u}_g$$

where

$$P_i = \frac{\varphi_i^{\mathrm{T}} \boldsymbol{M}}{\left(\varphi_i^{T} \boldsymbol{M} \varphi_i\right)} \tag{3.11.11}$$

This equation is similar to Eq. 3.7.1 for a damped free vibration of a SDOF system. Its solution can therefore be written as

$$q_i(t) = -\frac{P_i}{\omega_{id}} \int_0^t \ddot{u}_g(\tau)\, e^{-\xi\omega_i(t-\tau)} sin\ \omega_{id}(t-\tau)\, d\tau \quad i = 1 \text{ to } N \tag{3.11.12}$$

This is the response of the $N$ masses of the MDOF system vibrating in mode $i$ which can be represented as $\varphi_i q_i$. The total response of the system will be

$$u_i = \sum_{i=1}^{N} \varphi_i q_i \tag{3.11.13}$$

$\boldsymbol{M}_i$, $\boldsymbol{C}_i$ and $\boldsymbol{K}_i$ are termed as generalised mass, generalised damping and generalised stiffness, respectively.

## 3.7 Torsional Vibrations

Torsion is produced when the centre of mass and centre of rigidity do not coincide as is often the case. Analytical studies suggest that torsional effects are significant when the magnitude of torsion is large or when uncoupled lateral translational and torsional natural frequencies are close. Such coupling may cause large transverse displacements of structural supporting members.

### *3.7.1 Equations of Motion for an Undamped System*

Consider a rigid rectangular slab of uniformly distributed mass $m$ of a single-storey structure. Its centroid ($O$) undergoes displacements (Fig. 3.9) $u_x, u_y$ and $u_\theta$ relative to the ground along the $x$- and $y$-axes and about the vertical $z$-axis, respectively, in response to earthquake excitations $\ddot{u}_{gx}, \ddot{u}_{gy}$ *and* $\ddot{u}_{g\theta}$. As a result, the centroid shifts to location $O_1$. The centre of rigidity (shear centre) $S$ is located at radial distance $r$ and orthogonal distances $e_x$ and $e_y$ from $O$. It will also experience translations $u_x, u_y$ to reach location $S_1$.

Due to rotation $u_\theta$ the shear centre will experience an additional displacement $r.u_\theta$ which has components $u_\theta.r \sin\theta = e_y u_\theta$ and $u_\theta.r \cos\theta = e_x u_\theta$ along the $x$- and $y$-axes, respectively, to reach location $S_2$ (Wakabayashi 1986). Taking support stiffness as $k_x$ and $k_y$ along the two orthogonal axes, the resisting forces at the shear centre will be (Fig. 3.9 Det A)

$$F_x = k_x \left(u_x - e_y u_\theta\right) \text{ and } F_y = k_y \left(u_y + e_x u_\theta\right)$$

Their moments about the vertical axis through the centroid will be $-F_x e_y$ and $F_y e_x$. Taking torsional stiffness as $k_\theta$, the resistance to mass rotation will be $k_\theta u_\theta$.

Inertia forces are related to accelerations through the mass matrix, whereas the resisting forces and displacements are related through the stiffness matrix. Taking the mass moment of inertia about the centroidal axis as $m_\theta$, the equations of motion in directions $x$, $y$ and $\theta$ can be written in matrix form as

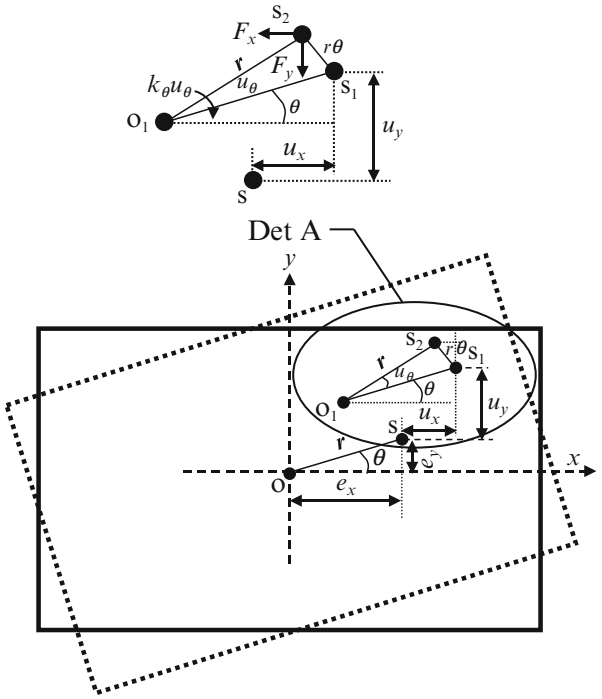


**Fig. 3.9** Torsional motion

$$\begin{pmatrix} m & 0 & 0 \\ 0 & m & 0 \\ 0 & 0 & m_\theta \end{pmatrix} \begin{Bmatrix} \ddot{u}_x \\ \ddot{u}_y \\ \ddot{u}_\theta \end{Bmatrix} + \begin{pmatrix} k_x & 0 & -k_x e_y \\ 0 & k_y & k_y e_x \\ -k_x e_y & k_y e_x & k_x e_y^2 + k_y e_x^2 + k_\theta \end{pmatrix} \begin{Bmatrix} u_x \\ u_y \\ u_\theta \end{Bmatrix} = -\begin{Bmatrix} m\ddot{u}_{gx} \\ m\ddot{u}_{gy} \\ m_\theta \ddot{u}_{g\theta} \end{Bmatrix} \tag{3.12.1}$$

These three equations are coupled through the stiffness matrix. By taking its solution in the form $u_x = \overline{u}_x e^{i\omega t}, u_y = \overline{u}_y e^{i\omega t}$ and $u_\theta = \overline{u}_\theta e^{i\omega t}$ and substituting in the above equations, the three frequencies and mode shapes can be obtained.

Consider a simpler case of having to determine the three frequencies of free vibrations with the shear centre being on the $x$-axis, i.e. $e_y = 0$, which leads to

$$\begin{pmatrix} m & 0 & 0 \\ 0 & m & 0 \\ 0 & 0 & m_\theta \end{pmatrix} \begin{Bmatrix} \ddot{u}_x \\ \ddot{u}_y \\ \ddot{u}_\theta \end{Bmatrix} + \begin{pmatrix} k_x & 0 & 0 \\ 0 & k_y & k_y e_x \\ 0 & k_y e_x & k_y e_x^2 + k_\theta \end{pmatrix} \begin{Bmatrix} u_x \\ u_y \\ u_\theta \end{Bmatrix} = \begin{Bmatrix} 0 \\ 0 \\ 0 \end{Bmatrix} \tag{3.12.2}$$

Clearly the equation for lateral displacement along the $x$-axis is uncoupled leading to two separate sets of equations

$$m\ddot{u}_x + k_x u_x = 0 \tag{3.12.3}$$

and

$$\begin{pmatrix} m & 0 \\ 0 & m_\theta \end{pmatrix} \begin{Bmatrix} \ddot{u}_y \\ \ddot{u}_\theta \end{Bmatrix} + \begin{pmatrix} k_y & k_y e_x \\ k_y e_x & k_y e_x^2 + k_\theta \end{pmatrix} \begin{Bmatrix} u_y \\ u_\theta \end{Bmatrix} = \begin{Bmatrix} 0 \\ 0 \end{Bmatrix} \tag{3.12.4}$$

These two coupled equations can be written as

$$m\ddot{u}_y + k_y u_y + k_y e_x u_\theta = 0 \tag{3.12.5}$$

and

$$m_\theta \ddot{u}_\theta + k_y u_y e_x + \left(k_y e_x^2 + k_\theta\right) u_\theta = 0 \tag{3.12.6}$$

$$\text{Introducing} \quad u_y = \bar{u}_y \mathrm{e}^{i\omega t};\ u_\theta = \bar{u}_\theta \mathrm{e}^{i\omega t}, \tag{3.12.7}$$

Eq. 3.12.5 can be written as

$$-\omega^2 m\bar{u}_y + k_y \bar{u}_y + k_y e_x \bar{u}_\theta = 0 \tag{3.12.8}$$

from which

$$\bar{u}_y = \left\{ \frac{k_y e_x}{m\omega^2 - k_y} \right\} \bar{u}_\theta \tag{3.12.9}$$

Utilising the value of $\bar{u}_y$ from Eq. 3.12.9 and substituting for $u_y$ and $u_\theta$ in Eq. 3.12.6,

$$m.m_\theta \omega^4 - \omega^2 \left[m_\theta k_y + m k_y e_x^2 + m k_\theta\right] + k_y.k_\theta = 0 \tag{3.12.10}$$

from which the two frequencies can be obtained. The procedure is explained with the help of *Ex*.3.9.4.

## 3.8 Rocking Motion

Consider a multistoreyed shear building with rigid floors supporting lumped masses subjected to lateral seismic ground acceleration $\ddot{u}_g$ (Fig. 3.10). The structure is assumed to be supported on two springs located at a distance $b$ on either side

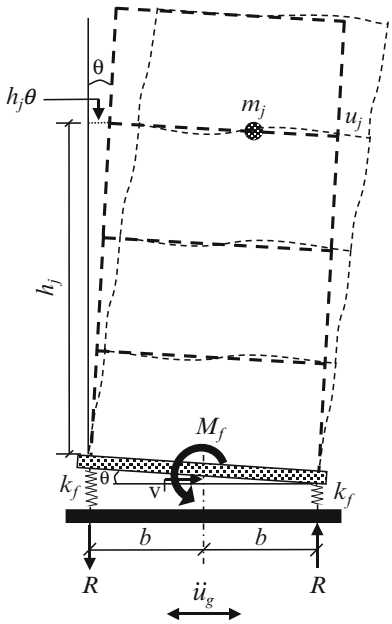


**Fig. 3.10** MDOF system on springs

of the centre line of a rectangular footing in the form of a massless plate of negligible thickness. Under the ground motion defined by acceleration $\ddot{u}_g$ the displaced configuration of the system at any time instant can be defined by lateral floor displacement $u_j$ of the mass at floor $j$ and rotation as well as vertical movement of the foundation mat by $\theta$ and $v$, respectively, at the foundation centre of gravity.

Considering viscous damping, the equations for lateral, rocking and vertical motions will be given by the following three equations, respectively: (Solomon et al. 1985)

$$\boldsymbol{M}\ddot{\boldsymbol{U}} + \boldsymbol{M}\boldsymbol{h}\ddot{\theta} + \boldsymbol{C}\dot{\boldsymbol{U}} + \boldsymbol{K}\boldsymbol{U} = -\boldsymbol{M}\ddot{\boldsymbol{U}}_{\boldsymbol{g}} \tag{3.13.1}$$

$$\boldsymbol{h}^{\mathrm{T}}\boldsymbol{M}\ddot{\boldsymbol{U}} + I_b\ddot{\theta} + M_f = -\boldsymbol{h}^{\mathrm{T}}\boldsymbol{M}\ddot{\boldsymbol{U}}_g \text{ and} \tag{3.13.2}$$

$$m_t\ddot{v} + R = -m_t g \tag{3.13.3}$$

where

$\boldsymbol{M}$ : diagonal matrix of the lumped masses
$\boldsymbol{K}$ : stiffness matrix of the building resting on a rigid foundation
$\boldsymbol{C}$ : viscous damping matrix on rigid foundation
$\boldsymbol{U}$ : floor displacement matrix
$h$ : floor height vector

$m_t$ : total mass $= \sum_{j=1}^{N} m_j$ where $m_j$ is the mass at storey $j$
$I_b$ : moment of inertia of all masses together, about the base, neglecting their inertias about their respective centroidal axes $= \sum_{j=1}^{N} m_j h_j^2$
$M_f$ : resistive moment provided by the springs against overturning
$R$ : resistive elastic force of each spring
$v$ : vertical displacement at centre of footing

Under seismic excitation, a tall building could rock on its foundation and may intermittently uplift over one portion of the footing or the other. If the structure uplifts from its support, it can have a significant effect on its response during an earthquake. In this case, various support conditions need to be considered for the system, viz.

- It stays in contact with the supports.
- It lifts off one of the supports and loses contact with it.
- It tries to lift off from one of the supports but is prevented by the support providing tensile restrain.
- Its foundation may slide.

Clearly, the overall motion would be nonlinear and needs to be studied as a three-dimensional structure. The response of such a system can be obtained by numerical methods, but such a rigorous analysis is highly complex and the reader should refer to specialist literature and take competent advice. Here, for demonstration purposes, a simple case is considered where it is assumed that throughout its rocking, the motion is linear and the base does not lift off the springs. It is also assumed that the base is not bonded to the springs which will preclude any downward pull on the undamped structure. It is also assumed that there is no horizontal slip between the base of the structure and the springs.

As shown in Sect. 4.6.2, a MDOF system can be replaced, in each mode $i$ with an equivalent SDOF oscillator of effective mass $M_i$ supported with a massless rod of effective height $h_i$ (Fig. 3.11). Values of $M_i$ and $h_i$ from Eqs. 4.15.6 and 4.16.1 are given by

$$M_i = \frac{\left[\sum_{j=1}^{N} m_j \varphi_{ji}\right]^2}{\sum_{j=1}^{N} m_j \left(\varphi_{ji}\right)^2} \quad \text{and} \quad h_i = \frac{\sum_{j=1}^{N} m_{ji} \varphi_{ji} h_j}{\sum_{j=1}^{N} m_{ji} \varphi_{ji}} \tag{3.13.4}$$

Since normally the response of the first mode is predominant, only this mode of vibration is considered hereafter. It is further assumed that the vertical displacement $v$ is negligible and damping is neglected. In the first mode, the modal mass will be $M_1$, and its lateral displacement due to inertia forces is taken as $u_1$ (Fig. 3.11). The suffix '1' denotes values of the parameters in the first mode. Substituting in

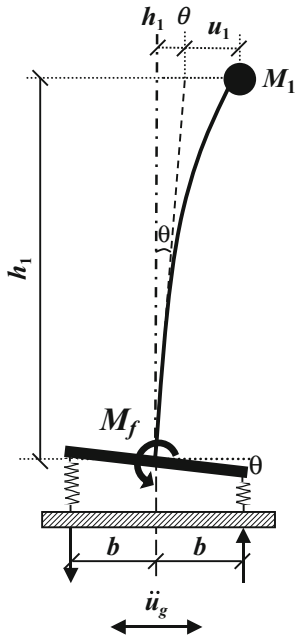


**Fig. 3.11** Rocking SDOF system

Eqs. 3.13.1 and 3.13.2,

$$M_1\ddot{u}_1 + M_1h_1\ddot{\theta} + k_1u_1 = -M_1\ddot{u}_g \tag{3.13.5}$$

and

$$M_1h_1\ddot{u}_1 + I_{b1}\ddot{\theta} + M_{f1} = -M_1h_1\ddot{u}_g \tag{3.13.6}$$

Taking $k_f$ as the stiffness of each elastic spring, the resistive force on each spring will be $k_f.b\theta$ and its couple about the centre of base mat $M_{f1} = 2k_f.b^2\theta$. The rotational stiffness can be taken as $k_\theta = 2k_f.b^2$.

The total lateral displacement of mass $M_1$ will be $(u_1 + h_1\theta)$ which, for small values of angle $\theta$, can be approximated as a total horizontal movement of $(u_1 + x_1)$ where $x_1 = h_1\theta$. Taking the moment of inertia of mass $M_1$ as $I_{b1} \approx M_1h_1^2$ and noting that $k_1 = M_1\omega_1^2$, the above equations reduce to

$$(\ddot{u}_1 + \ddot{x}_1) + \omega_1^2u_1 = -\ddot{u}_g \tag{3.13.7}$$

and

$$(\ddot{u}_1 + \ddot{x}_1) + \frac{k_\theta\theta}{M_1h_1} = -\ddot{u}_g \tag{3.13.8}$$

Subtracting Eq. 3.13.8 from Eq. 3.13.7 gives

$$u_1 = \frac{k_\theta x_1}{k_1 h_1^2} \quad \text{i.e.} \quad x_1 = \frac{k_1 h_1^2}{k_\theta}.u_1 \tag{3.13.9}$$

Introducing the total lateral displacement $s = (u_1 + x_1)$, (Psycharis 1982) the equation of motion can be written as

$$\ddot{s} + \left\{ \frac{{\omega_1}^2 k_\theta}{k_\theta + k_1 h_1^2} \right\} s = -\ddot{u}_g \tag{3.13.10}$$

Thus, the combined natural frequency of the structure in the first mode will be

$$\omega_s^2 = \left\{ \frac{{\omega_1}^2 k_\theta}{k_\theta + k_1 h_1^2} \right\}, \quad \text{i.e.} \quad \frac{\omega_s^2}{{\omega_1}^2} = \left\{ \frac{k_\theta}{k_\theta + k_1 h_1^2} \right\} \tag{3.13.11}$$

which leads to (Solomon et al. 1985)

$$T_s = T_1 \sqrt{1 + \frac{k_1 h_1^2}{k_\theta}} \tag{3.13.12}$$

It can also be said that the approximate rocking frequency is given by

$$\omega_\theta = \sqrt{\frac{k_\theta}{M_1 h_1^2}} = \sqrt{\frac{2k_f b^2}{M_1 h_1^2}} \tag{3.13.13}$$

Computation of rocking frequency is illustrated in *Ex* 3.9.5.

## 3.9 Illustrative Examples

***Ex 3.9.1*** A SDOF portal frame fixed at its base has a mass of 1,200 kg at roof level. Lateral stiffness of frame columns together is 27,000 N/m and viscous damping coefficient is 550 N s/m. Under free vibrations, find the natural period of oscillations and cyclic as well as circular natural frequencies for both damped and undamped conditions. For the damped condition, if the initial displacement and velocity are 15 mm and 17 mm/s, respectively, compute frame side sway after 1.1 s.

**Solution**

(a) *Undamped condition*
From Eq. 3.4.4

1. Circular natural frequency $\omega = \sqrt{\frac{k}{m}} = \sqrt{\frac{27,000}{1,200}} = 4.743$ rad/ s

2. Natural period $T = 2\pi/\omega = 1.325$ s
3. Cyclic natural frequency $f = 1/T = 0.755$ Hz (cycles/s)

(b) *Damped condition*

From Sect. 3.4.3,

$$\text{Damping factor } \xi = \frac{c}{2\sqrt{km}} = \frac{550}{2\sqrt{27,000 \times 1,200}} = 0.0483 = 4.83\ \%$$

1. Circular damped natural frequency

$$\omega_d = \omega\sqrt{1-\xi^2} = 4.743\ \sqrt{1-0.0483^2} = 4.737 \text{ rad/ s}$$

2. Natural damped period $T_d = \dfrac{2\pi}{\omega_d} = 1.326$ s
3. Cyclic natural damped frequency $f_d = 1/T_d = 0.754$ Hz.
4. Displacement (side sway) will be given by Eq. 3.5.8, viz.

$$u(t) = \mathrm{e}^{-\xi\omega t}\left\{u_0 cos\ \omega_d t + \frac{\dot{u}_0 + u_0\xi\omega}{\omega_d} sin\ \omega_d t\right\}$$

Substituting values, $u_0 = 15$ mm, $\dot{u}_0 = 17$ mm/s, $\xi = 0.0483$, $\omega = 4.743$ rad/ s

$$\text{and } \omega_d = 4.737 \text{rad/ s}, \quad t = 1.1 \text{ s}$$

$$\text{The side sway} = u_{1.1} = \mathrm{e}^{(-0.0483\times4.743\times1.1)} \times \left\{15\ \cos(4.737 \times 1.1) + \frac{17 + (15 \times 0.0483 \times 4.743)}{4.737} \sin(4.737 \times 1.1)\right\}$$

$$= 2.63 \text{ mm}$$

***Ex 3.9.2*** A SDOF system with 5% damping is as shown in Fig. 3.12a. Mass at roof level is $15 \times 10^5$ kg and the system is supported on two columns each with a

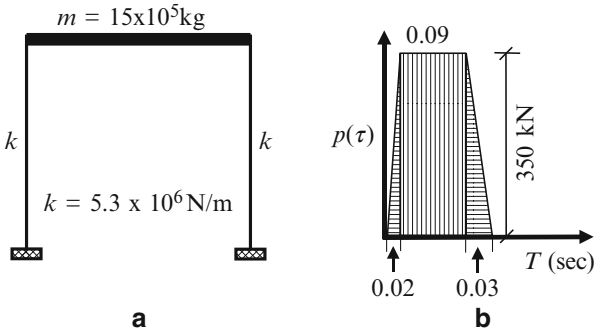


**Fig. 3.12** Impulse loading. (**a**) Structure. (**b**) Impulse

stiffness of $5.3 \times 10^6$ N/m. The nature and magnitude of an impulse experienced by the structure at base level is as shown in Fig. 3.12b. Determine the displacement after 2.5 s.

**Solution** Total lateral stiffness of two columns would be $10.6 \times 10^6$ N/m

From Eq. 3.4.4, $\omega = \sqrt{\dfrac{k}{m}} = \sqrt{\dfrac{10.6 \times 10^6}{15 \times 10^5}} = 2.658$ rad/ s

From Eq. 3.5.3, $\omega_d = \omega\sqrt{1-\xi^2} = 2.658\sqrt{1-(0.05)^2} = 2.655$ rad/s

The displacement will be obtained from Eq. 3.6.3, viz.

$$u(t) = \mathrm{e}^{-\xi\omega(t-\tau)} \left\{ \frac{p\,(\tau)}{m\omega_d} \right\} \sin\ \omega_d\,(t-\tau)\,d\tau$$

Total impulse value is

$$p\,(\tau)\,d\tau = \left[ \left\{ \frac{1}{2}(0.02) \times 350 \right\} + \left\{ \frac{1}{2}(0.03) \times 350 \right\} + (350 \times 0.09) \right] = 40.25 \text{ kN}$$

Substituting values in Eq. 3.6.3,

$$u(2.5) = \mathrm{e}^{-(0.05 \times 2.658 \times 2.5)} \left[ \frac{40.25 \times 10^3}{15 \times 10^5 \times 2.655} \right] \sin\,(2.655 \times 2.5) \times 10^3 = 2.515 \text{ mm}$$

***Ex 3.9.3*** A single-bay two-storey framed structure with 5 % damping and storey heights of 3.2 m, as shown in Fig. 3.13, is located in seismic zone IV as per IS 1893. Mass $m_1 = 21{,}000$ kg, and $m_2 = m_1/\beta$. The stiffness of the upper storey $k_2 = 4.43 \times 10^6$ N/m and that of the lower storey $k_1 = \alpha\, k_2$. Consider an importance factor of 1.0 and response reduction factor of 5.0. For the condition $\alpha = \beta = 1$, determine for the first mode: vibration period, lateral storey inertia forces, base shear, storey drifts and roof displacement.

**Solution** This is a two degree-of-freedom system where equations developed in Sect. 3.5.1 apply. Substituting $m_1 = \beta m_2$ and $k_1 = \alpha k_2$ in Eq. 3.8.10,

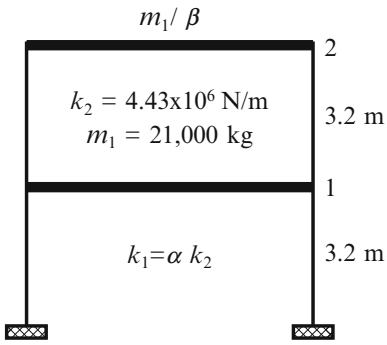


**Fig. 3.13** Two-storey frame

$$\omega^2{}_{2,1} = \frac{k_2}{2\beta.m_2}\left\{(1+\alpha+\beta) \pm \sqrt{(1+\alpha+\beta)^2 - 4\alpha\beta}\right\} \tag{3.14.1}$$

For the condition that $\alpha = \beta = 1.0$,

$$\omega_{2,1}^2 = \frac{4.43 \times 10^6}{42,000}[3 \pm 2.236] \quad \text{which gives} \tag{3.14.2}$$

$\omega_1 = 8.98$ rad/s, $\omega_2 = 23.5$ rad/s. $T_1 = 0.70$ s, $T_2 = 0.27$ s.

Mass and stiffness matrices, respectively, are

$$[\boldsymbol{M}] = 10^3 \begin{pmatrix} 21 & 0 \\ 0 & 21 \end{pmatrix} \quad \text{and} \quad [\boldsymbol{K}] = 10^4 \begin{pmatrix} 886 & -443 \\ -443 & 443 \end{pmatrix}$$

from which the first mode shape is $\varphi_1 = \begin{Bmatrix} 0.618 \\ 1.000 \end{Bmatrix}$

Substituting values in Eq. 4.6.1, the design horizontal seismic coefficient is

$$A_h = \frac{Z}{2} \cdot \frac{I}{R} \cdot \frac{S_a}{g} = \frac{0.24}{2} \cdot \frac{1}{5} \cdot \frac{S_a}{g} = 0.024\frac{S_a}{g} \tag{3.14.3}$$

Based on period of vibration for first mode evaluated above, the seismic acceleration coefficient (from response spectrum profile in IS1893) $S_a/g = 1.429$. From Eq. 3.14.3 $A_{h1} = 0.0343$.

As per codal stipulation, the peak inertia force at floor $i$ for the first mode will be

$$Q_{i\,1} = A_{h1} \cdot \varphi_{i1} \cdot P_1 \cdot W_1 \tag{3.14.4}$$

Substituting values in Eq. 4.14.1, the participation factor for the first mode is

$$P_1 = \frac{21\,(1.0 + 0.618)}{21\left(1^2 + 0.618^2\right)} = 1.1708$$

Substituting values in Eq. 3.14.4, for mode 1,

(a) *Inertia forces:*

At slab level 2, $Q_2$=0.0343 × 1.0 × 1.1708 × 21,000 × 9.81 × $10^{-3}$=8.273 kN.
Similarly at slab level 1, $Q_1 = 5.113$ kN.

(b) *Storey shears:*

At storey 2, $V_2 = Q_2 = 8.273$ kN.
At storey 1, $V_1 = Q_1 + Q_2 = 13.386$ kN.
Base shear = $V_1 = 13.386$ kN.

(c) *Storey displacements:*

Storey displacements $\Delta$ are given by

$$\{\boldsymbol{F}\} = \boldsymbol{K}.\,\boldsymbol{\Delta},$$

$$\text{i.e.} \quad \begin{Bmatrix} 5.113 \\ 8.273 \end{Bmatrix} 10^3 = \begin{pmatrix} 886 & -443 \\ -443 & 443 \end{pmatrix} 10^4 \times \begin{Bmatrix} \Delta_1 \\ \Delta_2 \end{Bmatrix}$$

which gives $\Delta_1 = 3.022$ mm and $\Delta_2 = 4.889$ mm.

(d) *Drifts:*

From displacement values, the drifts can be obtained as
At slab level 1, $\delta_1 = 3.022$ mm
At slab level 2, $\delta_2 = 1.867$ mm

***Ex 3.9.4*** Consider a 6m × 4m × 0.12 m thick rigid roof slab of a single-storey structure with support stiffness being $k_x = 400$ kN/m, $k_y = 600$ kN/m, $k_\theta = 2{,}000$ kN m along the *x, y* and $\theta$ vectors, respectively. The distances of the shear centre from the centroidal axis are $e_y = 0$ and $e_x = 1.0$ m. Determine the three natural frequencies and the two mode shapes.

**Solution** Mass of slab $m = 25{,}000\,(6.0 \times 4.0 \times 0.12)/9.81 = 7{,}340$ kg
Mass moment of inertia (Eq. 2.11.1)

$$m_\theta = \frac{m\left(a^2 + b^2\right)}{12} = \frac{7,340\,(36 + 16)}{12} = 31,807 \text{ kg m}^2 \tag{3.15.1}$$

For the *x* direction $m\ddot{u}_x + k_x u_x = 0$ and from Eq. 3.4.4,

$$\omega_x = \sqrt{\frac{k_x}{m}} = \sqrt{\frac{400,000}{7,340}} = 7.38 \text{ rad/ s} \tag{3.15.2}$$

For the other two frequencies,

$m.m_\theta = 7{,}340 \times 31{,}807 = 233.46 \times 10^6$ N$^2$s$^4$
$m_\theta\, k_y = 31{,}807 \times 600 \times 10^3 = 190.84 \times 10^8$ N$^2$s$^2$
$mk_y e_x{}^2 = 7{,}340 \times 600 \times 1^2 \times 10^3 = 440.40 \times 10^7$ N$^2$s$^2$
$mk_\theta = 7{,}340 \times 2 \times 10^6 = 146.80 \times 10^8$ N$^2$s$^2$
$k_y\, k_\theta = 600 \times 2 \times 10^9 = 120.00 \times 10^{10}$ N$^2$

Substituting values in Eq. 3.12.10,
$233.46\,\omega^4 - (19{,}084 + 4{,}404 + 14{,}680)\,\omega^2 + 120 \times 10^4 = 0$
from which

$$\omega_1 = 6.517 \text{ rad/s} \text{ and } \omega_2 = 11.0 \text{ rad/s} \tag{3.15.3}$$

Replacing $m\ddot{u}$ by $-m\omega^2 u$ in Eq. 3.12.4, for the first mode

$$\begin{pmatrix} -m\omega_1^2 + k_y & k_y e_x \\ k_y e_x & -m_\theta \omega_1^2 + k_y e_x^2 + k_\theta \end{pmatrix} \begin{Bmatrix} \varphi_{y1} \\ \varphi_{\theta 1} \end{Bmatrix} = \begin{Bmatrix} 0 \\ 0 \end{Bmatrix} \tag{3.15.4}$$

Substituting values in Eq. 3.15.4,

$$\begin{pmatrix} -\left(7.340 \times 6.517^2\right) + 600 & 600 \\ 600 & -\left(31.807 \times 6.517^2\right) + 600 + 2000 \end{pmatrix} \begin{Bmatrix} \varphi_{y1} \\ \varphi_{\theta 1} \end{Bmatrix} = \begin{Bmatrix} 0 \\ 0 \end{Bmatrix}$$

which yields $\varphi_{\theta\,1} = 1$, $\varphi_{y1} = -\,2.081$. Similarly proceeding for the second mode, $\varphi_{\,\theta 2} = 1$, $\varphi_{\,y2} = 2.081$ and the mode shapes are

$$\begin{Bmatrix} \varphi_{y1} \\ \varphi_{\theta 1} \end{Bmatrix} = \begin{Bmatrix} -2.081 \\ 1.000 \end{Bmatrix} \quad \text{and} \quad \begin{Bmatrix} \varphi_{y2} \\ \varphi_{\theta 2} \end{Bmatrix} = \begin{Bmatrix} 2.081 \\ 1.000 \end{Bmatrix}$$

***Ex 3.9.5*** For the structure and loading details as in *Ex* 4.9.3, determine the approximate rocking frequency for the fundamental mode if base dimension is 15 m and the spring resistance $k_f = 300$ kN/m.

**Solution** Modal mass for the first mode ($M_1$) is worked out in *Ex* 4.9.7 and its value is 3.1236 m.

The value of m in *Ex* 4.9.3 is $1.62 \times 10^5$ kg.
Hence, modal mass in the first mode will be
$= 3.1236 \times 1.62 \times 10^5 = 5.06 \times 10^5$ kg.
Modal height $h_1 = 6.593$ m from *Ex* 4.9.7.
Substituting values in Eq. 3.13.13,

$$\omega_\theta = \sqrt{\frac{2 \times 300 \times 10^3 \times 7.5^2}{5.06 \times 10^5 \times 6.593^2}} = 1.239 \text{ rad/ s}$$

# Chapter 4
# Response Evaluation

**Abstract** The purpose of this chapter is to explain the basic concepts underlying various response evaluation techniques and to demonstrate their use, with the help of illustrative examples, for analysing building structures subjected to seismic ground motion. It is shown how relationships between spectral quantities are derived and the utility of this relationship in plotting a tripartite chart. The design acceleration spectrum is described including its merits and limitations. It is shown how an inelastic acceleration spectrum can be derived from an elastic spectrum for a SDOF system. Modal analysis is covered in all its facets including derivation of mode shapes, modal frequencies, participation factor, modal mass and modal height. The importance of orthogonality of modes and how to combine modal responses is demonstrated. A large number of illustrative examples show how to evaluate various modal quantities and how to conduct a time history analysis both for a SDOF system and MDOF system in both the linear and nonlinear domains. The missing mass method of analysis is also included.

**Keywords** Elastic response spectrum • Tripartite plot • Inelastic response spectrum • Linear static procedure • Modal analysis • Time history analysis

## 4.1 Introduction

The preferred methods to evaluate structural response of a building subjected to dynamic base excitation can be grouped as:

(a) *Linear methods*

- Linear static procedure (LSP) – also known as seismic coefficient method
- Linear dynamic procedure (LDP) – usually modal analysis
- Time history analysis

(b) *Nonlinear methods*

- Inelastic time history analysis.
- Static pushover analysis – this method is explained in Sect. 11.3 of Chap. 11.



S. Manohar, S. Madhekar, *Seismic Design of RC Buildings*, Springer Transactions in Civil and Environmental Engineering, DOI 10.1007/978-81-322-2319-1_4

The method of analysis to adopt is decided on a case-to-case basis. For regular medium-rise buildings, the LSP is normally adopted. For irregular buildings and for tall buildings or where the response from higher modes becomes important, modal analysis procedure is preferred. Generally, only in very special cases, dictated by complexity or importance of the structure, a time history analysis is resorted to. The purpose of this chapter is (1) to explain the basic concepts underlying various response evaluation techniques and (2) to demonstrate the use of such techniques, with the help of illustrative examples, for analysing building structures subjected to seismic ground motion.

## 4.2 Elastic Response Spectrum

Response spectrum is a graphical representation of maximum response values such as acceleration, velocity or displacement of a SDOF system for a range (i.e. spectrum) of natural vibration periods for specific damping. By the 1960s, this technique had gained acceptance as a design tool and today, acceleration design response spectrum is in common use for analysis of linear systems under seismic excitation. Its popularity stems from the fact that it is simple to use and at the same time it is a relatively accurate static method of analysis. By using response spectrum an engineer is in effect designing for a range of earthquake ground motions and hence it is cost effective.

### *4.2.1 Concept*

Earthquake excitation being dynamic, the forces and displacements induced by it in a structure are naturally a function of time. One method to arrive at these values is by direct integration of the differential equations of motion to yield time-varying responses for a given seismic accelerogram. Such analysis has to be conducted for a range of earthquake signatures since one particular earthquake cannot represent the overall seismicity at a given location. While such computations are now possible with present-day fast computing power which can provide answers of considerable accuracy, the time required for analysis would be enormous and resulting data too voluminous to scrutinise.

During design, several responses of a structure have to be evaluated, viz. displacements, base shears, overturning moments, inter-storey drifts and others. It is difficult to accomplish this in a reasonable time frame because of the acute randomness of ground excitation which inhibits a closed-form solution of the equations of motion. To overcome these difficulties, the response spectrum method was proposed. M. A. Biot is generally credited (Trifunac 2006) for conceiving it in the early 1930s and G. W. Housner was instrumental in its wider recognition. However, its general acceptance and use by professionals had to wait for almost

three decades until fast digital computing capability and acceptable quality of strong motion earthquake records became available.

There is a unique response spectrum for a given time history but the reverse is not true. Also, it has not been possible to establish a globally acceptable correlation between the profile of an earthquake's time history and the extent of structural damage it can cause. Thus, it is apparent that for design purposes we need to include a range of estimated ground motion signatures in the response evaluation process in order to cover most of the likely peaks of ground motion for a given site. This is achieved through a response spectrum.

### *4.2.2 Relationship Between Spectral Quantities*

As mentioned earlier, the response spectrum could be in terms of either displacement or velocity or acceleration. Initially, the response displacements $u(t)$ are obtained for a range of seismic excitations of SDOF systems, with different vibration periods, by solving the Duhamel's integral for a damped SDOF system (Eq. 3.7.3) which is given by

$$u(t) = -\frac{1}{\omega_d}\int_0^t \ddot{u}_g(\tau)\, e^{-\xi\omega(t-\tau)} \sin\ \omega_d\,(t-\tau)\, d\tau \tag{4.1.1}$$

Differentiating Eq. 4.1.1,

$$\dot{u}(t) = -\xi\omega.\, u(t) - \int_0^t \ddot{u}_g(\tau)\, e^{-\xi\omega(t-\tau)} \cos\ \omega_d\,(t-\tau)\, d\tau \tag{4.1.2}$$

For building structures, the damping is low ($<<1$), and hence dropping the term in $\xi$, the maximum displacement of such a SDOF system subjected to an earthquake motion $\ddot{u}_g$ can be expressed as

$$|u|_{\max} = \left|\frac{1}{\omega}\int_0^t \ddot{u}_g(\tau) \sin\ \omega\,(t-\tau)\, d\tau\right|_{\max} \tag{4.1.3}$$

Ordinates of horizontal displacements $u$ so obtained are scanned and their normalised peak values form the displacement response spectrum denoted as $S_d = |u|_{\max}$.

Similarly,

$$S_v = |\dot{u}|_{\max} = \left|\int_0^t \ddot{u}_g(\tau) \cos\ \omega\,(t-\tau)\, d\tau\right|_{\max} \tag{4.1.4}$$

Considering maximum values, it follows that the velocity spectrum is given by

$$S_v = \omega S_d \tag{4.1.5}$$

For a damped system under seismic excitation, from Eq. 3.7.1,

$$m\ddot{u} + c\dot{u} + ku = -m\ddot{u}_g$$

Substituting $k = m\omega^2$ and $c = 2\, m\omega_d \xi$ from Sect. 3.4.3,

$$\ddot{u} + 2\omega_d \xi \dot{u} + \omega^2 u = -\ddot{u}_g$$

Neglecting damping for reasons mentioned earlier,

$$\ddot{u} + \omega^2 u \simeq -\ddot{u}_g \quad \text{or} \quad \left(\ddot{u} + \ddot{u}_g\right) \simeq -\omega^2 u \tag{4.1.6}$$

A mass $m$ of a building structure experiences the absolute acceleration, i.e. the sum of ground acceleration $\ddot{u}_g$ and that due to its displacement relative to the ground $\ddot{u}$.

Thus, the acceleration spectrum will be

$$S_a = \left|\ddot{u} + \ddot{u}_g\right|_{\max} \tag{4.1.7}$$

Introducing Eq. 4.1.6 into Eq. 4.1.7,

$$S_a = -\omega^2 |u|_{\max} = -\omega^2 S_d \tag{4.1.8}$$

Since these are maximum values, they are treated as positive although they may be algebraically positive or negative. Thus,

$$|\omega S_d| \simeq |S_v| \simeq \left|\frac{1}{\omega} S_a\right| \tag{4.1.9}$$

Because of the approximation ($\xi = 0$) involved in arriving at $S_a$, it is termed as a pseudo-acceleration which will equal the true acceleration if damping is zero. Since damping is low for buildings, it is commonly assumed that $S_a$ represents the maximum acceleration. In the case of displacement, since rigid body displacement of a building does not generate any inertia forces, the displacement spectrum represents true relative displacement of the mass with respect to the ground. The pseudovelocity spectrum values are relative to the base.

A response spectrum is a jagged plot with a sawtooth appearance having drastic variations in amplitude even for a small change in period. This is not suitable for design purposes because, for a particular vibration period, the ordinate may fall in a valley and with a slightly different period it may be at a crest of the response profile.

Since the time period of a vibrating body cannot be accurately estimated, it is clear that a jagged plot is unsuitable. This led to the creation of a design acceleration spectrum described below.

### 4.2.3 Linear Design Acceleration Spectrum

To overcome the above drawbacks, researchers came up with a design response spectrum. There is a clear distinction between a response spectrum and a design spectrum. The former represents the response of a SDOF system to a specific ground motion against a range of frequencies and damping ratios of the system. On the other hand, the latter represents the normalised response of a SDOF system to an ensemble of ground motions.

A design acceleration spectrum is a graphical representation of a smooth average envelope of peak accelerations of SDOF systems. It is presented as a function of the system's time period of vibration, for a specified damping ratio, for an ensemble of earthquake ground motion signatures (BIS 2002a). This is achieved through a process of statistical analysis and normalising and scaling to a chosen peak acceleration. With the aid of such a spectrum, the engineer would be designing for a likely maximum response for a range of earthquake ground motions.

Engineers are essentially interested in maximum response values (stresses, deflections, bending moments, shear forces and others) for which an envelope of inertial accelerations for different periods of a vibrating structure would be adequate. This information is available through a design acceleration response spectrum drawn against different damping values and types of founding soils. This technique can also be used for dynamic analysis of a MDOF system utilising the orthogonality property of modes, as explained in Sect. 4.6.5.

To estimate the likely maximum inertial acceleration that the mass of a structure will experience using a response spectrum, the only information required is the vibration time period of the building, the nature of founding soil and an estimate of damping in the system.

Thus, it forms a handy means to evaluate inertial forces for design of a structure. Therefore, a response spectrum is recognised as an ideal tool for evaluating the response of a linear system and forms the backbone for practical dynamic analysis.

### 4.2.4 Tripartite Plot

Consider a logarithmic plot of spectral velocity against the time period of vibration, i.e. log $S_v$ vs. *log* $T$, where, say $y = \log_{10} S_v$ and $x = \log_{10} T$.

From Eq. 4.1.9 $S_a = \omega S_v = \dfrac{2\pi}{T} S_v$

Taking logarithm of both sides and substituting for log $S_v$ and log $T$,

$$\log S_a = y + \log(2\pi) - x \tag{4.2.1}$$

For $S_a$ to be a constant (say log $S_a = a$ constant $C_1$), this equation reduces to

$$y = x + (C_1 - \log 2\pi)$$

This is an equation of a straight line with a slope $\frac{dy}{dx} = 1$. It implies that a constant $S_a$ line makes an angle of 45° with the $x$-axis. Its intercept on the $y$-axis depends on the value of $C_1$, i.e. that of $S_a$. Proceeding in a similar manner for displacement,

$$\log S_d = y - \log(2\pi) + x, \quad \text{i.e.} \quad y = -x + (C_2 + \log\ 2\pi) \tag{4.2.2}$$

where $C_2$ is a constant. It can be seen that for a constant value of spectral displacement, the equation is that of a straight line with a slope of (−1), i.e. the line subtends an angle of 135° with the abscissa.

As a result, all three spectral parameters $S_d$, $S_v$ and $S_a$, which are related through the circular frequency, can be plotted on a single quadric-logarithmic plot which is known as a tripartite plot (Betbeder-Matibet 2008). For a given period, the above three values can be determined from such a plot (Fig. 4.1). This is illustrated in *Ex* 4.9.1.

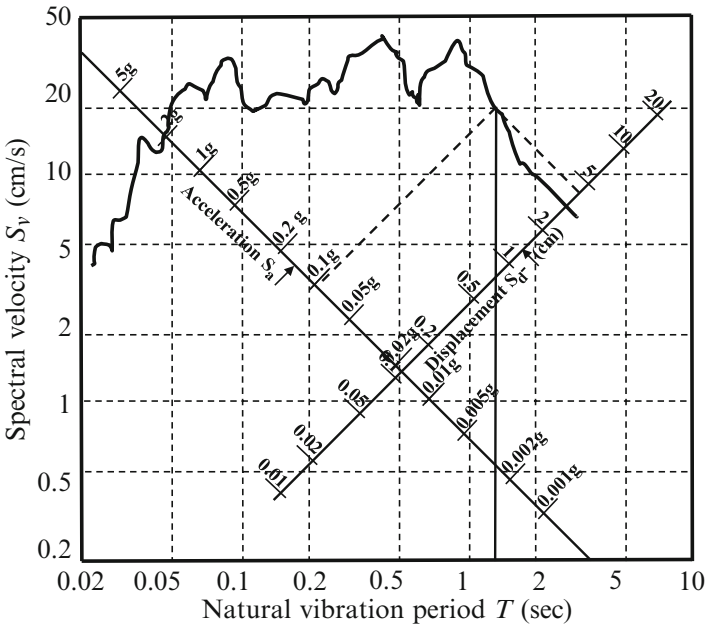


**Fig. 4.1** Tripartite (logarithmic) response spectra

Each of these quantities has a physical meaning. For instance, the deformation spectrum represents peak deformation values, the pseudovelocity spectrum gives a representation of peak strain energy stored in the system during a seismic event, and the pseudo-acceleration spectrum provides the peak base shear. Knowing the vibration period of the system, a designer can estimate all three parameters from a single tripartite plot.

### *4.2.5 Merits and Limitations of a Design Response Spectrum*

Engineers should be aware of the following principal merits and demerits of such a response spectrum:

1. *Merits*

- It is a user-friendly tool that enables a designer to arrive at the maximum acceleration response which forms the basis for determining the forces for which a structure needs to be designed.
- It provides appreciable computational benefits compared to other methods.
- It represents a graphic display of the relationship between expected response and vibration frequency. Thus, a designer has an indication of the resonant frequency range over which peak response may be expected.
- Its popularity stems from the fact that it provides a simple but relatively accurate static method of analysis to a problem which is basically a dynamic one.

2. *Limitations*

- It provides only maximum anticipated values of a particular response.
- An important constituent of the motion, viz. its duration is not reflected in a response spectrum. During a long-duration earthquake, structures could fail under low-cycle fatigue and saturated soils can liquefy.
- A major limitation is that it is applicable only to the design of linear systems.

### *4.2.6 Effect of Vertical Ground Motion*

It is commonly presumed that since a structure is designed to support vertical dead and live loads with a factor of safety, the additional vertical inertia forces are not likely to control structural design. However, care should be taken in designing structural members particularly vulnerable to damage by vertical acceleration – such as columns, cantilevers, prestressed concrete structures, transfer girders, long-span beams supporting substantial masses, members where stability is a design criterion and elements in which demand generated by dead and permanent live loads exceeds 80 % of the nominal capacity of the elements (FEMA 273 1997).

#### 4.2.6.1 Vertical Acceleration Spectrum

It is normally presumed, as an empirical approximation, that vertical acceleration is two-third the peak horizontal acceleration and that it has a similar spectral pattern (BIS 2002a). Secondly, as mentioned above, it is often assumed that since a structure is designed to support vertical dead and live loads with an abundant factor of safety, any additional vertical inertia forces will not control its structural design. In recent years more attention is being paid to vertical seismic effects as more data on near-field seismic records are becoming available.

For a near-field seismic event, there is increasing evidence (Collier and Elnashai 2001; Elnashai and Di Sarno 2008; Paulay and Priestley 1992) that the ratio of peak vertical to horizontal components of acceleration could be much more than the assumed value of two-third and in some instances may even exceed 1.0. In such an event, the vertical component of seismic acceleration could have a large destructive effect on structures. Secondly, the fundamental period of a tall building is usually larger than that of a medium-height building with the result that horizontal design acceleration is smaller for the former. However, vertical acceleration is not reduced. As a result the V/H acceleration ratio is larger for taller buildings (Aoyama 2001).

#### 4.2.6.2 Analysis for Vertical Response

A designer should be aware of the following issues (Collier and Elnashai 2001) resulting from likely high vertical acceleration in near-field earthquakes:

- In the vertical component, energy is likely to be concentrated in a narrow high-frequency band which can cause serious damage to buildings with vertical vibration periods within this band (Collier and Elnashai 2001).
- In lightly loaded columns and walls (e.g. those in higher storeys), the vertical stabilising load could be substantially reduced. This can be critical if stability is a consideration and it may result in net tension in vertical members. Such acceleration can alter the vertical forces in members which can reduce their shear capacity and ductility (Collier and Elnashai 2001).
- Normally the damping effect is small because the energy dissipation capacity is low.
- Vertical vibrations are not symmetrical (Elnashai and Papazoglou 1997) with respect to the horizontal plane.

For analysis purposes, the masses at floor level would need to be lumped at several locations along the horizontal members. As a result, a large number of modes will need to be included if 90 % of the mass is to be reflected in the modal analysis. Fardis (2009) has proposed that the approximate effects of vertical seismic forces may be ascertained by using a method similar to the LSP for lateral seismic effects.

## 4.3 Inelastic Response Spectrum

It is realised that, with proper detailing, a large amount of seismic energy can be dissipated in the inelastic range, if some degree of damage is accepted. Clearly, the reason for permitting the structure to go into the inelastic range during an earthquake is economic. A typical force – deformation relationship for a SDOF system (curve *a*) – is shown in Fig. 2.10. After the structure yields, its stiffness diminishes to $\alpha\ k$ ($\alpha < 1$) from the initial elastic stiffness, $k$. It is mathematically convenient to utilise curve 1 ($k = 0$) which is drawn such that areas under the two curves are same. This is a representation of an elasto-fully plastic system. For such a system it is further assumed that the loading, unloading and reloading take place along the elastic path as shown in Fig. 4.2.

### *4.3.1 Effect of Ductility*

During studies on SDOF systems, Newmark and Hall observed the following approximate relationships (Lam et al. 1998; Paulay and Priestley 1992):

(a) If a building has a short natural period of vibration ($T < \approx 0.03$ s), it exhibits an acceleration response nearly the same as that of ground motion irrespective of the ductile detailing incorporated. Thus, ductility does not help in reducing the response. As a result the reduction factor $R_\mu$ is essentially 1.0, where $\mu$ is the displacement ductility. This implies that the structure should be designed as remaining elastic (Fig. 4.3a).

(b) For buildings with moderate periods ($0.1 < T < 0.5$ s), the maximum energy responses are about the same for elastic and inelastic systems. To achieve

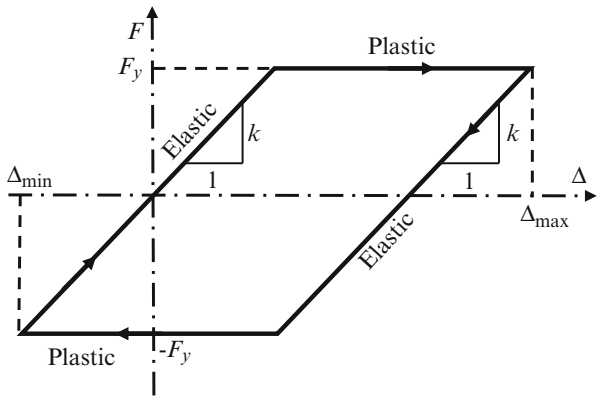


**Fig. 4.2** Elasto-fully plastic behaviour

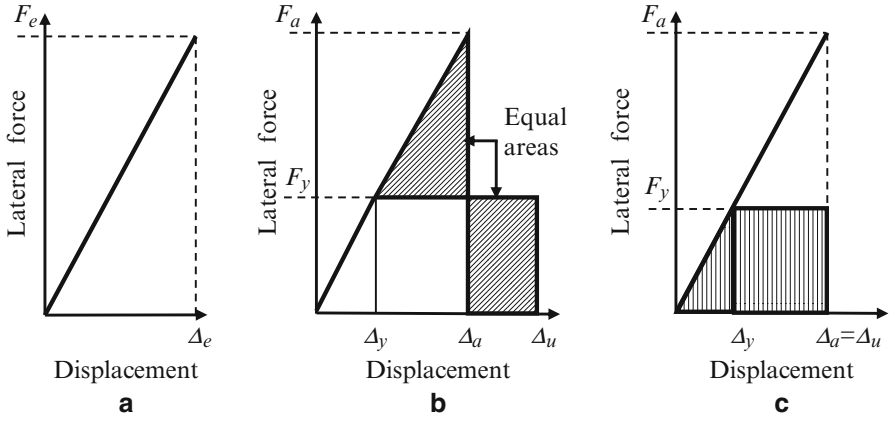


**Fig. 4.3** Load–displacement diagrams. (**a**) Elastic, (**b**) equal energy and (**c**) equal displacement

this, the structure must possess sufficient inelastic energy capacity to meet the seismic demand. In this case, areas under the respective load–displacement diagrams should be equal. From (Fig. 4.3b),

$$\frac{1}{2}F_a\Delta_s = \frac{1}{2}F_y\Delta_y + F_y\left(\Delta_u - \Delta_y\right)$$

$$F_y = \frac{F_a}{\sqrt{2\mu - 1}}, \quad \text{i.e.} \quad R_\mu = \sqrt{2\mu - 1} \tag{4.3.1}$$

where $\mu$ is the translational ductility of an elasto-perfectly plastic system.

(c) For long-period structures ($T > 0.5$ s), it is observed that the ultimate displacements of elastic and elasto-perfectly plastic systems are nearly the same irrespective of the value of yield force, i.e. $\Delta_u = \Delta_a$ (Fig. 4.3c), and the corresponding force-displacement relationship between the two systems can be written as

$$\frac{F_y}{\Delta_y} = \frac{F_a}{\Delta_a} = \frac{F_a}{\Delta_u}, \quad \text{i.e.} \quad F_y = \frac{F_a}{\Delta_u/\Delta_y} = \frac{F_a}{\mu} \tag{4.3.2}$$

It has been pointed out that this happens because during inelastic deformation the time period increases. This would lead to an increase in displacement but the force reduces and damping increases resulting in displacement being about the same as that for an elastic system. Thus, if a structure is detailed for ductility such that it can withstand large inelastic deformations without collapse, then it can be designed for the force at yield $F_y$ instead of its value $F_a$ for an elastic system near collapse. The response reduction factor $R_\mu$ due to ductility is then given by the ratio $F_a/F_y$ and can be written as

$$R_\mu = \frac{F_a}{F_y} = \frac{\Delta_u}{\Delta_y} = \mu \tag{4.3.3}$$

### 4.3.2 *Deducing Inelastic Design Response Spectrum*

Recent studies by researchers utilising many accelerograms recorded on rock and sites with alluvial or soft soils have demonstrated that the $R_\mu$ factor is dependent on characteristic period of the ground motion $T_g$. Using curve-fitting techniques, various relationships have been proposed. A general relationship now proposed, which provides a smooth transition of the value of $R_\mu$ from the equal acceleration response to the equal displacement response, is as (Lam et al. 1998; Paulay and Priestley 1992; US Army Corps of Engineers 2007) under:

$$\text{(a)} \quad For \quad T \leq 1.5\, T_g; \quad R_\mu = 1 + \frac{(\mu_\Delta - 1)\, T}{1.5\, T_g} \tag{4.4.1}$$

and

$$\text{(b)} \quad For \; T > 1.5\, T_g; \quad R_\mu = \mu$$

where $T$ is the natural period of vibration of the SDOF system.

This provides a mechanism by which the yield strength of a nonlinear elasto-fully plastic system on firm ground could be deduced from an elastic spectrum for a given ductility and damping. The inelastic spectrum developed as illustrated above could be used for an approximate determination of deformation of a SDOF system for an allowable displacement ductility ($\mu$) during a displacement-based design. The nature of inelastic response is complex and for a detailed analysis the reader may refer to Chopra (1995). The reduction in design lateral inertia force due to an inelastic behaviour is demonstrated through *Ex* 4.9.2.

## 4.4 Estimate of Fundamental Time Period of Vibration

To analyse a building using the linear static procedure (LSP) described below, the first requirement is to estimate the natural fundamental period of the building under free vibrations. For the period so estimated, the pseudo-response acceleration is read off the design acceleration response spectrum. This value is then used to calculate lateral forces and thereafter a classical static analysis is performed. If modal analysis is performed, then the response acceleration should be for a time period corresponding to the mode under consideration.

When a SDOF system is displaced laterally and then released, it will vibrate at what is known as its natural frequency. This is termed as free vibrations and the time required to complete one oscillation is called the natural period. For a building fixed at its base, there are four fundamental periods. There are three translational frequencies, one along each of the $x$ and $y$ axes and a vertical translation along the $z$-axis. In addition there will be a fundamental natural period for rotation about the vertical axis ($z$-axis).

For a MDOF system there will be a distinct period of vibration for each mode as explained in Sect. 4.6.4. The displaced profiles (or mode shapes) during such vibrations and their corresponding frequencies depend solely on system parameters, viz. magnitude and distribution of mass, ratio of stiffness to mass and type of supports. The mass of a body and not its weight is represented in the equations of motion. It is thus clear that the natural frequency is independent of the local gravitational field.

The calculation of vibration period of a building is fraught with uncertainties such as the values to consider for moment of inertia, modulus of elasticity of the materials used, contribution from infill walls and nonstructural members towards frame stiffness and such others. In view of the many uncertainties, the use of an empirical codal formula for evaluating the period $T$ is considered acceptable although there are limitations regarding its accuracy as demonstrated from many free vibration tests on buildings.

For concrete moment frames without infill panels, the codal (BIS 2002a) stipulation is that

$$T = 0.075\, h^{0.75} \tag{4.5.1}$$

### *4.4.1 Effect of Masonry Infill*

If the frames are infilled with brick masonry or equivalent, then the codal (BIS 2002a) formula for time period is

$$T = \frac{0.09\, h}{\sqrt{d}} \tag{4.5.2}$$

For both cases above, $T$ is the time period (s), $h$ is the height of the building (meter), and $d$ is the base dimension of the building (meter) along the considered direction of lateral force. The height $h$ excludes basement storeys when basement walls are connected with the ground floor deck or fitted between building columns. The contribution towards additional stiffness from infill walls will diminish rapidly once the brickwork cracks or if brickwork is omitted from some of the bays as an afterthought. Hence, the common practice is to ignore the stiffening effect of brick infill.

### 4.4.2 *Effect of Shear Walls*

There are many formulae proposed in literature for evaluating the period for shear wall-supported buildings. One of them is to consider the shear wall as a wide column with the moment of inertia reduced to 50 % of its gross value. Another suggestion is that, if concrete shear walls are used, the period may be determined (Jain et al. 2005) as under:

$$T = \frac{0.075}{\sqrt{A_w}} h^{0.75} \quad \text{where} \quad A_w = \sum A_{wi} \left\{ 0.2 + \left( \frac{L_{wi}}{h} \right) \right\}^2 \tag{4.5.3}$$

$h$ : height of building from foundation level (m). However, if there is a basement, then the basement storeys are to be excluded only in case the walls are connected with the ground floor deck.
$A_w$ : total effective wall area in the first storey of the building ($m^2$).
$A_{wi}$ : effective cross-sectional area of wall $i$ in the first storey of the building ($m^2$).
$L_{wi}$ : length of shear wall $i$ (m) in the first storey in the direction of seismic force but $L_{wi}/h$ not to exceed 0.9.

## 4.5 Linear Static Procedure (LSP)

This method is often used primarily because it is simple and elegant and gives sufficiently accurate results for low- to medium-rise regular buildings in moderate earthquake regions. It can also be used to have a first-order check on the results of dynamic analysis. Some of the important assumptions made in the LSP are:

- The building is regular and symmetrical.
- The stiffness and mass are nearly uniformly distributed.
- The torsion is small.
- Only the first mode of vibration is considered and higher mode effects are neglected.

In view of the above limitations, the LSP may be unconservative if applied to tall flexible structures or lateral load-resisting systems that are non-orthogonal or for systems where lateral and torsional modes are strongly coupled and buildings in which major irregularities prevail in terms of mass or stiffness distribution and similar cases.

### 4.5.1 *Design Horizontal Seismic Coefficient*

A design horizontal seismic coefficient is a dimensionless factor which when multiplied by the seismic weight supported by an element (including its own weight)

provides the horizontal inertia force on the element. Its birth is attributed (Betbeder-Matibet 2008) to an effort at codification following the major earthquakes in San Francisco, USA (1906), in Messina, Italy (1908) and in Kanto, Japan (1923). It had a humble beginning by way of a single coefficient, which was improved upon with growing knowledge in this field, and today it incorporates the influence of several factors, each with its own specific importance. The design horizontal seismic coefficient is calculated using the IS 1893 formula:

$$A_h = \frac{Z}{2} \cdot \frac{I}{R} \cdot \frac{S_a}{g} \tag{4.6.1}$$

with the proviso that for any structure with $T \leq 0.1$ s, the value of $A_h$ will not be taken less than $Z/2$ whatever be the value of $I/R$.

$Z$ zone factor. Its value, specified in IS 1893, is for the maximum considered earthquake (MCE) for the region. The latter is defined as the largest reasonably predicted earthquake for the tectonic region. This factor is divided by 2 since the design basis earthquake (DBE) is empirically taken as half the value for MCE (BIS 2002a; Jain et al. 2005).

$I$ importance factor. The use of importance factor is a way to recognise that certain categories of permanent buildings need to be designed for a higher safety level, e.g.

(a) Those buildings which house essential services, viz. fire stations, hospitals, power plants and other similar structures
(b) Places where a large number of persons may congregate, viz. schools and cinema halls, and those that may be required to house very large number of persons, post earthquake
(c) Structures whose collapse would have serious consequences, viz. dams, nuclear installations, etc.

$S_a/g$ seismic response acceleration coefficient. It is expressed as a fraction of the acceleration due to gravity, $g$. This figure is read off the design response spectrum against a calculated time period. If modal analysis is used, the coefficient $S_a/g$ has to be evaluated for each mode corresponding to its modal time period of vibration.

$R$ response reduction factor. This attribute is discussed in detail in Sect. 4.5.2.

For underground structures and foundations at 30 m depth or more, the code permits a reduction of 50 % in the value of $A_h$. For foundations at depth between ground level and 30 m, $A_h$ value shall be linearly interpolated between $A_h$ and $0.5\,A_h$. Note that this effects a reduction in inertia force on the substructure and not on the superstructure.

### 4.5.2 Response Reduction Factor

Since it is economically unviable to design buildings for elastic performance under strong earthquakes, a concept emerged of designing buildings for much lower inertia forces and accepting some degree of damage. In such an approach, advantage is taken of the substantial energy-absorbing capacity available in a structure during the inelastic regime while at the same time accepting limited damage that does not impair the vertical load-carrying capacity of the system, thereby avoiding collapse. Thus, the philosophy of design is to permit graded structural damage during an earthquake, corresponding to the limit state under consideration.

Reduction in force for design purposes is achieved through application of a factor termed as a response reduction factor $R$. It is the ratio of the seismic base shear for an elastic system to a value of the base shear for which the structure is to be designed. This factor is at best an engineering judgment and has little sound scientific basis although it plays a key role in arriving at the design forces. The estimated response reduction is brought about by:

- The inherent energy-absorbing capacity due to ductility which is incorporated through ductile detailing of the elements. This is expressed as a factor termed $R_\mu$.
- The existing overstrength capacity in the system represented by a factor $R_\Omega$.
- The redundancy existing in the system $R_R$.
- The effect of added damping $R_\xi$.

As depicted in Fig. 4.4, the response reduction factor enables a designer to use elastic design methods, which will cater to inelastic demands. Recent studies

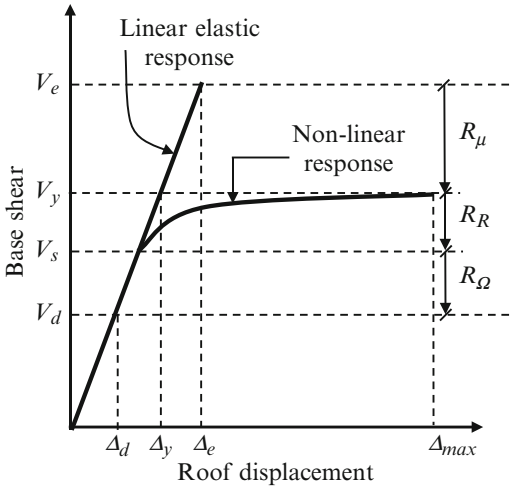


**Fig. 4.4** Response reduction factor

(Whittaker et al. 1999) support a formulation that the reduction factor may be expressed as

$$R = \frac{V_e}{V_y} \times \frac{V_y}{V_s} \times \frac{V_s}{V_d} \tag{4.7.1}$$

where

$V_e$: maximum elastic base shear
$V_y$: base shear corresponding to maximum load capacity
$V_s$: base shear corresponding to the first hinge formation in the structure
$V_d$: design base shear

$$\text{i.e.} \qquad R = R_\mu \times R_R \times R_\Omega \tag{4.7.2}$$

where

$R_\mu$: reduction factor due to ductility ($V_e/V_y$)
$R_R$: reduction due to redundancy ($V_y/V_s$)
$R_\Omega$: overstrength factor ($V_s/V_d$)

For structures wherein supplementary devices like dampers are provided to dissipate energy, an additional reduction factor $R_\xi$ is applicable. Herein, such addition is not considered and hence this factor is taken as 1.0 (Kumar and Sharma 2010).

#### 4.5.2.1 Reduction Due to Ductility

Force reduction component due to ductility $R_\mu$ is dependent on the ductility incorporated in the detailing of building elements. It is a function of the period of vibration of the structure and the predominant frequency of the supporting ground. This factor is used to reduce the elastic force demand to the level of yield force of the structure for a given ductility. It is obtained as shown in Sect. 4.3.1.

#### 4.5.2.2 Reduction Due to Overstrength

This parameter quantifies the ratio between the actual strength prevailing in the structure and the required strength demand. The reasons for overstrength are identified in Sect. 2.6.3. Various strength factors have been proposed, but there is a wide scatter in the results depending on building height, seismic zone applicable, margins prevailing in design, etc.

#### 4.5.2.3 Reduction Due to Redundancy

It has been observed that normally local yielding does not result in the failure of the structure as a whole. This is because the excess load in a particular element

gets distributed among redundant elements which provide reserve strength. This is termed as redundancy. If the failure of a component of a structure leads to failure of the entire system, then it is labelled as being nonredundant. Members that aid redundancy could be partly active or may be inactive. In the latter case they form a part of standby redundancy.

Redundancy can be considered as a feature in a multicomponent system whereby the failure of one component does not lead to the failure of the entire system. A redundant framing system should have multiple vertical lines of framing each designed and detailed to transfer lateral forces to the foundation. Although *structural redundancy* is recognised as a positive feature for enhancing seismic resistance, it is very difficult to quantify it.

The value of response reduction factor due to redundancy depends on many variables but in particular on the number of parallel paths and duality of framing systems provided for carrying loads to the foundations, under seismic conditions. Normally the reduction due to redundancy is clubbed with that due to overstrength. For the design of buildings, the total response reduction factor is taken as that specified in IS 1893 (BIS 2002a).

### 4.5.3 Evaluation of Base Shear

The static base shear is the summation of lateral inertia forces on the structure. It is given by

$$V_b = A_h W \tag{4.8.1}$$

where

$V_b$: base shear (N)
$A_h$: seismic coefficient as stipulated in Eq. 4.6.1
$W$: seismic weight of the building including part of the imposed loads (N)

### 4.5.4 Distribution of Base Shear

The distribution of the base shear over the height of a structure is quite complex. The code stipulated method presupposes that the fundamental mode response predominates, which is generally the case for regular buildings with regular distribution of mass and stiffness. While the fundamental vibration mode for such structures may lie between a straight line and a parabola, the code (BIS 2002a) specifies that the distribution of the base shear $V_b$ over the building height be taken as

$$Q_i = V_b \frac{w_i {h_i}^2}{\sum_{j=1}^{N} w_j {h_j}^2} \tag{4.9.1}$$

where

$Q_i$ : design lateral force at storey $i$
$w_i$, $w_j$: seismic weight at storey $i$ and $j$ respectively
$h_i$, $h_j$ : height of storey $i$ and $j$ respectively from base
$N$ : number of storeys at which masses are located

The distribution of storey lateral force among individual masses at a given floor level is proportionate to the mass distribution at that floor. For buildings with rigid diaphragms (which is normally the case), the design storey shear at storey $i$ is obtained from

$$V_i = \sum_{i}^{N} Q_i \tag{4.9.2}$$

This shear force should be distributed among lateral load-supporting vertical members in proportion to their lateral stiffness.

### *4.5.5 Linear Static Design Procedure*

For buildings with regular shapes and with nearly uniform distribution of mass and stiffness, which fall within the limitations specified in the code, this approach to design may be adopted. In summary form, the steps in this method are as under:

- Develop a mathematical model for the structure.
- Calculate load $w_i$ at each storey level $i$ which is the sum of gravity and code-specified imposed loads. The total weight to be considered is then $W = \sum_{i=1}^{N} w_i$.
- For the given building location, select the appropriate codal zone factor $Z$.
- Depending on the nature of use of the structure such as schools, day-care centers; or criticality of its post- earthquake functional need such as hospitals, power stations etc., importance factor $I$ can be chosen from the code. If the designer considers it necessary, a higher factor may be chosen.
- Commensurate with the nature of supporting framework and other factors, select a response reduction factor from those specified in the code.
- Estimate the first mode time period $T$ of the structure based on empirical codal formula as in Sect. 4.4.
- For this estimated time period and characteristics of the foundation soil, read off the seismic acceleration coefficient $S_a/g$ as stipulated in the code. Adjust this coefficient for assumed damping value, if different from 5 %.
- Determine the horizontal seismic coefficient $A_h$ from Eq. 4.6.1.
- Arrive at the base shear $V_b$ using Eq. 4.8.1.
- Distribute this base shear among various storey levels to arrive at storey forces $Q_i$ from Eq. 4.9.1 and storey shears $V_i$ from Eq. 4.9.2.

- Utilising the storey forces, a static analysis is to be conducted to determine forces and moments in frame members.
- Design the members.
- Check for inter-storey drifts and other parameters.

Application of this procedure is explained through *Ex* 6.10.1.

## 4.6 Modal Analysis

The dynamic analysis of a MDOF system is a complex task requiring enormous computational effort to solve a large set of coupled global equilibrium equations. While searching for simpler techniques, researchers evolved the modal analysis method for linear systems.

### *4.6.1 Basic Principles*

Modal analysis is an elegant, a powerful and an efficient computational technique for analysing linear dynamic systems. It enables the equations of motion to be written in a generalised form taking advantage of the invariant mode shape for each mode of vibration as explained in Sect. 4.6.3. This method involves breaking down of the response into several natural modes and determining the maximum response for each mode using a SDOF system response spectrum. The responses so obtained are then appropriately summed up to arrive at the total response.

This method admittedly falls short of capturing the total picture but the results are considered to be adequate for design. It is also an ideal method for determining natural dynamic characteristics of a structure, viz. frequencies and mode shapes. For evaluating the total response, it utilises the mode superposition technique which is not applicable to nonlinear systems. Hence, the use of this method is restricted to the analysis of linear systems only.

### *4.6.2 Modal Equation of Motion*

Consider a MDOF system under free vibrations. From Eq. 3.9.5,

$$\left[-\boldsymbol{M}\omega^2 + \boldsymbol{K}\right]\boldsymbol{A} = 0 \quad \text{and} \quad \left[-\boldsymbol{M}\omega^2 + \boldsymbol{K}\right]\boldsymbol{B} = 0$$

These equations have to be satisfied for each vibration frequency, so

$$\left[-\boldsymbol{M}\omega_i^2 + \boldsymbol{K}\right]\boldsymbol{A}_i = 0 \quad \text{and} \quad \left[-\boldsymbol{M}\omega_i^2 + \boldsymbol{K}\right]\boldsymbol{B}_i = 0 \tag{4.10.1}$$

Using Eq. 3.9.2, for each mode $i$, the total displacement can be written as

$$\boldsymbol{U}(t) = \sum_{i=1}^{N} \boldsymbol{A}_i \cos\ \omega_i t + \boldsymbol{B}_i \sin\ \omega_i t \tag{4.10.2}$$

From Eq. 4.10.1 it can be concluded that $\boldsymbol{A}_i$ and $\boldsymbol{B}_i$ must be proportional and hence it may be assumed that $\boldsymbol{A}_i = a_i\ \varphi_i$ and $\boldsymbol{B}_i = b_i \varphi_i$.

It follows that

$$\boldsymbol{U}(t) = \sum_{i=1}^{N} \varphi_i \{a_i \cos\ \omega_i t + b_i \sin\ \omega_i t\} = \sum_{i=1}^{N} \varphi_i\ q_i(t) \tag{4.10.3}$$

where

$$q_i(t) = a_i \cos\ \omega_i t + b_i \sin\ \omega_i t \tag{4.10.4}$$

Thus, the displacements for any mode $i$ can be represented as a product of a time-dependent variable $q_i$ and a displacement profile $\varphi_i$ which is invariant with time. Replacing this value of $\boldsymbol{U}(t)$ in Eq. 3.8.5 and specialising for mode $i$,

$$\left[-\boldsymbol{M}\omega_i^2 \varphi_i + \boldsymbol{K}\varphi_i\right]\ q_i(t) = 0 \tag{4.10.5}$$

Since $q_i(t) \neq 0$, it follows that

$$\boldsymbol{K}\varphi_i = \boldsymbol{M}\omega_i^2 \varphi_i \tag{4.10.6}$$

Premultiplying Eq. 4.10.5 by the transpose of mode shape $\varphi_j$, we get

$$\left[-\omega_i^2 \varphi_j^{\mathrm{T}} \boldsymbol{M} \varphi_i + \varphi_j^{\mathrm{T}} \boldsymbol{K} \varphi_i\right]\ q_i(t) = 0 \tag{4.10.7}$$

Utilising the mode orthogonality condition (described later in Sect. 4.6.5), the above equation reduces to

$$\left[-\omega_i^2 \varphi_i^{\mathrm{T}} \boldsymbol{M} \varphi_i + \varphi_i^{\mathrm{T}} \boldsymbol{K} \varphi_i\right]\ q_i(t) = 0 \tag{4.10.8}$$

and introducing terms $m_i = \varphi_i^{\mathrm{T}} \boldsymbol{M} \varphi_i$ and $k_i = \varphi_i^{\mathrm{T}} \boldsymbol{K} \varphi_i$ and noting that $-\omega_i^2 q_i = \ddot{q}_i$,

$$m_i \ddot{q}_i + k_i q_i = 0, \tag{4.10.9}$$

$$\text{i.e.} \quad \ddot{q}_i + \frac{k_i}{m_i} q_i = 0, \quad i = 1 \text{ to } N \tag{4.10.10}$$

The property of orthogonality of modes allows the $N$-coupled equations of motion of a MDOF system to be decoupled and solved independently for each vibration mode. The motion of a MDOF system can now be represented for each mode with the help of a single time-dependent coordinate $q_i$ which is known as the generalised coordinate. These constitute $N$-uncoupled modal equations of motion which results in a substantial reduction in computational effort.

### *4.6.3 Mode Shapes*

The number of natural frequencies of vibration of a MDOF system is equal to the number of degrees of freedom of the structure. During each natural frequency, the system vibrates in a particular invariant shape. It represents the magnitude of lateral storey displacements (viz. $\varphi_1$, $\varphi_2$, etc.) relative to that of any chosen storey. This forms a column matrix termed as a mode shape and each element of that matrix is known as the mode shape coefficient. Such coefficients for all modes together constitute a mode shape matrix denoted by $\Phi$.

Taking advantage of orthogonality of modes, the response of a multistorey building with $N$ floors can be considered as comprising of $N$ number of SDOF systems vibrating in their respective modes with their corresponding natural frequencies. Each such frequency is termed as a modal frequency and the deflected profile as the mode shape denoted by a column matrix $\varphi$ which remains invariant. In a given mode, the displacement vector varies harmonically with time and the deflection of storey $j$ vibrating in mode $i$ can be represented by

$$u_{ji}(t) = \varphi_{ji} q_i(t) \tag{4.11.1}$$

Such displacements for storey $j$ can be obtained for each frequency separately. Then by superimposition, the total displacement at storey $j$ for a MDOF system with $N$ degrees of freedom is given by

$$\sum u_{ji}(t) = \sum \varphi_{ji} q_i(t) \tag{4.11.2}$$

where $q_i(t)$ is the characteristic value or eigenvalue, while $\varphi_{ji}$, which is the modal amplitude that describes the vibrating pattern, is called the eigenvector.

Similar expressions can be written down for each storey of a MDOF system.

The following are some of the important characteristics of mode shapes.

(a) In each mode $i$, a MDOF structure vibrates at a particular frequency $\omega_i$ which is called its natural modal frequency. The mode with the lowest frequency is termed as the fundamental mode.
(b) There are $N$ mode shapes corresponding to $N$ degrees of freedom.

(c) Natural frequencies and mode shapes are dynamic characteristics of a structure which are a function only of the building properties, viz. stiffness matrix $\boldsymbol{K}$ and mass matrix $\boldsymbol{M}$.
(d) The relative floor displacements in each mode are fixed, i.e. the displacement profile in a particular mode does not change although the magnitude of floor displacements could vary.
(e) A normal mode is one in which the lumped masses attain maximum displacements at the same instant and also pass through equilibrium positions simultaneously, i.e. the nodes undergo synchronous motion.

### 4.6.4 Modal Frequencies

The eigenequation of motion for a building with N storeys is given by (Eq. 3.11.8)

$$\left[-\boldsymbol{M}\omega^2 + \boldsymbol{K}\right] = 0 \tag{4.12.1}$$

Introducing mass and stiffness values in Eq. 4.12.1 for a given $N$-degree MDOF system will result in an $N$th order equation in $\omega$. Solving these equations will yield $N$ natural modal frequencies of the structure. This is demonstrated in *Ex* 4.9.3. The lowest of these natural frequencies is called the fundamental natural frequency of the structure. The corresponding vibration period is termed the fundamental natural period.

Each of the masses in a MDOF system can move independent of each other. When all masses undergo a harmonic motion at the same frequency, then it is termed as the *natural frequency* of the system. At this frequency all masses will attain their maximum amplitudes at the same time although they may not be moving unidirectionally.

### 4.6.5 Orthogonality of Modes

Mode shapes of a lumped mass MDOF system have an important property of orthogonality which is demonstrated below. For an undamped MDOF system vibrating in the *i*th and *j*th modes, the corresponding eigenpair of equations (Eq. 3.11.8) would be

$$\boldsymbol{K}\varphi_i = {\omega_i}^2\boldsymbol{M}\varphi_i \quad \text{and} \quad \boldsymbol{K}\varphi_j = {\omega_j}^2\boldsymbol{M}\varphi_j \tag{4.13.1}$$

Premultiplying the first and second equations by $\varphi_j^T$ and $\varphi_i^{\mathrm{T}}$, respectively, we get

$$\text{(a)} \quad \varphi_j^{\mathrm{T}}\boldsymbol{K}\varphi_i = {\omega_i}^2\varphi_j^{\mathrm{T}}\boldsymbol{M}\varphi_i \quad \text{and} \quad \text{(b)} \quad \varphi_i^T\boldsymbol{K}\varphi_j = \omega_j^2\varphi_i^{\mathrm{T}}\boldsymbol{M}\varphi_j \tag{4.13.2}$$

Taking the transpose of both sides of the first of Eq. 4.13.2,

$$\left[\varphi_j^{\mathrm{T}} \boldsymbol{K} \varphi_i\right]^{\mathrm{T}} = {\omega_i}^2 \left[\varphi_j^{\mathrm{T}} \boldsymbol{M} \varphi_i\right]^{\mathrm{T}} \tag{4.13.3}$$

For the transpose of a scaler, $\{ABC\}^{\mathrm{T}} = C^{\mathrm{T}} B^{\mathrm{T}} A^{\mathrm{T}}$, and utilising symmetry of the $\boldsymbol{M}$ and $\boldsymbol{K}$ matrices, Eq. 4.13.3 reduces to

$$\varphi_i^{\mathrm{T}} \boldsymbol{K} \varphi_j = {\omega_i}^2 \varphi_i^{\mathrm{T}} \boldsymbol{M} \varphi_j \tag{4.13.4}$$

Subtracting Eq. 4.13.4 from Eq. 4.13.2(b),

$$\left({\omega_j}^2 - {\omega_i}^2\right) \varphi_i^{\mathrm{T}} \boldsymbol{M} \varphi_j = 0 \tag{4.13.5}$$

which implies that for the condition $\omega_j \neq \omega_i$; $\varphi_i^{\mathrm{T}} \boldsymbol{M} \varphi_j = 0$ and similarly it can be shown that for $\omega_j \neq \omega_i$; $\varphi_i^{\mathrm{T}} \boldsymbol{K} \varphi_j = 0$. It is then said that the two independent modes $i$ and $j$ are orthogonal with respect to both mass and stiffness matrices because for $\omega_j \neq \omega_i$,

$$\varphi_i^{\mathrm{T}} \boldsymbol{M} \varphi_j = 0 \quad \text{and} \quad \varphi_i^{\mathrm{T}} \boldsymbol{K} \varphi_j = 0 \tag{4.13.6}$$

Equations for vibratory motion of a structure in the $i$th and $j$th mode can now be written as two uncoupled equations, viz.

$$u_i(t) = q_i(t)\varphi_i \quad \text{and} \quad u_j(t) = q_j(t)\varphi_j \tag{4.13.7}$$

Inertia force generated in the $j$th mode will be $F_j = -\varphi_j m \ddot{q}_j(t)$. It is demonstrated by Chopra (1995) that work done by this force while going through the $i$th mode of displacements will be

$${F_j}^{\mathrm{T}} u_i = -\varphi_j^{\mathrm{T}} m \, \ddot{q}_j \, q_i \, \varphi_i = -\left\{\varphi_j^{\mathrm{T}} m \varphi_i\right\} \ddot{q}_j \, q_i = 0 \quad \text{(from Eq. 4.13.6)} \tag{4.13.8}$$

Thus, there is no work done by the $j$th mode inertia forces while traversing in the $i$th mode of displacements. It is also shown that the intermodal work done by static forces is also nil. From the above property of orthogonality of modes, a very important fallout is that it is possible to decouple the equations of motion. This greatly simplifies the vibration analysis of a MDOF system. The mode orthogonality property is demonstrated through *Ex* 4.9.4.

### *4.6.6 Normalisation of Modes*

Mode shapes are not absolute values but only relative ones and so can be normalised in different ways such as:

(a) To maintain roof or first-storey displacement as unity
(b) To designate the largest amplitude as unity
(c) To normalise with respect to mass matrix such that $\varphi_i^{\mathrm{T}} M \varphi_i = 1$

It is important to remember that whichever method is employed to normalise, the relative modal values within a given mode remain unchanged. The normalisation of mode shapes is for convenience and has no physical significance. These forms of normalisation are shown in *Ex* 4.9.5.

### 4.6.7 Modal Participation Factor

As per Eq. 3.11.10 the motion of a MDOF system vibrating in the *i*th mode is represented as $\ddot{q}_i + 2\omega_i \xi_i \dot{q}_i + \omega_i^2 q_i = -P_i \ddot{u}_g$ where $P_i = \frac{\varphi_i^{\mathrm{T}} \boldsymbol{M}}{\varphi_i^{\mathrm{T}} \boldsymbol{M} \varphi_i}$ which, for a symmetrical diagonal matrix $\boldsymbol{M}$, reduces to

$$P_i = \frac{\sum_{j=1}^{N} m_j \varphi_{ji}}{\sum_{j=1}^{N} m_j \left(\varphi_{ji}\right)^2} \tag{4.14.1}$$

The term $P_i$ is called the mode participation factor and it represents a mathematical ratio of the response of a MDOF system while vibrating in a particular mode to that of a SDOF system with the same mass and period. Its value depends on the manner in which modes are normalised and hence it is not unique. Also, it does not represent the extent of participation of the particular mode in structural response. For any storey *j* and considering all modes *i* to *N*,

$$\sum_{i=1}^{N} P_i \left\{\varphi_{ji}\right\} = 1 \tag{4.14.2}$$

This is demonstrated through *Ex* 4.9.6.

### 4.6.8 Modal Mass

The modal mass in mode *i* is that portion of the total mass which is effective in mode *i* of vibration. It is a codal requirement that the number of modes considered during analysis be such that they capture at least 90 % of the participating mass of a building along each of the two orthogonal principal horizontal axes.

Consider a MDOF linear system vibrating in the *i*th mode under seismic excitation. The displacement of mass $m_j$ at the *j*th storey (viz. $u_{ji}$) will be given by Eq. 4.13.7

$$u_{ji}(t) = \varphi_{ji}\, q_i(t)$$

and acceleration of mass $m_j$ will be

$$\varphi_{ji}\ddot{q}_i(t) = -\varphi_{ji}\omega_i{}^2 q_i(t) \tag{4.15.1}$$

The force acting on mass $m_j$ will be

$$F_{ji} = m_j \varphi_{ji} \ddot{q}_i = -m_j \varphi_{ji} \omega_i^2 q_i \tag{4.15.2}$$

and substituting value of $q_i$ from Eq. 3.11.12,

$$F_{ji} = \left[m_j \varphi_{ji} P_i\right] \omega_i \int_0^t \ddot{u}_g(\tau)\, e^{-\xi\ \omega_i\ (t-\tau)} \sin\ \omega_i\ (t-\tau)\, d\tau \tag{4.15.3}$$

From Eq. 3.7.4, a similar expression for a SDOF system will be

$$F = m\ \omega_i \int_0^t \ddot{u}_g(\tau)\, e^{-\xi\ \omega_i\ (t-\tau)} \sin\ \omega_i\ (t-\tau)\ d\tau \tag{4.15.4}$$

Comparing Eqs. 4.15.3 and 4.15.4, the terms in parentheses of Eq. 4.15.3 have units of mass. Hence, the modal mass at storey *j* in the *i*th mode of vibration will be

$$m_{ji} = m_j \varphi_{ji} P_i \tag{4.15.5}$$

Substituting for $P_i$ from Eq. 4.14.1, the modal mass in mode *i* will be

$$M_i = \frac{\left[\sum_{j=1}^{N} m_j \varphi_{ji}\right]^2}{\sum_{j=1}^{N} m_j \left(\varphi_{ji}\right)^2} \tag{4.15.6}$$

For a lumped mass linear system, $M_i$ represents the portion of total mass $M$ which is responding in vibration mode *i* and therefore is often termed as the effective modal mass in mode *i*. For each mode, the vertical distribution of modal masses will depend on the mode shape but their values are independent of the mode shape scaling. It is

easy to see that the sum of modal masses over all storeys $j$ and all modes $i$, viz. $\sum_{j=1}^{N}\sum_{i=1}^{N} M_{ji}$, will equal the total mass $M$ of the vibrating system.

### 4.6.9 Modal Height and Moment

The modal height provides a physical insight regarding the magnitude of base moment in each mode and height of the centroid of inertia forces in each mode. For a vibration period $T_i$ in mode $i$, the horizontal response coefficient will be $A_{hi}$. The force acting on a modal mass at storey $j$ in mode $i$ will be $A_{hi}\, w_{ji}\, \varphi_{ji}$. Its moment about the base will be $A_{hi} w_{ji} \varphi_{ji} h_j$ where $h_j$ is the height of storey $j$ above the base. Then, taking moments about the base, the modal height is given by

$$h_i = \frac{\sum_{j=1}^{N} m_{ji}\varphi_{ji}h_j}{\sum_{j=1}^{N} m_{ji}\varphi_{ji}} \tag{4.16.1}$$

Chopra (1995) has pointed out that for some of the higher modes, the modal height may be negative, signifying that the modal moment in that particular mode is subtractive. The evaluation of modal masses and modal height is demonstrated through *Ex* 4.9.7.

### 4.6.10 Combining Modal Responses

The results of a modal analysis for a MDOF system are in the form of peak values for the base shear, storey shears, base moment and such other response quantities, separately for each mode. These now have to be combined to arrive at the total value. These peak values do not occur simultaneously for all modes and so clearly the total response cannot be an algebraic sum of individual peaks. A commonly used approach is to utilise one of the following two methods:

1. Square root of the sum of the squares (SRSS) method
2. Complete quadratic combination rule (CQC) method

Both these methods are based on random vibration theory and the equations for combining modal responses by these two methods are given below.

#### 4.6.10.1 SRSS Method

When a total of $n$ modes are considered, then the total response $\lambda$ of a set of modal responses $\lambda_i$ is given by (BIS 2002a)

$$\lambda = \sqrt{\sum_{i=1}^{n} {\lambda_i}^2} \tag{4.17.1}$$

When combining modal response by the SRSS method, the sign is lost. This creates a problem while ascertaining whether a column is in residual compression. In such an event it is suggested that a static analysis may first be conducted for the first mode which invariably controls the maximum response. From this, the signs for forces are known. Thereafter, the quantity resulting from a combination of values using SRSS method may be assigned an appropriate sign.

This method is based on the assumption that the various modal values are statistically independent. It is not considered appropriate to adopt this method when the modal frequencies are close, i.e. when natural frequencies of two modes differ by less than 10 % of the lower frequency.

#### 4.6.10.2 CQC Method

In the complete quadratic combination (CQC) method (BIS 2002a),

$$\lambda = \left[ \sum_{i=1}^{n} \sum_{j=1}^{n} \lambda_i \rho_{ij} \lambda_j \right]^{1/2} \tag{4.18.1}$$

where

$n$ = number of modes being considered
$\lambda_i$ = response quantity in mode $i$ (including sign)
$\lambda_j$ = response quantity in mode $j$ (including sign)
$\rho_{ij}$ = cross mode coefficient which is given by

$$\rho_{ij} = \frac{8\xi^2 \left(1 + \beta_{ij}\right) {\beta_{ij}}^{1.5}}{\left(1 - {\beta_{ij}}^2\right)^2 + 4\xi^2 \beta_{ij} \left(1 + \beta_{ij}\right)^2} \tag{4.18.2}$$

where

$\xi$ = modal damping ratio
$\beta_{ij}$ = ratio of circular modal frequencies in $j$th and $i$th modes, i.e. $\beta_{ij} = \omega_j / \omega_i$

The CQC method is applicable, both when modes are well separated and when modes are closely spaced. A building could have only a few closely spaced modes among its many modes of vibration. In such an event, the combined response of these closely spaced modes can be obtained by direct summation to yield a response $\lambda^*$. This response can then be combined with responses for rest of the widely spaced modes by the CQC method to arrive at total response $\lambda$. When using the CQC method, it is important to correctly specify the damping factor which must match with the one used for response spectrum ordinate.

Whichever method is adopted, the rule should be applied to all computed response values such as bending moments, shear forces, displacements or any other response quantity. Considering that various modes contribute to the overall response, the maximum shear and moments at a level do not occur simultaneously with those at another level. Hence, moment and shear diagrams are envelopes and therefore cannot be treated as quantities in equilibrium. Secondly, the values obtained after combining modal values of a seismic analysis are peak values and have to be combined with those due to gravity and other responses as either positive or negative.

It is important to draw the reader's attention to the manner of combining modal responses. Consider that it is desired to obtain the total base shear of a two-storey building with storey forces $Q_{1i}$ and $Q_{2i}$ for mode $i$ and $Q_{1j}$ and $Q_{2j}$ for mode $j$, respectively. Then the total base shear for both modes together is evaluated by first obtaining the base shear for each mode separately [viz. $V_i = (Q_{1\mathrm{i}} + Q_{2i})$ and $V_j = (Q_{1j} + Q_{2j})$] and then combining $V_i$ and $V_j$ by using one of the above methods. The use of both these methods is explained in *Ex* 4.9.8.

### *4.6.11 Modal Analysis Procedure*

In brief, the modal analysis procedure for a regular shear building structure is described below:

- As for the LSP, determine the lumped masses $m_j$ at each floor and formulate the mass matrix $\boldsymbol{M}$.
- The stiffness of a single-storey column is $k = 12\ EI/h^3$ and the frame storey stiffness will be $\Sigma\ k$. From storey stiffness, create the stiffness matrix $\boldsymbol{K}$.
- Conduct an eigenvalue analysis for the structure using the specified stiffness and mass distribution. This will provide natural frequency, time period and mode shape for each mode
- Determine modal participation factors $P_i$ for each mode $i$ from Eq. 4.14.1
- Determine modal masses from Eq. 4.15.6. The codal provision states that the number of modes to be included in the analysis should be such that the sum of modal masses for all modes considered is at least 90 % of the total seismic mass. Check that this requirement is met.

- For each modal time period, read off the corresponding modal acceleration coefficient $S_{ai}/g$ from codal design response spectrum.
- For each mode evaluate the horizontal seismic coefficient $A_{hi}$ using Eq. 4.6.1 which is specialised for each mode *i*.
- Calculate the peak lateral force $Q_{ji}$ at storey $j$ in mode $i$ by the equation $Q_{ji} = A_{hi}\varphi_{ji}P_i w_j$.
- Calculate the base shear in each mode $i$ as $V_{bi} = \sum_{j=1}^{N} Q_{ji}$.
- Compute the total base shear for all modes given by $V_b = \sum_{1}^{n} V_{bi}$ using one of the established summation methods from Sect. 4.6.10.
- Evaluate $\overline{V}_b$, the base shear using LSP and Eq. 4.8.1.
- Check that $V_b \geq \overline{V}_b$. If not, all values obtained by modal analysis procedure have to be enhanced by the ratio $\overline{V}_b/V_b$.
- Using the values of storey forces (enhanced if found necessary due to previous condition), conduct a static analysis to determine the various parameters such as shears, moments, etc., separately for each mode.
- Combine modal values using one of the methods described in Sect. 4.6.10 to arrive at the final maximum values.

The procedure is illustrated in *Ex* 6.10.3 of Chap. 6.

A point of importance to note here is that, as per codal specifications, if the dynamic analysis results in a base shear $V_b$ which is less than that predicted by the LSP, viz. $\overline{V}_b$, based on an empirical codal time period, then all response values obtained from a dynamic analysis have to be scaled up by the ratio $\overline{V}_b/V_b$. The stipulated condition, in effect, specifies the minimum value of base shear to adopt for design. Nonetheless, in spite of the above limitation, a dynamic analysis is preferred since it results in a superior distribution of storey shears as compared to the LSP.

Researchers have pointed out that base shears corresponding to short-period structures produce relatively smaller overturning moments. Thus, a dynamic analysis which includes the effects of higher modes will produce a high base shear but smaller overturning moment. If moment values are scaled up as proposed above, it will result in lower overturning moments. Hence, moments should be scaled up with respect to the base moment obtained by the LSP.

For preliminary seismic dynamic analysis of buildings without irregularities, rudimentary stick models are widely employed because of their simplicity and acceptable level of accuracy. This can be achieved by stacking all column lines of a building structure while, at the same time, capturing their mass and stiffness characteristics. A detailed computer analysis of each framing system is then done for gravity and inertia loads including $P$-$\Delta$ effects. Thereafter, the structure is checked for strength, drift and other codal stipulations. Ideally a building should be modelled and analysed with a three-dimensional mathematical model.

### 4.6.12 Missing Mass Correction

When analysing a system with a large number of degrees of freedom using modal analysis technique, one needs to decide on the number of modes to consider in order to conserve computational effort. At the same time, an adequate number of modes need to be included such that the evaluated response reflects adequately the true behaviour of the system. For this purpose, IS 1893 requires that during analysis, 90 % of the modal mass should be captured in each orthogonal direction. Normally the desired result is achieved by considering the first few modes.

In some cases, however, it may be difficult to achieve this even when a reasonably large number of modes are considered or when the response of a dominant mass is controlled by a modal frequency that is at or near the rigid behaviour frequency. A typical example is when very stiff retaining walls of a basement form a part of the frame to be analysed. In such cases, a technique known broadly as the *missing mass correction* method can be employed (Dhileep and Bose 2008). It is a computational approach that is efficient and accurate.

The concept of this method is to undertake a modal analysis for all modes with frequencies below the zero period which is commonly taken as 33 Hz (BIS 2002a). For these modes, the sum of participating modal masses at each storey is evaluated. These values for each floor are subtracted from the lumped masses at corresponding floor levels to arrive at missing masses at individual floors. The response of these missing masses is then obtained as if they will respond with a rigid body frequency, i.e. the forces at a floor level will be the missing mass multiplied by peak ground acceleration in the acceleration spectrum. This response is then added to the earlier modal responses, using one of the methods described earlier, to arrive at the total response.

This approach is illustrated in *Ex* 4.9.9. Herein, the basement mass is not excited even after considering the first three modes. Hence, the masses participating at each floor level, for the first three modes, are first determined. Their modal summation gives the value of the participating masses at each floor. These values are deducted from the masses prevailing at each floor level. This gives the missing masses. The lateral forces on these missing masses are then calculated by applying the seismic acceleration appropriate for the highest mode.

## 4.7 Numerical Time History Analysis

Due to an earthquake ground acceleration $\ddot{u}_g$, the inertial forces acting on a structure vary arbitrarily with time. While the response to impulse excitation can be obtained by the Duhamel's integral (Sect. 3.4.5), it is not a practical medium to evaluate the dynamic response against such random excitation. Instead, in the time domain, numerical time-stepping methods can be used if a more precise response value is required than that obtained by modal analysis. Such an approach is commonly referred to as *time history analysis*.

It involves a step-by-step numerical evaluation of response to ground motion discretised typically at 0.01–0.02 s inputs. It is reported that in general, sufficient accuracy can be obtained if the time interval chosen is ≤ one-tenth of the natural period of the structure (Paz 1985). A simple method of assessing whether the time interval chosen is appropriate is to redo the sample calculations with half the time step. The result so obtained should not differ by more than 10 % from the earlier one.

It is important that time history signatures utilised to evaluate the response are reasonable representations of the ground motions anticipated at a given site. An approach commonly adopted is to evaluate the response for a number of time histories which should necessarily include those which may prove hazardous to the building. Such motions can be applied in one direction at a time along the two orthogonal directions or a pair of time histories can be applied simultaneously.

Numerical time history analysis is based on interpolation of excitation over short time steps which will, as closely as possible, reflect the likely true excitation. These methods provide approximate elastic solutions to the equations of motion at discrete time intervals. They may be generally classified as either explicit or implicit. In the former methods, the equation of motion is formulated for the commencement of a time step and then solved to project the response at end of the time step. In the latter case, equations of motion at the end of a time step include one or more values pertaining to that step.

There are different methods available, each with their own merits and demerits. The important aspects to be considered while choosing a particular method are:

- The capability of the solution to converge to the exact solution
- The stability of the method – the result should not blow off due to rounding-off errors
- The accuracy of results

The evaluation of forces and displacements in structural members at every time step during an earthquake calls for enormous computational effort even for a simple structure. With the advent of high-speed computers with large number-crunching capability and diminishing cost of computational aids, it is now possible, in special cases, to run time histories in a workable time frame. The preferred implicit methods are those proposed by Newmark – viz. (1) linear acceleration method and (2) average acceleration method – and hence only these are described below.

### *4.7.1 Newmark's Numerical Methods*

In 1959, N. M. Newmark (Chopra 1995) presented a family of time-stepping methods for linear SDOF systems utilising acceleration time histories as their base. For any vibrating system, all methods have to satisfy the equation of motion at commencement as well as at the end of a time step, viz. at $t = t_1$ and $t = t_2$ {i.e.

at $(t_1 + \Delta t)\}$, with corresponding inertia forces being $p_1$ and $p_2$. For a system with mass $m$, stiffness $k$ and damping $c$, from Eq. 3.7.1,

$$m\ddot{u}_1 + c\dot{u}_1 + ku_1 = p_1 \tag{4.19.1}$$

$$m\ddot{u}_2 + c\dot{u}_2 + ku_2 = p_2 \tag{4.19.2}$$

The terms $u_2$ *and* $\dot{u}_2$ were expanded using Taylor's series but were truncated (Wilson 2002) by Newmark for a time step $\Delta t$, as

$$u_2 = u_1 + (\Delta t)\,\dot{u}_1 + \frac{(\Delta t)^2}{2}\ddot{u}_1 + \beta(\Delta t)^3\dddot{u} + \cdots \tag{4.19.3}$$

and

$$\dot{u}_2 = \dot{u}_1 + (\Delta t)\,\ddot{u}_1 + \gamma(\Delta t)^2\dddot{u} + \cdots \tag{4.19.4}$$

For a time step $\Delta t$,

$$\dddot{u} = \frac{(\ddot{u}_2 - \ddot{u}_1)}{\Delta t} \tag{4.19.5}$$

Substituting Eq. 4.19.5 in Eqs. 4.19.3 and 4.19.4 (Chopra 1995),

$$u_2 = u_1 + (\Delta t)\,\dot{u}_1 + \left[(0.5 - \beta)\,(\Delta t)^2\right]\ddot{u}_1 + \beta(\Delta t)^2\ddot{u}_2 \tag{4.19.6}$$

and

$$\dot{u}_2 = \dot{u}_1 + (1 - \gamma)\,(\Delta t)\,\ddot{u}_1 + \gamma\,(\Delta t)\,\ddot{u}_2 \tag{4.19.7}$$

The parameters $\gamma$ and $\beta$ depend on the nature of variation of acceleration over the time step as detailed later. These equations form the basis of a family of Newmark's equations for linear system. Their use is explained in subsequent sections with due modification for nonlinear systems.

### *4.7.2 Linear Acceleration Method*

In this method it is assumed that the variation of acceleration is linear (Fig. 4.5a) during the time step $\Delta t$. As described by Chopra (1995), at any time $\tau$ from the commencement,

$$\ddot{u}\,(\tau) = \ddot{u}_1 + \frac{\tau}{\Delta t}\,(\ddot{u}_2 - \ddot{u}_1) \tag{4.20.1}$$

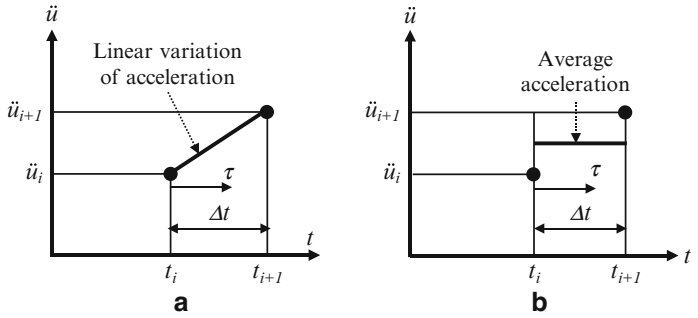


**Fig. 4.5** Concept of Newmark's methods (Based on Chopra 1995)

and with successive integration,

$$\dot{u}(\tau) = \dot{u}_1 + \ddot{u}_1\tau + \frac{\tau^2}{2\Delta t}(\ddot{u}_2 - \ddot{u}_1) \tag{4.20.2}$$

$$u(\tau) = u_1 + \dot{u}_1\tau + \ddot{u}_1\frac{\tau^2}{2} + \frac{\tau^3}{6\Delta t}(\ddot{u}_2 - \ddot{u}_1) \tag{4.20.3}$$

These equations can be obtained from Eqs. 4.19.6 and 4.19.7 by taking $\tau = \Delta t$, $\gamma = \frac{1}{2}$ and $\beta = \frac{1}{6}$.

Thus,

$$\dot{u}_2 = \dot{u}_1 + \frac{\Delta t}{2}(\ddot{u}_1 + \ddot{u}_2) \tag{4.20.4}$$

and

$$u_2 = u_1 + (\Delta t)\,\dot{u}_1 + (\Delta t)^2\left\{\frac{\ddot{u}_2}{6} + \frac{\ddot{u}_1}{3}\right\} \tag{4.20.5}$$

To make the solution of these equations non-iterative, it is suggested by Chopra (1995) to replace the variables by incremental operators leading to

$$\Delta u_1 = (u_2 - u_1) = (\Delta t)\,\dot{u}_1 + (\Delta t)^2\left\{\frac{\ddot{u}_1}{2} + \frac{\Delta\ddot{u}_1}{6}\right\} \tag{4.20.6}$$

$$\Delta\dot{u}_1 = (\dot{u}_2 - \dot{u}_1) = \frac{3\Delta u_1}{\Delta t} - 3\dot{u}_1 - \frac{\Delta t}{2}\ddot{u}_1 \tag{4.20.7}$$

$$\Delta\ddot{u}_1 = (\ddot{u}_2 - \ddot{u}_1) = \frac{6\Delta u_1}{(\Delta t)^2} - \frac{6\dot{u}_1}{\Delta t} - 3\ddot{u}_1 \tag{4.20.8}$$

For an incremental seismic force $m\Delta\ddot{u}_g$, the corresponding motion needs to satisfy the incremental equation

$$m\Delta\ddot{u}_1 + c\Delta\dot{u}_1 + k\Delta u_1 = -m\Delta\ddot{u}_g \tag{4.20.9}$$

Substituting Eqs. 4.20.6, 4.20.7 and 4.20.8 into Eq. 4.20.9, the incremental displacement will be

$$\Delta u_1 = \frac{\Delta\overline{p}_1}{\overline{k}} \tag{4.20.10}$$

where

$$\overline{k} = k + \frac{3c}{\Delta t} + \frac{6m}{(\Delta t)^2} \tag{4.20.11}$$

and

$$\Delta\overline{p}_1 = -m\Delta\ddot{u}_g + \left(\frac{6m}{\Delta t} + 3c\right)\dot{u}_1 + \left(3m + \frac{c\Delta t}{2}\right)\ddot{u}_1 \tag{4.20.12}$$

The incremental displacement $\Delta u_1$ can be evaluated from the known system parameters $m$, $k$ and $c$ and motion conditions, viz. $\dot{u}_1$ and $\ddot{u}_1$, at commencement of the assumed time step. Knowing $\Delta u_1$, the incremental velocity and incremental acceleration can be computed from Eqs. 4.20.7 to 4.20.8, respectively. The acceleration at the end of a time step should satisfy the condition

$$\ddot{u}_2 = \frac{p_2 - c\dot{u}_2 - ku_2}{m} \tag{4.20.13}$$

These values at the end of the first time step become the initial conditions for the next time step. As mentioned earlier, the method adopted should be stable. Newmark's linear acceleration method is stable (Chopra 1995) if $\frac{\Delta t}{T} < 0.551$ which is commonly met for SDOF systems. The procedure of conducting a time history analysis for a linear SDOF system using this method is shown in *Ex* 4.9.10.

### *4.7.3 Average Acceleration Method*

In this case, the acceleration during a time step is taken as the average of its values at the commencement and end of the time step as shown in Fig. 4.5b. The analysis procedure is similar to that described for linear acceleration method except for the nature of variation of acceleration between a time step $t_1$ to $t_2$. In this case $\gamma = \frac{1}{2}$ and $\beta = \frac{1}{4}$ leading to

$$\Delta u_1 = (u_2 - u_1) = (\Delta t)\,\dot{u}_1 + (\Delta t)^2\left\{\frac{\ddot{u}_1}{2} + \frac{\Delta\ddot{u}_1}{4}\right\} \tag{4.21.1}$$

$$\Delta \dot{u}_1 = (\dot{u}_2 - \dot{u}_1) = \frac{2\Delta u_1}{\Delta t} - 2\dot{u}_1 \tag{4.21.2}$$

$$\Delta \ddot{u}_1 = (\ddot{u}_2 - \ddot{u}_1) = \frac{4\Delta u_1}{(\Delta t)^2} - \frac{4\dot{u}_1}{\Delta t} - 2\ddot{u}_1 \tag{4.21.3}$$

The equations for incremental force and displacement are

$$\overline{k} = k + \frac{2c}{\Delta t} + \frac{4m}{(\Delta t)^2} \tag{4.21.4}$$

$$\Delta \overline{p}_1 = -\Delta m \ddot{u}_g + \left(\frac{4m}{\Delta t} + 2c\right)\dot{u}_1 + 2m\ddot{u}_1 \tag{4.21.5}$$

$$\Delta u_i = \frac{\Delta \overline{p}}{\overline{k}} \tag{4.21.6}$$

As per Chopra (1995) this method is unconditionally stable.

## 4.8 Nonlinear Time History Analysis

A system experiences inelastic behaviour when the lateral force exceeds the elastic resisting strength of vertical supporting members. The common nonlinearities during cyclic loading are those due to stiffness and damping. In the inelastic range the force–displacement profile could be assumed as bilinear or trilinear as desired. Newmark's methods described above can be extended to nonlinear systems with the assumption that during a time step the stiffness is the tangent stiffness corresponding to the displacement. This stiffness is assumed to remain constant over the time step.

A common approach is to assume secant stiffness over the elastic range up to the yield and a zero stiffness in the fully plastic state as shown in Fig. 4.2. Damping is considered unchanged over both the elastic and inelastic ranges and its effect on stiffness is ignored. In professional practice there is a premium on the use of computational time which restricts the use of a nonlinear dynamic analysis to the barest minimum.

### *4.8.1 Nonlinear SDOF System*

The analysis procedure is identical to a conventional elastic system except that at each stage of displacement of the element, its tangent stiffness at that displacement $k_t$ is used in lieu of a uniform elastic stiffness. As a result, the calculations are complicated by having to modify the stiffness at each time step when conducting a nonlinear analysis. Also, in this case, gravity loads must be considered concurrently

with seismic and other forces. As described by Datta (2010) the following four cases arise for an elasto - fully plastic frame system:

#### 4.8.1.1 Elastic to Elastic

The system remains elastic throughout the time step and the procedure is described in the case (a) of *Ex* 4.9.11.

#### 4.8.1.2 Elastic to Plastic

At commencement of a time step, the frame system is elastic with displacement $u_1$. At end of the time step, the incremental displacement $\Delta u_1$ results in total displacement being $(u_1 + \Delta u_1)$. At this stage, the elastic shear force in columns is evaluated. If that has exceeded the elastic limit of the columns' shear capacity, then it means that the system has passed into a fully plastic state within the time step $\Delta t$. It is then necessary to locate the incremental displacement $\lambda \Delta u_1$ (where $\lambda$ is a scalar) at which the change from elastic to plastic behaviour occurred. The plastic displacement is then obtained considering a balance force of $(1 - \lambda)\, \Delta \overline{p}_1$ acting on the system while taking the column stiffness $k_t$ as zero. The total incremental displacement at end of the time step is then the sum of elastic and plastic portions of the incremental displacements.

#### 4.8.1.3 Plastic to Plastic

In this case, the system remains plastic throughout the time step with column stiffness $(k_t)$ as zero. If the velocity of the system in positive at the end of a time step, then the system has continued to be in plastic state. The analysis is then continued further.

#### 4.8.1.4 Plastic to Elastic

While proceeding with the analysis as in 4.8.1.3 above, if it is observed that the system velocity is negative at the end of a time step, then it means that the system has passed back into the unloading portion of the elastic range. In this event, the location where velocity became zero has to be identified. For this purpose, the factored plastic incremental displacement $\lambda \Delta u_1$ has to be ascertained where velocity $\dot{u}(t) = 0$. Analysis is continued further with the balance force being $(1 - \lambda)\, \Delta \overline{p}_1$ and the balance elastic incremental displacement is obtained taking elastic column stiffness $(k_t)$. The total incremental displacement is then the sum of the two incremental displacements.

For a SDOF system the solution procedure utilising this method is illustrated through *Ex* 4.9.11. It covers the response history analysis, both in the elastic and

nonelastic ranges. For given initial conditions, the motion-related parameters are determined at the end of a time step for each of the four cases (4.8.1.1, 4.8.1.2, 4.8.1.3 and 4.8.1.4) described above.

For simplicity, the mass ($m$) is taken as 1 kg and the spring resisting lateral displacement is represented as the lateral stiffness of vertical members of a frame.

### *4.8.2 Nonlinear MDOF System*

The equations in Sect. 4.7 are also applicable here for each time step. The equation of motion for a MDOF system subjected to base excitation can be written as (Eq. 3.11.1)

$$\boldsymbol{M}\ddot{\boldsymbol{U}} + \boldsymbol{C}\dot{\boldsymbol{U}} + \boldsymbol{K}\boldsymbol{U} = -\boldsymbol{M}\{r\}\ddot{u}_g \tag{4.22.1}$$

$\boldsymbol{M}$ is the mass matrix, $\boldsymbol{K}$ is the stiffness matrix and $\boldsymbol{C}$ is the damping matrix. Proportional damping is assumed and the $\boldsymbol{C}$ matrix is given by

$$\boldsymbol{C} = \alpha\boldsymbol{M} + \beta\boldsymbol{K} \tag{4.22.2}$$

Proceeding as in the case of a SDOF system, the other equations for a MDOF system subjected to seismic excitation at a time step $i$ take the form

$$\boldsymbol{M}\ddot{\boldsymbol{U}}_{\boldsymbol{i}} + \boldsymbol{C}\dot{\boldsymbol{U}}_{\boldsymbol{i}} + \boldsymbol{K}_{\boldsymbol{i}}\boldsymbol{U}_{\boldsymbol{i}} = -\boldsymbol{M}\ddot{u}_{gi} \tag{4.22.3}$$

where $K_i$ is the stiffness matrix for time interval $\Delta t$

$$\Delta\overline{\boldsymbol{P}}_{\boldsymbol{i}} = -\boldsymbol{M}\Delta\ddot{u}_{gi} + \left[\frac{\boldsymbol{M}}{\beta\Delta t} + \frac{\gamma}{\beta}\boldsymbol{C}\right]\dot{\boldsymbol{U}}_{\boldsymbol{i}} + \left[\frac{\boldsymbol{M}}{2\beta} + \Delta t\left\{\frac{\gamma}{2\beta} - 1\right\}\boldsymbol{C}\right]\ddot{\boldsymbol{U}}_{\boldsymbol{i}} \tag{4.22.4}$$

$$\overline{\boldsymbol{K}}_{\boldsymbol{i}} = \boldsymbol{K}_i + \frac{\gamma}{\beta\Delta t}\boldsymbol{C} + \frac{1}{\beta(\Delta t)^2}\boldsymbol{M} \tag{4.22.5}$$

The incremental displacement will be

$$\Delta\boldsymbol{U}_{\boldsymbol{i}} = \frac{\Delta\overline{\boldsymbol{P}}_{\boldsymbol{i}}}{\overline{\boldsymbol{K}}_{\boldsymbol{i}}} \tag{4.22.6}$$

$$\Delta\dot{\boldsymbol{U}}_i = \frac{\gamma}{\beta\Delta t}\Delta\boldsymbol{U}_i - \frac{\gamma}{\beta}\dot{\boldsymbol{U}}_i + \Delta t\left[1 - \frac{\gamma}{2\beta}\right]\ddot{\boldsymbol{U}}_i \tag{4.22.7}$$

$$\Delta\ddot{\boldsymbol{U}}_i = \frac{1}{\beta(\Delta t)^2}\Delta\boldsymbol{U}_i - \frac{1}{\beta\Delta t}\dot{\boldsymbol{U}}_i - \frac{1}{2\beta}\ddot{\boldsymbol{U}}_i \tag{4.22.8}$$

The approach for analysing a MDOF system is explained below.

#### 4.8.2.1 Newmark's Linear Acceleration Method

The equations in Sect. 4.8.2 are specialised herein for linear variation of acceleration for a MDOF system by introducing

$$\gamma = \frac{1}{2} \text{ and } \beta = \frac{1}{6}$$

which leads to

$$\Delta \overline{\boldsymbol{P}}_i = -\boldsymbol{M}\,\Delta \ddot{u}_{gi} + \left[\frac{6\boldsymbol{M}}{\Delta t} + 3\boldsymbol{C}\right]\dot{\boldsymbol{U}}_i + \left[3\boldsymbol{M} + \frac{\Delta t}{2}\boldsymbol{C}\right]\ddot{\boldsymbol{U}}_i \tag{4.23.1}$$

$$\overline{\boldsymbol{K}}_{\boldsymbol{i}} = \boldsymbol{K}_{\boldsymbol{i}} + \frac{3}{\Delta t}\boldsymbol{C} + \frac{6}{(\Delta t)^2}\boldsymbol{M} \tag{4.23.2}$$

The incremental displacement will be

$$\Delta \boldsymbol{U}_i = \frac{\Delta \overline{\boldsymbol{P}}_i}{\overline{\boldsymbol{K}}_{\boldsymbol{i}}} \tag{4.23.3}$$

$$\Delta \dot{\boldsymbol{U}}_i = \frac{3}{\Delta t}\Delta \boldsymbol{U}_i - 3\dot{\boldsymbol{U}}_i - \frac{\Delta t}{2}\ddot{\boldsymbol{U}}_i \tag{4.23.4}$$

and

$$\Delta \ddot{\boldsymbol{U}}_i = \frac{6}{(\Delta t)^2}\Delta \boldsymbol{U}_i - \frac{6}{\Delta t}\dot{\boldsymbol{U}}_i - 3\ddot{\boldsymbol{U}}_i \tag{4.23.5}$$

#### 4.8.2.2 Newmark's Average Acceleration Method

By introducing $\gamma = \frac{1}{2}$ and $\beta = \frac{1}{4}$ for the average acceleration method, Eqs. 4.22.4, 4.22.5, 4.22.6, 4.22.7 and 4.22.8 take the following form:

$$\Delta \overline{\boldsymbol{P}}_{\boldsymbol{i}} = -\boldsymbol{M}\,\Delta \ddot{u}_{gi} + \left[\frac{4\boldsymbol{M}}{\Delta t} + 2\boldsymbol{C}\right]\dot{\boldsymbol{U}}_{\boldsymbol{i}} + 2\boldsymbol{M}\ddot{\boldsymbol{U}}_{\boldsymbol{i}} \tag{4.24.1}$$

$$\overline{\boldsymbol{K}}_{\boldsymbol{i}} = \boldsymbol{K}_i + \frac{2}{\Delta t}\boldsymbol{C} + \frac{4}{(\Delta t)^2}\boldsymbol{M} \tag{4.24.2}$$

The incremental displacement will be

$$\Delta \boldsymbol{U}_i = \frac{\Delta \overline{\boldsymbol{P}}_{\boldsymbol{i}}}{\overline{\boldsymbol{K}}_{\boldsymbol{i}}}, \tag{4.24.3}$$

$$\Delta \dot{\boldsymbol{U}}_i = \frac{2}{\Delta t}\Delta \boldsymbol{U}_i - 2\dot{\boldsymbol{U}}_i \tag{4.24.4}$$

and

$$\Delta \ddot{\boldsymbol{U}}_i = \frac{4}{(\Delta t)^2}\Delta \boldsymbol{U}_i - \frac{4}{\Delta t}\dot{\boldsymbol{U}}_i - 2\ddot{\boldsymbol{U}}_i \tag{4.24.5}$$

The method for undertaking a time history analysis for a MDOF system in both the elastic and inelastic regime is illustrated in *Ex* 4.9.12. The solution method broadly follows the procedure described by Datta (2010). As in the previous example, for simplicity, the masses ($m$) at each floor are taken as 1 kg and springs at floor levels resisting lateral displacement are represented as the lateral stiffness of vertical members of a frame.

## 4.9 Illustrative Examples

***Ex 4.9.1*** The SDOF system in *Ex* 3.9.1, under damped conditions, is subjected to a seismic ground motion. For purpose of this example, assume that the response tripartite plot is as given in Fig. 4.1. Find the pseudo-acceleration, maximum inertia force on the mass and maximum lateral spectral displacement.

**Solution** From *Ex* 3.9.1, the natural damped period $T_d = 1.326$ s and circular frequency is 4.737 rad/s.

From Fig. 4.1, for $T = 1.3$ s the spectral velocity is 200 mm/s. Dropping ordinates from this point, the seismic acceleration is $S_a \cong 0.095$ g and maximum roof displacement is 45 mm.

These values can also be obtained from Eq. 4.1.9 as under

$$S_a/g = \omega S_v/g = 4.737 \times 20/980.6 = 0.097$$

Maximum inertia force $= 1{,}200 \times 0.097 \times 9.806 = 1{,}141.418$ N

Lateral displacement $= S_v/\omega = 20 \times 10/4.737 = 42.22$ mm

***Ex 4.9.2*** A single-storey frame with a lumped weight $W$ at roof level has a natural vibration period of 0.24 s and is located in seismic zone V. The importance factor may be taken as 1.0. It is supported on rocky strata and has an estimated damping value of 5 %. Determine the percentage reduction in the design lateral force if it is to be designed for elasto-fully plastic behaviour with a displacement ductility factor ($\mu$) of 5 instead of being designed to remain elastic (use Eq. 4.3.1 for purpose of this example).

**Solution** For a time period of 0.24 s for a SDOF system on rocky strata with 5 % damping, the response acceleration coefficient from IS 1893 is 2.5. The zone

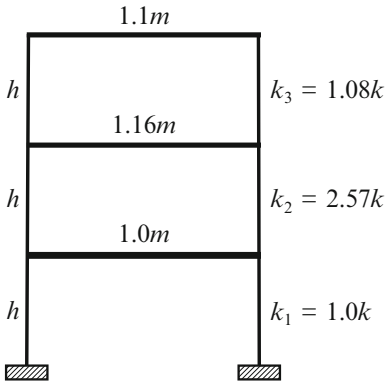


**Fig. 4.6** Three-storey frame

factor for zone V is 0.36 as specified in the code. For an elastic system the design horizontal acceleration coefficient would be *Ah*.

For a vibration period of 0.24 s, from Eq. 4.3.1, the reduction factor for elasto-plastic behaviour with a ductility factor of 5 would be $\sqrt{2\mu - 1} = \sqrt{2(5) - 1} = 3$

Introducing $R = 3$ in Eq. 4.6.1, value of $A_h$ will reduce from 4.415 (with $R = 1$) to,

$$A_h = \frac{Z}{2} \cdot \frac{I}{R} \cdot \frac{S_a}{g} = \frac{0.36}{2} \times \frac{1}{3} \times 2.5 \times 9.81 = 1.47$$

$$\text{Percentage reduction in lateral force} = \frac{(4.415 - 1.47)}{4.415} \times 100 = 66.7\ \%$$

***Ex 4.9.3*** Consider a frame under free vibrations with mass and stiffness values (for both columns together) as shown in Fig. 4.6. With $m = 1.62 \times 10^5$ kg, $k = 68.28 \times 10^6$ N/m and storey height $h = 3$ m, evaluate (1) mode shapes and (2) modal frequencies.

**Solution**

(a) *Evaluation of mode shapes*

Substituting values in Eq. 2.10.1,

the mass matrix is $\boldsymbol{M} = m \begin{pmatrix} 1.0 & 0 & 0 \\ 0 & 1.16 & 0 \\ 0 & 0 & 1.1 \end{pmatrix}$

From Eq. 2.7.2,

the stiffness matrix is $\boldsymbol{K} = k \begin{pmatrix} k_1 + k_2 & -k_2 & 0 \\ -k_2 & k_2 + k_3 & -k_3 \\ 0 & -k_3 & k_3 \end{pmatrix}$

$$= k \begin{pmatrix} 3.57 & -2.57 & 0 \\ -2.57 & 3.65 & -1.08 \\ 0 & -1.08 & 1.08 \end{pmatrix}$$

From Eq. 3.9.5, $\boldsymbol{K} - \boldsymbol{M}\omega^2 = 0$. Substituting values and taking $\frac{m\omega^2}{k} = \lambda$,

$$\begin{pmatrix} 3.57 & -2.57 & 0 \\ -2.57 & 3.65 & -1.08 \\ 0 & -1.08 & 1.08 \end{pmatrix} - \begin{pmatrix} \lambda & 0 & 0 \\ 0 & 1.16\lambda & 0 \\ 0 & 0 & 1.1\lambda \end{pmatrix} = 0, \tag{4.25.1}$$

$$\text{i.e.} \quad \begin{pmatrix} 3.57-\lambda & -2.57 & 0 \\ -2.57 & 3.65-1.16\lambda & -1.08 \\ 0 & -1.08 & 1.08-1.1\lambda \end{pmatrix} = 0 \tag{4.25.2}$$

Solving, $\lambda_1 = 0.2287$, $\lambda_2 = 1.6283$, $\lambda_3 = 5.8414$

For mode 1, from Eq. 4.13.1, taking $\lambda = \lambda_1$,

$$\begin{pmatrix} 3.57-0.2287 & -2.57 & 0 \\ -2.57 & 3.65-0.2653 & -1.08 \\ 0 & -1.08 & 1.08-0.2516 \end{pmatrix} \begin{Bmatrix} \varphi_{11} \\ \varphi_{21} \\ \varphi_{31} \end{Bmatrix} = 0$$

Let $\varphi_{31} = 1.0$;

$-1.08\varphi_{21} + 0.828431 = 0$, i.e. $\varphi_{21} = 0.7670654$ and

$-2.57\varphi_{11} + 3.384709\ \varphi_{21} - 1.08(1.0) = 0$, i.e. $\varphi_{11} = 0.5899972$.

Proceeding similarly for modes 2 and 3, the mode shape vectors can be written as

$$\varphi_1 = \begin{Bmatrix} 0.5899972 \\ 0.7670654 \\ 1.0000000 \end{Bmatrix}, \quad \varphi_2 = \begin{Bmatrix} -0.8714424 \\ -0.6584110 \\ 1.0000000 \end{Bmatrix}, \quad \varphi_3 = \begin{Bmatrix} 5.6002325 \\ -4.9495867 \\ 1.0000000 \end{Bmatrix} \tag{4.25.3}$$

(b) *Evaluation of modal frequencies*

$$\frac{k}{m} = \frac{68.28 \times 10^6}{1.62 \times 10^5} = 421.4815 \tag{4.25.4}$$

For the first mode, $\omega_1^2 = \left(\frac{k}{m}\right)\lambda_1 = (421.4815 \times 0.2287) = 96.3926$

Fundamental frequency $= \omega_1 = 9.818$ rad/s and the other two frequencies will be

$$\omega_2 = 26.197 \text{ rad/s} \quad \text{and} \quad \omega_3 = 49.619 \text{ rad/s}$$

***Ex 4.9.4*** For the structure with loading details as in *Ex* 4.9.3, demonstrate the orthogonality of modes.

**Solution** Considering the first two modes and substituting values,

$$\begin{aligned}\varphi_1^T\ \boldsymbol{M}\ \varphi_2 &= \{0.5899972\ \ 0.7670654\ \ 1.0\} \times m \begin{pmatrix} 1.0 & 0 & 0 \\ 0 & 1.16 & 0 \\ 0 & 0 & 1.1 \end{pmatrix} \begin{Bmatrix} -0.8714424 \\ -0.6584110 \\ 1.0000000 \end{Bmatrix} \\ &= m\,\{0.5899972 \quad 0.8897958 \quad 1.1\} \times \begin{Bmatrix} -0.8714424 \\ -0.6584110 \\ 1.0000000 \end{Bmatrix} \cong 0 \end{aligned} \tag{4.26.1}$$

Similarly, for modes 1 and 3 together and 2 and 3 together,

$$\varphi_1^T\ \ \boldsymbol{M}\varphi_3 = m\,\{0.5899972 \quad 0.8897958 \quad 1.1\} \times \begin{Bmatrix} 5.6002325 \\ -4.9495867 \\ 1.0000000 \end{Bmatrix} \cong 0 \tag{4.26.2}$$

and

$$\varphi_2^T \boldsymbol{M}\varphi_3 = m\,\{-0.8714424 \quad -0.7637567 \quad 1.1\} \times \begin{Bmatrix} 5.6002325 \\ -4.9495867 \\ 1.0000000 \end{Bmatrix} \cong 0 \tag{4.26.3}$$

This proves the mode orthogonality with respect to the mass matrix. Now considering the stiffness matrix,

$$\begin{aligned}\varphi_1^T\ \ \boldsymbol{K}\varphi_2 &= \{0.5899972 \quad 0.7670654 \quad 1.0\}\, k \begin{pmatrix} 3.57 & -2.57 & 0 \\ -2.57 & 3.65 & -1.08 \\ 0 & -1.08 & 1.08 \end{pmatrix} \\ &\quad \times \begin{Bmatrix} -0.8714424 \\ -0.6584110 \\ 1.0000000 \end{Bmatrix} \cong 0 \end{aligned} \tag{4.26.4}$$

With a similar procedure, it can be shown that

$$\varphi_1^T\ \boldsymbol{K}\varphi_3 = 0 \quad \text{and} \quad \varphi_2^T\ \boldsymbol{K}\varphi_3 = 0 \tag{4.26.5}$$

The above proves mode orthogonality with respect to both the mass and stiffness matrices.

***Ex 4.9.5*** Normalise, in different ways, the modal vector $\varphi_3$ obtained in *Ex* 4.9.3.

**Solution**

(a) The modal values for $\varphi_3$ in the above example are already normalised with respect to the roof displacement in Eq. 4.25.3, i.e.

$$\varphi_3 = \begin{Bmatrix} 5.6002 \\ -4.9496 \\ 1.0000 \end{Bmatrix} \tag{4.27.1}$$

(b) The values when normalised with respect to the maximum value read as under

$$\varphi_3 = \begin{Bmatrix} 1.0000 \\ -0.8838 \\ 0.1786 \end{Bmatrix}$$

(c) Normalising with respect to mass matrix.

$$\boldsymbol{M} = 1.62 \times 10^5 \begin{pmatrix} 1.0 & 0 & 0 \\ 0 & 1.16 & 0 \\ 0 & 0 & 1.1 \end{pmatrix} \text{ and } \{\varphi_3\}^T = \{5.6002 \quad -4.9496 \quad 1.0000\}$$

$$\varphi_3^T M \varphi_3 = 10^5 \{5.6002 \quad -4.9496 \quad 1.0000\} \begin{pmatrix} 1.6200 & 0 & 0 \\ 0 & 1.8792 & 0 \\ 0 & 0 & 1.782 \end{pmatrix} \times \begin{Bmatrix} 5.6002 \\ -4.9496 \\ 1.0000 \end{Bmatrix}$$

$$= 10^5 \{5.6002 \quad -4.9496 \quad 1.0000\} \begin{Bmatrix} 9.07238 \\ -9.30126 \\ 1.78200 \end{Bmatrix} = 98.6268 \times 10^5 \text{kg} \tag{4.27.2}$$

For $\varphi_3^T M \varphi_3 = 1$, we need to divide the modal values by $\sqrt{98.6268 \times 10^5} = 3,140.49$ and the normalised modal values become

$$\varphi_3 / 3140.49 = 10^{-3} \begin{Bmatrix} 1.7832 \\ -1.5761 \\ 0.3184 \end{Bmatrix} \tag{4.27.3}$$

To check whether $\varphi_3^T M \varphi_3 = 1$,

$$\varphi_3^T M \varphi_3 = 10^{-1} \begin{pmatrix} 1.7832 & -1.5761 & 0.3184 \end{pmatrix} \begin{pmatrix} 1.6200 & 0 & 0 \\ 0 & 1.8792 & 0 \\ 0 & 0 & 1.7820 \end{pmatrix} \times \begin{Bmatrix} 1.7832 \\ -1.5761 \\ 0.3184 \end{Bmatrix}$$

$$= \begin{pmatrix} 0.28888 & -0.29618 & 0.05674 \end{pmatrix} \begin{Bmatrix} 1.7832 \\ -1.5761 \\ 0.3184 \end{Bmatrix} \simeq 1.0 \tag{4.27.4}$$

***Ex 4.9.6*** The structure in *Ex* 4.9.3 is subjected to a seismic base acceleration. With the mode shapes evaluated therein, calculate the participation factors ($P_i$) for each mode and demonstrate that for node $j$ in all modes, $\sum_{i=1}^{n} P_i \varphi_{ji} = 1.0$

**Solution** From *Ex* 4.9.3, the mass matrix and mode shapes are as under

$$\boldsymbol{M} = m \begin{pmatrix} 1.0 & 0 & 0 \\ 0 & 1.16 & 0 \\ 0 & 0 & 1.1 \end{pmatrix} \quad \varphi_1 = \begin{Bmatrix} 0.5900 \\ 0.7671 \\ 1.0000 \end{Bmatrix}, \quad \varphi_2 = \begin{Bmatrix} -0.8714 \\ -0.6584 \\ 1.0000 \end{Bmatrix},$$

$$\varphi_3 = \begin{Bmatrix} 5.6002 \\ -4.9496 \\ 1.0000 \end{Bmatrix}$$

From Eq. 4.14.1 the participation factor in mode $i$ is given by

$$P_i = \frac{\sum_{j=1}^{n} m_j \varphi_{ji}}{\sum_{j=1}^{n} m_j \left(\varphi_{ji}\right)^2}$$

Substituting values, the participation factor for the first mode is

$$P_1 = \frac{\{(1.1 \times 1.0) + (1.16 \times 0.7671) + (1.0 \times 0.5900)\}}{\left\{\left(1.1 \times 1.0^2\right) + \left(1.16 \times 0.7671^2\right) + \left(1.0 \times 0.5900^2\right)\right\}} = \frac{2.5798}{2.1307} = 1.2108 \tag{4.28.1}$$

Proceeding in a similar manner, $P_2 = -\dfrac{0.5351}{2.3622} = -0.2265$ and $P_3 = \dfrac{0.9587}{60.8805} = 0.0157$

Using these values for participation factors and earlier obtained values for modal vectors,

$$P_1\varphi_{11} + P_2\varphi_{12} + P_3\varphi_{13} = \\ = (1.2108 \times 0.5900) + (0.2265 \times 0.8714) + (0.0157 \times 5.6002) = 1.0 \tag{4.28.2}$$

Proceeding similarly, it can be shown that the above identity holds good for modes 2 and 3 also.

***Ex 4.9.7*** For the structure and loading details in *Ex* 4.9.3, evaluate the modal masses for each mode and demonstrate that the sum of modal masses is equal to the total mass. Also determine the modal height for the first mode.

**Solution** From Eq. 4.15.6, the modal mass $M_i$ is given by

$$M_i = \frac{\left[\sum_{j=1}^{N} m_j \varphi_{ji}\right]^2}{\sum_{j=1}^{N} m_j \left(\varphi_{ji}\right)^2}$$

Using the values in Eq. 4.28.1,

$$M_1 = m \times \frac{2.5798^2}{2.1307} = 3.1236 \text{ m} \tag{4.29.1}$$

Proceeding similarly, we get $M_2 = 0.1212$ m and $M_3 = 0.0152$ m which demonstrates that the sum of modal masses $M_1 + M_2 + M_3$,
$= m\,(3.1236 + 0.1212 + 0.0152) = 3.260\,m =$ total mass.

From Eq. 4.15.5, the modal mass at the $j$th node in the $i$th mode is $m_{ji} = m_j \varphi_{ji} P_i$.

From Eq. 4.16.1, the modal height is given by

$$h_i = \frac{\sum_{j=1}^{N} m_j \varphi_{ji} h_j}{\sum_{j=1}^{N} m_j \varphi_{ji}}$$

**Table 4.1** Frequencies and storey forces

| Vibration mode | Roof shear (kN) | Frequency $\omega$ rad/s |
|---|---|---|
| 1 | 109.900 | 10.59 |
| 2 | −23.826 | 27.45 |
| 3 | 1.719 | 51.46 |

Substituting values from earlier calculations in Eq. 4.28.1, the modal height for the first mode comes to

$$h_1 = \frac{\{(1.1 \times 1.0 \times 9) + (1.16 \times 0.7671 \times 6.0) + (1.0 \times 0.59 \times 3.0)\}}{\{(1.1 \times 1.0) + (1.16 \times 0.7671) + (1.0 \times 0.59)\}} = \frac{17.009}{2.5798} = 6.593 \text{ m} \tag{4.29.2}$$

***Ex 4.9.8*** For a three-storey structure the shear forces at the roof level for the three modes of vibration and corresponding vibration frequencies are as shown in Table 4.1. Determine the combined effect of these modal shears at roof level using (1) SRSS method and (2) CQC method. The modal damping may be taken as 5 % for all modes.

**Solution** From Table 4.1, the shear forces and natural frequencies are as given below:

$V_1 = 109.9$ kN, $V_2 = -23.826$ kN and $V_3 = 1.719$ kN and $\omega_1 = 10.59$ rad/s, $\omega_2 = 27.45$ rad/s and $\omega_3 = 51.46$ rad/s.

(1) *Using SRSS method*

Combined value of roof shear

$$V = \sqrt{109.900^2 + 23.826^2 + 1.719^2} = 112.47 \text{ kN} \tag{4.30.1}$$

(2) *Using CQC method*

From the frequency values given above, the $\beta$ values are:

$$j = \begin{matrix} 1 & 2 & 3 \end{matrix}$$

$$\beta_{ij} = \begin{pmatrix} \omega_1/\omega_1 & \omega_2/\omega_1 & \omega_3/\omega_1 \\ \omega_1/\omega_2 & \omega_2/\omega_2 & \omega_3/\omega_2 \\ \omega_1/\omega_3 & \omega_2/\omega_3 & \omega_3/\omega_3 \end{pmatrix} = \begin{pmatrix} 1.000 & 2.592 & 4.859 \\ 0.386 & 1.000 & 1.875 \\ 0.206 & 0.533 & 1.000 \end{pmatrix} \tag{4.30.2}$$

Substituting these values in Eq. 4.18.2 and taking $\xi = 0.05$, for $i = j$, $\beta_{ij} = \beta_{ji} = 1$ and $\rho_{ij} = \rho_{ji} = 1$,

$$\rho_{12} = \frac{8(0.05)^2 \times (1 + 2.592)\,(2.592)^{1.5}}{\left(1 - 2.592^2\right)^2 + 4(0.05)^2 \times (2.592) \times (1 + 2.592)^2} = 0.0091 = \rho_{21}$$

$$\rho_{13} = \frac{8(0.05)^2 \times (1 + 4.859)\,(4.859)^{1.5}}{\left(1 - 4.859^2\right)^2 + 4(0.05)^2 \times (4.859) \times (1 + 4.859)^2} = 0.0025 = \rho_{31}$$

$$\rho_{23} = \frac{8(0.05)^2 \times (1 + 1.875)\,(1.875)^{1.5}}{\left(1 - 1.875^2\right)^2 + 4(0.05)^2 \times (1.875) \times (1 + 1.875)^2} = 0.0227 = \rho_{32}$$

$$\rho_{11} = \rho_{22} = \rho_{33} = 1.0$$

The cross modal coefficients are

$$\rho_{ij} = \begin{pmatrix} 1.000 & 0.0091 & 0.0025 \\ 0.0091 & 1.000 & 0.0227 \\ 0.0025 & 0.0227 & 1.000 \end{pmatrix} \tag{4.30.3}$$

From Eq. 4.18.1, the total roof shear, including for all modes, will be

$$V_{\text{roof}} = \left[ \begin{bmatrix} V_1 & V_2 & V_3 \end{bmatrix} \begin{pmatrix} \rho_{11} & \rho_{12} & \rho_{13} \\ \rho_{21} & \rho_{22} & \rho_{23} \\ \rho_{31} & \rho_{32} & \rho_{33} \end{pmatrix} \begin{Bmatrix} V_1 \\ V_2 \\ V_3 \end{Bmatrix} \right]^{1/2}$$

Substituting values, this reduces to

$$V_{\text{roof}} = \left[ \begin{bmatrix} 109.900 & -23.826 & 1.719 \end{bmatrix} \begin{pmatrix} 1.0000 & 0.0091 & 0.0025 \\ 0.0091 & 1.0000 & 0.0227 \\ 0.0025 & 0.0227 & 1.0000 \end{pmatrix} \begin{Bmatrix} 109.900 \\ -23.826 \\ 1.719 \end{Bmatrix} \right]^{1/2} \tag{4.30.4}$$

The shear force at the roof level by the CQC method $= V_{\text{roof}} = 112.25$ kN.

***Ex 4.9.9*** A special moment-resisting frame idealised in Fig. 4.7 is supported on soft soil in zone III as per IS 1893. The other parameters are:

$m = 2 \times 10^5$ kg, storey stiffness $k = 3 \times 10^9$ N/m, importance factor $I = 1.0$ and response reduction factor $R = 5.0$. Using the SRSS method, evaluate:

(a) The base shear considering all modes.
(b) The base shear by considering only the first three modes.
(c) The base shear while demonstrating the approach of the missing mass correction method. For the purpose of this example, the mass in the last two modes may be considered as the missing masses which experience a response acceleration equivalent to that of the fifth mode. (Normally this method is used for masses vibrating with a frequency > 33 Hz and experiencing the peak ground acceleration.)

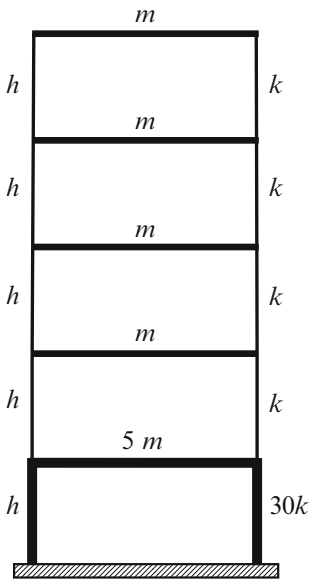


**Fig. 4.7** Frame with a stiff basement

**Table 4.2** Summary of mode shapes and frequencies

| Storey | Mode | | | | |
|---|---|---|---|---|---|
| j | 1 | 2 | 3 | 4 | 5 |
| 5 | 1.00000 | 1.00000 | 1.00000 | 1.00000 | 1.00000 |
| 4 | 0.88113 | 0.01295 | −1.32519 | −2.51889 | −5.25000 |
| 3 | 0.65752 | −0.98688 | −0.56906 | 2.82595 | 21.31247 |
| 2 | 0.35576 | −1.01261 | 1.51024 | −1.77343 | −85.32795 |
| 1 | 0.01170 | −0.03885 | 0.07795 | −0.13229 | 341.33109 |
| $\omega$ rad/s | 15.42 | 44.43 | 68.19 | 83.89 | 111.80 |

**Solution** After undertaking an eigenvalue analysis, the mode shapes and frequencies are as presented in Table 4.2. Evaluations of participation factor and modal mass participation for the first mode are shown in Table 4.3. Incidentally, the first row in Table 4.4 provides values of participation factors for all five modes. The modal mass participation for each mode has been computed and results are presented in Table 4.4.

Based on the modal vibration frequency, the horizontal seismic acceleration coefficient ($S_a/g$) is obtained for each mode from design response spectrum in IS 1893. Thereafter, the horizontal seismic coefficient $A_{hi}$ for each mode is calculated. Multiplying this coefficient with the total modal weight gives the base shear for each mode. A typical evaluation for the first mode is given below:

From Table 4.2, frequency $\omega_1 = 15.42$ rad/s

Time period $T_1 = 2\pi/\omega_1 = 2 \times \pi/15.42 = 0.407$ s (Table 4.5)

**Table 4.3** Modal participation factor and modal mass participation factor for the first mode

| $m$ | $\varphi$ | $m\varphi_1$ | $m\varphi_1{}^2$ | $P_1(m\varphi_1)$ |
|---|---|---|---|---|
| 1 | 1.00000 | 1.00000 | 1.00000 | 1.26410 |
| 1 | 0.88113 | 0.88113 | 0.77639 | 1.11384 |
| 1 | 0.65752 | 0.65752 | 0.43233 | 0.83117 |
| 1 | 0.35576 | 0.35576 | 0.12657 | 0.44972 |
| 5 | 0.01170 | 0.05850 | 0.00068 | 0.07395 |
| 9 m | $\Sigma$ | 2.95291 | 2.33597 | 3.73278 |
| $P_1 = 2.95291/2.33597 = 1.26410$ | | | | |
| Mass participation = (3.7328 m × 100/9 m) = 41.47 % | | | | |

**Table 4.4** Modal mass participation

| | | Modal mass = value × m | | | | | | | |
|---|---|---|---|---|---|---|---|---|---|
| | | Mode | | | | | | | |
| j | Mass | 1 | 2 | 3 | 4 | 5 | 1–3 | Missing | 1–5 |
| 5 | m | 1.2641 | −0.3927 | 0.1866 | −0.0608 | 0.0028 | 1.0580 | −0.0580 | 1.0000 |
| 4 | m | 1.1138 | −0.0051 | −0.2472 | 0.1531 | −0.0146 | 0.8615 | 0.1385 | 1.0000 |
| 3 | m | 0.8312 | 0.3876 | −0.1062 | −0.1717 | 0.0591 | 1.1126 | −0.1126 | 1.0000 |
| 2 | m | 0.4497 | 0.3976 | 0.2817 | 0.1078 | −0.2368 | 1.1290 | −0.1290 | 1.0000 |
| 1 | 5 m | 0.0740 | 0.0763 | 0.0727 | 0.0402 | 4.7368 | 0.2230 | 4.7770 | 5.0000 |
| Total | 9 m | 3.7328 | 0.4637 | 0.1876 | 0.0686 | 4.5473 | 4.3841 | 4.6159 | 9.0000 |

**Table 4.5** Evaluation of base shear ($V_i$)

| | | Mode | | | | | |
|---|---|---|---|---|---|---|---|
| Parameter | Unit | 1 | 2 | 3 | 4 | 5 | Missing |
| $T = 2\pi/\omega$ | s | 0.407 | 0.141 | 0.092 | 0.075 | 0.056 | |
| $S_a/g$ | | 2.500 | 2.500 | 2.380 | 2.125 | 1.840 | 1.840 |
| $A_{hi}$ | | 0.0400 | 0.0400 | 0.0381 | 0.0340 | 0.0290 | 0.0290 |
| $M_i$ | m | 3.7328 | 0.4637 | 0.1876 | 0.0686 | 4.5473 | 4.6159 |
| $V_i = A_{hi} \times W_i$ | kN | 292.95 | 36.39 | 14.02 | 4.58 | 258.73 | 262.64 |

For this $T_1$, the response acceleration from IS 1893 is 2.5 g and for zone III $Z = 0.16$.

Substituting values in Eq. 4.6.1, $A_{h1} = \frac{0.16}{2} \times \frac{1.0}{5} \times 2.5 = 0.04$ as in Table 4.5.

From Table 4.4, modal mass $M_1 = 3.7328 \times 2 \times 10^5 = 7.4656 \times 10^5$ kg.

Modal base shear $= A_{h1} \times W_1 = \left(0.04 \times 7.4656 \times 10^5 \times 9.81\right) \times 10^{-3} = 292.95$ kN

The values of base shear for other modes are listed in Table 4.5.

In the column 'Missing' in Table 4.4 are values of missing mass at each level, i.e. actual mass at that level less modal mass at the same level for the first three modes together. For instance, from Table 4.4, for the first mode,

Actual mass at level 1 = 1.0 $m$.

Modal mass at level 1 = 1.058 $m$ for modes 1–3 together.

Hence, the missing mass at level 1 is –0.058 $m$.

Similarly, the missing masses at each level are listed in Table 4.4 and their total value is $4.6159\,m$. For this missing mass, it is assumed that the seismic acceleration coefficient for the highest mode will apply (as specified for this example), i.e. 1.84.

The corresponding $A_h = 0.029$.

Hence, the base shear due to missing masses is

$$= 0.029 \times 4.6159 \times 2 \times 10^5 \times 9.81 \times 10^{-3} = 262.64 \text{ kN}$$

From the above, the base shears in the three cases, using the SRSS method, are as under:

(1) Considering all modes

$$\text{Base shear} = \left[292.95^2 + 36.39^2 + 14.02^2 + 4.58^2 + 258.73^2\right]^{\frac{1}{2}} = 392.81 \text{ kN} \tag{4.31.1}$$

(2) Considering the first three modes only

$$\text{Base shear} = \left[292.95^2 + 36.39^2 + 14.02^2\right]^{\frac{1}{2}} = 295.53 \text{ kN} \tag{4.31.2}$$

(3) Considering the first three modes and adding the balance for modes 4 and 5 using the missing mass correction

$$\text{Base shear} = \left[292.95^2 + 36.39^2 + 14.02^2 + 262.64^2\right]^{\frac{1}{2}} = 395.37 \text{ kN} \tag{4.31.3}$$

It will be seen that if only first three modes are considered, the effect of a large mass is not reflected in the results as it does not get excited in lower modes. This matter is set right through the missing mass correction approach.

***Ex 4.9.10*** A SDOF system as idealised in Fig. 4.8 is at rest when it is subjected to an earthquake with a random horizontal acceleration time history as shown in the fourth

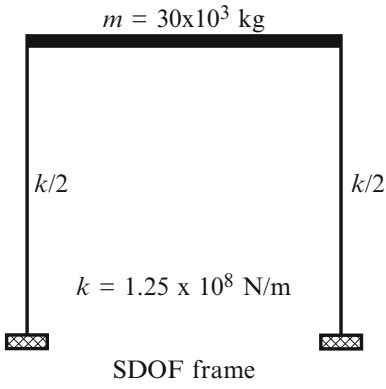


**Fig. 4.8** Time history analysis

column of Table 4.6 at every 0.02 s time step. Using Newmark's linear acceleration method, demonstrate the response history evaluation process by calculating the response quantities, viz. displacement, velocity and acceleration, of the system at the end of the first seven time steps. The given data are mass $m = 3 \times 10^4$ kg, lateral frame storey stiffness $k = 1.25 \times 10^8$ N/m and damping ratio $\xi = 5\ \%$.

**Solution** Time step $\Delta t = 0.02$ s

From Sect. 3.4.3, for a SDOF system,

$$\omega = \sqrt{\frac{k}{m}} = \sqrt{\frac{1.25 \times 10^8}{30{,}000}} = 64.54972 \text{ rad/s}$$
$$c = 2m\xi\omega = 2 \times 30{,}000 \times 0.05 \times 64.54972 = 1.93649 \times 10^5 \text{ N s/m}$$

Substituting values in Eq. 4.20.11,

$$\overline{k} = \left(1.25 \times 10^8\right) + \frac{\left(3 \times 1.93649 \times 10^5\right)}{0.02} + \frac{(6 \times 30{,}000)}{(0.02)^2} = 6.04047 \times 10^8 \text{ N/m}$$

Equation 4.20.12 can be written as $\Delta\overline{p}_1 = -m\Delta\ddot{u}_g + a\dot{u}_1 + b\ddot{u}_1$

where

$$a = \left(\frac{6m}{\Delta t} + 3c\right) = \frac{(6 \times 30{,}000)}{0.02} + 3(1.93649) \times 10^5 = 95.80948 \times 10^5 \text{ N s/m}$$
$$b = \left(3m + \frac{c\Delta t}{2}\right) = 3\,(30{,}000) + 0.01(1.93649)10^5 = 91{,}936.49 \text{ N s}^2/\text{m}$$
$$\therefore \Delta\overline{p}_1 = \Delta p_1 + \left(95.80948 \times 10^5\right)\dot{u}_1 + (91936.5)\ddot{u}_1 \text{ N} \tag{4.32.1}$$

Substituting $\Delta t = 0.02$ in Eqs. 4.20.7 and 4.20.8,

$$\Delta\dot{u}_1 = 150\Delta u_1 - 3\dot{u}_1 - 0.01\ \ddot{u}_1 \tag{4.32.2}$$

$$\Delta\ddot{u}_1 = 15{,}000\Delta u_1 - 300\dot{u}_1 - 3\ddot{u}_1 \tag{4.32.3}$$

*Analysis for the first time step*

Using value of $\Delta\ddot{u}_g$ from Table 4.6, for the first time step,

$$\Delta p_1 = -m\Delta\ddot{u}_g = \left(30 \times 10^3\right)(0.025212) = 756.351 \text{ N}$$

Since the structure is at rest,

$$u_1 = \dot{u}_1 = \ddot{u}_1 = 0. \tag{4.32.4}$$

Hence, $\Delta\overline{p}_1 = \Delta p_1 = 756.351$ N

**Table 4.6** Time history analysis using Newmark's linear acceleration method

| Step | t | $\ddot{u}_g/g$ | $\ddot{u}_g$ | $P_i$ | $\Delta p_i$ | $\Delta u_i$ | $\Delta \dot{u}_i$ | $\Delta \ddot{u}_i$ | $\Delta P$ | $u_{i+1}$ | $\dot{u}_{i+1}$ | $\ddot{u}_{i+1}$ |
|---|---|---|---|---|---|---|---|---|---|---|---|---|
| | s | | m/s$^2$ | N | N | m $\times 10^5$ | m/s $\times 10^3$ | m/s$^2$ | N | m $\times 10^5$ | m/s $\times 10^3$ | m/s$^2$ |
| 0 | 0.00 | −0.00257 | −0.0252117 | 0.000 | 756.351 | 0.12521 | 0.18782 | 0.01878 | 756.3510 | 0.00000 | 0.00000 | 0.00000 |
| 1 | 0.02 | −0.01980 | −0.1942380 | 756.351 | 5,827.140 | 1.54846 | 1.57140 | 0.11958 | 9,353.4016 | 0.12521 | 0.18782 | 0.01878 |
| 2 | 0.04 | −0.01850 | −0.1814850 | 6,583.491 | 5,444.550 | 5.79751 | 2.03503 | −0.07321 | 35,019.7000 | 1.67367 | 1.75922 | 0.13836 |
| 3 | 0.06 | −0.01620 | −0.1589220 | 12,028.041 | 4,767.660 | 7.79895 | −0.33577 | −0.16387 | 47,109.3080 | 7.47118 | 3.79425 | 0.06514 |
| 4 | 0.08 | −0.01740 | −0.1706940 | 16,795.701 | 5,120.820 | 4.83079 | −2.14204 | −0.01676 | 29,180.2692 | 15.27013 | 3.45848 | −0.09872 |
| 5 | 0.10 | −0.02200 | −0.2158200 | 21,916.521 | 6,474.600 | 1.40225 | −0.69112 | 0.16185 | 8,470.2632 | 20.10092 | 1.31644 | −0.11548 |
| 6 | 0.12 | −0.02610 | −0.2560410 | 28,391.121 | 7,681.230 | 2.96925 | 2.11418 | 0.11868 | 17,935.6499 | 21.50318 | 0.62533 | 0.04637 |
| 7 | 0.14 | −0.02350 | −0.2305350 | 36,072.351 | 6,916.050 | 8.00219 | 2.13429 | −0.11667 | 48,336.9767 | 24.47242 | 2.73951 | 0.16505 |

Note: The value of $\Delta \dot{u}_i$ at step 1 is $1.57140 \times 10^{-3}$ m/s

Substituting values in Eq. 4.20.10,

$$\Delta u_1 = \frac{756.351}{6.04047 \times 10^8} = 0.12521 \times 10^{-5} \text{ m} \tag{4.32.5}$$

*Second time step*

Substituting values from Eqs. 4.32.4 and 4.32.5 into Eqs. 4.32.2 and 4.32.3,

$$\begin{gathered} u_2 = u_1 + \Delta u_1 = 0.12521 \times 10^{-5} \text{ m} \\ \Delta \dot{u}_1 = 150 \left(0.12521 \times 10^{-5}\right) = 0.187815 \times 10^{-3} \text{ m/s} \\ \dot{u}_2 = \dot{u}_1 + \Delta \dot{u}_1 = 0.18782 \times 10^{-3} \text{ m/s} \end{gathered}$$

Similarly, $\ddot{u}_2 = \ddot{u}_1 + \Delta \ddot{u}_1 = 0.18782 \times 10^{-1} \text{ m/s}^2$.

Substituting value of the second impulse from row 2 of Table 4.6,

$$\Delta p_2 = \left(30 \times 10^3\right) (0.194238) = 5,827.14 \text{ N}$$

Substituting values in Eq. 4.32.1,

$$\begin{aligned} \Delta \overline{p}_2 &= 5,827.14 + 95.80948 \times 10^5 \left(0.18782 \times 10^{-3}\right) \\ &\quad + 91,936.492(0.01878) = 9,353.4016 \text{ N} \\ \Delta u_2 &= \frac{9,353.406}{6.04047 \times 10^8} = 1.54846 \times 10^{-5} \text{ m} \end{aligned}$$

The rest of the computations are summarised in Table 4.6. At the end of 0.14 s (7th time step), the values of motion parameters are

$$u_7 = 24.47242 \times 10^{-5} \text{ m}, \quad \dot{u}_7 = 2.73951 \times 10^{-3} \text{ m/s} \quad \text{and} \quad \ddot{u}_7 = 0.16505 \text{ m/s}^2$$

***Ex 4.9.11*** A SDOF system has an initial elastic behaviour until the storey shear force in the vertical members reaches a magnitude $F_e = 1.962$ N at a roof displacement $\Delta_e = 0.016$ m. Thereafter, the system follows a fully plastic behaviour as shown in Fig. 4.9. During the unloading stage, assume the load–displacement path to be parallel to that during loading. The analysis to be based on Newmark's average acceleration method with a time interval $\Delta t = 0.02$ s, for the following data:

Mass $m = 1$ kg, damping factor $\xi = 5$ % constant throughout all phases. The motion parameters at commencement are specified separately for each case. All values are chosen primarily only to emphasise the time history analysis procedure.

Determine the motion parameters at the end of one time step for each of the four cases, viz. (1) elastic to elastic, (2) elastic to plastic, (3) plastic to plastic and (4) plastic to elastic.

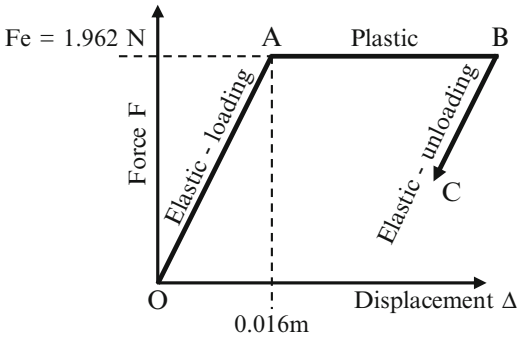


**Fig. 4.9** Elasto-fully plastic behaviour

**Solution** The elastic lateral storey stiffness during loading and unloading stages:

$$k_t = 1.962/0.016 = 122.625 \text{ N/m}$$

During the plastic state, for a fully plastic behaviour, $k_t = 0$.

Based on the initial stiffness, the natural frequency

$$\omega = \sqrt{\frac{k_t}{m}} = \sqrt{\frac{122.625}{1}} = 11.074 \text{ rad/s}$$

Damping coefficient $c = 2m\xi\omega = (2 \times 1 \times 0.05 \times 11.074) = 1.1074$ Ns/m

Substituting values in Eq. 4.21.4,

$$\begin{aligned} \overline{k}_e \text{ (during elastic range)} &= k_t + 100\text{c} + 10,000 \\ &= 122.625 + 100(1.1074) + 10,000 = 10,233.37 \text{ N/m} \end{aligned} \tag{4.33.1}$$

$$\overline{k}_p \text{ (during plastic range)} = 10,110.74 \text{ N/m} \quad \text{since } k_t = 0 \tag{4.33.2}$$

$$\Delta p_1 = -m\Delta\ddot{u}_g$$

Substituting values in Eqs. 4.21.2, 4.21.3, 4.21.4, 4.21.5 and 4.21.6 and with $m = 1$,

$$\Delta\overline{p}_1 = -\Delta\ddot{u}_g + 202.2148\dot{u}_1 + 2\ddot{u}_1 \tag{4.33.3}$$

$$\Delta u_1 = \Delta\overline{p}_1/\overline{k};\ \Delta\dot{u}_1 = 100\Delta u_1 - 2\dot{u}_1 \quad \text{and} \quad \Delta\ddot{u}_1 = 10,000\Delta u_1 - 200\dot{u}_1 - 2\ddot{u}_1 \tag{4.33.4}$$

It is required to ascertain the values of the various motion-related parameters at the end of a time interval of 0.02 s for each of the four cases identified above.

*Case (a) Elastic to elastic state*

The given initial conditions are

$$t_1 = 3.04s,\ \ u_1 = 0.00851 \text{ m},\ \ \dot{u}_1 = 0.01 \text{ m/s},\ \ \ddot{u}_1 = 1.148 \text{ m/s}^2,\ \ F_1 = 1.0435 \text{ N}$$

This system experiences an incremental ground acceleration due to the Koyna earthquake at 3.04 s of $\Delta\ddot{u}_g = 0.0312\ g = 0.30607 \text{ m/s}^2$

**Solution** Since $F_1 < F_e$ and $\dot{u}_1 > 0$, motion is in the elastic range on a loading path.

Substituting values in Eq. 4.33.3, the incremental force is

$$\Delta\overline{p}_1 = -0.30607 + 0.01(202.2148) + 2(1.148) = 4.01208 \text{ N}$$

From Eqs. 4.21.6 and 4.33.4, the incremental values of displacement, velocity and acceleration are

$$\Delta u_1 = \frac{\Delta\overline{p}_1}{\overline{k}_e} = \frac{4.01208}{10233.37} = 3.92058 \times 10^{-4} \text{ m}$$
$$\Delta\dot{u}_1 = 100\left(3.92058 \times 10^{-4}\right) - 2(0.01) = 0.019206 \text{ m/s}$$
$$\Delta\ddot{u}_1 = 10,000\left(3.92058 \times 10^{-4}\right) - 200(0.01) - 2(1.148) = -0.37542 \text{ m/s}^2$$
$$\Delta F = k_t.\Delta u_1 = 122.625\left(3.92058 \times 10^{-4}\right) = 0.04808 \text{ N}$$

The values at the end of time step (i.e. at 3.06 s) are obtained by adding these incremental values to those at commencement of the time step. Hence,

$$u_2 = u_1 + \Delta u_1 = \left(0.00851 + 3.9206 \times 10^{-4}\right) = 8.90206 \times 10^{-3} \text{ m}$$

Proceeding similarly,

$$\dot{u}_2 = 0.02921 \text{ m/s},\ \ \ddot{u}_2 = 0.77258 \text{ m/s}^2 \quad \text{and} \quad F_2 = 1.09158 \text{ N}$$

It will be observed that at $t_2 = (t_1 + \Delta t)$ ; $F_2 < F_e\,(1.962\ N)$ ; $\dot{u}_2 > 0$ and $u_2 < 0.016$ which implies that force and displacement are less than the upper limits for elastic behaviour and the velocity is positive. Thus, the system is in the elastic range at end of the time step.

*Case (b) Elastic to plastic state*

For this case, initial conditions at $t_1 = 4.12$ s are given as under:

$$u_1 = 0.0147 \text{ m},\ \ \dot{u}_1 = 0.16 \text{ m/s},\ \ \ddot{u}_1 = 0.806 \text{ m/s}^2,\ \ F_1 = 1.8026 \text{ N} \quad \text{and}$$
$$\Delta\ddot{u}_g = 0.02\ g = 0.1962 \text{ m/s}^2$$

**Solution** Since displacement $u_1 < \Delta_e$; $F_1 < F_e$ and $\dot{u}_1 > 0$, the system is elastic and on loading part of its force–displacement range. Proceeding exactly as in the earlier case,

$$\Delta\overline{p}_1 = -0.1962 + 202.2148(0.16) + 2(0.806) = 33.77017 \text{ N}$$
$$\Delta u_1 = \frac{\Delta\overline{p}_1}{\overline{k}_e} = \frac{33.77017}{10,233.37} = 33 \times 10^{-4} \text{ m}$$
$$\Delta\dot{u}_1 = 100\left(33 \times 10^{-4}\right) - 2(0.16) = 0.01 \text{ m/s}$$
$$\Delta\ddot{u}_1 = 10,000\left(33 \times 10^{-4}\right) - 200(0.16) - 2(0.806) = -0.612 \text{ m/s}^2$$
$$\Delta F_1 = k_t.\Delta u = 122.625\left(33 \times 10^{-4}\right) = 0.40466 \text{ N}$$

Then, the values of the above parameters at time $t_2$ $(t_1 + \Delta t) = 4.14$ s are

$$u_2 = u_1 + \Delta u_1 = 0.0147 + 0.033 = 0.018 \text{ m}$$

Similarly,

$$\dot{u}_2 = 0.17 \text{ m/s}, \quad \ddot{u}_2 = 0.194 \text{ m/s}^2 \quad \text{and} \quad F_2 = 2.20726 \text{ N}$$

This force exceeds the elastic force limit $F_e$ of 1.962 N. It implies that although the system was initially in the elastic range, it entered the plastic behaviour state prior to end of the time step. Hence, the incremental displacement value at which this stage change took place needs to be determined (Fig. 4.10). As a first step, the force causing elastic portion of the displacement has to be determined,

i.e storey shear force increment should be restricted to

$$\Delta F_e = (1.962–1.8026) = 0.1594 \text{ N}$$

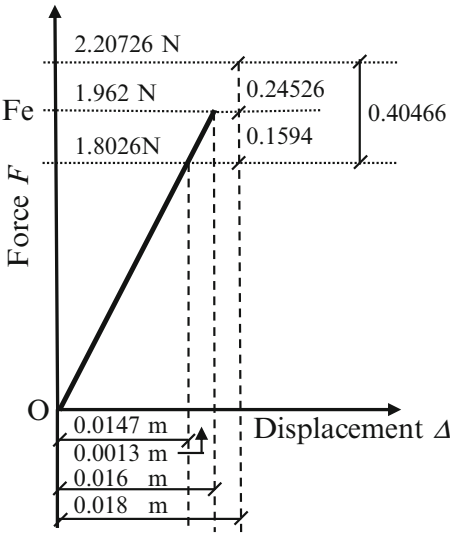


**Fig. 4.10** Elasto-fully plastic behaviour

The ratio of permissible force to incremental force, so that the system remains within elastic limit, is $\lambda = 0.1594/0.40466 = 0.39391$.

The elastic incremental displacement will be

$$\Delta u_{1e} = \lambda \left(33 \times 10^{-4}\right) = 0.0013 \text{ m}.$$

The balance seismic force applicable for plastic state will be $(1-\lambda)\,\Delta\overline{p} = 20.46776$ N and corresponding inelastic incremental displacement from Eq. 4.21.6 will be

$$\Delta u_{1p} = (1-\lambda)\,\Delta\overline{p} \,/\, \overline{k}_p = 20.46776/10110.74 = 2.0244 \times 10^{-3} \text{ m}.$$

The total incremental displacement (i.e. elastic $\Delta u_{1e}$ + plastic $\Delta u_{1p}$):

$$\Delta u_1 = \Delta u_{1e} + \Delta u_{1p} = 0.0013 + 0.0020244 = 3.3244 \times 10^{-3} \text{ m}$$

This leads to $u_2 = 0.0147 + 0.0033244 = 0.01802$ m.

Other incremental values will be

$$\begin{aligned}\Delta\dot{u}_1 &= 100\Delta u_1 - 2\dot{u}_1 = 100(0.0033244) - 2(0.16) = 0.01244\\ \Delta\ddot{u}_1 &= 10,000\,(\Delta u_1) - 200\dot{u}_1 - 2\ddot{u}_1\\ &= 10,000(0.0033244) - 200(0.16) - 2(0.806) = -0.368 \text{ m/s}^2\end{aligned}$$

Adding these incremental values to the corresponding ones prevailing at commencement of the time step, the resulting values are

$$u_2 = 0.01802 \text{ m},\ \ \dot{u}_2 = 0.17244 \text{ m/s},\ \ \ddot{u}_2 = 0.438 \text{ m/s}^2 \quad \text{and} \quad F_2 = 1.962 \text{ N}.$$

*Case (c) Plastic to plastic state*

For this case the given initial conditions at $t_1 = 8$ s are as under:

$$u_1 = 0.02 \text{ m},\ \ \dot{u}_1 = 0.12 \text{ m/s},\ \ \ddot{u}_1 = 0.898 \text{ m/s}^2,\ \ F_1 = 1.962 \text{ N} \quad \text{and}$$
$$\Delta\ddot{u}_g = 0.08\ g = 0.7848 \text{ m/s}^2$$

**Solution:** Since displacement $u_1 > \Delta_e$; $F_1 = F_e$ and $\dot{u}_1 > 0$, the system is in the plastic state and on loading part of the hysteresis loop. Proceeding as in case (b),

$$\Delta\overline{p}_1 = -0.7848 + 202.2148(0.12) + 2(0.898) = 25.2770 \text{ N}$$
$$\Delta u_1 = \frac{\Delta\overline{p}_1}{\overline{k}_p} = \frac{25.2770}{10,110.74} = 0.0025 \text{ m},\ \ \Delta\dot{u}_1 = 100(0.0025) - 2(0.12) = 0.01 \text{ m/s}$$
$$\Delta\ddot{u}_1 = 10,000(0.0025) - 200(0.12) - 2(0.898) = -0.796 \text{ m/s}^2$$
$$\text{and} \qquad \Delta F = 0 \quad \text{since } k_t = 0$$

The values of above parameters at $t_2 = (t_1 + \Delta t)$ (viz. 8.02 s) will be

$$u_2 = 0.0225 \text{ m}, \quad \dot{u}_2 = 0.13 \text{ m/s}, \quad \ddot{u}_2 = 0.102 \text{ m/s}^2 \quad \text{and} \quad F_2 = 1.962 \text{ N}$$

The system continues to remain in plastic state.

*Case (d) Plastic to elastic state*

For this case the given initial conditions at $t_1 = 3.02$ s are as under:

$$u_1 = 0.018 \text{ m}, \quad \dot{u}_1 = 0.016 \text{ m/s}, \quad \ddot{u}_1 = -0.345 \text{ m/s}^2,$$
$$F_1 = 1.962 \text{ N} \quad \text{and} \quad \Delta\ddot{u}_g = 0.15 \text{ g} = 1.4715 \text{ m/s}^2$$

Since displacement $u_1 > \Delta_e$; $F_1 = F_e$ and $\dot{u}_1 > 0$, the system is in plastic state and on loading part of the hysteresis loop. Proceeding as in case (c),

$$\Delta\overline{p}_1 = -1.4715 + 202.2148(0.016) + 2\,(-0.345) = 1.07394 \text{ N}$$
$$\Delta u_1 = \frac{1.073937}{10110.74} = 1.06217 \times 10^{-4} \text{ m}$$
and $$\Delta\dot{u}_1 = 100\left(1.06217 \times 10^{-4}\right) - 2(0.016) = -0.021378 \text{ m/s}$$
$$\dot{u}_2 = (\dot{u}_1 + \Delta\dot{u}_1) = -0.005378 \text{ m/s}^2$$

Since the velocity is negative at end of the time step, it implies that the system is on unloading branch of the hysteresis loop. Hence, it is necessary to ascertain the location at which velocity became zero where the system transitted from plastic to an elastic state. Assume that this occurs when incremental force utilised is $\lambda\overline{p}_1$ due to which incremental plastic displacement will be

$$\Delta u_{1p} = 1.06217 \times 10^{-4}\lambda$$

The incremental velocity will be

$$\Delta\dot{u}_{1p} = 100\lambda(1.06217) \times 10^{-4} - 2(0.016)$$

Since the velocity has to be zero,

$$\dot{u}_1 + \Delta\dot{u}_{1p} = (0.016) + \left(1.06217 \times 10^{-2}\right)\lambda - (0.032) = 0$$

This leads to $\lambda = 1.50635$.

The force causing plastic displacement will be $\lambda\overline{p}_1$ and the unloading elastic part will be due to a balance force of

$$(1 - \lambda)\,\Delta\overline{p}_1 = -0.50635\Delta\overline{p}_1$$

Utilising these factors, the incremental plastic displacement on loading part ($\Delta u_{1p}$) will be $\Delta u_{1p} = (1.50635 \times 1.06217) \times 10^{-4} = 1.6 \times 10^{-4}$ m

Similarly, the elastic incremental displacement on unloading part ($\Delta u_{1e}$) will be

$$\Delta u_{1e} = \frac{-0.50635(1.07394)}{10,233.37} = -5.31387 \times 10^{-5} \text{ m}$$

The gross incremental deflection will be $\Delta u_1 = \Delta u_{1p} + \Delta u_{1e} = (1.6 - 0.53139)\, 10^{-4}$
$= 1.06861 \times 10^{-4}$ m

$$u_2 = u_1 + \Delta u_1 = 0.018 + 1.068613 \times 10^{-4} = 0.018107 \text{ m}$$

$$\Delta \dot{u}_1 = (100 \Delta u_1 - 2\dot{u}_1) = (0.01068613) - 0.032 = -0.021314 \text{ m/s}$$

$$\dot{u}_2 = (\dot{u}_1 + \Delta \dot{u}_1) = (0.016 - 0.021314) = -5.314 \times 10^{-3} \text{ m/s}$$

During the unloading part, there will be a reduction of resisting force given by

$$\Delta F = 122.625\,(-0.531387) \times 10^{-4} = -0.006516 \text{ N.}$$
$$\text{Hence,} \qquad F_2 = 1.962 - 0.006516 = 1.95548 \text{ N}$$

$$\Delta \ddot{u}_1 = 10,000\,(\Delta u_1) - 200\dot{u}_1 - 2\ddot{u}_1$$
$$= 10,000\left(1.06861 \times 10^{-4}\right) - 200(0.016) - 2\,(-0.345) = -1.44139$$
$$\ddot{u}_2 = -0.345 - 1.44139 = -1.78639 \text{ m/s}^2$$

The motion parameters at the end of the time step will be

$$u_2 = 0.01811 \text{ m}, \quad \dot{u}_2 = -0.00531 \text{ m/s}, \quad \ddot{u}_2 = -1.78639 \text{ m/s}^2, \quad F_2 = 1.95548 \text{ N}$$

***Ex 4.9.12*** A multistorey frame as shown in Fig. 4.11 experiences a lateral ground acceleration impulse of ($-0.5396$ m/s$^2$). For the purpose of this example, it is considered that each vertical storey member can elastically sustain a maximum lateral shear of 1.75 N after which it's behaviour is fully plastic as shown in Fig. 4.12. The lateral elastic stiffness $k_t$ of the two vertical members together in each storey is 122.625 N/m and damping factor is 5 % throughout. The proportional damping matrix can be based on the first two frequencies of vibration and it can be assumed constant over both the elastic and inelastic ranges. Demonstrate the procedure, for a time step 0.02 s, nonlinear time history analysis of a MDOF frame using Newmark's average acceleration method. Consider for simplicity that each mass $m = 1.0$ kg. The initial motion parameters are as given below. As in *Ex* 4.9.11, all values are chosen primarily only to emphasise the time history analysis procedure.

**Data** Tangent stiffness during the elastic range, $k_{te} = 122.625$ N/m
Tangent stiffness during the inelastic range $k_{tp} = 0$
Limit of lateral elastic force carrying capacity of each vertical member in a storey $F_e = 1.75$ N

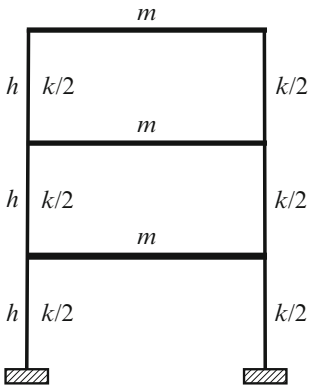


**Fig. 4.11** MDOF system

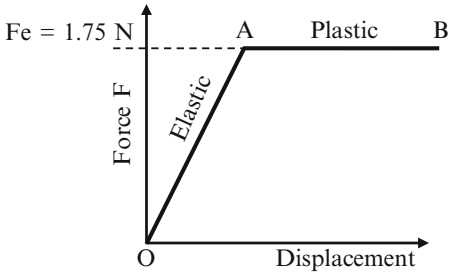


**Fig. 4.12** Elastoplastic behaviour of storey verticals

Time step $\Delta t = 0.02$ s, damping factor $\xi = 5$ %, mass $m = 1$ kg
The initial motion parameters and force ($F$) in the vertical members are as under:

$$\boldsymbol{U}_1 = 10^{-2}\begin{Bmatrix} 2.67534 \\ 5.51340 \\ 8.30616 \end{Bmatrix} \text{ m};\quad \dot{\boldsymbol{U}}_1 = \begin{Bmatrix} 0.1798 \\ 0.0782 \\ 0.1463 \end{Bmatrix} \text{ m/s};\quad \ddot{\boldsymbol{U}}_1 = \begin{Bmatrix} 0.8061 \\ 0.1045 \\ 1.1316 \end{Bmatrix} \text{ m/s}^2;$$
$$\boldsymbol{F}_1 = \begin{Bmatrix} 1.64032 \\ 1.74009 \\ 1.71231 \end{Bmatrix} \text{ N} \tag{4.34.1}$$

**Solution** Computations are done using high precision. However, results presented herein are to five significant places.

$$\text{Mass matrix } \boldsymbol{M} = \begin{pmatrix} 1 & 0 & 0 \\ 0 & 1 & 0 \\ 0 & 0 & 1 \end{pmatrix} \tag{4.34.2}$$

(a) *Elastic range*

The shear in vertical members is within the elastic limit and velocity is positive. Thus, the system is in elastic range.

Substituting values in Eq. 2.7.2, the elastic stiffness matrix is

$$\boldsymbol{K}_{te} = \begin{pmatrix} 245.25 & -122.625 & 0 \\ -122.625 & 245.25 & -122.625 \\ 0 & -122.625 & 122.625 \end{pmatrix} \tag{4.34.3}$$

From computer run, the three modal frequencies are

$$\omega_1 = 4.92822\,\text{rad/s}; \quad \omega_2 = 13.80857\,\text{rad/s}; \quad \omega_3 = 19.95397\,\text{rad/s} \tag{4.34.4}$$

Substituting values of the first two frequencies in Eq. 2.4.4 and with the given damping factor of 5 %, the proportional damping matrix is

$$\boldsymbol{C} = \begin{pmatrix} 1.67210 & -0.65445 & 0 \\ -0.65445 & 1.67210 & -0.65445 \\ 0 & -0.65445 & 1.01765 \end{pmatrix} \tag{4.34.5}$$

Substituting values into equations in Sect. 4.8.2.2 for Newmark's average acceleration method with a time step $\Delta t = 0.02$,

$$\Delta\dot{\boldsymbol{U}}_1 = 100\Delta\boldsymbol{U}_1 - 2\dot{\boldsymbol{U}}_1 \tag{4.34.6}$$

$$\Delta\ddot{\boldsymbol{U}}_1 = 10,000\Delta\boldsymbol{U}_1 - 200\dot{\boldsymbol{U}}_1 - 2\ddot{\boldsymbol{U}}_1 \tag{4.34.7}$$

$$\Delta\overline{\boldsymbol{P}} = -\boldsymbol{M}\,\Delta\ddot{u}_g + [200\boldsymbol{M} + 2\boldsymbol{C}]\,\dot{\boldsymbol{U}} + 2\boldsymbol{M}\ddot{\boldsymbol{U}} \tag{4.34.8}$$

$$\overline{\boldsymbol{K}} = \boldsymbol{K}_t + 100\boldsymbol{C} + 10,000\boldsymbol{M} \tag{4.34.9}$$

$$\ddot{\boldsymbol{U}}_2 = \frac{\boldsymbol{P}_2 - \boldsymbol{C}\dot{\boldsymbol{U}}_2 - n\boldsymbol{F}_2}{\boldsymbol{M}} \tag{4.34.10}$$

where $n$ is the number of vertical supporting members in a storey.

From Eq. 4.24.3, the incremental displacement will be

$$\Delta\boldsymbol{U}_1 = \frac{\Delta\overline{\boldsymbol{P}}_1}{\overline{\boldsymbol{K}}} \tag{4.34.11}$$

Substituting values from Eqs. 4.34.2, 4.34.3 and 4.34.5 into Eq. 4.34.9, the initial elastic value of $\overline{\boldsymbol{K}}$ is

$$\overline{\boldsymbol{K}}_e = \begin{pmatrix} 10412.46 & -188.07 & 0 \\ -188.07 & 10412.46 & -188.07 \\ 0 & -188.07 & 10224.39 \end{pmatrix} \tag{4.34.12}$$

Substituting values in Eq. 4.34.8,

$$\Delta\overline{\boldsymbol{P}}_1 = \begin{Bmatrix} 0.5396 \\ 0.5396 \\ 0.5396 \end{Bmatrix} + \begin{pmatrix} 203.3442 & -1.3089 & 0 \\ -1.3089 & 203.3442 & -1.3089 \\ 0 & -1.3089 & 202.0353 \end{pmatrix} \begin{Bmatrix} 0.1798 \\ 0.0782 \\ 0.1463 \end{Bmatrix} + 2 \begin{Bmatrix} 0.8061 \\ 0.1045 \\ 1.1316 \end{Bmatrix}$$

$$\Delta\overline{\boldsymbol{P}}_1 = \begin{Bmatrix} 38.61073 \\ 16.22328 \\ 32.25821 \end{Bmatrix} \tag{4.34.13}$$

Utilising values from Eqs. 4.34.12 and 4.34.13,

$$\Delta\boldsymbol{U}_1 = \begin{pmatrix} 10,412.46 & -188.07 & 0 \\ -188.07 & 10,412.46 & -188.07 \\ 0 & -188.07 & 10,224.39 \end{pmatrix}^{-1} \begin{Bmatrix} 38.61073 \\ 16.22328 \\ 32.25821 \end{Bmatrix}, \tag{4.34.14}$$

$$\text{i.e.} \qquad \Delta\boldsymbol{U}_1 = \begin{Bmatrix} \Delta u_1 \\ \Delta u_2 \\ \Delta u_3 \end{Bmatrix} = \begin{Bmatrix} 3.73853 \\ 1.68314 \\ 3.18599 \end{Bmatrix} \times 10^{-3} \tag{4.34.15}$$

The drift in each storey will be

$$\begin{Bmatrix} \delta_1 \\ \delta_2 \\ \delta_3 \end{Bmatrix} = \begin{Bmatrix} \Delta u_1 - 0 \quad \text{(base)} \\ \Delta u_2 - \Delta u_1 \\ \Delta u_3 - \Delta u_2 \end{Bmatrix} = \begin{Bmatrix} 3.73853 \\ -2.05539 \\ 1.50285 \end{Bmatrix} \times 10^{-3} \tag{4.34.16}$$

The corresponding storey shears in vertical members will be

$$\boldsymbol{\Delta F} = \frac{k_{te}}{2} \begin{Bmatrix} \delta_1 \\ \delta_2 \\ \delta_3 \end{Bmatrix} = 61.3125 \times \begin{Bmatrix} 3.73853 \\ -2.05539 \\ 1.50285 \end{Bmatrix} \times 10^{-3} = \begin{Bmatrix} 2.29218 \\ -1.26021 \\ 0.92144 \end{Bmatrix} \times 10^{-1} \tag{4.34.17}$$

Adding these incremental shear forces to those at commencement of the time step as given in Eq. 4.34.1, the shears at end of time step will be

$$\boldsymbol{F}_1 + \boldsymbol{\Delta F} = \begin{Bmatrix} 1.86954 \\ 1.61407 \\ 1.80445 \end{Bmatrix} = \begin{Bmatrix} > 1.75 \\ < 1.75 \\ > 1.75 \end{Bmatrix} \tag{4.34.18}$$

For the first and third storeys, the maximum permissible elastic stiffness of vertical members is exceeded. As a first step the drifts in these storeys are scaled by factors $\{\lambda\}$ so that the limiting elastic force value of 1.75 N is not exceeded. Hence,

$$\boldsymbol{F}_1 + \lambda \boldsymbol{\Delta F} = \left\{ \begin{array}{c} F_1 + \lambda_1 \Delta F_1 \\ F_2 + \lambda_2 \Delta F_2 \\ F_3 + \lambda_3 \Delta F_3 \end{array} \right\} = \left\{ \begin{array}{c} 1.75 \\ < 1.75 \\ 1.75 \end{array} \right\} \tag{4.34.19}$$

This leads to

$$\lambda_1 = 0.47851, \quad \lambda_2 = 1.0, \; \lambda_3 = 0.40909 \tag{4.34.20}$$

The incremental drifts, so that shears in vertical members remain within elastic limit, are

$$\lambda\delta = \left\{ \begin{array}{c} \lambda_1\delta_1 \\ \lambda_2\delta_2 \\ \lambda_3\delta_3 \end{array} \right\} = \left\{ \begin{array}{c} (0.47851) \times (3.73853) \\ (1.00000) \times (-2.05539) \\ (0.40909) \times (1.50285) \end{array} \right\} \times 10^{-3} = \left\{ \begin{array}{c} 1.78890 \\ -2.05539 \\ 0.61480 \end{array} \right\} \times 10^{-3} \tag{4.34.21}$$

The elastic incremental displacements will be

$$\Delta \boldsymbol{U}_{1e} = \left\{ \begin{array}{c} \Delta u_{e1} \\ \Delta u_{e2} \\ \Delta u_{e3} \end{array} \right\} = \left\{ \begin{array}{l} \lambda_1\delta_1 \\ \lambda_1\delta_1 + \lambda_2\delta_2 \\ \lambda_1\delta_1 + \lambda_2\delta_2 + \lambda_3\delta_3 \end{array} \right\} = \left\{ \begin{array}{c} 1.78890 \\ -0.26649 \\ 0.34831 \end{array} \right\} \times 10^{-3} \tag{4.34.22}$$

Introducing a factor $\psi$ such that

$$\{\psi\}\, \Delta \boldsymbol{U}_1 = \Delta \boldsymbol{U}_{1e}, \tag{4.34.23}$$

$$\Delta \boldsymbol{U}_{1e} = \left\{ \begin{array}{c} \psi_1 \Delta u_1 \\ \psi_2 \Delta u_2 \\ \psi_3 \Delta u_3 \end{array} \right\} = \left\{ \begin{array}{c} \Delta u_{e1} \\ \Delta u_{e2} \\ \Delta u_{e3} \end{array} \right\} \tag{4.34.24}$$

Introducing values from Eqs. 4.34.15 and 4.34.22 leads to

$$\psi_1 = 0.47850, \quad \psi_2 = -0.15833, \quad \psi_3 = 0.10933 \tag{4.34.25}$$

The corresponding force is $\{\boldsymbol{\psi}\}\, \boldsymbol{\Delta \overline{P}}_1$. The balance driving force causing displacement in the inelastic range will be

$$\{1 - \psi\}\, \boldsymbol{\Delta \overline{P}}_1 = \boldsymbol{\Delta \overline{P}}_p = \left\{ \begin{array}{c} 20.13531 \\ 18.79191 \\ 28.73151 \end{array} \right\} \tag{4.34.26}$$

(b) *Inelastic range*

Since storeys 1 and 3 are in plastic range, the stiffness matrix $\boldsymbol{K}_t$ has to be modified with $k_1 = k_3 = 0$. This leads to a stiffness matrix in the plastic range as

$$\boldsymbol{K}_{tp} = \begin{pmatrix} 122.625 & -122.625 & 0 \\ -122.625 & 122.625 & 0 \\ 0 & 0 & 0 \end{pmatrix} \tag{4.34.27}$$

Substituting values from Eq. 4.34.27 into Eq. 4.34.9,

$$\overline{\boldsymbol{K}}_{\boldsymbol{p}} = \begin{pmatrix} 10,289.84 & -188.07 & 0 \\ -188.07 & 10,289.84 & -65.445 \\ 0 & -65.445 & 10,101.77 \end{pmatrix} \tag{4.34.28}$$

The plastic incremental displacement:

$$\boldsymbol{\Delta U}_{1p} = \left[\overline{\boldsymbol{K}}_{\boldsymbol{p}}\right]^{-1} \Delta \overline{\boldsymbol{P}}_p = \begin{Bmatrix} 1.99119 \\ 1.88082 \\ 2.85639 \end{Bmatrix} 10^{-3} \tag{4.34.29}$$

The total incremental displacement will be

$$\begin{aligned} \boldsymbol{\Delta U}_1 = \boldsymbol{\Delta U}_{1e} + \boldsymbol{\Delta U}_{1p} &= \begin{Bmatrix} 1.78890 \\ -0.26649 \\ 0.34831 \end{Bmatrix} \times 10^{-3} + \begin{Bmatrix} 1.99119 \\ 1.88082 \\ 2.85639 \end{Bmatrix} \times 10^{-3} \\ &= \begin{Bmatrix} 3.78009 \\ 1.61433 \\ 3.20470 \end{Bmatrix} \times 10^{-3} \end{aligned} \tag{4.34.30}$$

(c) *At the end of the time step*

$$\boldsymbol{U}_2 = \begin{Bmatrix} 0.02675 \\ 0.05513 \\ 0.08306 \end{Bmatrix} + \begin{Bmatrix} 0.00378 \\ 0.00161 \\ 0.00320 \end{Bmatrix} = \begin{Bmatrix} 0.03053 \\ 0.05674 \\ 0.08626 \end{Bmatrix} \tag{4.34.31}$$

Utilising values in Eqs. 4.34.1 and 4.34.6, the velocity at end of time step will be

$$\dot{\boldsymbol{U}}_2 = \begin{Bmatrix} 0.19822 \\ 0.08323 \\ 0.17417 \end{Bmatrix} \tag{4.34.32}$$

$$\boldsymbol{P}_2 = -\boldsymbol{M}\Delta\ddot{u}_g + \boldsymbol{M}\ddot{\boldsymbol{U}}_1 + \boldsymbol{C}\dot{\boldsymbol{U}}_1 + 2\boldsymbol{F}_1 \tag{4.34.33}$$

Substituting values from Eq. 4.34.1 and given value of seismic impulse,

$$\boldsymbol{P}_2 = \begin{Bmatrix} 0.5396 \\ 0.5396 \\ 0.5396 \end{Bmatrix} + \begin{Bmatrix} 0.8061 \\ 0.1045 \\ 1.1316 \end{Bmatrix} + \begin{Bmatrix} 0.24947 \\ -0.08266 \\ 0.09770 \end{Bmatrix} + \begin{Bmatrix} 3.28064 \\ 3.48018 \\ 3.42461 \end{Bmatrix} = \begin{Bmatrix} 4.87581 \\ 4.04162 \\ 5.19351 \end{Bmatrix} \tag{4.34.34}$$

Substituting values, the acceleration at the end of time step will be

$$\ddot{\boldsymbol{U}}_2 = [\boldsymbol{M}]^{-1} \begin{Bmatrix} 4.87581 - 0.27697 - 3.50000 \\ 4.04162 + 0.10460 - 3.22814 \\ 5.19351 - 0.12282 - 3.50000 \end{Bmatrix} = \begin{Bmatrix} 1.09884 \\ 0.91808 \\ 1.57069 \end{Bmatrix} \tag{4.34.35}$$

Thus, the motion parameters at the end of time step are:

$$\boldsymbol{U}_2 = \begin{Bmatrix} 0.03053 \\ 0.05674 \\ 0.08626 \end{Bmatrix} \text{ m}; \quad \dot{\boldsymbol{U}}_2 = \begin{Bmatrix} 0.19822 \\ 0.08323 \\ 0.17417 \end{Bmatrix} \text{ m/s}; \quad \ddot{\boldsymbol{U}}_2 = \begin{Bmatrix} 1.09884 \\ 0.91808 \\ 1.57069 \end{Bmatrix} \text{ m/s}^2;$$

$$\boldsymbol{F}_2 = \begin{Bmatrix} 1.7500 \\ 1.6141 \\ 1.7500 \end{Bmatrix} \text{ N}; \quad \boldsymbol{P}_2 = \begin{Bmatrix} 4.87581 \\ 4.04162 \\ 5.19351 \end{Bmatrix} \text{ N}$$

# Chapter 5
# Planning for Aseismic Buildings

**Abstract** This chapter focuses on what constitutes a good configuration for a building structure and how to achieve it. Different types of irregularities are discussed together with their implications and methods to minimize their negative impact. The important question regarding evaluation of torsional moment in a multi-storey building is dealt with. This is followed by matters of concern to a designer such as pounding between buildings and effect of weakness in structural anatomy such as soft storeys and short columns. Measures to be taken to minimize the detrimental impact of these problems are also enumerated. Importance of load path integrity and the necessity to build in redundancy are emphasized. Some of the key factors in present day force-based design procedure are highlighted. Illustrative examples show how effect of soft storey and weak storey can be quantifiably gauged.

**Keywords** Pounding • Torsion • Soft storey • Weak storey • Force-based design • Irregularity

## 5.1 Introduction

Merely possessing inherent structural strength is not adequate for a building to successfully withstand a major seismic event. In addition to strength, the framework should meet codal limitations regarding permissible drift. Further, it should possess ductility as explained in Sect. 2.4, be stable and yet meet the challenges of aesthetic creativity. Clearly, to achieve all this we need to have a multidisciplinary integrated approach for creating aesthetically pleasing and efficient seismic resistant structures. For this reason, architects and engineers should work closely together right from the planning stage of a project because as the saying goes, *earthquakes do not respect division of responsibility between architect and engineer*.

In this chapter the discussion is focused on what constitutes a good configuration for a building structure and how to achieve it. Different types of irregularities are then discussed together with their implications and methods to minimize their negative impact. A method of evaluating torsional moment in multi-storey buildings is then explained. This is followed by matters of concern to a designer such as pounding between buildings and weakness in structural anatomy that can cause



S. Manohar, S. Madhekar, *Seismic Design of RC Buildings*, Springer Transactions in Civil and Environmental Engineering, DOI 10.1007/978-81-322-2319-1_5

infirmity such as soft storey and short columns. Measures to be taken to minimize impact of these problems are also enumerated.

Importance of load path integrity and the necessity to build in redundancy are emphasized. Some of the key factors in present-day force-based design procedure are highlighted together with their limitations. Illustrative solved examples are included.

## 5.2 Building Configuration

Configuration defines the size and shape of members of a building, their layout in plan and elevation as well as nature and location of the lateral force resisting elements. Thus it would include important aspects of architectural and structural planning that directly affect the performance of a building under seismic excitation. Examination of failures during past earthquakes has demonstrated that regular buildings perform better than irregular ones.

In practice, building configuration is invariably dictated by aesthetic considerations and guided by a desire to optimize utilization of available space. These two requirements are often at conflict. It is clear that configuration cannot be legislated upon, but the various considerations covered herein should receive careful attention by both architect and structural engineer, right at the planning stage. Even small improvements at the initial stage of planning a building can result in substantial improvement in earthquake resistance capability of a structure. Flaws in basic concepts cannot be rectified through sophisticated design.

Over the years, building footprints (i.e. total plan area of vertical supporting members such as walls and columns as a percentage of gross floor area) have reduced substantially due to stronger materials being available and advances in design and construction techniques. This calls for greater attention to be paid to efficient planning of architectural and structural systems as they are central to achieving satisfactory performance under seismic excitation. In addition, much attention needs to be focused on detailing of structures and on following sound construction practices. Past damages during an earthquake have demonstrated that many failures could be attributed to defective construction.

### *5.2.1 Architectural Planning for Earthquakes*

In general, architects shun uniform and regular structural grids as they tend to restrict aesthetic expression. On the other hand, from a structural engineer's standpoint, symmetrical structures with uniform mass and stiffness distribution are among the key requirements for satisfactory seismic performance. Thus a building design to resist earthquake damage is a compromise between aesthetic creativity,

functional demands as well as structural strength and ductility requirements; all to be achieved within a viable overall cost.

The use that a building will be put to is a major consideration in selecting its structural form. Modern offices require large open spaces which are ideal to subdivide into suitable modules with the help of lightweight partitions. On the other hand, residential premises call for smaller framing modules which are repeated over the height of a building. For the former, a central core with perimeter columns is an ideal framing layout whereas for the latter a moment frame or bundled tube structure will prove advantageous. Where moment frames are used there is a trend to use stiff exterior frames with relatively flexible interior columns designed to carry gravity loads. Exterior beams can be deeper and columns can be at closer centers without affecting floor to floor height.

The ratio of height to least lateral dimension of a building is termed as its slenderness ratio and that of its length divided by width (both in plan) as its aspect ratio. From seismic considerations, slenderness ratio of a building is more important than its absolute height. The larger the slenderness ratio, the greater is the need to check stability against overturning, impact of $P$-$\triangle$ effects, extent of storey drifts and consequence of large axial tensile and compressive forces prevailing in supporting columns. The redeeming feature of a tall building is that an increase in height generally leads to an increase in its natural period of vibration and thereby it attracts lesser inertia forces. In the horizontal plane, aspect ratio plays an important role from vibration response considerations.

From studies of building damage during past earthquakes, it is observed that medium height buildings are prone to seismic damage. Also, if the building size is very large so as to be comparable to or larger than the seismic wave length, then there is the danger that all supports may not simultaneously experience the same magnitude of ground movement which in itself can induce torsion. Finally, in a very long building, if a portion of the building experiences distress, then floor rigidity may not be adequate to distribute lateral forces among less damaged supporting elements (Arnold and Reitherman 1982). In such cases, the building should be split into two or more portions with provision of seismic gaps between them.

Architects need to bear in mind the following:

- It is important to maintain a uniform grid of columns placed orthogonally. Lack of such a layout can result in torsion in a building.
- Shear walls should be positioned in both orthogonal directions and preferably be located close to building periphery.
- Long narrow diaphragms can resonate with maximum energy containing portion of an earthquake spectrum and this can cause serious damage.
- Exit points from a building should be prominently displayed and staircases to be wide enough to accommodate sudden exodus of people wanting to exit a building.
- Architectural finishes should be well anchored to the parent structure. This is to avoid them from being separated and falling down which can cause serious injury and possibly block exit staircases with serious consequences.

**Picture 5.1** Beam and column are not aligned

- Columns and beams should be coaxial. Picture 5.1 depicts that the beam and column are not aligned.
- Improper layout of shear walls could result in domination of torsional modes of vibration causing large displacements particularly along a building periphery.
- Only a few columns should not be oriented differently from rest of them.
- For a given quality of construction, regular buildings perform well as compared to irregular ones. In addition, irregular buildings have a premium on cost and often lead to difficulties during construction.

We need to have a multidisciplinary integrated approach for efficient seismic resistant design. It should encompass an efficient structural design, meet the architectural compulsions and constructability demands and commensurate with economy. To achieve this, as mentioned earlier, it is important that an architect involves the structural engineer right from the time that structural framework is being conceptualized.

### *5.2.2 Structural Planning*

Efficient structural configuration is best achieved when lateral force resisting framework is simple and regular both in plan and in elevation and the building as a whole, along with its sub systems, is symmetrical about both orthogonal axes.

**Picture 5.2** Failure of columns supporting end wall

In addition, careful detailing of critical areas of the framework is of paramount importance. Listed below are some of the requirements which, if met, can lead to a sound structural plan.

- Maintain uniformity of stiffness, mass and strength distribution over the height of the structure.
- Since magnitude of inertia forces experienced by a building is proportional to its mass, it should be seen that the total building mass is kept to a minimum.
- Columns to be of uniform nominal sizes and preferably all columns should be oriented in the same direction along a particular axis.
- Beams and columns should be coaxial with beam width being preferably less than that of the face of a column into which it frames.
- Shear walls should extend from foundation to their top level along a single vertical axis. There have been frequent failures because shear walls were discontinued below first floor level. Picture 5.2 depicts failure of columns supporting an end wall that is stopped at an intermediate level
- Shear walls to be suitably located along both orthogonal directions.
- Parapet walls and large cornices to be firmly anchored to their main supporting structure.
- Adequate ties must exist so that the structure behaves as an integral unit and redundancy should be incorporated into the structural framing.
- Center of mass and center of rigidity to virtually coincide.

- Provide maximum lateral resistance through members located along outermost periphery.
- Foundations, which are not resting on rock, should be tied together either at plinth level or at foundation level.
- Multiple openings in slabs should not be located close to each other.
- A stiff structure is preferred over a flexible one. However a balance has to be achieved between the benefit of a stiff structure limiting excessive displacements and its demerit of attracting larger inertia forces.
- Nonstructural elements should be either separated from the lateral load-carrying system or alternately totally integrated with it.
- Columns should be continuous throughout, without offsets.
- Aim at avoiding abrupt changes in vertical geometry.
- Columns should be able to accommodate additional short-term dynamic loads without precipitating failure.
- Avoid large column spacing.
- Avoid floating columns and tapered columns with a smaller section at its base than at the top. Picture 5.3 depicts floating columns and that the columns are not aligned.

For a properly engineered earthquake-resistant structure, it is important to have a sound building layout with a simple structural framework. Apart from clearly identifiable load paths, parallel paths should exist to transfer loads so as to create a structure with redundancy. Meticulous detailing, a strong foundation and good quality of construction are equally important. One strategy is to ensure that the structure is robust, i.e. it is not susceptible to distress in key structural elements (such as transfer girders) or to small changes in distribution of loads. Thus there has to be a trade-off between reduction of risk and escalation of cost.

Desirable structural attributes are listed above. While efforts should be made to meet the same, this is difficult to achieve in practice. For any deviation from the above, it calls for the structural engineer to pay increased attention to member design and details.

### *5.2.3 Irregularity*

Irregularity can arise due to many factors such as nonuniform distribution of mass, or strength or stiffness; sudden change in geometry; or interruption in a load path which can result in ductility demands getting concentrated in weak areas. Clearly, these should be avoided. Assessment of damage during past earthquakes has demonstrated that buildings with symmetry in structural configuration in both plan and elevation and without significant discontinuities in stiffness and strength behave in a much better way. An irregularity in a building brings in uncertainties in design and calls for a more detailed analysis which is cost intensive.

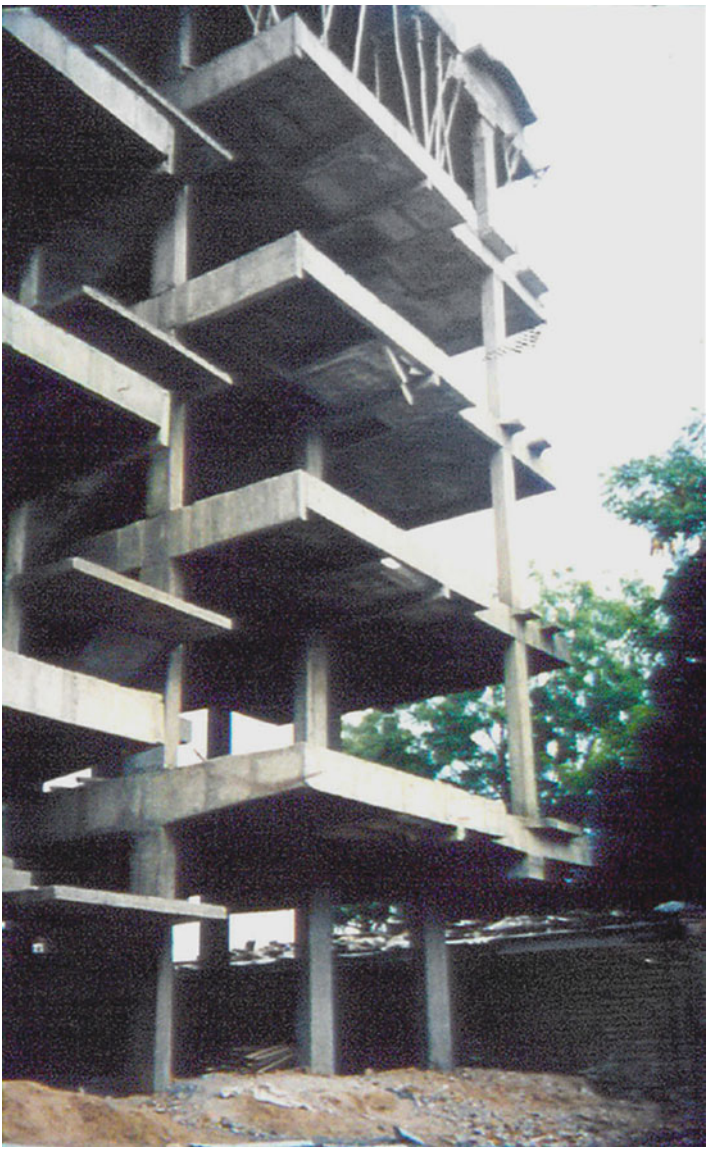

**Picture 5.3** Presence of floating columns and columns misaligned

#### 5.2.3.1 Horizontal Irregularity

There are many forms of horizontal irregularity which are widely covered in literature. Some of the key aspects are highlighted below:

(a) A figure is considered to be convex when any two points within it can be connected by a straight line which lies wholly within the figure. Such a configuration invariably promotes direct load paths and demonstrates superior performance during an earthquake. A building plan which is concave (Fig. 5.1a) often results in horizontal irregularity.

(b) Buildings with plan shapes such as L,Y, U, H etc. (Fig. 5.1b) are popular with architects as they encourage good lighting and ventilation and are ideal for hotels with perimeter rooms. These shapes lead to re-entrant corners where building wings meet. Individual wing tends to vibrate with different amplitudes which can also be out of phase with one another. This leads to differential motion between the wings and damaging stress concentrations could occur.

(c) There is a need to differentiate between geometric symmetry and seismic symmetry. Having geometrical symmetry in a building plan is not enough insurance against horizontal irregularity. For instance, a symmetrical crucifix shape of a building plan as shown in (Fig. 5.1c) is considered irregular since responses of its wings to a particular seismic motion are not identical which will create local stress concentrations.

(d) In T-shaped layouts the situation is compounded by planners preferring to locate large openings at re-entrant corners to accommodate lift shafts and/or stairwells to serve both adjoining wings. Such openings weaken the structure where it would be heavily stressed during an earthquake. Where such shapes are unavoidable, the resulting unfavourable position can be slightly redeemed by one of the following remedies.

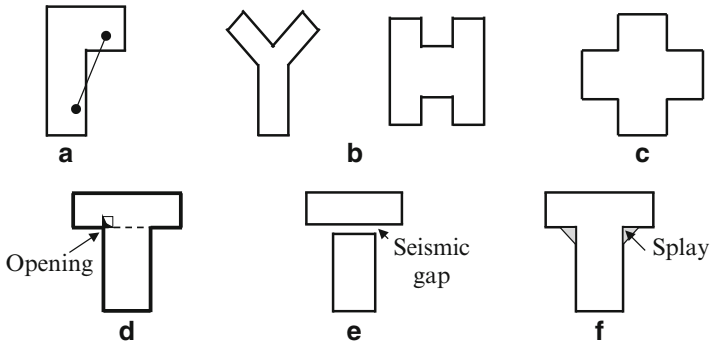


**Fig. 5.1** Horizontal irregularity. (**a**) Concave layout. (**b**) Re-entrant corners. (**c**) Seismic asymmetry. (**d**) Wings tied together. (**e**) Wings separated. (**f**) Splays provided

- Tie the different wings together (Fig. 5.1d).
- Separate the wings with a physical gap which should be wide enough to prevent pounding (Fig. 5.1e). When such separation is provided, each individual wing should be designed to resist full inertia forces commensurate with its mass.
- Provide a splay between adjoining wings (Fig. 5.1f).

(e) Horizontal irregularity will exist if there is significant difference in stiffness between different portions of a diaphragm at a given level. Such irregularity can lead to an alteration in distribution of lateral forces among vertical supporting elements thereby creating torsion (Arnold and Reitherman 1982)

(f) Other forms of horizontal irregularity are:

- A cut back in a rigid diaphragm (Fig. 5.2a). Large penetrations in a diaphragm, if unavoidable, should be located and detailed carefully such that they do not jeopardize its sound performance.
- A non-orthogonal vertical supporting system (Fig. 5.2b).
- Unsymmetrical location of shear walls (Fig. 5.2c).
- Imbalance in strength and stiffness along building perimeter which can have serious consequences due to resulting torsion (Fig. 5.2d).
- Irregularity in layout of infill walls between columns.

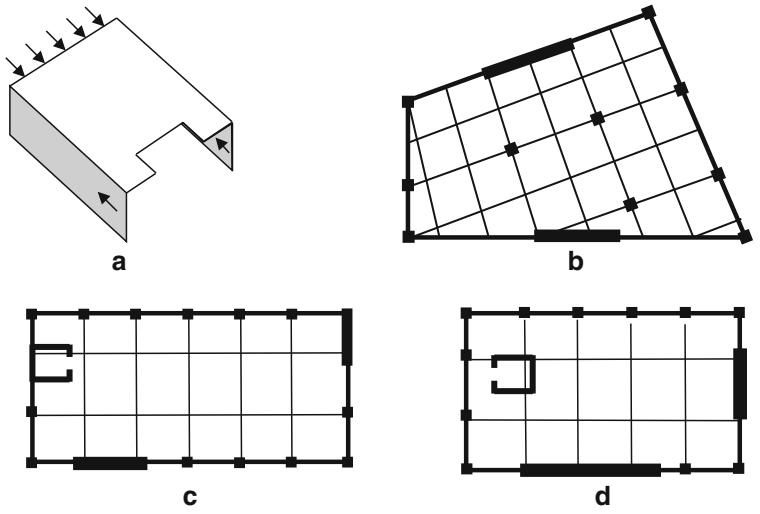


**Fig. 5.2** Other forms of horizontal irregularity. (**a**) Diaphragm cut back. (**b**) Non-orthogonal grid. (**c**) Shear walls – asymmetrical. (**d**) Perimeter strength imbalance

### 5.2.3.2 Vertical Irregularity

Vertical setback in a building can be looked upon as a vertical re-entrant angle around which loads are forced to flow. This is termed as geometrical irregularity (Fig. 5.3a). It will inevitably lead to stress concentrations at notches which will become focal points for potential damage during a major seismic event. It could also prevent distribution of inelastic seismic response over building height as is computationally envisaged

Vertical irregularity is often the result of:

- Sudden change in strength in elevation. Such changes can attract plastic deformations (Fig. 5.3b). This is apparent in Picture 5.4 which shows a single column supporting heavy superstructure load.
- Non-uniform distribution of mass even when structure is geometrically symmetrical, e.g. providing a swimming pool at an intermediate storey (Fig. 5.3c). If mass irregularity is small, it can be compensated to some extent by altering stiffness of supporting columns in the storey such that drift ratio between relevant storeys is not unduly high (Jain et al. 2005)
- Intermediate storey height or stiffness or both being substantially different from that of a storey above or below it (Fig. 5.3d).
- Introduction of a mezzanine floor over part of the building area (Fig. 5.3e).

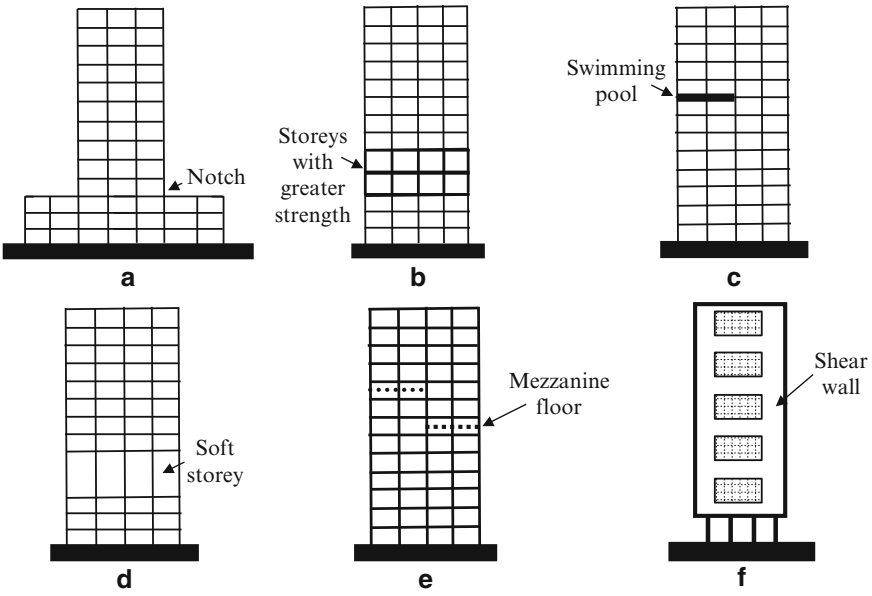


**Fig. 5.3** Vertical irregularity. (**a**) Geometrical irregularity. (**b**) Strength irregularity. (**c**) Mass irregularity. (**d**) Stiffness irregularity. (**e**) Mezzanine floor over part area. (**f**) Shear wall terminated at intermediate level

**Picture 5.4** Single column supporting heavy load – recipe for distress

- Shear walls not continuing from top right up to their foundations but being discontinued midway – say below first floor level. A shear wall is basically provided to transmit lateral loads from diaphragms to the supporting ground. Discontinuing a shear wall at mid height contradicts this intended purpose and it should be avoided (Fig. 5.3f).
- Irregular distribution of infill walls in elevation.
- Sudden reduction in length of a shear wall. For the building as a whole, this may not present itself as an apparent offset. Effect of mass and stiffness irregularities have been evaluated in illustrative example *Ex* 5.7.1.

## 5.3 Pounding

Under earthquake excitation, buildings sway laterally. Invariably, the dynamic characteristics of adjacent buildings being different, they tend to vibrate out of phase. If the gap between adjoining buildings (or between two portions of the same building) is small, then adjacent buildings could collide against each other which is termed as pounding. Resulting damage can be only local or it could also be quite severe particularly when the floor of one building hammers into columns between floors of an adjoining structure (Fig. 5.4). Damage due to pounding has been reported from metropolitan areas around the world, and even building collapses attributable to pounding have been reported in some cases.

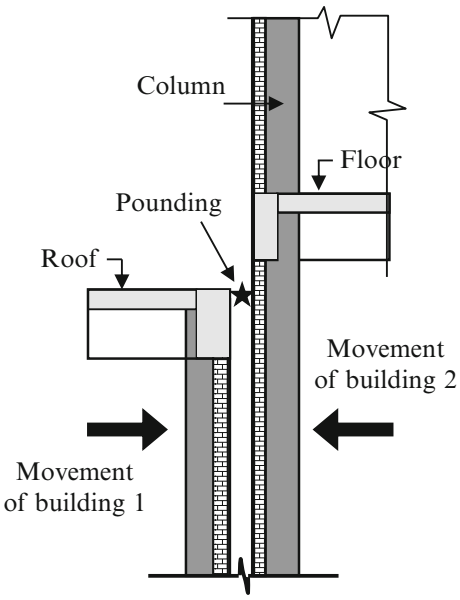


**Fig. 5.4** Pounding

Pounding is a highly complex phenomenon and resulting damage depends on many factors such as masses that impact during collision, location of impact and extent of momentum transfer. Pounding can occur at superstructure level or at mote level. It leads to an exchange of an enormous amount of kinetic energy among pounding buildings and alters their mode shapes and inertia forces at various levels. The easiest solution to this problem is to provide a gap (termed seismic gap) between concerned buildings. Prescribed quantum of separation to preclude pounding varies from one code/guideline to another.

Two of these are:

(a) It is stipulated in IS 4326 (BIS 2001) that buildings with height exceeding 40 m, the separation between adjoining buildings should not be less than the sum of their dynamic deflections at any level. The gap for pounding between two adjacent buildings or between parts of the same building with a separation joint between them should be $R$ times the sum of storey displacements evaluated with a partial load factor of 1.0. When floors of adjacent buildings are at same level, the multiplication factor can be $R/2$ (BIS 2002a).

(b) It can be assumed that that there will be incoherence of multimode response as it is unlikely that adjoining buildings will experience maximum response of all modes simultaneously. Taking advantage of this, the separation between buildings at any height could be the square root of the sum of the squares of estimated lateral responses of concerned two buildings (relative to the ground) at location being investigated. This value should not exceed 4 % (FEMA 273 1997) of height of likely impact above ground.

Total lateral displacement shall be computed taking into account inelastic displacement, $P$-$\triangle$ effect, torsion and soil–structure interaction whenever they enhance the response. Gap between buildings may have to be larger when adjacent structures are torsionally flexible and have similar vibration periods with torsionally coupled modes.

## 5.4 Horizontal Torsion

Structural members always have some degree of axial and bending stress when they are subjected to an earthquake which can induce a large amount of torsion. Hence an area of practical interest is to analyse the effect of torsion combined with axial and flexural stresses. Torsion could be static or dynamic. In addition, some open-ended members could experience warping torsion. These forms of torsion as well as dynamic inelastic torsion are highly complex subjects and are outside the scope of this book. Herein, the computations are limited to evaluation of static elastic torsion which is an approach that is commonly used in practice.

### *5.4.1 Torsion Computation for a Multi-storey Building*

At a given floor level, the resultant of lateral inertia forces may act eccentric to the centre of rigidity and as a result generate a torsional moment causing the structure to rotate. Centre of rigidity for a single-storey frame is a point through which the resultant of restoring forces acts when motion is purely translatory. This location is easy to determine since center of rigidity, shear center and center of twist are the same. For a multi-storey building (Fig. 5.5a) in a strict sense, the centre of rigidity is difficult to define. For obtaining floor torques, generalized centre of rigidity for each floor can be determined. For calculating the twisting moment at a floor in a multi-storey building, one of the following two approaches, indicated by Tso (1990) and Jain (2003), may be adopted.

#### 5.4.1.1 By Isolating a Floor (Option 1)

Consider a free body diagram of floor $i$ of a multi-storey building frame as shown in Fig. 5.5b. The building has $N$ floors and $n$ number of frames across $x$-axis, and it does not rotate. For simplicity, only a single bay width is considered with eccentricity only along $x$-axis and seismic forces $Q_i$ acting along $y$-axis. From compatibility of lateral forces, the force in frame $j$ at floor $i$ will be

$$F_{ji} = V_{j,i} - V_{j,i+1} \tag{5.1.1}$$

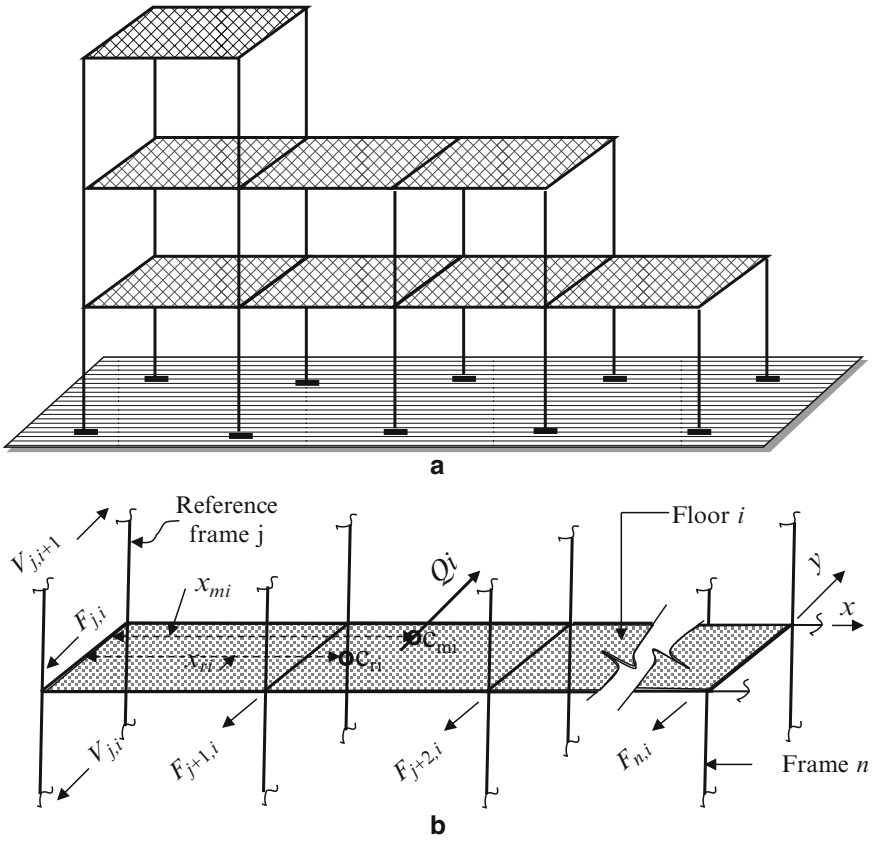


**Fig. 5.5** Torsion evaluation (option 1). (**a**) Multi-storey building frame. (**b**) Free body diagram – floor *i*

and

$$\sum_{j=1}^{n} F_{ji} = Q_i \tag{5.1.2}$$

Taking moments of forces $F_{ji}$ about the reference frame, its distance to generalized centre of rigidity $c_{ri}$ at floor *i* is given by

$$x_{ri} = \frac{\sum_{j=1}^{n} F_{ji}.x_{ji}}{Q_i} \tag{5.1.3}$$

Taking moments of inertia forces at floor $i$ about the reference frame, its distance ($x_{mi}$) to centre of mass ($c_{mi}$) at this floor can be readily obtained.

Load eccentricity is

$$e_i = (x_{mi} - x_{ri}) \tag{5.1.4}$$

and torque at floor $i$:

$$T_i = Q_i . e_i . \tag{5.1.5}$$

Torsional moment at storey $i$ is given by

$$M_{ti} = \sum_{i}^{N} T_i \tag{5.1.6}$$

$V_{j,i}$ : storey shear in frame $j$ at storey $i$
$V_{j,i+1}$ : storey shear in frame $j$ at storey $i+1$
$V_i$ : shear in storey $i$
$F_{ji}$ : storey force in frame $j$ at level $i$
$Q_i$, $Q_k$ : total inertia force at storeys $i$ and $k$, respectively
$M_{ti}$, $M_{tk}$: torsional moment at storeys $i$ and $k$, respectively
$N$ : number of storeys
$T_i$ : floor torque at storey $i$
$n$ : number of frames in the direction of inertia forces $Q$
$x_{mi}, x_{ri}$ : distance of centre of mass and center of rigidity respectively from reference frame at storey $i$
$x_{ji}$ : distance of storey force $F_{ji}$ and also storey frame shear $V_{ji}$ from reference frame
$x_{mk}$ : distance of centre of mass from reference frame at storey $k$
$x_{sk}$ : distance of shear centre from reference frame at storey $k$

#### 5.4.1.2 By Isolating a Storey (Option 2)

Consider a multi-storey structural framework as shown in Fig. 5.6a. Its free body diagram for storey $i$ is shown in Fig. 5.6b. Consider a similar free body diagram for storey $k$. Storey shear for storey $i$ can be written as

$$V_i = \sum_{k=i}^{N} Q_k \tag{5.2.1}$$

Let $x_{si}$ be the distance of storey shear centre from the reference frame for storey $i$. It follows that

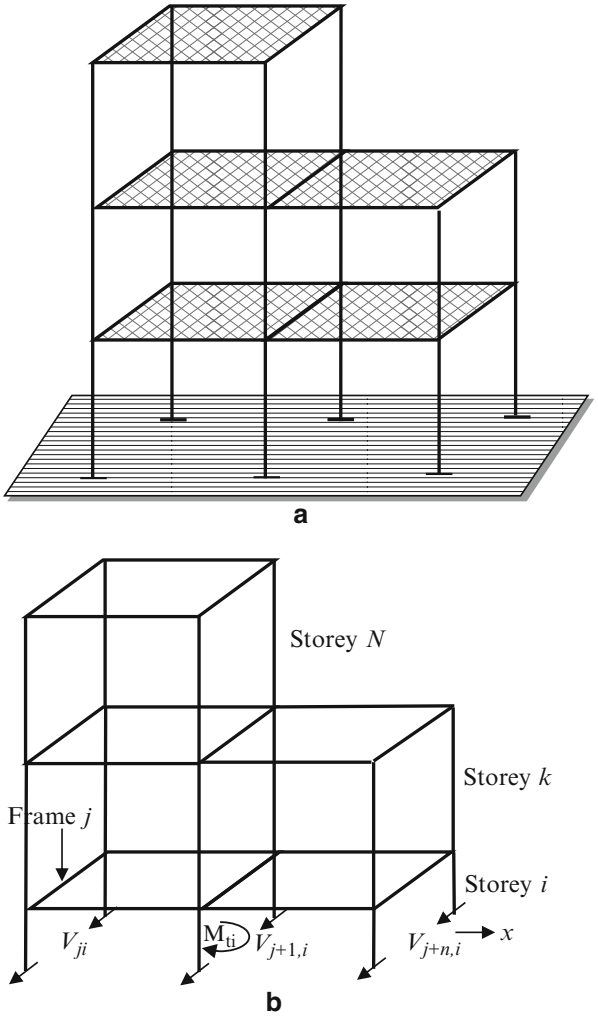


**Fig. 5.6** Torsion evaluation (option 2). (**a**) Multi-storey frame. (**b**) Free body diagram – storey *i*

$$x_{si} = \frac{\sum_{j=1}^{n} V_{ji}.x_{ji}}{V_i} \tag{5.2.2}$$

The moment required to maintain torsional equilibrium will be,

$$M_{ti} = \sum_{k=i}^{N} Q_k \{x_{mk} - x_{si}\} \tag{5.2.3}$$

Introducing $V_i$ from Eq. 5.2.1 into Eq. 5.2.3,

$$M_{ti} = \sum_{k=i}^{N} Q_k x_{mk} - V_i x_{si} \tag{5.2.4}$$

In the above equation, first term on the right represents a moment of all inertia forces (at and above storey $i$) about the reference frame. Hence, distance of equivalent centre of mass at storey $i$ from the reference frame will be

$$\overline{x}_{mi} = \frac{\sum_{k=i}^{N} Q_k . x_{mk}}{V_i} \tag{5.2.5}$$

Substituting value of $V_i$ from Eq. 5.2.1, torsional moment at storey $i$ is given by

$$M_{ti} = V_i \left[\overline{x}_{mi} - x_{si}\right] \tag{5.2.6}$$

Tso (1990) has shown that both methods yield the same result. For computer based analysis, the procedure as per Sect. 5.4.1.2 is considered to be more convenient. The evaluation of floor static torsional moment in a multi-storey building by both the above methods is illustrated in *Ex* 5.7.2.

### 5.4.2 *Design Forces Including for Torsion*

For design purposes IS 1893 stipulates that at level $i$, design eccentricity $e_d$ to be considered should be one of the following two, whichever gives the larger response.

$$\text{Condition 1}: \quad e_d = 1.5e_s + 0.05b_i \tag{5.3.1}$$

$$\text{Condition 2}: \quad e_d = e_s - 0.05b_i, \tag{5.3.2}$$

where $e_s$ is static eccentricity.

This implies that torsional moment at level $i$ would then be a sum of:

1. Torque $M_{ti}$ enhanced by a factor of 1.5, perhaps to allow for its dynamic amplification during possible coupling of torsional and translational modes of vibration
2. Additional accidental torsion $T_a$ by considering that the centre of mass at a floor is offset horizontally by 5 % of the horizontal dimension at a given floor level.

Thus $T_{ai} = 0.05.Q_i b_i$ where $b_i$ is the horizontal dimension of floor $i$ measured perpendicular to direction of inertia forces. This margin is provided possibly to account for many factors such as variation between assumed and actual weights, error in estimation of distribution of dead loads and imposed loads, inaccuracies in evaluating structural stiffness of components, random variation of torsional ground motion, etc.

To account for this requirement, Goel and Chopra (1993) have demonstrated an approach which may be adopted in a computer-based analysis using option in Sect. 5.4.1.2. This approach is broadly as under:

(a) Analyse the building as a 3D frame with lateral forces $Q_{ji}$ acting at centre of mass on all floors $i$ ($i = 1$ to $N$) and let the response be $R_1$. This response (either force or deformation) will relate to the condition when static eccentricity is taken into account along with lateral translation.
(b) Analyse the building with lateral forces $Q_{ji}$ acting at centre of mass on all floors $i = 1$ to $N$. However, in this case the structure is assumed to be restrained laterally by rollers (guided supports) such that floors do not rotate (Fig. 5.7). Let response quantity be $R_2$. This response will relate to a situation that lateral loads were applied at centre of rigidity of each floor since rotation of floors was disallowed.
(c) Evaluate the difference in above two responses (i.e. $R_1 - R_2$). This will provide the response due to static eccentricity. In order to enhance by 50 % the static eccentricity portion of response $R_1$, a value equal to $0.5(R_1 - R_2)$ has to be added to response $R_1$.
(d) Analyse the building for floor torques equal to $0.5b_i\ Q_i$ acting on it. Let the solution be $R_3$.

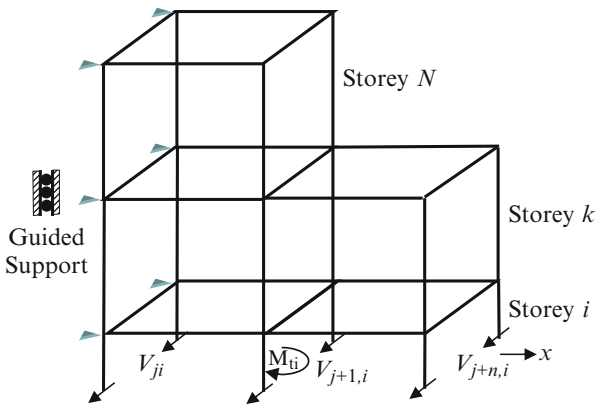


**Fig. 5.7** Frame held in position by rollers

Design torsional moment which will satisfy Eqs. 5.3.1 and 5.3.2 will be the larger of the two responses $R_a$ and $R_b$ given below:

$$(1) \quad R_a = R_1 + 0.5\ (R_1 - R_2) \pm R_3 \tag{5.3.3}$$

and

$$(2) \quad R_b = R_1 \pm R_3 \tag{5.3.4}$$

### 5.4.3 *Effects of Horizontal Torsion*

Analytical studies suggest that torsional effects are significant when uncoupled lateral translational and torsional natural frequencies are close. Effects of torsion are normally taken care of by static augmentation of member forces obtained from a 2D dynamic analysis. It is imperative that torsional effects are carefully evaluated because in present-day buildings, structural members are very slender with small safety margins.

Following aspects may be borne in mind:

- Torsion tends to distort the structure causing large displacement demands on vertical columns farthest away from center of rigidity.
- Perimeter columns will be subjected to biaxial displacements which will be more severe in corner columns. For this reason, corner columns should be conservatively designed with proper confinement of concrete and provision of ductile detailing.
- When lateral and torsional motions are strongly coupled, i.e. their frequencies are close or there exists a large eccentricity, at least three degrees of freedom per floor should be considered in the analysis.
- Where significant torsion is anticipated, the designer should preferably adjust stiffness of supporting members in order to reduce such torsion instead of designing for the high value.
- Effect of torsion is normally evaluated based on an elastic system with equilibrium and displacement compatibility.
- For a member subjected to torsion, diagonal tension exists on all four faces and hence top legs of stirrups have to be properly anchored.

An illustration of sharing of lateral forces among vertical members due to torsion is presented in *Ex* 5.7.1.

## 5.5 Structural Anatomy

The form, positioning and detailing of the structural skeleton requires careful consideration since it has an important bearing on performance of the structure during an earthquake. It will be observed from Fig. 5.8a, b that total length of shear walls in both layouts is identical. However alternative (b) is the superior option from seismic considerations because of its capacity to resist much greater torsion with shear walls being located along the periphery.

The structural skeleton must work in unison and not as a conglomerate of loose parts. For instance, even when the main frame is intact, lives can be lost due to canopies falling off, portions of cladding dropping down from a height, window frames separating and tumbling down and collapse of a staircase thereby blocking exit paths. Hence projecting parts should be well anchored to the main structure. Herein, different aspects are discussed to know how a structural form affects structural performance.

### *5.5.1 Soft and Weak Storeys*

A soft storey could occur at any floor. From architectural considerations, stiffening walls between columns are often removed at grade level for public access to reception lobbies or for other similar reasons or to provide for parking space which is often a functional necessity, particularly in an urban environment. This creates a sudden and significant reduction in lateral stiffness resulting in formation of a soft storey. Unfortunately, this occurs at a level where gravity and inertia loads from superstructure are highest. As a result, large deformations can occur causing

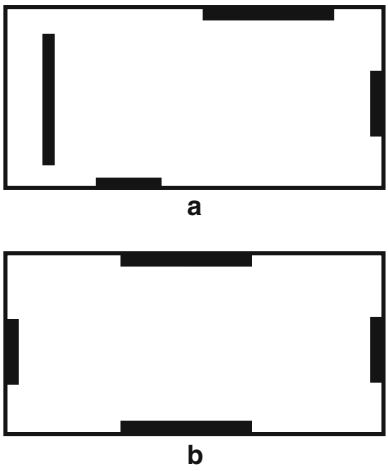


**Fig. 5.8** Location of shear walls. (**a**) Unfavourable. (**b**) Favourable

**Picture 5.5** Collapse of a soft storey

**Picture 5.6** Distress due to a soft storey

substantial $P$-$\Delta$ effects which can lead to plastic hinge formation in columns. If these members do not have adequate ductility, they could trigger progressive collapse of an entire storey – ref. Picture 5.5 – collapse of a soft storey. Also Picture 5.6 depicts the distress in a soft storey of a frame building with brick infill.

A similar situation arises if many lateral stiffening members are removed at an intermediate storey. As per IS 1893 (BIS 2002a), a storey may be labelled as a soft storey when its lateral stiffness is less than 70 % of that of the storey above or less than 80 % of average lateral stiffness of three storeys above it. On the other hand, a storey is termed as a weak storey when lateral strength of a storey is less than 80 % of that of the storey above. Thus soft storey qualification is based on stiffness irregularity, and a weak storey is a statement of capacity discontinuity.

In a complex frame it is sometimes difficult to determine stiffness of storeys. In such an event the storey drift indices, which are often a part of a computer output, may be used to determine existence of a soft storey. It should be noted that if we use drift indices, which are in terms of reciprocal of stiffness, then comparison factors will also need to be reciprocals. For evaluating drifts, elastic displacements ($\delta_i$) may be used as an approximation although, in fact, inelastic effects should be included. If drift index of storey $i$ is $(\delta_i - \delta_{i-1}) / h_i$, then as an approximation, this storey can be considered as a soft storey if either of the following two conditions are satisfied:

$$0.7\left[\frac{(\delta_i - \delta_{i-1})}{h_i}\right] > \left[\frac{(\delta_{i+1} - \delta_i)}{h_{i+1}}\right] \tag{5.4.1}$$

or

$$0.8\left[\frac{(\delta_i - \delta_{i-1})}{h_i}\right] > \frac{1}{3}\left[\frac{(\delta_{i+1} - \delta_i)}{h_{i+1}} + \frac{(\delta_{i+2} - \delta_{i+1})}{h_{i+2}} + \frac{(\delta_{i+3} - \delta_{i+2})}{h_{i+3}}\right] \tag{5.4.2}$$

Buildings, with a soft storey, require to be designed and detailed with much caution as they are the target of seismic damage. From among design options proposed in IS 1893, the preferred one would be to design the columns for storey seismic demand and provide shear walls symmetrically in both directions well away from building center and design them for 1.5 times storey shear. *Examples* 5.7.4 and 5.7.5 demonstrate how to check whether a soft storey or a weak storey exists.

### *5.5.2 Short Column*

A short column, as the name implies, is a column that is restrained from lateral movement over a part of its height. This could occur when nonstructural elements restrain lateral deformation of a column over part of its height. It could also occur due to structural reasons as described below. These are termed as captive columns and the terms *short* and *captive* are used interchangeably. Short columns invariably result from architectural requirements such as:

- Provision of part height walls between columns to accommodate slit windows to let in more natural light. A typical case is where such windows are provided for a small height of a basement wall that projects above ground level (Picture 5.7).

**Picture 5.7** Part height wall in few bays – short columns formed

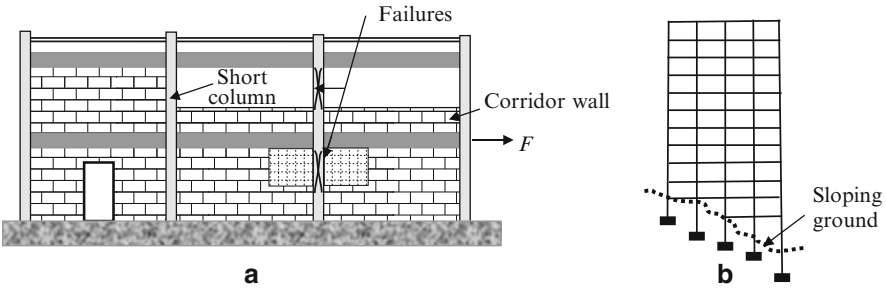


**Fig. 5.9** Short columns

- Provision of a watchman's cabin between columns in only a few bays at grade level. Such walls often stiffen the column over a part of its storey height. If infill is strong it may lead to shearing of the column top especially when infill is located only on one side of the column.
- Part height infill walls provided along corridors (Fig. 5.9a).
- Nonstructural elements subsequently added in some of the bays which impose a restrain on deformation profile of adjoining columns
- When perimeter beams are made deep over a bay to avoid a lintel over the window. There can also be structural reasons such as:
- Foundations being at different levels (Fig. 5.9b).
- Height of a column is broken by a beam supporting a stair landing or the introduction of a mezzanine floor.

- Perimeter columns of a building are supported off basement walls whereas the interior columns are much longer since they take off from the basement floor. This causes perimeter columns to carry much larger seismic forces.

In stiffness calculations, the full height of a column is considered. However, if a column is later stiffened either by deep spandrel beams or by intermediate bracing or by partial height infill walls or by stairways etc, then it's stiffness increases, with the result that it will attract larger shear forces which can result in shear failure. As shown in Fig. 5.9a, assume that lateral seismic shear at first floor level of a rigid slab is $F$ which is to be shared by four identical columns. If there were no openings, the shear carried by each column would be $0.25\,F$. However if one of the columns is stiffened by brickwork over only half its height, then it will behave as a short column with a height equal to half that of other columns.

Since lateral stiffness of these columns varies as the cube of their effective height, the stiffness of the short column will be eight times that of other columns. Since displacement of all columns at rigid first floor slab level has to be same, it will result in the short column carrying a load of $8\,F/11 = 0.727\,F$, i.e. an increase of nearly 290 %. There are many cases of severe damage to columns attributable to short column effect, and it is prudent to avoid them. When unavoidable, then the following care is advisable:

- Provide a sealed gap between brick infill and columns. In such an event, the infill wall may have to be confined to overcome out-of-plane stability problems.
- If a column supports a mezzanine floor, then it is advisable to design the column to take into account short column effect. In addition it is prudent to protect it with confining reinforcement over its full height.
- Where ground is sloping, shear walls may be provided to sustain lateral shear.

### *5.5.3 Floating Column*

A floating column can rest on an intermediate span of a continuous girder (Fig. 5.10a) or may be supported off the cantilever end of a continuous beam as shown in Fig. 5.10b. Invariably the latter type of floating columns is being used on projects primarily because they provide more circulation space at grade level. Their use should be discouraged in normal course, and they should preferably be avoided altogether under seismic conditions. There are problems associated with design of such columns and a few are enumerated below:

- Supporting beam is subjected to heavy shear and bending moments which can travel well beyond the first column support.
- Detailing of the beam–column joint is an arduous task.
- Codal inertia forces are much lower than what the building could experience during a major earthquake. Under such circumstances, structural integrity of the column and its supporting framework is difficult to evaluate and provide for.
- Effects arising from deflection of supporting beam is an area of serious concern.

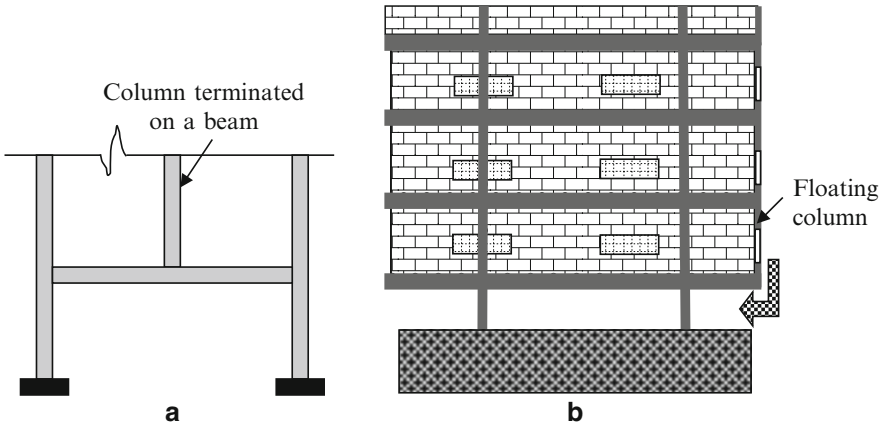


**Fig. 5.10** Floating columns

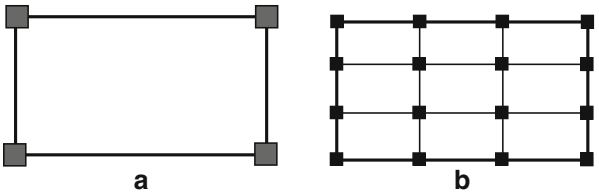


**Fig. 5.11** Redundancy. (**a**) Redundancy absent. (**b**) Redundancy present

- Evaluating the stability of such construction under vertical and bidirectional horizontal seismic acceleration is a complex exercise.
- A clear load path is not available which leads to heavy stress concentrations.
- Even ductile detailing at beam–column joint may not prove to be adequate.

### *5.5.4 Load Path Integrity and Redundancy*

An important consideration in seismic design of frames is to ensure redundancy to preclude the danger of an entire structure collapsing because of failure of a single lateral load-resisting element. Although the definition of redundancy is fuzzy, it is generally understood that a framed structure possesses redundancy when it is able to transmit lateral loads to the foundation through frames along multiple vertical lines. The difference between a structural framework that has no redundancy and one that has is brought out in Fig. 5.11a, b.

If redundancy is present, then yielding of a member at one location is unlikely to result in total collapse of the structure. In effect, presence of redundancy aids in localizing a failure and improves the reliability of a structure. While the concept

of redundancy in a seismic environment is generally understood, it is difficult to quantify it (Bertero and Bertero 1999). This is because it is not enough to incorporate only additional strength but to also have extra rotation and displacement capacity in members to withstand a major seismic event.

Nonstructural members performing as structural members during a major seismic event is not redundancy. The primary frame itself must have redundant load paths such that the structure can ride over local damage. The oft-quoted excellent example of redundancy is a spider's web which does not collapse even when a substantial number of its strands are broken. Structurally, one method to incorporate redundancy is to use dual forms of lateral load-resisting systems because dual systems, in most cases, possess redundancy (FEMA P 750 2009).

In codal provisions, presence of redundancy is taken into account by way of a force reduction factor. While redundancy is essential, it is not a sufficient safeguard against progressive failure. A force path identifies the route along which members will receive and transmit forces right from the location where they originate up to the resisting soil. A designer must ensure that all along such paths, the members are able to sustain these forces and deformations and transmit them to the next member along the path.

In the primary horizontal load resistance path, there should not be any lack of continuity which can be caused by improperly designed split level floors, missing collectors, discontinuous chords as a result of cut backs, inadequate connections or large openings pierced for accommodating stairways. A diaphragm plays an important role in the transfer of lateral forces, and hence, its continuity is paramount. Particular care should be taken for the proper transfer of loads between joints in precast elements, between precast and cast-in-situ portions and at locations where the transfer of shear takes place between diaphragms and their supporting walls. A few options to enhance redundancy are:

- Use closely spaced columns.
- Avoid structural discontinuities that can lead to local stress concentrations.
- Avoid large eccentricities.
- Divide the structure into independent load-resisting systems.
- Provide structural fuses such that horizontally spreading progressive collapse cannot be transferred from one section to another.
- In a tall building, provide strong floors at intermediate levels such that they can withstand the load of falling debris from failure at upper floors.
- Columns, their foundations and connections between them should be provided with additional design margins to cater to enhanced loads if a neighbouring column yields. Also it should be ensured that the soil bearing pressure does not exceed its limiting value.
- Two-way slabs are preferred to slabs spanning one way.
- When using flat plate floor systems, provide a strong perimeter frame and connecting spandrel girder.
- Provide adequate shear rebars in coupling beams and around openings in shear walls.

- Make the structure continuous with monolithic joints. This helps to generate more shear and thrust routes.
- Corner columns should be tied in two orthogonal directions to the structure they support.
- Thicker footings will improve resistance to punching failure at column connections.
- Floor slabs should be tied to walls.
- If due to site constraints it is not possible to maintain structural continuity for the entire building, then the structure can be subdivided into blocks with continuity in each block. Such blocks can be connected by flexible access ways, but there should be sufficient space between the blocks to avoid pounding.

After design work is complete, a check could be made regarding the structural framework's ability to bridge over potential damage areas. One of the tools for this is to remove, one at a time, key structural members that carry the highest force or shear in a storey, from locations where damage is most likely, and study its impact on the strength and stability, both locally and globally. If removal of such a member leads to substantial reduction in storey strength or an extreme torsional irregularity is created, then the structure needs to be strengthened. However, under such conditions large deformations from inelastic behaviour and damage short of precipitating collapse may be acceptable within reason.

### *5.5.5 Staircases*

The shape and location of a staircase is often dictated by architectural and functional considerations. Its detailing calls for special attention such as:

(a) Presence of a stairwell in one corner of a building will lead to structural asymmetry in an otherwise symmetrical structure.
(b) External staircases supported off cantilever brackets call for great care both in design and detailing (Fig. 5.12a). The supporting cantilever members should be adequate against both horizontal and vertical inertia forces. These members break the clear height of supporting column and could generate a short column. Picture 5.8 depicts the failure of a staircase – a lifeline for survival.
(c) If a flight of stairs rests on columns at an intermediate level, the columns need to be stiffened with infill walls. Secondly, where there is a change of slope as when a flight merges with a landing, the member should be appropriately confined.
(d) When staircases are rigidly tied to main frames, they act as braces and can attract heavy axial forces because they inhibit storey drift. Since they are not intended to be a part of the main lateral load-resisting system, they are normally not designed for such forces and partial or total collapse of a staircase could result. In such an event exit paths can get blocked trapping people within the building and also may prevent fire fighters from reaching upper floors. To overcome this defect, two easy options are available:

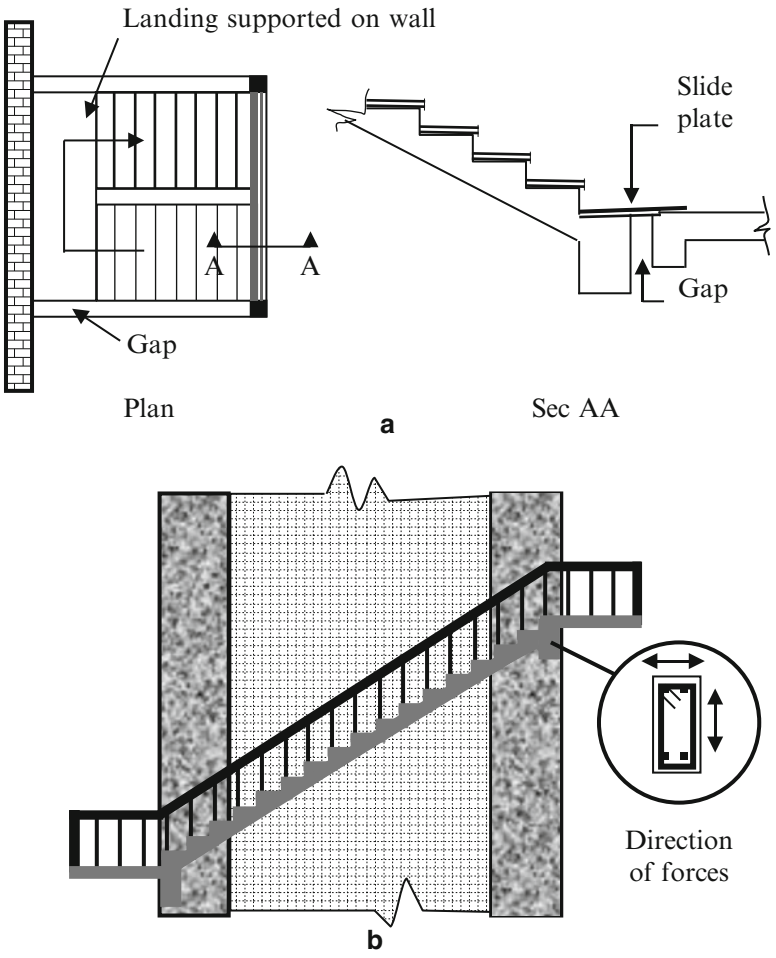


**Fig. 5.12** Staircases. (**a**) Dog – legged stairs. (**b**) Staircase supported on brackets

1. When an intermediate landing of a staircase is supported on a wall with the other ends resting on beams spanning between columns, a clear gap can be provided on three sides of the stairs as shown in Fig. 5.12a. This separates the stairs from the rest of the structure. At landings, the gap can be covered with a tread plate. Thus the staircase is able to slide and avoid attracting axial loads. The sliding arrangement should be such that it will allow inter storey drift in any direction.
2. Enclose the stairwell with rigid walls on at least two sides as suggested in IS 4326 (BIS 2001). These walls should extend from foundation level up to full height of the staircase. This will preclude the staircase from functioning as a bracing member.

**Picture 5.8** Staircase failure

## 5.6 Force-Based Design

Earthquakes are often described as minor, moderate or severe in intensity. While minor earthquakes may occur frequently, the severe ones could be rare, say even once in 500 years. This begs the question whether buildings need to be designed to remain undamaged under such rare earthquakes whose probable frequency of occurrence is well beyond design life of the building itself. On the other hand, it must be remembered that the one in 500 year earthquake could occur the next day.

### *5.6.1 Design Philosophy*

Faced with this dilemma, earthquake design philosophy that evolved and which is the basis of design today can be stated as under:

1. Minor but frequent shaking should not cause damage to primary load carrying members, but other members may sustain damage that could be repaired at small cost.
2. Moderate but occasional shaking may cause repairable damage to primary load carrying members.
3. Under strong but rare shaking, primary members may sustain severe damage, but the building should not collapse giving enough time for evacuating people, thereby saving lives.

Excursion of a structure into the inelastic range is accepted on the premise that such excursions occur during peaks which are for short durations. Hence, the code specifies design forces which are a fraction of what a structure would experience if it were to remain elastic throughout such a motion. It relies on inherent structural redundancy, overstrength and inelastic capacity of the structure to absorb shocks beyond yield point. Therefore, only providing structural strength cannot result in an adequate earthquake-resistant design. In addition, it must possess ductility as an essential ingredient. As a corollary to the above, it can be said that a structure should have adequate strength to withstand earthquake forces, have appropriate ductility to dissipate the energy input and be of sufficient stiffness to meet human comfort and other serviceability limits.

A dynamic analysis is required when a building is relatively flexible or because of its irregular shape, or its importance, or irregular mass distribution, etc. For initial dynamic analysis, gross concrete sections (neglecting steel) are assumed to arrive at relative member stiffness. Cracked section values should be used for final design. Effects of cracking in reinforced concrete members due to flexural tensile stresses are assumed representable by a reduced moment of inertia. For this purpose, gross inertias of members can be reduced as indicated in Sect. 2.5.1.1.

### 5.6.2 Selection of a Design Earthquake

There is considerable uncertainty associated with defining a design earthquake specific to a particular site since there are many imponderables including the nature and location of a future earthquake, random variations in duration, frequency and total energy content of any ground motion. As a result it is incumbent to consider an ensemble of probable different earthquake ground motions rather than to base design on a single ground motion signature. Creation of a site-specific ground motion spectrum is the domain of geotechnical experts and seismologists. It requires inputs from different branches of science, and even when all variables are assessed, the prediction of a likely ground motion at a site can, at best, be an informed guess.

### 5.6.3 Direction of Ground Motion

Earthquake ground motion is truly random, and as a result, the inertia forces also are highly random. Therefore a building needs to be designed for seismic forces that may act in any direction. To simplify the matter, measured ground accelerations in different directions are resolved along three orthogonal axes – two horizontal and one vertical. Simultaneous lateral inertia forces in more than one horizontal direction need to be considered for buildings that are not regular and for structural elements such as corner columns.

As per the code, this requirement is deemed to be satisfied if buildings are designed for 100 % excitation in one direction simultaneously with 30 % of projected force in the orthogonal direction. It implies that if $EL_x$ and $EL_y$ are the design earthquake loads in $X$ and orthogonal $Y$ direction, respectively, then by this empirical approach, building elements along principal axes should be designed for ($\pm EL_x$ $\pm 0.3EL_y$) and ($\pm EL_y$ $\pm 0.3EL_x$). For a building with a rectangular plan, a designer should also check the members for strength, with inertia forces acting at an oblique angle, usually taken at 45°.

### 5.6.4 Inertia Effects

A building superstructure is not subjected to any externally applied seismic force. Inertia forces are entirely due to dynamic response of the structure to ground motion. Their magnitude depends on response acceleration and building masses and their distribution over the building height. These aspects are discussed below.

#### 5.6.4.1 Lateral Load Magnitude

There is a fundamental difference between inertia forces and wind forces. The former are due to cyclic random movement of ground at base of the structure and are thus essentially dynamic in nature, where the oscillating component predominates. Wind load, on the other hand, is dependent on surface area of a structure that is exposed to wind and normally there is a large quasi-steady-state component. Secondly, seismic inertia effect manifests itself in the form of ground motion and not as an external force. It is cyclic in nature and random in terms of space, intensity, frequency, duration, etc.

The code IS 1893 specifies the percentage of imposed load that should be considered along with gravity load to arrive at seismic weight. In the LSP approach, the base shear is calculated as a product of this total building seismic weight and a horizontal seismic coefficient which is a function of response acceleration as read off the response spectrum. This shear is then distributed vertically among floors as specified in the code and thereafter among individual lateral load-resisting systems in proportion to their lateral stiffness.

#### 5.6.4.2 Lateral Load Transmission

In buildings, inertia forces generate largely at floor levels. Floor diaphragms act as mediums to transmit inertia loads to vertical supporting frameworks. Through such frameworks these forces are transmitted to the foundation. Diaphragm stiffness in relation to that of the vertical supporting system can range from flexible to rigid. If the diaphragm is flexible, then each frame is considered to support loads proportionate to tertiary slab areas it supports. On the other hand, if the diaphragm is rigid, which is most often the case, the lateral inertia load will be shared among frames in proportion to their stiffness.

To resist lateral loads, the commonly provided vertical systems for mid-rise buildings are concrete shear walls, moment frames, coupled shear walls or a combination of any two or three of the above. Among them, the favoured system is moment frames but when shear forces are large, a dual system comprising of shear walls and frames is the most popular system for mid-rise buildings. This form is discussed below

#### 5.6.4.3 Dual Systems

If inertia forces on a building are resisted by a combination of shear walls and moment frames (Fig. 5.13), then each will support a load in proportion to its stiffness. However, as per the code, if a system is to be qualified as a dual system, then frames have to be designed to carry at least 25 % of the lateral inertia forces. While this percentage is arbitrary, it does automatically provide an in-built

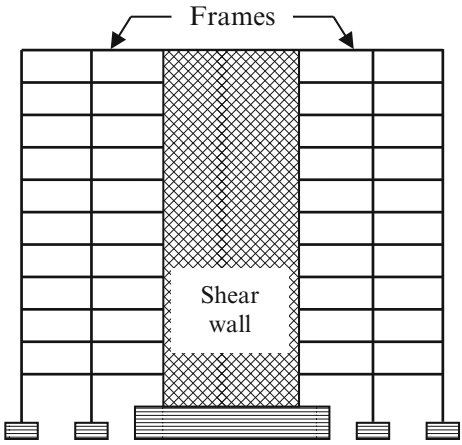


**Fig. 5.13** Dual system

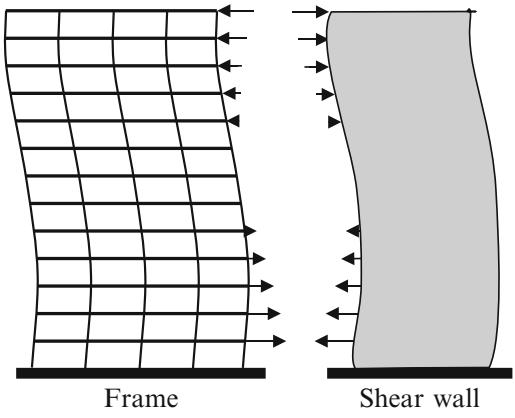


**Fig. 5.14** Shear wall – frame interaction

redundancy. Frames offer a second line of defence in the inelastic range when the base of a shear wall yields due to plastic hinge formation. Such a dual system displays superior seismic performance.

For tall buildings, such dual systems are often provided thereby taking advantage of the large stiffness of walls supplemented with high ductility and redundancy afforded by frames. A tall shear wall deflects like a cantilever whereas a frame deflects in a shear mode and a coupled shear wall in a mixed mode. Shear walls and moment frames must meet the requirement of deformation compatibility between them because of the rigid floor slabs. This act of the floor slabs leads to considerable redistribution of forces.

Such displacement compatibility between shear wall and frame results in shear wall restraining lateral displacement of the frame in lower reaches and converse is true in the upper reaches (Fig. 5.14). With wall pushing the frame laterally in the upper reaches, it may enhance prevailing inertia forces in the frame. This could

result in nearly uniform shear forces over the frame height. In such an event if the column section is maintained uniform over building height, it may call for a reduction in quantity of steel in the columns at the base because of higher axial compression prevailing there (Fardis 2009).

From an analysis of full height wall frame dual system, Smith and Coull (1991) has surmised that in a full height tall dual system comprising of shear wall and frame:

- In lower reaches of a building, both wall and frame resist external moment and shear.
- Above the point of contra-flexure, moment in the wall reverses with the result that frame moment can exceed the external moment.
- In uppermost reaches, above the point of zero shear, wall shear also reverses and as a result the frame shear can exceed external shear.

Consequently there is a case for stopping the shear wall short of its full height. However, validity of the above should be checked analytically in each case before implementation. Since dimensions of shear walls often change over height, it becomes imperative to use computer software to determine the distribution of load between shear walls and frames in a dual system. Even with this sophistication, the actual shear carried by a wall can be higher because of overstrength, strain hardening and the role of vertical web reinforcement.

Potential advantage of a dual system depends on the extent of interaction between the individual forms. This, to a large extent, depends on their relative lateral stiffness which is difficult to determine. Lateral deformation of a wall is strongly affected by foundation rotation which is difficult to assess because of uncertain inelasticity of soil. Foundation rotation does not affect a frame deflection to that extent as its primary deflection is in shear. The problem is further compounded when torsion prevails.

#### 5.6.4.4 Vertical Inertia Effects

As mentioned in Sect. 4.2.6.1, the ratio of vertical to horizontal response spectra varies. Its value depends on factors such as vibration period, distance to the fault, and earthquake magnitude. This ratio is larger if earthquake occurs in the near-field region. Some of the structural elements that are vulnerable to vertical seismic forces are listed in Sect. 4.2.6. Design for a vertical seismic condition is important for tall buildings as vertical gravity load is the only stabilizing force and large uplift forces could prove detrimental to stability of the structure. In such cases it is important to take into account vertical seismic forces particularly when addressing uplift and overturning concerns.

### 5.6.5 Load Combinations

As shown in Sect. 3.3, for linear systems, the responses for static and dynamic loads can be arrived at separately and then added algebraically. However this is not possible for non-linear systems where gravity and other loads need to be considered along with earthquake loads to arrive at total response. As per IS 1893 (BIS 2002a), earthquake and wind effects are not considered together. Further, horizontal load combinations considered for design are based on the assumption that peak ground accelerations do not occur simultaneously in two orthogonal directions.

For buildings with orthogonal supporting systems, the following load combinations (excluding torsion) need to be considered under normal conditions:

| | |
|---|---|
| 1. $1.5(DL + IL)$ | 5. $1.5(DL \pm EL_y)$ |
| 2. $1.2(DL + IL \pm EL_x)$ | 6. $0.9DL \pm 1.5\ EL_x$ |
| 3. $1.2(DL + IL \pm EL_y)$ | 7. $0.9DL \pm 1.5\ EL_y$ |
| 4. $1.5(DL \pm EL_x)$ | |

When lateral load-resisting systems are not oriented orthogonally or when a building is irregular about both orthogonal axes, then the system should be designed for following load combinations (excluding torsion):

| | |
|---|---|
| 1. $1.5(DL + IL)$ | 5. $1.5\{DL \pm (EL_y \pm 0.3EL_x)\}$ |
| 2. $1.2\{DL + IL \pm (EL_x \pm 0.3EL_y)\}$ | 6. $0.9DL \pm 1.5\ (EL_x \pm 0.3EL_y)$ |
| 3. $1.2\{DL + IL \pm (EL_y \pm 0.3EL_x)\}$ | 7. $0.9DL \pm 1.5\ (EL_y \pm 0.3EL_x)$ |
| 4. $1.5\{DL \pm (EL_x \pm 0.3EL_y)\}$ | |

It may be advisable to use these load combinations for evaluating stresses in corner columns even when column layout is regular. When considering response from three earthquake components, there are 73 load combinations that can occur as listed below (Jain et al. 2005):

| | |
|---|---|
| 1. $1.5(DL + IL)$ | 6. $1.5\{DL \pm (EL_y \pm 0.3EL_x \pm 0.3EL_z)\}$ |
| 2. $1.2\{DL + IL \pm (EL_x \pm 0.3EL_y \pm 0.3EL_z)\}$ | 7. $1.5\{DL \pm (EL_z \pm 0.3EL_x \pm 0.3EL_y)\}$ |
| 3. $1.2\{DL + IL \pm (EL_y \pm 0.3EL_x \pm 0.3EL_z)\}$ | 8. $0.9(DL) \pm 1.5(EL_x \pm 0.3EL_y \pm 0.3EL_z)$ |
| 4. $1.2\{DL + IL \pm (EL_z \pm 0.3EL_x \pm 0.3EL_y)\}$ | 9. $0.9(DL) \pm 1.5(EL_y \pm 0.3EL_x \pm 0.3EL_z)$ |
| 5. $1.5\{DL \pm (EL_x \pm 0.3EL_y \pm 0.3EL_z)\}$ | 10. $0.9(DL) \pm 1.5(EL_z \pm 0.3EL_x \pm 0.3EL_y)$ |

Alternatively, as per IS 1893 (BIS 2002a), the total magnitude of a particular response parameter to three components of an earthquake can be obtained by the SRSS method taking one direction at a time. Thus

$$EL = \sqrt{(EL_x)^2 + (EL_y)^2 + (EL_z)^2}$$

Although many loading cases are enumerated above, in practice only very few load cases need to be considered based on experience. It should be noted that the load combination of (0.9DL ± 1.5EL) often governs the quantity of bottom face reinforcement in floor beams near their supports. Also, there are cases where design of elements such as footings and columns is governed by the effect of horizontal load plus net axial tension.

## 5.7 Illustrative Examples

***Ex 5.7.1*** For the problem in *Ex* 3.9.3 and Fig. 3.13, determine the fundamental time period, storey forces, drifts, base shear and roof displacement. For this example analyse for different stiffness and mass ratios, given by ($\alpha = 1.0$; $\beta = 0.3$ and $\beta = 3.0$) and ($\beta = 1.0$; $\alpha = 0.5$ and $\alpha = 2.0$). Compare the results with those for a regular frame (i.e. with $\alpha = \beta = 1.0$) obtained in *Ex* 3.9.3.

**Solution** Procedure followed is the same as for *Ex* 3.9.3 and results are presented in Table 5.1. From comparison with values obtained for a regular frame, it will be observed that irregularities in mass and stiffness can have substantial effects on storey forces, base shear and drifts.

***Ex 5.7.2*** For an illustration of the method for evaluating static torsional moment in a multi-storey building, consider a frame as shown in Fig. 5.15a. The mass is spread evenly at all floors and the frame is subjected to lateral storey forces ($Q$) along the y axis. Columns in each storey of each frame are identical and the frame storey shears

**Table 5.1** Effect of irregularity

| | | Regular framing | Stiffness irregularity | | | | Mass irregularity | | | |
|---|---|---|---|---|---|---|---|---|---|---|
| | | $\alpha = 1.0$ | $\beta = 1.0$ | | | | $\alpha = 1.0$ | | | |
| | | $\beta = 1.0$ | $\alpha = 0.5$ | | $\alpha = 2.0$ | | $\beta = 0.3$ | | $\beta = 3.0$ | |
| Parameter | Unit | Value | Value | % | Value | % | Value | % | Value | % |
| Period T1 | s | 0.70 | 0.92 | 31.4 | 0.57 | −18.6 | 0.79 | 12.8 | 0.63 | −10.0 |
| Storey force Q1 | kN | 5.11 | 4.62 | −9.6 | 4.29 | −16.1 | 1.69 | −66.9 | 10.68 | 109.0 |
| Storey force Q2 | kN | 8.27 | 5.94 | −28.2 | 10.57 | 27.8 | 10.30 | 24.5 | 4.67 | −43.5 |
| Base shear Vb | kN | 13.39 | 10.56 | −21.1 | 14.86 | 11.0 | 11.99 | −10.5 | 15.35 | 14.6 |
| Drift $\delta 1$ | mm | 3.02 | 4.76 | 57.6 | 1.68 | −44.3 | 2.71 | −10.3 | 3.46 | 14.6 |
| Drift $\delta 2$ | mm | 1.87 | 1.34 | −28.3 | 2.39 | 27.8 | 2.32 | 24.1 | 1.05 | −43.9 |
| Deflection $\Delta 2$ | mm | 4.89 | 6.10 | 24.7 | 4.07 | −16.8 | 5.03 | 2.9 | 4.51 | −7.8 |

Note: % values refer to % change from corresponding value for framing with $\alpha = \beta = 1.0$

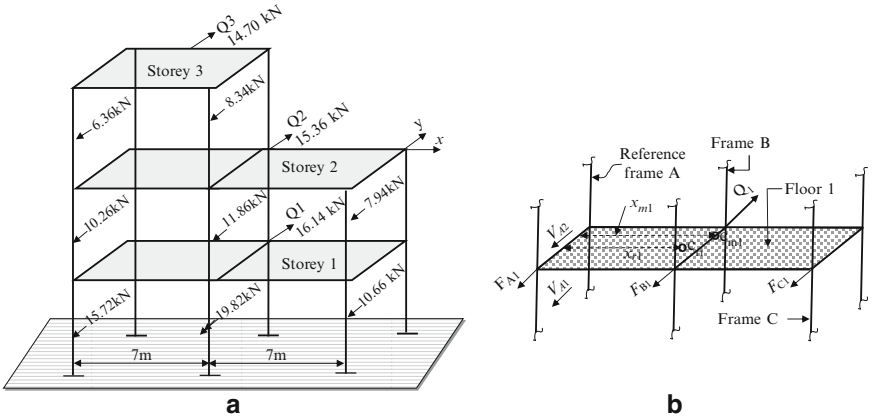


**Fig. 5.15** Evaluation of torsional moment. (**a**) Multi-storey frame. (**b**) Free body diagram – floor 1

(without rotation of the frames) are as shown. Determine the torsional moment at each storey using both the methods described in Sects. 5.4.1.1 and 5.4.1.2.

**Solution**

(a) *By isolating a floor* (*option* 1)

Consider a free body diagram of floor 1 as shown in Fig. 5.15b.
Using Eq. 5.1.1, force in reference frame A:

$$F_{A1} = V_{A1} - V_{A2}$$

Substituting values from Fig. 5.15a,

$$F_{A1} = 15.72–10.26 = 5.46 \text{ kN}$$

Similarly,

$$F_{B1} = 7.96 \text{ kN} \text{ and } F_{C1} = 2.72 \text{ kN}.$$

The storey frame shears and frame forces are listed in Table 5.2.

Taking moments of frame forces about reference frame A, the distance to generalized center of rigidity (Eq. 5.1.3) is given by

$$x_{r1} = \frac{5.46(0) + 7.96(7) + 2.72(14)}{5.46 + 7.96 + 2.72} = 5.81165 \text{ m}$$

Since masses at all floor levels are uniformly distributed, the distance to centre of mass at floor 1 (Fig. 5.15b) will be $x_{m1} = 7$ m

Load eccentricity (Eq. 5.1.4) will be

**Table 5.2** Frame shears and forces

| | Storey frame shears *Vj* | | |
|---|---|---|---|
| | Frame A | Frame B | Frame C |
| Storey | kN | kN | kN |
| 3 | 6.36 | 8.34 | 0 |
| 2 | 10.26 | 11.86 | 7.94 |
| 1 | 15.72 | 19.82 | 10.66 |
| | Frame forces *Fj* | | |
| | Frame A | Frame B | Frame C |
| Storey | kN | kN | kN |
| 3 | 6.36 | 8.34 | 0.00 |
| 2 | 3.90 | 3.52 | 7.94 |
| 1 | 5.46 | 7.96 | 2.72 |

**Table 5.3** Evaluation of torsional moment

| (a) | By isolating a floor (option1) | | | |
|---|---|---|---|---|
| Storey | Center of rigidity (m) | Floor eccentricity (m) | Floor torque (kNm) | Torsional moment (kNm) |
| 3 | 3.97143 | −0.47143 | −6.93002 | −6.930 |
| 2 | 8.84115 | −1.84115 | −28.28006 | −35.210 |
| 1 | 5.81165 | 1.18835 | 19.17997 | −16.030 |
| (b) | By isolating a storey (option2) | | | |
| Storey | Shear center (m) | Storey eccentricity (m) | Storey shear (kN) | Torsional moment (kNm) |
| 3 | 3.97143 | −0.47143 | 14.70 | −6.930 |
| 2 | 6.45975 | −1.17133 | 30.06 | −35.210 |
| 1 | 6.23333 | −0.34697 | 46.20 | −16.030 |

$$e_1 = (x_{m1} - x_{r1}) = 7.0 - 5.81165 = 1.18835 \text{ m}$$

Torque at floor 1 (Eq. 5.1.5):

$$T_1 = Q_1 e_1 = 16.14 \times 1.18835 = 19.17997 \text{ kNm}$$

Similarly, torques are evaluated at other floors and the same are tabulated in Table 5.3.

Substituting from Eq. 5.1.6 torsional moment at storey 1,

$$M_{t1} = \sum_{1}^{3} T_1 = (-6.93002 - 28.28006 + 19.17997) = -16.0301 \text{ kNm}$$

Similarly, the torsional moment at each storey is evaluated and presented in Table 5.3.

(b) *By isolating a storey* (*option* 2)

Values of $Q_k$ from Fig. 5.15a are

$$Q_1 = 16.14 \text{ kN}, \quad Q_2 = 15.36 \text{ kN}, \quad Q_3 = 14.70 \text{ kN},$$

Substituting above values in Eq. 5.2.1,

$$V_1 = 16.14 + 15.36 + 14.7 = 46.20 \text{ kN}$$

Taking values of $V_{j1}$ from Table 5.2 and substituting same in Eq. 5.2.2,

$$x_{s1} = \frac{15.72(0) + 19.82(7) + 10.66(14)}{46.2} = \frac{287.98}{46.2} = 6.23333 \text{ m}$$

Substituting values in Eq. 5.2.5,

$$\overline{x}_1 = \frac{14.7(3.5) + (15.36 \times 7) + (16.14 \times 7)}{46.2} = \frac{271.95}{46.2} = 5.88636 \text{ m}$$

Torsional moment at storey 1 will be (Eq. 5.2.6),

$$M_{t1} = V_1 \ [\overline{x}_{m1} - x_{s1}] = 46.2\,(5.88636 - 6.23333) = -16.0301 \text{ kNm}$$

This is the same value as that obtained by considering isolating a floor in option 1 above. Values of torsional moments for all floors are tabulated in Table 5.3.

***Ex 5.7.3*** A rigid diaphragm of uniform thickness is supported on four shear walls as shown in Fig. 5.16a. Wall stiffness values $k$ for displacement along their length are also shown. It is assumed that walls do not offer resistance to displacements perpendicular to their lengths. The diaphragm is subjected to lateral inertia forces $P = 100$ kN and $Q = 250$ kN along $x$ and $y$ axes, respectively. Locate the center of mass as well as center of stiffness and determine the lateral resisting forces generated in walls because of torsion due to forces $P$ and $Q$.

**Solution**

(a) *Locating centre of mass*

Since the diaphragm is uniform, its centre of mass ($c_m$) is located at its CG, i.e. distances from the origin $O$ are $c_{mx} = 13$ m and $c_{my} = 6.0$ m.

(b) *Locating centre of stiffness*

The distance along $x$-axis of centre of stiffness from origin $O$ is given by

$$c_{sx} = \frac{26k_1 + k_3(0)}{k_1 + k_3} = 11.818 \text{ m} \quad \text{and} \quad c_{sy} = \frac{12\,(k_4)}{k_2 + k_4} = 7.286 \text{ m}$$

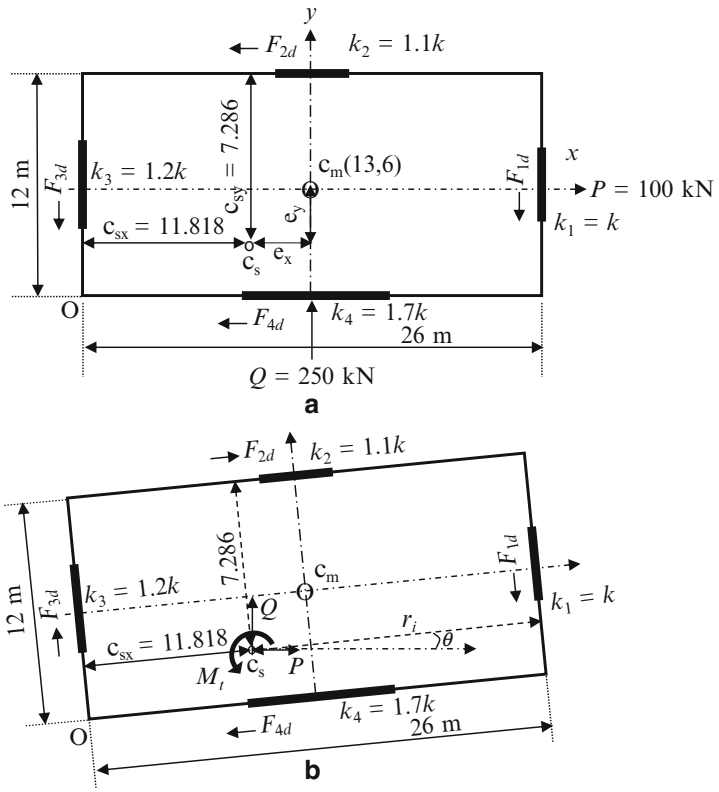


**Fig. 5.16** Forces due to torsion. (**a**) Plan view. (**b**) Slab after rotation

and eccentricities with respect to centre of mass will be

$$e_x = (13.0 - 11.818) = 1.182 \text{ m} \quad \text{and} \quad e_y = (7.286 - 6.0) = 1.286 \text{ m}$$

(a) *Wall forces due to displacements caused by P and Q*

For a rigid diaphragm, its supporting walls will displace by the same amount in $x$ and $y$ directions under forces $P$ and $Q$, respectively. Force in each wall will be proportional to its stiffness. Hence, wall forces caused by load $P$ will be

$$F_{2d} = \left\{ \frac{Pk_2}{k_2 + k_4} \right\} = \frac{100(1.1k)}{(1.1\text{k} + 1.7k)} = 39.29 \text{ kN}$$

$$F_{4d} = \left\{ \frac{Pk_4}{k_2 + k_4} \right\} = \frac{100(1.7k)}{(1.1\text{k} + 1.7k)} = 60.71 \text{ kN}$$

Similarly due to force $Q$ in the $y$ direction,

$$F_{1d} = 113.64 \text{ kN} \quad \text{and} \quad F_{3d} = 136.36 \text{ kN}$$

(b) *Wall forces due to twisting*

Eccentricities of lateral loads in $x$ and $y$ directions are $e_x = 1.182$ m and $e_y = 1.286$ m. These eccentricities cause the slab to rotate as shown in Fig. 5.16b. Net twisting moment about center of rigidity will be

$$M_t = Qe_x - Pe_y = \ 250(1.182) - 100(1.286) = 166.9 \text{ kNm}$$

Let perpendicular distance from center of stiffness to shear wall $i$ (Fig. 5.16b) be denoted as $r_i$ and its stiffness be denoted as $k_i$. If rigid body rotation of diaphragm in its own plane is $\theta$, then displacement of shear wall $i$ will be $\Delta_i = r_i\theta$ and restoring force in wall $i = F_{it} = k_i r_i \theta$ for small values of $\theta$.

$$\text{Restoring moment } M_{ti} = F_{it}\ r_i = k_i r_i^2 \theta.$$

Equating external moment to the restoring moment due to forces in $n$ walls,

$$M_t = \sum_{i=1}^{n} M_{ti} = \sum_{i=1}^{n} k_i r_i^2 \theta$$

it follows that force in wall $i$ will be

$$F_{it} = \frac{k_i r_i}{\sum_{i=1}^{n} k_i r_i^2} M_t$$

Accordingly, forces in the four walls are evaluated as shown in Table 5.4. Total restoring forces in walls due to both translation ($F_{id}$) and rotation ($F_{it}$) will be

$$\begin{aligned} F_1 &= F_{1d} + F_{1t} = 113.64 + 5.09 = 118.73 \text{ kN} \\ F_2 &= F_{2d} - F_{2t} = \ 39.29 - 2.88 = \ 36.41 \text{ kN} \\ F_3 &= F_{3d} - F_{3t} = 136.36 - 5.09 = 131.27 \text{ kN} \\ F_4 &= F_{4d} + F_{4t} = \ 60.71 + 2.88 = \ 65.59 \text{ kN} \end{aligned}$$

**Table 5.4** Evaluation of forces in shear walls

| Wall | $k_i$ (kN/m) | $r_i$ (m) | $k_i r_i$ (kN) | $k_i r_i^2$ (kNm) | $F_{it}$ (kN) |
|---|---|---|---|---|---|
| 1 | 1.0 k | 14.182 | 14.182 k | 201.129 k | 5.09 |
| 2 | 1.1 k | 7.286 | 8.015 k | 58.397 k | 2.88 |
| 3 | 1.2 k | 11.818 | 14.182 k | 167.603 k | 5.09 |
| 4 | 1.7 k | 4.714 | 8.014 k | 37.778 k | 2.88 |
| | | $\sum_{i=1}^{n} k_i\ r_i^2 = 464.907$ k | | | |

**Table 5.5** Deflection profile

| Storey no | Deflection (cm) |
|---|---|
| 6 | 7.79 |
| 5 | 6.72 |
| 4 | 5.76 |
| 3 | 4.78 |
| 2 | 3.81 |
| 1 | 2.46 |
| Base | 0 |

***Ex 5.7.4*** A six-storey frame is subjected to lateral seismic forces at each storey and displaces laterally at each storey by amounts as shown in Table 5.5. All storeys are 3 m high except for the ground storey which has a height of 3.5 m. Determine whether a soft storey exists at ground storey.

**Solution** The first step is to calculate storey drift indices:

$$\frac{\delta_1}{h_1} = \frac{2.46 - 0}{350} = 0.00703; \qquad \frac{\delta_2}{h_2} = \frac{3.81 - 2.46}{300} = 0.00450;$$

$$\frac{\delta_3}{h_3} = \frac{4.78 - 3.81}{300} = 0.00323; \qquad \frac{\delta_4}{h_4} = \frac{5.76 - 4.78}{300} = 0.00327;$$

Average drift ratio for three storeys (above the ground storey) will be

$$(0.00450 + 0.00323 + 0.00327)/3 = 0.00367$$

Checking the first condition (Eq. 5.4.1),

$$70\ \%\ \text{ of }\ \delta_1/h_1 = 0.7 \times 0.00703 = 0.00492 > 0.00450$$

Checking the second condition (Eq. 5.4.2),

$$80\ \%\ \text{ of }\ \delta_1/h_1 = 0.8 \times 0.00703 = 0.00562 > 0.00367$$

Hence a soft storey exists at ground floor under both checks.

***Ex 5.7.5*** A frame shown in Fig. 5.17 has a uniform storey height of 3 m. All beams have an end seismic moment capacity of 150 kNm. All columns, in addition to axial load capacity, have a seismic moment capacity of 175 kNm. Moment capacity at column bases is controlled by grade beam capacity which is 40 kNm on each side of a column. Determine whether a weak storey condition exists at ground floor level. Assume, for purpose of this example, that beam moment is shared equally by columns above and below a joint.

**Solution** First, it should be determined whether a strong column–weak beam or a weak column–strong beam condition exists.

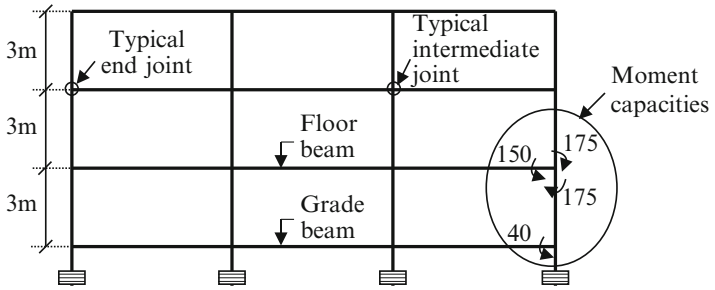


**Fig. 5.17** Check for weak storey

*At end joint*:

| | | |
|---|---|---|
| Moment capacity of columns at an end joint | = | $175 \times 2 = 350$ kNm |
| Moment capacity of a beam at an end joint | = | 150 kNm |
| Since $350 > 150$, a strong-column weak-beam condition exists | | |
| Moment capacity of columns at an intermediate joint | = | $175 \times 2 = 350$ kNm |
| Moment capacity of beams at an intermediate joint | = | $150 \times 2 = 300$ kNm |
| Since $350 > 300$, a strong-column weak-beam condition exists | | |
| Thus at all joints, capacity is controlled by that of beams at the joint | | |

*At ground storey*:

| | | | | |
|---|---|---|---|---|
| Limiting column shear at end joint | = | $[(150/2) + 40]/3$ | = | 38.3 kN |
| Limiting column shear at intermediate joint | = | $(150 + 80)/3$ | = | 76.7 kN |
| Limiting column shear at ground storey | = | $2(38.3) + 2(76.7)$ | = | 230.0 kN |

*At first storey*:

| | | | | |
|---|---|---|---|---|
| Limiting column shear at end joint | = | $[75 + 75]/3$ | = | 50.0 kN |
| Limiting column shear at intermediate joint | = | $[150 + 150]/3$ | = | 100.0 kN |
| Limiting column shear at first storey | = | $2(50.0) + 2(100.0)$ | = | 300.0 kN |
| 80 % of shear capacity at first storey | = | $0.8 \times 300$ | = | 240.0 kN |

$240 > 230$ (shear capacity at ground storey). Hence a weak storey condition exists at ground storey.

# Chapter 6
# Frames and Diaphragms: *Design and Detailing*

**Abstract** Structural frames, which are commonly adopted as the principal lateral load-carrying system, are dealt with in this chapter. Important facets of planning, design and detailing of structural elements of a frame such as beams and columns and importantly the joints between them, from seismic considerations, are explained. Issues normally associated with tall buildings such as drift, shear lag and $P$-$\triangle$ effects are also addressed. Response equations developed in Chap. 3 are utilised to analyse frames with both the linear static and linear dynamic methods. Examples are used to describe the design of a typical beam–column joint as well as evaluation of $P$-$\triangle$ effect. The different types of diaphragms are described, and it is detailed how flat slabs should be designed in a seismic environment. The role played by collectors and chords is covered. Then, through the solution of an example, it is shown how they are designed.

**Keywords** Moment-resisting frames • Diaphragms • Collectors • Chord elements • Beam–column joints • Tall frames • $P$-$\triangle$ effect

## 6.1 Introduction

In this chapter the common types of lateral load-resisting systems adopted for both medium- and high-rise concrete buildings and principal aspects associated with their seismic design and detailing are described. Also covered are designs and details of structural frame components that resist inertia forces – viz. diaphragms, beams, columns and more importantly beam–column joints. Issues normally associated with tall buildings such as drift, shear lag and $P$-$\triangle$ effects are also addressed. Analysis procedures for frames are explained with the help of illustrative examples. However, use of precast concrete elements is outside the scope of this book.

Past earthquakes have demonstrated, time and again, that lack of proper ductile detailing, absence of adequate confinement of concrete, poor quality of construction and non-use of capacity design approach as being the principal causes of structural failures. It follows that the key to success in achieving an efficient earthquake-



S. Manohar, S. Madhekar, *Seismic Design of RC Buildings*, Springer Transactions in Civil and Environmental Engineering, DOI 10.1007/978-81-322-2319-1_6

resistant design lies in careful planning, designing and detailing of structural elements so that likely locations of brittle failures are identified and precluded.

Towards this end, some key design and ductile detailing requirements for various building frame components have been specified in this chapter. In addition, it is recommended that in practice a designer should check all construction details for constructability.

## 6.2 Moment-Resisting Frames (MRFs)

For concrete buildings, moment frames are the commonly chosen framing system. They form a parallel array of bents in two orthogonal directions and thereby possess redundancy and create multiple load paths. They are inherently flexible and demonstrate adequate global ductility when designed by capacity design principles. Normally, rigid diaphragms in the form of floor slabs tie all frames together. The lateral loads are carried through flexure in columns and beams and propping action of columns.

Very long or very short beam spans should be avoided. In particular, the latter could lead to heavy reversing seismic shear forces at beam supports. For common storey heights and gravity loads, a beam span of 4–5 m is considered ideal under seismic conditions. Column foundations of frames are easier to deal with than those for walls particularly in high seismic zones. Design of corner columns deserves special attention.

### *6.2.1 Types of Moment-Resisting Frames*

Stiffness of a frame against lateral loads is provided primarily by bending resistance in girders, columns and beam–column joints (Fig. 6.1a), and hence they are termed as moment-resisting frames (MRFs). In the case of tall buildings, additional resistance is provided by axial rigidity of columns (Fig. 6.1b). Such frames should possess a stiff spine to limit drift, and their beam–column junctions should be stronger than the members that frame into them, but at the same time, they should permit joint rotation.

Minimum grade of concrete (BIS 2003) in frames is recommended as M20. For buildings exceeding 15 m in height in seismic zones III, IV and V, a concrete grade of M25 may be adopted. In any case, grade of concrete must meet the minimal grade specified in IS 456 (BIS 2000) based on exposure conditions. MRFs can be classified according to the degree of in-built ductility that they possess such as:

#### 6.2.1.1 Special Moment-Resisting Frame (SMRF)

These frames are specially detailed to meet the provisions of IS 13920 (BIS 2003) and thereby they respond in a ductile manner.

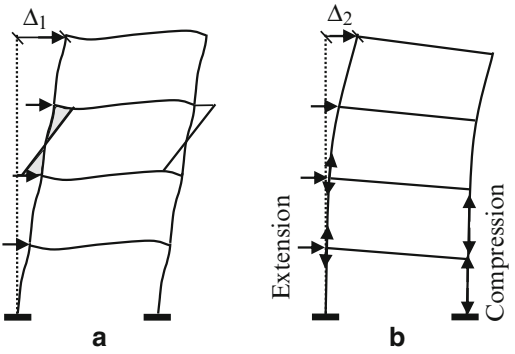


**Fig. 6.1** Deformation of MRFs. (**a**) Typical column moment diagram. (**b**) Column axial strain

#### 6.2.1.2 Ordinary Moment-Resisting Frame (OMRF)

These frames are not detailed to meet the special ductile detailing provisions of IS 13920. However, authors suggest that even in such cases, it may be prudent to detail both ends of columns for limited ductility to prolong the formation of a storey mechanism. As per IS 13920, all structural frames of buildings located in seismic zones III, IV and V have to be SMRFs. By inference, OMRFs could be adopted for buildings located in seismic zone II.

#### 6.2.1.3 Intermediate Moment-Resisting Frame (IMRF)

It is reported that based on lessons learnt from past earthquakes, a case may be made for reducing the toughness requirement for frames in seismic zone III. It is also argued that such frames may be permitted for minor structures, although this category has not been clearly defined. These are referred to as IMRFs. This translates into providing MRFs with less stringent detailing requirements compared to those specified for SMRFs. However, at the same time, it is argued that the response reduction factor for such frames be reduced to 3.5 or 4.0 as against 5 for SMRFs.

This aspect needs careful evaluation of likely enhancement of risk from brittle failure during a major seismic event of a magnitude corresponding to zone III. Towards this end, IMRFs could preferably form a part of a dual system with shear walls. It is brought to the reader's attention that so far, to the best of the author's knowledge, there is no codal stipulation in India in this respect. Hence, in this book, wherever ductile design or detailing of an MRF is mentioned, it refers to that for a SMRF.

### *6.2.2 Seismic Analysis Procedures*

Although normally MRFs are three-dimensional structures, it is often adequate to analyse regular MRFs as two dimensional with separate analysis being conducted in

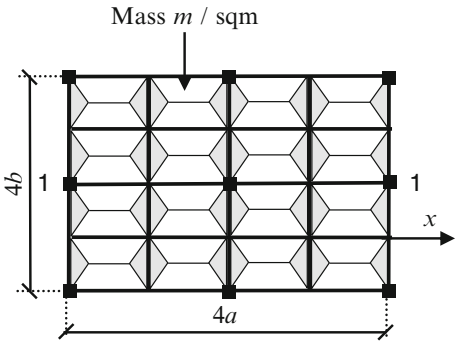


**Fig. 6.2** Beam tributary areas

each of the two orthogonal directions. Resulting response values are then combined using established methods. It should be noted that two translational and one torsional DOF per floor should be included when lateral and torsional motions are strongly coupled (i.e. when large eccentricities and/or closely spaced frequencies prevail). Secondly, when the slab is rigid and supported by frames of uniform stiffness, lateral storey shear is resisted by all frames. Hence, an MRF should not be designed for lateral forces based only on the tributary area that it supports. For instance, for a series of frames supporting a rigid slab (Fig. 6.2), the lateral seismic force on frame 1 in the $x$ direction should be $[mg\,A_h \times (16ab/5)]$ and not the tributary load of $[mg\,A_h \times 2b(2a - b)]$ on the inner beams.

Tall buildings behave as three-dimensional structures, and it is advisable to model them accordingly. This will permit irregularities in plan and elevation as well as torsional effects to be taken into consideration. Further, a three-dimensional analysis is recommended to ascertain the distribution of lateral forces between shear walls and other lateral force-resisting elements when shear wall layout is irregular. However, if the building is regular and has rigid diaphragms and torsion component is small, then a two-dimensional analysis may be adequate.

It is common practice, even today, to use an equivalent linear static analysis procedure in building design. However, over the years, structural members have become increasingly slender, rendering them vulnerable to vibration damage. This has sharpened the call for dynamic analysis, particularly under seismic conditions. Dynamic analysis will yield a more realistic characterisation of vertical distribution of lateral shear forces, particularly for unsymmetrical structures. As a result, such structures are expected to have superior earthquake resistance capability. IS 1893 stipulates the types of buildings when a dynamic analysis should be performed.

Analysis procedures that are in use can be divided into two groups – linear and nonlinear. These can be further subdivided as either static or dynamic. Commonly used procedures are linear. For the final design, a nonlinear procedure can be considered when estimating response of buildings with gross irregularity or when performance of an existing building is to be assessed for retrofitting purposes and other special cases. Merits of a nonlinear analysis are the following:

- It gives a more realistic estimate of forces and displacements.
- It takes into account the effects of stiffness degradation.
- It provides a better estimate of inter-storey drifts.

#### 6.2.2.1 Linear Static Procedure (LSP)

The linear static procedure is also known as seismic coefficient method. Herein, an elasto-static analysis procedure is adopted, but at the same time, it incorporates an element of dynamic analysis through the use of response spectrum. The method assumes an elastic stiffness and an equivalent viscous damping. Hence, it is suitable only for regular buildings in the elastic range. It is a popular method particularly because of its simplicity. IS 1893 stipulates the conditions when this method is not applicable. The steps involved in this method of analysis are listed in Sect. 4.5.5. Analytical process in using LSP is illustrated through *Ex* 6.10.1.

#### 6.2.2.2 Linear Dynamic Procedure (LDP)

In this method, member forces and distribution of base shear over the building height are determined using a linear dynamic procedure. Member stiffness is assumed constant during the design process, and an equivalent viscous damping coefficient is assumed. Response is evaluated using modal analysis technique as explained in Sect. 4.6.11. It can model regular and nominally irregular buildings in the elastic range and can account for higher mode effects.

IS 1893 stipulates that base shear value $V_b$ obtained by this method should not be less than the base shear $\overline{V}_b$ obtained by the LSP. If it happens to be so, then all results obtained from dynamic analysis have to be scaled up in the ratio $\overline{V}_b / V_b$. This is possibly to prevent inadvertent use of a very flexible structure with a large period with resulting inertial forces being undesirably low. This scaling can be different in the two orthogonal directions resulting in two different seismic amplitudes being used. Some researchers have pointed out that for short-period structures, it may be more appropriate to scale the moments upwards in the ratio of base moments rather than base shears.

Evaluation of two natural frequencies of vibration of a two-storey structure is demonstrated in *Ex* 6.10.2. The analytical process in using this linear dynamic procedure is illustrated through *Ex* 6.10.3.

#### 6.2.2.3 Nonlinear Static Procedure (NSP)

In the nonlinear static procedure, the overall building performance is evaluated at every incremental lateral displacement or incremental lateral load. The method is basically evolved for dealing with SDOF systems. It could be adapted for performance evaluation of MDOF systems with a predominant first mode of

vibration. It can evaluate the performance of buildings beyond the elastic range but is unable to capture dynamic effects of higher modes. It is a simplified technique which is also called the *pushover analysis.* It presents a building performance against an acceptable damage state. It is explained in Sect. 11.3.

#### 6.2.2.4 Nonlinear Dynamic Procedure (NDP)

The nonlinear dynamic procedure is applicable to all structures wherein the response values are determined using a time history analysis. At each incremental stage, stiffness of frame members is modified to include the effect of stiffness degradation as is explained in Sect. 4.8 and illustrated in *Ex* 4.9.12. The method is computationally highly demanding and is used only for very important or complex structures with unsymmetry and irregularities.

For frame analysis, typically the LSP or the modal LDP is used, both based on the response spectrum. Generally the latter method of analysis is adopted when the building is tall or nominally irregular either in terms of layout or flexibility or mass distribution.

### *6.2.3 Design and Ductile Detailing Principles*

MRFs should possess *toughness*, which is an ability to repeatedly sustain reversible stresses in the inelastic range without significant degradation. Both overstrength and understrength can prove to be detrimental to structural safety of a frame during an earthquake. From considerations of strength, performance and stability, the design requirements can be summarised as under:

(a) Strength: member stresses should be within permissible limits.
(b) Performance: specified displacement criteria must be met against a chosen hazard level.
(c) Stability: sufficient safety factor should be present against destabilising factors such as overturning moments and $P$-$\Delta$ effects.

An earthquake releases an enormous amount of energy, and when it strikes the base of a structure, a part of this energy enters the structure and gets released through inelastic deformations of structural elements. It is therefore desirable to identify a hierarchy in failure modes of structural elements which implies selecting a suitable energy-dissipating mechanism for the building. The common method adopted for this is to initiate flexural yielding (i.e. formation of plastic hinges) at specified locations. In the case of MRFs, the chosen locations are usually beam ends.

If plastic hinges form in columns before they form in beams, the curvature ductility demand can be very high, and it may not be possible to achieve it, leading to a storey mechanism (Fig. 6.3a). On the other hand, if yielding commences in beams,

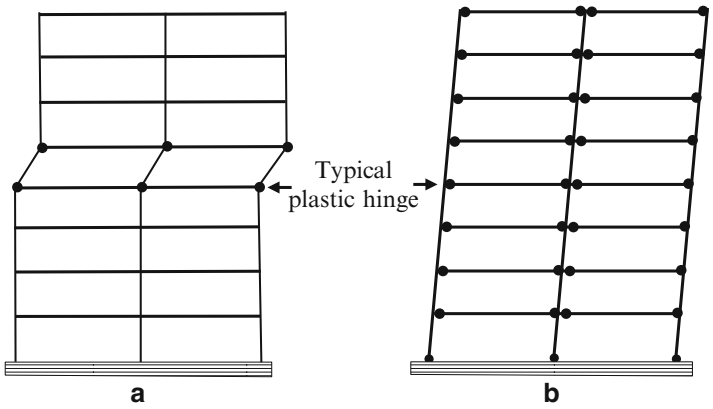


**Fig. 6.3** Sway mechanisms. (**a**) Storey sway. (**b**) Beam side sway

the curvature ductility demand is moderate and can be met by careful detailing (Fig. 6.3b). When seismic effects are combined with those due to gravity and other loads, IS 1893 permits an increase in permissible stresses in materials by 33.3 %. However, the stress in reinforcement has to be limited to the yield stress for steel with a definite yield point (BIS 2002a), and for steel without a definite yield point, the stress shall be limited to 80 % of its ultimate strength or 0.2 % proof stress, whichever is smaller.

At commencement of design, the engineer should clearly identify the locations in various elements where seismic energy should preferably be dissipated. These regions of limited length, known as plastic hinge regions, should be specially designed and detailed such that seismic energy release is achieved there through member rotations. It is important to distinguish between a plastic hinge and an elastic hinge. A plastic hinge is formed only at locations where yield moment $M_p$ is reached, i.e. when steel strain reaches yield point. On the other hand, an elastic hinge is a permanent feature with a given location, and it does not carry any moment.

Examination of earthquake failures has overwhelmingly demonstrated that unsatisfactory detailing has often been the cause of damage. Proper detailing of structural elements is vital to enable them to dissipate energy by inelastic deformations. Curvature ductility that should be available at location of a potential plastic hinge is dependent on many factors such as member geometry and relative member strengths. It is suggested that a curvature ductility of at least $3\,\mu$ (Park 1986) should be available where $\mu$ is the desired displacement ductility factor.

Detailing of stirrups deserves special attention because they assist in:

- Resisting shear forces and thereby limiting formation of diagonal shear cracks
- Protecting concrete from bulging outward due to compressive stresses
- Preventing buckling of compressed longitudinal bars

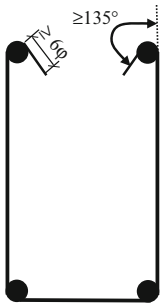


**Fig. 6.4** Typical stirrup end detail

For stirrups to perform satisfactorily, their ends should have 135° hooks and be well embedded in concrete by 10 bar diameters (but not <75 mm) (BIS 2003) (Fig. 6.4) so that they do not open up but continue to hold the concrete and rebars in position during major shaking. Stirrups ($\varphi \geq 6$ mm for beam span $\leq 5$ m and $\varphi \geq 8$ mm for larger beam spans) shall preferably be fabricated from plain round bars. There is an opinion (Jain et al. 2005), however, that the hook's minimum extension should be restricted to 65 mm instead of 75 mm as, based on tests, this is found to be adequate. Secondly, a longer length is a hindrance during construction.

IS 13920 has stipulated the minimum diameter for stirrups as 6 mm; but that it should be 8 mm for beams exceeding 5 m clear span. It would be preferable that stirrup diameter is specified as a function of diameter of the bar which it confines rather than relating it to beam span. Ductile detailing measures, although unpopular, should be implemented without fail. They include choosing appropriate rebar diameters, efficient distribution of bars in the section, location and details of splices and providing appropriate diameter, spacing and bending details of transverse reinforcement in critical regions. More details are covered in Sects. 6.4.5, 6.5.2 and 6.6.4 below.

## 6.3 Diaphragms

A diaphragm is a multipurpose horizontal element that is flexible out of plane. It has four primary functions to perform apart from supporting gravity loads, viz.:

- Tie the building together.
- Transmit heavy lateral inertia forces to vertical force-resisting systems even under extreme seismic conditions.
- Provide lateral restraint to vertical members.
- Transfer load from one load-resisting system to another when a dual system is adopted.

Diaphragm composition can take various forms, e.g. solid cast in place concrete slabs, precast planks with in situ concrete topping, cast in place waffle slabs,

ordinary or post-tensioned flat slabs, composite slabs in the form of thin concrete slabs laid over a steel deck and many others. In case of tall buildings, the choice of a particular floor system depends on many factors such as span, form the contractor is familiar with, ease and speed of construction attainable, etc. Depending upon the magnitude of in-plane rigidity of a diaphragm with respect to that of the vertical supporting members, it may be classified as (1) stiff, (2) flexible or (3) rigid.

A diaphragm is termed as stiff if its rigidity is close to that of the vertical elements and it can span over the supports as a continuous beam. It poses a complex problem of load distribution and may need to be modelled as a beam supported on springs. This approach is suited for single-storey buildings. However, for a multistorey building, the stiffness of springs is difficult to determine and would call for a computer model for the entire building. However, stiff diaphragms are not commonly used. Degree of rigidity of a diaphragm influences the lateral load distribution among its vertical supporting members, and this aspect is demonstrated in *Ex* 6.10.4 for all three types of diaphragms described above.

### *6.3.1 Flexible Diaphragm*

An intermediate floor diaphragm is termed as *flexible* if its maximum lateral displacement, against horizontal inertia forces, is more than twice the average inter-storey drift of lateral force-resisting vertical members of the storey immediately below the diaphragm (FEMA 356 2000). In such a case, load carried by each vertical member is a function of the tributary area it supports since a flexible diaphragm is assumed to be incapable of transmitting torsional shear stresses. The presence of a flexible diaphragm results in an increase in fundamental period of the building, and lateral deflection is significant. Such a diaphragm should be checked for possible failure in flexure, shear and buckling and for the adequacy of development length of rebars therein.

A flexible diaphragm acts as a simple beam spanning horizontally between vertical supporting members with the slab performing the function of its web. Stiffened edges perpendicular to the load act as its flanges. It relies on stiffness of its chord members to limit deflections. As the slab deforms under load, the chords carry axial forces that are alternately compressive and tensile as the load is reversible. Hence, splices along diaphragm chords should be confined if compressive stress is high.

### *6.3.2 Rigid Diaphragm*

If lateral displacement of a diaphragm due to horizontal forces is less than half the average inter-storey drift of lateral force-resisting vertical members of the associated

**Picture 6.1** Failure of slab–wall connections

storey, then the diaphragm is termed as rigid (FEMA 356 2000). This is the most common form of diaphragm adopted in buildings, and it is this form that is assumed throughout this book. A rigid diaphragm is considered to move as a rigid body. It does not change its shape in plan and has the capacity to transmit effects of torsion to vertical supporting elements.

During a major seismic event, the structure will experience forces much larger than those at first yield, and hence, it is important that diaphragms are capable of transmitting lateral forces to vertical supporting members, at maximum seismic demand. Secondly, diaphragms should be designed to be elastic at an earthquake level commensurate with serviceability criteria. Thirdly, under near-collapse condition, diaphragms need to remain substantially intact to carry gravity loads, although they may be highly stressed because of plastic hinge rotations at their junctions with beams. Picture 6.1 depicts failure of slab–wall connections

It is imperative that strong connections are provided between vertical members and diaphragms and collector elements. Ties from shear walls must extend well into the diaphragms to avoid tearing along the wall–diaphragm interface. As a step in this direction, in high seismic zones, diaphragm connections with shear walls may be designed without permitting a 33 % increase in permissible stresses supplemented with the concrete at joints being confined. The maximum span of a diaphragm should preferably be restricted to about five times its width as a larger span may lead to a weak diaphragm.

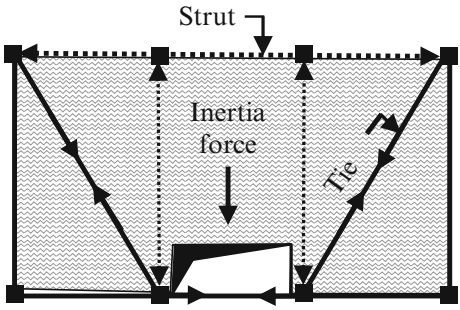


**Fig. 6.5** Struts and ties

#### 6.3.2.1 Effect of Openings

Diaphragms are commonly designed as deep beams, but such an approach could be compromised due to cut backs in them by way of large openings for services, stairwells, etc. In such cases, proper load paths have to be identified and detailed for faithful transfer of diaphragm forces to nodal points of the vertical load-resisting system. In the event that smooth integral load paths are not available, the diaphragm can be designed by strut and tie method. A typical layout for paths that form struts and ties is shown in Fig. 6.5. In such cases, Moehle et al. (2010b) have suggested that additional reinforcement should be provided to control cracking. Secondly, the tie force will be delivered to a joint close to the beam plastic hinge region and that calls for careful detailing.

For small openings (i.e. of dimension less than twice the diaphragm thickness), reinforcement is usually added on either side of the opening. Area of such additional reinforcement on each side of the opening is usually equal to half the area of reinforcement in that direction, disrupted by the opening. For a larger opening, proper load transfer mechanisms must be established as mentioned above. In addition, if a large opening in a diaphragm is positioned close to its junction with a wall, then it must be ensured that balance area of the junction is sufficient to transmit lateral shear forces from diaphragm to wall.

#### 6.3.2.2 Diaphragm Design Forces

In-plane lateral seismic load on a diaphragm is the product of response acceleration at respective floor and the distributed mass supported thereon. IS 1893 does not specifically stipulate the lateral load for which a diaphragm should be designed under seismic conditions. Storey forces obtained from a linear static or a linear dynamic analysis procedure are used for design of vertical supporting members. However, it is understood that storey forces do not necessarily reflect likely maximum force (Moehle et al. 2010b) induced at a particular diaphragm level. Under the circumstances, a diaphragm at level $i$ may be designed for higher of the following two forces (including the first one from Eq. 4.9.1) (Taranath 2010a):

$$\text{(a)} \quad Q_{ia} = \frac{w_i h_i^2}{\sum_{j=1}^{N} w_j h_j^2} V_b \quad \text{or} \tag{6.1.1}$$

$$\text{(b)} \quad Q_{ib} = \frac{\sum_{j=i}^{N} Q_j}{\sum_{j=i}^{N} w_j} w_i \tag{6.1.2}$$

with the proviso that $Q_{ib}$ shall not be less than 0.2 $S_s$ $I$ $w_i$ (Moehle et al. 2010b) and it need not exceed 0.4 $S_s$ $I$ $w_i$, where

$Q_{ia}$ : design diaphragm lateral force at level $i$ from analysis
$Q_{ib}$ : design diaphragm lateral force at level $i$ as per Eq. 6.1.2
$h_i$ : height of floor $i$
$I$ : importance factor
$S_s$ : short-period constant range seismic acceleration coefficient with 5 % damping
$V_b$ : base shear
$w_i$ : seismic weight tributary to the diaphragm at level $i$
$N$ : number of storeys

The lateral storey force $Q_j$ in Eq. 6.1.2 can be obtained either by the LSP approach or as a force at level $j$ with the LDP approach. The force $Q_{ib}$ should be applied to one floor at a time.

If the vertical supporting elements have varying stiffness from one floor to the next, then the diaphragm will experience additional transfer forces. It has to also sustain transfer forces between itself and the vertical supporting system. These two types of forces are coupled through stiffness and deformation compatibility between diaphragm and the vertical support system. Transfer forces could be quite large in magnitude which calls for careful detailing of the floors to ensure continuity of load paths and integrity of diaphragms.

A horizontal diaphragm is traditionally designed for both gravity and lateral loads. For the latter, it is commonly treated as a beam spanning between lateral supports in each of the two horizontal orthogonal directions. For situations where complexities are present, a finite element model may be adopted for analysis.

### *6.3.3 Flat Slab Diaphragm*

Flat slabs are beamless, like flat plates. The addition of column capitals increases their shear capacity, and if enhanced bending capability at supports is also desired, then drop panels can be added. This form of construction is very popular because it

permits architectural flexibility, results in smaller storey heights and needs simpler formwork which consequently leads to saving in construction time and cost.

Flat slabs typically run over columns and span in both orthogonal directions. The Achilles heel for this form of construction is to achieve effective transfer of shear from slab to columns. Flat slabs are susceptible to excessive lateral deformations in the absence of beams, and in some cases two-way punching shear may control slab design. In general, the performance of flat slabs under earthquake loading is reported to be poor (Erberik and Elnashai 2003). Some of the reasons attributed to this are the following:

- With small lateral stiffness of a flat slab, there can be excessive drift under a major seismic event resulting in large second-order $P$-$\Delta$ effects causing damage to structural and nonstructural components.
- Brittle punching failure at slab–column junction could occur under inelastic high unbalanced moment reversals near columns. The larger drop panel depth available locally is not effective in the case of inverted punching forces (Erberik and Elnashai 2003). One way to overcome this is by providing stud shear reinforcement and/or introduce liberally sized drop panels.
- It is vulnerable to progressive collapse as seen in Picture 6.2. Although punching failure is local, for flat slabs, it gains importance because such a failure can lead to total collapse of the structure. To avert this, a part of the bottom longitudinal reinforcement at slab–column junction should run continuous over the columns since it allows the slab to hang off the column support at a failed column–slab joint. This may be sufficient for the slab to temporarily carry gravity loads.

Such a structure is commonly analysed as a *column plus equivalent beam* framing system. While the analytical procedure is well established, there is considerable uncertainty regarding the effective width of such a slab that can actually perform as a beam under lateral loads. This effective width will depend on many factors such as column dimensions vis-à-vis slab panel spans, distribution of reinforcement in the slab, dimensions of drop panels, nature of orthogonal framing and so on. The equivalent beam width of flat slabs for a lateral load analysis should be chosen with great care since it will affect, in large measure, the lateral frame stiffness. There are many formulae that have been put forth, largely based on experimental studies.

Another difficulty is to decide on the effective stiffness of the slab section taking cognizance of slab cracking and effect of reinforcement distribution in both orthogonal directions. Overestimation or underestimation of assumed beam width is not desirable. Under the circumstances, a logical approach would be to undertake a refined finite element analysis to arrive at the width and stiffness of the slab acting as a beam. Some designers opine that even after such an analysis, flat slabs should be also coupled with shear walls to form the lateral load-resisting system. It may be appropriate to avoid flat slabs in high seismic zones.

**Picture 6.2** Progressive-type failure

### *6.3.4 Transfer Diaphragm*

If there is an offset at a floor in the vertical alignment of a lateral load-resisting system, then the slab at that level has to be designed for transfer of shear force from the element above to the one below the slab, e.g. a slab transferring lateral forces between a tower and its podium structure. Such a diaphragm is termed as a transfer diaphragm. It carries very heavy loads and normally requires additional concrete thickness and reinforcement. Any opening in such a diaphragm should be minimised.

### *6.3.5 Collectors and Chord Elements*

Often, shear walls are not continuous for full length of the slab they support. In such cases, the contact area between slab and wall may be inadequate to transfer horizontal shear, particularly in the inelastic range. To overcome this, the slab can be thickened along its edges to form collector members which will transfer the cyclic shear.

Other instances where collectors need be provided are as follows:

- When there are large penetrations through a diaphragm to accommodate service lines going through or for stairs, as a result of which the defined load path is interrupted.
- Whenever stiffness of a shear wall above a particular floor level is substantially different from that of the one below.
- At re-entrant corners of a building. These have to be designed to carry forces generated on an assumption that the wings may move either (1) in the same direction or (2) in opposite directions. Such forces, which generate a tearing action at corners, have to be ultimately transferred to the supporting structure.

Collectors can be looked upon as members gathering shear forces from a diaphragm and delivering them to vertical elements. They carry seismic forces in direct tension or compression in addition to bending due to gravity loads. Their connections need to be designed for transfer forces amplified (Taranath 2010a) by a factor (of say 2) to safeguard against their failure prior to lateral load-resisting members developing their full nonlinear capacity. Since collectors will be called upon to transmit heavy compressive forces during cyclic loading, there may be a need to provide confining stirrups.

A collector should be continuous. Reinforcement from collector and drag elements should extend well into the supporting wall such that relevant wall area can sustain the forces, and then these bars should be continued beyond that section for a sufficient distance to develop the reinforcement (SEAOC 1999). In cases where a diaphragm is connected to a wall through anchors, it is advisable to provide additional reinforcement that spreads itself out into the slab to avoid high concentration of tensile stresses in the diaphragm.

A typical arrangement of collectors and chords is shown in Fig. 6.6a. To transfer forces from diaphragm to vertical walls, shear-friction reinforcement has to be provided along their interface. Collectors may or may not fit within the wall width. In the event that they project beyond the wall, it will cause an eccentricity $e$ (Fig. 6.6b) for which the collector/wall interface will need to be designed. Effective width of such a collector is commonly assumed as width of wall plus half of wall length.

Chords, on the other hand, are components which may be provided along edges of a diaphragm orthogonal to the direction of inertia force. They can be in the form of beams or can form a zone of the diaphragm. They transmit forces generated due to in-plane bending of the diaphragm. Chords are reinforced both longitudinally and in transverse direction and carry forces through direct tension or compression, while the diaphragm needs to be designed for shear. Splices in tensile reinforcement in chords and collector elements should be capable of sustaining yield strength of the reinforcement (SEAOC 1999).

Chords must be continuous and have strong connections with the diaphragm. At re-entrant corners and around openings, chords should extend into the diaphragm sufficiently to transfer boundary stresses. Typical evaluation of forces in a collector and a chord is illustrated through *Ex* 6.10.5.

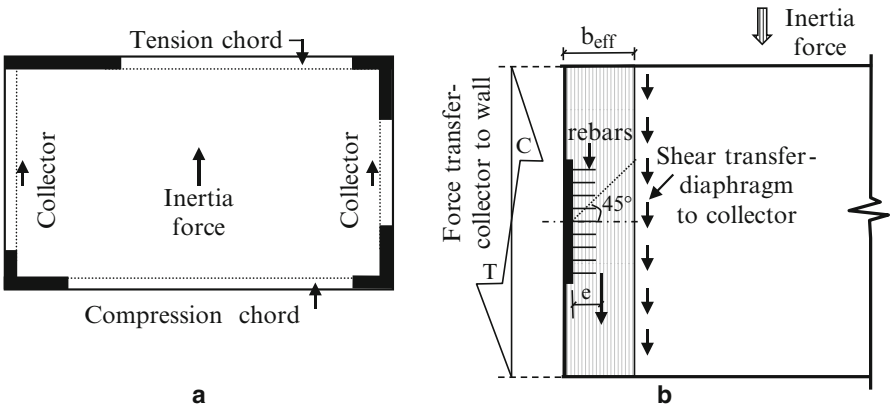


**Fig. 6.6** Collectors and chords. (**a**) General arrangement. (**b**) Collector wider than wall

## 6.4 Beams

From seismic considerations, the sizing of beams is important as it will dictate the strength of other framing members and components and indirectly affect frame cost. Beam end zones are often designed to yield under strong seismic demand because beams are more ductile than supporting columns as they do not carry significant compressive loads. It is important that the section chosen to yield reaches its flexure capacity before that in shear because hinging due to moment overload is ductile, whereas yielding in shear is brittle. Hence, a beam web should be well reinforced to preclude a shear failure through disintegration of web prior to yield failure of beam longitudinal rebars. Design and detailing requirements for a beam are specified in IS 13920 and hence are not repeated here in detail except for a few aspects listed below.

### *6.4.1 Design for Moment*

Procedure for design of a beam for a moment is well understood. However, some of the relevant aspects of design for seismic conditions are highlighted here.

(a) For SMRFs, plastic hinges are usually formed at beam ends and are distributed over the building height. Such hinges could be reversing or unidirectional. The former can occur under an extreme seismic event when very short span beams support light gravity loads. It can lead to yielding of both compression and tension steel alternately. In a unidirectional hinge, however, only the tension steel is likely to yield with stress in compression steel staying below yield point.
(b) It is recommended that the offset between beam and column centre lines should not exceed one-fourth the width of column (Elghazouli 2009) into which the

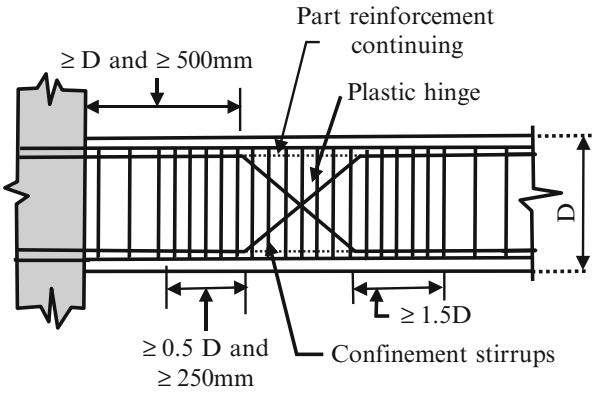


**Fig. 6.7** Shift in plastic hinge location

beam frames. This promotes efficient transfer of moments between beams and supporting columns.

(c) IS 13920 specifies that bottom reinforcement at a beam support should be at least half the top steel at that face. This is presumably to cater to longitudinal compressive forces. In addition, in the event of failure in a continuous beam, if the top reinforcement tears out of concrete, bottom rebars can provide catenary-type support and thereby prevent total collapse. These bars should be at least φ 12 mm.

(d) If a beam yields at a column face, such yielding could penetrate the column, thereby reducing anchorage length of beam rebars. Park (1986) has mentioned that sometimes the plastic hinge can be forced away from the column face as shown in Fig. 6.7. The special transverse confining reinforcement must commence (Park 1986) at least 0.5D or 250 mm (whichever is larger) before that section. As a variation, the confining stirrups should extend beyond the section into the span as shown in Fig. 6.7. At the shifted location of the plastic hinge, half the reinforcement could be bent as shown and the other half carried through.

(e) In beams, tension failure is preferred so that large increase in curvature can occur at near-constant moment, thus utilising ductility and preventing brittle failure in compression. IS 13920 specifies that maximum reinforcement ratio on any face at any section in beams shall not exceed 0.025. This could perhaps be to avoid congestion of reinforcement and to prevent compression failure in flexure.

(f) Sometimes, for architectural reasons, the concrete section provided could be much larger than that required from strength considerations. The quantity of steel in relation to concrete could then be low and may not be adequate to sustain the transfer of force from a cracked concrete section to steel. Perhaps for this reason, it is specified in IS 13920 (BIS 2003) that the tension steel ratio on any face, at any section, shall not be less than $0.24\sqrt{f_{ck}}/f_y$ where $f_{ck}$ and $f_y$ are in MPa.

(g) During an earthquake, it is difficult to establish the precise distribution of moment along a beam span, making it difficult to locate cutoff points for rebars. Perhaps to partially account for this uncertainty, IS code stipulates that two rebars be provided continuously on both faces of a beam and that this reinforcement should not be less than one-fourth of maximum negative steel provided at face of either joint. Rebars so provided should be at least of φ 12 mm.
(h) In the code, a minimum beam width to depth ratio is specified perhaps to ensure that there is no difficulty in confining concrete. Also, maximum depth to span ratio has been specified as ¼ to ensure that the beam does not behave as a deep beam.
(i) Longitudinal bars provided in beams should not be in excess of design requirement as this, in turn, will increase shear demand which could lead to brittle failure.
(j) ACI spells out details of reinforcement provision that can enhance the overall integrity of a structure. One of the recommendations to achieve this is to provide specified amount of continuous reinforcement at the top and bottom in perimeter beams along with closely spaced stirrups (Taranath 2010c).

### 6.4.2 Design for Shear

While the design of a beam for pure moment is routine, its design for shear is complex particularly in the inelastic range. One of the reasons for this is that there is wide scatter in results obtained from shear tests in comparison to those obtained from tests in flexure. It is very important to suppress the possibility of failure of a beam in shear as it is of a brittle nature. In other words, this implies that the strength of a beam in shear should exceed that in flexure.

For evaluating the design shear in a beam, consider a beam span as shown in Fig. 6.8a loaded with a factored gravity load of 1.2(DL + LL) which causes end shear forces of $V_a^{D+L}$ and $V_b^{D+L}$. Support moments under sway due to lateral inertia forces are shown in Fig. 6.8b, c. Design beam shear will need to be the larger of:

(a) Calculated factored shear force as per analysis
(b) Maximum of shear forces derived from beam's maximum capacity in flexure at corresponding end of the span, to be selected from

$$V_u^a = V_a^{D+L} - 1.4\left[\frac{M_u^{as} + M_u^{bh}}{L}\right];$$
$$V_u^b = V_b^{D+L} + 1.4\left[\frac{M_u^{as} + M_u^{bh}}{L}\right]; \quad \text{for sway to the right} \tag{6.2.1}$$

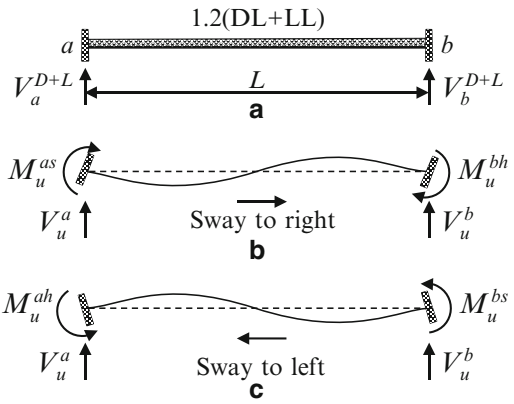


**Fig. 6.8** Sway moments and shear forces

$$
\begin{aligned}
V_u^a &= V_a^{D+L} + 1.4\left[\frac{M_u^{ah} + M_u^{bs}}{L}\right];\\
V_u^b &= V_b^{D+L} - 1.4\left[\frac{M_u^{ah} + M_u^{bs}}{L}\right] \quad \text{for sway to the left}
\end{aligned}
\tag{6.2.2}
$$

where

$V_u^a, V_u^b$ : design shear force at supports $a$ and $b$, respectively
$V_a^{D+L}, V_b^{D+L}$ : shear forces at $a$ and $b$, respectively due to gravity loads with a factor of 1.2
$M_u^{as}, M_u^{bs}$ : factored ultimate sagging moments at supports $a$ and $b$, respectively
$M_u^{ah}, M_u^{bh}$ : factored ultimate hogging moments at supports $a$ and $b$, respectively
$L$ : clear span of beam

The above is based on taking plastic moment as 1.4 times the calculated moment capacity with the usual partial safety factors. Because loading is cyclic, shear force can change direction. Hence, shear resistance of bent up bars and inclined stirrups cannot be considered.

### *6.4.3 Design for Bond*

From considerations of bond, it is advantageous to use deformed bars for longitudinal reinforcement in a beam. It is seen that with plain bars, the flexure cracks tend to be more concentrated in certain areas (Tanaka and Kono 2009), as a result of which cracks open wider. This leads to the possibility of increased corrosion of steel and lowers the durability quotient. Larger cracks also reduce stiffness of the member and become an avenue for a bond splitting failure.

The rebar diameter should not be unduly large as it can lead to difficulty while anchoring beam bars at joints. For proper anchorage length to transfer tensile force

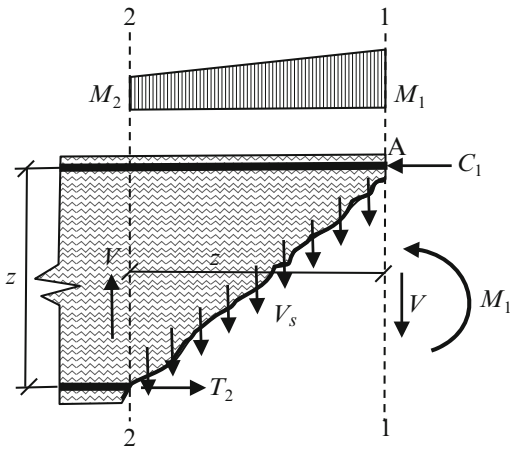


**Fig. 6.9** Tension shift effect

through bond, the effect of tension shift should be taken into account. This aspect is discussed below.

### *6.4.4 Tension Shift*

Whenever it is proposed to cut off some of the rebars, a designer should be aware of tension shift effect. To ascertain this, consider the free body diagram of a beam section under seismic effect as shown in Fig. 6.9 (the reader may also refer to Sect. 7.4.3.1). Plane of the crack may be taken at an angle of 45°, which leads to

$$M_1 = M_2 + V.z \tag{6.3.1}$$

Taking moments about point $A$ and neglecting forces due to resistance from dowel action and aggregate interlock, as their plane of action passes close to point A,

$$T_2.z = M_2 + V.z - 0.5V_s.z \tag{6.3.2}$$

where

$T_2$ : flexural tensile force at section 2
$M_1$, $M_2$: bending moment at sections 1 and 2, respectively
$V_s$ : shear force in stirrups crossing the crack
$V$ : total shear force on the section
$z$ : internal lever arm
$d$ : effective depth
$L_d$ : development length

It will be seen from the above that rebar tensile force $T_2$ is not proportional to moment $M_2$ at that section but to an enhanced moment of

$$M_2 + \left(1 - 0.5\frac{V_s}{V}\right) V.z \tag{6.3.3}$$

Stirrups provided near the plastic hinge zone are generally capable of sustaining the entire shear force, i.e. $V_s = V$. In such a case, the tensile force in rebar at section 2 is proportional to a moment given by $M_2 + 0.5V.z$.The value 0.5z is termed as *tension shift*.

Since $z \approx d$, it follows that beam rebars should extend a distance $(L_d + d/2)$ beyond the section at which they are required to develop full stress. As a limiting case, if concrete were to sustain the entire shear, then $V_s = 0$ and tension shift will be a distance $d$.

### 6.4.5 Ductile Detailing

The following aspects may be noted in respect of detailing:

- Locations where rebars may be spliced and where some of the rebars can be terminated should be worked out with much care. These should be specified on drawings.
- Wherever longitudinal bars are spliced, lap length should be the development length in tension and spacing of stirrups should not exceed 150 mm. Rebars should not be spliced (1) within a joint, (2) within $2d$ from joint face and (3) within a quarter span length from likely yield location where $d$ is effective depth of beam.
- Due to cyclic loading during a seismic event, beam bottom bars, near their junction with the column, may also develop tension. Hence, both top and bottom steel need to be fully anchored into column core concrete.
- Tension steel in a beam should be curtailed conservatively to allow for tension shift.
- Ductile detailing should be provided even if wind loads govern the design. This is because the structure has to withstand heavy inelastic demands during an earthquake.
- Mechanical couplers, if provided, should be thoroughly tested to demonstrate that they are capable of developing full strength of the bar and not be limited to $1.25 f_y$.
- At building corners, where two orthogonal beams terminate, careful detailing of rebars is required to ensure that they are adequately anchored. One option to overcome this difficulty is to have different depths and covers for the intersecting beams.

- To overcome non-availability of adequate space for anchoring beam top bars at a corner joint, provide a cross pin where the main bars bend. This pin should have a diameter preferably not less than that of the main bars. When another beam in the orthogonal direction frames into the column, its top steel can function as a pin.
- Confinement reinforcement in the form of stirrups should be provided over the entire lap length at a rebar splice.
- At beam ends, the first stirrup should be located no farther than 50 mm from column face.
- At an intermediate frame joint, beam bars shall run continuously through the column.
- At an end joint in a frame, the bars should be anchored a length from column face equal to the tension anchorage length plus ten times bar diameter, reduced by an allowance for the bend.
- Splicing of bars by welding could be considered only if great care is exercised to ensure that high-quality welding is feasible with the right electrodes and adequacy of splice strength is proven by regular testing. However, stirrups and ties required by design should not be welded to longitudinal rebars (Jain et al. 2005).
- Beam top longitudinal bars which terminate in a column should extend to the far face of the confined column core and then get anchored (ACI 318-08 2009).

## 6.5 Columns

Beams and columns are important elements of a frame wherein columns are normally the principal gravity compressive load-carrying members. Beams support loads from a particular floor, whereas columns support the entire building load above them. Any failure of a column can lead to a catastrophic failure, and hence it is a critical element for stability of a building. Columns should be dimensioned such that they do not fail in shear prior to failing in bending, and even after damage during a major seismic event, columns should have adequate capacity to sustain imposed gravity loads.

### *6.5.1 Column Design*

During preparation of a building layout, avoid creating a soft storey or a short column effect. If unavoidable, then relevant areas should be very carefully designed and detailed to safeguard against likely damaging consequences during an earthquake. A column should be designed on the strong column–weak beam philosophy, i.e. beam failure should precede column failure. Picture 6.3 demonstrates the concept of a weak beam–strong column. Flexibility of the beam is of vital importance. This


**Picture 6.3** Demonstration of strong column–weak beam

is because a plastic hinge at top of a column at its junction with a beam can cause storey-sway mechanism which can lead to a sudden collapse. Picture 6.4 depicts the formation of a typical storey-sway mechanism.

Here again, just like in beams, once design forces and moments are obtained from a computer analysis, the design of a column section is routine. Hence, a detailed column analysis is not repeated here, but emphasis is laid on the following important design aspects which should be noted:

(a) To achieve a strong column–weak beam configuration, as per ACI 318 (ACI 318-08 2009), the sum of column moments of resistance (calculated considering factored axial load) at a joint shall be at least 1.2 times the sum of moments of resistance of beams framing into the joint along each principal plane of the framework. New Zealand code calls for a much higher moment-carrying capacity in columns (Jain et al. 2005). IS 13920 presently is silent on this subject.

(b) Columns that rest on basement walls are sometimes detailed as pinned at their bases (Fig. 6.10). This results in an increase in the period of vibration with consequent reduction in inertia forces. However, with a pinned base, it is difficult to control inter-storey drift to within codal limits. This problem is heightened in the ground storey which is normally taller than the rest. For a pinned connection, the junction between column base and supporting wall should be capable of

**Picture 6.4** Storey sway mechanism

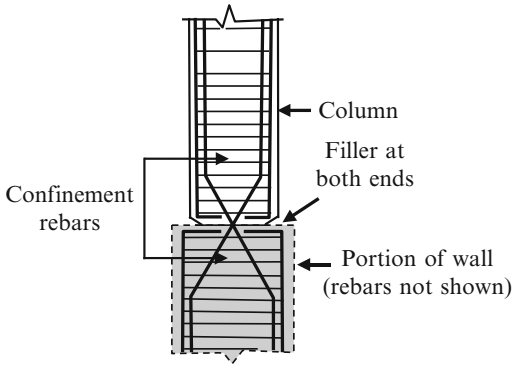


**Fig. 6.10** Column pinned at base

transferring the heavy shear. For this reason, hinge joint should be carefully detailed and constructed with utmost care.

(c) Normally the factored axial stress in a column under seismic conditions exceeds $0.1\,f_{ck}$, and it is designed as a member under axial force and flexure.

(d) Corner columns call for special attention of the designer. They are invariably heavily stressed and are vulnerable to simultaneous motion in both horizontal and vertical directions. Secondly, they could experience reversible axial forces due to overturning moments in tall buildings. Thirdly, it is at corners that deformations along one axis must interact with deformations along an orthogonal axis. Hence, it is prudent to provide a design margin in such columns to ride over any overload, and these biaxially loaded columns should be designed by capacity design approach.

(e) IS 13920 permits use of 200 mm column when beam spans are less than 5 m. However, the authors concur with the view expressed by many researchers that minimum column dimension should be 300 mm nor less than 15 times the largest beam bar diameter for its good performance as a ductile member. This will reduce congestion at beam–column joint and difficulties that are experienced during construction. Larger column size facilitates threading of beam rebars across more easily and bond and shear stresses at the joint can be met more readily.

(f) Storey shear causes frame columns to bend in double curvature with points of contraflexure close to mid-storey height. When combining modal responses by SRSS method, the sign is lost and point of contraflexure cannot be located. Secondly, forces obtained from a dynamic response analysis are always positive with the result that it is virtually impossible to check dynamic equilibrium. In such an event, it is suggested that a static analysis may first be performed for the first mode which invariably controls maximum response. From this, the signs for forces could be known and moments obtained from SRSS method may be assigned these signs. Normally this should be appropriate.

(g) A designer should focus on eliminating possible brittle failure of a column in axial compression as well as in bond and anchorage of rebars.

(h) Columns above and below a joint should be designed for shear forces which should be the higher of:

1. Factored shear force as per normal analysis.
2. A shear force in each direction required to equilibrate the sum of beam plastic moment capacities (inclusive of overstrength) at the joint as detailed in Sect. 6.4.2, i.e.

$$V_u^a\,(\text{col}) = 1.4\left[\frac{M_u^{ar} + M_u^{al}}{h}\right] \tag{6.4.1}$$

where $V_u{}^a$ is the column shear force at joint $a$, $M_u{}^{ar}$ and $M_u{}^{al}$ are ultimate factored beam moments to the right and left of joint $a$, respectively, and $h$ is storey height.

(j) Requirement in item (h) above does not apply to the junction with grade beams as the latter should not have plastic hinges.

### *6.5.2 Ductile Detailing*

In potential plastic hinge regions of a column, confinement of concrete is essential to permit development of required rotational ductility. Since column moment reduces sharply away from a joint, the region of plastic hinge is shorter than that of a beam framing into the joint. Column ends can experience heavy reversible moments under seismic conditions, and lateral shear forces can be much larger than those under gravity loads. Hence, the core concrete should be well confined to avoid sudden shear failure which can have catastrophic consequences. The following detailing aspects may be noted:

- Very small diameter bars should not be used for longitudinal reinforcement as they can easily buckle. Column links need to be of a size such that they are strong enough to prevent buckling of longitudinal steel and also are able to confine the concrete. Column longitudinal bars should be well anchored into foundations in order to avoid any tensile pull out.
- Laps in longitudinal bars should be within the middle half of column height with a splice length $L_d$ as for tension steel because of possibility of reversal of stresses. Not more than half the total reinforcement is to be spliced at any one section which implies that for a normal building, the column steel may have to be lapped in alternate storeys. This raises practical difficulties. However, any variation from this requirement can be looked into only if the column section is robust and workmanship is of a high quality. This is because, apart from bond considerations, it has to be ensured that strength of concrete itself, as cast, is adequate.
- Some of the codal stipulations regarding length over which confining stirrups need to be provided are:

  (a) Over the entire splice length at a spacing not exceeding 150 mm centres.
  (b) From column joints with beams and foundations, the confining stirrups should extend towards column mid height for a length, which shall be the larger of (1) 450 mm or (2) one-sixth of clear height of column or (3) longer side of a rectangular column.
  (c) Over full storey height, if in a particular storey the point of contraflexure, under the condition of gravity and earthquake loads, lies outside middle half of clear storey height.

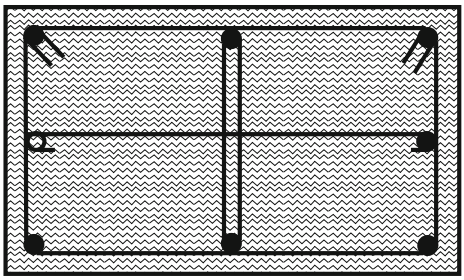

**Fig. 6.11** Typical column section

- It may be prudent to provide confining links over a larger length at locations where both axial and flexural demands are exceptionally high.
- Confining stirrups to extend at least 300 mm into footing or pile cap.
- If a shear wall is discontinued and then supported by columns, the latter should have confining reinforcement over their full height. Such reinforcement should continue into the wall for a height equal to development length of largest longitudinal bar in the columns. The same applies to columns supported on a wall. In author's view the terminating of a shear wall at part height should be avoided.
- A column that has significant variation in stiffness along its height should also be provided with special confining reinforcement over its full height.
- For circular columns, the longitudinal rebars should be uniformly distributed around its perimeter in order to assist confinement of concrete.
- It is recommended (Jain et al. 2005) that at least one intermediate bar shall be provided between corner bars along each column face and that every alternate longitudinal bar should be anchored by the corner of a stirrup. This helps to ensure integrity of the column joint as well as the column. Intermediate column bars should be restrained by using multiple stirrups or stirrups along with cross ties. The former are preferred. Typical details are shown in Fig. 6.11.
- Lap splices in columns cannot be located near column ends as spalling of concrete can occur there. Hence, splices have to be located near column mid height. Picture 6.5 depicts the failure of a column because of inadequate confinement.
- It is suggested (Jain et al. 2005) that if longitudinal column rebars are $>25$ mm diameter, then the stirrup diameter should be $\geq 10$ mm.

A typical section of a portion of a frame with ductile detailing for column and beam is shown in Fig. 6.12. Typical column failures are depicted in Picture 6.6.

## 6.6 Beam–Column Joints

A beam–column joint is normally defined as that portion of a column which is within the depth of the deepest beam that frames into it. Proper functioning of this zone

**Picture 6.5** Inadequate confining links

**Picture 6.6** Column failures

is critical for satisfactory performance of a MRF in the inelastic range during a major seismic event. The load flows through this region where moment gradient is very steep and any deficiency here will jeopardise the entire structure. Hence, much

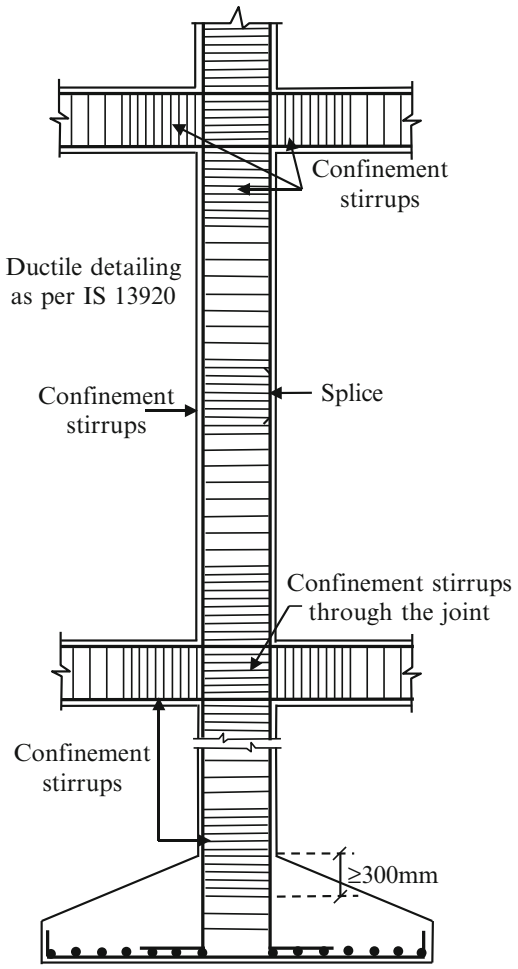


**Fig. 6.12** Typical frame confinement reinforcement

attention should be paid to the design, detailing and construction of such a joint. Picture 6.7 depicts failure of beam–column joints in a frame.

### *6.6.1 Joint Types*

In a MRF, it is common to classify a joint based on its geometrical configuration as under:

(a) *Interior joint* – where beams frame into all four faces of a column. Bars passing through such a joint face a pull–push effect as the force in a bar changes across the joint cyclically from tension to compression and vice versa. This imposes a

**Picture 6.7** Typical beam–column junction failure

severe demand on bond for which the bars need to have adequate development length so as to meet both tensile and compressive conditions in order to prevent bond failure.

(b) *Exterior joint* – where beams frame into opposite faces of a column and one orthogonal face. Repeated cyclic loading can cause splitting cracks in concrete (termed yield penetration) progressing into the concrete core. To meet this demand, beam rebars should have adequate development length within the column depth measured beyond region of penetration. This can be achieved by providing a hook, or a pin or extending bars beyond column exterior face as shown in Fig. 6.13. In practice this extension option is normally feasible only if it forms a part of the original architectural scheme.

(c) *Corner joint* – where two orthogonal beams frame into a column. Beam bars need to be well anchored as for an exterior joint.

(d) *Knee joint* – where a beam frames into a column at roof level. Each of these joint types is shown in Fig. 6.14a–d.

### *6.6.2 Joint Behaviour Mechanism*

Within the column/beam junction, concrete experiences a complex stress pattern due to bending, compression, tension and shear. A joint is subjected to both vertical and horizontal shear forces which in turn result in diagonal compression and tension in its core region. Failures at a beam–column joint are commonly due to (1) shear

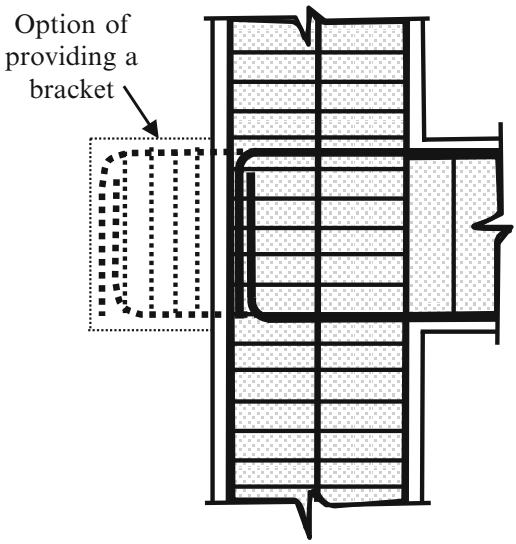


**Fig. 6.13** Exterior beam–column junction

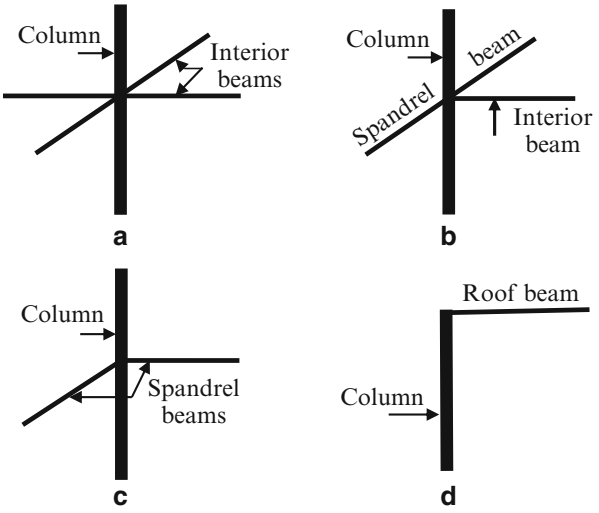


**Fig. 6.14** Joint types: (**a**) Interior. (**b**) Exterior. (**c**) Corner. (**d**) Knee

failure in panel zone, (2) anchorage failure of beam rebars and (3) bond failure of rebars going through the panel.

A cast in situ monolithic beam–column joint has to meet following challenges:

- Under serviceability limit state, the joint should be free of cracks induced by concrete compression and shear.

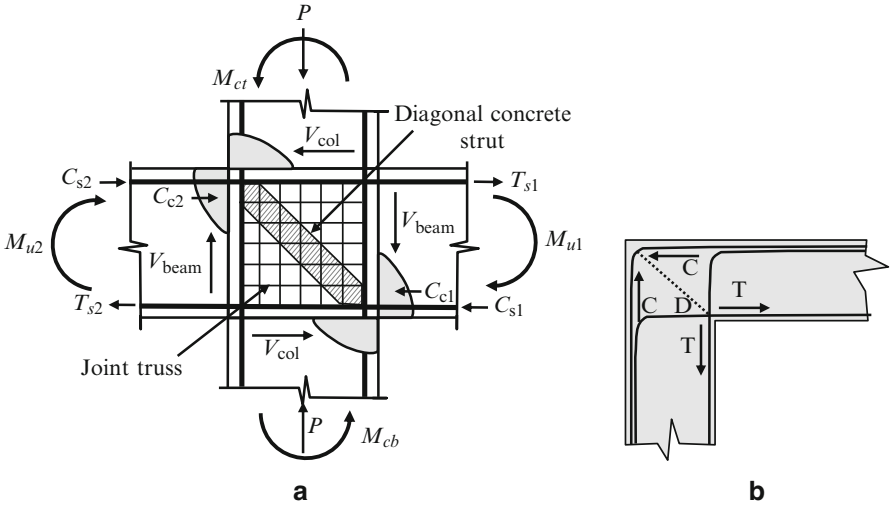


**Fig. 6.15** (**a**) Beam–column joint (sway to the *right*). (**b**) Corner joint

- Capacity of a joint in shear and flexure should be greater than that of the members it connects which will enable them to develop and sustain their ultimate capacities.
- There should not be over-congestion of reinforcement as it will preclude formation of sound and dense concrete.
- Horizontal shear stress should be less than the limiting nominal permissible shear stress in concrete.
- Column stirrups should extend right through beam–column joints to ensure that concrete there is properly confined and that column bars do not buckle within the joint.

Within the joint panel, a diagonal concrete strut is formed due to vertical and horizontal compressive forces as well as shear forces. It could be a single strut or there can be multiple struts. A truss mechanism is formed due to interaction between confining horizontal and vertical reinforcement and a diagonal compression field (Naeim 2001). These are shown in Fig. 6.15a.

A corner joint as shown in Fig. 6.15b deserves special attention. Compressive and tensile forces in rebars cyclically change from tension to compression. When inner bars are under tension, there is a tendency for rebars to pull open the inner corner of a joint. At the same time, rebars with compression will tend to force the upper corner out. It is desirable that diagonal bars D be provided to hold the joint together.

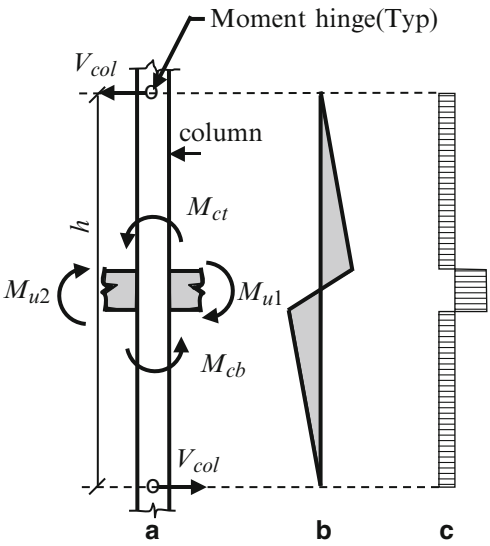


**Fig. 6.16** Joint moments and shears: (**a**) Force diagram. (**b**) Moment diagram. (**c**) Shear diagram

## *6.6.3 Joint Design*

The design process is explained for an interior joint under seismic conditions with sway towards right. For other types of joints and sway to the left, similar procedures can be readily adopted. Basis of design is the strong column–weak beam philosophy coupled with the requirement that a joint should be stronger than members that frame into it. A joint has to be designed for flexure, shear and bond which is discussed below.

### 6.6.3.1 Design for Flexure

An interior joint is subjected to a hogging moment $M_{u1}$ from beam on right and a sagging moment $M_{u2}$ from beam on left (Fig. 6.16a). The total moment being $M_b = \Sigma\ (M_{u1} + M_{u2})$. This moment is resisted by moments in top and bottom portions of the column, viz. $M_{ct}$ and $M_{cb}$, respectively. Total moment resisted by column at the joint will be $M_c = \Sigma\ (M_{ct} + M_{cb})$. Splitting of moment $M_c$ between $M_{ct}$ and $M_{cb}$ will be in proportion to relative stiffness of column portions above and below the joint. It is suggested (ACI 318-08 2009) that $M_c \geq 1.2\ M_b$. Upper and lower portions of the column are then designed for factored gravity load plus factored moment following well-established procedure.

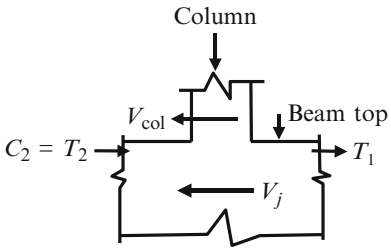


**Fig. 6.17** Joint free body diagram

### 6.6.3.2 Design for Shear

With forces transmitted from adjoining faming members, a joint is subjected to both vertical and horizontal shear (Jain and Murty 2005). The former is proportional to sum of beam moments at the joint divided by depth of column. Horizontal shear is proportional to sum of column moments at beam top and beam bottom sections divided by beam depth. External moment acting on the joint is $M_b$. This is resisted by forces acting at moment hinges located in the column above and below the joint. Distance between hinges is the storey height $h$ as shown in Fig. 6.16a. From this it follows that column shear can be obtained as

$$V_{\text{col}} = M_b / h \tag{6.5.1}$$

It will be observed from Fig. 6.16b that there exists a steep moment gradient through the joint which is much steeper than those in beams or columns that frame into it. With a steep change in moment across the joint, it is clear that shear forces are very large as can be seen from Fig. 6.16c. Typically, the forces acting on an intermediate joint are shown in the free body diagram (Fig. 6.17).

Considering equilibrium of forces at a joint, the joint shear is given by

$$V_j = T_1 + T_2 - V_{\text{col}} \tag{6.5.2}$$

A joint has to be designed for this horizontal shear force. Jain et al. (2005) have listed the effective width of a joint and nominal shear strengths of a joint as given below:

(a) For joints confined on all four faces, $1.5 A_j \sqrt{f_{ck}}$
(b) For joints confined on three faces or two opposite faces, $1.2 A_j \sqrt{f_{ck}}$
(c) For others, $1.0 A_j \sqrt{f_{ck}}$

where:

$A_j$: effective area of joint resisting shear $= b_j \times h_j$
$b_j$: effective width of joint which is the lesser of $b_c$ and $(b_b + 0.5h_j)$ in which $b_c$ is width of column and $b_b$ is width of beam for the condition when it is less than that of column

$f_{ck}$: characteristic strength of concrete, N/mm$^2$
$h_j$: depth of column in the direction of shear considered

Special confining reinforcement as required at end of a column should be continued right through the joint. A joint is considered as confined if beams frame into it on all four sides. For this purpose, each beam width should be at least three-fourth that of the column face into which it frames. In such an event, confinement reinforcement in the joint shall be half that at column ends (BIS 2003). However, spacing of stirrups should not exceed 150 mm.

#### 6.6.3.3 Check for Bond

Performance of a rebar in bond is primarily dependent on grade of concrete and degree of its confinement, bar spacing and surface texture of the rebar. When tensile force in beam reinforcement exceeds its yield strength, splitting cracks appear near its junction with the column. This is termed as *yield penetration*. To meet bond strength requirement, the bar development length has to exclude this penetration depth.

As mentioned above, a rebar passing through an interior joint experiences a pull–push effect. As a result, rebar development length must meet the compression as well as tension demand. To reduce bond stress, rebars of smaller diameter may be employed. Bond stress should be checked taking stress in the bar as $1.25 f_y$.

### *6.6.4 Ductile Detailing of a Joint*

Inadequate design provisions and detailing errors in a beam–column joint can jeopardise the entire structure, even when other structural members conform to codal requirements.

Judicious detailing is called for and following aspects may be noted:

- Do not anchor bars in the confined portion of a joint. When a longitudinal beam rebar is terminated in a column, it should extend to the far face of confined concrete core and then get anchored.
- Top beam rebars should be bent down and lower bars bent up. If length is inadequate, combine these bars into a U shape or else use screwed bars with anchor plates. This may be a must for a knee joint. Bent bars should not project into the column below the beam as this will prevent concreting of column up to beam bottom.
- Failure modes of a knee joint are typically brittle, i.e. in bond and shear. Therefore, it is important that confining stirrups continue through the joint.
- Rebars should not be spliced within a joint.

**Picture 6.8** Poor concrete at beam–column junction

- Joint details should take into account its practical implementation in the field such that there is no hindrance to production of concrete of sound quality. However, it is not advisable to substitute large diameter bars to decongest the zone at the expense of loss in bond.
- Joint section should not be very restricted. This is to limit horizontal joint stresses so as to prevent diagonal crushing of joint.
- It is desirable that the designer prepares a full size detail of beam–column connection with all the rebars and stirrups to ensure that such placement of rebars is easily possible and will be conducive to creating good concrete. Picture 6.8 depicts poor concrete quality at a beam–column joint.

### *6.6.5 Joint Constructability*

To avoid congestion of rebars in the joint region and to maintain joint shear stresses within limits, the following care is advisable:

- Column size should be ample with reinforcement ratio not exceeding 3 %.
- Rebars in beams should be in a single layer.
- Orthogonal beams meeting at a joint should have different covers.
- It is preferable that framing beams be narrower than the column within limits of aesthetics.
- It is advisable to use self-compacting concrete although there could be a cost premium. If this is not possible, then it should be explored whether it is possible to use 25 mm down aggregate with a higher cement content to maintain specified concrete strength.

One of the prime difficulties faced during construction is to provide horizontal stirrups within the joint portion. An approach that has been proposed (Joshi et al. 2001), applicable for small projects without much mechanisation, is as under:

- Lay beam bottom steel in either direction with the stirrups. Maintain rebar cage above slab level.
- Introduce confinement rings in column which will be required below beam bottom level.
- Over the beam bottom steel and within the joint portion, stack all the horizontal stirrups meant to be provided in joint portion.
- Thread beam top steel through vertical beam stirrups and rotate the beam top bars which were initially turned sideways.
- Lower the beam reinforcement cage into the formwork together with the loose links.
- Raise the stacked stirrups placed in joint portion and tie them at the right location The typical design of a beam–column joint is explained through *Ex* 6.10.6.

## 6.7 Facade Skin

Commonly, the facade skin is composed of (1) a rigid masonry infill or (2) a thin curtain wall. These form nonstructural components which are outside the scope of this book. However, since they have a significant effect on behaviour of a frame, their role during a seismic event is briefly discussed here.

### *6.7.1 Rigid Masonry Infill*

Use of rigid unreinforced masonry as an infill between frame columns to form a building envelope has been the practice for over a century. This form of building envelope contributes substantially to frame stiffness, thereby reducing drift. However, on the flip side, if masonry in some of the panels is unwittingly removed, it can lead to considerable irregularity with torsional imbalance and other unfavourable consequences.

In respect of incorporating infills in the seismic analytical model, there are two principal schools of thought (Fardis and Panagiotakos 1997) as listed below:

(a) Considerable experimental research has been done to model infill masonry as forming a single or multiple diagonal strut/s. A designer should take benefit of the outcome of such work and model infill in the analysis process as it often controls a building's seismic performance. With proper planning and maintenance, walls can be located to provide optimum benefits and steps can be taken to ensure that walls are maintained in their original positions throughout the life of a structure.

(b) Effectiveness of infill is suspect, and hence it is left out of the seismic analytical model. Some of the reasons put forth for this view are the following:

- Masonry is often punctured with openings (e.g. for windows), and in that event there is uncertainty attached to formation of diagonal struts as envisaged.
- Strength of infill masonry is not precisely known, and being brittle it has often cracked, spalled and got separated from the frame during a major earthquake.
- When main frames are designed to withstand large displacements without collapse, then rigid masonry infill needs to be separated from the frame to permit those deformations to occur. To achieve this, well-executed and long-life sealant joints have to be provided, which is a problem.
- Masonry has very little out-of-plane resistance and has often toppled over when shaken, and this can cause serious injury. Such a failure is seen in Picture 6.9.
- There is no certainty of masonry layout staying unchanged throughout the design process and during the life of the structure. Portions of it could be removed at some stage of its life.

Designers often forego the profit from beneficial effects of masonry infill and choose the second point of view. If masonry infills are present, they are considered to be nonstructural.

### *6.7.2 Curtain Wall*

Such a cladding may be of glass, sheet steel, plastic or aluminium panels or their combinations. It is much lighter than brickwork, thus reducing building weight and inertia forces. It is aesthetically pleasing and is amenable to quick erection, and hence it has come to stay. Such a cladding gives very little seismic resistance to the peripheral structure. It is reported that during seismic excitation, glass damage is largely due to in-plane deformation. Another area of concern is out-of-plane vibration. The designer should provide strong but flexible jointing details between glazing and its framing such that the glass develops out-of-plane resistance, is firmly held to prevent drop out if shaken but at the same time permits lateral drift without cracking of glass. Recently developed tests, for ensuring satisfactory performance during a seismic event, should be strictly adhered to. High cost of such detailing is another factor.

**Picture 6.9** Out-of-plane failure of infill walls

## 6.8 Tall Frames

Low-rise buildings are generally those where gravity loads predominate. There is no universally accepted definition of what constitutes a tall building since tallness cannot be defined either in terms of number of floors or total height. Hence, any definition per se will have to be transient on a time scale. From a structural engineer's point of view, the defining line separating a tall building is generally accepted as one which transforms its design from statics to dynamics, i.e. slenderness ratio of a building plays an important role in its design.

### *6.8.1 Introduction*

Tall buildings emerged on the horizon in the 1880s, but it is only in recent years that there has been a phenomenal spurt in their numbers. This is largely because of rapid urbanisation which has sent land prices skyrocketing coupled with the desire of residents to stay close to their work place and city centre. Thus, the engine for change has primarily been economic with an impetus from rapid technological development in vertical transport and advent of high-strength concrete. Introduction of digital computers in the 1950s and development of application software thereafter gave a major boost by reducing computerised analysis costs to affordable levels.

Mostly, seismic analysis of tall buildings is done utilising professional software with the result that approximate hand methods have been increasingly marginalised. Hence, no attempt has been made here to present such methods or to analyse a tall building in detail. The authors are of the opinion that a reader's interest will be better served by covering important aspects which a designer should be aware of while conceptualising or analysing the behaviour of a tall building under seismic conditions. Successful implementation of a tall building, as mentioned earlier, calls for close cooperation between multidisciplinary agencies right from planning stage. Secondly, construction methodology that is finally chosen can play an important role in achieving an economical solution.

Since high-frequency seismic waves attenuate much faster, tall buildings with their longer period of vibration can be more susceptible to distant earthquakes. On the other hand, due to near-field ground motion, a five- to ten-storey structure, whose period could be in the band width of seismic excitation, could experience high seismic forces. This is borne out in earthquake damage analysis of medium-rise (5–15 storeys) buildings.

It is common practice to assume that free-field ground motion is the exciting motion. However, in case of tall buildings, the foundations are often massive and are surrounded by deep stiff basement boxes with many subterranean levels. The structure's motion could, in such cases, be affected by that of its basement structure. Secondly, the fundamental period of a tall building is usually larger than that of a medium-height building, and as a result, the horizontal design acceleration

becomes relatively smaller. However, the vertical acceleration is not reduced. As a consequence, the V/H acceleration ratio is larger for taller buildings (Aoyama 2001).

### *6.8.2 Structural Forms*

Structural frameworks to support gravity loads and withstand lateral inertia forces in tall buildings have undergone many revolutionary changes over the past decade, and it is still a continuously evolving process guided by demand and performance. Some of the commonly adopted framing systems for concrete buildings are dual systems composed of MRFs and shear walls and more recently tubular systems. These can be further subdivided into coupled shear walls, slab–column frameworks, core supported structures, modular tubes, mega-frames, etc. Type of framing adopted is invariably a dual system formed by a combination of two or more of the above and other options.

The use that a building will be put to is a major consideration in selecting its structural form. Modern offices require large open spaces which are ideal to subdivide into suitable modules with the help of light weight partitions. On the other hand, residential premises call for smaller framing modules which are repeated from one floor to another. For the former, a central core with perimeter columns is an ideal framing layout, whereas for the latter a moment frame or bundled tube structure will prove advantageous.

#### 6.8.2.1 Moment Frame

This form consists of columns and girders joined by moment-resistant connections. They can be used in the form of a series of frames in both orthogonal directions, or they can be readily combined with shear walls to form dual systems. For MRFs, the bay widths adopted to support gravity loads can be suitable for resisting lateral loads also. This form of framework is covered in Sect. 6.2.

#### 6.8.2.2 Shear Wall

Shear walls are an efficient means of resisting lateral loads, and their design aspects are covered in Chap. 7. Initially in early 1950s, shear wall core systems with frames were adopted, but they proved uneconomic to resist lateral loads as buildings grew taller (Yilma 2005). Although core walls are quite effective in restricting the amount of drift, their efficiency diminishes with increasing building height. Secondly, such walls can experience excessive uplift forces on their foundations. This paved the way for introduction of outriggers into the framework.

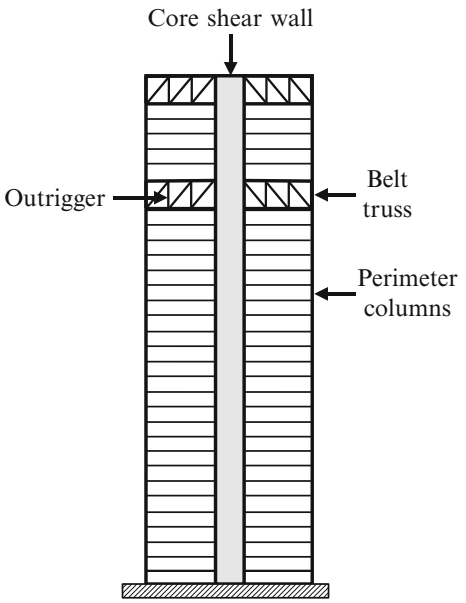


**Fig. 6.18** Outrigger with belt trusses

### 6.8.2.3 Core and Outrigger System

Outriggers are stiff trusses which span from the central core to external supporting building columns as shown in Fig. 6.18. These trusses mobilise resistance to overturning moments through axial forces in peripheral columns. This in turn leads to a reduction or complete elimination of net tension in shear core walls. The outriggers and belt trusses have to be adequately stiff in flexure and shear and hence could be even two-storey deep.

Outriggers are designed and detailed such that while being rigidly connected to core walls, they transmit only vertical loads to perimeter columns. In order to mobilise the peripheral columns that are not directly connected to outriggers, belt trusses can be added running along building perimeter. While outriggers effectively increase a structure's flexural rigidity thereby reducing bending moments and drifts below their level, they do not enhance shear resistance which is primarily carried by the core.

Outriggers are often one- or two-storey deep and can interfere with internal occupiable space in a building. This can be offset to some extent by locating outriggers in mechanical floors. To increase their effectiveness, outriggers may be employed in a multilevel configuration. If intermediate outriggers are also present, precise construction sequence has to be worked out for core walls. Also, a designer should evaluate the stresses developed because of differential shortening between core walls and external columns. The same is true with shear walls and adjoining frame columns.

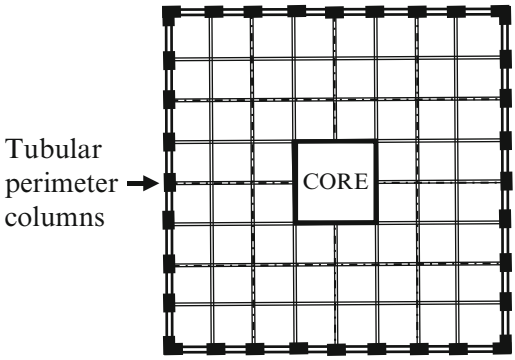


**Fig. 6.19** Schematic of a tubular frame

#### 6.8.2.4 Tubular Frame

A framed tube system comprises of frames along the building periphery formed by closely spaced columns connected by rigid spandrel beams at each floor level, thereby forming a tube-like structure. Introduction of tubular structural frames has been one of the most significant developments in high-rise structural forms, and Dr. Fazlur Khan is credited with their introduction (Fig. 6.19).

Perimeter columns parallel to the direction of lateral load act as webs of a large cantilever box and resist lateral shear. Frames perpendicular to the lateral force can be looked upon as its flanges. Webs and flanges are interconnected orthogonally by very stiff corner columns, while gravity loads are supported primarily on internal columns. Tubular structures have an advantage that they require less material, allowing freedom for internal space planning resulting in a column-free interior. However, the closely spaced perimeter columns are a hindrance for ingress and egress at grade level. This often results in perimeter building columns resting on large transfer girders which distribute the loads to widely spaced columns below.

For a structure to act as a tube, the closely spaced columns should be continuous along building periphery. Moments due to lateral forces on such systems are resisted by axial forces in flange columns which form an array perpendicular to the force direction. Shear is resisted by an array which is parallel to the forces direction. Since perimeter columns essentially carry axial loads, flange columns can be aligned such that their strong bending direction is along the building face. This enhances available rentable space within. These and other types of frames are normally analysed using computer software.

#### 6.8.2.5 Bundled Tube Framing

A tubular structure composed only of perimeter columns is not as stiff as a rigid tube because of shear lag effect as explained later. This can be overcome to some extent by introduction of bundled tubes. This form is created when framed tubes are bundled together so that common walls of contiguous tubes form single walls.

This brings about compatibility of forces at interfaces between these tubes. Such a framework has the added advantage that individual tubular modules could be terminated at intermediate levels without affecting basic structural integrity. Another feature is that internal tubes can be adapted to various polygonal shapes such as rectangular, hexagonal and so on.

A rigid floor slab constraints web panels of an inner tube to deform by the same amount as the external ones. They will thus carry a portion of external lateral load in proportion to their stiffness. The inner webs will now transfer their shear as loads onto inner perimeter columns. Thus, end columns of interior frames will be mobilised directly by internal frames, and these perimeter columns will carry loads that are higher than earlier, resulting in a reduction in shear lag effect. At the same time, a bundled tubular structure permits wider spacing of exterior tube columns, thus assisting functional and aesthetic planning.

## 6.9 Special Aspects Relevant to Tall Frames

Under seismic conditions, a tall building experiences large overturning moments and shears at its base coupled with large gravity loads. Meeting ductility demand at the base is difficult with the high compressive stress present. Other difficulties include restricting storey drifts, controlling foundation uplift forces and so on. Some of the relevant aspects that call for a designer's attention are discussed below.

### *6.9.1 Damping*

It is opined that (Wood 1973) damping diminishes with increase in building height. Thus, the usual 5 % damping assumed for concrete structures may be high for modern tall buildings because:

- Generally light cladding material is used which has a much lower energy-dissipating capacity and will thus play a smaller role in the magnitude of a building's damping.
- Radiation damping from the foundation is lower because rocking frequencies are very low.
- Role of other nonstructural components towards energy dissipation is also small.

While conducting time history analysis, a damping factor has to be assigned. However, the present state of art is not conclusive so as to clearly define the magnitude of damping to adopt. With the knowledge that damping cannot be predicted accurately, it has been suggested (PEERC 2010) that a default value of damping for tall buildings in all modes may be taken as 2.5 % for service level evaluation.

### 6.9.2 *Effect of Higher Modes*

It is traditional practice to focus attention on the first few translation modes while evaluating distribution of base shear for buildings. However, studies have shown that for tall buildings, the second or even higher modes can play a significant role in the building's response (PEERC 2010). To allow for greater participation of higher modes, most codes recommend that a portion of the base shear may be considered to be concentrated at roof level, thereby increasing shear at higher levels.

Magnitude of this force at roof level is to be taken as (SEAOC 1999) $Q_t = 0.07T.V_b$. However, $Q_t$ to be $\leq 0.25V_b$ if $T > 0.7$ s and $Q_t = 0$, if $T \leq 0.7$ s where $T$ is fundamental period of vibration of the building. With a base shear of $V_b$ for an $N$ storey building, a force $Q_t$ is considered to act at top floor level. Balance base shear (i.e. $V_b - Q_t$) can be distributed among all floors, including the top floor, in accordance with the formula

$$Q_i = \frac{(V_b - Q_t)\left(w_i h_i^2\right)}{\sum_{j=1}^{N} w_j h_j^2} \tag{6.6.1}$$

Storey shear and moment at level $j$ will be

$$V_j = Q_t + \sum_{i=j}^{N} Q_i; \text{ and } M_j = Q_t\left(h_N - h_j\right) + \sum_{i=j}^{N} Q_i\left(h_i - h_j\right) \tag{6.6.2}$$

where:

$Q_j$, $Q_i$ : shear force at storey $j$ and $i$, respectively
$Q_t$ : shear force at top storey $N$
$w_j$, $w_i$ : seismic weight at storey $j$ and $i$ respectively
$h_j$, $h_i$, $h_N$: height of storey $j$, $i$ and $N$ above the base respectively

### 6.9.3 *Reduction of Frames*

A large tall structural framework is first analysed by approximate methods. For this purpose, the imposed loads are assumed, and gravity loads are based on approximate sizing of members. Lateral loads are approximately allocated between frames. For such a preliminary analysis, a symmetrical frame with a repetitive floor system can be reduced in size so that computational time is substantially brought down. This approach is adequate to make a preliminary check on whether evaluated drift meets codal stipulations. If not, then member sizes can be revised. Such an approach is also useful for shear analysis of the frame.

The reduction can be either vertically or horizontally and can be implemented either separately or in combination. The process is described below, in brief, for a regular frame shown in Fig. 6.20a.

#### 6.9.3.1 Vertical Reduction

Consider a tall regular frame with uniform storey heights and identical girders at each floor level as shown in Fig. 6.20b. For a preliminary analysis to check drift, usually 3–5 number (say $n$) of identical girders (each with a moment of inertia $I_{gi}$) can be substituted by a single girder of moment of inertia $I_{gis}$. In that event, Smith and Coull (1991) has shown that

$$I_{gis} = \sum_{i=1}^{n} I_{gi} \tag{6.7.1}$$

With this substitution, the column height will increase to $nh$. It is well known that the approximate drift of a column in a storey will be

$$\delta_h = \frac{Vh^3}{12EI_c} \tag{6.7.2}$$

Since drift ($\delta_{nh}$) of the substituted columns of height $nh$ has to be the same as that of $n$ number of original columns each of height $h$,

$$\delta_{nh} = \frac{V(nh)^3}{12EI_{cs}} = \frac{Vh^3}{12E}\sum_{i=1}^{n}\frac{1}{(I_c)_i} \quad \text{i.e.} \quad I_{cs} = \frac{n^3}{\sum_{1}^{n}\left(\frac{1}{I_c}\right)_i} \tag{6.7.3}$$

where:

$\delta_{nh}$: drift of storey height $nh$
$I_{gi}$ : inertia of girder at floor $i$
$I_{gis}$: inertia of substituted girder
$I_{cs}$ : inertia of all substituted columns in the storey of height $nh$
$I_c$ : inertia of all columns in a storey of height $h$
$V$ : shear force
$h$ : height of a typical storey

Equivalent columns will have the same cross-sectional areas as that of the original columns since second moment of area about centroidal axis has to remain unchanged. Once the reduced frame is analysed, end moments in original girders, at the level of each substitute girder, are obtained on dividing the value of end moments in substitute girders by $n$. Thereafter girder end moments at intermediate

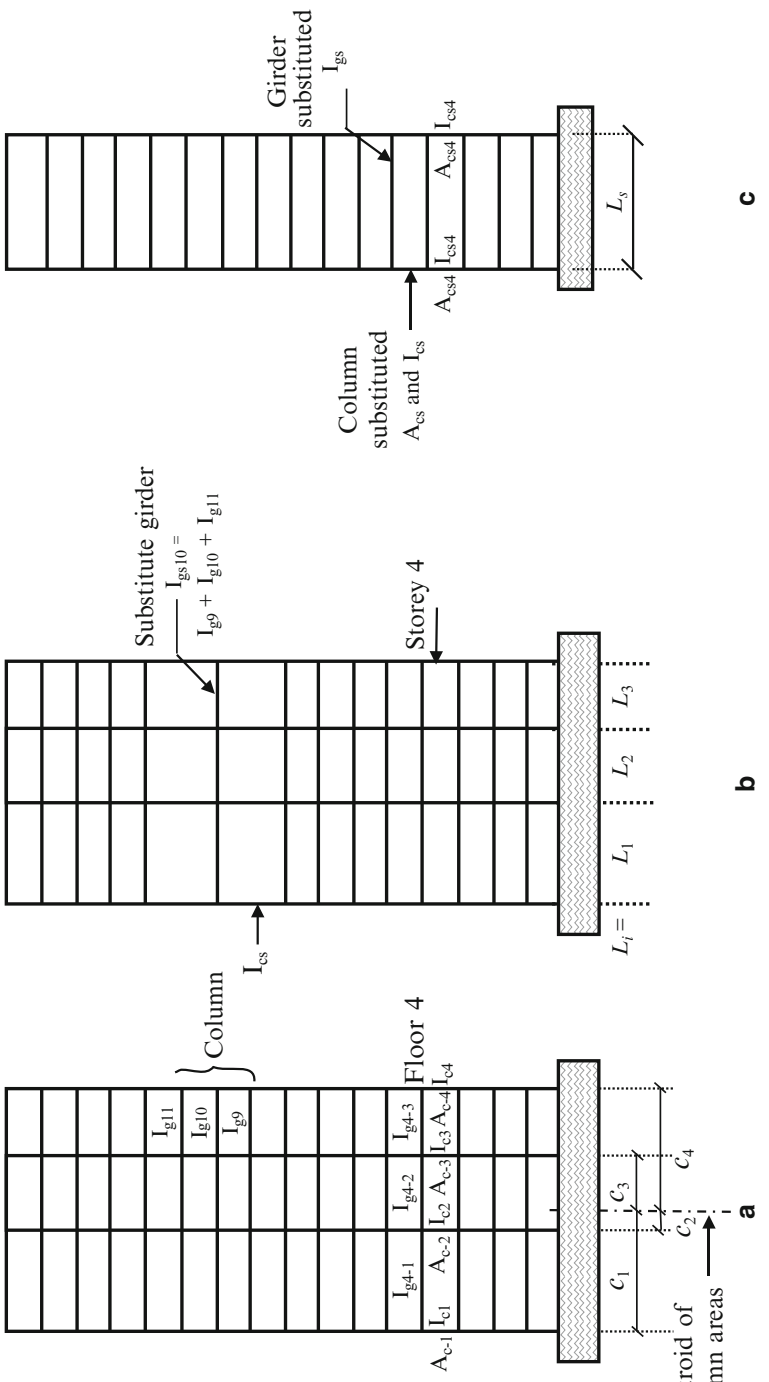


**Fig. 6.20** Frame reduction. (**a**) Frame. (**b**) Girders substituted. (**c**) Equivalent single-bay frame (based on Smith and Coull 1991)

floors between substitute girders are obtained by vertical interpolation. Shears in girders are obtained by dividing end moments by half the girder span.

Between two substitute girders, the storey shear at mid height of the original storey shall be obtained by interpolation. These shall be distributed among original columns in the same proportion as that in the substitute frame. End moments in each storey column shall be obtained by multiplying shear so obtained by half the storey height.

#### 6.9.3.2 Horizontal Reduction

Consider that a frame as in Fig. 6.20a is to be substituted by a single-bay frame of arbitrary span $L_s$ without a change in floor levels. Smith and Coull (1991) has shown that members of the substituted frame have to meet the following conditions to achieve same drift as that of the original frame:

(a) For same drift in storey $i$ due to double bending of girders, the moment of inertia of substitute girder at floor $i$ should be

$$\left(I_{gs}\right)_i = L_s \sum \left(I_g/L\right)_i \tag{6.8.1}$$

(b) For same drift due to double bending of columns, the equivalent single-bay column has to have a moment of inertia given by

$$(I_{cs})_i = \frac{1}{2} \sum (I_c)_i \tag{6.8.2}$$

(c) For same drift due to cantilever action, the sectional area of substitute columns should be

$$(A_{cs})_i = \frac{2}{L_s^2} \sum \left(A_c c^2\right)_i \tag{6.8.3}$$

With such substitution, Smith and Coull (1991) has suggested that the horizontal deflections will be reasonably accurate. In this case, however, member forces are not transferable back to the original frame. By this approach, for preliminary drift evaluation, a moment frame with many bays and several floors can be substituted in two stages with a single-bay frame with less number of floors. Often, in a tall building, storey heights are different for the bottom and top few levels. There, the points of contraflexure in columns are located differently from those in rest of the storeys. Hence, vertical reduction is normally restricted to intermediate storeys (Taranath 2010b).

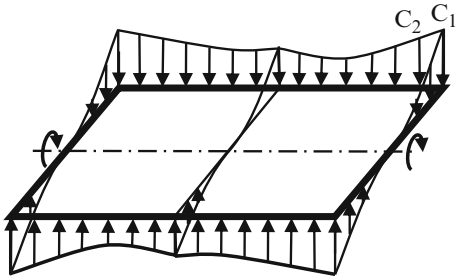


**Fig. 6.21** Shear lag effect

### *6.9.4 Shear Lag Effect*

Present-day high-rise buildings are often provided with a framed-tubular supporting system which is efficient because lateral load-resisting elements are placed along the outer perimeter. Such a structure can be looked upon as a vertical cantilever. However, its behaviour differs from that of an ideal cantilever because it violates two basic tenets of classical beam theory, viz. plane sections remain plane and stress distribution across the web is linear.

From each web of the framework, forces are transferred to flanges through corner supports, e.g. leeward flange column $C_1$ in Fig. 6.21, which undergoes axial compression $\delta$. Since the spandrel beam connecting flange columns has a finite stiffness, the adjacent column $C_2$ will compress less (say $\delta - \Delta\delta$) and so on. This leads to differential compression of flange columns with the result that inner columns will carry less axial load than those towards the ends. The axial stress distribution is then nonuniform with corner columns being more heavily loaded. The amount by which flange axial forces depart from uniform distribution is termed as positive shear lag.

This shear lag effect leads to a parabolic-type load distribution along flanges and a hyperbolic form along web frames. The extent of shear lag may vary considerably depending on configuration, geometry and elastic properties of the tubular structure. As a result of shear lag, capability of columns in the middle portion of a flange is not fully exploited, and thereby stiffness and moment of resistance of the tube get reduced.

Due to shear lag, there will be relative vertical displacement between columns which will cause vertical deformations of the rigid floor slab. Extent of shear lag varies along building height with maximum value being at the base (Singh and Nagpal 1994). There are various methods for evaluating shear lag, one among them being to use a 3D frame analysis software, although it is computationally intensive.

### 6.9.5 P-Δ Translational Effect

Lateral loads cause a horizontal deformation of the supporting frame with the result that gravity loads act eccentrically on the frame, causing an additional bending moment and increased deformation. This effect arising from eccentric gravity loads $P$ causing additional horizontal displacement $\Delta$ is known as $P$-$\triangle$ effect. The resulting additional drift needs to be evaluated to check whether it causes enhancement of member forces to a significant level. There are different methods to undertake such an analysis. For a shear frame building with rigid floor slabs, two methods are (1) direct method and (2) iterative gravity load method which are described below.

#### 6.9.5.1 Direct Method

This method is based on the premise that storey drift at $j$th level is proportional only to storey shear existing at that level. If storey shear due to external lateral loads is $V_j = \sum_{i=j}^{N} Q_i$, then the initial drift is $\delta_{j1} = V_j / k_j$. Because of this drift $(\delta_{j1})$ within storey $j$, the structure assumes a deformed shape (Fig. 6.22) causing an eccentricity $(\delta_{j1})$ of gravity load $P_j$ which produces a moment $P_j\,\delta_{j1}$ where:

$Q_i$ : storey forces obtained from an initial analysis using LSP or LDP
$P_j$ : total gravity load at and above level $j$
$\delta_{j1}$: initial storey drift at level $j$
$V_j$ : storey shear at level $j$
$h_j$ : height of storey $j$
$k_j$ : stiffness of storey $j$
$N$ : number of storeys

This moment causes an additional shear $P_j \delta_{j1}/h_j = \left(P_j V_j\right) / \left(h_j k_j\right)$ which leads to an additional drift $P_j V_j / k_j^2 h_j$ and the added drift then becomes $\delta_{j2} = V_j/k_j + P_j V_j / k_j^2 h_j$ and so on

Summing up incremental drifts, the final drift would be

$$\delta_j = \frac{V_j}{k_j}\left[1 + \frac{P_j}{h_j k_j} + \frac{P_j^2}{h_j^2 k_j^2} + \frac{P_j^3}{h_j^3 k_j^3} + \cdots\right] \tag{6.9.1}$$

Ratio of the moment due to initial *P-delta* ($P$-$\triangle$) effect to that due to initial storey shear is termed as a stability index $\theta$, where

$$\theta = P_j \delta_{j1} / \left(V_j h_j\right) \tag{6.9.2}$$

Equation 6.9.1 can be written as

**Fig. 6.22** *P*-Δ effect

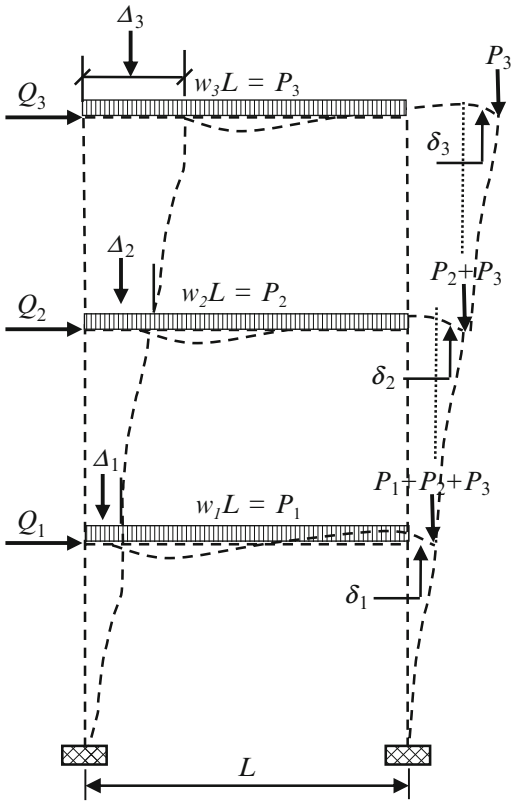


$$\delta_j = \delta_{j1}\left[1 + \theta + \theta^2 + \theta^3 + \cdots \theta^n\right] \tag{6.9.3}$$

which is an infinite geometric series. As $n \to \infty$, it converges to $1/(1-\theta)$ if $|\theta| < 1$ which is the case. Treating this as an enhancement factor ($\mu$) of initial drift, the final drift with $P$-$\Delta$ effect is $\delta_j = \mu\, \delta_{j1}$

$$\text{with} \quad \mu = \frac{1}{1-\theta} \tag{6.9.4}$$

Final deflection and moment at level $j$ will be obtained by multiplying their first-order values $\Delta_{j1}$ and $M_{j1}$, respectively, by this enhancement factor $\mu$.

This simplified approach ignores the effect of lengthening of natural periods due to second-order effects (Fardis 2009). The method is reasonably accurate for low- to medium-rise rigid frames which have a shear mode of deformation (Gaiotti and Smith 1989). For a building with significant flexural response, this method can be used for preliminary assessment, but it is advisable to use the iterative gravity load method.

#### 6.9.5.2 Iterative Gravity Load Method

In this method, the first-order horizontal frame displacement $\Delta_{j1}$ and storey moment $M_{j1}$ at storey $j$ are obtained using a standard frame analysis computer programme. Thereafter, gravity loads are applied to the unloaded structure with a deflected profile due to first-order displacements. Resulting incremental displacements $\delta_{j1}$ and moments $\delta M_{j1}$ are thus obtained. Gravity loads are again applied to the frame with deflected form $\delta_{j1}$ and resulting incremental displacement $\delta_{j2}$ and moments $\delta M_{j2}$ are obtained. This process is continued until incremental displacements $\delta$ become negligible. Final displacement and moment at storey $j$ are given by

$$\Delta^* = \Delta_{j1} + \delta_{j1} + \delta_{j2} + \delta_{j3} \cdots \tag{6.9.5}$$

and

$$M_j^* = M_{j1} + \delta M_{j1} + \delta M_{j2} + \delta M_{j3} \cdots \tag{6.9.6}$$

The above methods are for linear static $P$-$\Delta$ effect which needs to be evaluated about two orthogonal axes of the structure. For nonlinear procedures, this effect has to be considered directly in the time history analysis. Dynamic $P$-$\Delta$ effects can also be evaluated indirectly through an enhancement coefficient $C_3$ (chapter 11) during a pushover analysis (FEMA 273 1997).

#### 6.9.5.3 Analysis of P-Δ Effects

A $P$-$\Delta$ effect leads to an increase in both lateral displacements and storey moments as shown above. For evaluation, the gross properties of concrete should be reduced to allow for cracking (Smith and Coull 1991). Secondly, the additional shear due to $P$-$\Delta$ effect on columns not forming a part of the lateral load-resisting system needs to be transferred through diaphragms back to the latter. The above methods are approximate, and in a case where significant $P$-$\Delta$ effects exist, a more accurate analysis should be undertaken.

If $\theta < 0.1$ for every storey, then $P$-$\Delta$ effect may be ignored (FEMA 273 1997). For $0.1 < \theta < 0.25$ in any storey, the incremental increase in displacement, member forces and shears due to $P$-$\Delta$ effect can be obtained by multiplying corresponding initial values with a factor $1/(1-\theta)$ or any other rational method may be used. However, if $\theta > 0.25$ at any storey, the structure is potentially unstable (ASCE 2005) and it calls for a redesign.

Evaluation of translational $P$-$\Delta$ effect, by both the direct and iterative gravity method, is illustrated through *Ex* 6.10.7.

### 6.9.6 *P-Δ Torque Effect*

When a building distorts due to torsion from eccentric lateral loads, the centre of gravity of lateral loads becomes vertically displaced from its centre of rotation, and this causes an additional torque known as $P$-$\Delta$ torque. Due to this torque, the building further twists, and this carries on until $P$-$\Delta$ torque is in equilibrium with incremental torque. The procedure to follow is principally similar to that described above for translational $P$-$\Delta$ effect and will result in a torsional amplification factor.

### 6.9.7 *Drift and Deformation*

Inter-storey drift generally refers to lateral displacement of one floor with respect to the floor below. Drift index is the ratio of maximum lateral displacement at top of a building to the total building height. Magnitude of drift should be assessed early in the design stage. Control of drift is an important consideration particularly for limiting damage to nonstructural components. For this purpose, a shear wall–frame dual system is preferable to a purely moment-resisting frame. In tall buildings, it may even be the governing factor in selection of a suitable structural system (Naeim 2001).

Lateral deflection of any point in a structure is its absolute lateral displacement relative to its base. Limiting deflections is important such that they do not cause major distress in structural or nonstructural components. Permissible limit for drift specified in IS 1893 is 0.004 times storey height with a load factor of 1.0.

Deformation of a frame is the cumulative effect of:

1. Frame action – caused by lateral shear which causes beams and columns to bend in double curvature. Resulting deflection is termed as *racking component* and forms a large portion of the total sway of a SMRF.
2. Chord action – tall frames and tubular structures deform like a cantilever in response to a seismic overturning moment. The resulting axial deformation of columns causes an overall rotation of the frame which is termed as chord drift.
3. $P$-$\triangle$ effect – due to above deformations, vertical centreline of building deviates, laterally causing eccentricity of gravity loads. This creates an additional moment with consequent lateral deformation termed as $P$-$\Delta$ effect.
4. Lateral displacement arising from foundation rotation due to soil–structure interaction.
5. Torsional rotation of rigid slabs.
6. Inelastic deformations of the elements.

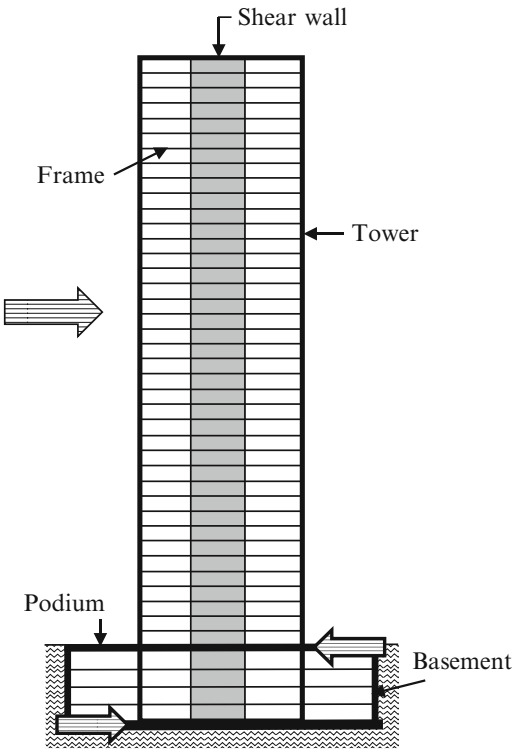


**Fig. 6.23** Backstay effect

### *6.9.8 Podium*

The footprint of the lower portion of a tall building is normally much larger than that of the rest of the structure, and this portion is often referred to as the podium. Tall upper portion, termed *the tower*, can be supported independently, or advantage may be taken of the podium structure to offer added resistance to seismic overturning moments. The podium can be below ground forming a basement for parking and other utilities. It can also be above grade level to house lobbies, shops and other retail. A typical tower with a podium is shown in Fig. 6.23.

A podium resists seismic forces and moments by two mechanisms:

(a) Part of the seismic resistance is provided by the tower foundation in the form of stiff subsoil or piles.
(b) The backstay effect is provided principally by diaphragms at the top and bottom of the basement and the perimeter wall of the podium.

A detailed analytical approach for the design of a podium is outside the scope of this book. However, a few observations, which may be helpful for a designer, are given below.

1. Diaphragms act as collectors and distributors to transfer forces from the tower to the perimeter basement walls. Thus, a couple is formed between ground floor slab and basement slab which resists seismic overturning moment. This is termed as *backstay effect* (ATC 72-1 2010).
2. For final design of tall buildings in high seismic zones, a capacity design approach is recommended, supported with perhaps a nonlinear response history analysis. For this purpose, it is necessary to carefully identify and detail the elements which will undergo nonlinear response.
3. A designer has to carefully estimate the stiffness, strength and behaviour of force-resisting elements under cracked conditions. Temperature, shrinkage and differential axial shortening of columns during construction have also to be allowed for.
4. Cast in situ diaphragms are commonly modelled as rigid. For design of backstay effect, a semi-rigid diaphragm is often recommended as it can result in a more economical design (ATC 72-1 2010).
5. Ramps that connect to different storeys in a parking lot need carefully planned design strategy as they can produce short column effect at their supports. Also they can attract axial forces, and further they can create flexible disconnected diaphragms.
6. Under lateral seismic forces, reversed shear forces can occur in basement columns when the basement storey does not drift as much as the first storey.

To apportion forces among these load paths, many assumptions have to be made such as stiffness and other properties. To overcome the problem of uncertainties, the use of bracketing assumptions is recommended. This approach provides an upper bound and lower bound range for the analysis.

## 6.10 Illustrative Examples

***Ex 6.10.1*** An SMRF in M 25 grade concrete with brick infill panels with loads and storey stiffness as shown in Fig. 6.24a rests on rock. It is located in seismic zone IV and has an importance factor of 1.0 and 5 % damping. Take stiffness factor $k$ (for all three columns together in a storey) $= 215.19 \times 10^3$ kN/m and $g = 9.81$ m/s$^2$. Determine the following using LSP (linear static procedure):

(a) Time period of natural vibration
(b) Horizontal seismic coefficient $A_h$
(c) Design base shear
(d) Lateral force at each storey
(e) Lateral deflection at each floor
(f) Storey drifts
(g) Storey shears

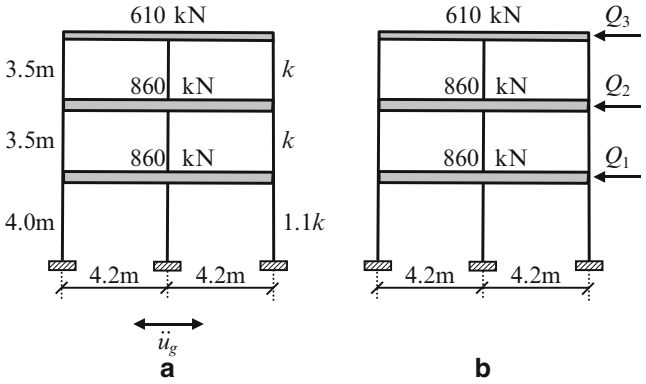


**Fig. 6.24** Three-storey SMRF

## Solution

(a) *Time period of natural vibration*

With brick infill, the vibration period, as per code IS1893, is given by

$$T = \frac{0.09h}{\sqrt{d}}$$

Substituting $h = 11$ m and $d = 8.4$ m in the above equation, $T = 0.342$ s.

(b) *Horizontal seismic coefficient* $A_h$

As per IS 1893, the horizontal seismic coefficient is given by

$$A_h = \frac{Z}{2}\frac{I}{R}\frac{S_a}{g} \tag{6.10.1}$$

From IS 1893, for seismic zone IV, $Z = 0.24$; response reduction factor $R = 5$ for a SMRF and for a time period of 0.342 s, $S_a/g = 2.5$. With the given importance factor $I = 1.0$, substituting values in Eq. 6.10.1, $A_h = \frac{0.24}{2} \times \frac{1}{5} \times 2.5 = 0.06$

(c) *Design base shear*

The base shear is given by

$$V_b = A_h \times W = \ 0.06\,\{610 + 860 + 860\} = 139.8 \ \text{kN}$$

(d) *Lateral force at each storey*

Base shear $V_b$ is distributed over the building height. Lateral force at each storey $j$ ($Q_j$), as per Eq. 4.9.1, has values as listed in Table 6.1.

(e) *Lateral deflection at each floor*

**Table 6.1** Evaluation of storey shear

| Storey | $w_j$ (kN) | $h_j$ (m) | $w_j h_j^2$ | $w_j h_j^2 / \Sigma\, w_j h_j^2$ | $Q_j$ (kN) |
|---|---|---|---|---|---|
| 1 | 860 | 4 | 13,760 | 0.10122 | 14.1506 |
| 2 | 860 | 7.5 | 48,375 | 0.35584 | 49.7464 |
| 3 (roof) | 610 | 11 | 73,810 | 0.54294 | 75.9030 |

Floor deflection is given by

$$[\boldsymbol{\Delta}] = [\boldsymbol{K}]^{-1}\,[\boldsymbol{Q}] \tag{6.10.2}$$

Substituting values from Table 6.1,

$$[\boldsymbol{Q}] = \begin{pmatrix} Q_1 \\ Q_2 \\ Q_3 \end{pmatrix} = \begin{pmatrix} 14.1506 \\ 49.7464 \\ 75.9030 \end{pmatrix} \text{ kN} \tag{6.10.3}$$

$$[\boldsymbol{K}] = k \begin{pmatrix} 2.1 & -1 & 0 \\ -1 & 2 & -1 \\ 0 & -1 & 1 \end{pmatrix} = 10^3 \begin{pmatrix} 451.90 & -215.19 & 0 \\ -215.19 & 430.38 & -215.19 \\ 0 & -215.19 & 215.19 \end{pmatrix} \text{ kN/m} \tag{6.10.4}$$

Substituting values from Eqs. 6.10.4 and 6.10.3 into Eq. 6.10.2, the horizontal deflections are

$$\begin{pmatrix} \Delta_1 \\ \Delta_2 \\ \Delta_3 \end{pmatrix} = \begin{pmatrix} 0.5907 \\ 1.1746 \\ 1.5273 \end{pmatrix} \text{ mm} \tag{6.10.5}$$

(f) *Storey drifts*

Storey drifts will be

$$\begin{pmatrix} \delta_1 \\ \delta_2 \\ \delta_3 \end{pmatrix} = \begin{pmatrix} 0.5907 \\ 0.5839 \\ 0.3527 \end{pmatrix} \text{ mm} \tag{6.10.6}$$

(g) *Storey shears*

From Eq. 6.10.3, the storey shear forces are

$$\begin{pmatrix} S_1 \\ S_2 \\ S_3 \end{pmatrix} = \begin{pmatrix} 14.2 + 125.6 = 139.8 \\ 49.7 + 75.9 = 125.6 \\ 75.9 = 75.9 \end{pmatrix} \text{ kN} \tag{6.10.7}$$

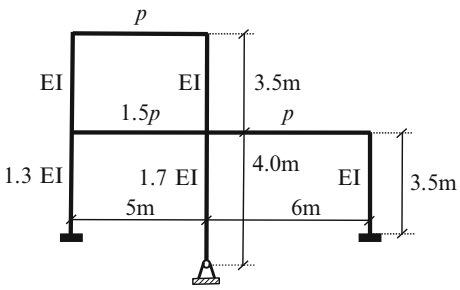


**Fig. 6.25** Two-bay frame

***Ex 6.10.2*** A two-storey OMRF with rigid floor diaphragms is shown in Fig. 6.25. Determine the two natural frequencies. Take flexural rigidity $EI = 27.728 \times 10^6$ N m$^2$ and mass $p = 1.3 \times 10^5$ kg.

**Solution** Stiffness of a column fixed at both ends is 12 EI/h$^3$.

Stiffness of a column fixed at one end and hinged at the other = 3 EI/h$^3$.

Substituting values, the total stiffness of columns at first storey is

$$= \frac{12\ \text{EI}\,(1.3\,)}{3.5^3} + \frac{3\ \text{EI}(1.7)}{4^3} + \frac{12\ \text{EI}}{3.5^3} = 0.7234\ \text{EI}$$

Proceeding similarly, stiffness of upper storey = 0.56 EI.

Substituting value of EI, the stiffness matrix is

$$[\boldsymbol{K}] = \begin{pmatrix} 35.586 & -15.528 \\ -15.528 & 15.528 \end{pmatrix} \times 10^6$$

$$\text{Mass matrix will be} \quad [\boldsymbol{M}] = \begin{pmatrix} 3.25 & 0 \\ 0 & 1.3 \end{pmatrix} \times 10^5$$

From the above, the two frequencies can be readily obtained as $\omega_1 = 6.23$ rad/s and $\omega_2 = 13.79$ rad/s.

***Ex 6.10.3*** Analyse the frame in *Ex* 6.10.1 using the LDP (linear dynamic procedure) and determine the following:

(a) Modal time periods of natural vibration
(b) Horizontal seismic coefficients $A_h$ for each mode
(c) Design base shear
(d) Lateral force at each storey
(e) Lateral deflection at each floor
(f) Storey drifts
(g) Storey shears

Thereafter, for some important parameters, compare the results obtained with those in *Ex* 6.10.1 using the LSP method.

**Table 6.2** Frequency and time period

| Mode | Frequency (rad/s) | Time period (s) |
|---|---|---|
| 1 | $\omega_1 = 24.6429$ | $T_1 = 0.255$ |
| 2 | $\omega_2 = 66.8773$ | $T_2 = 0.094$ |
| 3 | $\omega_3 = 91.8966$ | $T_3 = 0.068$ |

**Table 6.3** Evaluation of participation factor for the first mode

| Storey | Mass (kg) | $\varphi_1$ | $m_j \times \varphi_{j1} \times 10^3$ | $m_j \times \varphi_{j1}{}^2 \times 10^3$ |
|---|---|---|---|---|
| 1 | 87.666 | 0.4451 | 39.0200 | 17.3678 |
| 2 | 87.666 | 0.8245 | 72.2803 | 59.5951 |
| 3 | 62.181 | 1.0000 | 62.1814 | 62.1814 |
| | | Total | 173.4816 | 139.1443 |

$P1 = 173.4816/139.1443 = 1.2468$

(a) *Time period of natural vibration*

For loads shown in Fig. 6.24, the mass matrix will be

$$\boldsymbol{M} = 10^3 \begin{pmatrix} 87.6656 & 0 & 0 \\ 0 & 87.6656 & 0 \\ 0 & 0 & 62.1814 \end{pmatrix} \text{ kg} \tag{6.11.1}$$

Stiffness matrix will be as per Eq. 6.10.4,

$$\boldsymbol{K} = 10^3 \begin{pmatrix} 451.90 & -215.19 & 0 \\ -215.19 & 430.38 & -215.19 \\ 0 & -215.19 & 215.19 \end{pmatrix} \text{ kN/m} \tag{6.11.2}$$

Using MATLAB software, the frequencies and time periods of vibration obtained are given in Table 6.2, and the modal matrix is given below:

$$\boldsymbol{\Phi} = \begin{pmatrix} 0.4451 & -1.0520 & 1.0745 \\ 0.8245 & -0.2924 & -1.4403 \\ 1.0 & 1.0 & 1.0 \end{pmatrix} \tag{6.11.3}$$

For mode $i$, using Eq. 4.6.1, the horizontal seismic coefficient is obtained as

$$A_{hi} = 0.024 \left( \frac{S_{ai}}{g} \right) \tag{6.11.4}$$

The codal seismic acceleration coefficient ($S_{ai}$) and horizontal seismic coefficient ($A_{hi}$) are obtained for each mode. Participation factor ($P$) for each mode is obtained utilising Eq. 4.14.1, and steps for evaluating it are shown in Table 6.3. Results for all modes are summarised in Table 6.4.

**Table 6.4** Participation factors for all modes

| Mode | $S_a/g$ | $A_h$ | $P$ |
|---|---|---|---|
| 1 | 2.5000 | 0.0600 | 1.2468 |
| 2 | 2.4100 | 0.0578 | −0.3340 |
| 3 | 2.0260 | 0.0486 | 0.0872 |

**Table 6.5** Storey forces for first mode

| Mode1 | | | | | |
|---|---|---|---|---|---|
| Storey | Weight | $A_{h1}$ | $\varphi_{j1}$ | $P_1$ | $Q_{j1}$ |
| | kN | | | | kN |
| 1 | 860 | 0.0600 | 0.4451 | 1.2468 | 28.6355 |
| 2 | 860 | 0.0600 | 0.8245 | 1.2468 | 53.0441 |
| 3 | 610 | 0.0600 | 1.0000 | 1.2468 | 45.6329 |

**Table 6.6** Floor level forces

| Mode | 1 | 2 | 3 | kN |
|---|---|---|---|---|
| Storey | $Q_1$ | $Q_2$ | $Q_3$ | $Q$ |
| 3 | 45.6329 | −11.7762 | 2.5851 | 47.2 |
| 2 | 53.0441 | 4.8546 | −5.2493 | 53.5 |
| 1 | 28.6355 | 17.4658 | 3.9161 | 33.8 |

**Table 6.7** Storey shears

| Mode | 1 | 2 | 3 | kN |
|---|---|---|---|---|
| Storey | $V_1$ | $V_2$ | $V_3$ | $V$ |
| 3 | 45.6329 | −11.7762 | 2.5851 | 47.2 |
| 2 | 98.6770 | −6.9216 | −2.6642 | 99.0 |
| 1 | 127.3125 | 10.5442 | 1.2519 | 127.8 |

Modal storey forces are given by

$$Q_{ji} = A_{hi}\varphi_{ji}P_i w_j \tag{6.11.5}$$

where $\varphi_{ji}$ is obtained from Eq. 6.11.3.

For the first mode at level 1,

$Q_{11} = 0.06 \times 860 \times 0.4451 \times 1.2468 = 28.6355$ kN.

Similarly the storey forces for all levels for the first mode are obtained and summarised in Table 6.5 and for all storeys and modes in Table 6.6.

Storey shears for the three storeys for first mode are obtained as under:

$V_3 = 45.6329$ kN, $V_2 = 45.6329 + 53.0441 = 98.6770$ kN and $V_1 = 127.3125$ kN.

Similarly the storey shear forces are obtained at all levels and for all modes and summarised in Table 6.7.

Substituting values for $\boldsymbol{K}$ from Eq. 6.11.2 and $Q$ values from Table 6.5 into Eq. 6.10.2, the deflections for first mode at the three levels are obtained. Such deflection values for all modes and at all levels are summarised in Table 6.8. In the

**Table 6.8** Deflection and drift (mm)

| Mode | 1 | 2 | 3 | Deflection | Drift |
|---|---|---|---|---|---|
| Storey | $\Delta_1$ | $\Delta_2$ | $\Delta_3$ | $\Delta$ | $\delta$ |
| 3 | 1.2085 | −0.0423 | 0.0049 | 1.209 | 0.219 |
| 2 | 0.9964 | 0.0124 | −0.0071 | 0.997 | 0.460 |
| 1 | 0.5378 | 0.0445 | 0.0053 | 0.540 | 0.540 |

**Table 6.9** Comparative results from LSP and LDP analysis

| Linear static procedure (LSP) | Linear dynamic procedure (LDP) |
|---|---|
| $T = 0.342$ s | $T_1 = 0.255$ s |
| $\omega = 18.37$ rad/s | $\omega_1 = 24.64$ rad/s |
| Base shear | |
| 139.8 kN | 127.8 kN |
| Distribution of lateral forces | |
| Storey 1: 14.15 kN | Storey 1: 33.80 kN |
| Storey 2: 49.74 kN | Storey 2: 53.50 kN |
| Storey 3: 75.90 kN | Storey 3: 47.20 kN |
| Maximum deflection | |
| 1.527 mm | 1.209 mm |
| Storey drifts | |
| Level 1: 0.591 mm | Level 1: 0.540 mm |
| Level 2: 0.584 mm | Level 2: 0.460 mm |
| Level 3: 0.353 mm | Level 3: 0.219 mm |

last columns of Tables 6.6 and 6.7 are given values of storey forces and storey shears respectively obtained by the SRSS method. Similarly the deflection summation and corresponding drift values are given in Table 6.8.

The framework in Fig. 6.24 has been analysed by the linear static procedure (LSP) as well as the linear dynamic procedure (LDP). Comparative results are listed in Table 6.9.

***Ex 6.10.4*** A floor diaphragm is subjected to a uniformly distributed lateral force of 1,500 kN and is supported on three shear walls with stiffness as shown in Fig. 6.26a. Determine the load shared by each shear wall if the diaphragm is:

(a) Rigid
(b) Fully flexible, i.e. equivalent to being discontinuous at the central support
(c) Semi-flexible, i.e. it acts as a beam spanning over the central support

For case (c) take $E = 27{,}000$ N/mm$^2$, $k = 65 \times 10^3$ N/mm, slab thickness and depth as 100 mm and 5.5 m, respectively.

**Solution**

(a) Rigid slab

In this case, the load will be shared by walls in proportion to their stiffness, i.e.

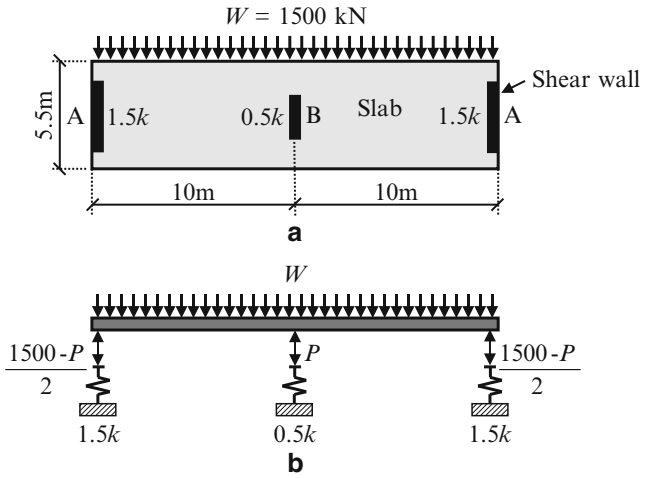


**Fig. 6.26** Influence of slab rigidity on load sharing. (**a**) Diaphragm under lateral load. (**b**) Beam on springs analogy

| | | | | |
|---|---|---|---|---|
| Load shared by each external wall (A) | = | (1,500 × 1.5)/3.5 | = | 642.86 kN |
| Load shared by central wall (B) | = | 1,500 – 2(642.86) | = | 214.28 kN |

(b) Fully flexible diaphragm

| | | | | |
|---|---|---|---|---|
| The tributary width supported by the central wall (B) | | | = | 10 m |
| Load shared by central wall (B) | = | 1,500 × 10/20 | = | 750 kN |
| Load shared by each external wall (A) | = | (1,500 – 750)/2 | | 375 kN |

(c) Semi-flexible (or stiff) diaphragm

This case can be represented as a vertical beam supported on three springs and loaded as shown in Fig. 6.26b. Stiffness of the springs at A and B shall be $1.5\,k$ and $0.5\,k$ respectively

The other data is as under:

$$W = 1.5 \times 10^6 \text{ N};\ E = 2.7 \times 10^4 N/mm^2;\ Length\ L = 2 \times 10^4 \text{ mm};$$
$$k = 6.5 \times 10^4\ N/mm$$

Let reaction of the central spring be $P$ kN:

$$\text{Depth } D = 5.5 \times 10^3\ mm;\ I = \frac{100 \times (5.5 \times 10^3)^3}{12} = 1.386 \times 10^{12}\ mm^4;$$
$$EI = 3.742 \times 10^{16}\ Nmm^2$$

$$\text{Mid span deflection of the slab as a beam} = \frac{5WL^3}{384EI} - \frac{PL^3}{48EI} = \frac{L^3}{384EI}(5W - 8P) = \frac{8 \times 10^{12}}{384 \times 3.742 \times 10^{16}}\left\{\left(5 \times 1.5 \times 10^6\right) - \left(8P \times 10^3\right)\right\}$$
$$= 4.175 - 0.00445P \tag{6.12.1}$$

**Table 6.10** Load sharing between walls

| Slab | Central wall | Each end wall |
|---|---|---|
| | kN | kN |
| Rigid | 214 | 643 |
| Flexible | 750 | 375 |
| Stiff | 294 | 603 |

**Fig. 6.27** Slab with collectors and chords

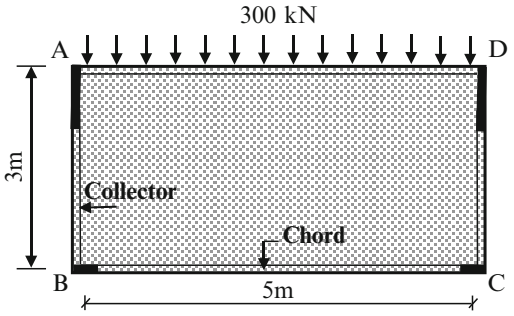


Relative deflection between spring at the centre and those at the two ends will be

$$\left\{\frac{P}{0.5k} - \frac{(1,500-P)}{2\times 1.5k}\right\}\times 10^3 = \frac{(7P-1,500)}{3k}\times 10^3$$
$$\text{Substituting value of } k, \quad = \frac{(7P-1,500)}{195} \tag{6.12.2}$$

Equating deflections obtained from Eqs. 6.12.1 and 6.12.2,

$$P = 294.13 \text{ kN}.$$

Accordingly, load shared by central wall = 294.13 kN and each of the end walls 602.94 kN. Loads shared by shear walls in each case are presented in Table 6.10.

***Ex 6.10.5*** Consider a rigid 150 mm thick M 25 concrete diaphragm as shown in Fig. 6.27 supported by two shear walls of length 1.2 m each along the direction of the force. The slab is reinforced with 0.25 % steel and transfers the lateral load of 300kN to these walls uniformly over their length through shear. However, the shear walls are not capable of resisting forces transverse to their length. Ascertain the forces for which the collectors along lines AB and CD should be designed with a load enhancement factor of 2.0. Also determine the force in the tension chord along line BC.

**Solution** The total lateral force is 300 kN. Hence, at each end, the force will be 150kN.

With 0.25 % steel and M25 concrete, the permissible shear stress as per IS 456 is 0.36 N/mm$^2$. Hence:

Force transferred to each shear wall = $(150\times 1{,}200)\times 0.36\times 10^{-3} = 64.8$ kN.
Allowing for a load enhancement factor of 2.0.

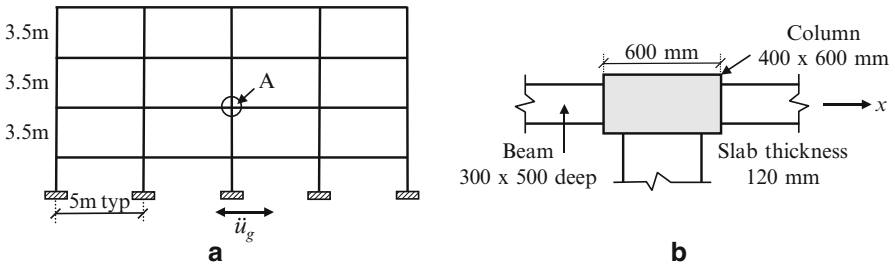


**Fig. 6.28** Frame joint design. (**a**) An SMRF. (**b**) Joint A (plan)

Force in each collector $= (150 \times 2) - 64.8 = 235.2$ kN in tension.
The section has to be designed suitably.
The horizontal bending moment is $300 \times 5/8 = 187.5$ kNm.
Chord tensile or compressive force will be $187.5/3 = 62.5$ kN.
With a load enhancement factor of 2.0, the design load will be 125 kN.

***Ex 6.10.6*** An array of multistorey SMRFs are placed orthogonally for a building with $400 \times 600$ mm columns and 3.5 m floor heights. A typical peripheral joint *A*, shown in Fig. 6.28a and b, is to be designed when the frame is subjected to a sway to the right due to seismic motion along the *x* direction. Longitudinal beams (300 mm × 500 mm deep) at the joint have 4- φ20 mm + 2- φ16 mm rebars at the top and 4- φ16 mm + 2- φ12 mm rebars at the bottom. Concrete is M25 grade and rebars are grade Fe 415. Design this joint for shear and flexure along *x* axis. Also determine the column reinforcement placed equally on all four sides if it is to support an additional factored axial load of 2,500 kN.

**Solution** Area of reinforcement provided in the beams is 1,659 mm$^2$ at top and 1,030 mm$^2$ at the bottom.

(a) *Evaluation of longitudinal beam moment capacities*

– *Hogging moment capacity*

From theory of limit state design, the moment capacity is given by

$$M_u = R_u b d^2 \tag{6.13.1}$$

For Fe 415 reinforcement and M25 concrete, $R_u = 3.45$ and $k_u = \dfrac{x_u}{d} = 0.48$

Substituting values in Eq. 6.13.1,

$$M_u^h = 3.45 \times 300 \times 460^2 \times 10^{-6} = 219 \text{ kNm} \tag{6.13.2}$$

Steel corresponding to this moment is

$$A_{st} = \frac{0.36 f_{ck}\ b\ k_u d}{0.87 f_y} = \frac{0.36 \times 25 \times 300 \times 0.48 \times 460}{0.87 \times 415}$$
$$= 1,651\ \text{mm}^2 \simeq 1,659\ \text{mm}^2$$

– *Sagging moment capacity*

The monolithic slab will act as a flange of a L-beam with $A_{sc} = 1030$ mm$^2$. As per standard analysis procedure for L beams, flange width will be 1042 mm and depth of the neutral axis is given by

$$x_u = \frac{0.87\ f_y\ A_{sc}}{0.36\ f_{ck}\ b_f} = \frac{0.87 \times 415 \times 1,030}{0.36 \times 25 \times 1,042} = 39.7 < 120\ \text{mm}$$

With neutral axis lying within the flange, the sagging moment will be

$$M_u^s = 0.87 \times 415 \times 1,030 \times 460 \left[1 - \frac{1,030 \times 415}{1,042 \times 460 \times 25}\right] \times 10^{-6} = 165\ \text{kNm} \tag{6.13.3}$$

Moments capacities are:

$$\text{Hogging moment } M_u^h = 219\ kNm$$
$$\textit{Sagging moment } M_u^s = 165\ kNm$$

(b) *Check for shear*

Areas of reinforcement at beam top and bottom are 1,659 mm$^2$ and 1,030 mm$^2$, respectively. Considering a tensile stress of 1.25 $f_y$, the tensile force capacities (Fig. 6.29) are

$$T_1 = 1.25 \times 415 \times 1,659 \times 10^{-3} = 861\ kN$$
$$T_2 = 1.25 \times 415 \times 1,030 \times 10^{-3} = 534\ kN$$

From Eq. 6.2.1, the shear force to be resisted by column is

$$V = 1.4\left[\frac{M_u^s + M_u^h}{h}\right]$$
$$= 1.4\,(219 + 165)\,/3.5 = 154\ kN \tag{6.13.4}$$

From Fig. 6.17, net shear in $x$ direction on the joint = 861 + 534 – 154 = 1,241 kN.

Joint width for shear is smaller of 400 mm and {300 + (600/2)} = 600 mm, i.e. 400 mm.

Joint shear area = $A_j = 400 \times 600 = 240 \times 10^3$ mm$^2$.

This joint is confined only on two faces. Hence, from Sect. 6.6.3.2,

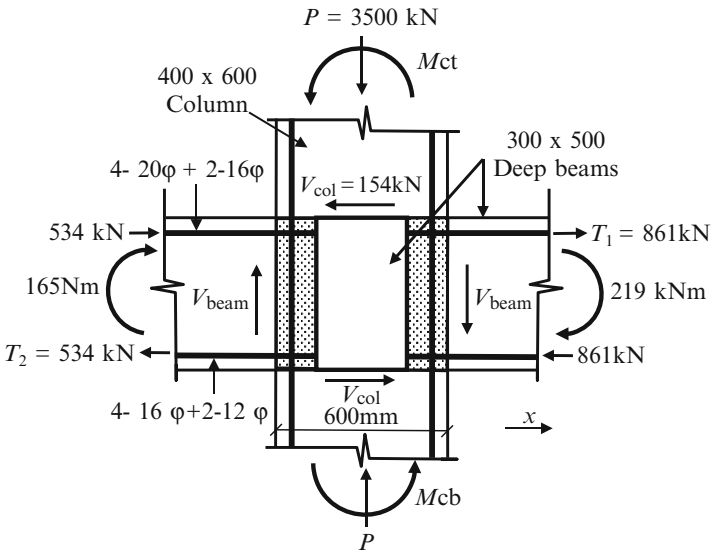


**Fig. 6.29** Interior peripheral joint

Permissible shear stress $= 1.2 A_j \sqrt{f_{ck}} = 1.2 \times 240 \sqrt{25} = 1,440\, kN > 1,241\, kN$

Hence safe.

Since the joint is not confined on all four sides, confining reinforcement has to be provided which is given by IS 13920 as

$$A_{sh} = \frac{0.18\, S\, h\, f_{ck}}{f_y} \left[ \frac{A_g}{A_k} - 1 \right] \tag{6.13.5}$$

With 40 mm cover, the unsupported legs of the stirrups are $(600 - 80) = 520$ mm and 320 mm. Both are $>300$ mm. Hence provide additional two links, one across the depth and one across the width. Maximum unsupported length will then be 260 mm.

Using φ 10 mm stirrups, area of stirrup $A_{sh} = 78.5$ mm$^2$, gross area of column $A_g = (400 \times 600) = 24 \times 10^4$ mm$^2$, and area of confined core, $A_k = 520 \times 320 = 16.6 \times 10^4$ mm$^2$. Substituting these values in Eq. 6.13.5,

$$78.5 = \frac{0.18 \times \mathrm{S} \times 260 \times 25}{415} \left[ \frac{24 \times 10^4}{16.6 \times 10^4} - 1 \right]$$

$$\text{Solving,} \qquad s = 62.5 \text{ mm}$$

Hence, provide φ 10 mm stirrups at 60 mm centres in the joint region.

(c) *Check for flexure*

Total moment in beams framing into the column joint is

$$M_b = (219 + 165) = 384 \text{ kNm}$$

Sum of the moments in upper and lower columns at the joint is required to be

$$M_c = 1.2 \times 384 = 460.8 \text{ kNm}$$

Since column stiffness above and below the joint is identical, this total moment will be shared equally between upper and lower column portions. Hence, the column section would have to be designed for a moment of 460.8/2 = 230.4 kNm.

Factored axial load is 2,500 kN. Using established design procedure,

$$\frac{P_u}{f_{ck}.b.d} = \frac{2,500 \times 10^3}{25 \times 400 \times 560} = 0.446 \text{ and } \frac{M_u}{f_{ck}.b.d^2} = \frac{230.4 \times 10^6}{25 \times 400 \times 560^2} = 0.074$$

Based on design charts with equal reinforcement on four sides, the quantity of reinforcement required will be 1.75 %, i.e. $1.75 \times 400 \times 600/100 = 4{,}200$ mm$^2$.

***Ex 6.10.7*** An 11-storey shear frame building (with rigid floor slabs) carries a gravity load of 960 kN per storey with each storey height being 3.75 m. The storey stiffness of columns is 154,000 kN/m for each of the first five storeys and 74,300 kN/m for rest of the upper storeys. Lateral seismic storey shears are as listed in the third column of Table 6.11 Determine the racking deflections at each floor including $P$-$\Delta$ effects. Also compare the final drifts at level 7, obtained by the *iterative gravity load method* and the *direct method.*

**Solution**

1. *Evaluation by iterative gravity load method*

Lateral storey shear at level 11 = 145.065 kN.

Drift at level 11 = (145.065 × 1,000)/74,300 = 1.9524 mm.

Moment due to eccentricity of gravity load,

$$P - \delta \text{ moment} = 960 \times 1.9524 = 1,874.326 \text{ kN mm}$$

Additional lateral shear at level 11 due to this moment = 1,874.326/3,750 = 0.4998 kN.

Additional drift due to this shear will be (0.4998 × 1,000)/74,300 = 0.0067 mm.

Proceeding similarly, the drift for the next cycle will be 0.00002 mm.

Evaluation process can be terminated at this stage since incremental drifts are negligible.

Total drift at level 11 = 1.9524 + 0.0067 + 0.00002 = 1.9592 mm.

The rest of the calculations for balance storey levels are summarised in Table 6.11.

Lateral deflection at level 1 = 4.1176 mm.

Deflection at level 2 = 4.1176 + 4.0973 = 8.4129 mm.

**Table 6.11** *P*-Δ effect

| Level | Storey Height m | Storey Shear kN | Stiffness kN/m | Drift $\delta_1$ mm | Σ P kN | Storey Shear kN | Drift $\delta_2$ mm | Storey Shear kN | Drift $\delta_3$ mm | Drift Total $\delta$ mm | Deflection Δ mm |
|---|---|---|---|---|---|---|---|---|---|---|---|
| 11 | 3.75 | 145.065 | 74,300 | 1.9524 | 960 | 0.4998 | 0.0067 | 0.0017 | 0.00002 | 1.95917 | 51.017 |
| 10 | 3.75 | 265.660 | 74,300 | 3.5755 | 1,920 | 1.8307 | 0.0246 | 0.0126 | 0.00017 | 3.60031 | 49.057 |
| 9 | 3.75 | 364.043 | 74,300 | 4.8996 | 2,880 | 3.7629 | 0.0506 | 0.0389 | 0.00052 | 4.95081 | 45.457 |
| 8 | 3.75 | 442.436 | 74,300 | 5.9547 | 3,840 | 6.0976 | 0.0821 | 0.0840 | 0.00113 | 6.03792 | 40.506 |
| 7 | 3.75 | 503.173 | 74,300 | 6.7722 | 4,800 | 8.6684 | 0.1167 | 0.1493 | 0.00201 | 6.89086 | 34.468 |
| 6 | 3.75 | 548.474 | 74,300 | 7.3819 | 5,760 | 11.3386 | 0.1526 | 0.2344 | 0.00315 | 7.53764 | 27.577 |
| 5 | 3.75 | 580.599 | 154,000 | 3.7701 | 6,720 | 6.7561 | 0.0439 | 0.0786 | 0.00051 | 3.81450 | 20.040 |
| 4 | 3.75 | 601.806 | 154,000 | 3.9078 | 7,680 | 8.0032 | 0.0520 | 0.1064 | 0.00069 | 3.96049 | 16.225 |
| 3 | 3.75 | 614.365 | 154,000 | 3.9894 | 8,640 | 9.1915 | 0.0597 | 0.1375 | 0.00089 | 4.04996 | 12.265 |
| 2 | 3.75 | 620.504 | 154,000 | 4.0292 | 9,600 | 10.3149 | 0.0670 | 0.1715 | 0.00111 | 4.09734 | 8.215 |
| 1 | 3.75 | 622.512 | 154,000 | 4.0423 | 10,560 | 11.3831 | 0.0739 | 0.2081 | 0.00135 | 4.11755 | 4.118 |

Proceeding similarly, lateral deflections at all storeys are summarised in the above table.

2. *Evaluation by direct method for level 7*

From Table 6.11, at level 7,
Gravity load $P_7 = 4{,}800.0$ kN; initial drift $\delta_{1-7} = 6.7722$ mm.
Storey shear $V_7 = 503.173$ kN; storey height $h_7 = 3{,}750$ mm.
Substituting in Eq. 6.9.2, $\theta = \dfrac{(4,800 \times 6.7722)}{(503.173 \times 3750)} = 0.01723.$
Enhancement factor as per Eq. 6.9.4, $\mu = \dfrac{1}{(1 - 0.01723)} = 1.0175.$

Hence, drift at level $7 = 6.7722 \times 1.0175 = 6.891$ mm, which matches with drift value obtained by the iterative gravity load method in Table 6.11.

# Chapter 7
# Shear Walls: *Aseismic Design and Detailing*

**Abstract** In this chapter are described various forms of shear walls such as cantilever walls, coupled walls, squat walls and walls with boundary elements and openings. The importance of adopting proper configuration of shear walls in a building layout is highlighted. Also in this chapter is described the commonly observed failure modes of shear walls. The theoretical background for their analysis under a seismic environment is described in detail. Capacity-based shear design of these walls is also dealt with. An important aspect of tension shift and its effect on wall reinforcement detailing is explained. The illustrative examples at end of the chapter include analysis and design of cantilever as well as squat shear walls and design of boundary elements.

**Keywords** Shear walls • Cantilever walls • Capacity-based shear design • Design of squat walls

## 7.1 Introduction

Shear walls are an efficient, easy to construct, economical and a popular means of resisting lateral inertia forces induced in a building, even though they pose aesthetic constrains. They are often termed as an insurance against building collapse due to their observed good performance in minimising damage during past moderate-level earthquakes (Fardis 2009). They have considerable in-plane stiffness and often form the backbone of a lateral load-resisting system in tall buildings. However, if a building is supported by only a few shear walls, then the structure would have limited redundancy as there would be only a few alternative load paths. The term shear wall, in a way, is a misnomer particularly so because tall cantilever walls (which are of common occurrence) primarily behave in flexure.

Since such walls form the primary vertical elements resisting lateral seismic forces, adequate ductility should be incorporated in their design. If the lateral load is sustained by only a few shear walls, then their foundation design can become problematic due to heavy uplift forces. To partially overcome this problem, during a strong seismic event, the use of a rocking foundation is an option. However,



S. Manohar, S. Madhekar, *Seismic Design of RC Buildings*, Springer Transactions in Civil and Environmental Engineering, DOI 10.1007/978-81-322-2319-1_7

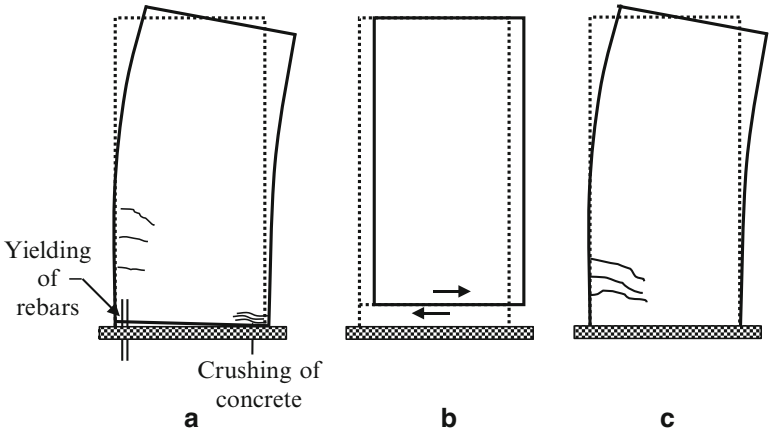


**Fig. 7.1** Typical failure modes of shear walls (**a**) Flexure failure, (**b**) Sliding failure, (**c**) Shear failure

the effect of rocking motion cannot be reliably accounted for during design and hence extreme care and sound engineering judgment needs to be exercised in such a venture.

The commonly observed failure modes (Fig. 7.1a–c) of shear walls are

1. Crushing of concrete in compression
2. Yielding of vertical reinforcement and inadequate anchorage of rebars
3. Horizontal sliding along construction joints
4. Diagonal tension or compression due to shear

On rare occasions failure can be attributed to overturning, instability conditions and rocking.

## 7.2 Functional Layout and Configuration

Geometry and location of shear walls are essentially dictated by architectural and functional considerations. It is important to locate shear walls such that they also function as bearing walls and support a portion of gravity loads so as to suppress, to the extent feasible, tensile forces generated due to bending. This also minimises chances of foundation uplift during a major earthquake. Walls do create barriers in plan layouts and one of the ways to minimise this problem is to couple adjacent walls to form flanged walls. When a shear wall extends monolithically from a column to its neighbouring column, a barbell shape is formed. The end columns are termed as *boundary elements* which significantly enhance both shear and flexural capacity of the wall. Different shear wall shapes that get formed are shown in Fig. 7.2.

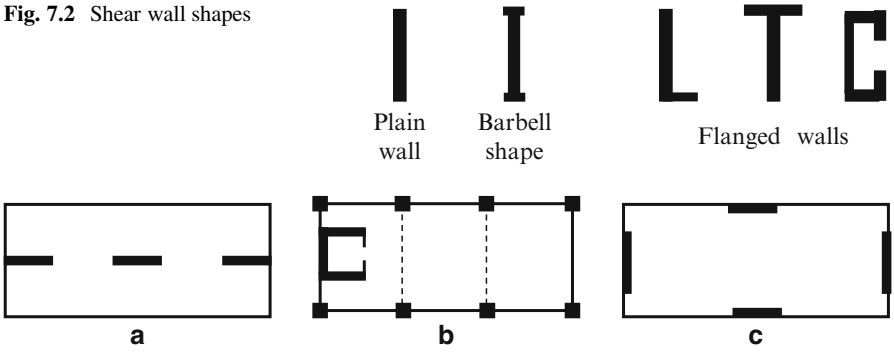


**Fig. 7.2** Shear wall shapes

**Fig. 7.3** Shear wall layouts (**a**) Collinear walls, (**b**) Unsuitable layout, (**c**) Preferred layout

Shear walls that form utility cores around elevator shafts and stairwells are punctured with openings. This weakens their flexural and torsional rigidity and leads to stress concentration at corners. Secondly, if a series of collinear walls (Fig. 7.3a) or an ill-located utility core wall (Fig. 7.3b) is the only means of resisting lateral forces, then there is likely to be heavy torsion. For best torsional stability, shear walls should be distributed along the building perimeter in both orthogonal directions (Paulay and Priestley 1992) so as to form an efficient means of resisting torsion and preventing instability (Fig. 7.3c). In short, the wall layout should be such that it leads to a flexurally and torsionally stiff building.

Shear walls have considerable rigidity in their own plane. For a building primarily supported on shear walls, one of the aims while developing the building layout should be to bring the centre of mass and centre of rigidity close together. This will minimise torsion. Secondly, these walls have to be sized to meet stipulated codal strength and drift limits. While doing so, there is often an urge to reduce wall thickness to the minimum to save cost. However, it is wiser to have a slightly thicker wall to improve constructability and seismic performance. From this consideration, IS 13920 stipulates that the minimum wall thickness should be 150 mm.

Shear walls should run continuously in a vertical line right from their foundation up to their top, and they should not have abrupt changes in stiffness and strength along the height. If they are provided from first floor level upwards, to accommodate access at grade level (e.g. for parking), then this will place a huge demand (in terms of axial forces, flexure and shears) on the lower supporting columns. During a major earthquake, such columns could experience significant alterations in their axial load coupled with heavy shear forces. There are many reports of failures of columns supporting shear walls which have been terminated at an intermediate level. Hence, such an arrangement should be avoided altogether (Fig. 7.4).

In tall buildings, shear walls should be used in conjunction with moment frames so as to increase overall stiffness in the upper reaches of a building. If collinear shear walls have varying inertia ratios between them, from one floor to another, then the

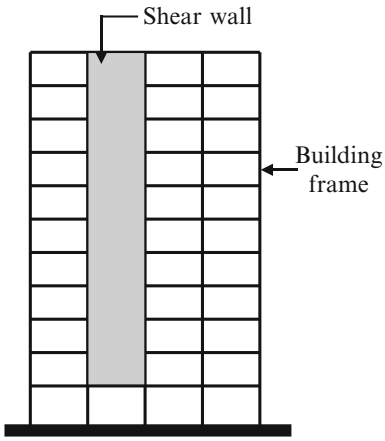


**Fig. 7.4** Shear wall terminated short

wall/slab interfaces need to be designed to carry heavy shear forces. Throughout this chapter it will be assumed that shear walls are provided with substantial foundations which are not subjected to partial uplift and that walls will counter in-plane shear and bending only, i.e. biaxial bending is not considered.

## 7.3 Classification of Shear Walls

A measure of the likely behaviour of a shear wall can be gauged from its aspect ratio and to some extent from its shape and ductility class. These walls may be classified in various ways as under:

### *7.3.1 Aspect Ratio*

An aspect ratio (AR) of a shear wall is its height divided by its length. On this criterion, the classification can be as under:

(a) *Slender Wall*

A wall is generally termed as slender if its aspect ratio, AR is $\geq 2$. The aspect ratio is self limiting to a value of about 7 for a shear wall supported building. Higher values could result in high $P$-$\Delta$ effects and difficulties in anchoring the tension side of its footing. A slender wall behaves essentially as a beam with lateral supports from rigid floor slabs and its design is largely controlled by flexure. Its primary deformation is in bending while deflection due to shear is small and hence often neglected. During cyclic loading from inertia forces, the vertical rebars are designed to yield near the base, as shown in Fig. 7.1a, and thus provide ductility.

(b) *Intermediate Wall*

If $1 < AR < 2$, the behaviour of such a wall is influenced by both shear and flexure and it is termed as an intermediate wall. In general, yielding of walls in shear should be prevented as it substantially diminishes its inelastic performance.

(c) *Squat Wall*

If $AR \leq 1$, the wall predominantly deforms in shear and functions more like a deep beam and is categorised as a squat wall. Failure of such walls can often be attributed to diagonal tension, horizontal sliding or diagonal compression, i.e. web crushing. Wall shear strength generally controls its design.

### *7.3.2 Shape in Plan*

Shear walls can also be classified as plain, flanged or core walls. Layout of shear walls in plan may generate different shapes such as T, L and I. In such cases they are termed as flanged walls. Flanges add substantially to the moment and shear capacities of a wall. Hence, even when a two-dimensional analysis is conducted, the effect of flange member in the third dimension has to be included. The extent of a flange that can be considered as part of the wall is specified in the code. When direction of the principal seismic force being considered is skew to the longitudinal axis of a flanged wall, then it needs to be analysed for bidirectional bending.

### *7.3.3 Ductility Class*

Similar to frames, one could also examine the possibility of different ductility levels for shear walls.

(a) *Elastically Responding Walls*

These are also termed as ordinary shear walls which operate in the elastic range. Such walls may be designed with a response reduction factor of 3.0 (BIS 2002a). The code specifies that ordinary shear walls cannot be used in seismic zones IV and V.

(b) *Ductile Walls*

These are walls designed for full ductility and a capacity design approach is recommended for their analysis. A response reduction factor of 4.0 (BIS 2002a) may be considered for their design. This value may be raised to 5.0 for coupled walls if energy dissipation is through suitably designed coupling beams.

## 7.4 Design of Cantilever Walls in Flexure

Most codes demarcate a wall from a column when the longer to shorter dimension exceeds 4.0. The design of even a simple cantilever shear wall is complex as its behaviour depends on many parameters such as its aspect ratio, shape, stiffness, strength, ductility and effective moment of inertia. Thus, simplifying assumptions need to be made, and the primary consideration, in a force-based design, is to ensure adequate strength, stiffness and ductility.

These walls are commonly designed as compression members under vertical loads and in-plane moment. They are usually restrained laterally by rigid floor slabs, and in such cases the effective height of a rectangular wall can be taken as 0.75 times storey height. As per IS 13920 the minimum thickness of any part of the wall shall be 150 mm. For coupled walls it would be advantageous to limit the minimum thickness to 300 mm to allow for placing of heavy reinforcement in coupling beams. As per IS 456, the ratio of effective wall height to its thickness shall not exceed (BIS 2000) 30.

### *7.4.1 Important Design Considerations*

While a wall is designed for flexure and ductility, it should also be protected against shear failure through capacity-based design. Some important design considerations, in addition to those enumerated in the code (IS 1893), are listed below:

- For tall buildings the long-term vertical movement of a shear wall, relative to adjoining vertical supporting elements, is an important consideration for the integrity of horizontal connecting elements between them.
- Shear walls need to be analysed both for maximum and minimum load conditions. The former condition is unfavourable when evaluating compressive strength and the latter when checking for tension and for possibility of foundation uplift.
- While tall slender shear walls may be analysed treating them as beams in flexure, for walls with large openings or with irregular changes in section over their height, a detailed analysis is recommended.
- If a shear wall rocks on its foundation under maximum earthquake conditions, the effects include (1) a reduction in the stiffness with consequent increase in its fundamental time period and a reduction in inertia forces and (2) an enhancement in drift as well as in overturning moment due to $P$-$\Delta$ effect.
- Walls resist lateral forces transmitted to them from the diaphragm. For this purpose utmost care should be taken in detailing the connection between diaphragm and shear wall so that it is strong enough to transmit seismic forces, shears and rotations from one to another.

- Wall foundation and soil bearing area should be able to support the yield capacity of a ductile wall (Paulay and Priestley 1992). Soil pressure should be restricted such that any inelastic deformations are negligible.
- Natural location to check for flexural stresses is at the base of a wall. However, stresses should also be checked at intermediate locations where there is considerable interaction between the wall and a frame in a dual system.
- Reinforcement along two faces is a good insurance against wall fragmentation under extreme inelastic cyclic loading.
- At locations where shear wall thickness changes along its height, the sharing of shear between walls alters and this will cause local shears in walls and that should be allowed for in design.
- For stress evaluation in flexure, advantage may be taken of a portion of the tributary flange area as specified in the code. However, when assessing the gravity load available to resist uplift, the entire tributary flange area may be used.
- When tension steel yields in a flanged shear wall supporting significant gravity load, the entire flange area may be in compression. As a result, confinement reinforcement has to be provided.
- With large flexural capacity, adequate horizontal and vertical shear reinforcement should be provided to prevent brittle shear failure.

### *7.4.2 Flexural Stress Analysis*

Consider a rectangular slender wall of thickness $t$ supporting an axial load and in-plane moment with uniformly distributed vertical web reinforcement as shown in Fig. 7.5a. For the purpose of analysis, the reinforcement is treated as a continuous

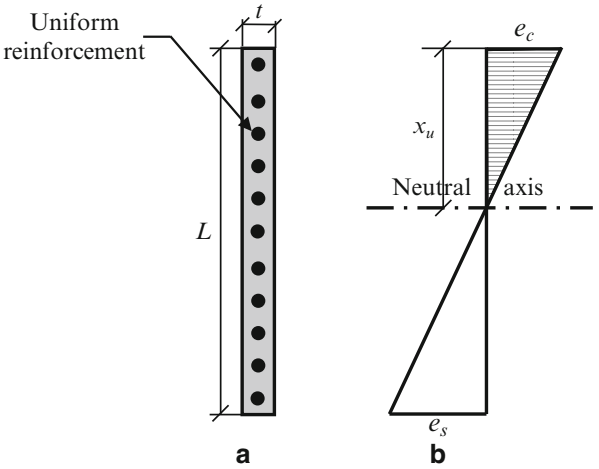


**Fig. 7.5** Slender wall in flexure (**a**) Wall plan, (**b**) Strain diagram

steel plate. Strain diagram is shown in Fig. 7.5b and analysis of such a wall section can be based on the same assumptions as those for a reinforced concrete beam.

#### 7.4.2.1 Balanced Design

For a balanced design, both steel and concrete are assumed to attain their maximum strain simultaneously, i.e. maximum concrete strain $e_{cu}$ will be 0.0035 and maximum strain in steel $e_{su}$ will be $0.87f_y/E_s$. It can be readily shown that depth of the nondimensional neutral axis for a balanced design will be given by

$$\frac{x_u^*}{L} = a^* = \frac{0.0035}{0.0035 + 0.87f_y/E_s} = \frac{1}{1+\beta} \tag{7.1.1}$$

In this case

$$\beta = 0.87f_y/0.0035E_s \tag{7.1.2}$$

In flexure, a shear wall may fail either in tension or in compression. Analysis for these two conditions is presented below.

#### 7.4.2.2 Tension Failure, i.e. When $a$ (i.e. $x_u/L$) $< a^*$

The strain, stress and force diagrams are shown in Fig. 7.6a–c respectively.

It has been shown (Medhekar and Jain 1993a) that forces acting on the section and their lever arms from the extreme tension fibre will be as given in Table 7.1 for which the nomenclature is as under:

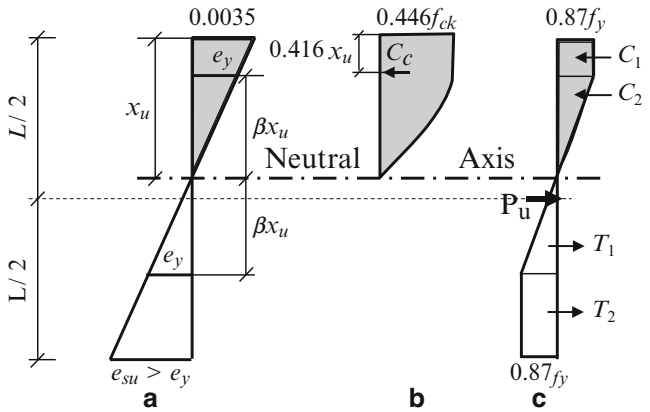


**Fig. 7.6** Slender wall in flexure Case 1: tension failure (**a**) Strain diagram, (**b**) Concrete stress and force diagram, (**c**) Steel stress and force diagram

**Table 7.1** Forces and their lever arms

| Force | Lever arm from the extreme tension fibre |
|---|---|
| $C_c = 0.36 f_{ck}.\, x_u.t$ | $L - 0.416 x_u$ |
| $C_1 = 0.87 f_y.t.p.x_u\,(1-\beta)$ | $L - x_u\,(1-\beta)\ /\ 2$ |
| $C_2 = \frac{0.87}{2} f_y.t.p.\beta.x_u$ | $L - x_u\left(1 - \frac{2\beta}{3}\right)$ |
| $T_1 = \frac{0.87}{2} f_y.t.p.\beta.x_u$ | $L - x_u\left(1 + \frac{2\beta}{3}\right)$ |
| $T_2 = 0.87 f_y.t.p\,\{L - x_u\,(1+\beta)\}$ | $\{L - x_u\,(1+\beta)\}/2$ |
| $P_u$ | $L/2$ |

$a$ : nondimensional depth of neutral axis (refer to Eq. 7.1.4)
$a^*$ : nondimensional depth of neutral axis for a balanced design
$A_s$ : area of vertical reinforcement
$C_c$ : compressive force in concrete
$C_1$ : compression in steel
$C_2$ : compression in steel below yield
$E_s$ : modulus of elasticity of steel
$e_y$ : yield strain in steel
$e_c$ : strain in concrete
$e_s$ : strain in steel
$e_{cu}$ : maximum strain in concrete = 0.0035
$e_{su}$ : maximum strain in steel = $0.87 f_y/Es$
$f_y$ : steel yield stress
$f_{ck}$ : characteristic strength of concrete
$L$ : length of wall
$M_u$ : moment of resistance of the wall
$p$ : vertical steel ratio = $A_s/t.L$
$P_u$ : external factored vertical axial load
$T_1$ : tension in steel before yield
$T_2$ : tension in steel after yield
$t$ : uniform thickness of rectangular wall
$x_u$ : depth of neutral axis
$x_u^*$ : depth of neutral axis for a balanced design
$\beta\, x_u$: distance from neutral axis where steel strain reaches $e_y$

Two parameters are introduced as

$$\varphi = \left\{\frac{0.87 f_y\ p}{f_{ck}}\right\};\quad \lambda = \left\{\frac{P_u}{f_{ck}\ t\ L}\right\} \tag{7.1.3}$$

From equilibrium of forces, the nondimensional depth of neutral axis is

$$a = \frac{x_u}{L} = \left\{\frac{\varphi + \lambda}{2\varphi + 0.36}\right\} \tag{7.1.4}$$

Taking moments about extreme tensile fibre, the moment of resistance of the section will be

$$\frac{M_u}{f_{ck}\,t\,L^2} = \varphi\left[\left(1+\frac{\lambda}{\varphi}\right)(0.5-0.416a) - a^2\left(0.168+\frac{\beta^2}{3}\right)\right] \tag{7.1.5}$$

#### 7.4.2.3 Compression Failure, i.e. When $a^* < a < 1$

In this case it is assumed that neutral axis lies within the section, i.e. $a < 1$. Stress, strain and force diagrams are shown in Fig. 7.7a–c respectively. Compressive forces $C_c$, $C_1$, $C_2$, and factored external load $P_u$ and their lever arms from extreme tensile fibre are the same as those for tension failure in Sect. 7.4.2.2. Steel tensile force $T_2$ is absent as the steel does not reach its limiting yield stress. Force $T_1$ and its lever arm will be

$$T_1 = \frac{\varphi}{2} f_{ck}\, t\, \frac{(L-x_u)^2}{\beta x_u}; \quad \text{Lever arm} = \frac{(L-x_u)}{3} \tag{7.1.6}$$

Proceeding as before, equilibrium of forces leads to the equation

$$a^2\alpha_1 + \left(\frac{\varphi}{\beta} - \lambda\right)a - \left(\frac{\varphi}{2\beta}\right) = 0 \tag{7.1.7}$$

The value of '$a$' can be obtained from the above quadratic equation.

Moment capacity of the section will be

$$\frac{M_u}{f_{ck}\,t\,L^2} = (\alpha_1.a) - \left(\alpha_2.a^2\right) - \alpha_3 - \frac{\lambda}{2} \tag{7.1.8}$$

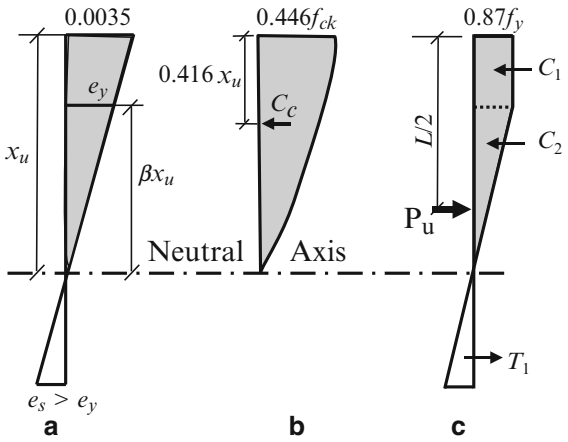


**Fig. 7.7** Slender wall in flexure Case 2: compression failure (**a**) Strain diagram, (**b**) Concrete stress and force diagram, (**c**) Steel stress and force diagram

where

$$\alpha_1 = 0.36 + \varphi\left(1 - \frac{\beta}{2} - \frac{1}{2\beta}\right); \quad \alpha_2 = 0.15 + \frac{\varphi}{2}\left(1 - \beta + \frac{\beta^2}{3} - \frac{1}{3\beta}\right);$$

$$\alpha_3 = \frac{\varphi}{6\beta}\left(\frac{1}{a} - 3\right)$$

The above analysis is for a uniformly reinforced rectangular wall. When boundary elements are provided, it would be appropriate to consider the composite section. However, commonly the rectangular portion of the wall is treated as above and boundary elements are considered as forming a short column. Results are then superimposed. A typical analysis of a cantilever wall in flexure is illustrated in *Ex* 7.9.1.

### *7.4.3 Detailing for Flexure*

Failure mode for tall slender walls is usually the yielding of tensile steel. Crushing of concrete with buckling of compression rebars can also follow. Slender walls need to be checked for out-of-plane bending as well. A cantilever shear wall effectively dissipates seismic energy through yielding at its base with plastic hinge formation under extreme seismic conditions. The following aspects may be noted in connection with shear wall detailing:

- Length of such a plastic hinge measured from the base is taken as specified in IS 13920. In this region, concrete should be confined.
- For walls with vertical reinforcement in two layers, the horizontal rebars should form a closed core by being placed external to the vertical rebars.
- Shear walls are often constructed using slip-form technique. In such construction, slab-to-wall junctions should be very carefully executed as per design to ensure proper moment and shear transfer.
- Spacing of vertical bars crossing potential horizontal sliding planes should not exceed three times the wall web thickness nor 1/5th the horizontal length of wall nor 450 mm (BIS 2003).
- Horizontal rebars should be anchored near wall edges. If boundary elements are provided, then horizontal rebars should be anchored in the confined core of boundary elements.
- Maximum reinforcement in the boundary element should preferably be restricted to 4 % from practical considerations to avoid congestion.
- Lap splices in vertical reinforcement should be avoided in areas of potential yielding.
- At location of vertical rebar splicing, the wall may get locally strengthened and care should be taken to protect against it yielding above or below the splice (Moehle et al. 2010a).

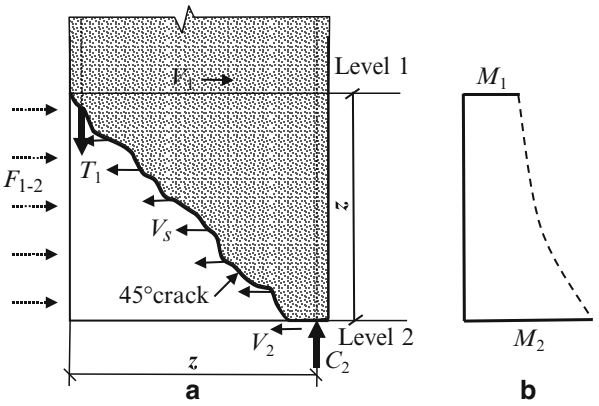


**Fig. 7.8** Tension shift. (**a**) Shear forces. (**b**) Bending moment diagram (Based on Sucuoglu and Akkar 2011)

#### 7.4.3.1 Tension Shift

This is an important aspect that requires careful attention in respect of curtailment of vertical rebars in shear walls. Consider the free body diagram of a shear wall near a crack close to the base (Fig. 7.8a). The bending moment diagram is shown (Sucuoglu and Akkar 2011) in Fig. 7.8b.

Taking moments about point 2, where the compression is $C_2$,

$$M_2 = z.T_1 + 0.5z.V_s \tag{7.2.1}$$

and considering equilibrium of portion between level 1 and level 2,

$$M_2 = M_1 + z\,V_1 + 0.5\,z\,F_{1-2} \tag{7.2.2}$$

where

$F_{1-2}$ : external lateral force acting on portions 1–2
$T_1$ : tension in longitudinal steel at section 1
$V_s$ : shear resisted by stirrups
$V_1$ : external shear at section 1
$z$ : moment arm $\approx$ wall length assuming a 45° crack
$M_1$ and $M_2$ : internal moments at sections 1 and 2, respectively

From Eqs. 7.2.1 and 7.2.2 it follows that

$$T_1 = \frac{M_1}{z} + [V_1 + 0.5\,(F_{1-2} - V_s)] \tag{7.2.3}$$

The value of $V_s$ is small compared to the external shear forces ($V_1 + 0.5F_{1-2}$), and hence ignoring it,

$$T_1 = \frac{M_1}{z} + [V_1 + 0.5F_{1-2}] = \frac{M_2}{z} \tag{7.2.4}$$

Hence, the tension at section 1 has to be calculated from the larger moment at section 2 and thus the tension shift (Paulay and Priestley 1992) is equal to the height $z$.

### 7.4.3.2 Design Bending Moment

For a tall cantilever wall, the bending moment diagram $M_d$ due to lateral static inertia forces, as calculated by the LSP, is depicted by line 1 in Fig. 7.9. Once the base section is designed for moment and axial load, the precise amount and distribution of rebars is determined. From this, the value of bending moment capacity $M_u$ that is actually provided is obtained. Research into the distribution of moment up the wall, based on inelastic time history analysis, has suggested (Mesa 2002) that a straight line joining the $M_u$ value for first mode at base, with the top of the wall, represents

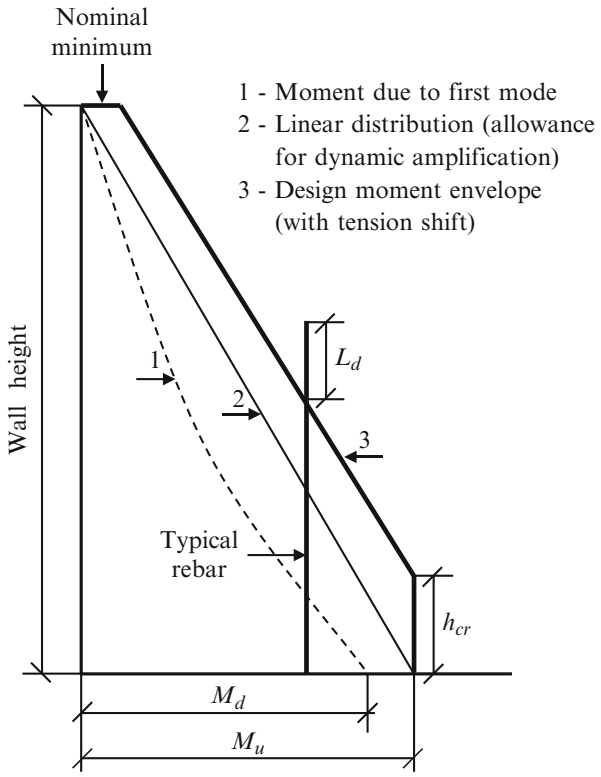


**Fig. 7.9** Design moment envelope (Based on Mesa 2002)

the moment (line 2 in Fig. 7.9) magnitude along the wall height which will allow for higher mode effects. This is subject to the condition that the structure does not have significant discontinuities of mass, stiffness or strength over its height.

Further, because of tension shift (refer Sect. 7.4.3.1), the bending moment diagram is shifted upwards (at the base) by a height $h_{cr}$ to create the bilinear moment envelope (line 3). This is the moment profile for which the wall should be designed. It is suggested (Sucuoglu and Akkar 2011) that height $h_{cr}$ above the base, termed as plastic hinge region, shall be taken as larger of $L$ and $H/6$ where $H$ is the building height. At the same time $h_{cr}$ must be $\leq$2 L (Sucuoglu and Akkar 2011).

As per IS 13920 it is the general practice to provide minimum reinforcement in the web of 0.25 % of gross concrete section of the web in each direction. Much of vertical steel resisting the moment should be concentrated in the wall extremities. This helps to increase rotational ductility considerably (Paulay 1972). Vertical bars are typically lap spliced for tension but splicing in the hinge region should be avoided because of their uncertain behaviour under cyclic loading in the inelastic range. These rebars should be curtailed only at a distance equal to their development lengths $L_d$ above the moment envelope (line 3) as shown in Fig. 7.9. Further, vertical rebars should have generous anchorage lengths extending into the footing.

In the plastic hinge region at base of a wall, the compression flange is heavily stressed due to load reversals and shear component from diagonal strut action. Hence, concrete in this portion needs to be confined. Horizontal stirrups are added to tie vertical rebars in the boundary elements or near edges for plain shear walls. The minimum horizontal and vertical reinforcement should be uniformly distributed in both directions as this helps to control width of inclined cracks. Secondly, a designer should not provide significantly more than required vertical reinforcement as this will lead to a reduction in overall ductility and will increase shear demand.

#### 7.4.3.3 Wall Piers

A wall pier is a narrow segment of a shear wall. Its dimensions do not satisfy requirements for a frame column (Fig. 7.10). A wall pier is generally one that has dimensions of $L_w/b_w \leq 6.0$ and $h_w/L_w \geq 2.0$. It should satisfy all requirements applicable to special moment frame columns. Additional horizontal rebars should be provided as shown in Fig. (7.10).

### *7.4.4 Boundary Elements*

Boundary elements are essentially thickened portions of a web at the edges of a shear wall (Fig. 7.11) which add substantially to flexural capacity of the wall. In these regions the stress levels are high and proper confinement of rebars and concrete is essential to delay buckling of rebars and consequent spalling of concrete.

**Fig. 7.10** Wall pier

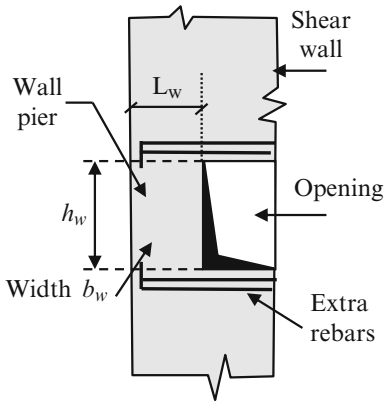


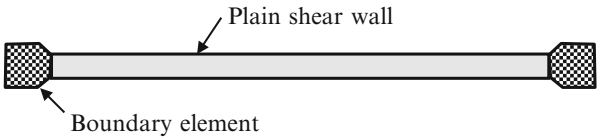


**Fig. 7.11** Shear wall with boundary elements

End portions of an un-thickened wall may also form boundary elements where additional rebars have to be provided and concrete needs to be confined.

Briefly, some of the codal requirements regarding boundary elements are:

- Boundary elements shall be provided along vertical edges of a shear wall when extreme fibre compressive stress in the wall due to factored gravity loads plus factored earthquake force exceeds $0.2f_{ck}$ (BIS 2003). Such elements may be discontinued where calculated compressive stress reduces to less than $0.15\,f_{ck}$. The compressive stresses are calculated using a linear elastic model and gross section properties.
- The size of a boundary element shall be such that it can carry imposed loads assuming a short column action.
- Under major seismic shaking, diagonal tension cracks can develop near the wall base which will induce truss action with consequent tensile stresses in horizontal web reinforcement. Hence, horizontal rebars should be well anchored in the edges of a rectangular wall or in the core of boundary elements.
- Other walls running at right angles to a shear wall can also provide some degree of confinement.
- Flanges act as boundary elements and boost the moment of resistance of slender walls. They also provide lateral stability against out-of-plane buckling in plastic regions of the wall.
- Boundary elements shall be provided with a minimum of 0.8 % reinforcement.
- Confining reinforcement at base of a boundary element needs to be continued into the footing or pile cap as the case may be (Fig. 7.12).

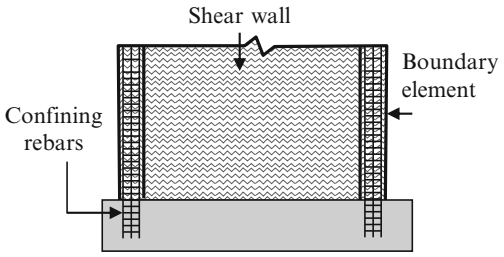


**Fig. 7.12** Confining bars extend into footing/pile cap

A boundary element should have an axial load carrying capacity, as a short column, equal to factored gravity load plus compression imposed on it by seismic moment. It should also be able to sustain the minimum gravity load coupled with seismic moment inducing tension. Compressive force on a boundary element due to seismic moment is calculated as

$$F_{cb} = \frac{M_u - M_{uw}}{C_b} \tag{7.3.1}$$

where

$F_{cb}$ : design compressive force on boundary element
$M_u$ : factored design seismic moment
$M_{uw}$: moment of resistance provided by vertical reinforcement in the web
$C_b$ : centre to centre distance between the two boundary elements

Factored gravity load on the boundary element can be obtained as being proportionate to the area of boundary element to that of the entire wall section. If however the gravity load adds to the strength of the wall, its load factor shall be reduced (BIS 2003) to 0.8. A typical design of a shear wall with boundary elements is demonstrated through *Ex* 7.9.1.

## 7.5 Capacity-Based Shear Design of Cantilever Walls

To achieve a ductile behaviour in shear walls during a severe seismic event, the designer should ensure that their lateral shear strength is higher than that required to develop flexural yielding in the vertical boundary reinforcement of walls. Consequently, the capacity-based approach should be adopted for design in shear.

### *7.5.1 Design for Diagonal Tension*

Cantilever walls need to be checked for diagonal tension due to shear. The nominal shear stress (BIS 2003) is given by

$$\tau_v = V_{uw}/t_w d_w \tag{7.4.1}$$

where

$V_{uw}$: factored shear force resisted by the wall concrete
$t_w$ : width of wall web
$d_w$ : effective depth of wall commonly taken approximately as 0.8 times the wall length for a rectangular wall

If $\tau_v >$ the maximum shear stress permitted by IS 456, $\tau_{max}$, the concrete section needs to be revised.

If $\tau_v <$ design shear strength of concrete $\tau_c$ specified in IS 456, then minimum shear reinforcement should be provided as specified in the code.

If $\tau_c < \tau_v < \tau_{max}$ then shear reinforcement has to be provided.

Shear resisted by the wall as per code is

$$V_{uw} = \tau_c \, (t_w d_w) + \frac{0.87 f_y A_{h\ w} d_w}{s_{vw}} \tag{7.4.1}$$

If boundary elements are provided, then their shear resistance should be added (Dasgupta et al. 2003). The latter will amount to

$$V_{ub} = n \left\{ \tau_c \, (t_b d_b) + \frac{0.87 f_y A_{hb} d_b}{s_{vb}} \right\} \tag{7.4.2}$$

The total shear resistance provided

$$V_u = V_{uw} + V_{ub} \tag{7.4.3}$$

where

$V_{uw}$ : shear force resisted by wall
$V_{ub}$ : shear force resisted by boundary elements
$V_u$ : total shear resisted commensurate with moment $M_u$
$t_b, t_w$ : thickness of a boundary element and rectangular wall, respectively
$d_b, d_w$ : effective depth of boundary element and rectangular wall, respectively
$A_{hw}$ : total area of horizontal shear reinforcement in web
$A_{hb}$ : total area of horizontal shear reinforcement in a boundary element
$s_{vw}, s_{vb}$ : vertical spacing of shear reinforcement in web and boundary elements, respectively
$n$ : number of boundary elements

For a capacity-based design, the shear force $V_u$, commensurate with moment $M_u$, has to be enhanced by a factor $\varphi_0$ to allow for overstrength and the section needs to be checked for this enhanced shear, viz:

$$V_\Omega = \varphi_o . V_u \tag{7.4.4}$$

where

$M_u$: moment capability provided at base
$V_u$: shear force commensurate with $M_u$
$\varphi_0$: overstrength factor

The overstrength factor is not known and any rational method may be used to determine it. One of the approaches could be to generate a *P-M* interaction diagram with steel overstrain taken into account. The steel stress corresponding to overstrain could be 1.25 $f_y$. Thereafter, the overstrength moment $M_\Omega$ can be read off the diagram corresponding to actual axial load $P_u$ expected on the section. Then $\varphi_0 = M_\Omega/M_u$. Clearly this approach is laborious. In the least, $\varphi_0$ may be taken as 1.4 by extrapolating from the code-specified factor for evaluating beam enhanced shear.

Near the wall base where a plastic hinge is likely to develop, the total shear should be resisted by horizontal steel which should be continued over full height of the estimated hinge region (Paulay 1972). In general, splices in transverse reinforcement should be staggered.

### 7.5.2 Design for Sliding Shear

Sliding shear failure is specially a feature of earthquake-induced loads and is often due to poorly detailed and executed construction joints. Another potential location for such a failure is the plastic hinge region where horizontal flexural cracks may form a weak plane after repeated inelastic load reversals. The resistance to this type of failure is essentially through aggregate interlock and dowel action of vertical reinforcement. For vertical reinforcement to be effective as dowels, it should be well anchored on both sides of the potential sliding interfaces.

The total quantity of clamping reinforcement provided across the joint should be able to meet the shear demand. For this, the area of vertical reinforcement required ($A_v$) may be obtained (Jain et al. 2005) from the following equation:

$$V_\Omega = \mu \left(0.8 P_u + 0.87 f_y A_v\right) \tag{7.5.1}$$

$V_\Omega$ : capacity-based shear demand force causing sliding.
$P_u$ : factored axial compressive load reduced by a factor of 0.8 to allow for possible effects of vertical acceleration.
$\mu$ : coefficient of friction whose value may be taken as 0.6 (Taranath 2010a) when the joint is not intentionally roughened. It can be close to 1.0 for a well-formed rough construction joint free of laitance.
$f_y$ : yield stress of steel.

The flexural wall reinforcement present in the concerned area could be utilised as part of total area required. This reinforcement should be distributed over full length of the wall. While the reinforcement provided should not be less than that stipulated by the code for construction joints, the joint should be so designed that its shear

strength exceeds that of wall itself. Diagonal rebars, placed in the web of a wall, will assist in resisting sliding shear. The methods of checking for diagonal tension and sliding shear are also demonstrated through *Ex* 7.9.1.

## 7.6 Design of Squat Walls

In design, it is intended that seismic energy dissipation in walls will be through ductility and the aim is to suppress any shear failure. While this is achievable in slender walls, squat walls tend to fail in a mixed flexure – shear mode or in pure shear. It is more often the latter. In squat walls with light horizontal reinforcement, a diagonal tension failure is also common. These walls tend to resist lateral forces through a diagonal strut mechanism (Moehle et al. 2010a). Their analysis commences with a design for shear, then for sliding and later for flexure.

### *7.6.1 Design for Flexure*

Squat walls are often provided in low-rise buildings. They may appear in tall buildings also, where wall height is restricted to a floor or two. For such walls, when their foundations are large enough to prevent rotations, they may respond in the elastic domain even during major shaking. These walls may fail either in diagonal tension or diagonal compression or sliding shear. One way to minimise chances of diagonal tension failure is to distribute more evenly the lateral load transfer at the top of wall through a capping beam after keeping the nominal shear stress low (Paulay and Priestley 1992).

Normally, in squat walls the vertical and horizontal rebars are uniformly distributed which helps in shear friction and dowel action against sliding shear. Their design is normally governed by shear, but if amount of vertical steel is low, its inelastic behaviour (FEMA 274 1997) may be controlled by flexure.

### *7.6.2 Design for Diagonal Tension*

Typical reinforcement in a squat wall is shown in Fig. 7.13. Base moment is given by $V_t$ x $h_w$. The base section may be designed for the analytically evaluated bending moment and shear. In this case also, sliding shear failure could occur (Medhekar and Jain 1993a) particularly at junction with foundation and at construction joints. In squat walls, clear horizontal shear cracks could open up over full wall length. To close such cracks, diagonal rebars may be provided to resist at least 50 % of the shear (Paulay and Priestley 1992).

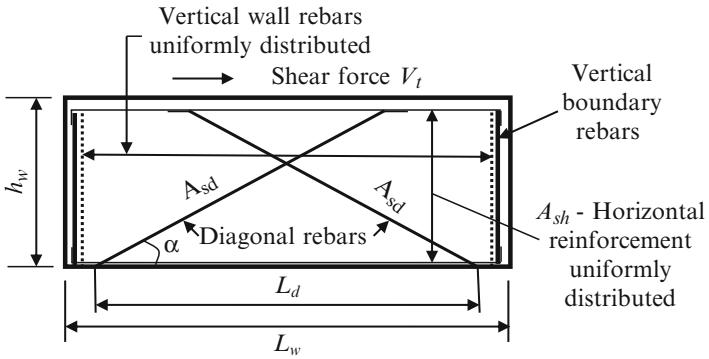


**Fig. 7.13** Typical reinforcement in a squat wall

Diagonal reinforcement in the web plus the well-confined boundary elements along edges have been shown to bring about significant improvement in resistance to sliding shear. In case where moment value is low and boundary elements are not provided, then a part of the force in diagonal reinforcement will be called upon to resist this moment and only the balance force will be available to resist shear. Since substantial portion of shear is resisted by vertical reinforcement, its quantity should not be less than the horizontal reinforcement.

Diagonal tension is resisted by both horizontal reinforcement and inclined bars, neglecting resistance of concrete. Their contribution, as shown by Paulay and Priestley (1992), is as under:

Shear resisted by horizontal rebars

$$V_{sh} = A_{sh}.f_{yh}.h_w/s_v \tag{7.6.1}$$

Shear resisted by inclined bars

$$V_{sd} = A_{sd}.f_{yd}\cos\ \alpha \tag{7.6.2}$$

The total resistance

$$V = V_{sh} + V_{sd} > \frac{h_w}{l_w}\varphi_o.V_t \tag{7.6.3}$$

$V_t$ : lateral shear force at top of wall
$A_{sh}$ : area of horizontal rebar
$A_{sd}$ : area of diagonal rebars
$f_{yh}$ : yield strength of horizontal rebars
$f_{yd}$ : yield strength of diagonal rebars
$h_w$ : height of wall

$l_w$ : length of wall $\geq h_w$
$\alpha$ : inclination of diagonal bars with the horizontal

The design of a squat wall for moment and diagonal tension is illustrated in *Ex* 7.9.2.

## 7.7 Coupled Shear Walls

Properly detailed coupled shear walls combine the lateral strength and stiffness of a shear wall and energy dissipating capacity of coupling beams. Two cantilever shear walls may be connected together at regular intervals vertically by deep beams termed as coupling beams (Fig. 7.14). When individual walls deform, they force connecting beams to rotate and deform vertically. This induces shear forces in beams that restrain the walls, thereby reducing bending moment in them. Coupled shear walls possess a great capability of being able to dissipate significant seismic energy through coupling beams. Any damage to coupling beams is easier to repair than that to the walls.

Shear in coupling beams varies over wall height and hence it should be planned such that critically stressed coupling beams yield first. Secondly, it should be borne in mind that individual walls are expected to develop plastic hinges at their bases during a severe earthquake. As a result the wall base moments developed may not be in the same proportion as in an elastic analysis. Presently, coupled walls are normally analysed using software with coupled walls being modelled either (1) as a frame with individual walls being interconnected by coupling beams or (2) as walls with coupling beams that are replaced by an equivalent continuum.

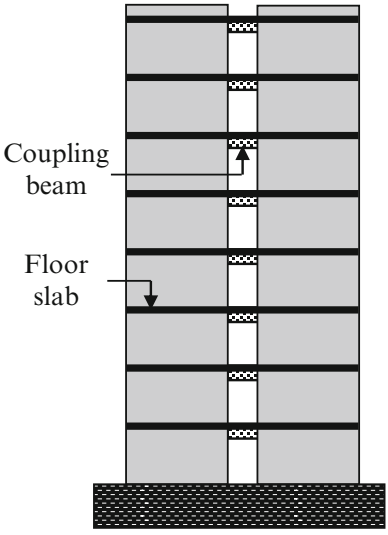


**Fig. 7.14** Coupled shear walls

Failure is often marked by:

1. Flexural failure of coupling beams when they are relatively shallow
2. Shear failure or diagonal splitting in moderately reinforced coupling beams
3. Compression crushing of a shear wall with very strong coupling beams

To couple shear walls effectively by dissipating substantial seismic energy through inelastic action, strong coupling beams are required with adequate ductility at their flexural overstrength capacity. Their depth should be greater than half their clear span. However, coupling beams should not be unduly stiff or strong as this could induce appreciable tension in coupled walls. Net tension will reduce the yield moment, shear resistance and ductility of the wall. On the contrary, if the walls are coupled through floor slabs or shallow beams, then coupling is not likely to be satisfactory and the two walls may need to be considered as independent walls.

### *7.7.1 Degree of Coupling*

Naeim (2001) has pointed out that stiff and strong beams are favoured but they should not be too strong flexurally. Hence, critically stressed coupling beams should yield prior to yielding of wall bases. Thus, a balance has to be struck between two opposing requirements. One of the ways to assess the degree of coupling is by the coupling factor $\lambda_c$ (Fig. 7.15) taken as

$$\lambda_c = \frac{TL}{M_1 + M_2 + TL} \tag{7.7.1}$$

where

$M_1$, $M_2$: resisting moments at base of shear walls 1 and 2, respectively
$T$ : axial resistive force due to coupling effect
$L$ : distance between wall centres

While there are differing views on the desired value of $\lambda_c$, Naeim (2001) has pointed out that as per the Canadian code, $\lambda_c$ should be $> 2/3$ for it to qualify as a fully effective coupled wall system.

### *7.7.2 Design of Coupling Beams*

Coupling beams are deep beams which resist a part of the overturning moment and thus reduce the moment that walls need to carry. Ends of such beams experience large rotational and vertical displacements during major shaking. Hence, the sections need to have adequate rotational ductility to dissipate seismic energy

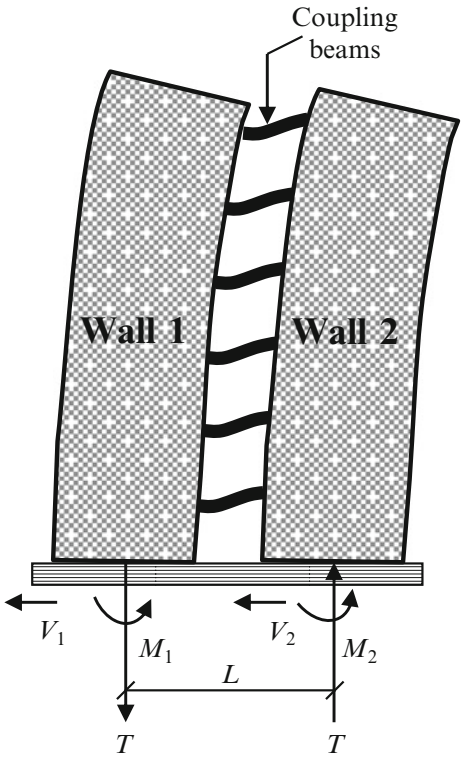


**Fig. 7.15** Coupling factor

through inelastic deformations and thus aid in the wall's ductile performance. For coupling beams in external walls covered with aesthetic finishes, the latter should withstand deformations experienced by coupling beams.

Coupling beams may be reinforced with parallel top and bottom bars that are well anchored into the walls and reinforced with closely spaced confinement bars. In addition they may be provided with diagonal rebars. Alternately they may be reinforced with only diagonal bars that are well confined over their full length and anchored into the walls. Such diagonal rebars are then designed to resist both bending moments and shear forces.

Experimental results from studies of inelastic behaviour of coupling beams have demonstrated (FEMA 273 1997) that compared to beams with conventional reinforcement; beams with full length diagonal reinforcement with adequate confining rebars have a superior performance.

Even when such beams are reinforced only with diagonal rebars, there is still a need for notional longitudinal bars with stirrups to confine the core. For clarity, a coupling beam with only diagonal reinforcement is shown in Fig. 7.16 and with only longitudinal reinforcement in Fig. 7.17. If span to depth ratio of a coupling beam >4.0, then diagonal reinforcement is not considered to be effective (Taranath 2010a). This corresponds to $\alpha \approx 13°$.

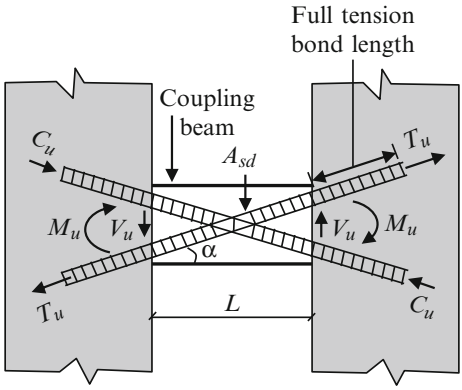


**Fig. 7.16** Coupling beam with diagonal reinforcement

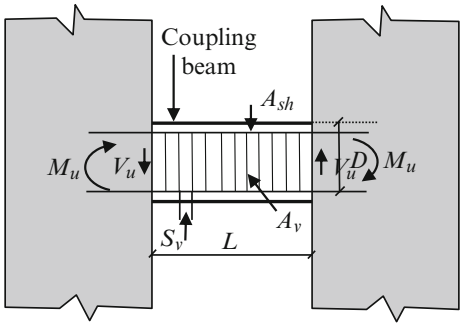


**Fig. 7.17** Regular reinforcement in coupling beam

As per IS code 13920, if earthquake-induced shear stress exceeds $0.1\frac{L}{D}\sqrt{f_{ck}}$, then the entire shear, moment and axial compression shall be resisted by diagonal rebars only. In this case it is assumed that shear forces can be resolved along the diagonals as tension and compression. Considering force magnitude $T$ along the diagonals, it follows that their capacity to resist shear is

$$V_u = 2\,T\,\sin\alpha \tag{7.8.1}$$

Replacing $T = 0.87 f_y A_d$, the area of reinforcement required along each diagonal ($A_d$) is given by

$$A_d = \frac{V_u}{1.74 f_y \mathrm{Sin}\alpha} \tag{7.8.2}$$

where

$V_u$ : factored shear force on coupling beam
$\alpha$ : angle of inclination of diagonals

The codal stipulation is that diagonal bars should extend into the walls a distance that is 1.5 times normal development length. This is presumably to allow for adverse

effect of reversed cyclic loading on a group of bars because there is a concentration of anchorage forces. These bars should be provided with confining reinforcement, in the form of stirrups, over their full lengths including anchorage portion to prevent premature buckling.

As mentioned earlier, in addition to diagonal rebars, a minimum quantity of reinforcement should be provided parallel as well as transverse to longitudinal axis of the beam (Paulay and Priestley 1992). This basketing reinforcement is meant to avoid spalling of concrete outside the diagonal core. Care should be taken in positioning of these diagonal bars so that they do not clash within the beam. With large quantity of reinforcement, constructability is an important consideration while detailing.

## 7.8 Walls with Openings

Openings are provided in shear walls for doors, windows, etc. Location of such openings should be decided with great care. Openings, when provided, should preferably have a regular pattern with uniform spacing and be such that they do not impede the efficient structural behaviour of a wall. Openings as shown in Fig. 7.18a permit proper stress flow around them and the designer can provide for ductile behaviour for dissipation of seismic energy. If openings are staggered in elevation (Fig. 7.18b), then large spaces should be left between them. With careful detailing and provision of additional reinforcement around openings, reasonably smooth flow of load can be achieved. When openings have only thin strips of wall between them, a *strut and tie model* may be used for the diagonal tension and compression fields to develop (Paulay and Priestley 1992). However, in such a case, it is difficult to avoid early damage during a seismic activity.

As per code, when openings are present, the shear strength should be checked at a plane passing through the openings. Moreover, additional reinforcement should be provided in walls along edges of opening and the area of such rebars should be equal that of the interrupted bars in both vertical and horizontal directions. Vertical bars

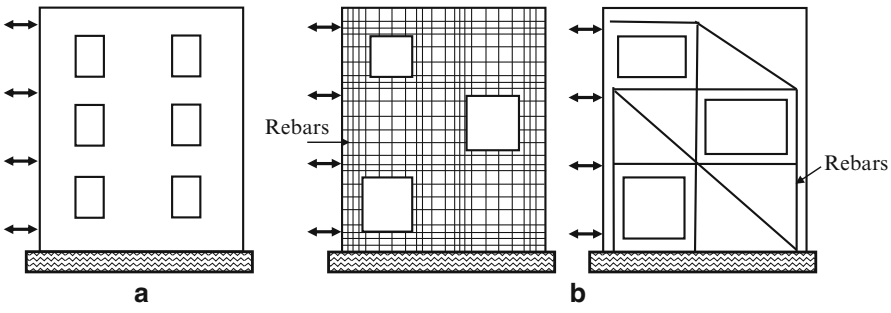


**Fig. 7.18** Openings in shear walls. (**a**) Regular openings. (**b**) Irregular openings

should run for the full storey height while horizontal bars should project beyond the openings by an amount equal to their development length in tension.

## 7.9 Illustrative Examples

***Ex 7.9.1*** The plan view at the base of a slender concrete shear wall is shown in Fig. 7.19a. It supports a factored (load factor 1.2) axial gravity load and moment and shear of 2,280 kN, 7100 kNm and 635 kN, respectively. Assume that the wall is to be provided with uniformly spaced rebars and the overstrength factor may be taken as 1.4. Assume that the entire shear force is to be resisted by the wall web only. Other details are as under:

$$f_y = 415\ \text{N/mm}^2;\ f_{ck} = 20\ \text{N/mm}^2;\ E_s = 2 \times 10^5 \text{N/mm}^2;\ \mu = 0.8$$

It is desired to:

(a) Ascertain whether boundary elements are required
(b) Design boundary elements, if they are required
(c) Design wall section for flexure
(d) Design wall for shear
(e) Design for sliding shear
(f) With capacity-based design check for diagonal tension

**Solution**

(a) *Need for Boundary Elements*

Area of wall section, $A = 5 \times 0.2 = 1.0\ \text{m}^2$. Modulus of section $Z = 0.833\ \text{m}^3$. Maximum compressive stress is

$$\frac{P_u}{A} + \frac{M_u}{Z} = \left[\frac{2,280 \times 10^3}{1 \times 10^6} + \frac{7,100 \times 10^6}{0.833 \times 10^9}\right] = 10.8\ N/\text{mm}^2 > 0.2 f_{ck}\ \left(= 4\ \text{N/mm}^2\right)$$

Hence, as per IS code 13920, boundary elements are required. Provide additional concrete elements at each end of the wall (Fig. 7.19b) of sizes as shown in Fig. 7.19c.

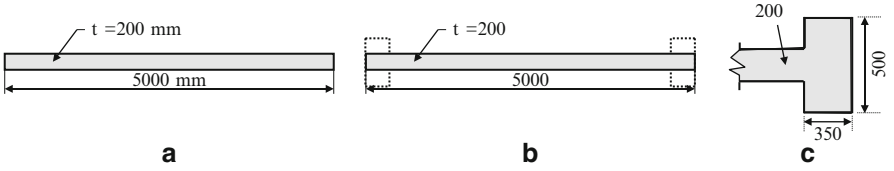


**Fig. 7.19** Shear wall with boundary elements. (**a**) Plain shear wall. (**b**) Boundary elements added. (**c**) Boundary element

(b) *Sharing of Load and Moment*

Area of web $= 4.3 \times 0.2 = 0.86\ \text{m}^2$.

Area of each boundary element $= 0.5 \times 0.35 = 0.175\ \text{m}^2$.

Area of wall with boundary elements $= 1.21\ \text{m}^2$.

Since the vertical gravity load adds to wall strength, the load factor to be considered is 0.8 on the unfactored gravity load.

Unfactored gravity load on wall $= 2{,}280/1.2 = 1{,}900$ kN.

Gravity load to be considered on wall with a load factor of 0.8 will be

$$= 1900 \times 0.8 = 1,520\ \text{kN}$$

Load shared by wall web $= 1{,}520 \times 0.86/1.21 = 1080.3$ kN.

Provide minimum reinforcement in wall of 0.25 % and substitute values in Eqs. 7.1.1, 7.1.2, 7.1.3, 7.1.4 and 7.1.5.

$$\varphi = \frac{0.87 \times 415 \times 0.25}{20 \times 100} = 0.045; \quad \lambda = \frac{1080.3 \times 10^3}{20 \times 200 \times 4300} = 0.0628$$

$$a = \frac{(0.045 + 0.0628)}{\{2(0.045) + 0.36\}} = 0.240; \quad \beta = \frac{0.87 \times 415}{0.0035 \times 2 \times 10^5} = 0.516;$$

$$a^* = \frac{1}{1 + 0.516} = 0.660$$

$a < a^*$, i.e. it is a tension failure. Hence,

$$\frac{M_u}{f_{ck} t_w L^2} = 0.045 \left[ \left\{ 1 + \frac{0.0628}{0.045} \right\} \{0.5 - (0.416 \times 0.24)\} - 0.24^2 \left\{ 0.168 + \frac{0.516^2}{3} \right\} \right]$$

$$= 0.0425$$

Moment supported by web:

$$M_{uw} = \left(0.0425 \times 20 \times 200 \times 4300^2\right) / 10^6 = 3143.3\ \text{kNm}$$

Moment to be supported by boundary elements $= 7100.0 - 3143.3 = 3956.7$ kNm

Axial load shared by each boundary element

$$= (1,520\text{–}1,080.3) / 2 = 219.85\ \text{kN}$$

(c) *Design of Boundary Elements*

Lever arm for boundary element to support the moment

$$= (5\text{–}0.35) = 4.650\ \text{m}$$

Axial load on boundary element due to moment
$$= \pm (3,956.7/4.65) = \pm 850.9 \text{ kN}$$

Maximum compressive force on boundary element = 219.85 + 850.9 = 1070.75 kN.

Minimum force on boundary element = 219.85−850.9 = −631.05 kN.

Minimum vertical reinforcement required in boundary element as per code is 0.8 %.

$$350 \times 500 \times 0.8/100 = 1,400 \text{ mm}^2.$$

Provide 8 φ 16 mm rebars, i.e. 1608 mm$^2$

$$\begin{aligned}\text{Compression capacity of boundary element} &= 0.4 f_{ck} A_c + \left(0.67 f_y – 0.4 f_{ck}\right) A_s \\ &= 10^{-3} \{0.4 \times 20 \times 350 \times 500\} + 1,608 \{(0.67 \times 415) \\ &\quad – (0.4 \times 20)\} \\ &= 1,834.2 \text{ kN} > 1,070.75 \text{kN}\end{aligned}$$

Tension capacity = $-10^{-3}(0.87 \times 415 \times 1{,}608) = -580.6$ kN < −631.05 kN.

Hence, reinforcement quantity needs to be increased.

Quantity of reinforcement required in a boundary element:

$$A_s = 631.05 \times 10^3 / (0.87 \times 415) = 1747.82 \text{ mm}^2$$

Increase reinforcement to 6 φ 16 mm plus 2 φ 20 mm rebars, i.e. 1835 mm$^2$ (i.e. 1.05 %).

Confining reinforcement in the boundary element is to be provided as per IS clause 7.4.8.

Consider φ 10 mm stirrups with a 30 mm cover.

Gross area of boundary element $A_g$ is 500 × 350 = 175,000 mm$^2$.

Core area of boundary element $A_k$ is 440 × 290 = 127,600 mm$^2$.

Ratio of above areas = 175,000/127,600 = 1.371.

Longer dimension of confining stirrups $h$ = 440/2 = 220 mm.

Spacing of stirrups not to exceed 350/4 = 87.5 mm.

Adopt stirrup spacing as 85 mm:

As per IS clause 7.4.8, stirrup diameter required
$$= 0.18 \times 85 \times 220 \times \frac{20}{415}\left[\frac{175,000}{127,600} - 1\right] = 60.26 \text{ mm}^2$$

Hence, provide φ 10 mm stirrups at 85 mm centres.

(d) *Design of Wall Section for Flexure*

As per IS 13920, vertical wall reinforcement can be in a single layer if the following two conditions are satisfied:

(a) Wall thickness does not exceed 200 mm.
(b) Factored shear stress does not exceed $0.25\sqrt{f_{ck}}$ i.e. $0.25\sqrt{20} = 1.12$ N/mm$^2$.

In the present case, with a factored shear stress of 0.923 N/mm$^2$ (refer para (e) below) and wall thickness of 200 mm, both the above conditions are satisfied. Hence, vertical minimum reinforcement in web of 0.25 % can be provided in a single layer:

$$\text{i.e. } (0.25 \times 200 \times 1,000)/100 = 500 \text{ mm}^2/\text{m}$$

Provide reinforcement in a single layer of φ 10 mm rebars at 150 mm centres, i.e. 523 mm$^2$/m.

(e) *Check Wall for Shear*

Factored shear force $= V_u = 635$ kN. Since only the wall web has to resist this shear,

Nominal shear stress $\tau_v = V_u/t_w\, d_w$=635,000/(200 × 0.8 × 4,300)=0.923 N/mm$^2$.

As per IS 456 (BIS 2000) code,

Permissible design shear stress $\tau_c = 0.36$ N/mm$^2$

Maximum permissible shear stress $\tau_{\max} = 2.8$ N/mm$^2$

$$\tau_c < \tau_v < \tau_{\max}$$

Hence, shear reinforcement has to be provided.

Shear resisted by concrete of the wall web $= 0.36(200 \times 0.8 \times 4300) \cdot 10^{-3}$ = 247.68 kN.

Shear to be resisted by reinforcement = 635−247.68 = 387.32 kN.

Provide minimum horizontal reinforcement of 0.25 %, i.e. same as vertical reinforcement.

This leads to 10 φ mm at 150 mm centres $Shear$ capacity

$$= \frac{\{0.87 \times 415 \times 78.54 \times (0.8 \times 4,300)\}}{150 \times 10^3} = 650.32 \text{ kN} > 387.32 \text{ kN}$$

Hence safe.

(f) *Check for Wall Against Sliding Shear*

Total shear inclusive of overstrength $V_\Omega \approx 635 \times 1.4 = 889$ kN.

Considering the web only, the total area of vertical reinforcement provided across the sliding surface = 78.54 × 4,300/150 = 2,251.5 mm$^2$.

Factored axial load supported by web = 2,280 × 0.86/1.21 = 1,620.5 kN.

From Eq. 7.5.1, shear that can be resisted, with reinforcement as provided, will be

$$V_j = \mu \{0.8P_u + 0.87 f_y A_v\} = 0.8 \{0.8\,(1,620.5) + (0.87 \times 415 \times 2,251.5)/10^3\} = 1,687.5 \text{ kN} > 889 \text{ kN}.$$

Hence safe.

(g) *Capacity-Based Design for Diagonal Tension*

Shear due to seismic effect inclusive of overstrength (from (f) above)

$$V_\Omega = 889 \text{ kN}$$

Nominal shear stress $\tau_v = V_\Omega / t_w\, d_w = 889{,}000/(200 \times 0.8 \times 4{,}300) = 1.292 \text{ N/mm}^2$.

In this case also, $\tau_c < \tau_v < \tau_{max}$.

Shear to be resisted by rebars $= 889 - 247.68 = 641.32$ kN.

Shear capacity provided (refer para (e) above) $= 650.32$ kN $> 641.32$ kN. Hence safe.

***Ex 7.9.2*** A squat wall of dimensions as shown in Fig. 7.20 carries a lateral factored uniformly distributed seismic shear of 675 kN at the top. The factored vertical load at its base is 150 kN. The other parameters are $f_{ck} = 20$ N/mm$^2$, inclined rebars have a yield strength of 415 N/mm$^2$, vertical and horizontal rebars in the web have a yield strength of 250 N/mm$^2$, and $E_s = 2 \times 10^5$ N/mm$^2$. Provisions of vertical, horizontal and inclined reinforcement are as shown in Fig. 7.20. Analyse the wall for flexure and diagonal tension with an overstrength factor $\varphi_o = 1.4$.

**Solution** From Fig. 7.20, the vertical reinforcement $= 2{,}714.34$ mm$^2$.

Vertical reinforcement coefficient $p = 2{,}714.34/(200 \times 5{,}000) = 0.002714$.

Utilising Eqs. 7.1.1, 7.1.2, 7.1.3, 7.1.4 and 7.1.5

$$\varphi = \frac{(0.87 \times 250 \times 0.002714)}{20} = 0.0295; \quad \lambda = \frac{150 \times 10^3}{20 \times 200 \times 5 \times 10^3} = 0.0075$$

$$a = \frac{0.0295 + 0.0075}{2(0.0295) + 0.36} = 0.0883$$

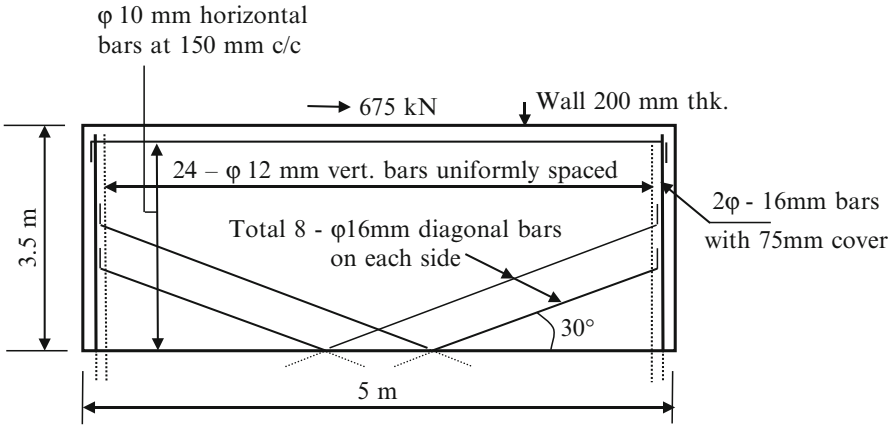


**Fig. 7.20** Squat wall

$$x_u = a.L = (0.0883 \times 5,000) = 441.5$$

$$\beta = \frac{0.87 \times 250}{0.0035 \times 2 \times 10^5} = 0.3107; \quad a^* = \frac{1}{1.3107} = 0.763$$

$a < a^*$ implies a tension failure case. Hence from Eq. 7.1.5,

$$\frac{M_u}{f_{ck}.t.L^2} = 0.0295\left[\left(1 + \frac{0.0075}{0.0295}\right)\{0.5 - (0.416 \times 0.0883)\} - 0.0883^2\left(0.168 + \frac{0.3107^2}{3}\right)\right] = 0.0171$$

$$M_u = \frac{(0.0171 \times 20 \times 200 \times 5^2 \times 10^6)}{10^6} = 1,710 \text{ kNm}$$

External moment = $675 \times 3.5 = 2362.5$ kNm.

Hence moment to be resisted by rebars in end zone of the wall
$= (2,362.5–1710) = 652.5$ kNm.

Assuming 75 mm effective cover, moment arm for rebars in end zone of the wall $\approx 4850$ mm.

Hence force to be resisted will be $= (652.5 \times 10^3)/4850 = 134.54$ kN.

Area of rebars required $= 134.54 \times 10^3/(0.87 \times 415) = 372.6$ mm$^2$.

Provide 2 nos 16 mm rebars (402.06 mm$^2$)

Moment capacity of rebars $= (0.87 \times 415 \times 402.06 \times 4,850)/10^6 = 704.04$ kNm

Total moment capacity $M_u = (1,710 + 704.04) = 2,414.04$ kNm.
$> 2,362.50$ kNm

Introducing values in Eqs. 7.6.1, 7.6.2 and 7.6.3,

Shear resistance by horizontal steel $= (78.54 \times 250 \times 3,500/150)\,10^{-3} = 458.15$ kN

Shear resistance by inclined bars $= (8 \times 201.06 \times 415 \times \text{Cos}30°)\,10^{-3} = 578.09$ kN

Total shear capacity provided $= 458.15 + 578.09 = 1,036.24$ kN

With an overstrength factor of 1.4 over the moment capacity value as provided, the shear capacity required at the base as per Eq. 7.6.3 will be:

Substituting values in Eq. 7.6.3,

$V_b = \frac{3.5}{5.0} \times 1.4 \times 675 = 661.5$ kN $< 1036.24$ kN. Hence safe.

# Chapter 8
# Substructure Design and Soil–Structure Coupling

**Abstract** In this chapter are described some of the key characteristics of seismic ground motion which can affect its behaviour during an earthquake. This, is turn, can affect the response of the superstructure. The need for providing tie beams under certain conditions is stressed. The analytical approach to analysis of retaining walls against lateral loads is explained using the M-O method. An approximate method for preliminary analysis of piles under lateral load is then described. If a structure is supported on soft soil of considerable thickness overlying rock, then the structure and soil interact with one another to influence the behaviour of both. Herein is described a simple practical method to assess the approximate impact of soil–structure coupling on the response of a SDOF structure as well as a MDOF structure where the fundamental mode predominates.

**Keywords** Soil–structure interaction • Subsoil parameters • Soil liquefaction • Open foundations • Piles • Retaining walls

## 8.1 Introduction

Normally, in dynamic analysis of a building under seismic conditions, base of the structure is considered to be fixed and subjected to the free field ground motion. Such ground motion is that which is not influenced by presence of the structure. This is applicable to rock formations because due to extremely high stiffness of rock, seismic wave motion therein is not constrained by the structure supported thereon. Hence, it can be termed as free field motion. However, if the structure is supported on soft soil of considerable thickness overlying the rock, then the structure and soil will interact with one another to influence the behaviour of both. This is termed as soil–structure coupling (or interaction) and it creates a new dynamic system.

Dynamic soil–structure coupling is a highly specialized interdisciplinary field, primarily involving geotechnical and structural engineering. Although the structural engineer will depend on inputs from a specialized geotechnical engineer, it is important that he is broadly familiar with the important facets of this subject and that is the purpose of this chapter.

As earthquake-induced ground motion traverses from its origin to the bedrock underlying a building; it undergoes modifications due to:



S. Manohar, S. Madhekar, *Seismic Design of RC Buildings*, Springer Transactions in Civil and Environmental Engineering, DOI 10.1007/978-81-322-2319-1_8

1. *Source effect*: During an earthquake, the ground vibrates in a complex manner and ensuing waves do not have uniform characteristics.
2. *Path effect*: Wave characteristics are modified during their transmission through variable topography from the source to bedrock at the building site.
3. *Local site effects*: Seismic waves are modified by properties of soil prevailing between bedrock and the building foundation. If this soil layer is very soft, then high frequency content of the motion may be filtered out and the foundation could experience long period motions.

Seismic ground motion at a building site is in the form of simultaneous multidirectional random pulses which cause translation in all three orthogonal directions as well as rocking about the horizontal axes and torsion about the vertical axis of the structure. In this chapter are described some of the key characteristics of seismic ground motion which affect a structure's response. Also described are the simple practical methods to assess the likely impact of soil–structure coupling (SSC) on the response of a SDOF as well as a MDOF structure. While doing so, it is assumed throughout that the soil is not liquefiable.

Considerable progress has been made in the last decade towards acquiring superior real-time ground motion data as well as in structural analysis techniques. This has lead to great strides being made in the understanding of soil characteristics and a structure's behaviour under dynamic loads as well as the effects of soil–structure coupling. In the near future, the present day techniques to analyse soil–structure interaction are likely to undergo major improvements through superior characterization of soil properties, and enhanced structural analysis capability supported by sophisticated software.

## 8.2 Parameters of Strong Ground Motion

Ground motion during an earthquake is composed of pulses which are random in frequency, amplitude and duration. Earthquake-induced ground motion can be captured in terms of displacement, acceleration or velocity. It can be synthesized into two orthogonal and one vertical component plus two rocking and one torsional component. The two horizontal components are normally considered for design, since they are often the predominant cause for building damage. With the limited dimensions of common building structures, the spatial variation in ground motion generally does not affect their seismic performance.

It has been shown that generally high-frequency components of seismic waves attenuate at a faster rate than their low-frequency components. Thus, the latter have a greater say in the performance of structures at large epicentral distances. Notwithstanding this broad observation, there is no accepted principle to relate the likely extent of building damage to an earthquake's signature.

The damage experienced by a building is a function of (1) peak ground acceleration, (2) duration of motion, (3) frequency content of ground motion, (4)

natural frequency of the structure, (5) characteristics of soil on which the structure is supported, (6) degree of structural and soil damping and (7) other factors. Under the circumstances, it is a specialized geotechnical exercise to select an appropriate earthquake signature for design. In spite of the highly sophisticated techniques available to predict the influence of all these factors on ground motion, the characteristics of ground motion as it may prevail at a given site can, at best, be an informed guess. Discussed in the following text are some of the important ground motion parameters in as far as they relate to interaction of the soil with a building structure.

### *8.2.1 Amplitude and Frequency Content*

As mentioned earlier, amplitude of ground motion can be expressed in terms of acceleration, velocity or displacement. Velocity may be a better indicator of the damage that a structure sensitive to motion in the intermediate frequency range (e.g. a tall building) is likely to experience (Kramer 2005). However, from a seismic response standpoint, ground acceleration determines the inertia forces that will be induced in a structure. For this reason, the peak horizontal ground acceleration (PGA) is the commonly used measure of ground motion.

The actual ground motion experienced at a particular site is a complex combination of vibrations of different frequencies. It can be decomposed into its harmonic components which provide amplitudes at different frequencies. Since energy is proportional to square of the amplitude, one can obtain a measure of energy content in a motion at different frequencies. Distribution of frequencies is referred to as *frequency content* of ground motion where some frequencies usually dominate.

Normally, ground motion contains a basket of frequencies and the motion amplitude varies randomly. For resonance to occur, the motion has to be within a narrow band of frequencies over a sustained period of time. Ground motion has a predominant period range of 0.4–2 s (FEMA 454 2006) with the higher end value pertaining to very soft ground and at the lower end to harder strata. Since this is within the period range of common building structures, there is the danger of response amplification even though resonance may not occur. If the dominant period of ground motion is very close to the natural period of the structure for some length of time, it can cause severe damage to the structure.

With increasing distance from the earthquake focus, the range of frequencies of a given earthquake gradually reduces to lower numbers because of preferential attenuation of higher frequencies. This means that a tall building (with its longer period) situated far from a fault can be damaged from distant earthquakes since high frequencies may be filtered out. Vertical components of ground motion, on the other hand, have a larger content of higher frequencies which will have a larger impact on low-rise structures.

### 8.2.2 *Effective Duration of Strong Motion*

An important constituent of ground motion, viz. its *duration*, is not reflected in the response spectrum. The damage potential of an earthquake is dependent not only on amplitude but also on duration of motion. A series of moderate acceleration pulses sustained over many cycles can prove to be more detrimental to a building than a single larger peak pulse (FEMA 454 2006). Firstly, for instance, under long duration shaking, a structure could fail under low cycle fatigue. Secondly, long duration of shaking can affect the extent of soil liquefaction which in turn will affect the likely magnitude of foundation settlement.

An accelerogram is generally composed of three segments – the build-up portion, followed by the strong motion and then the decay portion. There are many suggested definitions of duration of a seismic event – for instance, it could be the time between first and last peaks crossing a certain threshold level – but at present there is no unique definition of what constitutes duration. One that is popular is the time period over which the energy accumulates between 5 and 95 % of the total energy recorded, based on the square of acceleration history (Chen and Scawthorn 2003), i.e. $\int \left(\ddot{u}_t\right)^2 dt$. It is pointed out (Bommer and Martinez-Pereira 1999) that it may not be particularly useful to establish a single definition for duration of a strong motion, since the one that can be employed for hazard assessment may be less appropriate for assessment of building safety.

### 8.2.3 *Time History of Motion*

The chosen site-specific earthquake signature should at least represent the likely event in terms of its amplitude, frequency distribution and duration. However, there is considerable uncertainty in identifying these ground motion characteristics. For instance:

- Motions that appear reasonable in the time domain may not adequately reflect requirements in the frequency domain.
- Projected characteristics of ground motion at a particular site depend on filter function of the intervening media as well as on local site conditions. Both possess uncertain variability.
- Reasonable acceleration time history may produce unreasonable velocity and displacement profiles.
- Earthquake records with identical peaks can result in different building responses.
- Time histories in two orthogonal horizontal directions are normally not the same.

It has not been possible to establish a universally acceptable correlation between the form of an earthquakes time history and the degree of structural damage it

can cause. Hence, to assess the mean response of a structure, several time history records, which are scaled to a chosen peak acceleration, are generally used. This calls for time histories with similar durations and spectral properties, which are difficult to come by.

For this reason, synthetic (computer generated) time histories are used that will fit a predefined peak acceleration spectrum and time envelope. As a result, a family of site-specific earthquake time histories, based on an in-depth geological and seismological study, often need to be used. For such an analysis, the time step considered is important. It is recommended in literature that the time step should be $T/100$ where $T$ is the fundamental vibration period of the structure. Where there is a need to analyse conditions such as pounding, rocking and foundation uplift, this incremental time step may need to be even smaller.

## 8.3 Important Subsoil Parameters

The response of a building supported on compliant soil depends on characteristics of the soil intervening between building foundation and underlying bedrock. It plays a significant role in the magnitude of damage that an earthquake, of a particular signature, can cause. An important consideration in design is to obtain properties of soil such as stiffness, damping, density and others which affect dynamic soil–structure interaction. Of these properties, the first two play an important role in a structures' response and density in liquefaction potential.

In situ soils are commonly anisotropic and non-homogeneous. Their behaviour is non-linear and their properties can only be ascertained within a broad band because of problems in sampling, testing and interpretation of results. Field tests have the advantage that they do not require sampling which could alter the chemical and structural conditions of soil. There are many methods available to determine soil properties, each with their own advantages and limitations. Some of the important soil parameters that could affect seismic response of a building are outlined below.

### *8.3.1 Depth of Soil Overlay and Its Stratification*

Composition of the local soil and its characteristics have a profound influence on the response of a structure supported thereon. It is important to know the composition of each strata of subsoil up to bedrock. It has been shown that different modes of vibration are affected in differing manner when the strata are layered instead of being uniform. Layered soils can filter some or amplify other frequencies of incoming ground waves and thus the ground motion that reaches the foundation can be significantly different from that at bedrock level.

Depending on the change in ground motion caused by soil, the extent of damage in the superstructure could be different even for the same motion at bedrock. Many

characteristics of subsoil can be obtained through bore logs. The depth of bedrock can be conveniently determined through geophysical refraction surveys provided a low velocity layer does not lie below a high velocity one and the soil layers have sufficient thickness and they display detectable differences in velocities. The subsurface founding material can be broadly classified according to the shear wave velocity ($V_s$) passing through it, as indicated below (FEMA 450-1 2003):

- Hard rock: $V_s > 1{,}500$ m/s
- Rock: $760 < V_s \leq 1{,}500$ m/s
- Very dense soil or soft rock: $360 < V_s < 760$ m/ s
- Stiff soil: $180 < V_s < 360$ m/s

### 8.3.2 Dynamic Shear Modulus (G)

Secant shear modulus of soil is one of the most significant parameters affecting site response analysis. It is a measure of soil stiffness which is instrumental in modifying the natural frequency of the system. Soil shear modulus depends on strain amplitude, it being high at low strains. In the field, tests are conducted at low strain levels of the order of $10^{-5}$–$10^{-3}$ % (Dowrick 2009) compared with earthquake strains which range from $10^{-3}$ to $10^{-1}$ %. Hence measured values of $G$ need to be scaled down.

Shear wave velocity ($V_s$) is an important input to arrive at the soil shear modulus which is given by (Dowrick 2009) $G = \rho {V_s}^2$. In the field, $V_s$ can be determined by the up-hole or down-hole test in a borehole or by cross-hole technique using more than one borehole. Shear modulus can also be obtained in a laboratory through a cyclic triaxial test. In this test, the Young's modulus $E$ is obtained, which is converted to shear modulus through the relationship,

$$G = \frac{E}{2\,(1+\nu)} = \rho V_s^2 \tag{8.1.1}$$

### 8.3.3 Poisson's Ratio

This ratio is given by the equation,

$$\nu = \frac{V_p^2 - 2V_s^2}{2\left(V_p^2 - V_s^2\right)} \tag{8.1.2}$$

where

$V_p$: primary wave velocity (m/s)
$V_s$: shear wave velocity (m/s)

$\rho$ : mass density of soil (kg/m$^3$)
$\nu$ : Poisson's ratio
$G$: shear modulus (Pascal)
$E$: Young's modulus (Pascal)

In the absence of test data, Poisson's ratio may be taken as 0.3 for cohesionless soils and 0.4 for cohesive soils (Kameswararao 2011).

### *8.3.4 Particle Grain Size Distribution*

Distribution of grain size in a soil is related to its liquefaction potential. Also, it is one of the important parameters of soil that affects its response. Firstly, soils that are poorly graded are susceptible to loss of strength under cyclic loading and if soil grains are uniform but loose, they can collapse (Department of Defense, USA 1997). Secondly, the degree of clay fraction that is present in soil will determine the likely decrease in stiffness and strength of such soils under cyclic loads. It will, at the same time, also indicate the likely decrease in its tendency to liquefy.

### *8.3.5 Soil Damping*

This is an important parameter that affects response of the supported structure. Damping in soils is attributed to:

- Material damping: This is primarily due to hysteresis in the soil and leads to a decrease in vibration energy. It increases with the level of strain and decreases with confining pressure.
- Radiation damping: This causes energy dissipation through radiation of waves from the foundation and its effect is often ignored when the foundation rests on a shallow layer of soil on firm rock.

Material damping for small strains can be assessed in a laboratory by the resonant column test. A typical shear stress vs shear strain diagram that is the outcome from such a test is shown in Fig. 8.1. The critical material damping ratio, which is a measure of energy dissipated by the soil, is given by (Zhang et al. 2005):

$$\xi_{\text{soil}} = \frac{\Delta_1}{4\pi\Delta_2} \tag{8.1.3}$$

$\Delta_1$: area inside the hysteresis loop (energy dissipated in one cycle of loading)
$\Delta_2$: area of shaded triangle (maximum strain energy stored during the cycle)

Material and radiation damping are difficult to determine and any generalized data in this regard has to be used with circumspection.

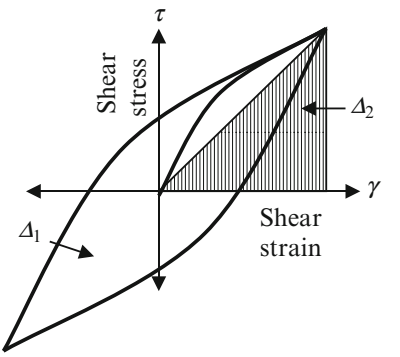


**Fig. 8.1** Hysteresis loop for a single cycle of loading

### *8.3.6 Relative Density*

This is a useful measure to determine the likely settlement of dry sand and potential for liquefaction of saturated cohesionless soils. SPT is a popular method for determining field density ($D_r$) from the equation,

$$D_r = \frac{e_{\max} - e}{e_{\max} - e_{\min}} \tag{8.1.4}$$

where $e_{\max}$ and $e_{\min}$ are values of maximum and minimum void ratios respectively and $e$ is the in situ void ratio.

For determining soil density, a Cone Penetration Test could also be used. It involves the steady penetration of a cone, of specified dimensions, into the ground. It is an inexpensive and quick test which will enable one to draw the continuous soil profile and thus detect depth of layers and seams. However, it is not possible to use this method in very stiff soils and gravels.

In the above discussions, it is assumed that the soil is a homogenous isotropic medium. However, in practice, the soil encountered is most likely to be layered. In such cases, other than for very important structures, the values of parameters $G$, $\rho$ and mass density are taken as the weighted average considering thicknesses of respective layers.

### *8.3.7 Water Depth*

Depth of water table can be conveniently measured in a borehole. This information is important since water table affects both shear modulus and damping of the soil. It also aids in determining liquefaction potential. If the soil is graded such that pore water can move freely in and out of the soil deposit, then the behaviour of such a layer is close to that of a partially saturated soil.

### *8.3.8 Soil Bearing Capacity*

Permissible increase in allowable pressure inclusive of seismic effects is laid down in IS 1893 (BIS 2002a). Common practice is to increase permissible bearing capacity by 33 % under seismic conditions, but it is suggested (Nagaraj et al. 2006) that such an increase should *not* be considered when:

- Soil is loose and is susceptible to liquefaction.
- When foundations are supported on soils composed of materials that weaken during seismic shaking such as sensitive and soft clays and organic soils subjected to plastic flow. In fact, in such cases, there could be a case for a reduction of bearing capacity under seismic conditions.

## 8.4 Soil Liquefaction

Liquefaction could lead to lateral spreading of soil and loss of bearing capacity which may cause the structure to tilt, settle or overturn. It can also induce differential settlements between foundations and create enhanced lateral pressures on retaining walls. Light structures can experience uplift. There have been many dramatic structural failures as a consequence of liquefaction of subsoil. The process of liquefaction, its causes and a method for its prediction are briefly discussed in the following text.

### *8.4.1 Causes of Liquefaction*

A soil deposit is an assemblage of its individual particles. The overlying weight is supported by these particles through contact forces between them. Shear strength of a cohesionless soil is directly proportional to the effective stress prevailing between sand particles. This effective stress is equal to the difference between downward overburden pressure and upward pore water pressure. During an earthquake, such a soil mass is shaken and the soil particles, over a wide range of relative densities (Idriss and Boulanger 2008), try to move into a denser configuration.

However, if there is not enough time for pore water to escape and it gets trapped inside the soil mass, then it prevents the particles from moving closer to each other. This reduces the contact forces between individual soil particles and these forces get transferred to pore water. With persistent oscillations, the magnitude of pore water pressure increases. When this upward pressure is equal to overburden pressure, the effective stress between soil grains is zero and the soil medium temporarily loses its strength to support the superstructure. This condition is known as liquefaction.

### 8.4.2 Determining Liquefaction Potential

Some of the governing factors that influence soil liquefaction are its grain size distribution, relative density, dynamic shear modulus and water table. Soils susceptible to potential liquefaction are saturated loose sands, silty sands, sandy silts, soils with low relative density and soils with low confining pressure. There are a variety of approaches available to access the potential for soil to liquefy. The most commonly used method is the Seed-Idriss simplified empirical procedure in which this susceptibility is measured as the ratio of cyclic resistance ratio (CRR) to cyclic stress ratio (CSR).

CRR represents the liquefaction resistance of in situ soil. For obtaining this value, Standard Penetration Test (SPT) results are commonly used where the blow counts are correlated with the cyclic resistance ratio. The CSR, which depends on peak horizontal ground acceleration, is evaluated using an empirical formula. Factor of safety $F_s$ against liquefaction is given by:

$$F_s = \text{CRR}/\text{CSR} \tag{8.2.1}$$

It is considered that liquefaction is likely if $F_s < 1.0$. It needs to be emphasised that determination of these values and their interpretation requires considerable experience and expertise. Also, even when the above ratio exceeds 1.0, liquefaction could still occur, such as when soil, below the layer under consideration, liquefies. Liquefaction usually is initiated at some depth below ground level and may then propagate downwards depending on the nature of soil, magnitude, duration of ground shaking, etc.

The subject of liquefaction is outside the scope of this book, and it is assumed that the subsoil is free from liquefaction. The issue is mentioned here for completeness and to create awareness among structural designers about how liquefaction potential can be assessed. Wherever liquefaction potential exists, adequate care should be exercised in structural design supported by expert geotechnical advice.

## 8.5 Open Foundations

A foundation is an important interface for transfer of loads from superstructure to the prevailing soil medium. Customarily, if depth below ground of an open foundation is less than its width, then it is termed as a shallow foundation. These foundations transmit vertical load to soil/rock by direct bearing. Lateral loads are resisted by friction at the foundation–soil interface plus lateral passive soil pressure acting against vertical face of the footing. Open foundations can be discrete pads, strip footings, combined footings, rafts etc.

Failure modes for which an engineer has to commonly design a shallow foundation are:

- Bearing capacity failure
- Permissible settlements
- Lateral sliding at soil–foundation interface
- Foundation strength

Soil behaviour varies from place to place and hence a detailed subsoil study, by a qualified and experienced geotechnical engineer, should be undertaken to define accurately the subsoil characteristics and bearing capacity. Foundations must be supported on undisturbed soil or well compacted engineered fill. A foundation has to be sized such that the maximum soil pressure due to vertical loads and moments is within allowable codal value under seismic conditions. However, it is often the case that permissible settlement controls the size of footing to adopt.

The frictional resistance at the base of footing should be able to provide adequate factor of safety against lateral shear. For this purpose, advantage may be taken of any lateral passive soil pressure, if it can be assured. Safety against sliding and overturning should be checked for the condition of minimum gravity load commensurate with maximum horizontal force. A foundation must be stable against the worst combination of overturning and uplift forces. Under seismic conditions, when dead loads and live loads as well as earth pressure are considered, the factor of safety against sliding and overturning (as per IS 1904) should be $>1.5$.

Foundations should be rigid and, to the extent possible, be of the same type and rest at one level for a given building. Structures that are supported partly on open foundations and partly on piles are vulnerable because of the inherent difference in both strength and stiffness between the two mediums. Since structures supported on open foundations are vulnerable to vertical ground motion and differential settlements; efforts should be made to get, as nearly as possible, uniform soil pressure under all footings so as to minimize this problem. In order to reduce the impact of likely differential movements, raft foundations are often resorted to.

At wall–foundation interface, confining reinforcement in boundary elements should extend full development length of the main reinforcement into the footing. It is argued that vertical reinforcement from the superstructure should extend full depth of the raft foundation. This would also be advantageous from constructability point of view. Foundations must satisfy *capacity design* requirements. The foundation of a ductile shear wall or frame should be designed to support overstrength capacity in moment and shear of the superstructure at its interface with the foundation (Paulay and Priestley 1992). The foundation should preferably remain elastic and soil pressure under the above conditions should be restricted such that any inelastic deformations are negligible. A foundation rotation can substantially alter the moment profile in ground storey columns.

The thorough design of a foundation is of paramount importance, since any damage to a foundation is often difficult to identify, cumbersome to access and extremely expensive to rectify. The design of open foundations is well understood and many software packages are available for undertaking their sophisticated analysis. Hence, only the aspects relevant to design under seismic conditions are mentioned here. The engineer has to make a judicious selection about the method of

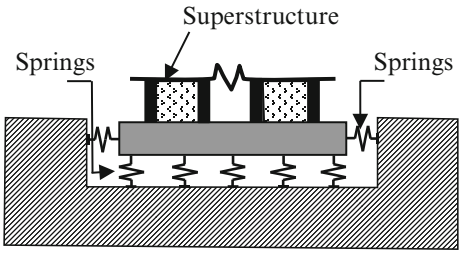


**Fig. 8.2** Raft foundation on springs

design to adopt so that it remains computationally viable but captures the important behavioural modes.

For analysis of raft foundations, the finite element method may be used or, alternatively, the simpler less precise approach of considering it as a plate resting on a series of springs may be adopted (Fig. 8.2). Settlement of each spring is assumed to be proportional to the force applied on it but independent of the stress applied or displacement at any other point. This approach was first proposed by Winkler in 1867 and this model has come to be known as a Winkler model.

The pressure displacement relationship of the spring will then be

$$q = k_s \delta \tag{8.3.1}$$

where

$q$ : bearing pressure (kN/m$^2$)
$k_s$: modulus of subgrade reaction (kN/m$^3$)
$\delta$ : soil settlement (m)

This method has the following principal limitations:

- A linear stress–strain behaviour is assumed. However, with the introduction of computer software packages, non-linear springs can also be introduced.
- Springs are not interdependent and there is no dispersion of load over increasing depth.
- There is an inherent assumption that a uniform soil underlying a uniformly loaded mat will settle uniformly which, in reality, is not the case. A foundation failure is depicted in Picture 8.1.

### *8.5.1 Tie Beams*

Isolated footings (not connected by a structural base slab) and pile caps should be tied together with the help of tie beams in two orthogonal directions. These ties should be at footing/cap level and not be tied to a column at any intermediate level as this can result in a short column. Tie beams should preferably be at the same

**Picture 8.1** Foundation distress

level, as per IS 4326 (BIS 2001) have a size of at least 200 mm × 200 mm with minimum reinforcement of 4–φ12 mm mild steel bars or 10 mm HYSD rebars.

These beams help the foundation system to work in unison by resisting differential foundation settlements through redistribution of column loads. They enhance foundation performance during seismic activity. Such beams are to be designed to resist a tensile as well as a compressive force not less than $A_h/4$ times the larger of the connected column or pile cap loads in addition to other computed forces. In practice, it is common to design tie beams for 5 % of the larger of the column or pile cap load.

Tie beams should be designed to withstand differential settlements between footings. Reinforcement in tie beams should be continuous and well anchored and splices should be for the full length required in tension. A grade slab may also be used as the connecting medium between footings provided it has substantial thickness and is appropriately designed and detailed. Tie beams in the form of a horizontal truss are seen in Picture 8.2.

**Picture 8.2** Foundation tie beams in form of a truss

## 8.6 Piles

Pile foundations are commonly adopted when a suitable foundation strata is not available within a reasonable depth. They assist in transferring loads through the unsuitable strata so as to support the load through end bearing at a lower level and/or skin friction with the soil. When a raft is supported on piles, there would be a reduction in its differential settlements and tilting. Also, if any pile in a group is slightly weak, the raft allows for redistribution of load among other piles in the group. Thus, it contributes to redundancy.

Vertical and lateral loads are carried to the soil through different mechanisms. Vertical loads are supported by skin friction and end bearing. Lateral loads are equilibrated by passive soil resistance mobilized around the pile.

### *8.6.1 Pile Loads*

Under seismic conditions (excluding liquefaction effects), piles are subjected to loads commonly termed as kinematic if induced by relative motion between pile

and the surrounding soil and inertial if caused by superstructure motion. Loads, which piles have to sustain, are:

***Vertical loads***:

(a) Gravity loads
(b) Vertical loads due to vertical inertia forces
(c) Axial forces due to seismic overturning moment

***Lateral loads***:

(d) Lateral shear at pile cap level due to horizontal seismic effect from the superstructure
(e) Kinematic forces because of movement of subsoil relative to the pile

Lateral loads induce lateral shear forces and moments in the piles. Lateral overturning moments on the superstructure could either enhance or diminish vertical loads. The latter could result in some piles being under tension.

### *8.6.2 Pile Design Criteria*

The design of piles for end bearing will be similar to that for vertical static loads. Against horizontal loads, the pile may be modelled as a vertical beam supported by a series of linear or non-linear horizontal springs. The design of a pile for axial and lateral loads should be based on the capacity design principle. A few limit states that could be adopted for the design of piles are:

(a) *Limit state of collapse*:

**Under This Condition:**

Pile shear stress should not exceed the permissible stress under lateral loads due to inertial or kinemaitc effects or their combination
Bending stresses should be within permissible limits
Piles should be safe against buckling due to vertical loads and loss of lateral confining pressure due to partial liquefaction
Soil around the pile shaft should not reach its ultimate capacity over a substantial portion of the pile length (Kameswararao 2011)

(b) *Limit state of serviceability*:

**Under This Condition:**

- Pile vertical settlement and lateral displacement should be within permissible values for the superstructure

### *8.6.3 Analysis of Laterally Loaded Piles*

Evaluation of dynamic response of a pile is a highly complex process which depends on inertial interaction between pile and superstructure, kinematic interaction between pile and ground, effects of pore water pressure, etc. This is further compounded because of multiple uncertainties regarding material non-linearity; variable soil properties; effects of piles being in a group, which increases their overall settlement and redistributes loads among them; and other factors.

A short pile will normally not bend but rotate and translate. Such piles are called *rigid* piles. Long and slender piles are termed *flexible* piles. There are a number of methods available to evaluate the response of pile foundations under lateral loads. Three-dimensional analysis techniques are also available for evaluating soil–pile interaction effects. These are outside the scope of this book. A pseudo-static design method, which is preferred because of its simplicity and which is known as the *p-y* method (proposed by Reese), for flexible piles is described below. In this method, kinematic interaction and effects of soil liquefaction are not accounted for.

#### 8.6.3.1 *p-y* Method

From among the various methods available, a popular method for analysis is to treat the pile as an elastic vertical beam supported laterally by a compliant foundation. The pile length is divided into small segments and each segment is laterally supported by elemental soil resistance which can be represented as a non-linear spring as shown in Fig. 8.3 for lateral load from the right. Shear transfer across soil layers is not considered.

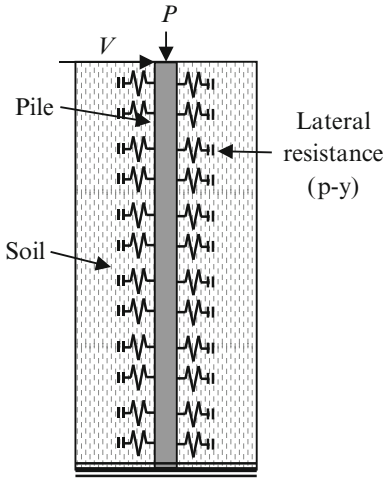


**Fig. 8.3** Pile supported by lateral springs

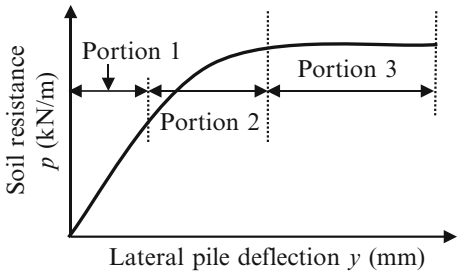


**Fig. 8.4** Typical *p-y* curve

The non-linear relationship between soil pressure and lateral displacement of a pile is termed as the *p-y* curve. Here *p* is the soil resistance pressure per unit length of pile and *y* is the pile lateral deflection. It is a two-dimensional soil–pile interaction. This curve, which is a back bone curve for elemental soil resistance, is a function of soil depth, nature of subsoil as well as stiffness and other properties of the pile. The ratio *p/y* at a given deflection is the soil secant stiffness at that deflection.

A typical *p-y* curve for cohesionless soil is shown in Fig. 8.4. Such curves generally have three portions – initially it is nearly a straight line implying that resistance is linearly proportional to pile displacement, followed by a portion where the soil resistance increases at a decreasing rate compared to pile deflection and finally a portion that depicts a plastic deformation of surrounding soil. The closeness with which the *p-y* curves represent true characteristics of existing soil will dictate the accuracy of analytical results.

As proposed by Hetenyi (Bull 2009), consider the free body diagram (Fig. 8.5) for an infinitely small pile element of length $dz$ at a soil depth $z$ subjected to an axial load, a moment and a shear force which are equilibrated by lateral soil resistance. It is assumed that the pile is straight, of uniform cross section, of homogeneous and isotropic material with the same modulus of elasticity in tension and compression. It is further assumed that loads lie in the $yz$ plane, that pile is symmetrical about $z$-axis and that pile deflection occurs only along $y$-axis (i.e. there is no out of plane deflection) and shear deflection is negligible. From moment equilibrium (Reese et al. 2006)

$$(M + dM) - M + P_z dy - V dz + p dz \frac{dz}{2} = 0 \tag{8.4.1}$$

In incremental form and ignoring second-order terms,

$$\frac{dM}{dz} + P_z \frac{dy}{dz} - V = 0 \tag{8.4.2}$$

Differentiating

$$\frac{d^2M}{dz^2} + P_z \frac{d^2y}{dz^2} - \frac{dV}{dz} = 0 \tag{8.4.3}$$

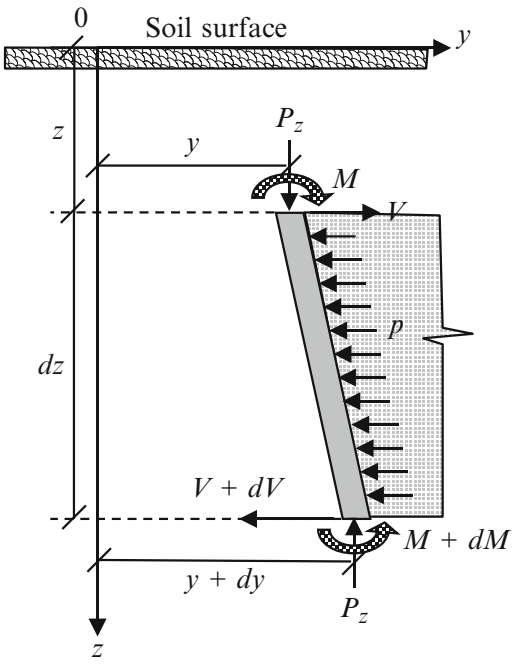


**Fig. 8.5** Pile element-free body diagram

Noting that

$$\frac{d^2M}{dz^2} = E_p I_p \frac{d^4y}{dz^4};\ \ \frac{dV}{dz} = k_s \text{ and } k_s = -E_s y \tag{8.4.4}$$

leads to

$$E_p I_p \frac{d^4y}{dz^4} + P_z \frac{d^2y}{dz^2} + E_s y = 0 \tag{8.4.5}$$

The moment and shear values are given by

$$M = E_p I_p \frac{d^2y}{dz^2};\quad \mathrm{V} = E_p I_p \frac{d^3y}{dz^3} + P_z \frac{dy}{dz} \tag{8.4.6}$$

where

$P_z$: vertical load (kN)
$p$ : soil resistance per unit length of pile (kN/m)
$E_p$: elastic modulus of pile material (kN/m$^2$)
$E_s$: horizontal soil modulus $= -p/y$
$I_p$ : moment of inertia of pile cross section with respect to the neutral axis (m$^4$)
$M$: pile moment (kNm)

$V$: pile shear (kN)
$k_s$: soil stiffness parameter per metre length of pile (kN/m)
$y$ : lateral deflection of pile or compression of soil (m)
$z$ : vertical distance along the pile (m)

The iterative and complex procedure for solving this equation makes it imperative to use an available computer software package wherein cohesive and cohesionless soils (under seismic conditions) can both be dealt with. To speed up the analysis process, the software replaces each non-linear *p-y* curve by a few linear portions. Accuracy of results depends, to a large extent, on the quality of data acquisition related to characteristics of subsoil at site.

Unit soil resistance $p$ depends on the soil characteristics. This in turn is a function of a passive pressure on the front of a pile, an active pressure from rear of the pile and soil friction along the pile surface (Kramer 1988). Clearly, the value of $p$ depends on many factors which are not amenable to easy quantification. Because of complexity of the problem, it is recommended that for important projects such data be based on instrumented field test results at site.

Lateral soil resistance can be modelled as a number of parallel springs, each with its own non-linear stiffness behaviour, i.e. its *p-y curve*. The given pile is analysed with specified loadings and the equations are solved for a selected value of the secant stiffness from the *p-y* curve. With the resulting pile deflections, an improved value of secant value is obtained. This is continued until convergence is obtained.

#### 8.6.3.2 Characteristic Load Method (CLM)

This method is the outcome of performing numerous non-linear *p-y* analyses for flexible piles (length $\geq 35$ pile diameters) with free as well as fixed-heads (Clarke and Duncan 2001) in clay and sand. The results were used to develop plots among dimensionless variables that would enable a designer to quickly arrive at lateral deflection at ground level and the maximum moment in a laterally loaded single pile as shown in Fig. 8.6. Variables are the lateral load and moment at ground level and pile lateral displacement at top. They are represented in a dimensionless format by dividing them by values of characteristic load, characteristic moment and pile diameter, respectively. The equations for determining characteristic values of lateral load and moment as given by Ruigrok (2010) are listed below:

*For cohesive soils*

$$V_c = 7.34D^2\left(E_p R_1\right)\left\{\frac{S_u}{E_p R_1}\right\}^{0.68} \tag{8.5.1}$$

$$M_c = 3.86D^3\left(E_p R_1\right)\left\{\frac{S_u}{E_p R_1}\right\}^{0.46} \tag{8.5.2}$$

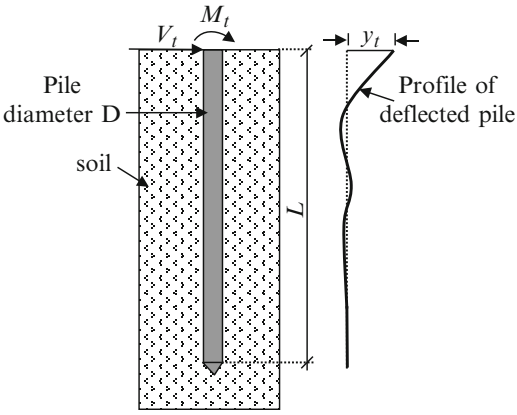


**Fig. 8.6** Pile with force and moment at ground level

*For cohesionless soils*

$$V_c = 1.57D^2\left(E_pR_1\right)\left\{\frac{\gamma' D\varphi' K_p}{E_pR_1}\right\}^{0.57} \tag{8.5.3}$$

$$M_c = 1.33D^3\left(E_pR_1\right)\left\{\frac{\gamma' D\varphi' K_p}{E_pR_1}\right\}^{0.4} \tag{8.5.4}$$

where

$D$ : pile diameter (m)
$E_p$ : pile modulus of elasticity (kN/m$^2$)
$I_p$ : moment of inertia of the pile (m$^4$)
$K_p$ : Rankine coefficient of passive earth pressure $= \tan^2\left(45 + \frac{\varphi'}{2}\right)$
$M_c$: characteristic moment (kNm)
$V_c$ : characteristic load (kN)
$R_1$ : moment of inertia ratio $= 64I_p/\pi D^4$
$S_u$ : undrained shear strength of clay (kN/m$^2$)
$\gamma'$ : effective unit weight of soil, which is total unit weight above ground water table and buoyant unit weight below ground water table (kN/m$^3$)
$\varphi'$ : effective stress friction angle of sand (degrees)

This method is based on the assumption that the pile is vertical, has a constant bending stiffness throughout its length and that the soil is uniform, i.e. its shear strength (as $S_u$ or $\varphi$) and unit weight are constant throughout the depth. The latter is a major limitation of this method. When soil properties vary with depth, as an approximation, they need to be replaced by an equivalent uniform soil profile based on averaging soil properties over a length of eight pile diameters from the top. Clarke and Duncan (2001) have stated that this is so because it is observed that within this length almost the entire lateral load is transferred from the pile to the soil.

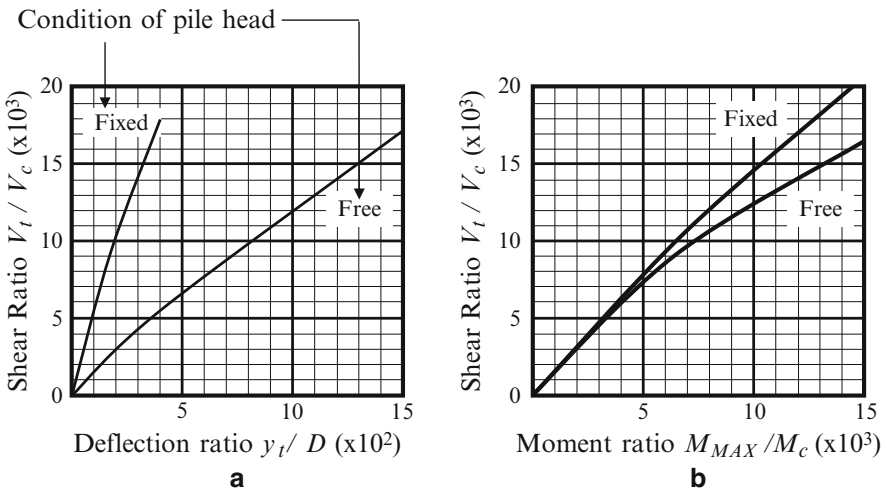


**Fig. 8.7** CLM procedure for non-dimensional relationships: (**a**) shear vs top displacement and (**b**) shear vs moment (Charts are only indicative)

Typical non-dimensional *indicative* relationship (for both fixed and free pile heads) between top shear ratio and top lateral deflection ratio is shown in Fig. 8.7a. Similarly, *indicative* relationship between top shear ratio and maximum moment ratio in the pile is depicted in Fig. 8.7b. Similar relationships are available in literature for a moment $M_t$ applied at the top of a pile. This is an approximate method which has the advantage that maximum moment and top deflection in a pile due to lateral shear at the top can be obtained directly without trial and error. The method may be used, while exercising caution and under the guidance of a geotechnical expert, only for an initial preliminary analysis of pile foundation. A typical evaluation of pile top displacement and maximum bending moment in a pile due to a lateral force ($V_t$) at the top is shown in *Ex* 8.9.1.

### *8.6.4 Pile Group Effect*

It is common to support a structure on a group of piles connected through a pile cap. The behaviour of a pile in a group is different from that of the same pile if it were isolated. This is because of many factors such as soil disturbance during installation of other piles, sequence of installation and interaction between piles of a group, which depends on pile spacing, their orientation, soil type, etc. As the leading pile deflects laterally, it relieves some of the stress on the soil behind it. This results in a lowering of soil resistance on the following pile and thus each pile will have a different *p-y* curve. This is termed as pile–soil–pile interaction or *shadowing effect*.

For piles spaced more than six pile diameters apart, the shadowing effect is reported to be negligible. However, in the case of closely spaced piles in a group, the resulting lateral pile deflections are larger. From among the two soil–pile interactions, viz. inertial and kinematic, it is seen from numerical investigations that kinematic interaction for pile groups is about the same as that for individual piles (Pecker 2007). For a comprehensive dynamic analysis of a pile group, a three-dimensional non-linear numerical analysis is required. Such a procedure is highly complex and computationally demanding.

A number of simplified methods have been proposed to analyse the response of laterally loaded pile groups, each with its own advantages and limitations of applicability. In one of the proposed methods, the pile grouping effect is accounted for by use of *p-multipliers*, i.e. the soil resistance $p$ in the $p$-$y$ curve is reduced by multiplying it with a factor which is $\leq 1.0$ (Basu et al. 2008). Based on the study of limited field and laboratory tests, values of these multipliers (which depend on pile spacing and their positions) are provided by Clarke and Duncan (2001).

### *8.6.5 Pile and Pile Cap Details*

Some other aspects to be considered during pile design are as follows:

- In the range where soil may liquefy, a pile should be designed for strength and detailed for ductility assuming loss of lateral soil support, i.e. it should be designed as an unsupported column over that region.
- Upper portion of a pile at its junction with the pile cap should be confined to allow for a plastic hinge formation.
- Ductile detailing should be followed in the zone where there is an abrupt and marked change in stiffness of soil strata.
- Lateral rigidity of a pile is important and so opting for fewer larger diameter piles as compared to a large number of smaller diameter piles seems to be the better solution.
- It is recommended that a pile be embedded in the pile cap so that there is a direct transfer of shear and the pile reinforcement should be fully anchored in the pile cap.
- Raker piles should be avoided as they have been found to be particularly susceptible to failure in earthquakes and they induce large forces on pile caps.
- Pile should be well embedded in soil below the liquefiable depth.
- Piles should be reinforced along their whole length even if this is not a requirement through analysis.
- Pile caps should be checked for shear and punching.
- It is advisable to provide an enveloping band of rebars that will tie pile heads together in a pile cap as shown in Fig. 8.8.

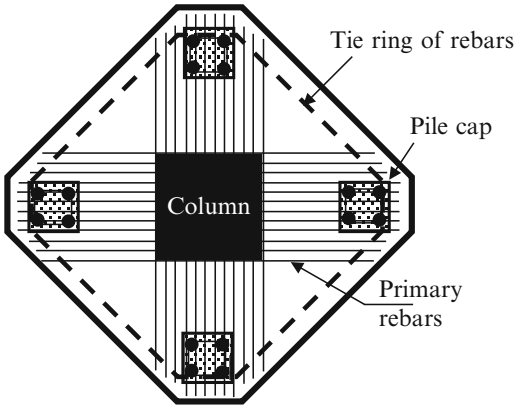


**Fig. 8.8** Typical pile cap detail

## 8.7 Retaining Walls

There are various structural forms for retaining walls such as gravity walls, rigid walls, cantilever walls, braced walls, anchored walls, etc. The evaluation of dynamic response of even the simplest type of retaining wall is highly complex as it depends on a number of factors such as variable input motion, response of both backfill and wall, which are not amenable to precise quantification, and so on. Besides, there is the uncertain variability of composition of retained soil and also the dynamic interaction that takes place between retaining wall and retained soil. Hence, design is normally based on theories which involve simplifying assumptions.

Earth retaining walls at a building project fall broadly under two categories:

1. Yielding walls – such as cantilever walls which may deform sufficiently either by translation, rotation or through flexibility, so as to develop a state of active soil pressure
2. Non-yielding walls – such as basement walls which are often transversely held in position with floor slabs

Given below are the simple methods for an approximate analysis of both the above types of walls.

### *8.7.1 Yielding Walls (Cantilever Walls)*

Cantilever walls generally fall under this category. Several researchers have proposed methods for computing dynamic earth thrust on such walls. Pioneering work in this area has been done by Okabe (1926) and Mononobe & Matsuo (1929) who proposed a pseudo-static method (Nimbalkar 2006) which is popularly known as the M-O method. It assumes the following:

- The retaining wall is of the yielding type such that active earth pressure can generate during an earthquake.
- The backfill is made up of dry cohesionless soil.
- Seismic acceleration is uniform throughout the soil mass.
- Liquefaction does not occur.

The procedure, which is based on Coulomb's theory of static pressure for cohesionless soils, is the often used method of analysis primarily because of its simplicity. As per this method, for linear backfill surfaces without surcharge, the pseudo-static pressure is evaluated as given in the following text.

#### 8.7.1.1 Active Thrust

An earthquake increases the active lateral earth pressure on retaining walls. In the M-O method of analysis, a dry cohesionless backfill material is assumed and the force diagram is as shown in Fig. 8.9. The total active thrust per unit width of wall (Dowrick 2009; Kramer 2005) is given by

$$P_{AE} = \frac{1}{2} K_{AE} \gamma H^2 (1 - k_v) \tag{8.6.1}$$

in which the total dynamic active earth pressure coefficient ($K_{AE}$) is

$$K_{AE} = \frac{\cos^2(\varphi - \theta - \psi)}{\cos\ \psi \cos^2\theta\ \cos(\delta + \theta + \psi)\left[1 + \sqrt{\frac{\sin\ (\delta+\varphi)\sin(\varphi-\beta-\psi)}{\cos(\delta+\theta+\psi)\ \cos(\beta-\theta)}}\right]^2} \tag{8.6.2}$$

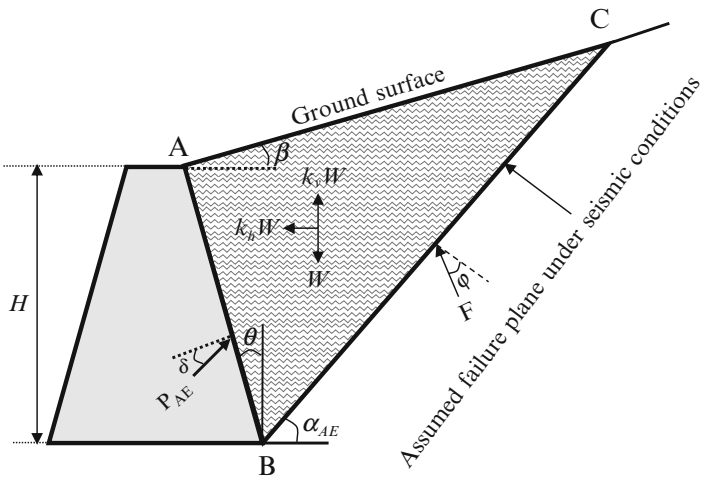


**Fig. 8.9** M-O method - Seismic active earth pressure

where

$$\psi : \text{arc tan}\,[k_h/(1-k_v)] \tag{8.6.3}$$

$P_{AE}$: maximum dynamic active earth thrust per unit wall width (N/m)
$\varphi$ : angle of internal friction of soil (degrees)
$\theta$ : slope of earth retaining face of wall relative to the vertical (degrees)
$\delta$ : angle of internal friction between wall and soil (degrees)
$\beta$ : slope of backfill top surface (degrees)
$\gamma$ : unit weight of retained soil (kN/m$^3$)
$H$ : backfill height (m)
$k_h$ : pseudo-static horizontal acceleration/g, at base of wall
$k_v$ : pseudo-static vertical acceleration/g, at base of wall
W : weight of retained wedge of material (kN)

While in the M-O method it is implied that the thrust would act at $H/3$ from the base, experimental evidence suggests (Kramer 2005) that the thrust acts at a higher elevation. To account for this, in an approximate way, Kramer points out that the total active thrust may be considered as composed of two components:

1. A static earth pressure component $P_A$ (utilizing static earth pressure coefficient $K_A$), as given by Coulomb's equation for static pressure on retaining walls. This component is known to act at $H/3$ from the base of the wall.
2. A dynamic incremental component $\Delta P_{AE}$, as suggested by Seed and Whitman (utilizing earth pressure coefficient $K_{AE}$), that is assumed to act at $0.6H$ from the base

Thus, the total thrust

$$P_{AE} = P_A + \Delta P_{AE} \tag{8.6.4}$$

It follows that value of base moment will be given by

$$P_A\,(H/3) + \Delta P_{AE}(0.6H) \tag{8.6.5}$$

The equations for static earth pressure coefficient ($K_A$) and earth thrust ($P_A$) are same as above for $K_{AE}$ and $P_{AE}$, respectively, but with $\psi = 0$ and $k_v = k_h = 0$. The procedure to obtain active thrust and base moment is illustrated through *Ex* 8.9.2.

#### 8.7.1.2 Passive Thrust

The maximum earth pressure on a wall generally occurs when the wall has translated or rotated towards the retained earth. Total passive resistance by the M-O method (Fig. 8.10) is given by (Kramer 2005)

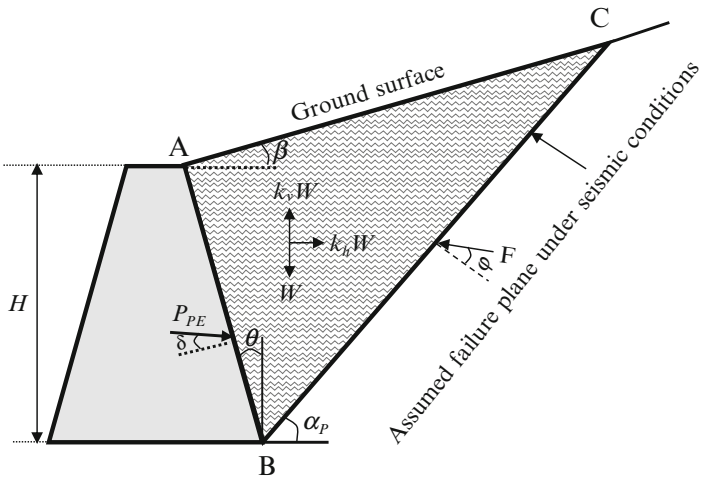


**Fig. 8.10** M-O method - Seismic passive earth pressure

$$P_{PE} = \frac{1}{2} K_{PE} \gamma H^2 (1 - k_v) \tag{8.7.1}$$

where passive earth pressure coefficient ($K_{PE}$) is

$$K_{\mathrm{PE}} = \frac{\cos^2(\varphi + \theta - \psi)}{\cos\ \psi\ \cos^2\theta\ \cos(\delta - \theta + \psi)\left[1 - \sqrt{\frac{\sin(\delta+\varphi)\ \sin(\varphi+\beta-\psi)}{\cos(\delta-\theta+\psi)\ \cos(\beta-\theta)}}\right]^2} \tag{8.7.2}$$

Kramer has pointed out that this total passive thrust can also be divided (as in Sect. 8.7.1.1) into two components, viz. static ($P_P$) and dynamic ($\Delta P_{PE}$). Thus,

$$P_{PE} = P_P + \Delta P_{PE} \tag{8.7.3}$$

Here again the equations to compute $K_P$ and $P_P$ are identical to those for $K_{PE}$ and $P_{PE}$ above but with $\psi = 0$ and $k_v = k_h = 0$. This static component is known to act at $H/3$ from the base. The dynamic component $\Delta P_{PE}$ reduces the total passive resistance, since it acts in opposite direction to the static component. The above seismic coefficients can vary over the wall height due to factors such as frequency characteristics of input ground motions, stiffness contrast between backfill and foundation soils, wall slope, etc. However, because of uncertainties in quantifying the effect of such factors, $k_h$ is assumed to be applicable uniformly to the soil over the entire wall height.

#### 8.7.1.3 Effect of Water Table

Often drains are provided in retaining walls, which prevent water build-up behind a wall. However, this is not possible for walls in water front areas. Presence of water in the backfill will alter the wall thrust. For low permeability soils with restrained pore water conditions, which is often the case ($k \leq 10^{-3}$ cm/s), Kramer (2005) has stated that the total active thrust on the wall can be obtained by modifying the M-O method. The active thrust on the wall will be the sum of:

1. Active thrust from buoyant soil which can be computed using Eq. 8.6.1 but replacing $\gamma$ and $\psi$ with $\gamma'$ and $\psi'$, respectively, where

$$\gamma' = \gamma_{\mathrm{b}}\,(1 - r_u) \quad \text{and} \quad \psi' = \text{arc}\ \tan\left[\frac{\gamma_{\mathrm{sat}} k_h}{\gamma'\,(1 - k_v)}\right] \tag{8.8.1}$$

   and
2. An equivalent fluid thrust of

$$P_w = \frac{1}{2}\gamma_{\mathrm{eq}} H^2 \mathrm{N/m} \tag{8.8.2}$$

   where

$$\gamma_{\mathrm{eq}} = \gamma_{\mathrm{w}} + r_{\mathrm{u}}\gamma_{\mathrm{b}} \tag{8.8.3}$$

If the soil is partially submerged for a height $\lambda H$ from the base, then according to Kramer, the lateral thrust may be calculated for an average unit weight given by

$$\overline{\gamma} = \lambda^2 \gamma_{\mathrm{sat}} + \left(1 - \lambda^2\right)\gamma_{\mathrm{d}}$$

$\lambda$ : coefficient defining height of water table above base ($\lambda < 1$)
$\gamma_{\mathrm{b}}$ : buoyant weight of soil (N/m$^3$)
$\gamma_{\mathrm{sat}}$: saturated weight of soil (N/m$^3$)
$\gamma_{\mathrm{d}}$ : dry unit weight of soil (N/m$^3$)
$\gamma_{\mathrm{w}}$ : density of water (N/m$^3$)
$r_{\mathrm{u}}$ : pore pressure ratio, i.e. pore pressure divided by the effective confining pressure

This procedure is demonstrated through *Ex* 8.9.3.

Further, in order to minimize hydrostatic pressure build-up, the backfill should be granular, free of clay, with drainage provided at bottom and an impervious clay layer being provided at top.

#### 8.7.1.4 Effect of Soil Cohesion

Analytical expressions are available to predict total active pressure on walls retaining $c$-$\varphi$ soil (Kumar and Sharma 2010). It is observed that cohesion has a

tendency to reduce the earth pressure on the wall. However, it is difficult to include this reduction in design practice because of uncertainty regarding the degree of cohesion present in backfill material with mixed c-φ conditions. At the same time, it is suggested that clay backfills should be avoided as they are susceptible to swelling which can enhance lateral pressure unpredictably (Jalla 1999).

### *8.7.2 Non-yielding Walls (Basement Walls)*

Tall buildings usually have subterranean levels to provide accommodation for parking of vehicles and to locate other facilities. The surrounding walls may be constructed partially or fully below ground level and form a strong box like structure (Fig. 8.11). These walls support dynamic forces transmitted from the superstructure as well as lateral pressure from retained subsoil. Basement walls can spread the impact of overturning forces over a large region and thereby enhance rotational resistance.

Due to restraint at its top, the wall behaves as a rigid wall and the lateral earth pressure approaches that predicted by elastic theory (Wood 1973). This pressure is substantially greater than that predicted by the M-O method. As a result, the elastic method appears more appropriate. For low-frequency input motions, in which many practical problems lie, Wood showed that dynamic amplification was negligible. Hence, in such cases, the pressure can be obtained from utilizing the elastic solution. In other cases, the incremental dynamic force and moment (above those predicted by static theory) for smooth walls are given by (Kramer 2005)

$$\Delta P_{eq} = \gamma H^2 k_h F_p \quad \text{and} \quad \Delta M_{eq} = \gamma H^3 k_h F_m \tag{8.9.1}$$

and this thrust acts at a height above the base given by

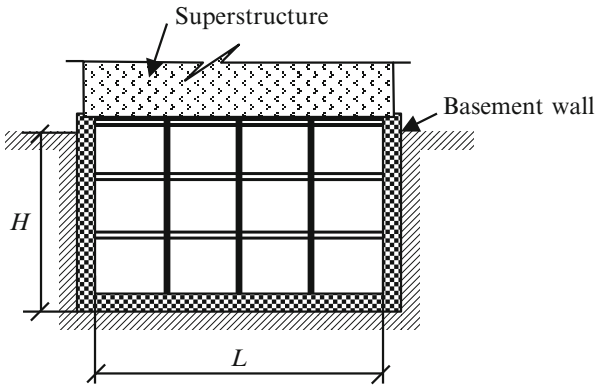


**Fig. 8.11** Basement structure

**Table 8.1** Dimensionless thrust ($F_p$) and moment ($F_m$) factors

| $L/H$ | $F_p$ | $F_m$ |
|---|---|---|
| 0 | 0.00 | 0.00 |
| 1 | 0.45 | 0.23 |
| 2 | 0.72 | 0.40 |
| 3 | 0.87 | 0.49 |
| 4 | 0.96 | 0.54 |
| 5 | 1.00 | 0.56 |
| 6 | 1.02 | 0.57 |
| 7 | 1.03 | 0.58 |
| 8 | 1.04 | 0.59 |
| 9 | 1.05 | 0.59 |

Extract from Wood (1973)

$$h_{eq} = \Delta M_{eq} / \Delta P_{eq} \tag{8.9.2}$$

where

$\Delta P_{eq}$ : dynamic force (N/m)
$\Delta M_{eq}$: dynamic base moment (Nm/m)
$\gamma$ : unit weight of soil (N/m$^3$)
$H$ : wall and backfill height (m)
$k_h$ : pseudo-static horizontal acceleration/g, at base of wall
$F_p$ : dimensionless dynamic thrust factor
$F_m$ : dimensionless dynamic moment factor

Wood (1973) has provided charts for variation of $F_p$ and $F_m$ as a function of the $L/H$ ratio and Poisson's ratio ($\nu$). Representative values for $\nu = 0.4$ interpolated from these charts are presented in Table 8.1 for information.

If a wall is designed as a non-yielding wall, then it must be ensured that the top restraining slab is in position prior to backfilling. Such walls are often designed as pinned at top and bottom and so would be reinforced on basement side as against backfill side for cantilever walls. In general, retaining walls need to be also checked for serviceability and ultimate limit states using the static at rest pressure which may control the design.

## 8.8 Soil–Structure Coupling (SSC)

The seismic response of a structure at a particular location depends on many factors such as follows:

- Characteristics of ground motion at source.
- Filter function of intervening media from source to the site, i.e. effects of wave attenuation, etc.

- Modifications to input motion due to nature and extent of soil overburden on the underlying rock. Soil layers in the overburden can filter some or amplify other frequencies of incoming ground waves. Thus the ground motion that reaches the foundation can be significantly different from that at bedrock level.
- Modified mode shapes and vibration periods because of SSC.
- Possible response amplification when vibration period of the structure is close to that of the input ground motion modified by local soil conditions.
- A significant portion of vibration energy may be dissipated through material and radiation damping of the soil supporting medium.

SSC is a process wherein the structure and its supporting soil medium interact with one another to influence the behaviour of both. For example, when a rigid foundation rests on a soft soil medium, then it will influence the free field ground motion. At the same time, deformation of ground will affect the response of the structure. SSC normally leads to:

- An increase in natural period of the structure
- Increased damping
- An increase in lateral displacements of the structure

The degree of these increases depends, among other factors, on mass of the structure, on stiffness of the soil and that of the structure and natural period of vibration of the structure. It is common to assume the input motion at base of a building structure to be same as the free field motion, i.e. the effect of SSC is commonly ignored. This is probably because it is often a valid assumption plus the usual presumption that such effects are beneficial as they lengthen the period of vibration and enhance damping. However, it is reported (Mylonakis and Gazetas 2000) that such effects can, in particular circumstances, be detrimental to the structure.

### *8.8.1 Dynamics of Soil–Structure Coupling*

Normally, in dynamic analysis the base is assumed as fixed, which can be considered as realistic only if the building is supported on solid rock or when stiffness of subsoil is very high in comparison with that of the superstructure. Conditions under which the impact of SSC should be allowed for in design can at best be described in a general way as:

- For structures where P-$\triangle$ effect can play a significant role
- Where the foundations are massive and deep
- For tall slender structures
- Where the supporting soil layer is both very soft (average shear wave velocity $<$100 m/s) and of considerable depth
- In cases where the supporting piles pass through alternating very stiff and very soft soil layers

Dynamic SSC can be distinguished in two forms, viz. kinematic, which is due to difference in stiffness between soil and structure, and inertial, which is due to mass of the structure. These are discussed in the following text.

#### 8.8.1.1 Kinematic Interaction

Due to an earthquake, the soil undergoes motion. When such movements are not influenced by presence of any structure, they are known as free field motions. A rigid foundation does not mimic the free field motion and there is a slip at the soil–foundation interface. As a result, the input motion gets modified and this is known as kinematic interaction.

The actual motion input into the foundation depends on its geometry and its relative stiffness with respect to the soil. This is a complex phenomenon with no simple solution to evaluate its effect. Tall buildings often have massive multi-level deep basements which form a box. In such cases, the building will be excited by motion of the basement (PEERC 2010) rather than that of the free field soil. However, for normal building structures, it is common to consider the input as the free field motion unless the structure is massive or is very important.

#### 8.8.1.2 Inertial Interaction

The mass of a structure induces inertia forces and causes the super structure to vibrate. In doing so, it transmits inertial forces, in the form of base shear and moment, to the soil. If the supporting soil is compliant, then dynamic interactions, in the form of displacements and rotations, occur at the base level and these influence final response of the structure. This is termed as inertial interaction. It is this form of interaction which will be examined further. While the soil adjacent to the foundation vibrates, some quantity of energy from soil is lost in moving the soil mass.

### *8.8.2 Evaluating Effect of Soil–Structure Coupling*

It is common to design structures on the fundamental assumption that the base is fixed and that ground motion experienced by its base is the same as free field ground motion at base level. For structures supported on soft soil, the base motion experienced by a structure is generally different from the free field motion as it could include:

- Possible sliding and rocking motion of the flexible medium
- Dissipation of vibration energy through the soil in the form of material damping and radiation damping

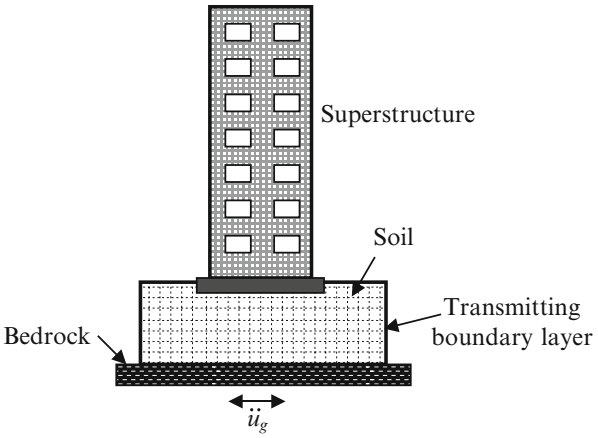


**Fig. 8.12** Direct approach

- Effects of foundation stiffness
- Extent of foundation embedment in the supporting medium

There are various methods available to evaluate the impact of SSC. Each has its own merits and demerits. The two general approaches (Stewart et al. 1998) for a soil–structure analysis are categorized as direct approach and substructure approach. All methods suffer from a basic problem of uncertainties associated with the dynamic properties to adopt for soil. In the discussion in the following section, the effect of foundation embedment is not considered.

#### 8.8.2.1 Direct Approach

In this approach, the soil (in the near field) and the structure together with its foundation are modelled and analysed as a single system (Fig. 8.12). Normally, FEM may be used for this purpose. Herein, the properties of the embedded footings as well as variation in properties of soil layers can be accounted for. However, to incorporate effect of damping, there is a need to incorporate absorbing/transmitting boundary elements so that the total energy is not trapped inside the model. This permits simulation of seismic energy radiating away from problem domain. In this approach, the model size becomes very large and the approach is computationally expensive. If there is a change, in say the superstructure, the entire analysis would have to be repeated.

#### 8.8.2.2 Substructure Approach

In this approach, the soil and structure (Fig. 8.13a) are modelled separately. The structure is idealized through a finite element grid and the base shear and moment

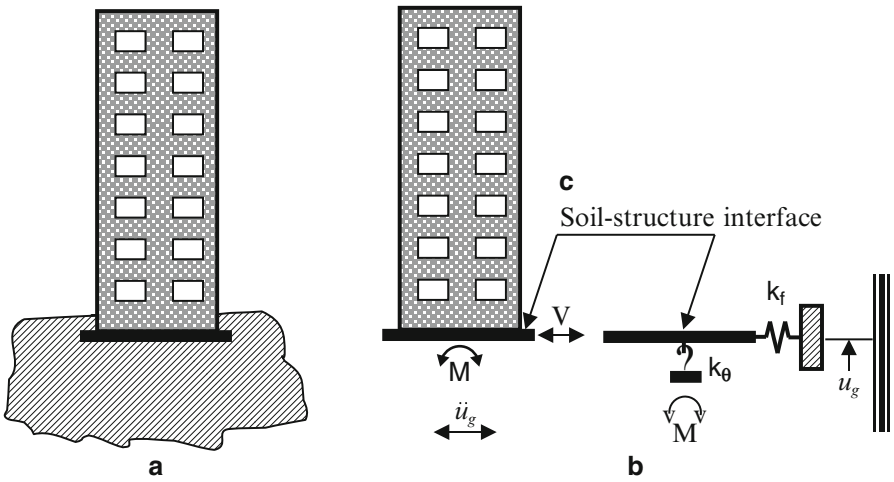


**Fig. 8.13** Substructure approach (**a**) Shear vs top displacement, (**b**) Shear vs Moment

are obtained (Fig. 8.13b). Next, the soil is discretized with the help of Winkler springs which can model horizontal, rocking and other impedance functions of the soil and dashpots may be used for viscous damping (Fig. 8.13c). The two models are connected by imposing compatibility conditions along the foundation and soil interface.

Both the above methods involve extensive complex modelling and analysis and are treated as being outside the scope of this book. The method described in the following text is a simplified approach which can give a reasonable insight into the effect of SSC for buildings where the primary response is from the first mode.

### 8.8.2.3 Simplified Method for a SDOF System

Consider a simple system (Fig. 8.14) which represents a SDOF system with mass $m$ and height of the structure $h$. The system has three degrees of freedom:

- Horizontal displacement of mass $m$, i.e. $(u_s + u_f)$
- Horizontal displacement of the foundation $u_f$, relative to the ground
- Rotation of foundation $\theta$

The system is subjected to a free field ground horizontal displacement $u_g$ and acceleration $\ddot{u}_g$ at a frequency $\omega$. Under this ground motion, the system displaces bodily by an amount $u_g$ along with the ground. Further, the foundation displaces horizontally by an amount $u_f$ relative to the ground and rotates by an angle $\theta$. The latter causes the superstructure mass $m$ to displace by $h\theta$ as shown in Fig. 8.15. The other parameters are:

$u_s$: elastic horizontal displacement of mass $m$ as a fixed base structure
$k_s$: lateral elastic stiffness of the fixed base structure

**Fig. 8.14** SDOF system

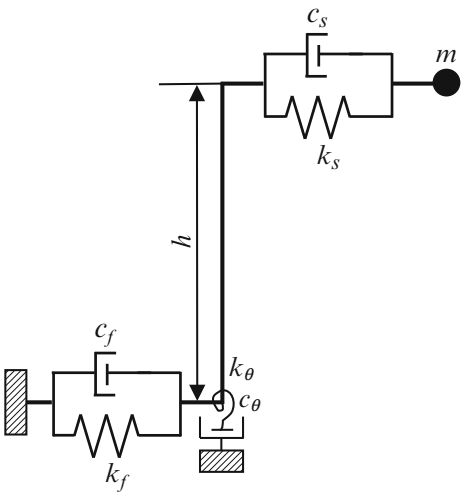


**Fig. 8.15** Displacement of a SDOF system

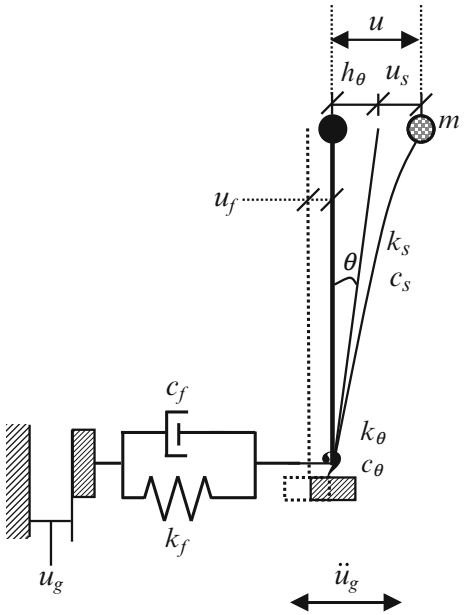


$k_f$ : lateral stiffness of the foundation against horizontal motion
$k_\theta$ : rotational stiffness of the foundation
$\xi_f$ : ratio of viscous radiation damping in the horizontal direction
$c_s$, $c_f$, $c_\theta$: damping coefficients for corresponding motions

Impedance functions ($k_f$, $k_\theta$) are complex-valued and frequency-dependent. Hence, for a simple formulation like the present one, their values at the predominant frequency of the soil–structure system are selected. The equations of motion in the

elastic range for this soil–structure system, in coupled horizontal translation and base rotation modes, considering (1) lateral motion of mass $m$, (2) lateral displacement of the foundation $u_f$ and (3) base rotation $\theta$, can be written, respectively, as (Stewart and Fenves 1998):

$$m\left(\ddot{u}_f + h\ddot{\theta} + \ddot{u}_s\right) + c_s\dot{u}_s + k_s u_s = -m\ddot{u}_g \tag{8.10.1}$$

$$m\left(\ddot{u}_f + h\ddot{\theta} + \ddot{u}_s\right) + m_f\ddot{u}_f + c_f\dot{u}_f + k_f u_f = -\left(m + m_f\right)\ddot{u}_g \tag{8.10.2}$$

$$mh\left(\ddot{u}_f + h\ddot{\theta} + \ddot{u}_s\right) + I\ddot{\theta} + c_\theta\dot{\theta} + k_\theta\theta = -mh\ddot{u}_g \tag{8.10.3}$$

Following approximations are introduced:

(i) $\ddot{u} = -\omega^2 u$
(ii) Material damping is neglected
(iii) Foundation mass ($m_f$) and the centroidal moment of inertia ($I$) of the top mass are neglected (Rodriguez and Montes 2000)
(iv) For a harmonic excitation it can be readily shown that, ignoring second-order terms in $\xi$, $\dot{u} = i\omega u$

Noting from Sect. 3.4.2, Sect. 3.4.3 and (iv) above that $k = m\omega^2$, $c = 2m\xi\omega$ and $\dot{u} = i\omega u$, respectively, it follows that

$$c_s\dot{u}_s = \frac{2k_s\xi_s}{\omega}\left(i\omega u_s\right) = 2i\xi_s k_s u_s$$

Substituting these approximations (Wolf 1985) into Eqs. 8.10.1, 8.10.2, and 8.10.3 above,

$$-m\omega^2\left(u_f + h\theta + u_s\right) + \ k_s\left(1 + 2i\xi_s\right)u_s = m\omega^2 u_g \tag{8.10.4}$$

$$-m\omega^2\left(u_f + h\theta + u_s\right) + k_f\left(1 + 2i\xi_f\right)u_f = m\omega^2 u_g \tag{8.10.5}$$

$$-m\omega^2 h\left(u_f + h\theta + u_s\right) + k_\theta\left(1 + 2i\xi_\theta\right)\theta = mh\omega^2 u_g \tag{8.10.6}$$

Introducing uncoupled circular natural frequencies due to (1) oscillations of the superstructure, (2) lateral motion of the foundation and (3) rocking oscillations of the base, the following identities can be written down:

$$\omega_s = \sqrt{k_s/m}; \omega_f = \sqrt{k_f/m} \text{ and } \omega_\theta = \sqrt{k_\theta/mh^2} \tag{8.10.7}$$

Eliminating $u_f$ and $h\theta$ from Eqs. 8.10.4– 8.10.6 leads to

$$u_f = \frac{\omega_s^2}{\omega_f^2}.\frac{(1+2i\xi_s)}{(1+2i\xi_f)}u_s \quad \text{and} \quad h\theta = \frac{\omega_s^2}{\omega_\theta^2}.\frac{(1+2i\xi_s)}{(1+2i\xi_\theta)}u_s \tag{8.10.8}$$

Introducing these values into Eq. 8.10.4,

$$\left[1+2i\xi_s - \frac{\omega^2}{\omega_s^2} - \frac{\omega^2}{\omega_f^2}\frac{(1+2i\xi_s)}{(1+2i\xi_f)} - \frac{\omega^2}{\omega_\theta^2}\frac{(1+2i\xi_s)}{(1+2i\xi_\theta)}\right]u_s = \frac{\omega^2}{\omega_s^2}u_g \tag{8.10.9}$$

**Equivalent SDOF System**

Consider an equivalent fixed base oscillator with stiffness $\tilde{k}$ and damping coefficient $\tilde{c}$, with its characteristic frequency $\tilde{\omega}$ such that the same mass $m$ will have the same structural displacement $u_s$ as that of the of the coupled system when excited by an acceleration $\tilde{u}_g$ at a frequency $\omega$. The equation of motion of such a SDOF system can be written down as

$$m\ddot{u}_s + \tilde{c}\dot{u}_s + \tilde{k}u_s = -m\ddot{\tilde{u}}_g \tag{8.11.1}$$

Substituting $\tilde{k} = m\tilde{\omega}^2$, and $\tilde{c}\dot{u}_s = 2\tilde{k}\tilde{\xi}/\tilde{\omega} = 2m\tilde{\omega}^2\tilde{\xi}iu_s$ (Pecker 2007) into Eq. 8.11.1,

$$\left(1+2i\tilde{\xi} - \frac{\omega^2}{\tilde{\omega}^2}\right)u_s = \frac{\omega^2}{\tilde{\omega}^2}\tilde{u}_g \tag{8.11.2}$$

For undamped free vibrations, $\xi_s = \xi_f = \xi_\theta = \tilde{\xi} = 0$ and $\ddot{u}_g = 0$.

Introducing the above values in Eq. 8.10.9 and for this equation to be satisfied, setting the coefficient of $u_s$ equal to zero,

$$\left[-\frac{1}{\omega_s^2} - \frac{1}{\omega_f^2} - \frac{1}{\omega_\theta^2} + \frac{1}{\omega^2}\right] = 0 \tag{8.11.3}$$

Similarly from Eq. 8.11.2,

$$\left[-\frac{\omega^2}{\tilde{\omega}^2} + 1\right]u_s = 0 \tag{8.11.4}$$

For the above equation to be satisfied, again the coefficient of $u_s$ has to be set equal to zero, resulting in

$$\omega = \tilde{\omega} \tag{8.11.5}$$

Substituting from Eq. 8.11.5 into Eq. 8.11.3,

$$\frac{1}{\tilde{\omega}^2} = \frac{1}{\omega_s^2} + \frac{1}{\omega_f^2} + \frac{1}{\omega_\theta^2} \tag{8.11.6}$$

Substituting values from Eq. 8.10.7,

$$\frac{1}{\tilde{\omega}^2} = \frac{1}{\omega_s^2}\left[1 + \frac{k_s}{k_f} + \frac{h^2 k_s}{k_\theta}\right] \tag{8.11.7}$$

Hence, period of the equivalent SDOF system is,

$$\tilde{T} = T_s\sqrt{1 + k_s\left[\frac{1}{k_f} + \frac{h^2}{k_\theta}\right]} \tag{8.11.8}$$

This demonstrates that period of the equivalent system with SSI is always larger than that of the fixed base structure. $\tilde{T}/T_s$ is referred to as period lengthening ratio.

**Equivalent Damping**

There is a change in the amount of damping because of energy dissipation through soil radiation and material damping. Wolf (1985) has pointed out that "with hysteritic damping the dissipated energy (which is independent of the frequency of excitation) is proportional to the product of damping ratio and strain energy". By equating the dissipated energy of the structure and the soil in the horizontal and rocking modes to that of the equivalent SDOF system, the equivalent damping ratio can be obtained.

For the SDOF oscillator, the deformation strain energies ($E$) due to a lateral force $F$ applied at a height $h$ above the base are (Betbeder-Matibet 2008)

$$\text{For horizontal displacement of structure} \quad E_s = \frac{1}{2}k_s u_s^2 = \frac{1}{2}\frac{F^2}{k_s} \tag{8.12.1}$$

$$\text{For rotational displacement} \quad E_\theta = \frac{1}{2}k_\theta \theta^2 = \frac{1}{2}\frac{F^2 h^2}{k_\theta} \tag{8.12.2}$$

$$\text{For lateral foundation motion} \quad E_f = \frac{1}{2}k_f u_f^2 = \frac{1}{2}\frac{F^2}{k_f} \tag{8.12.3}$$

By multiplying the strain energy in each mode with the corresponding damping ratio and summing up, the total dissipated energy of the coupled system will be

$$E = \frac{F^2}{2}\left[\frac{\xi_s}{k_s} + \frac{\xi_f}{k_f} + \frac{\xi_\theta h^2}{k_\theta}\right] \tag{8.12.4}$$

For the equivalent SDOF oscillator, the strain energy will be

$$\tilde{E} = \frac{\tilde{\xi}}{2}\tilde{k}\tilde{u}_s^2 = \frac{\tilde{\xi}}{2}\frac{F^2}{\tilde{k}} \tag{8.12.5}$$

With $\tilde{k} = m\tilde{\omega}^2$ and utilizing the expression for $\tilde{\omega}$ from Eq. 8.11.7,

$$\tilde{E} = \frac{\tilde{\xi}F^2}{2}\left[\frac{1}{k_s} + \frac{1}{k_f} + \frac{h^2}{k_\theta}\right] \tag{8.12.6}$$

Equating the dissipated energies in Eqs. 8.12.4 and 8.12.6, the equivalent damping for the combined system is

$$\tilde{\xi} = \left[\frac{\xi_s}{k_s} + \frac{\xi_f}{k_f} + \frac{\xi_\theta h^2}{k_\theta}\right] \Big/ \left[\frac{1}{k_s} + \frac{1}{k_f} + \frac{h^2}{k_\theta}\right] \tag{8.12.7}$$

The lateral force is then determined using the acceleration response spectrum for a period $\tilde{T}$ and damping value $\tilde{\xi}$. From the above, it will be observed that effect of SSC is generally to:

- Decrease frequency of vibration from $\omega_s \; to \; \tilde{\omega}$
- Enhance damping ratio from that of a fixed base structure $\xi \; to \; \tilde{\xi}$
- Decrease amplitude of input motion from $u_g \; to \; \tilde{u}_g$

#### 8.8.2.4 Simplified Method for a MDOF System

The method described earlier can be conveniently used to ascertain the approximate effect of SSC on the response of a MDOF system where the first mode response is predominant. The MDOF system vibrating in the first mode is replaced by an equivalent SDOF system with a mass equal to that of the first mode as given by Eq. 4.15.6. Thus, the SDOF system will have a lumped mass equivalent to the modal mass for the first mode of the MDOF system. The height $h_1$ of the equivalent SDOF oscillator is obtained from Eq. 4.16.1 specialized for the first mode, i.e.

$$h_1 = \frac{\sum_{j=1}^{N} m_{j1}\varphi_{j1}h_j}{\sum_{j=1}^{N} m_{j1}\varphi_{j1}} \tag{8.13.1}$$

where

$m_{j1}$: seismic mass at node $j$ in the first mode
$\varphi_{j1}$: displacement amplitude of the first mode at node $j$

$h_j$: height of node $j$ above the base
$h_1$: height of mass of the equivalent oscillator above the base

Rest of the analysis is identical to that explained earlier for a SDOF system. From Eq. 8.11.8, the vibration period of the oscillator equivalent to the first mode of the MDOF system will be given by:

$$\tilde{T}_1 = T_1 \sqrt{1 + \tilde{k}_1 \left[ \frac{1}{k_f} + \frac{h_1^2}{k_\theta} \right]} \tag{8.13.2}$$

where

$$\tilde{k}_1 = 4\pi^2 \left( \frac{M_1}{T_1^2} \right) \tag{8.13.3}$$

and $M_1$ and $T_1$ are modal mass and period of the fundamental mode of the MDOF system, respectively.

Once the vibration period of the equivalent SDOF system $\tilde{T}_1$ is obtained, the horizontal acceleration can be read from codal stipulations which will provide the modified first mode base shear $\tilde{V}_1$ using the modified damping value $\tilde{\xi}$. ASCE 7-05 (ASCE 2005) places a restriction that $\tilde{V}_1$ shall in no case be $<0.7\,V_1$ where $V_1$ is the first mode base shear for the fixed base MDOF structure.

Steps involved in the analysis process to determine the approximate effect of SSC for a MDOF system are listed below:

1. After a detailed geotechnical investigation, obtain soil parameters $k_f$ and $k_\theta$.
2. Using the LDP modal analysis technique, undertake an eigenvalue analysis which will provide values of frequencies $\omega_i$, time periods $T_i$ and mode shapes $\varphi_{ji}$.
3. For each mode, determine modal masses $M_i$, modal floor masses ($m_{ji}$) and modal participation factors $P_i$.
4. From codal design response spectrum, read off acceleration coefficient $S_{ai}/g$ corresponding to each modal time period $T_i$.
5. Next, determine horizontal seismic coefficient $A_{hi}$ followed by lateral storey forces $Q_{ji}$ and base shears $V_i$.
6. With values of $Q_{j1}$ for the first mode, determine the base moment $M_{b1}$ for this mode which will be given by $M_{b1} = \sum Q_{j1} h_j$
7. Determine floor displacements $u_{ji}$ for each mode based on storey shear forces $Q_{ji}$ and the stiffness matrix.
8. For the oscillator equivalent to first mode of the MDOF system, evaluate equivalent height $h_1$ from Eq 4.16.1 for $i = 1$.
9. For the equivalent oscillator with SSC, determine stiffness $\tilde{k}$ from Eq. 8.13.3, and first mode time period ($\tilde{T}_1$) using Eq. 8.13.2.

10. For the time period $\tilde{T}_1$ read off the acceleration coefficient Sa/g from the response spectrum and then arrive at acceleration coefficient $\tilde{A}_{h1}$ for 5 % damping.
11. Calculate equivalent damping $\left(\tilde{\xi}_1\right)$ utilizing Eq. 8.12.7.
12. Modify value of $\tilde{A}_{h1}$ in step 10 for the increased stiffness damping $\left(\tilde{\xi}_1\right)$ due to SSC taking values from IS 1893.
13. Obtain base shear of the oscillator equivalent to the first mode of vibration of the MDOF structure by the equation

$$\tilde{V}_1 = \tilde{A}_{h1}\, M_1\, g \tag{8.13.5}$$

14. Check that $\tilde{V}_1 > 0.7V_1$. If not, the value $\tilde{V}_1$ needs to be enhanced accordingly.
15. Obtain total base shear for the MDOF structure with SSC by SRSS method. First mode base shear being taken as $\tilde{V}_1$ and values for other modes being included in the summation without any modification for SSC.
16. The modified lateral deflection at floor $j$ in the fundamental mode "1" taking SSC into account (i.e. $\tilde{u}_{j1}$) is then obtained (ASCE 2005) as

$$\tilde{u}_{j1} = \frac{\tilde{V}_1}{V_1}\left[\frac{M_{b1}h_j}{k_\theta} + u_{j1}\right] \tag{8.13.6}$$

where

$M_{b1}$: overturning base moment for the fundamental mode of a fixed base structure using the unmodified modal floor forces determined in step 5
$h_j$ : height of storey $j$ above the base
$u_{j1}$ : lateral deflection of floor $j$ for the fundamental mode as for the fixed base structure using the unmodified modal base shear $V_1$ as obtained in step 7

17. This deflection in step 16 is to be combined by SRSS method with deflections for higher modes obtained in step 7. These are to be included without modification for SSC.

The process of evaluating base shear including SSC by the simplified method is explained through *Ex* 8.9.4. There are other extensions to this method to deal with higher mode responses, each with its own advantages and limitations. Modelling for SSC is expected to witness major improvements as a result of growing capability to model soil characteristics and with increasing computing power.

## 8.9 Illustrative Examples

***Ex 8.9.1*** A 400 mm dia., M40 concrete flexible pile in dry cohesionless soil ($\varphi' = 32°$) is subjected to a lateral shear force at its fixed head of 95 kN at top (i.e. ground level). Soil density is 1,950 kg/m$^3$. Determine the horizontal pile

displacement at the top and maximum bending moment in the pile using the CLM procedure. For the purpose of this example, utilize the *indicative* Fig. 8.7a, b.

Data: $D = 400$ mm, $f_{ck} = 40$ N/mm$^2$, $\varphi' = 32°$, $\gamma' = 1{,}950$ kg/m$^3$, $V_t = 95$ kN

**Solution** From IS 456, modulus of elasticity of pile $E_p = 5{,}000\sqrt{40} = 3.162 \times 10^4$ N/mm$^2$

From nomenclature for Eq. 8.5.4,

$$R_1 = 1.0 \text{ and } K_p = \tan^2\left(45° + 16°\right) = 3.255$$

Substituting values in Eqs. 8.5.3 and 8.5.4,

$$\frac{\gamma' D \varphi' K_p}{E_p R_1} = \frac{(1950 \times 9.81) \times 0.4 \times 32 \times 3.255}{3.162 \times 10^4 \times 10^6} = 2.5206 \times 10^{-5}$$

$$V_c = 1.57 \times 0.4^2 \times 3.162 \times 10^{10}\left(2.5206 \times 10^{-5}\right)^{0.57}/10^3 = 1.9 \times 10^4 \text{ kN}$$

$$M_c = 1.33 \times 0.4^3 \times 3.162 \times 10^{10}\left(2.5206 \times 10^{-5}\right)^{0.4}/10^3 = 3.895 \times 10^4 \text{ kNm}$$

$$V_t / V_c = 95/1.9 \times 10^4 = 0.005$$

From Fig. 8.7a for a pile with a fixed head, $y_t/D = 0.01$.

Hence lateral deflection at the top of pile $= 0.01 \times 400 = 4$ mm.

From Fig. 8.7b, $M_{max}/M_c = 0.0032$.

Hence maximum bending moment in the pile $= 0.0032 \times 3.895 \times 10^4 =$ 124.6 kNm.

***Ex 8.9.2*** A 5.5 m high yielding wall with a vertical back retains a cohesionless fill level with its top. Using the M-O method, compute the active earth pressures on wall and moment at the base of the wall under seismic conditions. Assume mass density of soil $\rho = 1{,}700$ kg /m$^3$, $\varphi = 35°$, $\delta = 15°$, $k_h = 0.15$, $k_v = 0.1$.

**Solution**

***Active earth pressure***

From the given data,

$$\gamma = (1{,}700 \times 9.81)/1{,}000 = 16.677 \text{ kN/m}^3$$

From Eq. 8.6.3, $\psi = \tan^{-1}[0.15/(1 - 0.1)] = 9.46^0$

For a vertical faced wall with level backfill $\theta = \beta = 0$.

Introducing the above values in Eqs. 8.6.2 and 8.6.1,

$$K_{AE} = \frac{\cos^2(35° - 9.46°)}{\cos\ 9.46° \cos(15° + 9.46°)\left[1 + \sqrt{\frac{\sin(15°+35°)\sin(35°-9.46°)}{\cos(15°+9.46°)}}\right]^2} = 0.353$$

$$P_{AE} = \frac{1}{2}(0.353)(16.677)\ \left(5.5^2\right)(1 - 0.1) = 80.14\ \text{kN/m}$$

The static component is obtained by introducing $\psi = 0°$ in Eq. 8.6.2 and $k_v = 0$ in Eq. 8.6.1.

Thus, static component of active pressure on the wall will be obtained as follows:

$$K_A = \frac{\cos^2(35°)}{\cos\ 15°\left[1 + \sqrt{\frac{\sin(15°+35°)\sin(35°)}{\cos(15°)}}\right]^2} = 0.248$$

and

$$P_A = \frac{1}{2}(0.248)(16.677)\left(5.5^2\right) = 62.56\ \text{kN/m}$$

Hence the dynamic component $\Delta P_A = P_{AE} - P_A = 17.58$ kN/m.

***Base moment***

From Eq. 8.6.5, the base moment is given by

$$\begin{aligned} M &= P_A(H/3) + \Delta P_A(0.6H) = 62.56(5.5)/3 + (17.58)(0.6 \times 5.5) \\ &= 172.7\ \text{kNm/m} \end{aligned}$$

***Ex 8.9.3*** In *Ex* 8.9.2 evaluate the active pressure on the wall if the backfill, which has a specific gravity $G_s$ of 2.65, is fully saturated and the pore pressure ratio $r_u = 0.45$.

The buoyant weight $\gamma_b = \gamma\left[\frac{G_s - 1}{G_s}\right] = 16.677 \times 0.6226 = 10.384\ \text{kN/m}^3$

From Eqs. 8.8.1, 8.8.2, and 8.8.3,

$$\gamma' = \gamma_b(1 - r_u) = 10.384(1 - 0.45) = 5.71\ \text{kN/m}^3$$

$$\gamma_{\text{sat}} = (\gamma_b + \gamma_w) = (10.384 + 9.81) = 20.194\ \text{kN/m}^3$$

$$\psi' = \tan^{-1}\left[\frac{20.194 \times 0.15}{(10.384)(1 - 0.45)(1 - 0.1)}\right] = 30.51°$$

Then dynamic active earth pressure coefficient is

$$K_{AE} = \frac{\cos^2(35^\circ - 31.5^\circ)}{\cos(30.51^\circ)\cos(15^\circ + 30.51^\circ)\left[1 + \sqrt{\frac{\sin(15^\circ+35^\circ)\sin(35^\circ-30.51^\circ)}{\cos(15^\circ+30.51^\circ)}}\right]^2} = 0.985$$

$$P_{AE} = \frac{1}{2}(0.985)(5.71)\left(5.5^2\right)(1 - 0.1) = 76.56\,\text{kN/m}$$

$$\gamma_{\text{eq}} = (\gamma_w + r_u.\gamma_b) = \left[\left(9.81 + (0.45 \times 10.384)\right] = 14.483\ \text{kN/m}^3\right.$$

$$P_w = \frac{1}{2}\gamma_{\text{eq}}H^2 = \frac{1}{2}(14.483)(5.5)^2 = 219.06\ \text{kN/m}$$

Total thrust $= P_{AE} + P_w = 295.62$ kN/m

***Ex 8.9.4*** For a MDOF frame of dimensions with mass and stiffness parameters as shown in Fig. 8.16, the following data is provided:

$m = 120{,}000$ kg, $k = 5{,}500$ kN/m; seismic zone IV, importance factor = 1, response reduction factor 5, damping $\xi_s = 5$ %. Soil parameters are $k_f = 225{,}000$ kN/m, $k_\theta = 1{,}800{,}000$ kNm/radian; damping $\xi_f = 10$ %; $\xi_\theta = 15$ %

Calculate the base shear and lateral displacement of the roof, taking soil structure coupling into account.

**Solution**

(a) *Fixed based MDOF system*

To commence, consider the fixed based structure shown in Fig. 8.16 and supported on soft soil as per given data

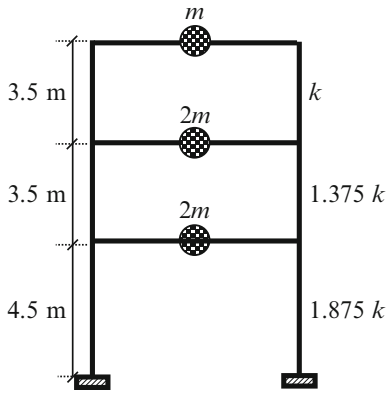


**Fig. 8.16** MDOF system

**Table 8.2** Evaluation of base shear

| Mode | $T$ (s) | $S_a/g$ | $A_h$ | Mass (kg) | $V$ (kN) |
|---|---|---|---|---|---|
| 1 | 2.000 | 0.835 | 0.02004 | 528,640 | 103.926 |
| 2 | 0.811 | 2.059 | 0.04944 | 53,137 | 25.773 |
| 3 | 0.614 | 2.500 | 0.06000 | 18,223 | 10.726 |

1. *Base shear:*

The mass and stiffness matrices are:

$$\boldsymbol{M} = m\begin{pmatrix} 2 & 0 & 0 \\ 0 & 2 & 0 \\ 0 & 0 & 1 \end{pmatrix} \text{ and } \boldsymbol{K} = k\begin{pmatrix} 3.250 & -1.375 & 0 \\ -1.375 & 2.375 & -1 \\ 0 & -1 & 1 \end{pmatrix} \tag{8.16.1}$$

Solving the eigen problem, the three frequencies and periods are as follows:

$\omega_1 = 3.140$ rad/s, $\omega_2 = 7.746$ rad/s, $\omega_3 = 10.241$ rad/s and $T_1 = 2.0$ s, $T_2 = 0.811$ s, $T_3 = 0.614$ s.

The modal matrix is as follows:

$$\begin{pmatrix} 0.382720 & -0.672615 & 1.335355 \\ 0.784834 & -0.309080 & -1.288253 \\ 1.000000 & 1.000000 & 1.000000 \end{pmatrix} \tag{8.16.2}$$

Modal masses in each mode are obtained from Eq. 4.15.6. Substituting values, modal mass for the first mode will be

$$M_1 = \frac{[(240 \times 0.382720) + (240 \times 0.784834) + (120 \times 1)]^2 \times 10^3}{(240 \times 0.382720^2) + (240 \times 0.784834^2) + (120 \text{x} 1^2)} = 528.64 \times 10^3 \text{ kg} \tag{8.16.3}$$

Similarly, modal masses for all modes are evaluated and these are presented in Table 8.2.

Base shear for each mode is given by $V_i = A_{hi} \times M_i \times g$.

Introducing values of $A_h$ and modal mass $M$ for first mode from Table 8.2, base shear for the first mode is

$$V_1 = 0.02004 \times 528,640 \times 9.81 \times 10^{-3} = 103.926 \text{ kN}. \tag{8.16.4}$$

Proceeding accordingly, base shear for other two modes are obtained and are given in Table 8.2. Combining these modal values by SRSS method, the total base shear for the fixed base structure is,

$$\text{Base shear} = \sqrt{103.926^2 + 25.773^2 + 10.726^2} = 107.610 \text{ kN} \tag{8.16.5}$$

2. *Modal Floor masses*

Participation factors for the three modes are obtained using Eq. 4.14.1. Substituting values in this equation, the first mode participation factor will be,

$$P_1 = \frac{(240 \times 0.382720) + (240 \times 0.784834) + (120 \times 1)}{\left(240 \times 0.382720^2\right) + \left(240 \times 0.784834^2\right) + (120 \times 1^2)} = 1.3209 \quad (8.16.6)$$

Similarly, participation factors for the other modes will be,

$$P_2 = -0.459658, \quad P_3 = 0.138792$$

From Eq. 4.15.5, the modal mass ($m_{ji}$) at floor $j$ in mode $i$ will be, $m_j \varphi_{ji} P_i$

Substituting values, the modal mass at floor 1 in mode 1 will be,

$$\mathrm{m}_{11} = 240,000 \times 0.382720 \times 1.3209 = 121.328 \times 10^3 \mathrm{kg} \quad (8.16.7)$$

Modal floor masses for first mode are:

$$m_{11} = 121.3283 \times 10^3 \mathrm{kg}, m_{21} = 248.8047 \times 10^3 \mathrm{kg}, m_{31} = 158.5079 \times 10^3 \mathrm{kg}$$

3. *Storey Shear Forces*

For the given data, viz. Zone IV, importance factor of 1.0 and with a reduction factor of 5, from Eq. 4.6.1, the seismic horizontal coefficient is

$$A_h = 0.024 S_a / g \quad (8.16.8)$$

Reading off values for $S_a/g$ from codal response spectrum for each modal time period evaluated earlier, the $A_h$ values for each mode are obtained and presented in Table 8.2.

Storey force for floor $j$ in mode $i$ will be

$$Q_{ji} = A_{hi}\, m_j\, \varphi_{ji}\, P_i g \quad (8.16.9)$$

which for the first mode will be

$$Q_{11} = 0.02004 \times 121.3283 \times 10^3 \times 9.81/1,000 = 23.852\,\mathrm{kN} \quad (8.16.10)$$

Similarly, forces are evaluated for the other two modes and listed in Table 8.3.

**Table 8.3** Storey forces

| Storey force (kN) | Mode | | |
|---|---|---|---|
| | 1 | 2 | 3 |
| $Q_1$ | 23.852 | 35.988 | 26.181 |
| $Q_2$ | 48.913 | 16.537 | −25.258 |
| $Q_3$ | 31.161 | −26.752 | 9.803 |

4. *Base Moment for First Mode*

Moment of storey forces about the base in the first mode is obtained by

$$M_{b1} = \sum_{1}^{3} Q_{j1} h_j \tag{8.16.10}$$

Utilizing values of storey forces for the first mode from Table 8.3 and storey heights from Fig. 8.16,

$$\text{Base moment } M_{b1} = (31.161 \times 11.5) + (48.913 \times 8.0) + (23.852 \times 4.5) = 857 \text{ kNm} \tag{8.16.11}$$

5. *Floor Displacements*

Floor displacements will be given by,

$$[\boldsymbol{U}] = [\boldsymbol{K}]^{-1} [\boldsymbol{Q}] \tag{8.16.12}$$

Substituting values for the first mode,

$$\begin{Bmatrix} u_{11} \\ u_{21} \\ u_{31} \end{Bmatrix} = \begin{pmatrix} 17875.0 & -7562.5 & 0 \\ -7562.5 & 13062.5 & -5500.0 \\ 0 & -5500.0 & 5500.0 \end{pmatrix}^{-1} \begin{Bmatrix} 23.852 \\ 48.913 \\ 31.161 \end{Bmatrix} = \begin{Bmatrix} 10.078 \\ 20.666 \\ 26.332 \end{Bmatrix} \times 10^{-3} \text{m}$$

Proceeding similarly for the other modes, roof deflections for modes 1, 2 and 3 are

$$u_{31} = 26.332 \text{ mm}, \; u_{32} = -3.716 \text{ mm and } \; u_{33} = 0.779 \text{ mm}$$

(b) *Equivalent First Mode SDOF system with SSC*

For the MDOF structure under consideration, we need to arrive at the equivalent oscillator for first mode. Utilizing Eq. 8.13.1, height of such a system is

$$h_1 = \frac{(158.508 \times 11.5) + (248.804 \times 8) + (121.328 \times 4.5)}{528.64} = 8.246 \; m$$

From Eq. 8.13.3, the equivalent oscillator stiffness will be

$$\tilde{k}_1 = M_1 \omega_1^2 = 528.64 \times 10^3 \times 3.14^2 / 1,000 = 5,212 \text{ kN/m}$$

Vibration period of the equivalent oscillator with SSC is obtained by substituting values in Eq. 8.13.2.

$$\tilde{T}_1 = 2.0 \times \sqrt{1 + 5,212 \left\{ \frac{1}{225,000} + \frac{8.246^2}{1,800,000} \right\}} = 2.21 \text{ s}$$

For this time period, from the codal response spectrum, $S_a/g = 0.756$ for 5 % damping.

*Equivalent Damping*

Substituting values in Eq. 8.12.7, the equivalent damping is given by,

$$\tilde{\xi} = \frac{\left[ \frac{5}{5212} + \frac{10}{225,000} + \frac{15 \times 8.246^2}{1,800,000} \right]}{\left[ \frac{1}{5212} + \frac{1}{225,000} + \frac{8.246^2}{1,800,000} \right]} \times 10^{-2} = 6.71 \text{ \%}$$

For this value of damping, the IS 1893 stipulated reduction factor is 0.915.

Substituting values in Eq. 4.6.1, the horizontal seismic force coefficient is,

$$\tilde{A}_{h1} = 0.024 \times 0.756 \times 0.915 = 0.0166$$

Base shear of the equivalent oscillator with SSC corresponding to the first mode of the MDOF system will be,

$$\tilde{V}_1 = (528.640 \times 0.0166 \times 9.81) = 86.087 \text{ kN}$$

$$\tilde{V}_1 \ (86.087 \text{ kN}) > 0.7 V_1 \ (0.7 \times 103.926 = 72.75 \text{ kN}) \ .\text{Hence safe}$$

This modified first mode base shear value $\tilde{V}_1$ is now combined with base shear values for the other two modes for a fixed base structure without SSC. The total base shear with SSC will be,

$$\text{Base shear (with SSC)} = \sqrt{86.087^2 + 25.773^2 + 10.726^2} = 90.50 \text{ kN}$$

Roof displacement in the first mode is obtained by substituting values in Eq. 8.13.6,

$$= \frac{86.087}{103.926} \left[ \frac{857 \times 11.5}{1,800,000} + 26.332 \right] = 21.817 \text{ mm}$$

Combining this value with roof displacement values for other two modes calculated earlier,

$$\text{Roof displacement} = \sqrt{21.817^2 + (-3.716)^2 + 0.779^2} = 22.145 \text{ mm}$$

# Chapter 9
# Confined and Reinforced Masonry Buildings

**Abstract** Masonry structures would continue to be built in large numbers in spite of masonry not being an ideal material under seismic impact. As a result, a large population in rural India will continue to live in such abodes. Hence, it is important to provide guidelines which, if followed, can minimise damage and save many lives in the event of an earthquake. One of the less expensive approach to achieve this is the use of confined masonry. This form is described in detail together with sizes and reinforcement to be used in confining members. Another approach is to fortify masonry with steel reinforcement supported by a proven design procedure. This chapter covers in detail confined masonry as well as reinforced masonry structures. Detailed analytical techniques are described for design of masonry shear walls subjected to in-plane and out-of-plane inertia forces. It is shown how the magnitude of lateral force shared among shear walls can be evaluated.

**Keywords** Confined masonry • Reinforced masonry • Design of masonry shear walls

## 9.1 Introduction

Stone and brick masonry buildings have been in use for many years. Early construction was without the bedding mortar and it was only much later that mortar was introduced between masonry units. The binding material in mortars has undergone changes from mud to lime and then to a mixture of lime and cement. Building bricks came in assorted sizes for a long time and the era of modern bricks commenced with the introduction of extrusion machines for brick manufacture in the mid-nineteenth century (FEMA 274 1997). It paved the way for standardisation of brick unit sizes. This was followed, in the early twentieth century, with the entry of concrete masonry blocks as a substitute for clay bricks.

The design of brick/block masonry buildings is used to be based on experience. Such buildings were often severely damaged during earthquakes due to their heavy weight, low tensile strength and brittle behaviour. This was compounded by the use of poor-quality materials and lack of seismic-resistant details in their construction. For instance, the walls were poorly knit together and they were not adequately tied to the roof. An example of this is seen in Picture 9.1. This was an invitation for out-of-



S. Manohar, S. Madhekar, *Seismic Design of RC Buildings*, Springer Transactions in Civil and Environmental Engineering, DOI 10.1007/978-81-322-2319-1_9

**Picture 9.1** Walls not tied together

plane instability to occur. Whenever buildings were damaged during a seismic event, it was treated as an accepted phenomenon and the problem was rarely addressed comprehensively.

Over the past few decades however, extensive research has been conducted on the behaviour of brick and block masonry work under seismic conditions. This has led to significant advances in design and construction methods such as introduction of confined masonry wherein the building is tied together with strong horizontal and vertical concrete bands. Another major improvement was fortification of masonry with steel reinforcement supported by a proven design procedure. Both these forms of construction are discussed below.

Even today, most of the low-income rural population resides in unreinforced adobe buildings and their total number is large and growing. There is enough evidence to suggest that unreinforced masonry buildings will continue to be used even in high-risk seismic areas because of their low cost, durability and good thermal and fire resistance properties coupled with the advantage of local availability of materials. This approach is reinforced with the knowledge that an earthquake is a rare phenomenon. Hence, much greater importance than at present should be given to bringing about improvements in such buildings so as to increase their resistance to an earthquake. This has to be done by educating the users, scientific selection of proper building layouts, accurate designs, insistence on high quality of construction in the field and incorporating seismic-resistant details in buildings.

## 9.2 Seismic Considerations

The design principles for masonry structures are well understood. Hence, the emphasis herein is primarily to stipulate the requirements and design principles relevant to achieving a masonry building's improved seismic performance. The lateral inertia forces are primarily generated at floor levels and are carried down to the foundations through shear walls. Thus, in a masonry building, structural shear walls are the key components whose proper location and distribution over the building plan is vital for seismic safety. Accordingly, given below are some of the important aspects that must receive attention during planning and implementation of such buildings so that earthquake-induced damage is minimised.

### *9.2.1 Building Configuration*

Under seismic conditions, a building's overall shape, size and distribution of its mass are parameters that gain significance. From studies by several researchers, the following empirical recommendations have emerged for improving seismic resistance of masonry buildings:

- A box-shaped building is inherently stronger than a L or U or similarly shaped building.
- Layout should be simple with a regular footprint and walls at different floor levels should be vertically aligned.
- At least two walls in each of the two orthogonal directions should be fully confined.
- Length to width ratio of a building should ideally be <4 (Brzev 2007). If it exceeds, then the structure should be broken up into modules with large enough movement joints between them to obviate pounding.
- Ensure strong inter connections (Schacher 2007) between longitudinal and transverse walls.
- In load-bearing construction, exterior walls should have robust pilasters or cross walls at regular intervals.
- Avoid top heavy construction. An example of failure of a heavy canopy roof is seen in Picture 9.2.
- A building should not have masonry load-bearing walls for one floor and a reinforced concrete frame in the next upper storey.
- Wall openings should be symmetrically located in the building and they should not interrupt beam bands.

**Picture 9.2** Canopy failure

### *9.2.2 Walls*

Often, walls fail because of too many openings, lack of structural integrity, very long walls with weak cross connections, unsymmetrical plan and poor workmanship. In-plane and out-of-plane stability of walls is crucial for survival of a building during an earthquake. To achieve this:

- Walls should have strong connections with their foundations.
- Concrete foundations under transverse and longitudinal walls should be tied together.
- Longitudinal and transverse walls should be stitched together with rebars or weld mesh at their junctions.
- Walls should be well anchored to the roof and at all intermediate floor levels.

- Walls are often punctured with openings for doors and windows. Such openings should be small and as few as architecturally admissible.
- Openings should be vertically aligned from one storey to another and the top ends of openings in a storey should be horizontally aligned.
- Piers between openings should be stronger than the spandrels.
- As far as possible, confined load-bearing walls should not be slender both vertically and horizontally. IS 1905 stipulates that for masonry walls in 1:3(H1 grade) or 1:4 (H2 grade) cement/mortar ratio, the H/t ratio should be $\leq$27. It is suggested by Meli et al. (2011) for load-bearing masonry H $\leq$ 3 m.

### *9.2.3 Roofs*

The following precautions are important:

- Roofs should be well anchored to walls. An example of failure due to inadequate roof–wall connection is seen in Picture 9.3.
- Roofs should be of light construction since heavy roofs will attract large inertia forces that can cause them to slide off the walls. Such a damage is more likely to occur when roof slab and the wall that supports it vibrate out of phase.

**Picture 9.3** Roof slid off the wall

- Purlins and bottom ties of trusses should be braced through horizontal bracing. Gable walls must be designed for possible out-of-plane inertia loads from the roof.
- Partition walls should be nominally reinforced by rebars which are anchored into the main walls.
- Parapets should be reinforced vertically and horizontally and vertical rebars should be anchored into the eaves tie beams.

## 9.3 Confined Masonry

Unreinforced masonry is brittle. Even when walls are well constructed and keyed together, it is observed that during an earthquake, cracks open up in the walls particularly at corners and at wall intersections. When this happens the masonry, being brittle, rapidly loses its rigidity and load-carrying capacity. This can lead to instability and eventual collapse. Under seismic conditions, the wall is exposed to racking shear which can cause brittle failure in masonry with serious consequences. Hence, concerted efforts were made to find a means of confining masonry to prevent it from disintegrating.

The first reported use of confined masonry dates back to 1908 (Brzev 2007). The principle in this type of construction is to confine the brick masonry panels in a manner that will enhance their resistance to earthquake effects. Confined masonry quickly gained popularity the world over because of its observed satisfactory performance during earthquakes (Meli et al. 2011) particularly when the wall density in both orthogonal directions was adequate. Wall density ratio is defined as a ratio of the cross-sectional area of walls in one direction to the total floor plan area of all floors in a building. The suggested (Brzev 2007) adequate density ratio is 2 % in low seismic areas and 4–5 % in high seismic areas.

Confined masonry can be looked upon as load-bearing unreinforced masonry which is confined with vertical and horizontal reinforced concrete bands around openings and also around masonry panels. The horizontal bands help to tie the walls together and prevent their separation at vertical joints, thereby augmenting their resistance to inertia forces. Confinement of masonry improves substantially both its strength and ductility. It is rated as a seismically superior construction at an economical cost as compared to ordinary masonry construction and is a suitable option for low- to medium-rise buildings.

The concrete bands, referred to above, are termed as tie columns and tie beams. They are not intended, nor designed, to act as moment resisting frames against lateral loads. Hence, their effect is ignored during wall design with the result that their recommended sizes and spacing are empirical. From a wide body of literature on this subject, the following suggestions emerge for tie columns and tie beams so that they can assist in confining brick walls.

### *9.3.1 Tie Columns*

(a) Their width should preferably be the same as that of the wall and their dimension parallel to the wall should be at least 150 mm (Meli et al. 2011). Each column may be reinforced with 4 φ 10 mm deformed bars lapped at mid-height but lapping in ground floor column is to be avoided. The bars to have φ 6 mm stirrups at 150 mm c/c with this spacing reduced to 100 mm near both ends of the tie columns.
(b) They should be introduced on either side of sizeable openings, at door jams, at wall ends and at wall intersections. This helps to prevent cracks forming at corners of openings.
(c) Walls on both sides of a tie column should have toothed ends where they engage with the brick walls so as to enhance confinement effect.
(d) Tie column spacing should preferably not exceed 4 m (Brzev 2007).

### *9.3.2 Tie Beams*

(a) They should also be of the same width as the wall and 150 mm thick reinforced with 4 φ10 mm deformed bars with φ 6 mm mild steel stirrups at not more than 200 mm c/c. The rebars therein should be connected with rebars from tie columns and they should also be anchored into transverse tie beams.
(b) They should be provided at eaves, lintel, sill and plinth levels to bind the building together. In the case of pitched roofs, gable tie beams should be provided.
(c) Even if there are no windows in a particular wall, tie beams should be provided at lintel and sill levels, of which the former band is the more important.
(d) A band is not required if there is a rigid slab at that level.
(e) Bands should be continuous without any break. An example of the benefit from use of a confining band is seen in Picture 9.4.

A typical arrangement of confining elements is shown in Fig. 9.1 and details in Fig. 9.2. Typical connections between tie beams and also between a tie beam and a wall are shown in Fig. 9.3a, b, respectively. The prescriptive suggestions in respect of member sizes and of reinforcement details of tie beams and tie columns vary since they are essentially empirical. Their representative values that are generally acceptable are given above.

## 9.4 Sharing of Lateral Force Among Co-planer Walls

The procedure for evaluating lateral shear forces at floor levels due to an earthquake motion is similar to that described earlier for framed structures in Sect. 4.5 of Chap. 4 and hence is not repeated here. In buildings, most of the inertia forces are


**Picture 9.4** Benefit of using confining bands

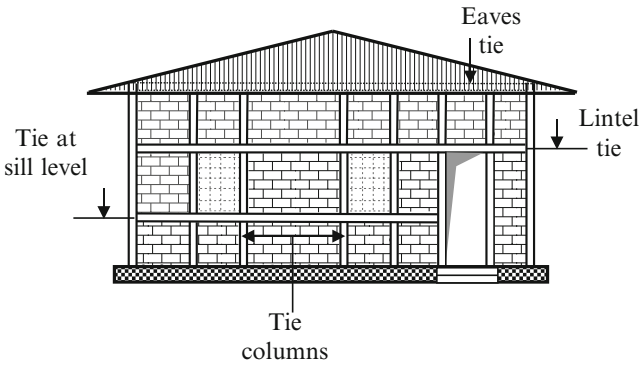


**Fig. 9.1** Typical arrangement of confining elements

concentrated at slab (i.e. diaphragm) level. The quantum of inertia load carried by a wall will depend on flexibility of the diaphragm, degree of symmetry in building layout, rigidity of individual walls, etc. As mentioned earlier, in this book it is assumed throughout that diaphragms are rigid as that is of common occurrence in buildings.

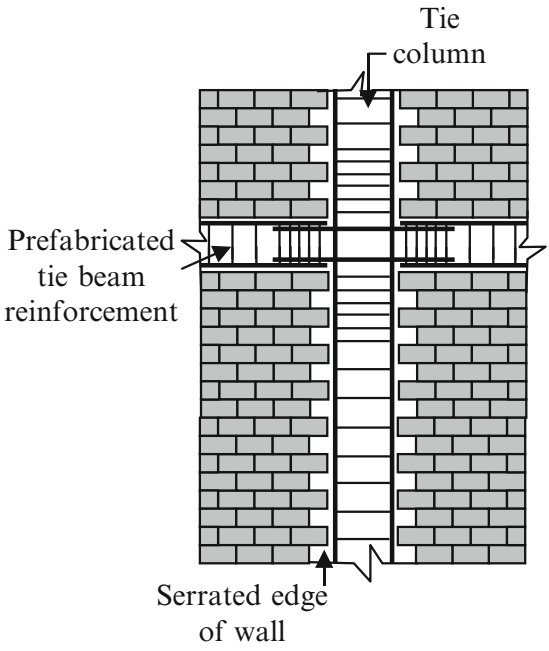


**Fig. 9.2** Typical tie beam and tie column

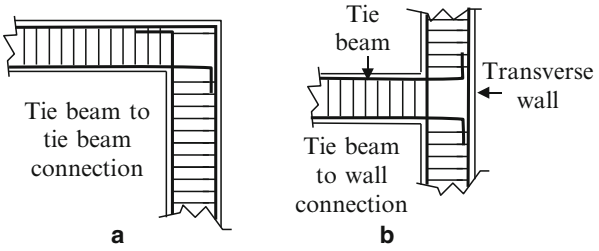


**Fig. 9.3** Tie beam connections (vertical rebars not shown for clarity)

First, the load shared by a group of co-linear walls is evaluated assuming the diaphragm to be rigid. Then the in-plane lateral load is shared among co-linear walls in proportion to their rigidities.

### *9.4.1 Rigidity of a Solid Cantilever Shear Wall*

Lateral top deflection, of a rectangular cantilever wall of thickness $t$ subjected to a unit lateral load at the top, is given by

$$\Delta = \frac{h^3}{3EI} + \frac{1.2h}{GA} + \theta_f.h \tag{9.1.1}$$

where

$h =$ wall height, $I =$ wall moment of inertia, and $E$ and $G$ are modulus of elasticity and of rigidity respectively. $A =$ area of wall section, $L =$ wall length, and $\theta_f$ is extent of wall rotation at its base.

The first term represents deflection due to bending. For calculating moment of inertia, the contribution of flanges in the form of pilasters, if provided, has to be taken into account. The second term is due to shear wherein, however, area $A$ is that of the web portion only neglecting pilasters, if any. The third term is due to rotation which is normally neglected.

For a rectangular wall of thickness $t$ and length $L$,

$$\text{Area } A = L.t \text{ and moment of inertia } I = Lt^3/12$$

Substituting for $E$, $I$, $G$ ($= 0.4$E) and $A$ in Eq. 9.1.1, the top lateral deflection (ignoring effect of rotation) due to a unit load there will be

$$\Delta = \frac{1}{Et}\left[4(h/L)^3 + 3\,(h/L)\right] \tag{9.1.2}$$

Thus, rigidity of a cantilever wall (Rai et al. 2005b) which is the inverse of flexibility will be given by

$$R = \frac{1}{\Delta} = \frac{Et}{\left[4(h/L)^3 + 3\,(h/L)\right]} \tag{9.1.3}$$

### 9.4.2 *Rigidity of a Wall with Openings*

Consider a cantilever wall of uniform thickness with openings as shown in Fig. 9.4a. To obtain its rigidity against lateral top displacement, the wall is considered to be composed of five portions as shown in Fig. 9.4b–f. Evaluation procedure to obtain the rigidity of such a wall could be as under (Agarwal and Shrikhande 2006):

(a) Obtain the top lateral displacement $\Delta_s$ of the solid wall as a cantilever without openings (Fig. 9.4b).

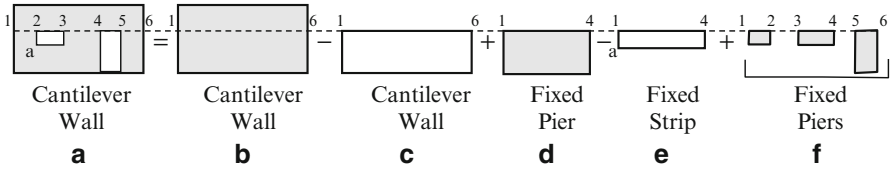


**Fig. 9.4** Evaluation of lateral displacement at roof

(b) Identify the strip having dimensions equal to the wall length and height up to the topmost opening (Fig. 9.4c). Obtain its lateral displacement $\Delta_{\text{strip1}}$ assuming it to be a cantilever and subtract the result from earlier value obtained in (a) above.
(c) Obtain lateral displacements of individual wall strips and wall piers of dimensions as shown in Fig. 9.4d–f considering their top and bottom ends as fixed. These displacements have to be added and/or subtracted as shown in Fig. 9.4. Net displacement of all piers and strips taken together will be $\Delta_p$.
(d) The top deflection of the wall with openings will be

$$\Delta_{\text{wall}} = \Delta_s - \Delta_{\text{strip1}} + \Delta_p$$

### *9.4.3 Distribution of Lateral Force Among Masonry Piers*

A masonry pier in a building may be defined (Rai et al. 2005b) as an isolated vertical member whose length to thickness ratio is >4 and height to length ratio is <5. Piers are generally considered as members that are fixed at both top and bottom. In that event the first term in Eq. 9.1.1 will be $h^3/12EI$. Rigidity of a pier with both top and bottom ends fixed will be

$$R = \frac{1}{\Delta} = \frac{Et}{\left[(h/L)^3 + 3\,(h/L)\right]} \tag{9.2.1}$$

#### 9.4.3.1 Piers in Series

Piers are generally formed as a result of a wall being punctured by openings. Shear force $F$ at the top of such openings will have to be resisted by a series of masonry piers (Fig. 9.5a). The shear component resisted by an individual masonry pier will be a function of its rigidity $R_i$. If these piers are of identical height, thickness and material (as is often the case), then combined rigidity of all the piers (Rai et al. 2005b) will be

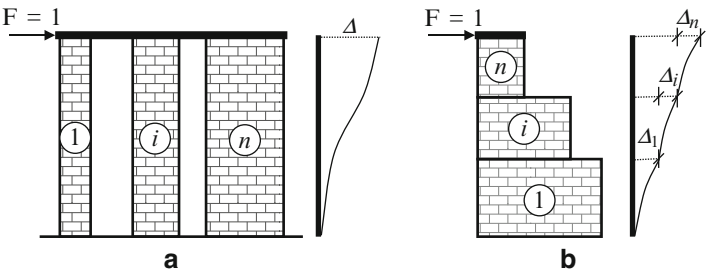


**Fig. 9.5** Distribution of lateral load among piers (**a**) Piers in series (**b**) Piers stacked vertically

$$R = \sum_{i=1}^{n} R_i . \tag{9.2.2}$$

#### 9.4.3.2 Piers Composed of Vertical Segments

A pier may comprise of segments of rigidities $R_1$, $R_2, \ldots R_i, \ldots R_n$ stacked one above the other. When such a pier is subjected to a unit lateral force $F$ at the top (Fig. 9.5b), lateral deflections of individual segments will be $\triangle_1, \triangle_2, \ldots \triangle_i, \ldots \triangle_n$ etc., neglecting the effect of rotations between segments. The combined rigidity of the stack will be (Rai et al. 2005b)

$$R = \frac{1}{[\Delta_1 + \Delta_2 + \cdots \Delta_i + \cdots \Delta_n]} = \frac{1}{\left[\frac{1}{R_1} + \frac{1}{R_2} + \cdots \frac{1}{R_i} + \cdots \frac{1}{R_n}\right]} = \frac{1}{\sum_{1}^{n} \frac{1}{R_i}} \tag{9.2.3}$$

In both the above cases, load shared by wall $i$ will be in the proportion $R_i/R$ of total load $F$.

Transverse load at top of cantilever walls will be shared between them in proportion to their rigidities evaluated according to Eq. 9.1.3. For squat walls, the evaluated rigidity based on shear deformation alone is reasonably accurate, whereas for walls with $h/L > 4$, rigidity based on bending alone may prove to be adequate. For walls with an intermediate range of $h/L$, both bending and shear deformation have to be considered. The manner of distribution of a lateral shear force among wall piers is demonstrated through *Ex* 9.8.1.

### *9.4.4 Walls Connected by a Drag Member*

Masonry walls may be connected by a drag member at their top. The purpose of this member would be to transfer the lateral force to co-planer walls. The force in such a member will vary along its length. Its value at any location will depend on wall rigidities. A method of calculating forces in drag members is given in *Ex* 9.8.2.

### *9.4.5 Design of a Wall Pier*

Wall piers are subjected to lateral shear force at their tops from seismic and wind effects. In addition, overturning moment on the building due to above lateral forces causes vertical forces in these piers which are determined by the well-known cantilever method. Thereafter, each pier is checked for stresses at its base which is also explained in *Ex* 9.8.3.

## 9.5 Reinforced Masonry

The poor performance of unreinforced masonry and limitation on the height of confined masonry construction led to a search for a better product. It is said that the first major application of reinforcing masonry was attempted in 1825 by Brunel. However, a scientific approach to modern reinforced masonry had to wait until the efforts by Brebner in 1923 (Taly 2000). Commonly, reinforced masonry is formed by placing reinforcement in the wall by either of the following means:

1. Reinforcement is placed in hollow clay or concrete block walls and then fully or partially grouted.
2. Thin walls are constructed with a cavity formed between them. Reinforcement is placed in this cavity and then grouted.

Masonry, when it is strengthened with reinforcement, possesses ductility and demonstrates a significant increase in its capacity to withstand inertia forces. Reinforcement also restricts potential cracking at corners of openings. Herein it is assumed that the reinforced brickwork is undertaken by a qualified engineer and is of sound quality executed under directions of an experienced supervisor.

### *9.5.1 Wall Formation*

In the case of walls made up of hollow units, vertical reinforcement is woven into the voids which are subsequently grouted as construction progresses (Anderson and Brzev 2009). The arrangement is shown in Fig. 9.6a. With solid blocks, the vertical reinforcement can be placed at intervals along the wall length by adopting a Quetta bond. Horizontal rebars are laid in mortar bed joints and run continuously for the full length of a wall. Horizontal reinforcement could be prefabricated in ladder or truss shapes as shown in Fig. 9.6b. These rebars are to be tied to vertical rebars as well as to ties in transverse walls.

For reinforced grouted cavity walls, two single-leaf masonry walls (each about 100 mm wide) are constructed with a cavity of about 60–100 mm between them. Reinforcement is then introduced into the bed joints as well as in the cavity created between the two leaves of brickwork (Fig. 9.7). This form has the advantage that reinforcement placed in the cavity can be bonded with that in floor slabs. Additional vertical reinforcement has to be provided, as required, at wall junctions and around openings. Grout has to be dense to ensure a good bond with both the rebar and the blockwork and also to avoid rebar corrosion. To achieve integrity, the two leaves of a wall are tied across with standard wall ties or rebars. The latter should be at least 4 φ 6 mm bars per square meter of wall area.

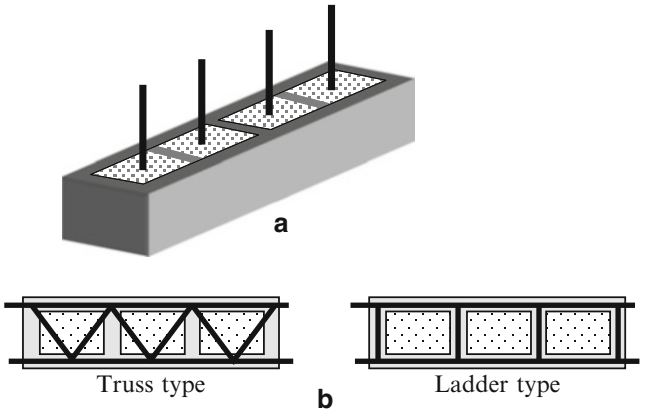


**Fig. 9.6** Rebars grouted in hollow blocks and in bed joints (**a**) Grouted vertical rebars, (**b**) Horizontal rebars in bed mortar joints

**Fig. 9.7** Cavity wall

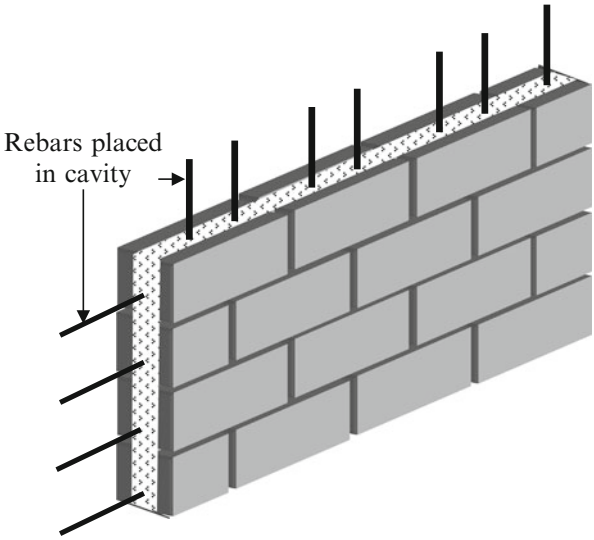


### *9.5.2 Special Reinforced Masonry Shear Wall*

Unlike in confined masonry, here the vertical reinforcement resists axial load and bending stresses, while horizontal reinforcement resists shear. In order that masonry shear walls meet the seismic demands of zones IV and V, they need to have energy dissipating capacity. For this purpose it has been suggested (Rai et al. 2005b) that reinforcement disposition be as under:

- Masonry to have uniformly distributed reinforcement in both directions totaling not less than 0.2 % of gross sectional area of the wall. Of this, at least 0.07 % shall be in any one direction.
- Maximum spacing of reinforcement in both directions shall be lesser of (1) one-third length of shear wall or (2) one-third height of shear wall or (3) 1.2 m.
- Minimum cross-sectional area of reinforcement in vertical direction shall be one-third of the required shear reinforcement.
- Shear reinforcement shall be anchored around vertical bars with 135° hooks.
- The response reduction factor as per IS 1893 is 3.0.

## 9.6 Shear Wall: Working Stress Design

During an earthquake, the building structure has to respond to both in-plane and out-of-plane forces. Hence, design for both these conditions is covered here. The procedure for analysis is quite well established and so it is depicted below in a brief manner for rectangular walls. Masonry walls subjected to a vertical load and in-plane bending moment (which is the common scenario) need to be analysed for three failure modes, viz:

(a) Compression or tension failure under vertical flexure
(b) Shear failure in the form of diagonal tension
(c) Sliding failure when a portion of a wall moves laterally (in the direction of inertia forces) with respect to its lower portion

Further, from seismic considerations, reinforced masonry needs to be detailed such that, particularly, the following types of failures are avoided:

- Separation between walls at their junctions
- Separation of roof from walls
- Unsatisfactory transfer of forces between a wall and its foundation
- Out-of-plane flexure

### *9.6.1 Design Parameters*

The compressive strength of masonry is determined by testing a prism built from the same masonry units and with the same mortar as is going to be used in the actual structure. As per IS 1905, the prism shall be at least 400 mm high and it shall have a height to thickness ratio of at least 2 but not more than 5. Effective area of a hollow unit is the gross area less the cellular space. However, it is opined (Rai et al. 2005b) that often alignment of cross webs is not complete and hence, as a conservative measure, the net area may be taken as that of the face shells only.

The relevant design parameters for working stress design of a reinforced masonry wall are indicated below:

#### 9.6.1.1 For Masonry

- Minimum acceptable compressive strength of masonry units (BIS 2002c): $f_m = 7.0\ \text{N/mm}^2$
- Permissible axial compressive stress in masonry (BIS 2002b): $F_a = 0.25\ f'_m$
- Permissible compressive stress due to combined axial load and flexure: $F_b = 0.313 f'_m$

The following values are as proposed by Rai et al. (2005b):

- Modulus of elasticity of masonry $E_m = 550 f'_m\ \text{N/mm}^2$
- Modulus of rigidity of masonry $G = 0.4 E_m\ \text{N/mm}^2$
- Maximum compressive axial force $= k_s \left(0.25 f'_m A_n + 0.65 A_s F_s\right)$
- Permissible shear stress (with $M/Vd > 1$) $F_v = 0.125\sqrt{f'_m}\ \text{N/mm}^2$ but not to exceed 0.4 N/mm$^2$

where:

$f'_m$ = prism strength of masonry.
$k_s$ = stress reduction factor as per Table 9 of IS 1905 and $A_n$ and $A_s$ are net area of masonry and area of rebars, respectively.

#### 9.6.1.2 For Reinforcement

The following values are as per IS 456 (BIS 2000):

- Permissible stress in HYSD bars (IS 1786) in tension $F_s = 230\ \text{N/mm}^2$
- Permissible stress in HYSD bars (IS 1786) in compression $F_s = 190\ \text{N/mm}^2$
- Permissible stress in MS bars (IS 432) in compression $F_s = 130\ \text{N/mm}^2$
- Permissible stress in MS bars (IS 432) in tension for $\varphi \leq 20$ mm $F_s = 140\ \text{N/mm}^2$
- Permissible stress in MS bars (IS 432) in tension for $\varphi > 20$ mm $F_s = 130\ \text{N/mm}^2$
- Modulus of elasticity of steel $E_s = 2 \times 10^5\ \text{N/mm}^2$

#### 9.6.1.3 Other Parameters

The following parameters are as indicated by Rai et al. (2005b):

- Slenderness ratio of load-bearing walls should not exceed values given in Table 9.1.

**Table 9.1** Maximum slenderness ratio for reinforced load bearing walls – span/effective depth

| | |
|---|---|
| Simply supported | 35 |
| Continuous | 45 |
| Spanning in two directions | 45 |
| Cantilever | 18 |

Source: Rai et al. (2005b)

- Development length for HYSD rebars shall be $L_d = 0.25\ d_b\ F_s$ but not less than 300 mm where $d_b$ is nominal diameter of bar (mm). This length shall be increased by 60 % for MS rebars.
- Maximum spacing of shear reinforcement shall be $\leq 0.5d$ or 1.2 m, whichever is less.
- For rebars placed in masonry pockets, the clear cover shall be 10 mm.
- For rebars in bed joints minimum cover shall be 15 mm from masonry face.
- Maximum spacing of horizontal and vertical reinforcement in special reinforced masonry shear wall shall be lesser of (1) L/3 (2) H/3 and (3) 1.2 m where $L$ and $H$ are length and height of wall.

## *9.6.2 Design of a Wall Subjected to Axial Load and In-Plane Flexure*

In general, masonry shear walls are subjected to axial load and in-plane bending and shear. The theory of design for such walls is essentially the same as that for concrete walls. To ascertain the stresses in such walls, there is no closed form solution available and engineers have to use design charts for this purpose.

### 9.6.2.1 Check for Flexure

This is the usual condition for shear walls resisting lateral seismic loads. Consider a rectangular wall of length $L$ and width $t$ subjected to an axial load $P$ and a bending moment $M$ as shown in Fig. 9.8a. The main reinforcement is assumed to be provided at two ends of the wall. With reference to Fig. 9.8b,

*Case (a)* $k = 1$

In this case, $T = 0$ and $C = P$. Taking moments about centroid of tensile steel,

$$P\ (2d/3) - P\alpha d\ = M\ \text{ i.e. }\ \frac{M}{Pd} = \frac{2}{3} - \alpha. \tag{9.3.1}$$

Thus, if $\frac{M}{Pd} \leq \frac{2}{3} - \alpha$, then compression in masonry will govern.

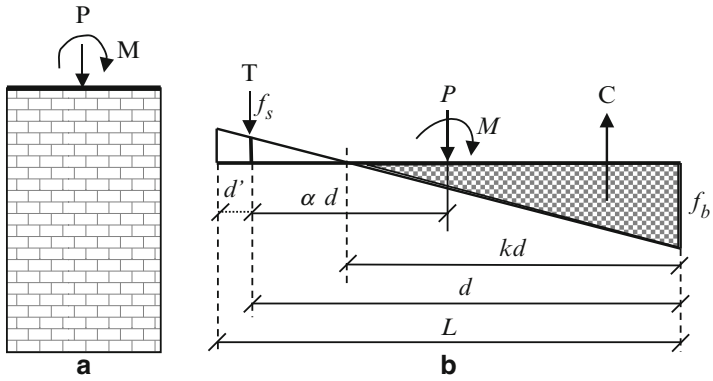


**Fig. 9.8** Wall under axial load and in-plane moment (**a**) Elevation, (**b**) Stress diagram

$C$ : compressive force in masonry
$d$ : effective depth of section $= L - d'$
$d'$ : distance of rebar centroid from extreme tensile fibre
$f_b$ : flexural compressive stress in masonry
$f_s$ : tensile stress in steel
$k$ : coefficient which specifies location of neutral axis as $kd$
$M$ : external moment
$P$ : external axial vertical load
$T$ : tensile force in steel
$\alpha$ : ratio defining distance of axial load from centroid of tensile force
$E_s$ : elastic modulus of steel
$E_m$ : elastic modulus of masonry
$m'$ : modular ratio $= E_s/E_m$
$L$ : length of wall
$t$ : thickness of rectangular wall

*Case (b)* $k < 1$

The method of design is iterative since distance $d'$ has to be initially assumed. If it is found that for chosen value of $d'$ any of the stresses are exceeded, then calculations have to be repeated with a new assumed value of $d'$. Stress diagram will be linear as shown in Fig. 9.8b and total compressive force will be

$$C = \frac{1}{2} f_b t\, kd \tag{9.3.2}$$

and taking moments about location of the centroid of tensile steel,

$$C\left[L - d' - \frac{kd}{3}\right] = P\left[\frac{L}{2} - d'\right] + M \tag{9.3.3}$$

Substituting for $C$ from Eq. 9.3.2 and $L - d' = d$ yields a quadratic equation in $k$, viz:

$$k^2 - 3k + \frac{6\left[P\left(\frac{L}{2} - d'\right) + M\right]}{f_b.t\,d^2} = 0 \tag{9.3.4}$$

Solving this equation gives the value of $k$, and from compatibility of strains, the stress in steel

$$f_s = \left(\frac{1-k}{k}\right) m'\ f_b \tag{9.3.5}$$

If $f_s$ exceeds the permissible steel stress, then calculations have to be repeated with a revised assumption for the value of $d'$.

#### 9.6.2.2 Check for Shear

The commonly observed form of failure in masonry walls is in shear. It generally occurs when the wall is under significant vertical load coupled with large lateral forces. Although masonry and steel both play a part in resisting longitudinal shear, either the masonry alone or steel alone is proposed (Rai et al. 2005b) to be considered as resisting shear. In the former case, the area of masonry section in tension is neglected (Rai et al. 2005b) and masonry shear stress can be approximately obtained as

$$f_v = V/td \tag{9.3.6}$$

When it is considered that shear is resisted by reinforcement, then the area of reinforcement required in the direction of shear force is given by

$$A_v = Vs/F_s.\ d \tag{9.3.7}$$

where

$A_v$ : area of shear reinforcement required in the direction of shear
$V$ : shear force along the wall
$f_v$ : shear stress in masonry
$s$ : spacing of shear steel
$d$ : distance of extreme compression fibre from centroid of tension steel
$t$ : wall thickness
$F_s$.: permissible stress in steel

#### 9.6.2.3 Check for Sliding Shear

For a conventional shear wall and in particular a squat wall, horizontal sliding shear could control its design. The maximum shear causing sliding $V$ should be less than the resistance to sliding, between masonry surfaces. Ignoring the effect of reinforcement, this resistance is given by $V_r = 0.6\,P$, where $P = 0.9$ (dead load) and the coefficient of friction between masonry surfaces is taken as 0.6.

A typical design of a cantilever masonry shear wall is depicted in *Ex* 9.8.4.

### 9.6.3 Design of a Wall Subjected to Out-of-Plane Forces

Walls would experience out-of-plane lateral inertia force during an earthquake. They are then designed as spanning vertically between plinth and eaves level, but the vertical span could be broken by intermediate supports provided by tie beams. For analysis, one may take recourse to the well-established analysis procedure according to which the location of neutral axis is given by $kd$ where

$$k = \left\{\sqrt{(m'p)^2 + 2m'p}\right\} - m'p \tag{9.4.1}$$

where

$p$ : $A_s/td$
$A_s$ : area of reinforcement
$m'$ : modular ratio

Thereafter, for compression failure, stresses in masonry and steel are obtained as

$$f_b = \frac{2M}{k\ t\ jd^2} \quad \text{where } j = 1 - k/3 \tag{9.4.2}$$

and

$$f_s = \frac{m'\ f_b\,(1-k)}{k} \tag{9.4.3}$$

These stresses should be within permissible limits as shown in *Ex* 9.8.5.

### 9.6.4 Flanged Wall

Rectangular walls may intersect other walls to form T, L or other sections. In that event the effective flange width formed by the intersecting wall can be taken into

account. The effective flange overhang on either side of a T-shaped wall shall not exceed (BIS 2002b) one-sixth of the total wall height above the level being considered nor 6 $t$ where $t$ is the thickness of flange portion. If an L- or a channel-shaped section is formed, then the flange width on one side of the wall shall not exceed the same stipulations as above. The section so obtained can be analysed under applied forces and moments. Secondly, the vertical shear stress at the interface between the rectangular and flange portions should be checked to ensure that it is within permissible shear stress.

## 9.7 Slender Shear Wall: Strength Design

Masonry walls are normally designed in India by the working stress method at service loads. This could be due to a combination of reasons such as difficulties of obtaining a consistent supply of high-quality bricks, shortfalls in achieving superior workmanship in the field, etc. Secondly, the compressive stress block to adopt for masonry is not available based on research in India. Thirdly, to the best of our knowledge, there are no codal provisions in India for strength design of masonry. As a result, engineers should continue to use the proven time tested working stress method of design.

With the introduction of factory-made precast concrete blocks and fly ash bricks, the reliability and consistency in quality of such bricks/blocks is likely to improve over the years. In due course, codal provisions will also be developed here. Only thereafter strength design for masonry can be considered. The information given below (Sects. 9.7.1, 9.7.2, 9.7.2.1, and 9.7.2.2) for strength design is based on international literature and only for knowledge and completeness purposes. These are not applicable for Indian conditions.

### *9.7.1 Limit States*

Considering the external moment as a quantifiable variable, the following three structural limit states can be readily defined:

(a) *Serviceability Limit State*

At this stage, cracking is induced in masonry and maximum stress in masonry is equal to its modulus of rupture. Until this state is reached, a reinforced masonry wall can be designed by the working stress method with linear elastic behaviour. Masonry in the compressive region and steel in the tensile regions provide the necessary resistance to external loads and moments.

(b) *Damage Control Limit State*

At this stage, steel reinforcement reaches its yield strain. It is assumed that hereafter the steel behaves in a plastic manner. Since masonry will have cracked in the tension zone, this portion is ignored while evaluating bending strength of the section. Deflections increase at a more rapid rate thereafter.

(c) *Ultimate Limit State*

At this stage the maximum strain in masonry is reached and steel has reached its yield strain. Masonry crushes and the wall reaches its ultimate capacity.

The structural engineer may be called upon to design a shear wall for any of these limit states or more states such as those relevant to damage caused to nonstructural components, permissible deflections, etc. However, in strength design, the focus is on designing for the ultimate limit state where the governing equation would be

$$M_u \leq \varphi \, M_n \tag{9.5.1}$$

where

$M_u$: factored moment due to external loads
$M_n$: nominal moment capacity of the wall based on masonry strength, modulus of elasticity, reinforcement category, etc.
$\varphi$ : partial safety factor considered

## *9.7.2 Strength Design for Flexure*

In such a design process, it has to be ensured that the stress and strain levels are within prescribed limits. In addition it is also important to check that drift is within code-specified limits. Also, in this approach to design, it is required that deflections be based on cracked section properties. The detailed procedure is amplified below.

### 9.7.2.1 Stress and Strain Diagrams

Based on tests, the masonry compression stress block has evolved. For mathematical convenience, this is replaced by a rectangular stress block (Brandow et al. 1993). Both are typically as shown in Fig. 9.9. For steel, an elastoplastic behaviour is assumed. The strain diagram is assumed to be linear with an assumed ultimate strain level in compression for masonry of 0.0025–0.003 when the ultimate masonry prism strength of $f'_m$ is attained.

Other factors to be considered are:

- Tensile strength of masonry is neglected in design.
- Codes impose an upper strength limit for grade of steel which is close to 415 N/mm$^2$.

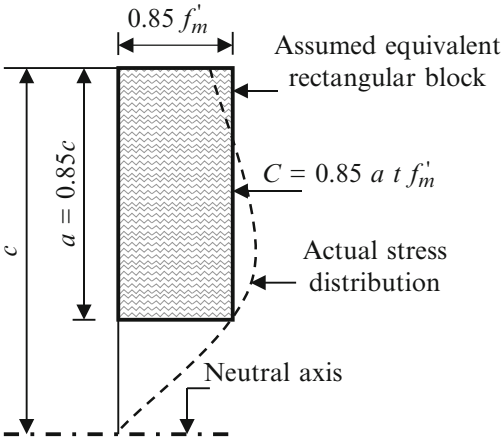


**Fig. 9.9** Equivalent stress block (indicative only)

- Rebars could be distributed over the length of the wall. In that event, the stress in a rebar is taken as $E_s$ times the masonry strain at that location. Whenever the resulting stress ≥ yield stress of steel $f_y$, then the steel stress is taken as $f_y$ (Brandow et al. 1993).

### 9.7.2.2 Load–Moment Interaction Diagram

The nominal capacity of a rectangular wall section subjected to axial load and bending can be obtained from an interaction diagram as depicted in Fig. 9.10. Such a diagram can be constructed by evaluating section capacities for different magnitudes of axial load and bending moment. It thus depicts a relationship between the nominal moment capacity ($M_n$) of a section for a given nominal axial load ($P_n$) and vise versa. For instance, point *1* on this diagram gives the value of $P_n$ when $M_n$ is zero and point *4* depicts value of $M_n$ when the section is under pure bending.

Two other important intermediate points on the diagram would be (1) point *2* which signifies that the maximum stress in masonry is equal to the modulus of rupture and (2) point *3* where steel reaches its yield stress. A fair impression of the diagram can be obtained by locating a few points on this diagram such as 1, 2, 3 and 4. At point 1, the section is subjected to an axial load $P_n$ but there is no moment. At this section, the nominal compression capacity of the section will be

$$P_n = 0.85 f'_m (A_m - A_s) + A_s f'_y \tag{9.6.1}$$

Point 4 on the interaction diagram signifies that the section is subjected to a pure moment only. The nominal capacity of the member in pure bending would be

$$M_n = 0.85 f'_m a.t \left(d - \frac{a}{2}\right) \tag{9.6.2}$$

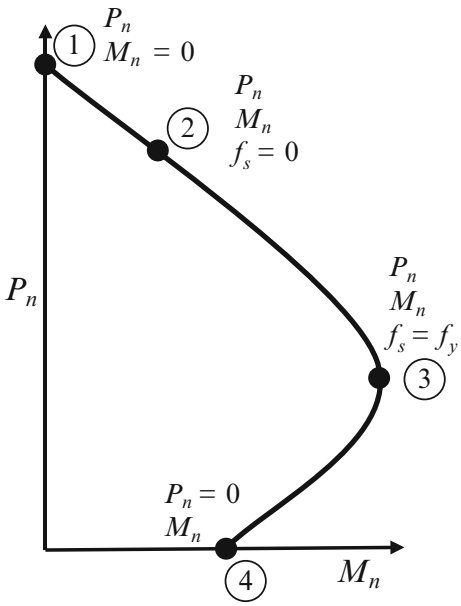


**Fig. 9.10** Typical P–M interaction diagram

The nominal values obtained above have to be reduced by applying a reduction factor whose value depends on whether the section is under pure axial force or under combined axial force and moment.

$a$ : depth of rectangular stress block
$A_m$ : net area of masonry cross section
$A_s$ : area of steel
$f'_m$ : compressive prism strength of masonry
$f_y$ : yield stress of steel
$f'_y$ : compressive stress in steel
$t$ : wall thickness
$d$ : wall depth

The common requirement is to design the section of a shear wall under the combined action of a vertical load and a moment. The procedure for analysis of such a load condition is illustrated in *Ex* 9.8.6.

## 9.8 Illustrative Examples

***Ex 9.8.1*** For a 230 mm thick masonry wall of a three-storey building, the summation values of dead and live loads up to its ground floor lintel level are 480 kN and 103 kN, respectively. Values of lateral inertia forces at storey levels are as shown

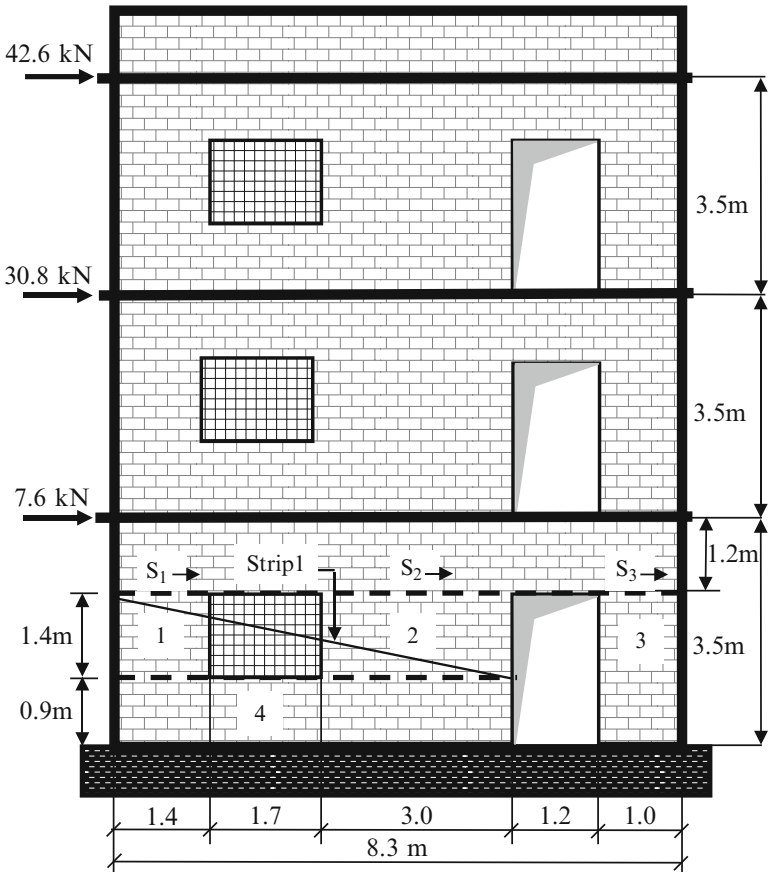


**Fig. 9.11** Inertia forces

in Fig. 9.11. Determine the inertia force component resisted by each of the piers 1, 2 and 3. Assume the ground floor wall and its piers to be fixed at both top and bottom.

**Solution** To determine the distribution of lateral force among piers 1, 2 and 3, we need to first evaluate their relative rigidities. Parameters required for this purpose are listed in Table 9.2. For wall segments fixed at both ends, relative rigidities can be determined by inserting values from this Table into Eq. 9.1.3. For a uniform value of Et = 1, evaluated values of lateral displacements at pier top are also given in Table 9.2.

Deflection of pier 1 + pier 2:

$$\Delta_{p1+2} = \frac{1}{(R_1 + R_2)} = \frac{1}{(0.25 + 0.6659)} = 1.0918$$

**Table 9.2** Determination of rigidity

| Pier/wall | Height $h$ (m) | Length $L$ (m) | $h/L$ | $\Delta$ | Relative rigidity $R$ |
|---|---|---|---|---|---|
| 1 | 1.4 | 1.4 | 1.0000 | 4.0000 | 0.2500 |
| 2 | 1.4 | 3.0 | 0.4667 | 1.5016 | 0.6659 |
| 3 | 2.3 | 1.0 | 2.3000 | 19.0670 | 0.0524 |
| Wall – 1,2,4 | 2.3 | 6.1 | 0.3770 | 1.1848 | 0.8441 |
| Strip 1 | 1.4 | 6.1 | 0.2295 | 0.7006 | 1.4273 |

and

$$\Delta_{1,2,4} = \Delta_{\substack{\text{solid} \\ 1,2,4}} - \Delta_{\text{strip1}} + \Delta_{p1+2}$$

Inserting values from Table 9.2,

$$\Delta_{1,2,4} = 1.1848 - 0.7006 + 1.0918 = 1.5760$$

Taking reciprocals of deflection, the following rigidity values are obtained

$$R_{1,2,4} = 0.6345, \quad R_3 = 0.0525$$

and

$$R_{1,2,3,4} = R_{1,2,4} + R_3 = 0.6345 + 0.0525 = 0.687$$

Lateral shear to be resisted by the three piers (Fig. 9.11):

$$S = 42.6 + 30.8 + 7.6 = 81 \text{ kN}$$

Shear force shared by piers 1 and 2:

$$S_{1+2} = S\left\{\frac{R_{1,2,4}}{R_{1,2,4} + R_3}\right\} = 81\left\{\frac{0.6345}{0.6870}\right\} = 74.810 \text{ kN}$$

$$S_3 = 81\text{–}74.810 = 6.19 \text{ kN}$$

$$S_1 = S_{1+2}\left\{\frac{R_1}{R_1 + R_2}\right\} = 74.810\left\{\frac{0.25}{0.25 + 0.6659}\right\} = 20.420 \text{ kN}$$

Similarly

$$S_2 = 54.390 \text{ kN}$$

Thus, shear forces shared by the three piers are

$$S_1 = 20.420 \text{ kN},\ S_2 = 54.390 \text{ kN and } S_3 = 6.190 \text{ kN}$$

***Ex 9.8.2*** Three cantilever masonry walls of the same width and height are connected at the top by a drag member of a rigid slab as shown in Fig. 9.12(a). A total lateral force of 300 kN is transmitted uniformly throughout the length of the drag member. Calculate forces in drag member at locations A, B, C and D. Wall segments are fixed at both ends.

**Solution** Proceed as in *Ex* 9.8.1. The rigidity of each wall, pier and strip is determined and presented in Table 9.3. From these values,

$$\Delta_{2,3} = \frac{1}{R_2 + R_3} = 0.873$$

$$\Delta_{1,2,3} = \Delta_{\text{strip1}} - \Delta_{\text{strip3}} + \Delta_{2,3} = 1.306 - 0.596 + 0.873 = 1.583 \; i.e.\; R_{1,2,3} = 0.632$$

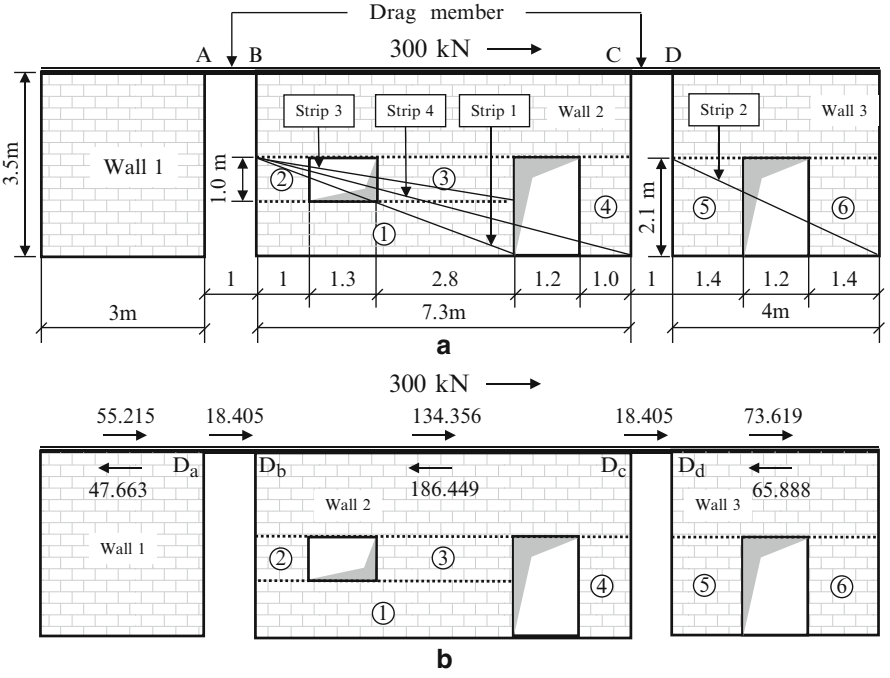


**Fig. 9.12** (**a**) Walls connected by drag members. (**b**) External forces and wall resistances

**Table 9.3** Evaluation of deflection and rigidity

| Element | $H$ (m) | $L$ (m) | $H/L$ | $\lambda(H/L)^3$ | $3(H/L)$ | $\Delta$ (m) | $R$ ($m^{-1}$) |
|---|---|---|---|---|---|---|---|
| 1 | 1.1 | 5.1 | 0.2157 | 0.0100 | 0.6471 | 0.6571 | 1.5219 |
| 2 | 1.0 | 1.0 | 1.0000 | 1.0000 | 3.0000 | 4.0000 | 0.2500 |
| 3 | 1.0 | 2.8 | 0.3571 | 0.0456 | 1.0714 | 1.1170 | 0.8953 |
| 4 | 2.1 | 1.0 | 2.1000 | 9.2610 | 6.3000 | 36.0000 | 0.0278 |
| 5 | 2.1 | 1.4 | 1.5000 | 3.3750 | 4.5000 | 7.8750 | 0.1270 |
| 6 | 2.1 | 1.4 | 1.5000 | 3.3750 | 4.5000 | 7.8750 | 0.1270 |
| Strip 1 | 2.1 | 5.1 | 0.4118 | 0.0698 | 1.2353 | 1.3060 | 0.7657 |
| Strip 2 | 2.1 | 4.0 | 0.5250 | 0.5788 | 1.5750 | 2.1540 | 0.4643 |
| Strip 3 | 1.0 | 5.1 | 0.1961 | 0.0075 | 0.5882 | 0.5960 | 1.6779 |
| Strip 4 | 2.1 | 7.3 | 0.2877 | 0.0952 | 0.8630 | 1.0080 | 0.9921 |
| Wall 1 | 3.5 | 3.0 | 1.1667 | 6.3519 | 3.5000 | 9.8530 | 0.1015 |
| W2 solid | 3.5 | 7.3 | 0.4795 | 0.4409 | 1.4384 | 2.0000 | 0.5000 |
| W3 solid | 3.5 | 4.0 | 0.8750 | 2.6797 | 2.6250 | 5.3050 | 0.1885 |

$\lambda = 1$ for all cases except for walls 1, 2 and 3 and strips 2 and 4 for which $\lambda = 4$

$$\Delta_{1,2,3,4} = \frac{1}{R_{1,2,3} + R_4} = \frac{1}{0.632 + 0.0278} = 1.516$$

$$\Delta_{\text{wall2}} = \Delta_{\substack{\text{solid} \\ \text{wall2}}} - \Delta_{\text{strip4}} + \Delta_{1,2,3,4}$$

$$= 2.0 - 1.008 + 1.516 = 2.508 \;\; i.e. \;\; R_{\text{wall2}} = 0.399$$

Proceeding similarly for wall 3,

$$\Delta_{5,6} = \frac{1}{R_5 + R_6} = \frac{1}{2(0.127)} = 3.937$$

$$\Delta_{\text{wall3}} = \Delta_{\substack{\text{solid} \\ \text{wall3}}} - \Delta_{\text{strip2}} + \Delta_{5,6}$$

$$= 5.305 - 2.154 + 3.937 = 7.088$$

$$R_{\text{wall3}} = 1/7.088 = 0.141$$

From Table 9.3, $R_{\text{wall1}} = 0.102$

In summary, $R_{\text{wall1}} = 0.102$, $R_{\text{wall2}} = 0.399$, $R_{\text{wall3}} = 0.141$

and total rigidity of all three walls $R = \sum_{i=1}^{3} R_i = 0.642$

The total force of 300 kN will be resisted by the walls in proportion to their rigidities. Hence, the forces shared by each wall are:

Force resisted by wall 1, $F_1 = 300.\frac{0.102}{0.642} = 47.663$ kN.

Proceeding similarly, forces resisted by the other two walls will be

$$F_2 = 186.449 \text{ kN}, \quad F_3 = 65.888 \text{ kN}$$

Total drag force = 300 kN. This is spread uniformly over the total length of three walls and two drag members between the walls, i.e. 16.3 m.

Uniform drag force = 300/16.3 = 18.405 kN/m.

External forces over each wall and on each drag member between the walls are shown in Fig. 9.12b.

The force in a drag member will keep changing along its length as given below.

For drag member A–B, forces at it's two ends will be

$$D_a = 55.215 - 47.663 = 7.552 \text{ kN}$$
$$D_b = 7.552 + 18.405 = 25.957 \text{ kN}$$

For drag member C–D, forces at the two ends will be

$$D_c = 134.356 + 25.957 - 186.449 = -26.136 \text{ kN}$$
$$D_d = -26.136 + 18.405 = -7.731 \text{ kN}$$

***Ex 9.8.3*** For the structure in *Ex* 9.8.1, check adequacy of pier 2.

**Solution**

(a) *Dead and Live Loads*

Dead and live loads are distributed among the piers in proportion to their tributary wall lengths

Total length of wall = 8.3 m

Tributary length of pier 2 = 3.0 + (1.7 + 1.2)/2 = 4.450 m

Hence dead load on pier 2 = $P_D = (4.45 \times 480)/8.3 = 257.349$ kN

Similarly, live load on pier 2 = $P_L = (4.45 \times 103)/8.3 = 55.223$ kN

(b) *Loads Due to Overturning Moment*

The overturning moment causes axial forces in piers. These are evaluated by first locating the neutral axis by taking moments ($A \times y$) of each wall pier sectional areas ($A$) about the left vertical edge of the wall (Table 9.4).

Distance of neutral axis from the left edge of the wall is given by

$$\sum (A \times y) / \left(\sum A\right) = 5.1934/1.242 = 4.181 \text{ m}$$

Distance of centerline of pier 2 from the neutral axis = $x_2 = 4.181 - 4.60 = -0.419$ m

A similar procedure is used to determine distances of pier centres of piers 1 and 3 from the neutral axis. These are listed as $x_n$ in Table 9.5.

Moment of inertia of pier 2 about the neutral axis:

**Table 9.4** Locating the neutral axis

| Pier | $L$ (m) | $h$ (m) | $A = L \times t$ (m$^2$) | $y$ (m) | $A\,y$ (m$^3$) |
|---|---|---|---|---|---|
| 1 | 1.4 | 1.40 | 0.322 | 0.70 | 0.2254 |
| 2 | 3.0 | 1.40 | 0.690 | 4.60 | 3.1740 |
| 3 | 1.0 | 2.30 | 0.230 | 7.80 | 1.7940 |
| | | Σ | 1.242 | | 5.1934 |

Note: All piers have the same thickness of 230 mm
$A$: area of pier in plan
$y$: distance of centre of pier from left vertical edge of wall
$Ay$: moment of the area about the left vertical edge of wall

**Table 9.5** Evaluation of axial load due to moment

| Pier | $A$ (m)$^2$ | $x_n$ (m) | $A\,x_n$ (m$^3$) | $Ax_n{}^2$ (m$^4$) | $I_g$ (m$^4$) | $I_n$ (m$^4$) | $\lambda = A\,x_n/\Sigma\, I_n$ | $P_E = M^*\lambda$ |
|---|---|---|---|---|---|---|---|---|
| 1 | 0.3220 | 3.4810 | 1.1209 | 3.9018 | 0.05259 | 3.95438 | 0.14719 | 82.41282 |
| 2 | 0.6900 | −0.4190 | −0.2891 | 0.1211 | 0.51750 | 0.63864 | −0.03797 | −21.25680 |
| 3 | 0.2300 | −3.6190 | −0.8324 | 3.0123 | 0.01917 | 3.03152 | −0.10931 | −61.19998 |
| | | | | | Σ | 7.62453 | | |

$x_n$: distance of pier centre from neutral axis
$I_n$: moment of inertia about the neutral axis $= A\,x_n{}^2 + Ig$
$Ig$: moment of inertia of pier about its axis

$$I_{n2} = \left(A_2 \times x_2{}^2\right) + I_{g_2} = 0.1211 + 0.5175 = 0.6386\ \text{m}^4$$

Values for all piers are shown in Table 9.5.

The axial force in the pier $n$ due to external moment $M_{E1}$ will be given by

$$P_{E\text{n}} = \frac{M_{E1}}{\sum I_n} \times A_n.x_n^2$$

where

$I_g$ : moment of inertia of pier section about its axis
$I_\text{n}$ : moment of inertia of the section about neutral axis of all piers
$A_n$: area of cross section of pier $n$
$x_n$ : distance of pier $n$ from neutral axis

External overturning moment about first floor level:

$$M_{E\,1} = (42.6 \times 7.0) + (30.8 \times 3.5) = 406\ \text{kNm}$$

Taking moments up to mid-height of piers, the overturning seismic moment for evaluating axial force in piers $(P_E) = 406 + 81(1.2 + 0.7) \cong 559.9$ kNm.

From Table 9.5, axial force in pier 2, $P_{E2} = 0.03797 \times 559.9 = \pm 21.259$ kN.

The seismic shear force resisted by pier 2 (*Ex* 9.8.1), i.e. $S_2 = 54.390$ kN.

This force causes a bending moment ($M_{E2}$) in pier 2, given by

$$S_2 \times (h/2) = 54.390 \times 1.4/2 = 38.073\ \text{kNm}$$

(c) *Design of Pier 2*

The design loads and moments for pier 2 are as under

| $P_D$ | $P_L$ | $P_E$ | $M_{E2}$ |
|---|---|---|---|
| kN | kN | kN | kNm |
| 257.349 | 55.223 | ±21.259 | 38.073 |

This pier has to be designed for three load cases as under

1. $P_D + P_L$
2. $P_D + P_L + P_E + M_{E2}$
3. $0.9\,P_D - P_E - M_{E2}$

Pier 2 is checked for different load cases as below:

*Load Case (i)* $P_D + P_L$

From Sect. 9.6.1,

with $f'_m = 10\text{N/mm}^2$; allowable basic compressive stress $F_a = 0.25 f'_m$

$= 2.50\text{N/mm}^2$

Under seismic conditions, its value will be $F_a = 1.33 \times 2.5$

$= 3.32\text{N/mm}^2$

Allowable compressive stress in bending $F_b = 1.25 \times 3.32$

$= 4.15\text{N/mm}^2$

$$\text{Slenderness ratio(SR)} = \text{height/thickness} = \frac{1.4}{0.23} = 6.087$$

From Table 9 of IS 1905, for SR = 6.087, the stress reduction factor $k_s = 0.998$.
Allowable compressive stress $F_a = 0.998 \times 3.32 = 3.313\ \text{N/mm}^2$.

$$\text{Compressive stress} = f_a = \frac{(P_D + P_L)}{A} = \frac{(257.349 + 55.223)\,10^3}{(0.69)10^6} = 0.453\ \text{N/mm}^2$$

$$\frac{f_a}{F_a} = \frac{0.453}{3.32} = 0.136 < 1.\ \text{Hence safe.}$$

*Load Case (ii)* $P_D + P_L + P_{E2} + M_{E2}$

Max $(P_D + P_L + P_E) = 333.829$ kN, $M_{E2} = 38.073$ kNm

$$\text{Compressive stress } f_a = \frac{333.829 \times 10^3}{0.69 \times 10^6} = 0.484\ \text{N/mm}^2$$

From Tables 9.5 and 9.2, for pier 2, $Z = \frac{I_g}{L/2} = \frac{0.5175}{1.5} = 0.345\ \text{m}^3$

$$\text{Bending stress} = f_b = \frac{38.073}{0.345} \times 10^{-3} = 0.110\ \text{N/mm}^2$$

For the combined action of direct load and bending,

$$\frac{f_a}{F_a} + \frac{f_b}{F_b} = \frac{0.484}{3.32} + \frac{0.110}{4.15} = 0.172 < 1.\ \text{Hence safe.}$$

*Load Case (iii)* $0.9P_D - P_{E2} - M_{E2}$

minimum load $= (0.9P_D - P_{E2}) = 231.614 - 21.259 = 210.355$ kN

and

$$M_{E2} = 38.073 \text{ kNm}$$

$$f_a = \frac{210.355}{0.69} \times 10^{-3} = 0.305 \text{ N/mm}^2$$

As before

$$f_b = 0.110 \text{ N/mm}^2$$

$$\frac{f_a}{F_a} - \frac{f_b}{F_b} = \frac{0.305}{3.32} - \frac{0.110}{4.15} = 0.065 \text{ which is positive}$$

Hence, pier 2 is safe for all three load cases.

***Ex 9.8.4*** The base section of a block masonry shear wall 200 mm thick and 3.0 m long supports an axial load of 285 kN and is subjected to a seismic moment of 1,050 kNm due to an in-plane shear of 200 kN. Masonry blocks have a prism strength of 15 N/mm$^2$ and HYSD rebars with a permissible stress ($F_s$) of 230 N/mm$^2$ are used. Check adequacy of the section (by the working stress method) and amount of tension and shear reinforcement to be provided. Assume reduction and modification factors as per IS 1905 (BIS 2002b) to be 1.0.

*Data*: $P = 285$ kN, $M = 1{,}050$ kNm, $f'_m = 15$ N/mm$^2$, $t = 0.19$ m (bedding width for 0.2 m wide blocks), $E_s = 2 \times 10^5$ N/mm$^2$

**Solution** Provide 2- φ16 mm vertical bars (at both ends) as shown in Fig. 9.13 ($A_s = 402$ mm$^2$).

Effective depth of section $d = 3.0 - 0.2 = 2.8$ m.

From Sect. 9.6.1, the permissible stresses under seismic conditions, taking 33 % increase, will be as under:

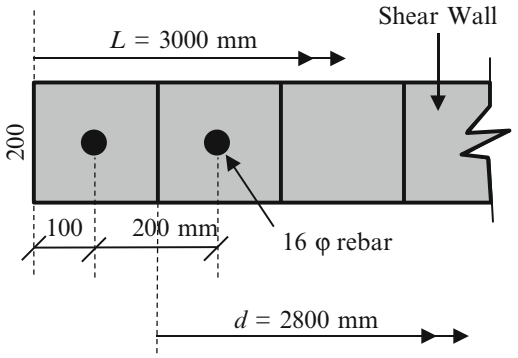


**Fig. 9.13** Rebar positioning in wall

Permissible bending stress in masonry $F_b$=1.25 ×0.25× 15 × 1.33=6.23 N/mm$^2$.
Permissible stress in steel $F_s = 230 \times 1.33 = 306$ N/mm$^2$.
Also, other values are
Modulus of elasticity for masonry $E_m$=550$f'_m$=550 × 15=0.0825 × 10$^5$ N/mm$^2$ and modular ratio $m' = E_s/E_m = 24.2$.
For a stress block as shown in Fig. 9.8, $kd$ is the depth of neutral axis.
From Eqs. 9.3.1 and 9.3.3, $C = \frac{1}{2} \times 6.23 \times 0.19 \times 2.8k \times 10^3 = 1657k$ kN
and

$$P\left(\frac{L}{2} - d'\right) = 285\,(1.5 - 0.2) = 370.5\,\text{kNm}$$

Substituting the above values in Eq. 9.3.2 yields $k = 0.346$.
From Eq. 9.3.5,

$$f_s = \frac{(1-k)}{k}.m'.f_b = \frac{(1-0.346)}{0.346} \times 24.2 \times 6.23 = 285\ \text{N/mm}^2 < 306\ \text{N/mm}^2$$

$$\text{Tensile force } T = f_s \times A_s = 285 \times 402 \times 10^{-3} = 115\ \text{kN}$$
$$C = T + P = 115 + 285 = 400\ \text{kN}$$

From Eq. 9.3.2,

$$f_b = \frac{400 \times 2 \times 10^{-3}}{0.19 \times 2.8 \times 0.346} = 4.35\ \text{N/mm}^2 < 6.23\ \text{N/mm}^2$$

*Check for Shear*
Shear force $V = 200$ kN
$M/Vd = 1{,}050/200 \times 2.8 = 1.875 > 1.0$
From Sect. 9.6.1,
Allowable shear stress $= 0.125\sqrt{15} = 0.484$ N/mm$^2$ or 0.4 N/mm$^2$ whichever is lower
Shear stress $= \frac{V}{bd} = \frac{200 \times 10^{-3}}{0.19 \times 2.8} = 0.375$ N/mm$^2$ < 0.4 N/mm$^2$
Provide φ 10 mm HYSD bars at 500 mm c/c horizontally and φ12 mm HYSD bars at 200 c/c vertically. The horizontal shear reinforcement area:

$$= \frac{78.5 \times 100}{500 \times 190} = 0.08\ \%\ \text{ and vertical reinforcement} = \frac{113.1 \times 100}{200 \times 190} = 0.29\ \%$$

Total amount of shear steel = 0.08 + 0.29 = 0.37 % > 0.2 %

***Ex 9.8.5*** A 150 mm thick hollow grouted block masonry partition wall is 4.6 m high. Assume this wall to be hinged at the top and that it does not support any vertical load. It experiences an earthquake causing a horizontal out-of-plane inertia force equivalent to 0.16 times the weight of the masonry. Masonry density is 1,800 kg/m$^3$ and its prism strength is 10 N/mm$^2$. Design the wall section with the use

of mild steel reinforcement. Also check for safety against sliding shear at the base assuming that the wall rests on a slab with a coefficient of friction of 0.6 between them.

**Solution** The values and permissible bending stress as listed in Sect. 9.6.1 under seismic conditions will be

$$f_b = 1.25 \times 0.25 \times 10 \times 1.33 = 4.15 \text{ N/mm}^2$$

$$E_m = 550 f'_m = 550 \times 10 = 0.055 \times 10^5 \text{ N/mm}^2$$

$$m' = E_s / E_m = 2.0/0.055 = 36.36$$

Weight of masonry $= 150 \times 1,800 \times 9.81 \times 10^{-3} = 2,649 \text{ N/m}^2$

Lateral seismic force (considered uniform over the height) $= 2{,}649 \times 0.16 = 424 \text{ N/m}^2$

Maximum bending moment $M = 424 \times 4.6^2/8 = 1{,}121$ Nm/m.

Assume φ10mm reinforcement at 300 mm c/c $= 0.175$ %.

$$m' p = 36.36 \times 0.175 \times 10^{-2} = 0.0636$$

Inserting this value in Eq. 9.4.1,

$$k = \left\{\sqrt{(0.0636)^2 + 2(0.0636)}\right\} - 0.0636 = 0.3 \text{ and } \mathrm{j} = 1 - \frac{\mathrm{k}}{3} = 0.9$$

With reinforcement placed in the pockets, the effective depth may be taken as 75 mm

Substituting values in Eq. 9.4.2 and Eq. 9.4.3, the maximum stresses are

$$f_b = \frac{2 \times 1,121 \times 10^3}{0.3 \times 1,000 \times 0.9 \times 75^2} = 1.47 \text{ N/mm}^2 < 4.15 \text{ N/mm}^2$$

$$f_s = \frac{36.36\,(1 - 0.3) \times 1.47}{0.3} = 124.7 < 172.9 \text{ N/mm}^2$$

*Check for Sliding Shear*

Base reaction $= 424 \times 4.6/2 = 975.2$ N/m length

Self weight $= 2{,}649 \times 4.6 = 12{,}185$ N/m length

Lateral friction $= (0.9 \times 12{,}185) \times 0.6 = 6{,}580$ N/m > actual shear 975.2 N/m

Hence safe against sliding

***Ex 9.8.6*** A 200 mm thick 5.8 m long block masonry shear wall with $f'_m = 15 \text{ N/mm}^2$ is reinforced as shown in Fig. 9.14a. The rebars are Fe 415 of φ 25 mm with $E_s = 2 \times 10^5 \text{ N/mm}^2$. It is subjected to an axial factored load of 365 kN. Determine the value of the factored design bending moment that it can sustain at

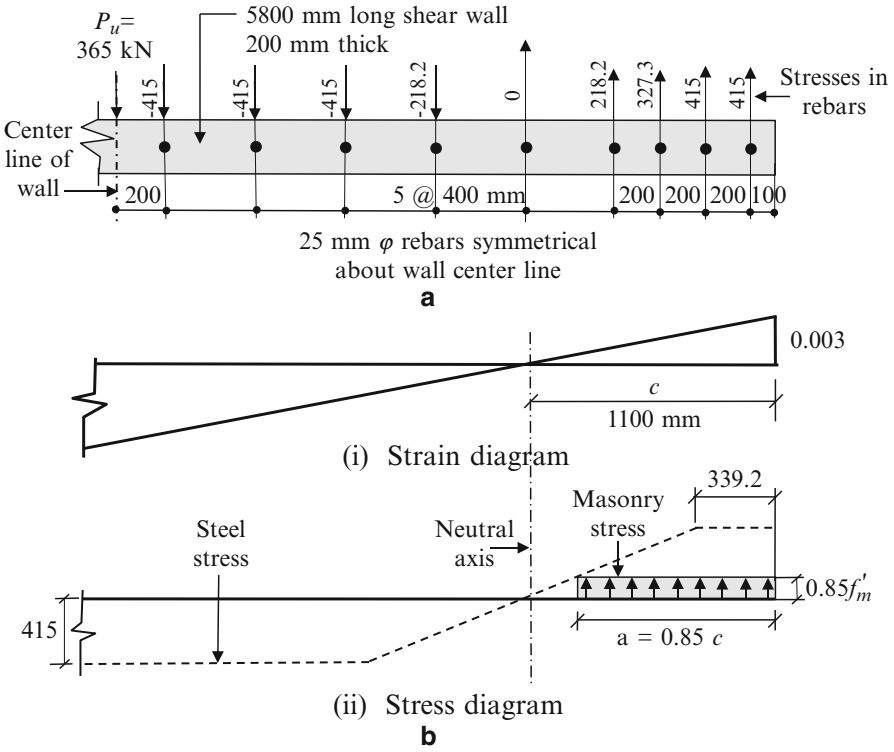


**Fig. 9.14** (**a**) Shear wall with rebars. (**b**) Stress and strain diagrams – ultimate limit state

ultimate strength limit state with a reduction factor of 0.65. The ultimate masonry strain may be taken as 0.003.

**Solution** The net width ($t$) of a 200 mm thick block is 190 mm.

Area of one φ 25 mm rebar ≈ 490 mm$^2$

*Vertical Force Compatibility*

The first requirement would be to achieve compatibility of vertical forces.

Assume (after a few iterations) that the depth of neutral axis ($c$) is 1,100 mm from the maximum compression face and the maximum masonry strain at ultimate limit state is 0.003 as shown in Fig. 9.14b.

Strain in the first rebar on the compression side = 0.003×1,000/1,100 = 0.002727

Stress in this rebar = 0.002727 × 2 × 10$^5$ = 545 N/mm$^2$. Since this stress exceeds $f_y$, i.e. 415 N/mm$^2$, it is taken as 415 N/mm$^2$. Accordingly, the stresses in all the rebars are evaluated. Wherever the stress commensurate with prevailing strain at the section is less than 415 N/mm$^2$, the stress considered is ($E_s$ × strain) and is shown in Fig. 9.14a.

From Fig. 9.9 the length of masonry stress block a = 0.85 × 1,100 = 935 mm

Compressive force in masonry (Fig. 9.14b) (ii),

$$C_m = 0.85 f'_m (A_m - A_{sc}) = (0.85 \times 15)\{(935 \times 190) - (4 \times 490)\} \times 10^{-3}$$
$$= 2,240 \text{ kN}$$

where

$A_m$: compressive area of masonry
$A_{sc}$: area of steel in the compressive zone

As mentioned earlier, compressive forces in steel rebars are evaluated based on the strain diagram. Thus, the total compressive force in steel:

$$C_s = 0.49\left\{2(415) + 327.3 + 218.2\right)\} = 674 \text{ kN}$$

On the tension side, 12 bars will be having a stress of 415 N/mm$^2$ and one will have 218.2 N/mm$^2$. Hence tensile force in steel:

$$T_s = 0.49\{218.2 + 12(415)\} = 2,547 \text{ kN}$$

$$\text{Net force} = C_m + C_s - T_s = 2,240 + 674 - 2,547 = 367 \text{ kN}$$

This is close to the actual factored load of 365 kN. Hence the location of neutral axis, as assumed, is in order.

*Evaluation of Moment*

Taking moments about neutral axis:

(a) Moment of compression forces in masonry

$$= 2,240 \times 10^{-3}\{1,100 - (935/2)\} = 1,416.8 \text{ kNm}$$

(b) Moment of compressive forces in steel rebars

$$= 490\left\{\left(415\,(1 + 0.8) + (327.3 \times 0.6) + \left(218.2 \times 0.4\right)\right\} \times 10^{-3}$$
$$= 505.02 \text{ kNm}$$

(c) Moment of tensile forces in steel rebars

$$= \left(490 \times 10^{-3}\right)\left[\begin{array}{l} 218.2(0.4) + 415\Big(0.8 + 1.2 + 1.6 + 2.0 + 2.4 \\ \quad + 2.8 + 3.2 + 3.6 + 4.0 + 4.2 + 4.4 + 4.6\Big) \end{array}\right]$$
$$= 7,119.34 \text{ kNm}$$

(d) Moment due to factored axial load

$$= 365\{(5,800/2) - 1,100\} \times 10^{-3} = 657 \text{ kNm}$$

The nominal moment capacity

$$M_n = (1,416.8 + 505.02 + 7,119.34 + 657.0) = 9,698.2 \text{ kNm}$$

Factored design moment capacity $M_u = 0.65 \times 9{,}698.2 = 6{,}304$ kNm

# Chapter 10
# Base Isolation

**Abstract** This chapter covers a brief history of base isolation and basic concepts of such a system. Elastomeric as well as sliding (friction pendulum system [FPS]) isolators are covered. Important merits and demerits of isolators are then listed. The theoretical background for design of a building on such isolators is described including developing the equations of motion. The purpose herein is to acquaint the reader with some of the principal facets of design of isolator supported buildings. The methodology of analysis is elaborated through illustrative examples, which cover evaluation of frequency of a framework supported on an elastomeric isolator and the sizing of an FPS isolator.

**Keywords** Base isolation • Elastomeric isolators • Sliding isolators • Friction pendulum system

## 10.1 Introduction

The conventional approach to seismic-resistant design is to incorporate adequate strength, stiffness and inelastic deformation capacity into the building structure so that it can withstand induced inertia forces. This was with the presumption that during strong ground motion, whenever inertia forces exceed their design earthquake levels, the structure will dissipate this excess energy through deformations at predefined locations scattered over the structural framework. It was observed that, even with members designed for ductility, the structures did not always perform as desired, which could be because of reasons such as:

- Strong-column weak-beam mechanism failed to develop as a result of stiffening effect of walls being present
- Creation of short columns because of changes in wall layout, introduced later
- Poor concreting at joints due to reinforcement congestion

On experiencing failures during earthquakes, it was realized that a design based only on the principle of incorporating ductility as a safeguard against seismic effects needs a critical review. In their search for alternative design strategies to minimize magnitude of inertia forces, engineers came up with the innovative idea of



S. Manohar, S. Madhekar, *Seismic Design of RC Buildings*, Springer Transactions in Civil and Environmental Engineering, DOI 10.1007/978-81-322-2319-1_10

introducing a flexible medium between supporting ground and the building, thereby decoupling the structure from energy-rich components of seismic ground motion. This strategy came to be known as the *base isolation method*.

This chapter covers a brief history of base isolation as well as basic concepts of such a system together with its principle benefits and limitations. Also described are the prevailing approaches for design of structures supported on both the elastomeric and sliding isolators. The purpose herein is to acquaint the reader with some of the principal facets of design of isolator supported buildings. The methodology of design is elaborated through illustrative examples. It should be recognized that the design and implementation of an isolator system is highly complex and calls for considerable practical experience and expertise.

## 10.2 Brief History

The frequency of vibration of low- to medium-rise buildings falls in the range where earthquake energy is high. This has often resulted in considerable damage to such buildings due to the enormous destructive strength of an earthquake. The prevailing earthquake-resistant design methods tacitly accept that during a major earthquake, structural damage, sometimes substantial in magnitude, is unavoidable. However, the extremely high cost of repairing and rebuilding damaged structures motivated designers to re-look at the concept of incorporating a flexible medium between ground and the building, which was first attempted in its rudimentary form, over a century earlier.

After many years of research to find a reliable flexible medium, rubber was first used as an isolating medium for protection against earthquakes in Skopje, Yugoslavia, in 1969 (Kelly 1986). Later, a building in Sebastopol in Crimea was supported on steel bearings. It is reported to have performed satisfactorily during an earthquake in 1977. Such satisfactory performance of this and other initial attempts established that *base isolation* is a viable, and in some cases a superior option, to conventional design methods. This prompted scientists and equipment manufacturers to put in considerable research and development efforts that brought about improvements and practical solutions in the last quarter of the twentieth century.

In parallel in the 1980s, efforts got under way to develop codes specifically applicable to seismically isolated buildings and in due course, codal provisions were introduced commencing with the publication in 1986 of "Tentative Seismic Isolation Design Requirements" by Seismology Committee of Structural Engineers Association of California (SEAOC). These guidelines and their subsequent revisions proved to be the precursor to the introduction of design guidelines by Federal Emergency Management Agency (FEMA) followed by the "Uniform Building Code" and "International Building Code". In all these documents, the underlying design philosophy has been life safety under major earthquake and acceptable performance of the building and its constituents under design earthquake.

Rapid development of this technology saw the introduction of newer and newer rubber products that possessed the desired elasto-plastic characteristics (i.e. high stiffness at low strains and low stiffness at high strains) which propelled base isolation to become an internationally accepted method of reducing earthquake-induced inertia forces. Availability of high-speed computing capability supported by reliable software to efficiently tackle complex design issues complemented by large shake table testing facilities played a major contributory role in base isolation technology gaining a firm foothold.

In 1995, a magnitude 7.1 earthquake struck Kobe, Japan. From records of two 6-storey fully instrumented buildings in each other's proximity, the following was observed (Mayes et al. 2012):

1. Earthquake forces across the isolator were reduced by a factor of 3.5 and there was no amplification up the building.
2. In the fixed based building the earthquake forces were amplified by a factor of 3 at roof level. Thus, the earthquake forces at roof level were reduced by a factor of about 10 due to isolators.

A building supported on isolators has a much lower fundamental frequency than that of a building with fixed bases. Also, this frequency is much lower than the predominant frequencies of ground motion. Further, it has been pointed out that the higher modes are orthogonal to the first mode and consequently to the ground motion (Kelly 1986). As a result, the high energy in ground motion at these higher frequencies does not get transmitted to the building framework vibrating in higher modes. Since this approach is still evolving, the codes lay down conservative design requirements and strict testing and acceptance procedures for isolators.

## 10.3 Concept of Base Isolation

To diminish vulnerability of a building to damage during an earthquake, base isolation has emerged as a viable structural option. It is a sophisticated practical solution to improve seismic response of a building by minimizing the structural damage, which was earlier taken to be unavoidable during strong ground motion. Because of the low horizontal stiffness of this deformable medium, it alters the fundamental period of a stiff structure such that it is significantly higher than that of the high energy imparting ground motions. As a result, for its fundamental mode of vibration, the superstructure is subjected to much lower inertia forces with consequent reduction (Fig. 10.1) in base shear.

On the flip side, if the founding stratum is soft, then there is a distinct possibility of the enhanced period due to base isolation being close to the period where an earthquake is likely to have considerable energy. Such a situation can lead to an increase in the response. Thus, it can be said that base isolation is best suited for buildings with a high natural fundamental frequency ($T$ less than about 1 s)

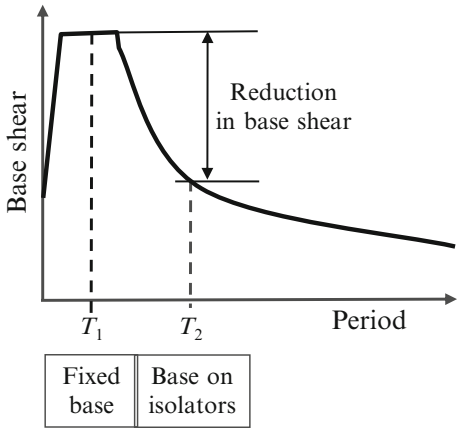


**Fig. 10.1** Effect of increased period (representative diagram)

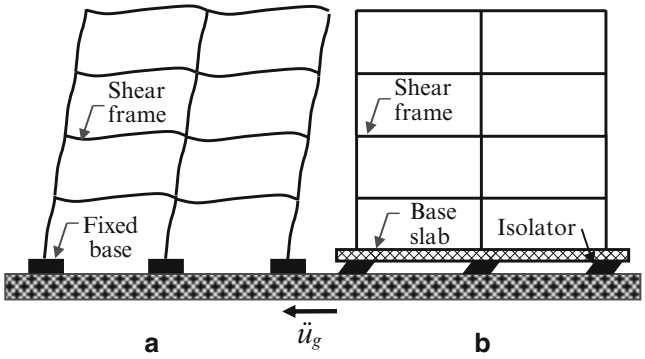


**Fig. 10.2** Displaced MDOF system: (**a**) fixed based and (**b**) on isolators

and preferably those supported on rock or stiff soils. Reinforced concrete moment framed buildings up to about 8–10 storeys and those with shear walls up to 12–15 storeys are said to be ideal candidates for base isolation (Naeim 2001).

If a framed structure were supported on hard strata, it would deform as in Fig. 10.2a. However, when supported on isolators, the lateral displacement in the first mode is concentrated at isolator level while the superstructure behaves almost like a rigid body (Fig. 10.2b). As a result, for buildings supported on base isolators, there is less need to provide ductile energy dissipating regions (e.g. near beam-column joints) as in conventional fixed based structures. However, in view of limited experience of such systems and as a matter of abundant precaution, codes recommend retention of the present form of ductile detailing. This is also to obviate possible brittle failure under a maximum credible earthquake (MCE) in the region or earthquakes with long period energy inputs. In addition, codes also call for rigorous testing of the proposed isolators and peer review of the design, since it is an emerging technology and failure of an isolator system could prove catastrophic.

Isolators should be located such that there is ample access to them for maintenance, repair and replacement, if necessary. A full diaphragm should be employed to distribute lateral loads as uniformly as possible to the isolators. Generally, isolators can be placed at the bottom of columns at basement slab level. This location has the advantage that no special treatment is required for elevator or service lines as they traverse the bearing level. On the other hand, if they are placed at top of basement, then elevator shaft and internal staircase and cladding details may require special treatment below first floor level.

Isolators do substantially enhance the fundamental period of a stiff structure but at the expense of increased building displacements. The first mode deformation occurs at the isolation level only. The real challenge while designing a base isolated structure is the need to control displacements during a major earthquake while maintaining good performance for moderate level earthquakes. Since the superstructure will function essentially as linearly elastic, the structural framework is expected to remain undamaged even during a moderate-level earthquake.

## 10.4 Passive Base Isolators

Base isolation is a passive control technique against lateral vibrations. As discussed earlier, an isolation system should be able to support gravity loads (including those due to vertical seismic acceleration), be sufficiently stiff to minimize displacements under repeated small magnitude lateral loads such as those due to wind, be highly flexible to absorb the energy during strong motion earthquakes and possess capability to self-centre after an earthquake event. Passive isolators that meet these requirements are preferred. Quite clearly, this means that the isolator should possess non-linear stiffness characteristics. It should also possess adequate damping characteristics to assist dissipation of seismic energy and not have excessive lateral displacement across the isolator interface.

Even with all their advantages, passive base isolation systems may not be adequate to prevent extensive damage to building superstructures when they experience a near field earthquake with long period, high peak acceleration and velocity pulse. If this is likely to occur, then a passive system is combined with passive dampers such as viscous or friction dampers or alternatively with semi-active control devices. These devices help to control seismic response through appropriate adjustments within the structure, as the seismic excitation changes. In other words, active control systems introduce elements of dynamic control, thereby augmenting the isolator's capability to resist a range of dynamic motions. Any form of dual control system, including a passive system combined with active or semi-active dampers, is outside the scope of this book.

There are two types of passive isolators which are commonly used, viz. elastomeric based (high-damping rubber, lead-core rubber, etc.) and friction based (e.g. friction pendulum system). Each type is briefly described in the following text.

### 10.4.1 Elastomeric Isolators

Rubber isolators can be of heavy-duty rubber or alternatively rubber stiffened with metal plates. The latter consists of layers of natural rubber vulcanized and bonded to thin stainless steel plates under heat and pressure. Steel plates prevent bulging of rubber under vertical load and also provide large vertical stiffness to support heavy gravity loads. Such a laminated rubber bearing with the addition of a central lead plug, called as Lead Rubber Bearing, is an ideal solution.

Rubber provides adequate horizontal flexibility to sustain large strains during a major earthquake coupled with the ability to generate the much desired restoring force. On the other hand, the lead plug provides higher initial stiffness and hysteresis damping to deal with low strains caused by wind forces. An elastomeric bearing has no moving parts, has good aging properties and has good resistance against environmental degradation.

### 10.4.2 Sliding Isolators

When sliding isolators are provided, the building is supported on surfaces of stainless steel sliding against a very low friction material like teflon. This permits transmission of shear forces across isolator interface only to the extent of frictional resistance between sliding layers. Such a system is relatively less expensive and is ideal for retrofitting. It is effective over a wide range of frequencies normally prevalent in input ground motions. Another advantage is that the maximum transmissibility of acceleration to the superstructure is limited to the maximum force that can generate at the frictional interface.

Among them, a pure friction (P-F) system is the simplest device to function as an isolator. This consists of a slider that moves laterally over a low friction flat surface. However, it is important that after an earthquake event, the slider should return to its pre-slide position. In a P-F system, since there is no restoring mechanism, there will be residual displacement after every seismic event which will result in lesser margin being available for sliding at the next event. From this practical consideration a P-F slider is not deemed suitable and hence is not discussed further.

A friction pendulum system (FPS) overcomes this deficiency. Its motion resembles that of a pendulum in the presence of friction and hence the name FPS. It consists of a curved articulated slider moving on a spherical stainless steel surface. During an earthquake, the building slides horizontally and due to the slider curvature, it is raised vertically as it slides. Tangential component of gravity load acts as a restoring force which pushes the slider back to its original position after an earthquake. However, there is the lurking danger that during a large earthquake, such an isolator could lift off the plate.

In a sliding isolator, since the frictional force generated is proportional to the weight it supports, the centre of mass and centre of resistance naturally coincide. As a result, these systems are less sensitive to torsional coupling. Many variations of

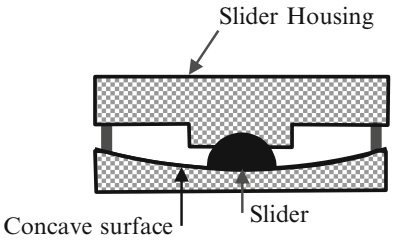


**Fig. 10.3** Typical sliding oscillator

this fundamental system have been developed, which include a sliding surface with varying curvature, two cylindrical sliding surfaces with different curvatures which are placed perpendicular to each other, etc. However, the system most frequently adopted and described herein is an isolator with a single spherical sliding surface. A schematic of such an isolator is shown in Fig. 10.3.

### *10.4.3 Primary Isolator Requirements*

There are strict codal stipulations in respect of both static and dynamic design as well as testing of isolators for which the reader should refer specialist literature and international codes. A few of the principal stipulations in respect of isolators are enumerated here:

1. It should resist static and dynamic loads under worst dead and live load combinations coupled with lateral and vertical forces expected during MCE while undergoing maximum lateral deformation.
2. Any isolation system should possess:
   - Adequate lateral flexibility in order to increase a structure's time period to the desired value
   - Capability to self-centre after a seismic event, i.e. return to its initial position
   - Reasonably high stiffness at low excitation in order to overcome undesirable frequent vibrations due to wind and at the same time should have low stiffness at large displacements to safeguard the structure during a major earthquake
3. An adequate gap should exist around both the isolator and the building to allow their unhindered relative lateral translation.
4. Final design should be based on results of mandatory tests which need to be conducted on the proposed isolation-system hardware to ascertain, among other things, the following:
   - That it functions satisfactorily under anticipated displacements
   - To confirm its actual force-deformation characteristics and degree of damping
   - That it remains stable when subjected to repeated cyclic loading
5. Since in a FPS isolator, the slip process is intrinsically non-linear, the final design should be a non-linear dynamic one.

6. In addition to the above, while designing an isolator system, designers need to pay attention to the following areas:
   - That there is allowance for differential movement between the parent structure and various building elements such as stairs, elevator shaft, piping, etc. which traverse the isolator interface.
   - There has to be easy access to and sufficient space around isolators for ease of maintenance and repair. Also, there has to be provision to temporarily support the structure without an isolator, if the latter is to be removed for maintenance.
   - Isolators should be housed in a fire-resistant enclosure.
   - A sufficiently rigid diaphragm above the isolator level will prevent relative displacement between isolator nodes.

## 10.5 Merits and Demerits of Isolators

Seismic isolation may be looked upon as an approach towards damage prevention rather than its cure. The principal merits and demerits of an isolator system can be summarized as follows:

### *10.5.1 Merits*

- Because of its low stiffness, use of an isolator system leads to an increase in the natural period of a structure as compared to that for a fixed base structure. This moves the system away from the period at which ground motion contains substantial energy. This results in lower inertia forces that the structure has to withstand leading to cost saving.
- In the first mode of vibration (which is often the predominant mode) primary displacements occur only at isolator level while the superstructure behaves almost like a rigid body.
- The floor accelerations are reduced which result in reduced inter-storey drifts.
- Hinge regions in fixed base structures need to have the capacity to deform into an inelastic range over many reversible cycles while maintaining adequate strength and stiffness to ensure stability and integrity of the structure. Such plastic deformations could be large resulting in significant damage to structural and non-structural components. This is minimized in an isolator protected structure.
- In the case of a larger than assessed seismic event, the damage gets concentrated in the isolation system which can be restored relatively easily. As a result, the structure can often be commissioned into service in a short time. This is of immense importance for buildings such as hospitals and those that house emergency service providers.
- It is an ideal and, sometimes, the only means of retrofitting buildings of historical importance.

### *10.5.2 Demerits*

Following are some of the demerits of supporting a building on isolators:

- An isolator system does not significantly help an already flexible structure. As a result, when used singly it has limited application for high-rise structures. However, this limitation is becoming secondary as minimizing damage to very expensive equipment (e.g. in hospital buildings and other structures) to ensure business continuity is gaining in importance.
- With a base isolation system, peak base displacements are large calling for adequate rattle space to be provided to prevent the structure colliding against adjacent elements.
- Caution is called for in the design of buildings with high aspect ratio as there could be net uplift forces on isolators brought about by large overturning moments.
- It is less effective for a building supported on soft soil.
- Since isolation systems are vertically stiff, vertical acceleration amplification is not prevented. Thus, it is advisable to protect equipment through secondary systems to guard against vertical earthquake motion.
- Special flexible joints have to be built into supply lines to sustain the displacements while transiting across the isolator interface. Also rigid structures crossing the interface (e.g. stairs, walls) should have the capability to absorb lateral displacements.
- There is additional expenditure towards foundation costs.
- The $P$-$\Delta$ moment on an isolator can be large because of isolator displacement. This moment will need to be considered at both top and bottom of the isolator interface (FEMA 274 1997).

## 10.6 Characteristics of Elastomeric Isolators

In general, base isolated buildings are designed such that the superstructure remains elastic. Designing a base isolation system is a fairly complex activity and hence only the basic principles are explained here. Prior to undertaking a detailed analysis of an isolator based structure, a key requirement is to estimate the effective stiffness that the proposed isolator should possess. For this purpose, a choice has to be made from one of the following three options:

- Target natural period desired for the isolator supported structure
- Maximum displacement permissible at isolator level
- Upper limit of the desired spectral acceleration

Assuming that the third option is selected, rest of the procedure is explained through the help of *Ex* 10.11.1. The codes lay down minimum and maximum displacements for which isolators need to be designed. They also stipulate the design

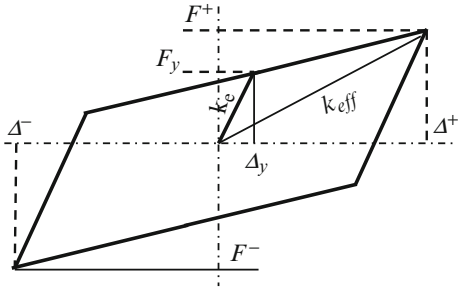


**Fig. 10.4** Bilinear force displacement

lateral seismic forces to be used for portion below the isolator interface and that above it. From seismic considerations, the three structural characteristics which are important for design are lateral stiffness of the isolator, its damping capability and fundamental time period of the isolated building. Each of these is discussed in the following text.

### *10.6.1 Isolator Stiffness*

Isolator performance is commonly non-linear with stiffness and damping being dependent on magnitude of lateral displacement. Without considering cyclic deterioration, a generic force–displacement diagram for an elastomeric isolator is bilinear as shown in Fig. 10.4. Initially, the design is based on assumed (Naeim 2001) values of effective stiffness from earlier test results available for similar isolators.

Thereafter, the preliminary design is checked with actual values obtained from cyclic tests. At each stage of displacement $\Delta$ of the isolation system, the corresponding force value $F$ is noted. The equivalent stiffness is taken as secant stiffness $k_{eff}$ evaluated for each cycle of deformation from the equation (FEMA 273 1997).

$$k_{\text{eff}} = \frac{|F^+| + |F^-|}{|\Delta^+| + |\Delta^-|} \tag{10.1.1}$$

where $F^+$ and $F^-$ are lateral forces at isolator test displacements $\Delta^+$ and $\Delta^-$ respectively. The maximum and minimum effective stiffness at design and maximum displacements, $\Delta_D$ and $\Delta_M$ respectively, are given by Eqs. 10.1.2 and 10.1.3:

$$k_D\,(\max) = \frac{\left|F_D^+\right|_{\max} + \left|F_D^-\right|_{\max}}{2\Delta_D} \quad \text{and} \quad k_D\,(\min) = \frac{\left|F_D^+\right|_{\min} + \left|F_D^-\right|_{\min}}{2\Delta_D} \tag{10.1.2}$$

$$k_M\,(\max) = \frac{\left|F_M^+\right|_{\max} + \left|F_M^-\right|_{\max}}{2\Delta_M} \quad \text{and} \quad k_M\,(\min) = \frac{\left|F_M^+\right|_{\min} + \left|F_M^-\right|_{\min}}{2\Delta_M} \tag{10.1.3}$$

where $\Delta_D$ and $\Delta_M$ are anticipated displacements at design basis earthquake (DBE) and maximum considered earthquake (MCE), respectively. $k_D$ (max) and $k_D$ (min) and $k_M$ (max) and $k_M$ (min) are based on cycles of prototype testing at displacements of $\Delta_D$ and $\Delta_M$, respectively, that produce the largest and least value of effective stiffness.

### *10.6.2 Isolator Damping*

Damping represents the energy dissipating capability of an isolator. The effective damping values at DBE ($\beta_D$) and MCE ($\beta_M$) are evaluated (Naeim 2001) from:

$$\beta_D = \frac{1}{2\pi}\left[\frac{\text{Total area of hysteresis loop}}{k_{D,\max}{\Delta_D}^2}\right]$$

and

$$\beta_M = \frac{1}{2\pi}\left[\frac{\text{Total area of hysteresis loop}}{k_{M,\max}{\Delta_M}^2}\right] \tag{10.1.4}$$

### *10.6.3 Time Period of Isolator Supported Building*

The effective time periods of the isolated building at the design and maximum displacements (FEMA 273 1997) may be taken, respectively, as:

$$T = 2\pi\sqrt{\frac{W}{k_{D\ \min}\cdot g}} \quad \text{and} \quad T = 2\pi\sqrt{\frac{W}{k_{M\ \min}\cdot g}} \tag{10.1.5}$$

where $W$ is the weight of the structure supported by the isolator.

## 10.7 Analysis of a SDOF Frame on Elastomeric Isolators

Consider a SDOF frame supported on isolators as shown in Fig. 10.5a, and its corresponding displacement diagram under a lateral earthquake motion $\ddot{u}_g$ is depicted in Fig. 10.5b. As mentioned earlier, an isolator displacement is non-linear; hence, use of a linear theory is only an approximation which is useful for preliminary design.

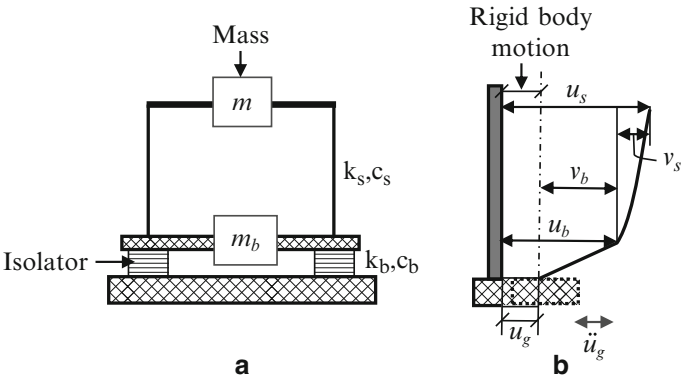


**Fig. 10.5** SDOF system on isolators: (**a**) frame on isolator and (**b**) displacement diagram (Based on Kelly 1997)

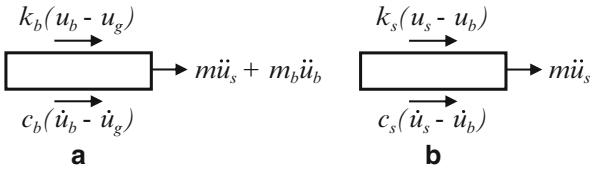


**Fig. 10.6** Free body diagrams: (**a**) base slab and (**b**) roof slab

## *10.7.1 Equation of Motion*

Denoting coefficients by suffix *s* for the structure and *b* for the base isolator:

$k_b$, $k_s$: lateral stiffness of isolator and structure, respectively, considered to be proportional to lateral displacement

$c_b$, $c_s$: damping coefficient for isolator and structure, respectively, considered proportional to lateral velocity

$u_b$, $u_s$: lateral displacement of the base and roof slabs, respectively, with respect to the condition at rest

$m_b$, $m$: mass of base slab and roof, respectively, of a SDOF frame

Free body diagrams for the base slab and frame roof are shown in Fig. 10.6a, b, respectively. From these diagrams, the equations of motion can be written as:

$$m\ddot{u}_s + m_b\ddot{u}_b + c_b\left(\dot{u}_b - \dot{u}_g\right) + k_b\left(u_b - u_g\right) = 0 \tag{10.2.1}$$

$$m\ddot{u}_s + c_s\left(\dot{u}_s - \dot{u}_b\right) + k_s\left(u_s - u_b\right) = 0 \tag{10.2.2}$$

For a base isolated structure, it is important to check storey drifts and isolator displacement. Hence, it is convenient to work with relative displacements for which the actual displacements $u$ are replaced by relative displacements $v$ as follows:

$$v_s = (u_s - u_b), \quad v_b = (u_b - u_g) \tag{10.2.3}$$

This substitution has the advantage that $v_s$ will represent drift and $v_b$ the isolator displacement. Following the procedure detailed by Kelly (1997) and Naeim and Kelly (1999) the above equations lead to,

$$\boldsymbol{M}^*\ddot{\boldsymbol{V}} + \boldsymbol{C}\dot{\boldsymbol{V}} + \boldsymbol{K}\boldsymbol{V} = -\boldsymbol{M}^*\boldsymbol{r}\ddot{u}_g \tag{10.2.4}$$

where

$$\begin{bmatrix} M & m \\ m & m \end{bmatrix} = \boldsymbol{M}^*, \quad \begin{bmatrix} c_b & 0 \\ 0 & c_s \end{bmatrix} = \boldsymbol{C}, \quad \begin{bmatrix} k_b & 0 \\ 0 & k_s \end{bmatrix} = \boldsymbol{K} \quad \begin{Bmatrix} v_b \\ v_s \end{Bmatrix} = \mathbf{V} \text{ and } \begin{Bmatrix} 1 \\ 0 \end{Bmatrix} = \boldsymbol{r} \tag{10.2.5}$$

and $M = m + m_b$.

This forms the equation of linear motion of a SDOF system supported on base isolators.

### *10.7.2 Evaluation of Natural Frequencies*

For evaluating frequencies, damping matrix is ignored and placing $\ddot{u}_g = 0$, Eq. 10.2.4 reduces to

$$\boldsymbol{M}^*\ddot{\boldsymbol{V}} + \boldsymbol{K}\boldsymbol{V} = 0 \tag{10.3.1}$$

This system is identical to the two-DOF system dealt with in Sect. 3.5.1 for which the natural frequencies are given by Eq. 3.8.9. The isolator and superstructure frequencies are taken as $\omega_b$ and $\omega_s$, respectively. Substituting values for the present case, i.e. $m_1 = m_b$, $m_2 = m$, $k_1 = k_b = (m + m_b)\ {\omega_b}^2$, $k_2 = k_s = m{\omega_s}^2$, and introducing a term $\gamma = m/(m + m_b)$ in Eq. 3.8.9, the natural frequencies will be given by

$$\omega^2_{n=1,2} = \frac{\omega_s^2}{2(1-\gamma)}\left[\left(1 + \frac{\omega_b^2}{\omega_s^2}\right) \mp \left\{1 + \left(\frac{\omega_b}{\omega_s}\right)^4 + (4\gamma - 2)\frac{\omega_b^2}{\omega_s^2}\right\}^{1/2}\right] \tag{10.3.2}$$

where $\omega_s$ and $\omega_b$ are frequencies of the superstructure and base slab, respectively.

Noting that normally $\omega_s >> \omega_b$ as pointed out by Kelly (1990), Eq. 10.3.2 leads to the two frequencies being given by

$$\omega_1{}^2 = \omega_b^2 \left\{ 1 - \gamma \left( \frac{\omega_b}{\omega_s} \right)^2 \right\} \quad \text{and} \quad \omega_2{}^2 = \frac{\omega_s^2}{(1-\gamma)} \left\{ 1 + \gamma \left( \frac{\omega_b}{\omega_s} \right)^2 \right\} \tag{10.3.3}$$

Introducing $\lambda = \left( \frac{\omega_b}{\omega_s} \right)^2$,

$$\omega_1{}^2 = \omega_b^2 \{1 - \lambda\gamma\} \quad \text{and} \quad \omega_2{}^2 = \frac{\omega_s^2}{(1-\gamma)} \{1 + \lambda\gamma\} \tag{10.3.4}$$

where $\omega_1$ and $\omega_2$ are the two frequencies for superstructure and isolator vibrating as a combined two-DOF system.

### *10.7.3 Mode Shapes*

The undamped equation for free vibrations is,

$$\boldsymbol{M}^* \ddot{\boldsymbol{V}} + \boldsymbol{K}\boldsymbol{V} = 0 \tag{10.4.1}$$

From Eq. 4.11.1, the relative displacement can be written as,

$$v(t) = \varphi_i q_i(t)$$

it follows that

$$\left| \boldsymbol{K} - \boldsymbol{M}^* \omega_i^2 \right| \varphi_i q_i = 0 \tag{10.4.2}$$

Substituting for $\boldsymbol{K}$ and $\boldsymbol{M}^*$ and noting that since $q_i$ cannot be zero,

$$\left[ \begin{pmatrix} k_b & 0 \\ 0 & k_s \end{pmatrix} - \omega_i^2 \begin{pmatrix} M & m \\ m & m \end{pmatrix} \right] \begin{Bmatrix} \varphi_{bi} \\ \varphi_{si} \end{Bmatrix} = 0 \tag{10.4.3}$$

where

$\omega_i$ : frequency for mode $i$
$\varphi_s$, $\varphi_b$: mode shape coefficients at roof and isolator levels, respectively

Substituting for $k_b$, $k_s$ and $\gamma$, as given above, for the first mode we have

$$-\omega_1^2 \{M\varphi_{b1} + m\varphi_{s1}\} + M\omega_b^2 \varphi_{b1} = 0 \tag{10.4.4}$$

Substituting value of $\omega_1$ from Eq. 10.3.4 and normalizing with respect to the isolator node, the first mode shape is

$$\varphi_1 = \left\{ \begin{matrix} \varphi_{\mathrm{b1}} \\ \varphi_{\mathrm{s1}} \end{matrix} \right\} = \left\{ \begin{matrix} 1 \\ \lambda \\ \hline 1 - \lambda\gamma \end{matrix} \right\} \tag{10.4.5}$$

Proceeding similarly for the second mode we have

$$-\omega_2^2 \, \varphi_{b2} + \left(\omega_s^2 - \omega_2^2\right) \varphi_{\mathrm{s2}} = 0 \tag{10.4.6}$$

and the second mode shape will be

$$\varphi_2 = \left\{ \begin{matrix} \varphi_{b2} \\ \varphi_{s2} \end{matrix} \right\} = \left\{ \begin{matrix} 1 \\ -(1 + \lambda\gamma) \\ \hline \gamma \, (1 + \lambda) \end{matrix} \right\} \tag{10.4.7}$$

### *10.7.4 Roof Displacement*

There will normally be a substantial difference between the degree of isolator damping and that of the SDOF system supported on it. This will result in equations of motion being coupled and will necessitate the use of complex modal analysis. However, for the reader, to get a broad picture of the behaviour of an isolated structure, classical damping is assumed. From Eq. 3.11.10,

$$\ddot{q}_i + 2\omega_i \xi_i \dot{q}_i + \omega_i^2 q_i = -P_i \ddot{u}_g \quad i = 1, 2 \tag{10.5.1}$$

where $P_i = -\dfrac{\varphi_i^{\mathrm{T}} M \, \{r\}}{\varphi_i^{\mathrm{T}} M \varphi_i}$

Solution to the above equation is

$$q_i = -\frac{P_i}{\omega_i} \int_0^t \ddot{u}_g \, (\tau) \, \mathrm{e}^{-\omega_i \xi_i (t-\tau)} \sin \, \omega_i \, (t - \tau) \, d\tau \tag{10.5.2}$$

If the earthquake time history is known, time stepping methods may be used to find $q_{i.}$.

## 10.8 Analysis of a MDOF Frame on Elastomeric Isolators

Consider a multistorey building of total mass $m$ with $n$ degrees of freedom fixed to a base slab which in turn is supported on isolators. This is shown in Fig. 10.7a.

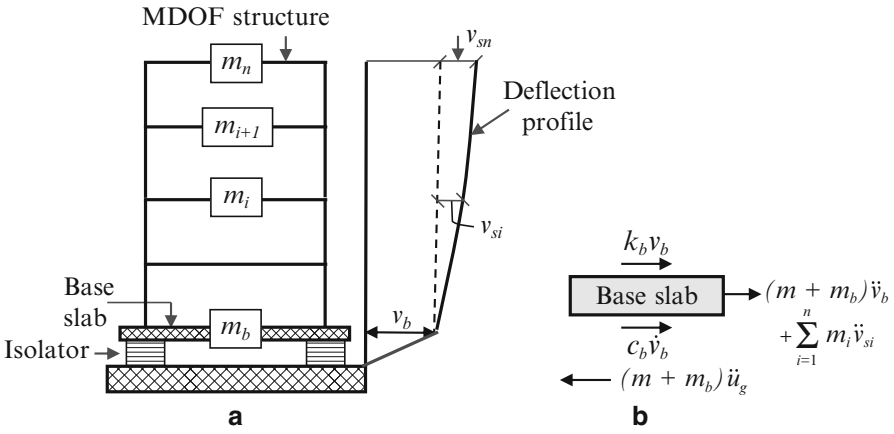


**Fig. 10.7** Model of a MDOF system: (**a**) model and (**b**) free body diagram

### *10.8.1 Equations of Motion*

Force–deformation relation of the superstructure is assumed to be linear. We adopt suffixes *s* and *b* for the superstructure portion and isolator base slab, respectively. It is convenient to write superstructure displacement with respect to the base slab ($v_s$), and that of the isolator slab with respect to the ground ($v_b$). Next, the superstructure is represented by the mass matrix $\boldsymbol{M_s}$, damping matrix $\boldsymbol{C_s}$ and stiffness matrix $\boldsymbol{K_s}$. Considering first that the superstructure is fixed at base slab level, its motion can be written as

$$\boldsymbol{M_s}\ddot{\boldsymbol{V}}_s + \boldsymbol{C_s}\dot{\boldsymbol{V}}_s + \boldsymbol{K_s}\boldsymbol{V_s} = -\boldsymbol{M_s}\{\boldsymbol{r}\}\left(\ddot{u}_g + \ddot{v}_b\right) \tag{10.6.1}$$

Consider the free body diagram for base slab as shown in Fig. 10.7b. Taking into account the shear from the superstructure at base slab level, the equations of motion for the base slab will be

$$\boldsymbol{r}^T\boldsymbol{M_s}\ddot{\boldsymbol{V}}_s + M_t\ddot{v}_b + c_b\dot{v}_b + k_b v_b = -M_t\{\boldsymbol{r}\}\ddot{u}_g \tag{10.6.2}$$

where $M_t$ is the total mass of the *n* DOF superstructure plus the base slab at isolator level, i.e.

$$M_t = \left\{\sum_{i=1}^{n} m_i\right\} + m_b = m + m_b \tag{10.6.3}$$

Above equations define the motion of the entire system which can be represented in matrix form as

$$\boldsymbol{M}^*\ddot{\boldsymbol{V}}^* + \boldsymbol{C}^*\dot{\boldsymbol{V}}^* + \boldsymbol{K}^*\boldsymbol{V}^* = -\boldsymbol{M}^*\{\boldsymbol{r}^*\}\ddot{u}_g \tag{10.6.4}$$

where

$$\boldsymbol{M}^* = \begin{pmatrix} M_t & \boldsymbol{r}^{\mathrm{T}}\boldsymbol{M}_s \\ \boldsymbol{M}_s\{\boldsymbol{r}\} & \boldsymbol{M}_s \end{pmatrix}, \quad \boldsymbol{C}^* = \begin{pmatrix} c_b & 0 \\ \boldsymbol{0} & \boldsymbol{C}_s \end{pmatrix}, \quad \boldsymbol{K}^* = \begin{pmatrix} k_b & 0 \\ \boldsymbol{0} & \boldsymbol{K}_s \end{pmatrix}$$

$$\ddot{\boldsymbol{V}}^* = \begin{Bmatrix} \ddot{v}_b \\ \ddot{\boldsymbol{V}}_s \end{Bmatrix} \quad \boldsymbol{r}^* = \begin{Bmatrix} 1 \\ \boldsymbol{0} \end{Bmatrix} \quad \boldsymbol{V}^* = \begin{Bmatrix} v_b \\ \boldsymbol{V}_s \end{Bmatrix} \quad \text{and} \quad \dot{\boldsymbol{V}}^* = \begin{Bmatrix} \dot{v}_b \\ \dot{\boldsymbol{V}}_s \end{Bmatrix}$$

Undertaking modal analysis for the superstructure considering it as fixed at isolator top level, its equation of motion for mode $i$ (based on Eq. 3.11.10) takes the form

$$\ddot{q}_i + 2\omega_i\xi_i\dot{q}_i + \omega_i^2 q_i = -P_i\left(\ddot{v}_b + \ddot{u}_g\right) \quad i = 1 \text{ to } n \tag{10.6.5}$$

where $P_i$ are the participation factors for the superstructure which are given by

$$P_i = \frac{\varphi_i^{\mathrm{T}}\boldsymbol{M}_s\{\boldsymbol{r}\}}{\varphi_i^{\mathrm{T}}\boldsymbol{M}_s\varphi_i} \tag{10.6.6}$$

in which modal masses are represented by

$$M_i = \varphi_i^{\mathrm{T}}\boldsymbol{M}_s\varphi_i \tag{10.6.7}$$

The equation of motion of the superstructure in mode $i$ can be written as

$$P_i\ddot{v}_b + \ddot{q}_i + 2\omega_i\xi_i\dot{q}_i + \omega_i^2 q_i = -P_i\ddot{u}_g \quad i = 1 \text{ to } n \tag{10.6.8}$$

For the base slab, its motion is represented by

$$\sum_{i=1}^{n} r^{\mathrm{T}}\boldsymbol{M}_s\varphi_i\ddot{q}_i + M_t\ddot{v}_b + c_b\dot{v}_b + k_b v_b = -M_t\ddot{u}_g \tag{10.6.9}$$

Substituting values of $P_i, M_i, c_b, k_b$ into the above equation,

$$\sum_{i=1}^{n}\frac{P_i M_i}{M_t}\ddot{q}_i + \ddot{v}_b + 2\omega_b\xi_b\dot{v}_b + \omega_b^2 v_b = -\ddot{u}_g \tag{10.6.10}$$

Equations 10.6.8 and 10.6.10 define the motion of a MDOF frame supported on isolators.

### *10.8.2 Evaluation of Natural Frequencies*

The classical natural modes can be obtained if we consider the undamped free vibrations. In that case, Eqs. 10.6.8 and 10.6.10 reduce to,

$$\ddot{q}_i + P_i \ddot{v}_b + \omega_i^2 q_i = 0 \tag{10.7.1}$$

$$\sum_{i=1}^{n} \frac{P_i M_i}{M_t} \ddot{q}_i + \ddot{v}_b + \omega_b^2 v_b = 0 \tag{10.7.2}$$

When the oscillators and the MDOF system are both vibrating in one of their common natural modes $\omega$, then each of their elements will vibrate at this frequency (Kelly 1997). Hence introducing

$$q_i = \overline{q}_i e^{i\omega t} \quad \text{and} \quad v_b = \overline{v}_b e^{i\omega t} \quad \text{and} \tag{10.7.3}$$

noting that $\ddot{q}_i = -\omega^2 \overline{q}_i e^{i\omega t}$ and $\ddot{v}_b = -\omega^2 \overline{v}_b e^{i\omega t}$ leads to

$$\left(-\omega^2 + \omega_i^2\right) \overline{q}_i - \omega^2 P_i \overline{v}_b = 0 \tag{10.7.4}$$

and

$$-\omega^2 \sum_{i=1}^{n} \frac{P_i M_i}{M_t} \overline{q}_i + \left(\omega_b^2 - \omega^2\right) \overline{v}_b = 0 \tag{10.7.5}$$

from Eq. 10.7.4,

$$\overline{q}_i = \frac{\omega^2 P_i \overline{v}_b}{\omega_i^2 - \omega^2} \tag{10.7.6}$$

Substituting value of $\overline{q}_i$ from Eq. 10.7.6 into Eq. 10.7.5 and for the condition $\overline{v}_b \neq 0$, as detailed by Kelly (1997), leads to the characteristic equation for $(n+1)$ frequencies as

$$\sum_{\mathrm{i}=1}^{n} \frac{P_i^2 M_i}{M_t} \frac{1}{\left(1 - \dfrac{\omega_i^2}{\omega^2}\right)} = \left(1 - \frac{\omega_b^2}{\omega^2}\right) \tag{10.7.7}$$

$$\text{i.e.} \quad \sum_{i=1}^{n} \frac{\gamma_i}{\left(1 - \dfrac{\omega_i^2}{\omega^2}\right)} = \left(1 - \frac{\omega_b^2}{\omega^2}\right) \quad \text{where} \quad \gamma_i = \frac{P_i^2 M_i}{M_t} \tag{10.7.8}$$

The $(n+1)$ frequencies can be obtained through iteration. Kelly (1997) pointed out that great precision is required while undertaking the calculations, since one of the elements in the stiffness matrix is much smaller in value than the others. For a detailed iteration procedure for obtaining frequencies the reader may refer Kelly (1997). The frequencies can also be obtained directly using any of the standard

eigenvalue methods. However, here again there could be difficulties because one of the diagonal elements of the stiffness matrix is likely to be orders of magnitude smaller than the others.

On obtaining the frequencies, their values can be substituted in Eq. 10.7.5 to yield displacements $\overline{q}_i$ for the $j$ common frequencies ($\omega_j$) given by Eq. 10.7.6, i.e.

$$\overline{q}_i = \frac{{\omega_j}^2 P_i \overline{v}_b}{\omega_i^2 - {\omega_j}^2} \quad i = 1 \text{ to } n; \quad j = 1 \text{ to } N \tag{10.7.9}$$

where $N = (n + 1)$. The above methodology is adopted in the solution of Ex 10.11.2.

## 10.9 Analysis of a SDOF Building Frame on Sliding (FPS) Isolators

A sliding isolation device, in its simplest form, consists of a friction device that can slide over a low friction concave spherical surface. An advantage of this form of isolator over the P-F system is that a self-centring force reduces the residual deflection after a seismic event. The isolator increases a structure's natural period and filters out the primary input earthquake forces (Scheaua 2011) through a frictional interface that also provides damping. These isolators are relatively insensitive to frequency content prevailing in ground motion.

### *10.9.1 Evaluation of Slider Parameters*

Consider an FPS isolator with a spherical surface of radius $R$ supporting a vertical load $W$ (Fig. 10.8). At an instant during its motion, it subtends an angle $\theta$ at the centre of curvature with a horizontal displacement $u$. Because of slider curvature, the load will be raised by an amount $\delta_v$ and a self-centring force $F_r$ will be generated.

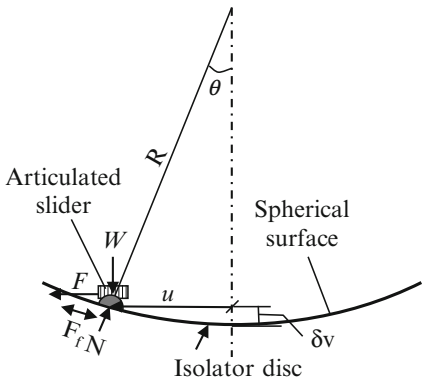


**Fig. 10.8** Model of FPS isolator

Let $N$ be the reaction normal to the disk surface and $\mu$ the coefficient of dynamic friction which, for preliminary analysis, is assumed constant. The frictional force is then given by $F_f = \mu N sgn\ \dot{u}$ where $sgn$ is a signum function, i.e. its value is $+1$ or $-1$ depending on the direction of motion.

#### 10.9.1.1 Inertia Force

Resolving forces vertically and horizontally including inertia force $F$, the equilibrium equations are:

$$W - N\cos\ \theta + F_f \sin\ \theta = 0 \tag{10.8.1}$$

and

$$F - N\sin\ \theta - F_f \cos\ \theta = 0 \tag{10.8.2}$$

Solving these equations,

$$F = W\frac{\sin\ \theta}{\cos\ \theta} + \frac{F_f}{\cos\ \theta} \tag{10.8.3}$$

Noting that for small values of $\theta$,

$$\sin\ \theta = \frac{u}{R},\ \cos\ \theta \simeq 1, \quad \text{and}\ \ F_f = \mu W; \tag{10.8.4}$$

$$F = W\left\{\frac{u}{R} + \mu\right\} \tag{10.8.5}$$

#### 10.9.1.2 Effective Stiffness

Effective horizontal secant stiffness of the isolator mechanism is

$$k_{\text{eff}} = \frac{F}{u} \quad = \frac{W}{u}\left\{\frac{u}{R} + \mu\right\} = \frac{W}{R}\left(1 + \frac{\mu R}{u}\right) \simeq \frac{W}{R} \tag{10.8.6}$$

#### 10.9.1.3 Time Period of Vibration

The circular frequency of vibration $\omega$ is given by the equation,

$\omega = \sqrt{\frac{k_{\text{eff}}}{m}} \simeq \sqrt{\frac{mg}{mR}} = \sqrt{\frac{g}{R}}$ and target period (Hamidi et al. 2003) of motion is given by

$$T_D = 2\pi\sqrt{\frac{R}{g}} \tag{10.8.7}$$

#### 10.9.1.4 Curvature of Sliding Surface

From Eq. 10.8.6, it will be observed that slider stiffness is directly proportional to the supported weight. From Eq. 10.8.7, it will be observed that natural period of vibration is independent of building weight. Thus, once a time period ($T_D$) for an isolator is chosen, the radius of curvature of the spherical surface can be readily determined as

$$R = g\left(\frac{T_D}{2\pi}\right)^2 \tag{10.8.8}$$

#### 10.9.1.5 Estimating Vertical Displacement

From Fig. 10.8, vertical displacement $\delta_v = R\,(1 - \cos\theta)$

Expanding, $\cos\ \theta\ =\ 1\ -\ \frac{\theta^2}{2!}$ (ignoring balance terms), and introducing this value in the above equation, $\delta_v = R\frac{\theta^2}{2}$ and for small values of $\theta$; $\sin\ \theta\ =\ \frac{u}{R}$,

thus

$$\delta_v \cong R\frac{\theta^2}{2} = \frac{u^2}{2R} \tag{10.8.9}$$

#### 10.9.1.6 Re-centring Capability

Assuming that for small values of $\theta$, the inertia force does not affect the normal force at the sliding surface, for the slider to re-centre, the centring force should be greater than the frictional resistance, i.e.

$F_r > F_f$ i.e. $W \sin\ \theta > \mu W \cos\ \theta$ which, for small values of $\theta$, will lead to

$$\frac{u}{R} > \mu \text{ i.e. } u > \mu R \tag{10.8.10}$$

If the above condition is satisfied, the isolator will re-centre.

#### 10.9.1.7 Effective Damping Ratio

The effective damping ratio is given by (Chen and Scawthorn 2003)

**Table 10.1** Damping coefficient at design displacement

| % of critical damping (ξ) | Damping coefficient ($B_D$) |
|---|---|
| 10 | 1.2 |
| 20 | 1.5 |

Extract from FEMA (FEMA 450-1 2003)

$$\xi = \frac{\text{Area of the hysterisis loop}}{4\pi\,(0.5k_{\text{eff}}u^2)} = \frac{4\mu W u}{2\pi k_{\text{eff}}u^2} = \frac{2\mu R}{\pi\,(\mu R + u)} \tag{10.8.11}$$

#### 10.9.1.8 Isolator Displacement

The isolator design displacement can be obtained from (Chen and Scawthorn 2003)

$$\Delta_D = \left(\frac{g}{4\pi^2}\right)\frac{S_D T_D}{B_D} \tag{10.8.12}$$

where

$S_D$ = maximum considered 5 % damped spectral acceleration at 1 s period
$T_D$ = period at target displacement of isolator
$B_D$ = damping factor to reflect the effective damping $\beta_D$ at maximum displacement (ref Table 10.1)

### *10.9.2 Equations of Motion in Different Phases*

Consider a SDOF system supported on a concave isolator surface. Motion of an isolated structure is discontinuous and highly non-linear, which is a challenge for modelling. Its motion is governed by different equations of motion depending on the phase of motion it is in. There are essentially two phases: a non-sliding phase (when the structure does not displace relative to the slider surface) and a sliding phase. The notation adopted here is the same as that stipulated in Sect. 10.7.1.

*Phase I: Non-sliding Phase (or Stick Phase)*

A structure is at rest prior to an earthquake, so the sliding motion always commences from a non-sliding phase. During this phase, the superstructure does not move relative to the isolator surface and can be considered as a fixed based structure. The equations of motion governing this phase are:

$$\text{(a)}\quad \text{for the superstructure}: \quad \ddot{v}_s + 2\xi_s\omega_s\dot{v}_s + \omega_s^2 v_s = -\ddot{u}_g \tag{10.9.1}$$

$$\text{(b)}\quad \text{for the isolator}: \quad \ddot{v}_b = 0;\ \ \dot{v}_b = 0 \ \text{ and } \ v_b = \text{constant} \tag{10.9.2}$$

The principle aim of providing an isolator is to diminish a structure's response such that it stays within the elastic range. Assuming this to be the case and further assuming classical damping, the magnitude of forces, displacements, etc. during this phase can be readily obtained by using solutions for a fixed base structure.

*Phase II: Transition Condition*

The structure will remain in Phase I as long as the sum of tangential components of inertia and restoring forces do not exceed the absolute value of interface friction force (Murnal and Sinha 2000).

$$\text{i.e.} \qquad \left|\left\{m\ddot{v}_s + M_t\ddot{u}_g\right\}\cos\ \theta + M_t g\ \sin\theta\right| \leq \mu M_t g\ \cos\theta \tag{10.9.3}$$

Dividing by $\cos\theta$, the slider will begin to move as soon as

$$\left|m\ddot{v}_s + M_t\ddot{u}_g + M_t g\ \tan\ \theta\right| \geq \mu M_t g \tag{10.9.4}$$

Substituting $\omega^2 = \frac{g}{R}$ from Eq. 10.8.7 and $u \simeq R\ \tan\ \theta$ from Eq. 10.8.4 (for small values of $\theta$), $g$ from Eq. 10.8.7 and introducing $\gamma = \frac{m}{M_t}$, the condition for sliding to commence can be written as

$$\left|\gamma\ddot{v}_s + \ddot{u}_g + \omega^2 u\right| \geq \mu g \tag{10.9.5}$$

Once above condition is met, the slider will commence to slide in a direction opposite to that of the net sum of inertia and restoring forces (Murnal and Sinha 2002) at isolator level. This is termed as the sliding phase in which the slider will remain until relative velocity of the base mass reduces to zero, i.e. $\dot{v}_b = 0$. Thereafter, depending on nature of ground motion, it may revert to a non-sliding phase or it may reverse its direction of sliding or it could also momentarily pause and then continue to slide in the same direction. It is important to have a significant restoring force to prevent permanent displacement offset. Hence, typically, a restoring force mechanism is coupled with such bearings.

For determining the precise juncture at which the slider will change its phase of motion, the reader may refer to a procedure described by Murnal and Sinha (2002), where they have suggested the use of *Time History Analysis* with a small time step of the order of $2 \times 10^{-4}$. This makes it computationally expensive.

*Phase III: Sliding Phase*

During this phase, the structure behaves as a two-DOF system. Utilizing Eq. 10.9.1 and adding a term for inertia force due to base acceleration, the first equation of motion can be expressed as

$$\ddot{v}_s + 2\xi_s\omega_s\dot{v}_s + \omega_s^2 v_s = -\ddot{u}_g - \ddot{v}_b \tag{10.9.6}$$

Considering free body diagram of the base slab, the second equation of motion will be,

$$m\ddot{v}_s + M\ \ddot{v}_b + k_b v_b = -M\ \ddot{u}_g - F_f \tag{10.9.7}$$

Introducing value of $F_f$ from Eq. 10.8.4,

$$\gamma\ddot{v}_s + \ddot{v}_b + \omega_b^2 v_b = -\ddot{u}_g - \mu g\ sgn\,(\dot{v}_b) \tag{10.9.8}$$

The function $sgn\,(\dot{v}_b)$ decides the direction in which the force of friction acts, which in turn depends on direction of the velocity of excitation. The slider will continue sliding until $\dot{v}_b = 0$. Thereafter, the slider motion could be from any one of the possibilities as detailed under *Phase II*. During the approximate analysis, the coefficient of friction is assumed, as a simplification, to be independent of the relative velocity at sliding interface.

## 10.10 Analysis of a MDOF Building Frame on Sliding (FPS) Isolators

Consider a MDOF system (with $N$ degrees of freedom excluding that of the base mass) supported on an FPS isolator. In this case also, the system will experience different phases of motion as described for a SDOF system in Sect. 10.9.2. It is extremely difficult to model the precise behaviour of such an isolator supported structure, firstly, since its motion is highly non-linear as it shifts from the non-sliding to the sliding phase. Secondly, its response depends on many variables such as coefficient of friction, bearing pressure, sliding velocity, etc. Its approximate response for a preliminary analysis may be evaluated as described in the following text.

### *10.10.1 Equation of Motion in Different Phases*

The equations of motion for this system in different phases will be as follows:

*Phase I: Non-sliding Phase* (*or Stick Phase*)

During this phase, the MDOF structure can be considered as a fixed based elastic structure and its response evaluated using modal analysis techniques for classically damped structures as described in Chap. 3. The equation of motion from Eq. 10.6.1, with $\dot{v}_b = \ddot{v}_b = 0$, will be

$$\boldsymbol{M_s}\ddot{\boldsymbol{V}}_s + \boldsymbol{C_s}\dot{\boldsymbol{V}}_s + \boldsymbol{K_s}\boldsymbol{V}_s = -\boldsymbol{M_s}\{\boldsymbol{r}\}\ddot{u}_g \tag{10.10.1}$$

For mode $i$ this equation can be written as (Chaudhry 2004),

$$\ddot{q}_i + 2\omega_i\xi_i\dot{q}_i + \omega_i^2 q_i = -P_i\ddot{u}_g \tag{10.10.2}$$

This equation is identical to Eq. 3.11.10 for a damped vibration of a MDOF system. Its solution can, therefore, be written as

$$q_i(t) = -\frac{P_i}{\omega_d}\int_0^t \ddot{u}_g(\tau)\, e^{-\xi\ \omega(t-\tau)} \sin\ \omega_d\,(t-\tau)\,d\tau \quad i = 1\ \text{to}\ n \qquad (10.10.3)$$

This is the response of the $n$ nodes of a MDOF system vibrating in mode $i$ which can

be represented as $\varphi_i\, q_i$. The total response of the system will be $u_i = \sum_{i=1}^{N} \varphi_i q_i$. This position will continue with the structure remaining at rest until the frictional resistance is overcome.

*Phase II: Transition Condition*

The condition to be met before sliding commences will be similar to Eq. 10.9.4 and can be readily written down as

$$\left|\left\{\sum_{i=1}^{n} m_i\left(\ddot{v}_{si} + \ddot{u}_g\right) + m_b\ddot{u}_g\right\} + M_t\omega_b^2 v_b\right| \geq \mu M_t g \qquad (10.10.4)$$

*Phase III: Sliding Phase*

During this phase, the structure may be analysed as a $(n+1)$ degree of freedom system (Murnal and Sinha 2002) with its equations of motion being similar to Eqs. 10.6.1 and 10.6.2, viz.

$$\boldsymbol{M_s}\ddot{\boldsymbol{V}}_s + \boldsymbol{M_s}\{\boldsymbol{r}\}\ddot{v}_b + \boldsymbol{C_s}\dot{\boldsymbol{V}}_s + \boldsymbol{K_s}\boldsymbol{V_s} = -\boldsymbol{M_s}\{\boldsymbol{r}\}\ddot{u}_g \qquad (10.10.5)$$

$$\boldsymbol{M_s r^T}\ddot{\boldsymbol{V}}_s + M_t\ddot{\boldsymbol{v}}_{\boldsymbol{b}} + k_b v_b = -M_t\{\boldsymbol{r}\}\ddot{u}_g - \mu M_t g\ sgn\,(\dot{v}_b) \qquad (10.10.6)$$

These equations of motion can be expressed in matrices of the order $n+1$ as

$$\boldsymbol{M^*}\ddot{\boldsymbol{V}} + \boldsymbol{C}\dot{\boldsymbol{V}} + \boldsymbol{K}\boldsymbol{V} = -\boldsymbol{M^*}\{\boldsymbol{r^*}\}\ddot{u}_g - \mu M_t g\{\boldsymbol{r^*}\}sgn\,(\dot{v}_b) \qquad (10.10.7)$$

where

$$\boldsymbol{M^*} = \begin{pmatrix} \boldsymbol{M_s} & \boldsymbol{M_s r_s} \\ [\boldsymbol{M_s r_s}]^T & M_t \end{pmatrix},\quad \boldsymbol{C} = \begin{pmatrix} \boldsymbol{C_s} & 0 \\ \boldsymbol{0} & 0 \end{pmatrix},\quad \boldsymbol{K} = \begin{pmatrix} \boldsymbol{K_s} & 0 \\ \boldsymbol{0} & k_b \end{pmatrix},\quad \ddot{\boldsymbol{V}} = \begin{Bmatrix} \ddot{\boldsymbol{V}}_s \\ \ddot{v}_b \end{Bmatrix}$$

$$\dot{\boldsymbol{V}} = \begin{Bmatrix} \dot{\boldsymbol{V}}_s \\ \dot{v}_b \end{Bmatrix},\quad \boldsymbol{V} = \begin{Bmatrix} \boldsymbol{V}_s \\ v_b \end{Bmatrix} \quad \boldsymbol{r^*} = \begin{Bmatrix} \boldsymbol{0} \\ 1 \end{Bmatrix}$$

The function $sgn\,(\dot{u}_b)$ decides the direction in which the force of friction acts which in turn depends on the direction of ground motion excitation. In this phase, all natural modes participate in the response with the fundamental frequency (which

is the predominant one) being that of the isolator. The behaviour of the structure is highly non-linear and complex particularly as it moves from the sliding phase to the non-sliding phase, which is beyond the scope of this book. Ex 10.11.3 explains the procedure for sizing of an isolator spherical disk.

## 10.11 Illustrative Examples

***Ex 10.11.1*** A SDOF system founded on rock is to be supported on elastomeric isolators. Its fixed base fundamental period is 0.51 s with a damping of 5 %. The roof mass is $p$ and that of the base raft above isolator level is $9p$. Estimate the stiffness required of the proposed isolators (as a fraction of superstructure stiffness) if the spectral acceleration in the fundamental mode is to be limited to 20 % of its fixed base value. For purposes of this example, assume damping of the isolated structure to be 10 %.

**Solution** For a fixed base SDOF system with 5 % damping and $T = 0.51$ s, the value of $S_a/g$ is 1.96 from response spectrum of IS 1893. Since the spectral acceleration desired is to be limited to 20 % of this value, the target acceleration coefficient is $S_a/g = 1.96 \times 0.2 = 0.392$.

For 10 % damping, the reduction factor is 0.8 as per Table 3 of IS 1893. Hence the value of $S_a/g$ with 5 % damping should be $0.392/0.8 = 0.49$. This will correspond to the desired acceleration considering 10 % damping. The corresponding period would be 2 s and the fundamental frequency $\omega_1 = \frac{2\pi}{2} = 3.14$ rad/s

For the SDOF system with $T = 0.51$ s, the frequency will be $\omega_s = 12.32$ rad/s.

From Sect. 10.7.2,

$$k_b = (m + m_b)\,\omega_b^2, \quad k_s = m\omega_s^2, \quad \text{and} \quad \gamma = m/(m + m_b) = p/10p = 0.1$$

Taking $\alpha = k_b/k_s$; $\omega_b^2/\omega_s^2 = \alpha\gamma$, Eq. 10.3.2 becomes

$$\omega_1^2 = \frac{\omega_s^2}{2(1-\gamma)}\left[(1+\alpha\gamma) - \sqrt{(1-\alpha\gamma)^2 + 4\alpha\gamma^2}\right]$$

Substituting values,

$$3.14^2 = \frac{12.32^2}{(2 \times 0.9)}\left[(1 + 0.1\alpha) - \sqrt{(1-0.1\alpha)^2 + 0.04\alpha}\right]$$

Solving, $\alpha = 0.656$,

that is, isolator stiffness required is 65.6 % of that of the superstructure.

***Ex 10.11.2*** A two storey framed structure is supported on a base slab which rests on isolators. The mass at each level and stiffness characteristics of the supports are

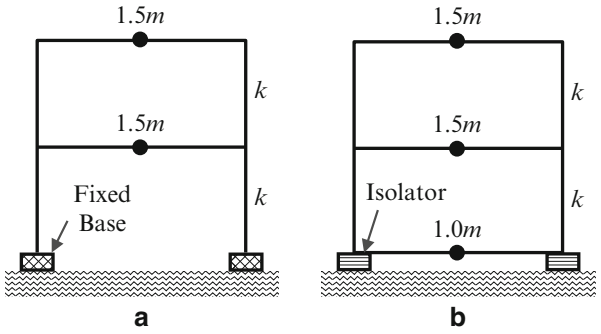


**Fig. 10.9** Moment frame: (**a**) fixed base and (**b**) on isolators

shown in Fig. 10.9. Take mass $m$ as 16,310 kg, stiffness $k = 10.115 \times 10^6$ N/m and isolator period as 2.5 s. Determine

(a) The frequencies of the two storey structure without base slab and isolators as if it was fixed at the base slab level (Fig. 10.9a).
(b) The three natural frequencies of the two-storey structure supported on isolators (Fig. 10.9b).
(c) The % reduction in first mode seismic base shear with 5 % damping as a result of placing the frame on isolators.
(d) Demonstrate that natural frequencies evaluated in item (b) above satisfy the characteristic equation 10.7.8.

**Solution**

(a) *Fixed Base Structure* (Fig. 10.9a).

The mass and stiffness matrices will be as follows:

$$\boldsymbol{M} = \begin{pmatrix} 1.5m & 0 \\ 0 & 1.5m \end{pmatrix} \quad \text{and} \quad \boldsymbol{K} = \begin{pmatrix} 2k & -k \\ -k & k \end{pmatrix}$$

Substituting values, the characteristic equation becomes

$$10^6 \begin{pmatrix} 20.23 & -10.115 \\ -10.115 & 10.115 \end{pmatrix} - \omega^2 \begin{pmatrix} 24{,}465 & 0 \\ 0 & 24{,}465 \end{pmatrix} = 0$$

which yields the two natural frequencies,

$$\omega_1 = 12.567 \text{ rad/s and } \omega_2 = 32.900 \text{ rad/s} \tag{10.11.1}$$

The mode shapes can be readily determined and these are,

$$\varphi_1 = \begin{Bmatrix} 1.000000 \\ 1.618034 \end{Bmatrix} \quad \text{and} \quad \varphi_2 = \begin{Bmatrix} 1.000000 \\ -0.618034 \end{Bmatrix}$$

**Table 10.2** Reduction in base shear

| Item | Fixed base | On isolator |
|---|---|---|
| $\omega_1$ (rad/s) | 12.567 | 2.478 |
| $T_1$(s) | 0.5 | 2.536 |
| $S_a/g$ | 2 | 0.394 |
| Mass (kg) | 3 m | 4 m |
| Base shear (N) | 6.000 mg | 1.576 mg |

(b) *Isolator Supported Structure*

Isolator bay period is 2.5 s. Hence, $\omega_b = 2.5133$ rad/s. From Sect. 10.7.2, the stiffness of isolator bay will be $k_b = (m + m_b)\,\omega_b{}^2$, i.e.

$$k_b = 4 \times 1.631 \times 10^4 \times 2.5133^2 = 0.41209 \times 10^6 \text{ N/m}$$

The mass and stiffness matrices are

$$\boldsymbol{M} = \begin{pmatrix} m & 0 & 0 \\ 0 & 1.5m & 0 \\ 0 & 0 & 1.5m \end{pmatrix}, \boldsymbol{K} = \begin{pmatrix} k + k_b & -k & 0 \\ -k & 2k & -k \\ 0 & -k & k \end{pmatrix}$$

Substituting values and solving, the frequencies are
$\omega_1 = 2.47768$ rad/s, $\omega_2 = 22.71360$ rad/s and $\omega_3 = 36.92867$ rad/s (10.11.2)

(c) *Reduction in Base Shear*

Base shear for the fundamental mode for the two storey fixed base frame and that supported on an isolator are obtained as shown in Table 10.2. Thus, reduction in base shear by placing the frame on an isolator

$$= \frac{(6.0 - 1.576)}{6.0} \times 100 = 73.7\ \%$$

(d) *Satisfaction of the Characteristic Equation*

The characteristic Eq. 10.7.8 is,

$$\sum_{i=1}^{n} \frac{\gamma_i}{\left(1 - \dfrac{\omega_i^2}{\omega_j{}^2}\right)} = \left(1 - \frac{\omega_b^2}{\omega_j{}^2}\right)$$

Represented as $A = B$

***Evaluation of $P_i$ and $\gamma_i$***, Utilising Eqs. ***in*** Sect. 10.8.1

$$\varphi_1^T \boldsymbol{M}\,\{\boldsymbol{r}\} = \{1.0 \quad 1.618034\} \begin{pmatrix} 24,465 & 0 \\ 0 & 24,465 \end{pmatrix} \begin{Bmatrix} 1.0 \\ 1.0 \end{Bmatrix} = 64,050.201 \text{ kg}$$

$$M_1 = \varphi_1^T \boldsymbol{M} \varphi_1 = \{1.0 \quad 1.618034\} \begin{pmatrix} 24,465 & 0 \\ 0 & 24,465 \end{pmatrix} \begin{Bmatrix} 1.000000 \\ 1.618034 \end{Bmatrix} = 88,515.201 \text{ kg}$$

$$P_1 = \frac{64,050.201}{88,515.201} = 0.7236067; \quad \gamma_1 = \frac{{P_1}^2 M_1}{4m} = 0.71041;$$

Proceeding similarly,

$P_2 = 0.276393$, $M_2 = 33809.798$ kg and $\gamma_2 = 0.039598$ and the three frequencies for the isolator supported structure are given in (b) above as $\omega_{j1} = 2.47768$ rad/s, $\omega_{j2} = 22.71360$ rad/s and $\omega_{j3} = 36.92867$ rad/s

$$A = \sum_{i=1}^{2} \frac{\gamma_i}{\left(1 - \frac{\omega_i^2}{{\omega_j}^2}\right)} = \frac{\gamma_1}{\left(1 - \frac{\omega_1^2}{{\omega_j}^2}\right)} + \frac{\gamma_2}{\left(1 - \frac{\omega_2^2}{{\omega_j}^2}\right)}$$

For the first frequency of the isolator supported frame ($\omega_{j1}$), $\omega_{j1}^2 = 6.1389$

The square of the fixed base frame frequencies from Eq. 10.11.1, are given by $\omega_1^2 = 157.9230$ and $\omega_2^2 = 1,082.42$.

Substituting values for the first common frequency,

$$A_1 = \sum_{i=1}^{2} = \frac{0.71041 \times 6.1389}{(6.1389 - 157.9231)} + \frac{0.0396 \times 6.1389}{(6.1389 - 1,082.421)} = -0.0290$$

Proceeding similarly, $A_2 = 0.9877, A_3 = 0.9954$ and for the first common frequency,

$$B_1 = \left(1 - \frac{\omega_b^2}{{\omega_j}^2}\right) = 1 - \left(\frac{2.5133^2}{6.1389}\right) = -0.0290$$

Proceeding similarly, $B_2 = 0.9877, B_3 = 0.9954$

This demonstrates that $\omega_1$, $\omega_2$ and $\omega_3$ satisfy the characteristic equation obtained by the method used in Sect. 10.8.2. Clearly, the same solution can be readily obtained by solving the characteristic equation in the first place, provided the matrix elements are not highly imbalanced.

***Ex 10.11.3*** A rigid spherical (FPS) slider supports a vertical load of 600 kN. The target period at design conditions $T_D = 2.4$ s with a design horizontal displacement of 250 mm. Damping reduction factor may be taken from Table 10.1. With a coefficient of friction $\mu = 0.06$ and spectral design acceleration coefficient $S_D = 0.5$, determine:

(a) Dimensions of spherical disc at design displacement
(b) Effective stiffness
(c) Effective damping ratio
(d) Whether the slider has self-centring capability
(e) Lateral force at design displacement to be resisted by substructure and superstructure, respectively, with a reduction factor $R = 2.0$

(a) *Dimensions of Disc*

From Eq. 10.8.8, the radius of curvature of disc

$$R = g\left(\frac{T_D}{2\pi}\right)^2 = (9.81)\left(\frac{2.4}{2\pi}\right)^2 = 1.43 \text{ m}$$

Provide a disk with a radius $R = 1.45$ m

From Eq. 10.8.9, $\delta_v = \dfrac{u^2}{2R} = \dfrac{0.25^2 \times 1,000}{2 \times 1.45} = 21.5$ mm

Provide a disk depth of 25 mm

With reference to Fig. 10.8; $\cos\ \theta = \dfrac{R - \delta v}{R} = \dfrac{(1.45 - 0.025)}{1.45} = 0.9828$

Disc diameter $= 2R \sin\theta = 2 \times 1.45 \times 0.1849 = 0.536$ m

Spherical disc required at design displacement will be of 600 mm diameter having a radius of curvature of 1.45 m and a depth of 25 mm

Check that for the diameter provided, vertical depth $\geq \delta_v$

Check $\dfrac{(0.6/2)^2}{2 \times 1.45} \times 1,000 = 31$ mm $> 25$ mm

(b) *Effective Stiffness*

From Eq. 10.8.6,

$$k_{\text{eff}} = \frac{W}{R}\left[1 + \frac{\mu R}{u}\right] = \frac{600}{1.45}\left[1 + \frac{0.06 \times 1.45}{0.25}\right] = 558 \text{ kN/m}$$

(c) *Effective Damping Ratio*

From Eq. 10.8.11,

$$\xi = \frac{2\mu R}{\pi\ (\mu R + u)} = \left[\frac{2 \times 0.06 \times 1.45}{\pi\ \{(0.06 \times 1.45) + 0.25\}}\right] = 0.1645$$

that is, damping ratio is 16.5 %

(d) *To Check Self-centring Capability*

$u = 250$ mm and $\mu R = 0.06 \times 1.45 \times 1{,}000 = 87$ mm

From Eq. 10.8.10 since $u > \mu R$, the slider will be able to re-centre itself.

(e) *Design Displacement*

From Table 10.1, for $\xi = 16.5$ % damping, the reduction factor is 1.4

From Eq. 10.8.12, slider horizontal displacement will be

$$\Delta_D = \frac{g}{4\pi^2}\frac{S_D T_D}{B_D} = \frac{9810}{4\pi^2}\left[\frac{0.5 \times 2.4}{1.4}\right] = 213 \text{ mm} < 250 \text{ mm}$$

Minimum base shear $V_b = k_{\text{eff}}.\ u$

$= 558 \times 0.25 = 139.5$ say 140 kN

Base shear for the superstructure $= V_b/R = 140/2 = 70$ kN

# Chapter 11
# Performance-Based Seismic Design

**Abstract** Performance-based seismic design, which is a relatively new concept, came into existence as a means to ascertain the likely performance of an existing building structure during an earthquake. However, this approach is equally applicable to new buildings being designed. Herein is explained why there is a growing consensus among designers to follow this approach as a replacement of the existing force-based design procedures. It is explained as to what constitutes a performance objective which relates the desired performance level to a perceived hazard level. The analytical approach calls for a nonlinear seismic analysis for which the simpler nonlinear static method is often adopted. This is termed as the pushover analysis which is described in detail. Both subsets of this method, viz., the capacity spectrum method and the seismic coefficient method, are explained in detail. The merits and limitations of this method of analysis are also pointed out. The recent drive for use of performance-based approach for design as well as assessment of building structures has led to rapid developments to enhance the reliability of this analytical approach.

**Keywords** Pushover analysis • Performance-based design • Performance levels • Nonlinear static procedure • Capacity spectrum method • Seismic coefficient method

## 11.1 Introduction

Performance-based seismic design is a relatively new concept which was initially developed for use in predicting the upgrade strategy needed for existing buildings. However, it is equally applicable to checking the design of new buildings and is a paradigm shift in seismic engineering design moving away from the *prescriptive code* approach. It is presently an evolving methodology with the key difficulties being to arrive at globally acceptable precise definitions of performance objectives and to quantify performance levels.

It is now accepted that lateral displacements, and not forces alone, invariably lead to structural damage during an earthquake. This understanding has propelled the demand for performance-based design. While enumerating the salient features of such a design principle, the concept of a pushover analysis is covered in detail. Both the popular methods used to conduct a *pushover analysis* are explained.



S. Manohar, S. Madhekar, *Seismic Design of RC Buildings*, Springer Transactions in Civil and Environmental Engineering, DOI 10.1007/978-81-322-2319-1_11

## 11.2 Description of the Procedure

The emphasis in a performance-based approach is to ascertain how a building is likely to reliably perform in terms of permissible damage against a selected potential hazard. This procedure helps in deciding the likely hierarchy of resistance of different structural elements, towards dissipation of seismic energy. The description given below is for regular building structures without overriding torsional or higher mode effects (ATC - 40 1996).

### *11.2.1 Need for This Approach*

Much effort, both theoretical and experimental, has been devoted over the last six decades to find solutions to minimise seismic damage. It was observed during examination of the after-effects of earthquakes that, in several cases, the buildings survived earthquakes that were estimated to generate inertia forces many times greater than the elastic strength of the structures. It was realised that the presence of ductility enabled the buildings to dissipate seismic energy without failure and consequently that an elastic force-based design concept was inadequate. There was a need to revisit the elastic design assumption that all structures of a given type have the same ductility and that their members can be forced to yield simultaneously.

It was concluded that the ability of a structure to survive an earthquake is more a matter of its inherent inelastic displacement capacity rather than its initial yield strength. Elastic force-based methods cannot predict the possible extent of inelastic deformations in a structure or its components nor can they predict the locations where critical displacements are likely to occur. While elastic analysis provides a good estimate of the elastic capacity of a structure, it cannot represent the deterioration in elastic capacity as well as failure mechanism of a structure during progressive yielding (ATC - 40 1996). Secondly, there is a drawback that the response reduction factors used in force-based design are independent of building period and ground motion characteristics. As a result, a need arose for an alternative approach resulting in the development of a performance-based design method.

In this method, the concept is to lay down performance objectives for the structure. Such objectives relate the degree of damage acceptable (performance level) against a specified seismic hazard (hazard level). It is considered that deformations are a better measure than forces to assess likely performance of a structure during an earthquake. Hence, a structure and its components are analysed for maximum permissible inelastic displacements (termed target displacements or performance points) rather than purely for their strength. It is only after the structure meets the stipulated performance criteria that it is checked for strength at global and component levels. The availability of sophisticated analytical tools and the advent of large computing capability have enabled the introduction and progress of this approach.

Nonetheless, force-based design approach will continue to be used because it is a procedure designers are familiar with, and displacement demand design criteria are still being fine-tuned. Secondly, for loads other than seismic, it is generally sufficient to design structures to have adequate stiffness and strength. Hence, for the present, structures continue to be designed for elastic forces but with an inbuilt provision which will make the structure ductile.

### *11.2.2 Performance Levels*

For generations, concrete structures have been designed primarily to avoid failure in flexure, shear, compression, tension, bond, buckling and anchorage. It is now recognised that during a major seismic event (hazard), some degree of damage is inevitable. The extent of damage tolerable is normally specified through performance levels (FEMA 424 2004). There is a growing realisation that the structure as a whole should be checked for adequacy under various performance levels. Both the performance and hazard levels are extremely difficult to quantify due to uncertainties associated with stipulating primarily the following:

- The magnitude, duration and frequency characteristics of the next likely earthquake
- The nature and variability of ground strata between the possible earthquake focus and the location of the structure
- The precise ground motion signatures for which the structure should be designed
- Specifying characteristics such as stiffness, ductility and damping capacities of structural elements
- Estimating the cost of damage repair, business downtime and other losses relevant to a particular damage and the cost that society is willing to bear to repair a projected damage
- The approximations inherent in structural modelling for dynamic analysis

The damage suffered by a building could be both structural and nonstructural, but herein we shall deal with only structural performance. Structural systems and their members must possess sufficient stiffness to limit deflections, lateral drift, vibration, etc. which could have an adverse effect on the intended utilisation and performance of a building. The performance level is normally stipulated in terms of limit states. While there could be many limit states for which a structure could be designed, there is no globally agreed specific stipulation of what constitutes an acceptable level of damage (i.e. performance level) for which structures are to be designed. The three commonly employed limit states are shown in Fig. 11.1 and are described below based on ATC 58-2 (2003).

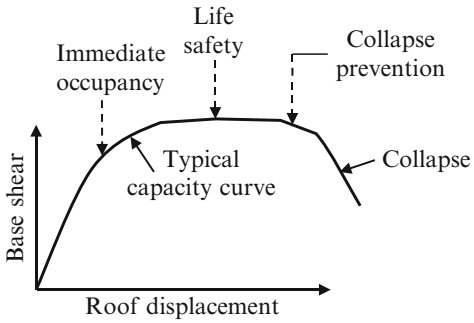


**Fig. 11.1** Qualitative performance levels (Limit States)

#### 11.2.2.1 Immediate Occupancy

As its name implies, under immediate occupancy limit state, post-earthquake condition shall be such that the building can be immediately and safely occupied and be functional. This means that no member of the primary frame should have yielded and members retain their elastic stiffness and strength. There could be hairline cracking of concrete, minor cracking and spalling of plaster in brick infill walls. Risk of life-threatening injury is very low, and the building should be operational with minimal repairs. Transient drift may be limited to 1 % with negligible permanent drift (FEMA 273 1997). Nonstructural elements should not be damaged.

In shear walls, there can be hairline cracks $<1.5$ mm wide and in coupling beams up to 3 mm. There can be some evidence of sliding at construction joints. Transient drift shall be $<0.5$ % with negligible permanent drift. Reinforced masonry shear walls could experience cracks up to 3 mm wide but no out-of-plane offsets. Transient and permanent drift could be up to 0.2 %. Foundations may experience minor settlement but negligible tilting. Overall, there may be a need for some minor structural repairs but not necessarily before reoccupation.

#### 11.2.2.2 Life Safety

Under life safety limit state, the primary structure would have suffered significant distress, e.g. beams may be damaged due to spalling (Priestley et al. 2007) of concrete cover and wide cracks may appear at location of plastic hinges requiring injection grouting to prevent corrosion, but such damage would be repairable. There will remain some margin against either partial or total structural collapse. Egress routes would not be extensively blocked but may be impaired by lightweight debris. Stairways would be safe for use. There could be extensive cracking and some degree of crushing of brick infill walls, but the walls would stay in place.

A few structural elements and components could be severely damaged but without the likelihood of falling debris causing life-threatening injury, and there would remain some margin against even partial structural collapse. The structure may need to be provided with temporary bracings, and it should be possible to

repair the structure, though expensive. Here, plastic hinges could form at identified locations with rotations being within acceptable limits, and there should not be any yielding at other locations nor should there be any brittle failure. Transient and permanent drift in frame members may be 2 % and 1 % (FEMA 273 1997), respectively.

There could be distress at some locations in the boundary elements of shear walls with bucking of rebars and damage of concrete in coupling beams and sliding at joints and damage around openings. Transient and permanent drift in shear walls may be 1 % and 0.5 %, respectively. Reinforced masonry would experience extensive cracking (<6 mm wide) throughout the wall with some isolated crushing. The transient or permanent drift may be <0.6 %. Total settlement of foundations is to be <50 mm and differential settlements to be <12 mm in a length of 10 m.

The probability of a threat to life will remain extremely low. However, the problem remains in representing this picture to the owner who is more interested to know the likely downtime, cost of repairs and degree of risk to occupants.

#### 11.2.2.3 Collapse Prevention

During this condition, extensive damage to the structure may have occurred including heavy cracking with large rotations at plastic hinges and some permanent drift. However, supports should not have yielded, and they should be able to sustain permanent gravity loads. Major amount of cracking in flexure and shear, damage in boundary elements of shear walls with buckling of reinforcement and severe damage of coupling beams may have occurred. There could be extensive cracking and crushing of brick infill walls, and these could dislodge themselves due to out-of-plane bending. However, there should not be a collapse or loss of life. The structure would not be safe to reoccupy, as aftershock activity could induce collapse.

This condition demands that the system must possess appropriate ductility and redundancy such that the inertia loads may get distributed and structural collapse avoided although the structure per se may not be repairable. During seismic analysis, the $P$-$\Delta$ effects need to be included so also material overstrength. This is an extremely important design criterion since it relates to the preservation of life which has always remained the principal concern in seismic design. Drift may be limited to 4 %, transient or permanent.

The readers are reminded that the above values are indicated for their broad information. In any particular case where it is proposed to use this method, expert advice should be sought.

### *11.2.3 Hazard Levels*

The likely ground motion and its characteristics are difficult to quantify although it is a critical part of any performance-based design. While a comprehensive

**Table 11.1** Performance objectives

| Event | Performance level<br>Limit state to which it usually corresponds | Hazard level<br>Recurrence interval years | <br>Probability of its exceedance |
|---|---|---|---|
| Frequent | Operational | 43 | 50 % in 30 years |
| Occasional | Immediate occupancy | 72 | 50 % in 50 years |
| Design earthquake | Life safety | 475 | 10 % in 50 years |
| Maximum earthquake | Collapse prevention | 2,475 | 2 % in 50 years |

Source: ATC - 40 (1996)

site-specific seismic hazard analysis is desirable, it is a highly complex exercise, requiring involvement of experts from many fields and is outside the scope of this book. In simple terms, a seismic hazard is commonly expressed as the maximum likely magnitude of an earthquake capable of occurring at the site, qualified with a probability of its exceedance in a given time frame. For simplistic practical design purposes, this is represented in codes through the zone factor and response spectrum as in IS 1893.

### *11.2.4 Quantifying Performance Objectives*

A performance objective is a statement that identifies the desired building performance for an expected seismic ground motion. The performance stipulated may be a single level one or a multilevel one, and it would depend on many factors such as type of occupancy, cost of repairing damage, life safety, etc. At the structural level, a performance objective is a coupling of anticipated damage state (i.e. performance level) against a likely idealised seismic hazard level.

A performance-based design aims at creating an appropriate design solution which meets the given objectives. There could be many performance levels that a designer may want to examine for a range of seismic hazard levels which can be termed as dual or multiple performance objectives. These should be agreed upon among the stakeholders prior to design. Commonly reported performance and hazard levels are given in Table 11.1 for information (ATC - 40 1996).

### *11.2.5 Preliminary Building Design*

The process commences with choosing a performance level in terms of a limit state with corresponding limiting deflections, rotations, deformations and other important responses. Next, the hazard level can be chosen in terms of zone factors given in IS

1893. Once a performance level and corresponding hazard level are chosen (i.e. a performance objective is defined), preliminary member sizes are selected based on a trial elastic design and engineering judgment.

Thereafter, a mathematical model of the building is developed. It should be loaded with gravity and other live and imposed loads as per codal requirements. The seismic inertia forces should then be added. A linear dynamic eigenvalue analysis is undertaken to arrive at frequencies and mode shapes. Thereafter, member forces, moments and displacements are evaluated for immediate occupancy performance level. With these results, a preliminary check on member dimensions, inter-storey drift ratios and other responses is made. If that is satisfactory, then the design can progress further; otherwise, member sizes may need to be altered.

The structure is configured such that yielding and inelastic behaviour of members occur at identified locations in certain preselected members. This is an attempt to ensure that the structure, if it fails, should be restrained to do so according to a preferred collapse mechanism. By doing so, these members will permit other elements to remain essentially elastic while responding to an earthquake.

## 11.3 Nonlinear Static Procedure (NSP) – *Pushover Analysis*

To estimate the inelastic displacements, a time history analysis is the most accurate method. However, it is computationally expensive and needs a large effort to carefully scrutinise the resulting voluminous output. Through extensive studies, approximate nonlinear methods were evolved to predict inelastic behaviour of structures. Using such a method, the three primary steps in a performance assessment are:

(a) Capacity evaluation
(b) Demand evaluation
(c) Determining the performance

Each of these steps is discussed below.

### *11.3.1 Capacity Evaluation*

A comprehensive nonlinear time history evaluation is the ultimate solution for the analysis of a complex building structure. As mentioned earlier, such an analysis is dogged by many uncertainties in terms of accuracy of input ground motion, member characteristics, modelling limitations and analysis of an essentially three-dimensional structure under cyclic loading. A capacity curve (i.e. pushover curve) described below is a representation of inelastic behaviour of a SDOF system expressed as base shear vs roof displacement. What an LSP method is in analysing approximately an elastic dynamic problem; the pushover method is to analysing a dynamic inelastic problem.

#### 11.3.1.1 Description of a Pushover Analysis

Pushover analysis is a simple and elegant static method for evaluating the nonlinear response of a SDOF system to strong ground motion. Although this method does not have a rigorous theoretical foundation (Krawinkler 1996), it is recognised as a useful tool in seismic engineering to obtain nonlinear force–displacement relationship of a structure and thus determine the load-carrying capacity of an inelastic system. Admittedly such a procedure would be an approximate one, but it serves the purpose because it can capture the essential features of inelastic behaviour of a structure and thus has an important bearing in predicting satisfactory performance of the system.

For analysis, a mathematical model is displaced by monotonically increasing lateral force or displacement, in gradual discrete increments (pushing the structure), until either a target displacement is exceeded or the collapse condition of a building is reached. At each discrete interval, the effect of existing gravity loads is taken into account. The base shear at each incremental loading is plotted against corresponding lateral roof displacement. Also, at each stage, the resulting internal deformations and forces are determined and recorded, i.e. in the pushover curve, sequential elastic analysis is inbuilt. The resulting load displacement relationship is termed the capacity curve.

Recent advent of performance-based design has pushed the nonlinear static pushover analysis procedure to the forefront. It has gained wide acceptance and is considered a valid alternative (of course with limitations) to dynamic nonlinear analysis of building frames to evaluate likely structural performance of existing and new buildings under seismic conditions. Pushover analysis is applicable to structures whose response is dominated by its first mode of vibration. In recent years, several methods have been proposed, with limited success, to enhance the capability of this method so that it can adequately account for higher mode effects.

#### 11.3.1.2 Merits and Limitations of a Pushover Analysis

In recent years, pushover analysis is gaining popularity for predicting the likely inelastic performance of a building. Some of the important merits and limitations of this method are summarised below:

*Merits*

- It is a simple procedure compared to nonlinear dynamic analysis.
- It can determine the load-carrying capacity of an inelastic system and the likely failure mechanism under progressive yielding.
- It provides an insight into the nonlinear behaviour of a structure which cannot be obtained either from elastic – static or dynamic – analysis.
- It can help identify the locations of potential weakness prevailing in a structure where failure could occur.
- It provides a good estimate of local and global inelastic demands for inter-storey drifts.

- A designer can observe the sequential formation of plastic hinges.
- It provides indirect information about completeness and adequacy of load paths within the structure as a whole.
- It gives an estimate of force demands on potentially brittle elements.
- It enables a designer to compare the capacity of a structure against the seismic demand at a given performance level.

*Limitations*

- It is assumed that the mode shape remains constant throughout the analysis regardless of the quantum of deformation.
- This method is not recommended where irregularities are present either vertical or horizontal or where there is uneven mass distribution or where torsional coupling prevails.
- It is reported that it does not provide a reliable estimate of deformation demands when higher mode effects are significant.
- Force distribution is based on the fundamental mode shape, and it is held constant.
- Much work still needs to be done until this method can be applied to asymmetric 3D systems, with stiffness or mass irregularities.
- The technique needs to be extended to address combined lateral and vertical ground motion effects.
- It is not applicable to tall buildings where significant portion of lateral drift is controlled by axial deformation of columns as compared to raking deformation.

In this method, it is assumed that the response of a MDOF structure can be related to that of a SDOF structure as described in Sect. 11.3.1.4. These aspects are discussed below.

#### 11.3.1.3 Selecting a Lateral Load Pattern

In the conventional method of nonlinear static analysis, the lateral storey inertial load pattern is maintained invariant with time although in a vibrating structure, the distribution of storey inertial forces varies with time. Secondly, the maximum of different responses do not occur simultaneously, and hence it follows that no single inertial load pattern will yield maximum responses. Some codes call for two separate nonlinear static analyses to be conducted each using different invariant lateral load vectors for load distribution at floor levels. Then the envelope of their responses can be used to verify performance. One distribution could be a uniform lateral load pattern distribution consisting of lateral forces at each level proportional to the total mass at that level. The other may be the first mode distribution provided that the modal mass in this mode exceeds 75 % of the total mass of the structure. This is generally a valid assumption for a structure with a fundamental vibration period up to (ATC - 40 1996) about 1 s.

In recently proposed adaptive methods, the lateral inertial load pattern depends on instantaneous mode shapes of the structure determined from eigenvalue analysis at each stage as the structure deforms. These methods, though they have merits, do not provide a distinct advantage (Antoniou and Pinho 2004) to offset their heavy computational demand in relation to that for a fixed load pattern. Hence, they are not included here. It may be mentioned that this is a subject of ongoing research directed towards improving predictive capabilities of a pushover analysis.

#### 11.3.1.4 Characterisation of an Equivalent SDOF System

The next step in the design process is the evaluation of maximum displacement at roof level. Herein, it is assumed that the dynamic response of a MDOF system in an uncoupled mode can be predicted from that of a corresponding equivalent SDOF system with an elastoplastic stiffness. This implies that the dynamic response of a MDOF system in a particular mode is determined with the shape factor $\varphi$ remaining constant throughout the deformation process.

For a MDOF system, the uncoupled equation of motion for mode $i$ using mode orthogonality is given by Eq. 3.11.10 as

$$\ddot{q}_i + 2\omega_i \xi_i \dot{q}_i + \omega_i^2 q_i = -P_i \ddot{u}_g \tag{11.1.1}$$

Substituting an equivalent SDOF system (identified with *) for mode $i$ of the MDOF system, its equation of motion from Eq. 3.7.1 would be

$$m_i^* \ddot{u}_i^* + c_i^* \dot{u}_i^* + k_i^* u_i^* = -m_i^* \ddot{u}_g^* \tag{11.1.2}$$

Substituting $c_i^* = 2m_i^* \xi_i \omega_i$; $\quad k_i^* = m_i^* \omega_i^2$ and dividing by $m_i^*$,

$$\ddot{u}_i^* + 2\omega_i \xi_i \dot{u}_i^* + \omega_i^2 u_i^* = -\ddot{u}_g^* \tag{11.1.3}$$

Comparing Eqs. 11.1.1 and 11.1.3,

$$q_i = P_i u_i^*$$

Since lateral displacement of a MDOF system in mode $i$ is given by $u_i = q_i \varphi_i$, it follows that

$$u_i = P_i u_i^* \varphi_i \tag{11.1.4}$$

Thus, to obtain the lateral roof displacement of a MDOF system ($u_i$), the displacement for a SDOF system $u_i^*$ should be multiplied by $P_i \varphi_i$. If $P_1$ and $M_1$ are the participation factor and mass of the first mode, respectively, then it can be readily shown that

$$\text{Displacement at roof of a SDOF system i.e. } u_1^* = \frac{u_{\text{roof}}\ (\text{MDOF system})}{P_1 \varphi_{1,\text{roof}}} \tag{11.1.5}$$

With this, the pushover curve displacement of a MDOF system in the fundamental mode can be transformed into that for a SDOF system.

### *11.3.2 Demand Evaluation*

For practical design, the country has been divided into four zones depending on the perceived magnitude of a future earthquake in these zones. For each zone, the code specifies a coefficient based on the maximum credible earthquake (MCE) at the reference location. Design is based on 50 % MCE, and hence the zonal coefficient (Z) is halved. Thereafter, depending on the empirical time period of the vibrating building, the seismic acceleration coefficient can be read off the codal response spectrum. This coefficient is modified to account for nature of founding soil and degree of damping inherent in the structure. This modified coefficient is then used to evaluate the seismic demand in terms of forces induced and deformations experienced by various structural members.

### *11.3.3 Conducting a Pushover Analysis*

The reader is urged to carefully study the quality literature widely available on this subject (ATC - 40 1996; FEMA 356 2000; FEMA 440 2005; Spacone and Martino 2009) and particularly the stipulations and limitations of this method before its use for analysis. The procedure outlined below is for a MDOF system with a fixed base, i.e. soil structure interaction effects are not included. Only the first mode is considered where the modal mass in the first mode exceeds 75 % of the total seismic mass of the structure. Basic steps involved in undertaking a pushover analysis of a moment resistant framed building are:

1. Load an elastic mathematical model of the structure with gravity loads and determine the approximate values of desired parameters, e.g. forces, moments, displacements, etc., of the frame elements. This gravity load effect has to be included with each increment of lateral load during a pushover analysis.
2. Conduct an eigenvalue analysis to determine fundamental frequency and mode shapes. The latter should be normalised for 1.0 at roof level.
3. With the fundamental frequency evaluated, determine corresponding seismic acceleration from the response spectrum in IS 1893.
4. For the specified hazard level (i.e. zone factor), obtain base shear and from there, the storey forces. For these forces, make a preliminary check on inter-

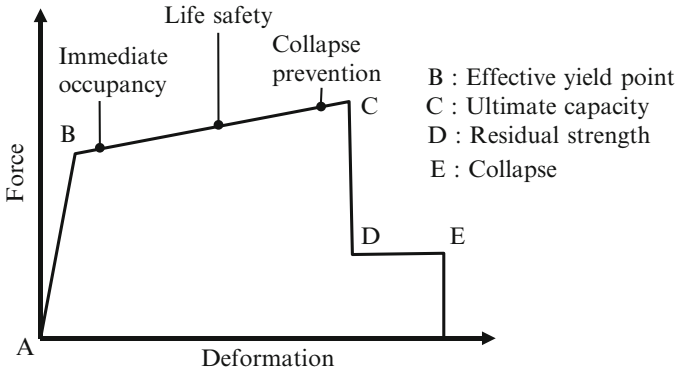


**Fig. 11.2** Force deformation characteristic for a hinge

storey drifts and forces in members. If there is any deficiency, the member sizes may be modified and modal analysis conducted again.

5. Thereafter, obtain base shear for the fundamental mode. This base shear should be distributed as forces at storey levels. In the subsequent analysis, this load pattern is considered as invariant.
6. In the model, incorporate nonlinear load–deformation characteristics of individual members. For instance, for a moment resisting frame, based on experience and engineering judgment, select likely locations in beams and columns where inelastic energy dissipating conditions may occur. At these locations, introduce hinges with preselected moment rotation characteristics. Hinges with default properties are available in computer programmes to choose from. A typical force–deformation relationship for a hinge is shown in Fig. 11.2
7. Later, the structural elements are designed and detailed for energy dissipation, and the balance structural elements are designed for strength. Modelling is an important step. It must capture the inherent nonlinear strength and deformation properties of each element of the structure.
8. Pushover analysis can be conducted as a force controlled or a displacement controlled approach. In the former case, the model is subjected to the invariant load pattern in small increments. Similarly, in a displacement controlled option, the roof is displaced in small incremental values.
9. Load or displacement increments are to be continued gradually until the yield strength of one of the elements is reached. At each incremental step, the base shear, displacements, rotations, member forces, moments and other parameters are recorded as these will be required while conducting a performance check.
10. The stiffness properties of the yielded member are modified (i.e. to their post-yield behaviour) to reflect the consequence of its yielding. The analysis is then continued incorporating post-yield behaviour of members as they progressively yield.

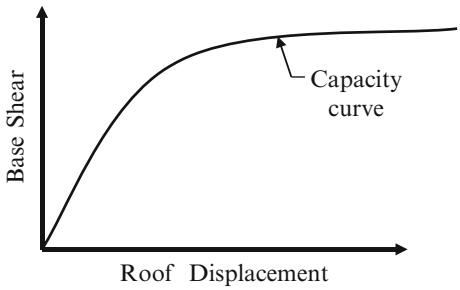


**Fig. 11.3** Pushover curve

11. This process is to be continued until an ultimate limit is reached, viz., instability from $P$-$\Delta$ effects or deformation beyond the estimated target displacement of the control node (i.e. mass location at roof level) or loss of gravity load-carrying capacity (ATC - 40 1996). On reaching the ultimate limit, the values at each incremental stage are plotted as a base shear vs roof displacement curve which is the pushover or capacity curve as shown in Fig. 11.3.
12. Obtain the responses of interest from the pushover analysis corresponding to the target displacement.

The control node is located at the centre of the mass at the roof of a building. If the building has a penthouse, then the control node shall be positioned at penthouse floor. Pushover analysis provides the capacity curve in a form of lateral roof displacement against base shear. It also provides a designer with an opportunity to know the sequence of element yielding. The performance evaluation flow chart is shown in Fig. 11.4. There are many approaches to arrive at the performance point of the system, and the two prominent methods are (1) capacity spectrum method, which is a form of equivalent linearization technique, and (2) seismic coefficient method. Both the methods are described below:

## 11.4 Capacity Spectrum Method

It is a graphical method for evaluation of seismic performance of structures. It is based on the assumption that maximum elastic plus inelastic displacement of a SDOF oscillator can be approximated from the maximum deformation of a linear elastic SDOF system with enhanced period and damping (FEMA 440 2005). Both these enhanced values depend on the location of the performance point which in turn is dependent on the enhanced values. Hence, an iterative process has to be employed. The reader is urged to carefully study specialist literature available on this subject to fully appreciate the nuances, approximations and limitations of this method prior to its use (ATC - 40 1996).

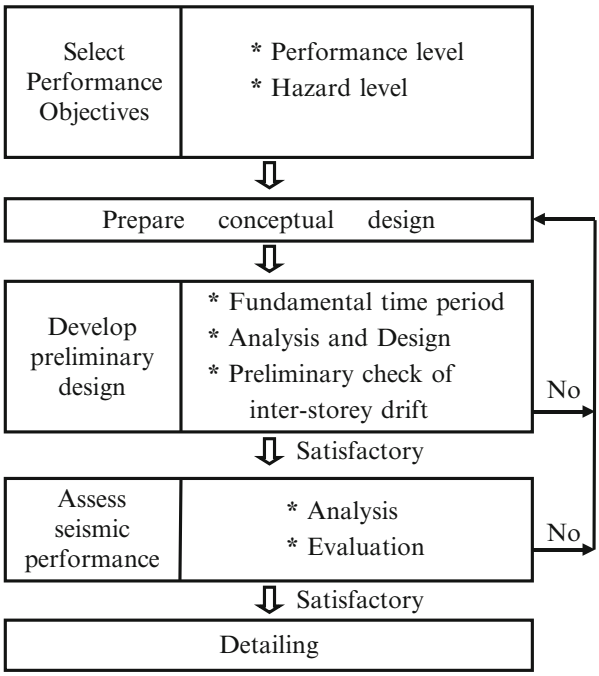


**Fig. 11.4** Flow chart of performance-based design

### *11.4.1 Conversion of Spectra to ADRS Format*

In this method, a performance point is the displacement at which the demand required meets the capacity available (Fig. 11.5). This can be achieved graphically for which both the response spectrum (which is in terms of acceleration vs period) and the capacity curve from a pushover analysis (which is in terms of base shear vs roof displacement) need to be converted to a capacity spectrum format. This resulting format is in the spectral acceleration vs spectral displacement domain, i.e. as acceleration–displacement response spectra (ADRS) format.

### *11.4.2 Conversion of Demand Spectrum*

The demand needs are to be determined from the estimated hazard level from a detailed site-specific analysis. However, for routine design work, the appropriate codal elastic response spectrum forms the base. Such a plot depicts the *acceleration* ($S_a/g$) vs *time period* ($T$). For points on the elastic response spectrum, one can read the acceleration coefficient $S_a/g$ against each time period $T$. Multiplying the former

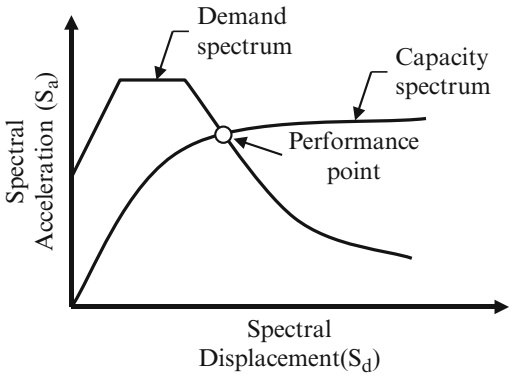


**Fig. 11.5** Performance point

by $g$, the spectral acceleration $S_a$ is obtained. The time period can be converted to frequency as $\omega = 2\pi/T$ and from Eq. 4.1.9, the spectral displacement is given by

$$S_d = \frac{S_a}{\omega^2} = \frac{S_a T^2}{4\pi^2} \tag{11.2.1}$$

This enables the demand response spectra to be plotted in the acceleration vs displacement (i.e. in the ADRS) format.

### *11.4.3 Conversion to Capacity Spectrum*

For converting the pushover curve, which is in a *displacement vs base shear* format, into ADRS format, each point on the pushover curve needs to be converted to the first mode spectral value. From Eq. 11.1.5 (Oguz 2005)

$$\Delta_{\text{SDOF}} = \frac{\Delta_{\text{roof-MDOF}}}{P_1 \varphi_{1,\text{roof}}} \quad i.e. \quad S_{d1} = \frac{\Delta_{\text{roof}}}{P_1 \varphi_{1,\text{roof}}} \tag{11.2.2}$$

This enables the roof displacement to be represented in the spectral format. The lateral base shear in the first mode ($V_1$) will be the product of mass in the first mode and first mode acceleration, i.e.

$$V_1 \text{ (for MDOF system)} = M_1 \left\{ \frac{S_{a1}}{g} \right\} .g$$

and if $M$ is the total seismic mass of the loaded structure, then

$$\frac{M_1}{M} \left\{ \frac{S_{a1}}{g} \right\} = \frac{V_1}{W}$$

Introducing $C_m$ as the mass factor $= M_1/M$ and noting that the total load $W = M.g$

$$\frac{S_{a1}}{g} = \frac{V_1/W}{C_m} \tag{11.2.3}$$

With the aid of the above equations, the pushover curve can be represented as a capacity spectrum. The demand and capacity spectra in ADRS format are shown in Fig. 11.5.

### *11.4.4 Locating the Performance Point*

Steps in arriving at the performance point are enumerated below:

To begin with, draw the response spectrum (for 5 % damping) in ADRS format (refer Sect. 11.4.2) to represent the demand spectrum. On this, superimpose the pushover capacity curve also in ADRS format (refer Sect. 11.4.3).

*Step 1: Select an Initial Performance Point*

An initial performance point is selected on the capacity spectrum. This can be based on judgment or as is usually done on the equal displacement criteria (Fig. 11.6). For the latter, a tangent is drawn to the initial portion of the capacity spectrum to meet the demand spectrum (with 5 % damping) at a point which defines the initial period $T_o$. A perpendicular dropped from there will meet the capacity spectrum at the initial performance point $p_1$ with coordinates $\mathrm{ap}_1$, $\mathrm{dp}_1$.

*Step 2: Modify the Capacity Spectrum*

The capacity spectrum needs to be converted to a bilinear form to estimate effective damping and consequent reduction in spectral demand. This is achieved by first drawing a straight line from the origin at the initial stiffness of the building. Then drawing another line backwards from the trial performance point such that the areas above and below the capacity spectrum (viz., $A_1$ and $A_2$ as shown in Fig. 11.6) are approximately equal. This identifies the point $d_y$, $a_y$ which represents the yield displacement and acceleration, respectively, as depicted in Fig. 11.6.

*Step 3: Modify the Demand Spectrum*

When a structure progresses into the inelastic range, then the damping increases due to hysteretic damping ($\xi_o$). This can be converted to an equivalent viscous damping as explained in ATC - 40 (1996). The value of $\xi_o$ has to be further multiplied by a factor $\kappa$ to allow for departure of the hysteresis curve from the ideal. Values of $\kappa$ are also given in ATC - 40. This value has to be added to the prevailing viscous damping (normally 5 %), and the total effective damping (%) will be

$$\xi_{\mathrm{eff}} = \kappa \xi_o + 0.05 \tag{11.2.4}$$

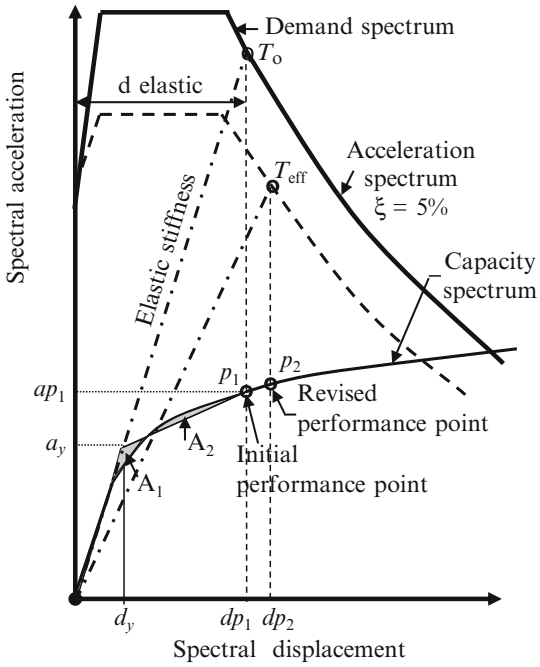


**Fig. 11.6** Capacity spectrum method

The ADRS spectral acceleration demand has to be reduced to account for the increase in damping (when the structure is pushed into the inelastic range) which, in this procedure, is taken as the sum of viscous damping and hysteretic damping, i.e. $\xi_{\text{eff}}$. This reduction is accomplished by using spectral reduction factors given in ATC - 40. The revised demand curve is shown in dash lines in Fig. 11.6.

*Step 4: Iteration to Arrive at a Performance Point*

Thereafter, determine the next estimate of maximum displacement demand ($d_{p2}$) by dropping a perpendicular from the intersection of the radial effective period ($T_{\text{eff}}$) with the acceleration spectra duly modified for effective damping ($\xi_{\text{eff}}$). If the new performance point ($dp_2$) is close (i.e. to within acceptable tolerance) from the previous chosen value ($dp_1$), then it identifies the performance point, and the corresponding acceleration is the maximum acceleration. ATC - 40 (1996) stipulates that the acceptable tolerance is given by $0.95dp_1 \leq dp_2 \leq 1.05dp_1$.

If the above condition is not met, then repeat the process from drawing a new bilinear representation of the capacity curve using the revised performance point $p_2$. This process is to be continued until the new performance point chosen is close to the previous performance point within the tolerance indicated above.

## 11.5 Seismic Coefficient Method

This method is based on statistical evaluation of results of time history analysis of different types of SDOF models. Initially an elastic displacement is estimated which is equal to the pseudo-acceleration divided by the square of the fundamental circular frequency of the structure. This is then enhanced to predict approximately the inelastic displacement. Alternatively, the permissible drift index may be utilised. Thereafter, a pushover curve is generated using available computer software. The first step in the analysis is the evaluation of equivalent stiffness and equivalent time period of the structure.

### *11.5.1 Equivalent Stiffness and Equivalent Time Period*

The pushover curve represents a nonlinear relationship between base shear and roof displacement of the control node. The latter is the centre of mass at the roof level. This is converted to an idealised bilinear force displacement curve in order to obtain the effective lateral stiffness and effective yield strength $V_y$ of the building. This is achieved by a graphical iterative procedure. A line segment is drawn (to represent roughly the post-elastic stiffness) by judgment from the target displacement where the structural strength has levelled off. This is the upper line segment. The lower line segment commences at the origin. The ordinate where the upper and lower line segments meet is the effective base shear at first yield $V_y$. This location also determines the yield displacement $\delta_y$.

These line segments have to be adjusted such that the following two requirements are satisfied:

(a) Areas intercepted by the two line segments above and below the pushover curve are approximately equal, i.e. ($A_1 = A_2$), as shown in Fig. 11.7.
(b) During the iteration process, it needs to be ensured that the lower line segment of the bilinear curve cuts the pushover curve at 60 % of the effective yield shear $V_y$ (FEMA 356 2000). This process is iterative because the value of $V_y$ is not known at the beginning.

Through this process, the elastic lateral stiffness ($K_i$) and effective lateral stiffness ($K_e$) are identified as well as the yield shear $V_y$. The effective fundamental period ($T_e$) is taken as (FEMA 356 2000),

$$T_e = T_i \sqrt{\frac{K_i}{K_e}} \quad \text{where} \tag{11.3.1}$$

$K_i$: elastic lateral stiffness of the building taken as the initial stiffness of the pushover curve

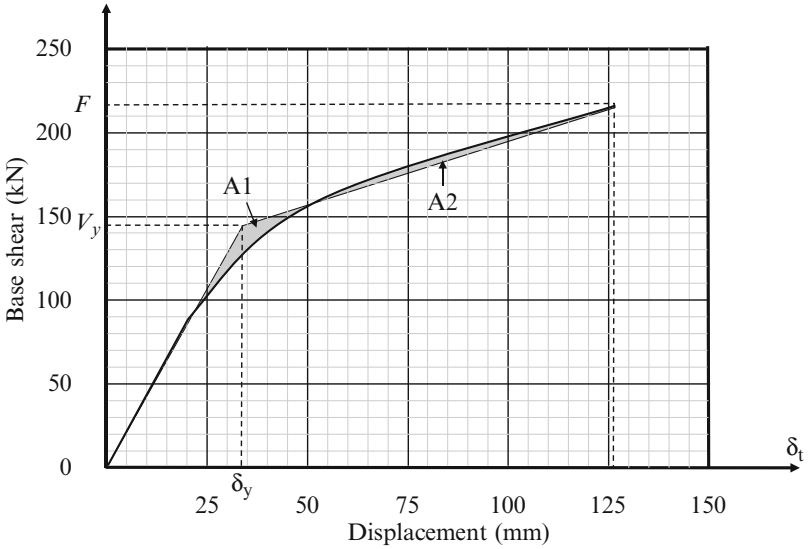


**Fig. 11.7** Capacity curve

$K_e$: effective lateral stiffness of the building defined as the slope of a line that connects the point of intersection of the above referred two line segments with the origin of the pushover curve

$T_i$: elastic fundamental period (in s) calculated by elastic dynamic analysis

The effective stiffness represents linear stiffness of the equivalent SDOF system. This effective period is then adopted to read off corresponding acceleration coefficient $S_a/g$ from the elastic acceleration response spectrum for 5 % damping. This value is then converted to spectral displacement by using Eq. 4.1.8

$$S_d = \frac{T_e^2}{4\pi^2}\frac{S_a}{g}.g \tag{11.3.2}$$

### *11.5.2 Prediction of Target Displacement*

The above spectral displacement is then modified by a set of empirically derived coefficients to arrive at total elastic plus inelastic displacement which is termed as the target displacement. The target displacement is intended to represent the maximum likely roof displacement of the structure at its centre of mass during the design earthquake associated with a certain performance level. In this method, the target displacement is taken as (FEMA 356 2000)

$$\delta_t = C_0.C_1.C_2.C_3 \frac{T_e^2}{4\pi^2} \left\{ \frac{S_a}{g} \right\} g \tag{11.3.3}$$

$C_o$: coefficient that converts spectral displacement of an equivalent SDOF system to roof displacement of a MDOF system. It is taken as the first mode participating factor ($P_1$) (FEMA 440 2005) when using a fixed first mode lateral load pattern with the mode shape normalised as 1.0 at the roof.

$C_1$: enhancement ratio for peak inelastic displacement of a SDOF system to peak elastic displacement of the system (Goel 2011) which may be taken as (FEMA 356 2000)

$$\begin{aligned} &= 1.0 \text{ for } T_e \geq T_s \\ &= [\{1 + (R-1)\, T_s / T_e\}] / R \text{ for } T_e < T_s \\ &= 1.5; \text{ for } T_e < 0.1 \text{ s} \end{aligned}$$

$C_2$: factor to represent effect of stiffness degradation and strength deterioration = 1.0 for non-degrading systems. For degrading systems, the recommendations in FEMA 440 (2005) may be followed.

$C_3$: factor to make allowance for dynamic $P$-$\Delta$ effect. Since commonly for structures, the post-yield stiffness is positive (i.e. $\alpha \geq 1$), this value may be taken as 1.0.

$T_s$: characteristic period of the response spectrum. It is defined as the period at the transition from a constant pseudo-acceleration region to constant pseudo-velocity region of the response spectrum (sec).

$V_y$: yield strength of the building estimated from pushover curve of the building (N).

$R$: ratio of elastic to yield strength of the structure $= \frac{S_a/g}{V_y/W}.C_m$

$C_m$: effective mass factor to account for higher mode mass participation effects. For a concrete moment frame, its value may be taken as 0.9 and as 1.0 if fundamental period >1.0 s (FEMA 356 2000).

$\alpha$: ratio of post-yield stiffness to effective elastic stiffness with a bilinear stiffness characteristic.

$W$: effective seismic weight (N).

For a three-storey frame as in Fig. 11.8, a typical pushover curve using the seismic coefficient method is shown in Fig. 11.7, and the progressive formation of plastic hinges can be observed as indicated in Fig. 11.9.

### *11.5.3 Evaluation of Performance*

As mentioned earlier, the demand is given by the amount of displacement at the performance point in the capacity spectrum method and the target displacement in the seismic coefficient method. Member displacements and forces computed at this displacement are used as the inelastic demand and checked against available capacities.

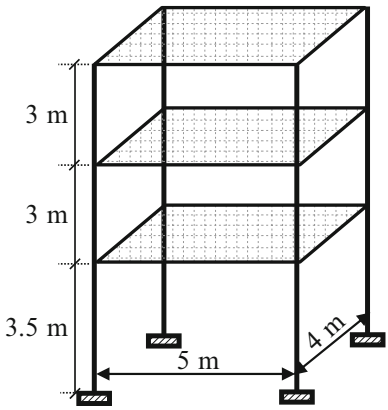


**Fig. 11.8** Three-storey frame

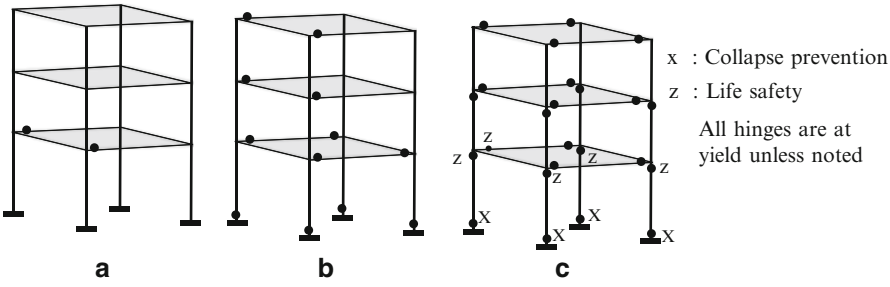


**Fig. 11.9** Progressive hinge formation

It can then be ascertained whether the responses meet global performance objective, e.g. stability against lateral loads, inter-storey drifts, plastic hinge rotations, floor displacements, strength, slab–column connections in flat plates, etc. Thereafter, the check can be at component level, viz., beams, columns, floor slabs, diaphragms, foundations and other structural elements. This portion of the design process needs to be done with utmost care supported by sound engineering judgment.

# References


ACI 318-08 (2009) Building code requirements for structural concrete and commentary. ACI, Farmington Hills, MI, USA

Agarwal P, Shrikhande M (2006) Earthquake resistant design of structures. PHI Learning Pvt Ltd., Delhi

Anderson D, Brzev S (2009) Seismic design guide for masonry buildings. Canadian Concrete Masonry Producers Association, Toronto

Antoniou S, Pinho R (2004) Advantages and limitations of adaptive and non adaptive force based pushover procedures. J Earthq Eng 8:497–522

Aoyama H (ed) (2001) Design of modern high rise RC structures, vol 3. Imperial College Press, London

Ari Ben Menahem (1995) A concise history of mainstream seismology, origins, legacy and perspectives. Bull Seismol Soc Am 85(4):1202–1225

Arnold C, Reitherman R (1982) Building configuration and seismic design. Wiley, New York

ASCE (2005) Minimum design loads for buildings and other structures, ASCE standard 7-05. ASCE, Reston

ATC - 40 (1996) Seismic evaluation and retrofit of concrete buildings, vol 1, Report No SSC 96-01. Seismic Safety Commission, Redwood City

ATC 58-2 (2003) Preliminary evaluation of methods for defining performance. ATC, Redwood City

ATC 72-1 (2010) Modelling and acceptance criteria for seismic analysis and design of tall buildings. PEERC and ATC, Redwood City

Basu D, Salgado R, Prezzi M (2008) Analysis of laterally loaded piles in multilayered soil deposits. JTRP tech report, Purdue University, West Lafayette, Indiana

Beards CF (1996) Structural vibration – analysis and damping. Butterworth – Heinemann, Oxford

Bertero RD, Bertero VV (1999) Redundancy in earthquake resistant design. ASCE J Struct Eng 125:81–88

Betbeder-Matibet J (2008) Seismic engineering. ISTE Ltd/Wiley, London/Hoboken

BIS (2000) IS 456, Plain and reinforced concrete – code of practice

BIS (2001) IS 4326- Ed 3.2, Earthquake resistant design and construction of buildings – code of practice

BIS (2002a) IS 1893 (Part1), Criteria for earthquake resistant design of structures – part 1

BIS (2002b) IS 1905, Code of practice for structural use of unreinforced masonry

BIS (2002c) IS 2222 Ed 5.1, Specification for burnt clay perforated building bricks

BIS (2003) IS 13920, Ductile detailing of RC structures subjected to seismic forces – code of practice




S. Manohar, S. Madhekar, *Seismic Design of RC Buildings*, Springer Transactions in Civil and Environmental Engineering, DOI 10.1007/978-81-322-2319-1

BIS (2005) IS 2185 (Part 1), Concrete masonry units – Specifications part I-Hollow and solid concrete blocks
BIS (2013) IS 15988, Seismic evaluation and strengthening of existing RC buildings – guidelines.
Bommer JJ, Martinez-Pereira A (1999) The effective duration of earthquake strong motion. J Earthq Eng 3(2):127–172
Booth E, Key D (2006) Earthquake design practice for buildings. Thomas Telford Ltd., London
Bozorgnia Y, Bertero VV (eds) (2004) Earthquake engineering, from engineering seismology to performance based engineering. CRC Press, New York
Brandow GE, Hart GC et al (1993) Design of masonry structures. Concrete Masonry Association of California & Nevada, Citrus Heights
Brooke N, Megget L, Ingham J (2005) Factors to consider in the use of grade 500E long. reinf. etc. J Struct Eng Soc NZ 18(1):14
Brzev S (2007) Earthquake resistant confined masonry construction. NICEE, Kanpur
Bull DK (2004) Understanding the complexities of designing diaphragms in buildings for earthquakes. Bull NZ Soc Earthq Eng 37(2):70–88
Bull JW (ed) (2009) Linear and non linear numerical analysis of foundations. Spon Press, New York
Chaudhry N (2004) Earthquake resistant design of structures using friction isolation systems. M. Tech. thesis, IIT, Mumbai
Chen WF, Scawthorn C (eds) (2003) Earthquake engineering handbook. CRC Press, New York
Chopra AK (1995) Dynamics of structures. Prentice Hall of India, New Delhi
Choudhury D (2007) Computations of seismic earth pressures for design of earth retaining structures. In: Bhattacharya S (ed) Design of foundations in seismic areas. NICEE, Kanpur
Chowdhury I, Dasgupta SP (2007) Dynamic earth pressure on rigid unyielding wall under earthquake force. Indian Geotech J 37(2):81–93
Clarke JA, Duncan JM (2001) Revision of the CLM spreadsheet for lateral load analysis of deep foundations. Virginia Polytechnic Institute, Blacksburg
Clough RW, Penzien J (2003) Dynamics of structures. Computers and Structures, Berkeley
Collier CJ, Elnashai AS (2001) A procedure for combining vertical and horizontal seismic action effects. J Earthq Eng 5(4):521–539
Dasgupta MK, Murty CVR et al (2003) Seismic shear design of RC structural walls – Part II, Proposed improvements in IS 13920, 1993 provisions. Indian Concrete Journal (ICJ) 77(11):105–113, Mumbai
Datta TK (2010) Seismic analysis of structures. Wiley, Singapore
Department of Defense, USA (1997) Soil dynamics and special design aspects. Department of Defense, USA, Washington, DC
Dhileep M, Bose PR (2008) A comparative study of missing mass correction methods for RS method of seismic analysis. Comput Struct 86:2087–2094
Dowrick D (2009) Earthquake resistant design and risk reduction. Wiley, Chichester
Elghazouli AY (ed) (2009) Seismic design of buildings to Eurocode 8. Spon Press, London
Elnashai AS, Di Sarno L (2008) Fundamental of earthquake engineering. Wiley, Chichester
Elnashai AS, Mwafy AM (2002) Overstrength and force reduction factors of multistorey RC buildings. Struct Des Tall Build 11:329
Elnashai AS, Papazoglou AJ (1997) Procedures and spectra for analysis of RC structures subjected to strong vertical earthquake loads. J Earthq Eng 1(1):121–155
Englekirk RE (2003) Seismic design of reinforced and precast concrete buildings. Hoboken, New Jersey
Erberik MA, Elnashai AS (2003) Seismic vulnerability of flat slab structures. Tech report Dec, DS9 project, University of Illinois. MAE Center, University of Illinois at Urbana, Champaign
Fardis MN (2009) Seismic design, assessment & retrofitting of concrete bldgs. Springer, London
Fardis MN, Panagiotakos TB (1997) Seismic design and response of bare & masonry infilled RC bldgs. Part II -Infilled structures. J Earthq Eng 1(3):475–503
FEMA 273 (1997) NEHRP guidelines for seismic rehabilitation of buildings. FEMA, Washington, DC

FEMA 274 (1997) NEHRP commentary on guidelines for seismic rehabilitation of buildings. FEMA, Washington, DC
FEMA 306 (1998) Evaluation of earthquake damaged concrete and masonry wall buildings. FEMA, Washington, DC
FEMA 356 (2000) Prestandard and commentary for the seismic rehabilitation of buildings. ASCE and FEMA, Washington, DC
FEMA 424 (2004) Design guide for improving school safety during earthquakes etc. FEMA, Washington, DC
FEMA 440 (2005) Improvement of non linear static seismic analysis procedures. FEMA, Washington, DC
FEMA 450-1 (2003) NEHRP recommended provisions for seismic regulations of new bldgs and other structures. FEMA, Washington, DC
FEMA 451B (2007) Inelastic behaviour of materials and structures. FEMA, Washington, DC
FEMA 454 (2006) Designing for earthquakes – a manual for architects. FEMA, Washington, DC
FEMA P 750 (2009) NEHRP recommended seismic provisions for new buildings and other structures. FEMA, Washington, DC
Gaiotti R, Smith BS (1989) P – delta analysis of building structures. ASCE J Struct Eng 115: 755–770
Goel RK (2011) Variability and accuracy of target displacement from NSPs. ISRN Civil Eng 2011:1–16. doi:10.5402/2011/582426
Goel RK, Chopra AK (1993) Seismic code analysis of buildings without locating centers of rigidity. ASCE, J Struct Eng 119(10)
Hamidi M, El Naggar MH et al (2003) Seismic isolation of buildings with sliding concave foundation (SCF). Earthq Eng Struct Dyn 32:15–29
Hanks TC, Kanamori H (1979) A moment magnitude scale. J Geophys Res 84(B5):2348–2350
Hart GC, Wong K (2000) Structural dynamics for structural engineers. Wiley, New York
Idriss IM, Boulanger RW (2008) Soil liquefaction during earthquakes, MNO 12. EERI, Oakland
Jain SK (2003) Review of Indian seismic code IS 1893(Part1):2002. ICJ 77:1414
Jain SK, Murty CVR (2005) Proposed draft provisions and commentary on IS 1893 (Part 1). IITK/GSDMA, EQ 05 v4, EQ15, v3 – IIT, Kanpur
Jain SK, Murty CVR et al (2005) Proposed draft provisions and commentary on ductile detailing of RC structures subjected to seismic forces. IITK/GSDMA, EQ11- v4 & EQ16- v3 IIT, Kanpur
Jain SK, Ingle RK, Mondal G (2006) Proposed codal provisions for design and detailing of beam-column joints in seismic regions. ICJ 80:27–35
Jalla R (1999) Basement wall design – geotechnical aspects. ASCE J Arch Eng 5:89–91
Joshi DS, Nene RL, Mulay MD (2001) Design of RC structures for EQ resistance. Indian Society of Structural Engineers, Mumbai
Kameswararao NSV (2011) Foundation design theory and practice. Wiley, Singapore
Kelly JM (1986) Aseismic base isolation: review and bibliography. Soil Dyn Earthq Eng 5(3):202–216
Kelly JM (1990) Base isolation: Linear theory and design. Earthq Spectra 6(2)
Kelly JM (1997) Earthquake resistant design with rubber. Springer, London
Kelly JM, Konstantinidis DA (2011) Mechanics of rubber bearing – for seismic and vibration isolation. Wiley, Chichester
Kheyroddin A, Naderpour H (2007) Plastic hinge rotation capacity of RC beams. J Inst Civil Eng 5(1):30–47
Kramer SL (1988) Development of p-y curves for analysis of laterally loaded piles in western Washington. Research project, Washington (TRAC) 1988, no WA RD 153.1. Olympia: Washington State Dept. of Transportation, at Seattle, Washington
Kramer SL (2005) Geotechnical earthquake engineering. Pearson Education (Singapore) Private Limited, Singapore
Krawinkler H (1996) Pushover analysis: Why, how, when and when not to use it. In: Proceedings of the SEAOC convention, Maui, Hawaii

Kumar A, Sharma ML (ed) (2010) Earthquake engineering, vol 1. In: Proceedings of the 14th symposium on EQ engineering, IIT Roorkee, Elite Publishing House, Pvt Ltd, Delhi
Lam N, Wilson J, Hutchinson G (1998) The ductility reduction factor in the seismic design of buildings. Earthq Eng Struct Dyn 27:749–769
Mayes RL et al (2012) Using seismic isolation and energy dissipation to create earthquake resilient buildings. NZSEE 45:117–122
Medhekar MS, Jain SK (1993a) Seismic behaviour, design & detailing of RC shear walls – Part I: Behaviour & strength. ICJ 67:311–318
Medhekar MS, Jain SK (1993b) Seismic behaviour, design & detailing of RC shear walls – Part II: Design & Detailing. ICJ 67:451–457
Meli R et al (2011) Seismic design guide for low rise confined masonry buildings. Oakland, USA
Mendis PA, Panagopoulos C (2000) Applications of high strength concrete in seismic regions. In: 12th world conference on earthquake engineering, Auckland
Mesa ADA (2002) Dynamic amplification of seismic moments and shear forces in cantilever walls. Masters dissertation, Rose School, IUSS
Moehle JP et al (2010a) Seismic design of cast in place concrete, special structural walls and coupling beams. NIST, GCR 11-917-11 Rev1
Moehle JP, Hooper JD et al (2010b) Seismic design of cast in place concrete diaphragms, chords and collectors. Tech brief 3, NEHRP, NIST GCR 10- 917-4
Murnal P, Sinha R (2000) VFPI-an isolation device for aseismic design. Earthq Eng Struct Dyn 29:603–627
Murnal P, Sinha R (2002) Earthquake resistant design of structures using VFPI. ASCE J Struct Eng 128:870–880
Mylonakis G, Gazetas G (2000) Seismic soil – structure interaction: beneficial or detrimental? J Earthq Eng 4(3):277–301
Naeim F (ed) (2001) The seismic design handbook. Springer, Dordrecht
Naeim F, Kelly JM (1999) Design of seismic isolated structures. Wiley, New York
Nagaraj HB, Murty CVR, Jain SK (2006) Review (draft) of geotechnical provisions in IS 1893; 2002.IITK/GSDMA, EQ 13, v 1, IIT, Kanpur
Nimbalkar SS (2006) Seismic analysis of retaining walls by pseudo dynamic method. PhD thesis, IIT, Mumbai
Oguz S (2005) Evaluation of pushover analysis procedures for frame structures. MSc thesis at Middle East Technical University, Ankara
Otani S (2003) Dawn of earthquake engineering. In: 5th US-Japan workshop on performance based earthquake engineering, Hakone, Japan, 10–11 Sept
Park R (1986) Ductile design approach for RC frames. Earthquake Spectra 2(3):565–619
Paulay T (1972) Some aspects of shear wall design. Bull NZSEE 5(3):89–105
Paulay T, Priestley MJN (1992) Seismic design of RC and masonry buildings. Wiley, New York
Paz M (1985) Structural dynamics – theory and computation. Van Nostrand Reinhold, New York
Pecker A (ed) (2007) Advanced earthquake engineering analysis. Springer Wien, New York
PEERC (2010) Guidelines for performance based seismic design of tall buildings. PEERC, University of California, Berkeley
Priestley MJN, Calvi GM et al (2007) Displacement based seismic design of structures. IUSS Press, Pavia
Psycharis IN (1982) Dynamic behaviour of rocking structures allowed to uplift. PhD thesis, Cal Institute of Technology, Pasadena
Rai DC et al (2005a) Structural use of unreinforced masonry. IITK-GSDMA EQ 12, 19 & 25; IIT, Kanpur
Rai DC et al (2005b) Draft guidelines for structural use of reinforced masonry. IITK-GSDMA, IIT, Kanpur
Reese LC, Isenhower WM et al (2006) Analysis and design of shallow and deep foundations. Wiley, New York
Rodriguez ME, Montes R (2000) Seismic response and damage analysis of buildings supported on flexible soils. Earthq Eng Struct Dyn 29:647–665

Ruigrok JAT (2010) Laterally loaded piles. Thesis, TU Delft, Faculty of Civil Engineering
Schacher T (2007) Confined masonry – a guidebook for technicians and artisans. NICEE, Kanpur
Scheaua F (2011) Seismic base isolation of structures using friction pendulum bearings. Annales of University of Galati, Mechanical Engineering. Univ of Galati, Romania
SEAOC (1999) Recommended lateral force requirements and commentary. SEAOC, Sacramento
Singh Y, Nagpal AK (1994) Negative shear lag in framed tube buildings. ASCE J Struct Eng 120(11):3105–3121
Smith BS, Coull A (1991) Tall building structures: analysis and design. Wiley, New York
Solomon CS, Yim AM et al (1985) Simplified earthquake analysis of multistorey structures with foundation uplift. ASCE J Struct Eng 111(12):2708–2731
Spacone E, Martino R (2009) Non linear push over analysis of RC structures. Colorado advanced software Institute, University of Colorado, Boulder
Stewart JP, Fenves GL (1998) System identification for evaluating SSI effects in buildings from strong motion recordings. Earthq Eng Struct Dyn 27:869–885
Stewart JP, Seed RB et al (1998) Empirical evaluation of inertial SSI effects. PEERC, University of California, Berkeley
Sucuoglu H, Akkar S (2011) Introduction to earthquake engineering – lecture notes. Department of CE, Middle East Technical University, Ankara
Taly N (2000) Design of reinforced masonry structures. McGraw Hill, New York
Tanaka H, Kono S (2009) RC Structures – Design for shear and bond (+ flexure). International Institute of Seismology & Earthquake engineering, Kyoto, Lecture Note
Taranath BS (2010a) Reinforced concrete design of tall buildings. CRC Press, London
Taranath BS (2010b) Structural analysis and design of tall buildings. McGrawHill, New York
Taranath BS (2010c) Wind and earthquake resistant buildings. Marcell Decker, New York
Trifunac MD (2006) Biot response spectrum. Soil Dyn Earthq Eng 26:491–500
Trifunac MD, Brady AG (1975) A study on the duration of strong earthquake ground motion. Bull Seismol Soc Am 65:581
Tso WK (1990) Static eccentricity concept for torsional moment estimations. ASCE J Struct Eng 116(5):1199–1212
Uma SR, Meher Prasad A (2006) Seismic behaviour of beam-column joints in RC moment resisting frames – a review. ICJ 80:33–42
US Army Corps of Engineers (2007) Earthquake design and evaluation of concrete hydraulic structures. EM1110 – 2-6053. Department of the Army, Washington, DC
Wakabayashi M (1986) Design of earthquake resistant buildings. McGraw Hill, New York
Whittaker A, Hart G, Rojahn C (1999) Seismic response modification factors. J Struct Eng 125:438–444
Wilson EL (2002) Three dimensional static and dynamic analysis of structures. Computers and Structures Inc., Berkeley
Wolf JP (1985) Dynamic soil – structure interaction. Prentice – Hall Inc., Upper Saddle River
Wood JH (1973) Earthquake induced soil pressure on structures. Caltech EERL 73-05
Wood A (ed) (2008) Recommendations for the seismic design of high rise buildings. Council on Tall Buildings and Urban Habitat, Chicago
Yilma A (2005) Evaluation of analysis of framed tube and tube-in-tube structural systems for high rise buildings. MSc (Struct) thesis, Adis Ababa University
Zhang J, Andrus RD et al (2005) Normalized shear modulus and material damping ratio relationships. ASCE J Geotech Geo Environ Eng 131:453–464

# Index


**A**
Architectural planning, 156–158

**B**
Base isolation
  concept of, 389–391
  history of, 388–389
  merits and demerits of isolators, 394–395
  passive base isolators, 391
  primary isolator requirements, 393–394
Base shear, 36, 86, 90, 95, 103–106, 114, 116, 117, 135–138, 186, 190, 203, 210, 243, 253, 254, 256, 259, 331, 332, 339, 340, 343, 344, 347, 389, 413, 414, 416, 423, 424, 427–431, 434
Beam–column joints
  ductile detailing of a joint, 233–234
  joint behaviour, 228–231
  joint constructability, 234–235
  joint design, 231–233
  joint types, 237–238
Beams
  design for bond, 217–218
  design for moment, 214–216
  design for shear, 216–217
Bond and shear, 19–20, 35, 223, 233
Boundary elements, 270, 279, 282–285, 288, 294–296, 311, 332, 421
  codal requirements, 283
Building configuration, 156–165, 351–352

**C**
Cantilever shear walls
  balanced design, 276
  compression failure, 278–279
  design for sliding shear, 286–287
  detailing for flexure, 279–282
  flexural stress analysis, 275–276
  important design considerations, 274–275
  rocking foundation, 269
  tension failure, 276–278
Capacity based shear design, 284–287
Capacity spectrum method
  conversion to ADRS format, 430
  conversion to capacity spectrum, 431–432
  demand spectrum, 430–431
  locating the performance point, 432–433
Chord elements, 212–214
Collectors, 180, 208, 212–214, 261, 262
Columns
  corner, 223
  design, 220–224
  size, 223–224
  strong column–weak beam, 221
Combining gravity and dynamic loads, 60–61
Complete quadratic combination (CQC) method, 114–116, 134–135
Concrete
  hysteresis loop, 145, 146, 307, 308, 397
  stress strain curves, 17
  yogic concrete, 16–18
Confined masonry
  tie beam connections, 357
  tie beams, 355
  tie columns, 355
Core and outrigger system, 240–241




S. Manohar, S. Madhekar, *Seismic Design of RC Buildings*, Springer Transactions in Civil and Environmental Engineering, DOI 10.1007/978-81-322-2319-1

Coupled shear walls
degree of coupling, 290
design of coupling beams, 290–293
CQC method. *See* Complete quadratic combination (CQC) method

**D**
Damped free vibrations, 58, 64–69, 76
Damping
critical, 23–24
damped natural frequency, 49
damped period of vibration, 49
damping coefficient, 49
damping ratio, 22
energy dissipation, 50
magnitude of, 26
nature of, 48
proportional, 26–28
Rayleigh damping, 27, 51
types of, 21–22
viscous, 22
Deformation, 28–30, 33, 35–37, 39, 95, 97–99, 172, 174, 176, 177, 180, 181, 187, 188, 201, 204, 205, 210, 211, 223, 236, 247–249, 251–252, 272, 275, 291, 311, 317, 330, 337, 360, 387, 391, 393, 394, 396, 418, 422, 424–429
Degrees of freedom (DOF)
description of, 46–47
vibration frequencies in six, 47–48
Design earthquake, 7, 185, 388, 435
Design for diagonal tension, 284–289, 298
Design parameters
for masonry, 364
other parameters, 364–365
for reinforcement, 364
Detailing of stirrups, 205
Diaphragms
design forces, 209–210
flat slab, 210–212
flexible, 207
rigid, 207–208
transfer, 212
Distribution of lateral force among masonry piers
piers composed of vertical segments, 360
piers in series, 359–360
Drag member, 360, 375, 377
walls connected by, 360
Drift, 5, 15, 16, 36, 38, 43, 57, 73, 85, 87, 90, 107, 117, 150, 151, 155, 157, 164, 176, 181, 182, 190, 196, 199, 200, 203, 207, 211, 221, 235, 236, 239, 240, 242–244, 246, 248, 249, 251–253, 255, 256, 259, 265–267, 271, 274, 370, 394, 399, 419–421, 423–425, 428, 434, 437
Dual systems, 186–188, 201, 206, 239, 251, 275
Ductile detailing, 3, 43, 97, 103, 173, 179, 200, 201, 204–206, 219–220, 224–225, 233–234, 322, 390
Ductility
curvature, 30–32
displacement, 33–34
effect of, 97–99
importance of, 28–29
joint, 32–33
material, 30
rotational, 32–33
section, 30–32
structural, 29–30
Dynamic loads, 60–61, 160, 302, 393
Dynamic soil structure coupling
equivalent damping, 337
equivalent fixed based oscillator, 336
impedance functions, 334

**E**
Earth interior, 4
Earthquake effects, 7–8, 354
Earthquake excitation, 58, 67–69, 75–77, 90, 165
Elastomeric isolators
isolator damping, 397
isolator stiffness, 396–397
time period of isolator supported building, 397
Epicenter, 8–11, 14

**F**
Facade skin
curtain wall, 236–237
masonry infill, 235–236
Faults, 1, 6–7, 13, 14, 188, 303
Flanged wall, 270, 273, 368–369
Floating column, 160, 161, 178–179
Focus, 3, 9, 10, 43, 155, 223, 243, 303, 370, 419
Force based design, 28, 156, 184–190, 274, 418, 419
Frame side sway, 83

Friction pendulum system (FPS)
curvature of sliding surface, 407
effective damping ratio, 407–408
evaluation of slider parameters, 405–408
isolator displacement, 408
motion in different phases, 408–410
re-centring capability, 407

**G**
Gravity load, 43, 45, 60, 61, 123, 186, 188, 200, 206, 208, 211, 213, 214, 216, 217, 220, 224, 231, 238, 239, 241–243, 248, 250, 251, 265, 267, 270, 283, 284, 294, 295, 311, 315, 391, 392, 421, 424, 427
Ground motion
amplitude of, 303
direction of, 185
duration of, 304
frequency content, 303
local site effects, 302
path effect, 302
source effect, 302
time history of motion, 304–305
vertical, 95–96

**H**
Hazard levels, 204, 418, 419, 421–423, 427, 430
Historical review of seismic design, 1–4
Horizontal seismic coefficient, 86, 101–102, 106, 117, 136, 186, 253, 254, 256, 257, 339
Horizontal torsion
design forces including for torsion, 171–173
effects of, 173

**I**
Impulse loading, 58, 66–67, 84
Inertia effects, 185–188
Inertial interaction, 316, 331
Intensity scale, 12
Irregularity
geometrical, 164
horizontal, 162–163
mass, 164
stiffness, 164
strength, 164
vertical, 164–165

**K**
Kinematic interaction, 316, 322, 331

**L**
Laterally loaded piles
bending moment in a pile, 321
characteristic load method, 319–321
pile design criteria, 315–316
pile group effect, 321–322
pile top displacement, 321
*p*-multipliers, 322
*p-y* method, 316–319
Lateral stiffness
degradation of stiffness, 36
elastic-fully plastic, 36
nature of stiffness, 35–38
Linear dynamic procedure, 89, 203, 204, 256, 259
Linear static procedure
base shear, 105
distribution of base shear, 105–106
Load combinations, 189–190
Load path integrity, 156, 179–181
Logarithmic decrement, 24–26, 49
Lumped mass, 39, 44–46, 53, 69, 79, 80, 110, 113, 116, 118, 338

**M**
Magnitude scale, 13–14
Masonry buildings, 15, 349–385
Masonry components
brick units, 20
concrete blocks, 20
masonry mortar, 21
masonry reinforcement, 21
Masonry piers, 359–360
Masonry shear walls
reinforced grouted cavity walls, 361
special reinforced, 362
walls made up of hollow units, 361
Mass moment of inertia, 45–47, 55, 77, 87
Measuring ground motion, 11–12
Medvedev, Sponheuer and Karnik (MSK) scale, 12, 14
Missing mass correction, 118, 135, 138
Modal analysis
modal equation of motion, 107–109
modal frequencies, 110
modal height and moment, 114
modal mass, 112–114
modal participation factor, 112
mode shapes, 109–110

Modal analysis (*cont.*)
normalization of modes, 111–112
orthogonality of modes, 110–111
procedure, 116–117
Modulus of elasticity, 31, 38, 100, 277, 317, 320, 341, 358, 364, 370, 381
Moment magnitude, 13, 14
Moment of inertia, 37, 42, 46, 53, 55, 81, 82, 100, 101, 184, 244, 246, 274, 318, 320, 335, 358, 377, 378
Moment resisting frames (MRFs)
design and ductile detailing principles, 204–206
intermediate, 201
ordinary, 201
special MRFs, 200
M-O method of analysis, 323–325, 328, 341
Multi degree of freedom (MDOF) system, 39–40, 47, 51, 58, 69, 73–77, 80, 81, 93, 100, 107, 109–114
building fame on sliding (FPS) isolators, 410–412
frame on elasotomeric isolators
evaluation of natural frequencies, 403–405
motion of the entire system, 402–403

**N**

Newmark's numerical methods
average acceleration method, 122–123
linear acceleration method, 120–122
Non linear dynamic procedure (NDP), 204
Non linear MDOF system, 125–127
Non linear SDOF system, 123–125
Non linear static procedure, 203–204, 423–429
Non linear time history analysis, 123–127, 147
Non yielding walls, 323, 328–329

**O**

Open foundations, 310–314
ties, 312–314

**P**

P-Δ effects
direct method, 248–249
iterative gravity load method, 250
torque effect, 251
Performance based seismic design
collapse prevention, 421
evaluation of performance, 436–437
immediate occupancy, 420
life safety, 420–421
performance levels, 419–421
performance objectives, 422
zonal coefficient, 427
Piles
flexible, 316, 319, 340
pile cap details, 322–323
pile loads, 314–315
rigid, 316
Plastic hinge, 18, 29, 32–34, 52, 175, 187, 204, 205, 209, 214, 215, 219, 221, 224, 279, 282, 286, 289, 322, 420, 421, 425, 436, 437
progressive hinge formation, 437
Plate tectonics, 4–5
Pounding, 35, 155, 163, 165–167, 181, 305, 351
Predicting earthquake occurrence, 6–7
Pushover analysis
capacity curve, 423, 424, 429, 430, 432, 433, 435
capacity evaluation, 423–427
conducting, 427–429
control node, 429, 434
demand evaluation, 427
equivalent SDOF system, 426–427, 435, 436
lateral load pattern, 425–426, 436
merits and limitations of a, 424–425
pushover curve, 423, 424, 427, 429, 431, 432, 434–436

**R**

Redundancy, 44, 103–105, 156, 159, 160, 179–181, 184, 187, 200, 269, 314, 421
Reinforced masonry, 21, 235, 349–385, 420, 421
Relationship between spectral quantities
pseudo acceleration spectrum, 92
pseudo velocity spectrum, 92
Resonance, 69, 303
Response reduction factor
reduction due to ductility, 104
reduction due to overstrength, 104
reduction due to redundancy, 104–105
Response spectrum
acceleration spectrum, 92
design acceleration spectrum, 93
inelastic, 97–99
spectral displacement, 94
spectral velocity, 93
vertical acceleration spectrum, 96

Retaining walls, 118, 323–329
Rigidity of a pier, 359
Rigidity of a solid cantilever shear wall, 357–358
Rocking motion, 79–83, 270, 332
  rocking frequency, 83, 88

**S**
Seismic analysis procedures, 201–203
Seismic coefficient method
  equivalent stiffness, 434–435
  equivalent time period, 434–435
  target displacement, 435–436
Seismic considerations, 157, 174, 214, 351–354, 363, 396
Seismic waves
  body waves, 9
  surface waves, 9
Seismic zoning, 8
Sharing of lateral force, 173, 355–360
Shear lag effect, 241, 242, 247
Shear walls
  aspect ratio, 272–273
  classification of shear walls, 272–273
  ductile walls, 273
  functional layout, 270–272
  shape in plan, 273
Short column, 156, 176–178, 181, 253, 279, 283, 312, 387
Simple harmonic motion, 58–60
Single degree of freedom (SDOF) systems, 2, 23, 25, 29, 39, 46, 48, 58, 62–69, 75, 76, 81–83, 90, 91, 93, 97, 99, 100, 107, 109, 112, 113, 119, 122
  equation of motion of, 62–63
  frame on elasotomeric isolators
    frequencies for superstructure, 399–400
    roof displacement, 401
  frame on sliding (FPS) isolators, 405–410
Sliding isolators, 388, 392–393
Soft storey, 156, 174–176, 196, 220
  existence of, 176
Soil liquefaction
  causes of liquefaction, 309
  liquefaction potential, 310
Soil–structure coupling
  approximate effect of SSC, 339
  direct approach, 332
  simplified method for a MDOF system, 338–340
  simplified method for a SDOF system, 333–338
  sub-structure approach, 332–333
Square root of the sum of the squares (SRSS) method, 114, 115, 134, 135, 138, 189, 223, 253, 340, 344
Squat walls, 273, 287–289, 298, 360, 368
  design for flexure, 287
Staircases, 157, 174, 181–183, 391
Steel reinforcement, 15, 18–19, 43, 350, 382
  strain hardening, 18, 19, 36, 188
Stiffness values
  column stiffness, 39, 41, 54
  stiffness in torsion, 41–42
  stiffness matrix, 40
  stiffness of load bearing masonry wall, 41
  wall of uniform thickness, 40, 45
Storey drift, 16, 36, 85, 157, 176, 181, 196, 207, 242, 248, 253, 255, 256, 259, 266, 428
Storey shear, 73, 86, 106, 114, 117, 144, 150, 169, 176, 190, 192, 202, 223, 243, 246, 248, 253, 255, 256, 258, 259, 265, 267, 339, 345
Strength
  characteristic strength, 43
  overstrength, 43–44
  target strength, 43
Strength design of masonry shear wall
  equivalent stress block, 371
  interaction diagram, 371–372
  structural limit states, 369
Structural anatomy, 155, 174–183
Structural planning, 158–160
Subsoil parameters
  depth of soil overlay, 305–306
  dynamic shear modulus, 306
  grain size distribution, 307
  Poissons ratio, 306–307
  relative density, 308
  soil bearing capacity, 309
  soil damping, 307–308
  stratification, 305–306
  water depth, 308

**T**
Tall frames
  bundled tube framing, 241–242
  effect of higher modes, 243
  podium, 252–253
  reduction of frames, 243–247
  special aspects, 242–253
  tubular frame, 241

Tension shift, 218–219, 280–282
Time history analysis, 89, 90, 118–123, 127, 138, 140, 141, 147, 204, 242, 250, 281, 409, 423, 434
Time period of vibration
  effect of masonry infill, 100
  effect of shear walls, 101
Torsional vibrations, 77–79
Torsion computation for a multi-storey building
  centre of mass, 168, 169
  centre of rigidity, 167, 168
  by isolating a floor, 167–169
  by isolating a storey, 169–171
  torsional moment, 167, 169, 171
Tributary area, 202, 207
Tripartite plot, 93–95, 127
Two degree of freedom (Two-DOF) system, 69–73

**U**
Undamped free vibrations, 64–65, 69–74, 336, 403

**V**
Vertical response, 96
Vibration concepts, 57–88

**W**
Wall piers, 37, 282, 283, 359, 360, 375, 377
Wall subjected to axial load and in-plane flexure, 365–368
Wall subjected to out of plane forces, 368
Walls with openings, 293–294
Weak storey, 174–176, 196–198
  existence of a weak storey, 176
Working stress design
  check for flexure, 365–367
  check for shear, 367
  check for sliding shear, 368

**Y**
Yielding walls
  active thrust, 324–325
  dynamic incremental component, 325
  effect of soil cohesion, 327–328
  effect of water table, 327
  passive thrust, 325–326